IntechOpen

Liposomes

Edited by Angel Catala

LIPOSOMES

Edited by **Angel Catala**

Liposomes
http://dx.doi.org/10.5772/66243
Edited by Angel Catala

Contributors

Rajeev K. Tyagi, Yamnah Hafeji, Kunjal Agrawal, Vishwa Vyas, Anna Angela Barba, Sabrina Bochicchio, Gaetano Lamberti, Ting Wang, Ning Wang, Ann Mari Holsæter, Ulrich Massing, Natasa Skalko-Basnet, Sveinung G. Ingebrigtsen, Dieter Haemmerich, Anjan Motamarry, Mahmoud Ibrahim, Anroop B. Nair, Bandar E. Aldhubiab, Tamer M. Shehata, Alina Porfire, Marcela Achim, Lucia Tefas, Bianca Sylvester, Anna Timoszyk, Rita Milagros Nieto Montesinos, Sergey Kazakov, Gina Manda, Daniela Baconi, Anne-Marie Ciobanu, Maria Barca, George Traian Alexandru Burcea Dragomiroiu

Notice

First published in Croatia, 2017 by INTECH d.o.o.
eBook (PDF) Published by IN TECH d.o.o.
Place and year of publication of eBook (PDF): Rijeka, 2019.
IntechOpen is the global imprint of IN TECH d.o.o.
Printed in Croatia

Legal deposit, Croatia: National and University Library in Zagreb

Additional hard and PDF copies can be obtained from orders@intechopen.com

Liposomes
Edited by Angel Catala
p. cm.
Print ISBN 978-953-51-3579-1
Online ISBN 978-953-51-3580-7
eBook (PDF) ISBN 978-953-51-4622-3

Meet the editor

Angel Catalá was born in Rodeo (San Juan, Argentina). He studied chemistry at the Universidad Nacional de La Plata, Argentina, where he received a PhD degree in chemistry (Biological Branch) in 1965. From 1964 to 1974, he worked as an assistant in Biochemistry at the School of Medicine,
Universidad Nacional de La Plata, Argentina. From 1974 to 1976, he was a fellow of the National Institutes of Health (NIH) at the University of Connecticut, Health Center, USA. From 1985 to 2004, he served as a full professor of Biochemistry at the Universidad Nacional de La Plata, Argentina. He is a member of the National Research Council (CONICET), Argentina, and Argentine Society for Biochemistry and Molecular Biology (SAIB). His laboratory has been interested for many years in the lipid peroxidation of biological membranes from various tissues and different species. Professor Catalá has directed 12 doctoral theses and published over 100 papers in peer-reviewed journals, several chapters in books, and 11 edited books. Angel Catalá received awards at the 40th International Conference Biochemistry of Lipids 1999: Dijon (France). He is the winner of the Bimbo Pan-American Nutrition, Food Science and Technology Award 2006 and 2012, South America, Human Nutrition, Professional Category. In 2006, he received an award in pharmacology, Bernardo Houssay, in recognition of his meritorious works of research. Angel Catalá belongs to the Editorial Board of Journal of Lipids, International Review of Biophysical Chemistry, Frontiers in Membrane Physiology and Biophysics, World Journal of Experimental Medicine and Biochemistry Research International, World Journal of Biological Chemistry, Oxidative Medicine and Cellular Longevity, Diabetes and the Pancreas, International Journal of Chronic Diseases and Therapy, and International Journal of Nutrition.

Contents

Preface

Liposomes have received increased attention in recent years. Nevertheless, liposomes, due to their various forms and applications, require further investigation. These structures can deliver both hydrophilic and hydrophobic drugs. Preparation of liposomes results in different properties for these systems. In addition, there are many factors and difficulties that affect the development of liposome drug delivery structure.

The purpose of this book is to concentrate on recent developments on liposomes. The articles collected in this book are contributions by invited researchers with a long-standing experience in different research areas. We hope that the material presented here is understandable to a broad audience, not only scientists but also people with general background in many different biological sciences. This volume offers you up-to-date, expert reviews of the fast-moving field of liposomes. The book is divided into three major sections:

1. Liposome Preparation
2. Liposomes for Drug Delivery
3. Liposomes in Therapy

In the first chapter, Dr. Massing has described "Dual Centrifugation: A Novel "In-Vial" Liposome Processing Technique." In Chapter 2 "Phenomenological and Formulation Aspects in Tailored Nanoliposome Production" is described by Dr. Bochicchio. "Lipobeads" are summarized by Dr. Kazako in Chapter 3. In Chapter 4, Dr. Timoszyk described "Application of Nuclear Magnetic Resonance (NMR) to Study the Liposome Properties." Dr. Wang described "Liposomes Used as a Vaccine Adjuvant-Delivery System" in Chapter 5. In Chapter 6, "Hydrogels and Their Combination with Liposomes, Niosomes, or Transfersomes for Dermal and Transdermal Drug Delivery" is described by Dr. Ibrahim. In Chapter 7, Dr. Motamarry analyzed "Thermosensitive Liposomes." "Liposomal Drug Delivery to the Central Nervous System" is described in Chapter 8 by Dr. Montesinos. In Chapter 9, Dr. Porfire described "Liposomal Nanoformulations as Current Tumor Targeting Approach to Cancer Therapy." In Chapter 10, Dr. Ciobanu described "Methotrexate Liposomes: A Reliable Therapeutic Option." Finally, in Chapter 11, Dr. Agrawal described how "Liposome-Mediated Immunosuppression" plays an instrumental role in the development of "humanized mouse" to study *P. falciparum*.

I would like to express my gratitude to Ms. Romina Skomersic, the Publishing Process Manager, and Intech Open Access publisher for their efforts in the publishing process.

Angel Català
Instituto de Investigaciones Fisicoquímicas Teóricas y Aplicadas
(INIFTA-CCT La Plata-CONICET),
Facultad de Ciencias Exactas,
Universidad Nacional de La Plata,
La Plata, Argentina

Liposome Preparation

Chapter 1

Dual Centrifugation - A Novel "in-vial" Liposome Processing Technique

Ulrich Massing, Sveinung G. Ingebrigtsen,
Nataša Škalko-Basnet and Ann Mari Holsæter

Additional information is available at the end of the chapter

http://dx.doi.org/10.5772/intechopen.68523

Abstract

Conventional liposome preparation methods bear many limitations, such as poor entrapment efficiencies for hydrophilic drugs, batch size limitations, and limited options for aseptic manufacturing. Liposome preparation by dual centrifugation (DC) is able to overcome most of these limitations. DC differs from normal centrifugation by an additional rotation of the samples during the centrifugation process. Thus, the direction of the centrifugal forces changes continuously in the sample vials. The consequential powerful sample movements inside the vials result in powerful homogenization of the sample. Since this "in-vial" homogenization is optimal for viscous samples, semisolid "vesicular phospholipid gels" (VPGs) are preferred intermediates in the liposome manufacturing by DC. The DC method easily enables aseptic preparation and is gentler as compared to other methods, such as high-pressure homogenization. The method allows very small samples to be prepared, and VPG batches down to 1–5 mg scale have been prepared successfully. VPGs have several applications; they are attractive as depot formulations, or as stable storage intermediates, and can be easily transferred into conventional liposomal formulations by simple dilution. Here, we aim to present the novel DC-liposome technique; the concept, advantages, and limitations; and provide an overview of the experiences of liposome preparation by DC so far.

Keywords: dual centrifugation, dual asymmetric centrifugation, liposomes, vesicular phospholipid gels, homogenization, aseptic manufacturing

1. Introduction

Liposomes as a drug delivery system are considered to be one of the most successful developments regarding the transfer from laboratory research to actual products on the market.

From the first liposome drug delivery system approved for human use by the Food and Drug Administration (FDA) in 1995 (Doxil®), the field has expanded and, currently, 15 liposome- or lipid-based drug formulations are approved for human use [1]. Moreover, in 2013, there were 589 interventional drug studies focusing on liposomal drug formulations, of which at least 107 were active (ClinicalTrials.gov). The development in the field of liposome technology for extensive clinical studies requires industrial scale production not only due to the larger quantities but also under quality assurance and Good Manufacturing Practice guidelines [2].

The aim of this chapter is to provide an overview over the state-of-the-art of a novel liposome preparation technique: "in-vial" homogenization using dual centrifugation (DC). First, we explain the concept of the new method and why highly concentrated lipid dispersions, usually named vesicular phospholipid gels (VPGs), offer several advantages to this method. Second, we comment on the potential of this method and on our own experiences when applying DC for the preparation of VPGs or liposome dispersions. Finally, we compare the two dual centrifuges that have been used for liposome production so far: the Speedmixer DAC 150 FVZ (Hauschild GmbH & Co KG, Hamm, Germany), used in the first liposome manufacturing by this technique, as well as the recently constructed ZentriMix 380 R (Andreas Hettich GmbH & Co KG, Tuttlingen, Germany).

2. Liposome preparation by dual centrifugation: concept and mode of action

One of the most important and easy ways to prepare liposomes is to homogenize membrane-forming lipids together with an aqueous phase like a buffer and the drug substance to be entrapped. As homogenization tools, high-pressure homogenizers [3, 4], the "French press" [5, 6], microfluidizers [7, 8], and related devices can be used. For entrapping water-soluble drugs into liposomal vesicles with the highest possible entrapping efficiency (EE), it is of advantage to homogenize highly concentrated lipid-water-drug mixtures. Since this is also the preferred way to make liposomes by DC, the characteristics of this strategy will be discussed first, followed by the presentation of the concept of DC and its use to make liposomes.

2.1. Background: preparation of liposomes from highly concentrated lipid-water mixtures by homogenization

Homogenization of membrane-forming lipids together with an amount of water that is only sufficient to hydrate the polar head groups of the lipids (typically 50–70% water) results in highly concentrated, vesicular phospholipid gels (VPG) [3, 9]. Since the water used for VPG production is not sufficient to fill the inner core of the liposomes, it can be suggested that VPGs does not contain vesicular liposomes, but preliposomes that are expected to be flat structures without an aqueous core (**Figure 1**). The amount of water, which is sufficient only to hydrate the polar head groups, depends on the lipids used for VPG production. If bulky water-binding

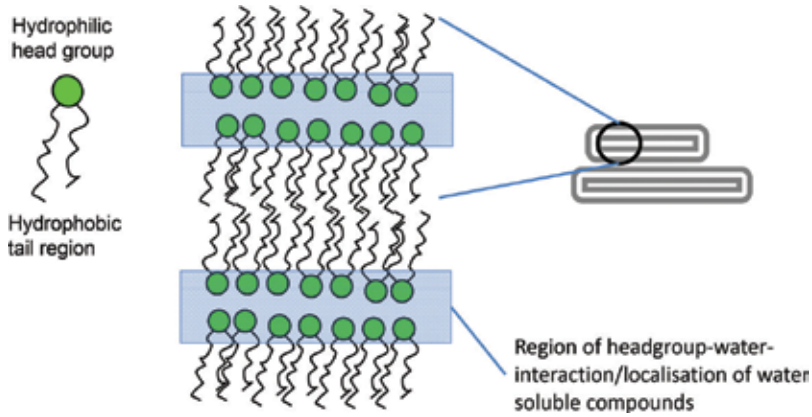

Figure 1. Schematic view of a VPG consisting of preliposomes without an aqueous core. Roughly, all water molecules—together with water-soluble drug compounds—are in use for hydrating the polar head groups of the membrane forming lipids.

structures like PEG-chains are part of the lipid membranes, more water is needed in contrast to lipids carrying only phosphocholine head groups [10].

VPGs have a creamy consistency [11] and can directly be used as depot formulations, e.g., as subcutaneous injectable depots [12, 13] or can be dispersed in an excess of water to get normal aqueous liposomal formulations [14]. Dispersion of the VPGs allows the formation of normal liposomes by filling the preliposomes with additional water molecules, which can easily diffuse across the lipid membranes (**Figure 2**). Since in preliposomes the water molecules together with the water-soluble drug molecules were only distributed over the surfaces of the polar membranes, and since the surface area inside the liposomes is nearly as large as outside, it becomes clear that EE values up to 50% can be reached in the dispersed liposomal formulations [10, 15–17].

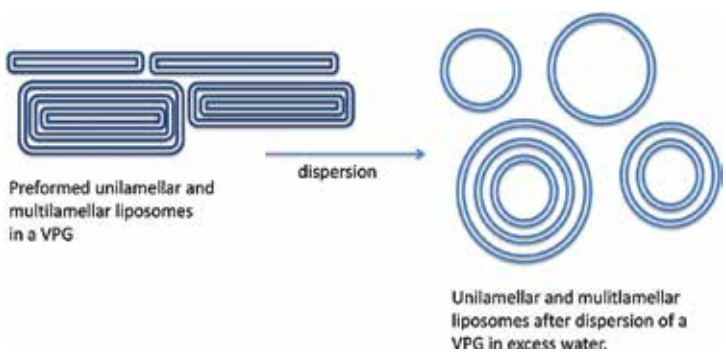

Figure 2. Schematic drawing of preliposomes in a VPG made by homogenization of a highly concentrated lipid-water mixture. The amount of water is sufficient to hydrate the phospholipid head groups, but is not sufficient to form vesicular, water-filled liposomes. The flat preliposomes became vesicular after dispersion of the preliposomes in an excess of water.

However, EE values higher than 50% for VPG-derived liposomes have been reported. This "overload" of water-soluble drugs is most probably due to the formation of multilamellar preliposomes and—after dispersion—of multilamellar liposomes (MLVs) (**Figure 2**). In MLVs, more of the membrane-associated, water-soluble drug molecules are entrapped due to the "entrapment" of additional membranes. Unfortunately, only a few articles reporting EE values >50% present also data on lamellarity—e.g., EM pictures [10, 17] or NMR studies.

Liposomes made by homogenization via VPG intermediates tend to have a higher lamellarity as seen by EM pictures [10, 17]. The lamellarity can somewhat be influenced by the type of lipids used [10]. Using lipids that ease the interactions between the surfaces of two membranes like PEG-carrying phospholipids leads to a higher lamellarity [17], whereby this interaction is further supported by the close vicinity of the membranes due to the low amount of water in the VPGs. In addition, also compounds to be entrapped may have an influence. Especially charged or very polar compounds that help to enable membrane-surface interactions like the multivalent-charged DNA molecules or divalent cations result preferably in the formation of MLVs during VPG production [16], and thus in very high EE-values.

In summary, the formation of liposomes with high EE values for water-soluble drug molecules as well as the formation of MLVs depends largely on the high lipid/water ratio used. Using an excess of water, EE as well as lamellarity goes down. Vice versa, using only the minimal necessary amount of water, EE is at its maximum, but lamellarity will be high as well.

Theoretically, reduction of the liposome diameter might help to reduce lamellarity, simply because in small liposomes there is only limited space to accommodate additional membranes. However, the average sizes of liposomes made by homogenization of highly concentrated lipid mixtures are small, but seldom below 100 nm with PI values > 0.2 (PCS (Photon Correlation Spectroscopy), intensity weighted[1]) [10, 16–21]. At a first glance, this appears somewhat confusing, since it is known that the liposome diameters clearly depend on the energy by which the highly concentrated lipid-water mixture has been treated and thus, liposomes made by HPH would have been expected to be very small.

The limited possibility of making very small liposomes via a VPG intermediate can be discussed as an intrinsic property of its high lipid concentration, typically >40% (w/v). During homogenization, the bigger membrane vesicles, which resulted from the initial hydration of the lipids, are broken into smaller membrane fragments, which spontaneously form smaller vesicles by self-organization. These smaller vesicles are disrupted again, forming even smaller vesicles. However, below a certain size, these lipid fragments not only form smaller vesicles by self-organization but also start to recombine into bigger vesicles. This process of recombination is more probable at an immediate vicinity of these fragments—or, in other words—at higher lipid concentrations as used for VPG-preparation.

To sum up, homogenization of highly concentrated lipid blends has been the preferred way to make liposomes with high EE for water-soluble drugs. The liposome sizes are still small enough even for parenteral use as well as for tumor accumulation via the so-called enhanced

[1]Many articles about liposomes made by HPH or DC present number-weighted PCS results, which values are much lower than the respective intensity-weighted PCS values.

permeability and retention effect (EPR-effect) [22]. The rather high content of multilamellar liposomes contributes to reach EE values of >50%. It has to be mentioned that multilamellarity of liposomes has never been reported as a problem in preclinical studies, e.g., in mice [14]. Furthermore, a high lipid load is sometimes of advantage. It has been found that liposomes made from hydrogenated phospholipids (PL) have anti-metastatic properties [23, 24] and that this effect is due to the high load of hydrogenated PL [25].

Despite the above-described advantages of liposomes made by homogenization, the homogenization tools currently in use have its limitations, especially for making liposomes in small batch sizes, under gentle and aseptic conditions. There is, therefore, a need for an alternative method that might overcome these limitations, which are listed below:

2.1.1. Batch sizes

Most of the homogenizers that are in use for liposome preparation have been developed to process bigger batches or at least batch sizes of several grams and very small batches are not possible due to the relatively high dead volumes of the devices. These "high" minimum batch sizes are a problem when only small amounts of liposomes are needed, i.e., for cell culture or animal experiments, and especially when the raw material applied is expensive or rare, like siDNA.

2.1.2. Harsh conditions

Since the samples in the normal homogenizers are in direct contact with the homogenizing unit (e.g., the homogenizing valve in HPH) for only a very short period of time (milliseconds), a large quantity of energy is needed to successfully homogenize the sample in that moment (VPG production with HPH: typically >700 bar, 10 cycles). Thus, the samples will heat up, which might damage the samples.

2.1.3. Cleaning/metal contamination

During homogenization, the liposomes are in contact with various parts of the homogenizers. Thus, a careful device cleaning prior to the liposome preparation is necessary. Furthermore, since the liposomes are squeezed through pumps and valves during homogenization, there is always the danger of product contamination with metal abrasion.

2.1.4. Number of samples

None of the known homogenizers is able to process more than one sample at once, which makes screening approaches burdensome, e.g., the screening for an optimal lipid composition for a new liposomal formulation.

2.1.5. Sterile formulations

The dimensions of the known homogenizers are rather big, only a few of them can be placed into a sterile bench. Thus, the production of sterile liposome formulations that are needed for cell culture, animal experiments, or for human use is difficult.

The above-listed limitations can be overcome by using dual centrifugation (DC) as a homogenization technique [15]. DC easily allows the gentle preparation of liposomes and other lipid nanoparticles in very small batch sizes. The use of closed and disposable vials avoids metal contamination as well as cleaning of the homogenization device ("in-vial" homogenization). Using sterile vials allows production of sterile formulations. Furthermor, since the vials are tihgtly closed during DC, safe handling of particles with toxic compounds is possible. Many samples can be produced in parallel, which allows effective formulation screening.

2.2. Principles of dual centrifugation (DC)

DC is based on centrifugation. But in contrast to normal centrifugation where samples are turned around a central axis, during DC, the sample vials are additionally turned around a second rotation axis (**Figure 3**). Due to that the direction of high centrifugal acceleration in the sample vials changes continuously, which result in high frequent and very powerful sample movements. In contrast to normal centrifugation, DC is not a separation technique. DC is simply the opposite, a process which can be used for extremely powerful sample mixing, milling, extraction, dissolution, and homogenization, which is the central theme of this chapter.

While using DC for mixing purposes is well known for decades (e.g., for the mixing of two-component dental filling materials), its usefulness for homogenization and for the preparation of lipid nanoparticles was first described in 2008 [15]. Homogenization power of a DC depends on the rotating speed and the diameter of the dual rotor (→ centrifugal acceleration) as well as the rotating speed around the second axis (→ frequency of changing the direction of centrifugal acceleration in the sample vial). Furthermore, the shape and the orientation of the sample vial placed in the dual rotor strongly influence the homogenization power.

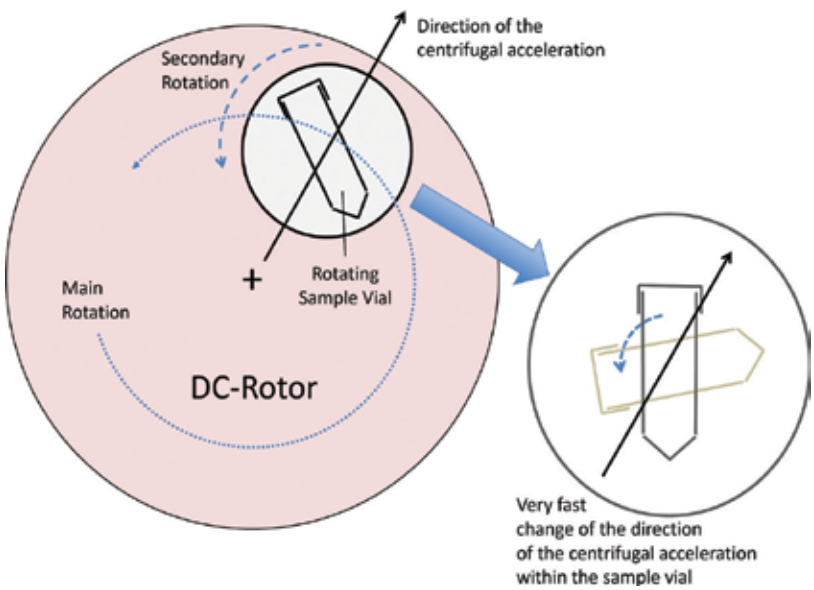

Figure 3. Principles of dual centrifugation (DC). Left: Dual rotor with a vial turning around its own axis (only one vial is shown). Right: Visualization of the changing direction of the centrifugal forces in a sample vial.

Homogenization power can also be increased by adding homogenization aids to the samples like ceramic beads.

2.2.1. Speed of main and secondary rotation

These parameters strictly depend on the type of dual centrifuge used for liposome preparation. Until now, two different dual centrifuges have been successfully used for this purpose, the ZentriMix 380R and the Speedmixer DAC 150. Despite being different in many aspects (the technical features of both DC devices are compared in Section 5), both devices are able to reach roughly the same maximum acceleration (about 600-700 × g) and have about the same ratio between the main and secondary rotation (about 3-4:1), which is sufficient for making liposomes from highly concentrated lipid dispersions.

2.2.2. Vial orientation during DC

Vials with a rather longish shape can be placed into the dual rotor in two different orientations—vertical or horizontal in relation to the plane of the second rotation unit (**Figure 4**). These different orientations result in two different homogenization processes.

2.2.2.1. Vertical vial orientation

Using the vertical vial orientation, the rotating vessel walls are always equally distant from the secondary rotation axis. Processing highly concentrated lipid dispersions, the viscous and sticky material adheres to the rotating vessel wall, whereby it is transported against the

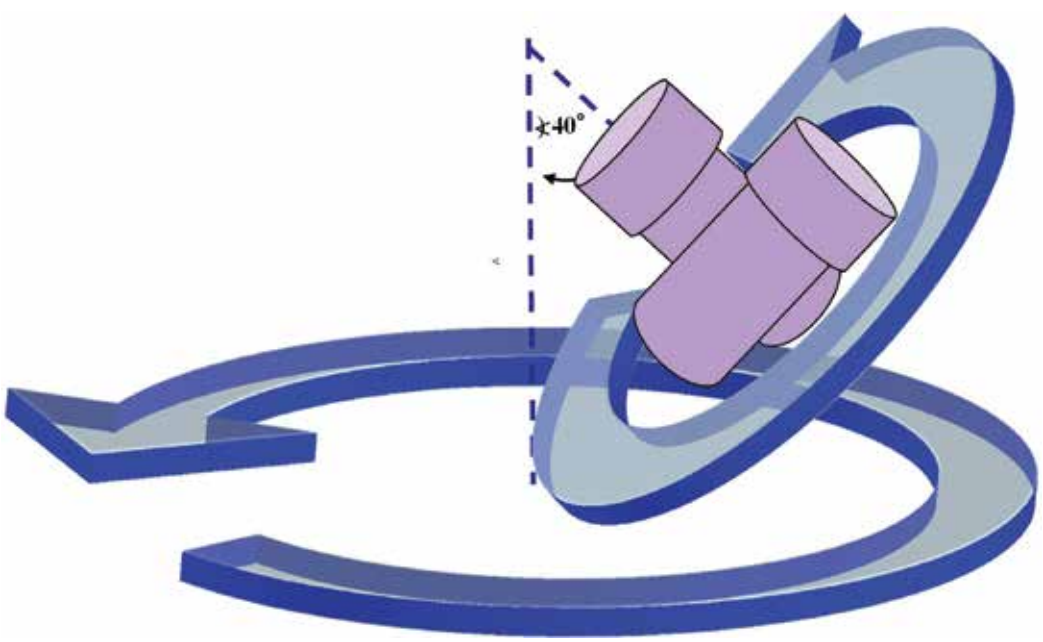

Figure 4. Vertical and horizontal orientation of long-shaped vials into a dual rotor.

centrifugal forces (inward movement). At the same time, the centrifugal force pushes the sample material that is not in close contact to the vessel wall in the opposite direction (outward movements). Both contrary movements results in strong friction and shear forces within the viscous material and thus, in homogenization (**Figure 5**, left). Homogenization using vertical vial orientation is especially effective in vials with a rather large diameter, e.g., 150 ml disposable PP beakers for the homogenization of bigger batches (**Figure 5**, right).

2.2.2.2. Horizontal vial orientation

Using the horizontal vial orientation, the position of the vial in relation to the centrifugal acceleration changes continuously while turning around the second axis (**Figure 6**). Having the lengthy vial parallel to the acceleration vector allows the material to gain speed and kinetic energy over a rather long distance, thus clashing to the top or the bottom of the vial with high impact. Within the next forth of rotation, nothing happens until the vial turns into an angel, which allows the movement of the sample material again. "From the vials point of view," the sample material constantly moves from the bottom to the top of the vial with high acceleration, including a soft transition in between. This type of movement is similar to that in a horizontal ball mill, with the difference that the acceleration of the sample material (and the balls) in DC is much higher and always constant (up to 1.000 × g). Especially when very small amounts of sample material will be homogenized in small vials (e.g., PCR tubes or 2 ml PP vials), the horizontal orientation is much more effective than the vertical orientation.

2.2.3. Homogenization aids

Despite liposome preparation by DC-homogenization is possible without any homogenization aids, the outcome gets better and the process faster if homogenization aids, in the form of heavy beads, are added. Those beads work in two ways: on the one side, the beads help to bring the sticky and viscous lipid blends rapidly in motion—simply by increasing the density

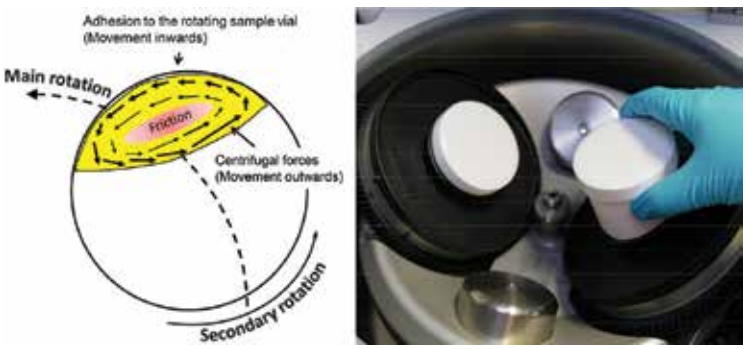

Figure 5. Left: Schematic view into a rotating vial in a dual rotor. At the same time, the viscous sample material (e.g., VPGs)—is transported against the centrifugal forces due to adhesion to the vessel wall, and in the opposite direction due to centrifugal acceleration of sample material rather distant to the vessel wall. Both contradictory movements result in shear forces and inner friction of the viscous sample material and thus, homogenization and formation of small liposomes. Right: Using standard PP beakers in a dual centrifuge placed in vertical orientation (view from top).

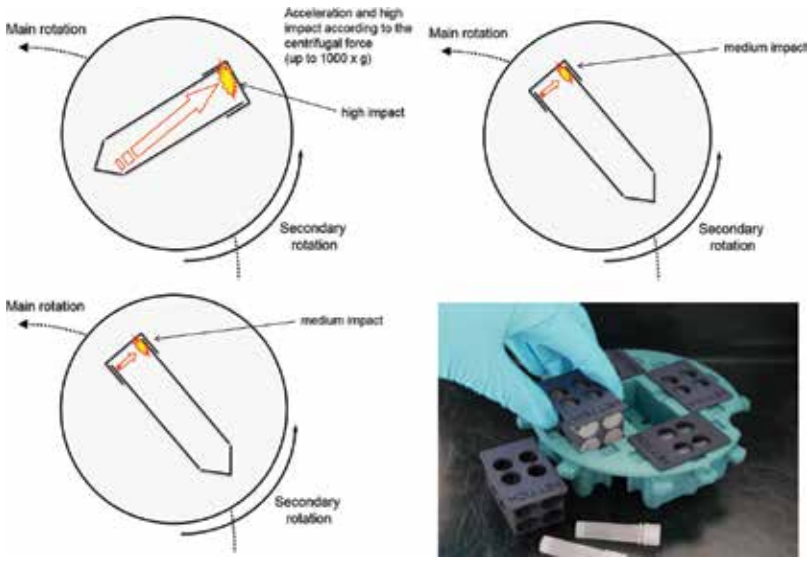

Figure 6. Schematic view into a lengthy vial in a dual rotor in "horizontal orientation," showing the movement of sample material (for detailed description of the process, see text). Below and left: Adapter for placing 20 × 2 ml vials in a dual centrifuge in horizontal position (only one of the two possible adapters is shown).

of the bead-lipid-water mixture and thus its potential energy which is not only a function of the centrifugal force but also of the weight of the accelerating material. On the other side, DC-homogenization is more effective due to the collision between the beads—with the viscous lipid mixture in between. That the bead-bead interactions play an important role for effective homogenization is supported by the finding that an increase in the number of beads while keeping the bead mass constant (smaller beads) results in the best DC-homogenization (more beads—more bead-bead interactions). Possible bead materials are glass, stainless steel, or ceramic.

2.2.3.1. Glass beads

At the onset of the development of DC-homogenization, glass beads which are cheap, easy to sterilize, and believed to be inert have been used. However, it turned out that glass beads get rapidly smaller during DC, which can be explained by their rather soft surface and the very frequent bead-bead interactions. In addition, depending on the intensity of the DC process and the processing time, samples developed an unpleasant smell of fish, a phenomenon which unfortunately was reproducible. We concluded that the frequent interactions between the glass beads results in micro- and nano-sized glass particles (dust) with a huge and, of course, fresh basic surface, e.g., due to the potassium oxide within the glass. We propose that due to these polar and basic particles, a so-called Hoffmann elimination of phosphatidylcholines takes place (**Figure 7**), resulting in phosphatidic acid, acetaldehyde, and trimethylamine, explaining the fishy smell. The reaction proposed here belongs to the field of heterogenic catalysis and has not been seen so far with phospholipids. Beside chemically of interest, even a little degradation of phospholipids due to the use of glass beads might be a problem. Thus, after a few initial studies, we completely avoided glass beads in DC for making liposomes.

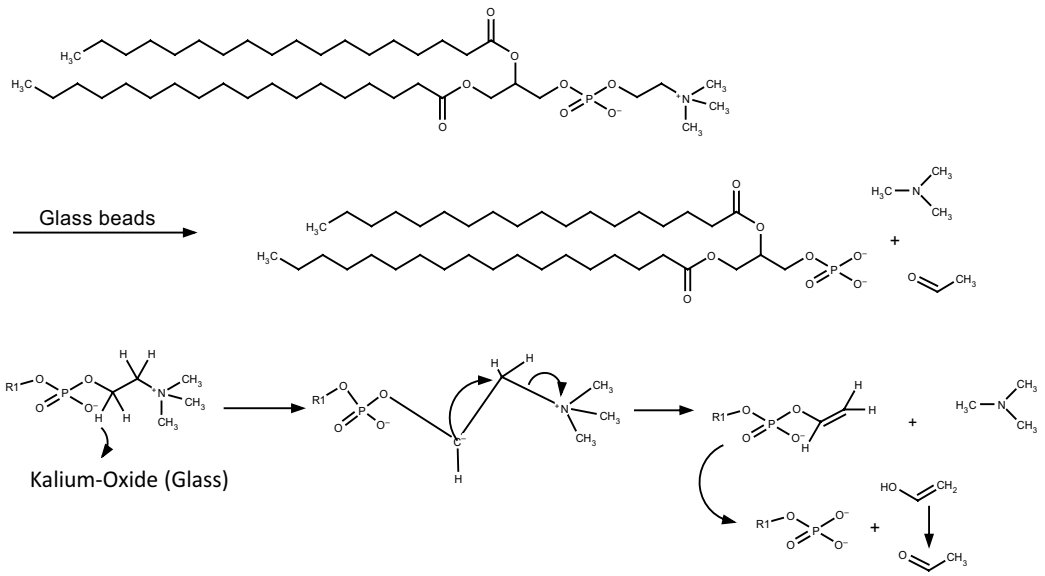

Figure 7. Proposed mechanism of the degradation of phosphatidylcholine during DC of phospholipid blends with glass beads as homogenization aids (top: Overview of the Hoffmann elimination of phosphatidylcholine. Below: Mechanism of the Hoffmann elimination of the phosphocholine unit).

2.2.3.2. Stainless steel beads

The biggest advantage of steel is its high density of typically > 7.5 kg/l, which would be ideal to support the process of the "in-vial" homogenization. Unfortunately, steel has a rather soft surface, resulting in steel abrasion that is not acceptable for formulations used in cell culture, animal experiments, or in men. Generation of lipophilic steel abrasion can easily be seen by the resulting yellowish-colored liposome preparations.

2.2.3.3. Ceramic beads

Ceramic is the material of choice, and there is a lot of experience for beads made of zircon oxide stabilized with yttrium (ZY-beads). ZY-beads have a density of > 6 kg/l, which is about three times higher than glass. In contrast to glass and steel, the surface is extremely hard (microhardness: 1.200 HV [hardness according to Vickers, corresponding to a Mohrs-hardness between 7 and 8]). ZY-beads are commercially available, even in food and pharmacy grade. Finally, using ZY-beads resulted in the best DC-homogenization so far (unpublished data). A typical procedure for making liposomes is to add the same weight of beads, as the weight of the lipid-water mixture in the respective vial. A typical diameter of ZY-beads used for liposome preparation is 1.5 mm which is big enough to subsequently remove the beads by filtration, or—after dispersion of the resulting VPG—by simply removing the liquid dispersion by a standard pipette, the beads are too big to be sucked into the pipette.

It has to be mentioned that zirconia-containing particles are in use to remove traces of phospholipids from extracts of biological samples to reduce the matrix effects during MS-analytics.

Thus, it can be assumed that the ZY-beads used for DC-homogenization also interact with the phospholipids during VPG production, an effect—if real—which obviously has no negative effect on liposome production.

3. Potential of the DC-liposome technique

Manufacturing of liposomal dispersions destined for human use and biomedical research should fulfill some important criteria, and the resulting liposomes should (i) be uniform/homogeneous, (ii) have a reproducible particle size range, (iii) be sterile, and (iv) be free of any traces of harmful substances such as organic solvents or glass residues. Not related to the manufacturing process, but very helpful for its acceptance would be an adequate shelf life of the liposomes [1]. In addition, the cost- and time-effectiveness of the manufacturing process should be considered. Based on these criteria, we discuss the potential of the newly developed DC-homogenization in liposome production in relation to

I. its reproducibility and robustness (Section 3.1),
II. the possible batch sizes and the sample capacity (Section 3.2),
III. the gentleness of the DC method as compared to other liposome preparation methods (Section 3.3) and
IV. the cost-effectiveness relative to other methods (Section 3.4)

In addition to these issues, we also discuss the potential of applying DC for the dilution of VPGs to normal liposomal dispersions (Section 3.5).

3.1. Reproducibility and robustness of the DC method (liposome size, PI, and EE)

3.1.1. Lipid concentration and composition

As already stated in Section 2, efficient homogenization and size reduction by DC demand concentrated and thus viscous lipid dispersions. With increasing lipid concentrations from 10% (w/v) up to 35% (w/v), an improved efficiency of DC-homogenization was observed, which was illustrated by decreasing vesicle sizes [15]. The reproducibility of the process was also improved with higher lipid contents, resulting in a lower variability of the liposome sizes between the batches. However, there is a threshold lipid concentration, and VPGs made from 50% (w/v) lipids showed a small increase in size and a poorer reproducibility [15]. Thus, a lipid concentration range between 35 and 45% (w/v) seemed advisable regarding the applied DC processing conditions; EPC3/cholesterol (55:45 mole/mole; 0.5 g batches in 30 ml injection vials plus 0.5 g glass beads (Ø = 1 mm); DC for 30 minutes at 3540 rpm (Speedmixer DAC 150 FVZ). However, different threshold values have been reported with different lipids applied. When a phospholipid mix with 80% phosphatidylcholine (Lipoid E-80) was the applied lipid raw material, VPGs with up to 50% lipids were successfully prepared [26]. Here, the 50% (w/v) VPGs enabled smaller liposomes (163.4 ± 58.2 nm) with lower standard deviation and

batch-to-batch variations, as compared to VPGs containing less lipids (30% (w/v): 486.2 ± 92.8 nm; 40% (w/v): 216.5 ± 76.3 nm). In addition, the more concentrated VPGs gave higher EE values and a lower polydispersity index (PI), with a PI of 0.287 ± 0.065 and 0.186 ± 0.044, in the 30 and the 50% (w/v) VPGs, respectively [26].

The effect of lipid composition on the liposome size has also been demonstrated for VPGs with the same lipid concentration and processing conditions. Using a more rigid lipid blend containing saturated phosphatidylcholine (HSPC/CHOL/DSPE-PEG) resulted in bigger liposomes than a more fluid mixture containing an unsaturated phosphatidylcholine (POPC/DDAB/DSPE-PEG) in 35% (w/v) VPGs [10]. Similarly, the morphology of the liposome vesicles was affected by the lipid composition, with more lamellas formed in more rigid lipid formulations [10]. The same effect was observed when propylene glycol was added to the lipid mixtures (PG-Lip) [18]. PG obviously reduces the lipid interactions in the lipid bilayers and makes the membranes more flexible than the conventional liposome formulation without PG (C-Lip). This gave a significant shorter DC processing time required to reach the aimed liposome sizes of 200–300 nm, the optimal liposome size for topical drug deposition [27], with a processing time of 3 minutes with PG vs. 50 minutes without PG [18]. In these experiments, the standard deviation of the vesicle sizes, and the PI values were higher for the PG-Lip formulation because of the reduced processing time. However, the reproducibility of the processing method was still found acceptable; PI = 0.31 ± 0.03 (PG-Lip) and PI = 0.13 ± 0.02 (C-Lip), mean liposome sizes and standard deviation (n ≥ 3) = 278 ± 66 nm (PG-Lip) and 282 ± 30 nm (C-Lip), respectively [19].

3.1.2. Processing time

As expected, but only up to a certain extent, the DC processing time affects the vesicle size [15]. When using a rather rigid lipid blend consisting of saturated phosphatidylcholine and cholesterol (55:45 [mole/mole]), 5 minutes of DC-homogenization at maximum speed gave a mean liposome size of 105 nm (measured by PCS, number weighted), and after 30 minutes of DC processing, the size was further reduced to 62 nm with a reduced standard deviation. Since longer DC processing (up to 60 minutes) gave no further size reduction, a processing time of 30 minutes was recommended as optimal [15].

3.1.3. Mixing aids

In the first DC-experiments, the addition of glass beads as a mixing aid has been demonstrated to increase the efficiency of the particle size reduction by DC-homogenization [15]. Regarding the amount of glass beads (Ø = 1 mm), the addition of 50–100% (w/w), relative to the total weight of the VPG, enabled the most efficient particle size reduction, as well as a more homogeneous size distribution [15].

Recently, alternative materials to glass as mixing aids have been tested and found more appropriate (see also Section 2.2.3). Even if glass beads have been the most applied mixing aid in DC [10, 15–19, 21, 28–32], and the minor amounts of glass particles found in the preparation postprocessing was judged acceptable [15]; new findings reported in Section 2.2.3 show that even a small amount of glass abrasion will catalyze the degradation of PC. Thus, ceramic beads

made of zircon oxide stabilized with yttrium (ZY-beads) seem to be the material of choice. The higher density of the ZY-beads, as compared to glass beads, results in a smaller volume of ZY-beads necessary to support DC-homogenization. In addition, since the ZY-beads are heavier and available in very small diameters, the number of beads can be increased to gain the aimed bead-bead interactions needed for efficient size reduction, whereas keeping the bead volume constant. However, successful preparation of liposomes by DC was also demonstrated without any mixing aid present [13, 33, 34].

3.1.4. Drug entrapment efficiency

In general, entrapping water-soluble drugs into VPGs does not seem to affect the liposome vesicle sizes [10, 15, 18]. The water-soluble fluorescence dye calcein has been used in several studies to investigate the entrapment efficiency of water-soluble drugs into DC-manufactured liposomes [15, 16, 21]. These studies, as well as a study where the fluorescence dye 5,6-carboxyfluorescein (CF) was used [35], demonstrate that the DC-VPGs enable a high EE of hydrophilic drugs compared to what is achievable with other techniques, and typically > 50% EE is reported. From the previous experience with VPGs made by HPH [36], the high EE of water-soluble drugs in the VPGs made by DC is somewhat expected. However, EE of calcein into VPGs made by HPH was surprisingly lower than into VPGs made by DC-homogenization (56.0 ± 3.3% vs. 36.0 ± 3.2%) [15]. This difference might be explained by the bigger size of the liposomes produced by DC (60 ± 5 nm [DC] vs. 36 ± 4 nm [HPH], both number weighted), and the suggested advantages of having liposomes with higher number of lipid lamellar bilayers (see Section 2.1.). Also in accordance with the suggestions made in Section 2.1, a higher drug entrapment of water-soluble drugs with increased lipid content has been demonstrated in several studies. As an example, EE values for the anticancer drug cytarabin (Ara-C) were 31.7 ± 0.31% in 30% (w/v) VPGs and 72.1 ± 0.25% in 50% (w/v) VPGs, respectively [6].

Also more lipophilic drugs, such as chloramphenicol (CAM), have been entrapped into liposomes by DC-homogenization and EE values close to 50% were found [18, 19]. When comparing this value with EE values obtained with the conventional liposome production techniques, probe sonication and filter extrusion, when using the same lipids and CAM-to-lipid ratio, a 70% increase in EE was achieved by using DC, even though the resulting liposomes were smaller (282 ± 30 nm) compared to those getting from sonication (836 nm) or extrusion (667 nm). Thus, the higher EE values were suggested to be due to the increased lipid concentration and the less available aqueous media for the drug to diffuse into, as CAM will be in an equilibrium between the dissolved portion of the drug present in the aqueous phase and the portion located in the lipid bilayer [18]. This is in agreement with the previous suggestions, claiming that VPGs that contain drugs that tend to diffuse through and from the liposome bilayers into the aqueous phase of the liposomal dispersion must be stored as VPGs to achieve an acceptable shelf life. This is because liposomal dispersions are characterized by a huge extravesicular water phase where these drugs will participate, and thus the EE of the drug will be reduced as soon as the VPGs are diluted into liposome dispersions [36].

To summarize, the most important factors affecting the size distribution for liposomes made by DC-homogenization are processing time, type, and size of the mixing aid, lipid concentration, and lipid composition. The polydispersity index (PI) obtained for liposomes made

by DC is rather low compared to that of HPH, reflecting a homogeneous size distribution, and PI values <0.2 are frequently reported [19–21, 28, 30, 35]. However, PI increases when bigger liposomes are obtained due to the formulation and/or processing conditions selected [15, 18, 26]. Regarding the entrapping efficiency of drugs into liposomes, DC seems to be advantageous over other manufacturing techniques, independently of the charge or solubility characteristics of the drug, and the DC method turned out to be robust and highly reproducible.

3.2. Batch sizes/sample capacity in DC

The batch sizes processed by DC homogenization depend on the capacity of the DC instrument used. So far, the DC technology in liposome production has been demonstrated at the laboratory scale, and the development of this technology for industrial scale production of liposomes remains to be confirmed. However, some progress has been made lately, with the new DC prototype ZentriMix 380 R that has a higher capacity compared to the Speedmixer DAC 150 FVZ which has been used for the basic developments of DC-homogenization (compared in Section 5 of this chapter). With the new ZentriMix 380 R, the maximum cargo has been substantially increased from 150 to 1000 g, but maybe more important, the number of the typically used 2 ml vials has been increased from 4 to 40.

The possibility of processing up to 40 samples with different compositions in the same run is a big advantage when conducting screening experiments, e.g., for comparing different liposome formulations. But also when using bigger vials, e.g., 10 ml injection vials for preparing liposomes for potential human use, 10 vials can be prepared in parallel (see **Table 1**, Section 5).

Beside the advantages of DC processing of many small sample vials in one run, the possibility to prepare very small batches significantly helps to save costs, e.g., when doing experiments with expensive materials such as siRNA [10, 16], or when compounds to be entrapped or special lipids are only available in small amounts [35, 37]. Thus, the typical batch sizes applied in the DC-homogenization are usually < 500 mg (2 ml vials), and batch sizes down to 20 mg [16] and 1–5 mg [37] have been reported as well. These small batch sizes significantly differ from the minimal batch sizes when using HPH. Even with one of the smallest HPH devices, the APV Micron Lab 40 lab-scale homogenizer, relatively huge amounts of lipids and drugs were necessary. Producing a VPG with a final lipid concentration of 40% would demand 16 g lipids and 24 g buffer to fill the 40 ml homogenization vessel [38]. Thus, with the sample material for one HPH experiment, 400 DC experiments (á 100 mg) can be performed, which allows efficient screening of the optimal conditions.

However, one can discuss that small batch sizes will reduce EE values for water-soluble compounds since such an effect was observed when siRNA was entrapped in conventional liposomes. Reduction of the batch size from 60 to 20 mg VPG resulted in a reduction of siRNA entrapment from 71 to 55% [16]. The same effect was observed for siRNA in sterically stabilized liposomes. Since it is known that nucleic acids have an affinity to polar glass surfaces, this batch size effect was explained by a possible unspecific binding of the siRNA to the vials surface [16]. Therefore, absorption of active ingredients onto the vial surface or to the surface

of the mixing aids (glass beads) might reduce EE values, especially when very small batches are processed. However, in the same study, entrapment of calcein, which has virtually no affinity to polar glass surfaces, was found not to be affected by the samples size [16].

Small batch sizes are also advantages when toxic materials, such as cytostatic or radioactive compounds, are used as ingredients in liposomes formulation. Since the DC method also facilitates handling samples in the closed container, it is advantageous to the environmental and personnel safety concerns. Thus, DC was the method of choice and enabled successful preparation of Ara-C containing VPGs for a local injection into the brain tissue, to provide a sustained drug release in treatment of gliomas, and *in vivo* studies in rat and mice models [26].

3.3. Gentleness of the DC method and advantages of closed container in DC

3.3.1. Temperature

All homogenization methods suitable for liposome size reduction are based on bringing energy into the sample through applying shear forces, which also contribute to a temperature increase of the sample. Rise in temperature will accelerate any hydrolytic degradation processes and should be avoided to protect phospholipids and other constituents from degradation. Since the Speedmixer DAC 150 FVZ has no cooling unit, the temperature and gentleness of the processing method were investigated carefully [15]. For comparison, VPGs were also prepared by the HPH performing 10 homogenization cycles at 700 bars. Both, DC- and HPH-liposomes were analyzed for phospholipid hydrolysis by measuring the content of the hydrolysis product, lyso-phosphatidylcholine (lyso-PC). The results showed that there was only a slight increase in lyso-PC during the DC processing (<0.1%), whereas the liposomes processed by HPH had a lyso-PC increase of approximately 1% when autoclaved, which is necessary to get sterile formulations [15]. The temperature of the sample during the DC was also monitored and found not to exceed 50 ± 1°C during the 30 minutes processing time (6 × 5 minutes, interrupted by mandatory breaks for downcooling) [15].

When 40% (w/w) DC-VPGs, containing Ara-C and added sodium sulfite as a preservative, were autoclaved, no chemical degradation was noticed after autoclaving, as no degradation products neither for the Ara-C drug nor for the E80 lipids applied in the formulation were found. The only change observed was an improved viscosity [26]. These results are in accordance with the earlier studies on autoclaving of VPGs made by HPH that was also proven stable during autoclaving [39].

The gentleness of the DC method opens new applications for VPGs and liposomes, namely, to incorporate highly sensitive drugs such as proteins, i.e., References [13, 28, 34]. As regards to the lack of a cooling unit, the short-run cycles are a common way to control the temperature rise, and Tian et al. [13] made 1.5 minutes of centrifugation steps interrupted by a cooling at 2–8°C every 6–8 runs, which gave a successful incorporation of model protein erythropoietin (EPO) into the VPGs. However, the new DC device ZentriMix 380 R is equipped with a powerful cooling unit, which allows also longer runtimes without cooling down breaks.

3.3.2. Closed container

Since DC homogenization is carried out in closed container(s), the sample vial(s) can be flushed with inert gas to reduce oxidation of sensitive components. This is however not the normal praxis, but sealing of the vials under nitrogen prior to autoclaving of VPGs has been reported [26]. Others have stored DC vials prefilled with beads and lipids (lipid film) under argon at RT until use [17]. The concept of making a homogeneous lipid film (molecular dispersed lipid mixture) directly in the DC vials for subsequent hydration and DC-homogenization has been demonstrated and found highly useful to optimize the "in-vial" performance of the method, avoiding material transfer and possible material loss [18, 19]. This is contrary to other liposome processing methods such as the HPH, membrane extrusion, or sonication. The high material recovery has been demonstrated by phosphorous determination in the liposomes after DC-homogenization and removal of the nonentrapped drug by filtration and or/or dialysis [19]. These results show a lipid recovery of about 100% after the DC-homogenization, and a lipid loss of approximately 13% after dialysis and filtration (0.22 μm filter). Thus, if acceptable EE values are obtained and a removal of nonentrapped drug is avoided, a close to 100% recovery is achievable.

The protection of light-sensitive drugs from light during liposome preparation is also possible by DC. In addition to the dark conditions provided in the locked DC machine, brown injection vials have been applied for extra protection during handling [15, 16, 18]. For comparison, when liposomes are prepared by the HPH, open handling is necessary to move the sample content from the receiver reservoir to the feeding reservoir in between every homogenization cycles (typically 10 cycles). Thus, to protect the sample from light during the processing, one would have to operate the instrument in the dark. Closed containers are also of advantage when toxic materials, such as cytostatic or radioactive compounds, are used as ingredients in liposomes formulation (environmental and personnel safety).

3.3.3. Bedside preparation

Since liposomal formulations contain water and since most low molecular weight drug molecules (e.g., conventional cytostatics) are able to diffuse through liposomal membranes from one aqueous compartment into the other, the liposome shelf life is limited to hours, days, or sometimes weeks. Furthermore, drug molecules sensitive to hydrolysis, like alkylants, might also hamper stability. Some drug molecules are also shown to promote phospholipid hydrolysis, like gemcitabine [40] and camptothecin [41]. Taken together, shelf life is a major problem when developing liposomal formulations. Since DC-homogenization allows fast and straightforward preparation of liposomes in sterile containers, bedside liposome preparations for patient treatments might be one potential application of DC in the future [15]. Applying readymade kits—containing the dry lipid mixture, the drug molecule, and mixing aid— would make the liposome preparation easy, as only adding the aqueous media before the subsequent DC processing to form VPGs, remains. This strategy might facilitate personalized medicine and bedside preparation to take place without any need for dedicated production rooms, as the DC method is performed with locked containers. Subsequent dilution (dispersion) of the VPGs and dosing of the resulting liposomes into an infusion bag would be one potential way of administering the drug, where the rapid infusion into the patient would complete the bedside preparations process. DC instruments are bench-top

machines, which fit into any hospital pharmacy, where the bedside preparation and the subsequent dosing can be performed. However, not only liposomes with a limited shelf life can be made assessable for the patients, also liposomal formulations carrying short living isotopes, e.g., PET tracers—for a better tumor visualization due to an improved tumor accumulation of the liposomes due to the EPR effect—might be a promising application for DC-homogenization. If necessary, the DC instruments are small enough to be placed into a sterile bench [15].

3.4. Cost-effectiveness of the DC-liposome technique

3.4.1. Easy and fast DC-homogenization

Many of the already mentioned advantages of the DC in liposome processing, such as high material recovery [19], small sample sizes [35], and straightforward and fast procedure [19], will also save material cost and personnel expenses in the laboratory. As compared to the more time-consuming techniques such as the filter extrusion [42], HPH homogenization [36], and ultrasound [43], the relatively higher drug EE obtained with concentrated lipid dispersions (VPGs) may make the time-consuming separation step, removing nonentrapped drug from the liposome drug carrier, unnecessary before the administration [18]. Especially when drugs are entrapped into liposomes to be protected from degradation in the blood stream, one might argue that the resulting liposome dispersions with high entrapment might be administered without removing the nonentrapped drug, as the free drug will be destroyed immediately after administration into the blood stream [11]. An example is liposomal gemcitabine, where the free gemcitabine has a half-life of 9 minutes, while the liposomal gemcitabine has a half-life of 13 hours [40].

3.4.2. Device cleaning

It is not only the fast homogenization procedure that is saving time to the operator as compared to other liposome techniques. With disposable and closed containers, the cleaning of the machine is avoided. This eliminates also the risk of cross contamination, which might happen during other methods resulting from a nonsufficient cleaning of the instrument (i.e., the probe applied in probe sonication—and instrumentation applied during extrusion—or HPH).

3.5. Mixing of liposomes into secondary vehicles

As DC is not only an "in-vial" homogenization tool but also an "in-vial" mixing or dispersion tool, DC machines are also suitable for dispersing the highly concentrated VPGs to normal liposomal dispersions. VPGs-dispersion in an aqueous media like a buffer can easily be performed by simply adding the required volumes of aqueous media to the VPGs, using the same vials already used for DC-homogenization, and continuing the DC process for typically 1–5 minutes [17, 28].

However, if topical liposome administration is the target application, there might be a need to disperse liposomes into more semisolid, viscous vehicles, such as hydrogels, to gain the wanted qualities of the product, such as texture, stability, drug release profile, and bioadhesion [44–47]. The DC technique has been proven suitable for both liposome processing and further

mixing of the liposomes into hydrogels, and the topical preparations as liposome-in-hydrogels was reported to be homogeneous after DC for 5 minutes at 3500 rpm in the Speedmixer [18]. The DC technique has also been applied to prepare liposomes for further embedding into gelatin [21]. Here, the DC technique was useful for both the size reduction of the liposomes forming VPGs and for the direct dispersion of liposomes into gelatin. Solid matrix liposomes in gels are obtained from the gelatin-VPG mass after the cooling [21].

4. Dual centrifugation: current application in liposome research

Since DC-homogenization was first introduced as an innovative method for liposome preparation in 2008 [15], a number of publications have appeared reporting on this technology for different liposome applications. However, the most appreciated advantages of the method seem to be its gentleness, the unusual high EE values for water-soluble drug molecules, and the small batch sizes. Moreover, the majority of the publications concern the entrapment of heat labile peptides and proteins. These proteins and peptides have been entrapped into VPGs and liposomes for different routes of administration: oral [21, 30, 31], nasal [33], and iv injection [17, 20, 28, 29], or as VPG-depot formulations [13, 34, 48]. Various organs were targeted as therapeutic sites: cancerous tissue [10, 26, 35], the central nervous system (CNS) and brain [28, 32, 33], liver [31], and skin [18, 19].

The DC "in-vial" liposome technique has facilitated a straight forward preparation method for entrapment of siRNA under sterile and RNase-free conditions, with EE close to 50% EE [16, 49]. Targeting of the siRNA-liposomes to neuroblastoma cells through applying DC in a combination with a sterol-based postinsertion technique was demonstrated *in vitro* [10].

Recently, the antitumor effect of anticancer drug cytarabin (Ara-C) loaded into VPGs was evaluated *in vivo* in nude mice bearing U87-MG glioma cells, as compared to empty VPGs and free drug in solution. The formulations were injected subcutaneously around the tumor. For the same Ara-C-VPG formulation, the *in vivo* drug release was studied in rat plasma and the *in vivo* biodistribution in rat brain evaluated for 28 days using the UPLC-ESI-MS/MS quantification assay [26]. Here, a sustained release of Ara-C from the VPGs was confirmed as the drug (Ara-C) administered as free drug in solution could be detected in rat plasma already after 7 hours postinjection into the brain, whereas no drug was detected after 7 days from the Ara-C-VPG formulation. Moreover, the therapeutic effect lasted at least for 28 days for the Ara-C loaded VPGs, and VPGs were thus suggested as a promising local delivery system for postsurgical sustained chemotherapy of gliomas [26].

The DC liposome technique has also been applied to explore new polymeric amphiphiles, so-called polyether lipids or polymer-lipid conjugates, for obtaining multifunctional liposomes. Here, DC was offering the benefit of testing the rationally designed polymer architectures in a microscale [35, 50].

In a different study, a simple and reproducible method for preparing immune-magneto-liposomes (ML-liposomes), with iron oxide particles (SPIOS) was developed applying the DC liposome "in-vial" technique. After the liposomes were formed, antigen binding to the surface of the

liposomes was successfully carried out applying a postinsertion technique [17]. The antigen should facilitate targeting of the activated platelets in atherothrombosis, and thus form a contrast agent for timely detection and diagnosis [17].

The DC technique has also been proven useful in preparing so-called liposomes-in-hydrogel formulations intended for topical application for local deposition of active ingredients and for a sustained release into the skin [18, 19]. In this production procedure, not only the homogenization and size reduction of the liposomes but also the mixing of the liposomes into the hydrogel vehicle was facilitated by the DC [18].

5. Description and comparison of the dual centrifuges used for liposome preparation

Until now, two different DC devices have been used for liposome production (compared in **Table 1** and **Figure 8**). The process of DC-homogenization was first discovered using the

	Speedmixer DAC 150	**ZentriMix 380 R**
Number of rotation units	1	2
Diameter of the rotation unit/usable area of the rotation unit	7.5 cm/44 cm^2	14.7 cm/170 cm^2
Distance between turning-point rotor and turning-point rotation unit	4.5 cm	10.0 cm
Primary rotation (minimum−maximum)	300–3450 rpm	50–2500 rpm
Ratio of primary and secondary rotation	~4:1	~3:1
Maximum centrifugal acceleration at the turning point of the rotation unit	600 × g	700 × g
Time to maximum speed (empty)	ca. 5 seconds	ca. 1 minutes
Maximum cargo (sample plus adapter)	150 g	1000 g (2 × 500 g)
Cooling unit (temperature range)	Nonexistent	Yes (−20 to 40°C)
Runtime	5 seconds–5 minutes	1 minutes–99 hours (30 minutes recommended)
Dimension (width × depth × height; weight); d	27.5 × 49.5 × 41.0 cm; 25 kg	47.0 × 76.0 × 40.0 cm; 82 kg
Maximum number of samples		
Twist top vials, 2 ml	4	40
Injection vials, 10 ml	1	10
Beakers, 150 ml	1	2
Centrifuge tubes, 15 or 50 ml	0*	6

*Tubes are too long for the diameter of the rotation unit.

Table 1. Properties of the dual centrifuges already used for liposome preparation.

Figure 8. Pictures of the two dual centrifuges: the Speedmixer DAC 150 FVZ (left) and the ZentriMix 380 R (right). Their respective rotors with typical vial holders are shown in the small pictures.

Speedmixer DAC 150 FVZ (Hauschild GmbH & Co KG, Hamm, Germany), which was predominantly constructed for the effective mixing of two-component dental filling materials as well as for other mixing tasks, e.g., in the field of printing inks. To better meet the requirements of DC-homogenization for the production of liposomes—which in particular are longer processing times and the need for efficient temperature control—a new dual centrifuge has been developed, the ZentriMix 380 R (Andreas Hettich GmbH & Co KG, Tuttlingen, Germany).

5.1. Speedmixer DAC 150 FVZ

The Speedmixer is a so-called "dual asymmetric centrifuge" (DAC), meaning that the dual rotor is asymmetrically built and carries only one rotation unit. The resulting imbalance during operation is compensated by a fix or by variable counter weights. Thus, the allowed total cargo is fixed at 5–150 g in predefined steps. In earlier versions of the Speedmixer, for each different sample type a special sample vial adapter had to be used which own weight plus the sample weight has to be 100–150 g. This type of construction is of advantage if the number of samples to be processed is only one. The diameter of the vial holder is approximately 7 cm which limits the number of 2 ml vials that can be processed in parallel to 4. Typical lab PP beakers with a volume of 150 ml can be processed easily, but not vials longer than 7 cm (e.g., 15 or 50 ml disposable centrifuge tubes).

Due to its powerful engine and the rather low weight of the dual rotor, the Speedmixer needs only seconds to reach its maximum speed. The second rotation for the DC process and the

main rotation are mechanically couplet by a v-belt, which has advantages in compensating the forces during acceleration, but also contributes to the rapid contamination of the rotor unit with rubbed-off parts of the v-belt.

The Speedmixer is constructed for rather short runs, and the effective mixing of the mentioned dental filling materials needs only 15 seconds. Longer runtimes resulted in a significant and rapid development of heat caused by the powerful engine and the used mechanic elements (v-belt mechanics and the bearings are deeply embedded in the rotor case). Since the heat production is intense, and no cooling unit is implemented, the maximum allowed and adjustable runtime is 5 minutes. Thus, reaching a runtime of 20–30 minutes needed for making liposomes by DC-homogenization, the Speedmixer has to be restarted at least 4–6 times. If temperature-sensitive samples have to be processed, it is necessary to patiently allow the Speedmixer as well as the samples to cool down between the 5-minute runs. For very sensitive samples, shorter runs have to be performed allowing intermediate downcooling of the Speedmixer and—more important—the samples. Running the Speedmixer in a cool place (cooling chamber) is of advantage.

5.2. ZentriMix 380 R

To improve the in-vial homogenization process in terms of temperature control, longer processing times and flexibility in the number, shape, and size of the sample vials, a new type of dual centrifuge (ZentriMix 380 R) was developed. In contrast to the Speedmixer, the ZentriMix is a symmetric dual centrifuge, meaning that the dual rotor carries two symmetrically placed rotation units. However, the abbreviation of this type of dual centrifugation is simply DC, but one might discuss if DSC would be more appropriate—as the opposite of the abbreviation DAC.

The dual rotor of the ZentriMix is rather heavy (≈15 kg), very robust, and can process cargos from a few milligrams up to 1 kg (2 × 500 g). Due to its higher weight, acceleration of the ZentriMix rotor is comparable to that of a normal centrifuge.

The ZentriMix is superior for long runtimes, the technical limit being 99 hours. This was not only achieved through the robust rotor case but also by a very robust mechanical coupling between the rotation units and the main rotation. This coupling has been realized through cogwheels made of polyamide, which also keeps the operation noise in an acceptable range. Furthermore, accumulation of heat is almost entirely prevented by a powerful cooling unit. For an optimal heat transport, sample vial holders made of aluminum are available (sample vial holders are usually made of polyamide), which further helps to keep the sample temperatures in acceptable ranges for most applications, even when 40 samples were processed at once.

6. Conclusion

DC has proven to be a straightforward and reproducible method for the production of various types of liposomes carrying a broad variety of drugs/active compounds. The method allows the preparation of different batch sizes. Especially interesting is the possibility to produce sterile liposomes; it is attractive for the immediate preparation of liposomes for *in vitro* cell culture or

in vivo animal experiments. The new dual centrifuges with improved manufacturing features and ability to control the in-vial homogenization process (e.g., by temperature control) will further contribute to the success of DC in the field of liposome preparation.

Acknowledgements

The publication charges for this article have been funded by a grant from the publication fund of University of Tromsø, the Arctic University of Norway. We also like to thank Vittorio Ziroli for making the pictures applied in this chapter.

Abbreviations

Chol	Cholesterol
DC	Dual centrifugation
DAC	Dual asymmetric centrifugation
EE	Entrapping efficiency
EPR effect	Enhanced permeability and retention effect
EPC3	Hydrogenated phosphatidylcholine
HPH	High-pressure homogenization
MLV	Multilamellar liposome
P.I.	Polydispersity index
VPG	Vesicular phospholipid gel

Author details

Ulrich Massing[1], Sveinung G. Ingebrigtsen[2], Nataša Škalko-Basnet[2] and Ann Mari Holsæter[2]*

*Address all correspondence to: ann-mari.holsater@uit.no

1 Andreas Hettich GmbH & Co KG, Freiburg, Germany

2 University of Tromsø–The Arctic University of Norway, Tromsø, Norway

References

[1] Kraft JC, Freeling JP, Wang Z, Ho RJY. Emerging research and clinical development trends of liposome and lipid nanoparticle drug delivery systems. Journal of Pharmaceutical Sciences. 2014;**103**:29-52. DOI: 10.1002/jps.23773

[2] Wagner A, Vorauer-Uhl K. Liposome technology for industrial purposes. Journal of Drug Delivery. 2011;**2011**:1-9. DOI: 10.1155/2011/591325

[3] Brandl M, Bachmann D, Drechsler M, Bauer KH. Liposome preparation by a new high pressure homogenizer Gaulin Micron Lab 40. Drug Development and Industrial Pharmacy. 1990;**16**:2167-2191. DOI: 10.3109/03639049009023648

[4] Dürr M, Hager J, Löhr J. Investigations on mixed micelle and liposome preparations for parenteral use based on soya phosphatidylcholine. European Journal of Pharmaceutics and Biopharmaceutics. 1994;**40**:147-156

[5] Purmann T, Mentrup E, Kreuter J. Preparation of SUV-liposomes by high-pressure homogenization. European Journal of Pharmaceutics and Biopharmaceutics. 1993;**39**: 45-52

[6] Barenholzt Y, Amselem S, Lichtenberg D. A new method for preparation of phospholipid vesicles (liposomes)—French press. FEBS Letters. 1979;**99**:210-214

[7] Mayhew E, Lazo R, Vail WJ, King J, Green AM. Characterization of liposomes prepared using a microemulsifier. BBA-Biomembranes. 1984;**775**:169-174. DOI: 10.1016/0005-2736(84) 90167-6

[8] Gregoriadis G, da Silva H, Florence AT. A procedure for the efficient entrapment of drugs in dehydration-rehydration liposomes (DRVs). International Journal of Pharmaceutics. 1990;**65**:235-242. DOI: 10.1016/0378-5173(90)90148-W

[9] Brandl M. Vesicular phospholipid gels. In: Weissig V. editors. Liposomes—Methods and Protocols. Vol. 1. Pharmaceutical Nanocarriers. New York: Humana Press; 2010. pp. 205-212. DOI: 10.1007/978-1-60327-360-2_14

[10] Adrian JE, Wolf A, Steinbach A, Rössler J, Süss R. Targeted delivery to neuroblastoma of novel siRNA-anti-GD2-liposomes prepared by dual asymmetric centrifugation and sterol-based post-insertion method. Pharmaceutical Research. 2011;**28**:2261-2272. DOI: 10.1007/s11095-011-0457-y

[11] Bender J, Michaelis W, Schubert R. Morphological and thermal properties of vesicular phospholipid gels studied by DSC, rheometry and electron microscopy. Journal of Thermal Analysis and Calorimetry. 2002;**68**:603-612. DOI: 10.1023/A:1016008306952

[12] Grohganz H, Tho I, Brandl M. Development and *in vitro* evaluation of a liposome based implant formulation for the decapeptide cetrorelix. European Journal of Pharmaceutics and Biopharmaceutics. 2005;**59**:439-448. DOI: 10.1016/j.ejpb.2004.10.005

[13] Tian W, Schulze S, Brandl M, Winter G. Vesicular phospholipid gel-based depot formulations for pharmaceutical proteins: Development and *in vitro* evaluation. Journal of Controlled Release. 2010; **142**:319-325. DOI: 10.1016/j.jconrel.2009.11.006

[14] Moog R, Burger A, Brandl M, Schüler J, Schubert R, Unger C, Fiebig H, Massing U. Change in pharmacokinetic and pharmacodynamic behavior of gemcitabine in human tumor xenografts upon entrapment in vesicular phospholipid gels. Cancer Chemotherapy and Pharmacology. 2002;**49**:356-366. DOI: 10.1007/s00280-002-0428-4

[15] Massing U, Cicko S, Ziroli V. Dual asymmetric centrifugation (DAC)—A new technique for liposome preparation. Journal of Controlled Release. 2008;**125**:16-24. DOI: 10.1016/j.jconrel.2007.09.010

[16] Hirsch M, Ziroli V, Helm M, Massing U. Preparation of small amounts of sterile siRNA-liposomes with high entrapping efficiency by dual asymmetric centrifugation (DAC). Journal of Controlled Release. 2009;**135**:80-88. DOI: 10.1016/j.jconrel.2008.11.029

[17] Meier S, Pütz G, Massing U, Hagemeyer CE, von Elverfeldt D, Meißner M, Ardipradja K, Barnert S, Peter K, Bode C, Schubert R, von zur Muhlen C. Immuno-magnetoliposomes targeting activated platelets as a potentially human-compatible MRI contrast agent for targeting atherothrombosis. Biomaterials. 2015;**53**:137-148. DOI: 10.1016/j.biomaterials.2015.02.088

[18] Ingebrigtsen SG, Škalko-Basnet N, Holsæter AM. Development and optimization of a new processing approach for manufacturing topical liposomes-in-hydrogel drug formulations by dual asymmetric centrifugation. Drug Development and Industrial Pharmacy. 2016;**42**:1375-1383. DOI: 10.3109/03639045.2015.1135940

[19] Ingebrigtsen SG, Škalko-Basnet N, de Albuquerque Cavalcanti Jacobsen C, Holsæter AM. Successful co-encapsulation of benzoyl peroxide and chloramphenicol in liposomes by a novel manufacturing method—dual asymmetric centrifugation. European Journal of Pharmaceutical Sciences. 2017;**97**:192-199. DOI: 10.1016/j.ejps.2016.11.017

[20] Tremmel R, Uhl P, Helm F, Wupperfeld D, Sauter M, Mier W, Stremmel W, Hofhaus G, Fricker G. Delivery of copper-chelating trientine (TETA) to the central nervous system by surface modified liposomes. International Journal of Pharmaceutics. 2016;**512**:87-95. DOI: 10.1016/j.ijpharm.2016.08.040

[21] Pantze SF, Parmentier J, Hofhaus G, Fricker G. Matrix liposomes: A solid liposomal formulation for oral administration. European Journal of Lipid Science and Technology. 2014;**116**:1145-1154. DOI: 10.1002/ejlt.201300409

[22] Maeda H, Wu J, Sawa T, Matsumura Y, Hori K. Tumor vascular permeability and the EPR effect in macromolecular therapeutics: A review. Journal of Controlled Release. 2000;**65**:271-284. DOI: 10.1016/S0168-3659(99)00248-5

[23] Jantscheff P, Ziroli V, Esser N, Graeser R, Kluth J, Sukolinskaya A, Taylor LA, Unger C, Massing U. Anti-metastatic effects of liposomal gemcitabine in a human orthotopic LNCaP prostate cancer xenograft model. Clinical & Experimental Metastasis. 2009;**26**:981-992. DOI: 10.1007/s10585-009-9288-1

[24] Graeser R, Bornmann C, Esser N, Ziroli V, Jantscheff P, Unger C, Hopt UT, Schaechtele C, Von Dobschuetz E, Massing U. Antimetastatic effects of liposomal gemcitabine and empty liposomes in an orthotopic mouse model of pancreatic cancer. Pancreas. 2009;**38**:330-337. DOI: 10.1097/MPA.0b013e31819436e6

[25] Raynor A, Jantscheff P, Ross T, Schlesinger M, Wilde M, Haasis S, Dreckmann T, Bendas G, Massing U. Saturated and mono-unsaturated lysophosphatidylcholine metabolism in tumour cells: A potential therapeutic target for preventing metastases. Lipids in Health and Disease. 2015;**14**:69. DOI: 10.1186/s12944-015-0070-x

[26] Qi N, Cai C, Zhang W, Niu Y, Yang J, Wang L, Tian B, Liu X, Lin X, Zhang Y, Zhang Y, He H, Chen K, Tang X. Sustained delivery of cytarabine-loaded vesicular phospholipid gels for treatment of xenografted glioma. International Journal of Pharmaceutics. 2014;**472**:48-55. DOI: 10.1016/j.ijpharm.2014.06.005

[27] Duplessis J, Ramachandran C, Weiner N, Muller D. The influence of particle size of liposomes on the deposition of drug into skin. International Journal of Pharmaceutics. 1994;**103**:277-282. DOI: 10.1016/0378-5173(94)90178-3

[28] Helm F, Fricker G. Liposomal conjugates for drug delivery to the central nervous system. Pharmaceutics. 2015;**7**:27-42. DOI: 10.3390/pharmaceutics7020027

[29] Pohlit H, Bellinghausen I, Schömer M, Heydenreich B, Saloga J, Frey H. Biodegradable pH-Sensitive Poly(ethylene glycol) Nanocarriers for allergen encapsulation and controlled release. Biomacromolecules. 2015;**16**:3103-3111. DOI: 10.1021/acs.biomac.5b00458

[30] Parmentier J, Hofhaus G, Thomas S, Cuesta LC, Gropp F, Schröder R, Hartmann K, Fricker G. Improved oral bioavailability of human growth hormone by a combination of liposomes containing bio-enhancers and tetraether lipids and omeprazole. Journal of Pharmaceutical Sciences. 2014;**103**:3985-3993. DOI: 10.1002/jps.24215

[31] Uhl P, Helm F, Hofhaus G, Brings S, Kaufman C, Leotta K, Urban S, Haberkorn U, Mier W, Fricker G. A liposomal formulation for the oral application of the investigational hepatitis B drug Myrcludex B. European Journal of Pharmaceutics and Biopharmaceutics. 2016;**103**:159-166. DOI: 10.1016/j.ejpb.2016.03.031

[32] Fülöp A, Sammour DA, Erich K, von Gerichten J, van Hoogevest P, Sandhoff R, Hopf C. Molecular imaging of brain localization of liposomes in mice using MALDI mass spectrometry. Scientific Reports. 2016;**6**:33791. DOI: 10.1038/srep33791

[33] Chen KH, Di Sabatino M, Albertini B, et al. The effect of polymer coatings on physicochemical properties of spray-dried liposomes for nasal delivery of BSA. European Journal of Pharmaceutical Sciences. 2013;**50**:312-322

[34] Buchmann S, Sandmann GH, Walz L, Reichel T, Beitzel K, Wexel G, Tian W, Battmann A, Vogt S, Winter G, Imhoff AB. Growth factor release by vesicular phospholipid gels: In-vitro results and application for rotator cuff repair in a rat model. BMC Musculoskeletal Disorders. 2015;**16**:82. DOI: 10.1186/s12891-015-0542-1

[35] Fritz T, Hirsch M, Richter FC, Müller SS, Hofmann AM, Rusitzka KAK, Markl J, Massing U, Frey H, Helm M. Click modification of multifunctional liposomes bearing hyperbranched polyether chains. Biomacromolecules. 2014;**15**:2440-2448. DOI: 10.1021/bm5003027

[36] Brandl M. Vesicular phospholipid gels: A technology platform. Journal of Liposome Research. 2007;**17**:15-26. DOI: 10.1080/08982100601186490

[37] Fritz T, Voigt M, Worm M, Negwer I, Müller SS, Kettenbach K, Ross TL, Roesch F, Koynov K, Frey H, Helm M. Orthogonal click conjugation to the liposomal surface reveals the stability of the lipid anchorage as crucial for targeting. Chemistry—A European Journal. 2016;**22**:11578-11582. DOI: 10.1002/chem.201602758

[38] Brandl M. Vesicular phospholipid gels. Methods in Molecular Biology. 2010;**605**:205-212. DOI: 10.1007/978-1-60327-360-2_14

[39] Tardi C, Drechsler M, Bauer KH, Brandl M. Steam sterilisation of vesicular phospholipid gels. International Journal of Pharmaceutics. 2001;**217**:161-172. DOI: 10.1016/S0378-5173(01)00605-6

[40] Moog R, Brandl M, Schubert R, Unger C, Massing U. Effect of nucleoside analogues and oligonucleotides on hydrolysis of liposomal phospholipids. International Journal of Pharmaceutics. 2000;**206**:43-53. DOI: 10.1016/S0378-5173(00)00497-X

[41] Sætern AM, Skar M, Braaten Å, Brandl M. Camptothecin-catalyzed phospholipid hydrolysis in liposomes. International Journal of Pharmaceutics. 2005;**288**:73-80. DOI: 10.1016/j.ijpharm.2004.09.010

[42] Berger N, Sachse A, Bender J, Schubert R, Brandl M. Filter extrusion of liposomes using different devices: Comparison of liposome size, encapsulation efficiency, and process characteristics. International Journal of Pharmaceutics. 2001;**223**:55-68. DOI: 10.1016/S0378-5173(01)00721-9

[43] Woodbury DJ, Richardson ES, Grigg AW, Welling RD, Knudson BH. Reducing liposome size with ultrasound: Bimodal size distributions. Journal of Liposome Research. 2006;**16**:57-80. DOI: 10.1080/08982100500528842

[44] Mourtas S, Fotopoulou S, Duraj S, Sfika V, Tsakiroglou C, Antimisiaris SG. Liposomal drugs dispersed in hydrogels. Effect of liposome, drug and gel properties on drug release kinetics. Colloids Surfaces B Biointerfaces. 2007;**55**:212-221. DOI: 10.1016/j.colsurfb.2006.12.005

[45] Hurler J, Žakelj S, Mravljak J, Mravljak J, Pajk S, Kristl A, Schubert R, Škalko-Basnet N. The effect of lipid composition and liposome size on the release properties of liposomes-in-hydrogel. International Journal of Pharmaceutics. 2013;**456**:49-57. DOI: 10.1016/j.ijpharm.2013.08.033

[46] Elnaggar YSR, El-Refaie WM, El-Massik MA, Abdallah OY. Lecithin-based nanostructured gels for skin delivery: An update on state of art and recent applications. Journal of Controlled Release. 2014;**180**:10-24. DOI: 10.1016/j.jconrel.2014.02.004

[47] Mourtas S, Haikou M, Theodoropoulou M, Tsakiroglou C, Antimisiaris SG. The effect of added liposomes on the rheological properties of a hydrogel: A systematic study. Journal of Colloid and Interface Science. 2008;**317**:611-619. DOI: 10.1016/j.jcis.2007.09.070

[48] Breitsamer M, Winter G. Needle-free injection of vesicular phospholipid gels—A novel approach to overcome an administration hurdle for semisolid depot systems. Journal of Pharmaceutical Science. 2017;**106**:968-972. http://dx.doi.org/10.1016/j.xphs.2016.12.020

[49] Camenzind A, Schweizer T, Sztucki M, Pratsinis SE. Structure & strength of silica-PDMS nanocomposites. Polymer. 2010;**51**:1796-1804. DOI: 10.1016/j.polymer.2010.02.030

[50] Müller SS, Fritz T, Gimnich M, Worm M, Helm M, Frey H. Biodegradable hyperbranched polyether-lipids with in-chain pH-sensitive linkages. Polymer Chemistry. 2016;**7**:6257-6268. DOI: 10.1039/c6py01308b

Chapter 2

Phenomenological and Formulation Aspects in Tailored Nanoliposome Production

Sabrina Bochicchio, Gaetano Lamberti and
Anna Angela Barba

Additional information is available at the end of the chapter

http://dx.doi.org/10.5772/intechopen.68157

Abstract

Liposomes as cell-mimetic system have attracted wide attention of researchers in various branches of the drug delivery topic as they can be highly functionalized and personalized, thus solving the major drawbacks of bioactive molecules linked to their low stability, limited membrane permeability, short half-life and low bioavailability. The development of sustainable processes able to produce ad hoc liposomes in a rapid manner through the use of not-laboured techniques, avoiding drastic conditions, is of great relevance for the industrial sector. In this chapter, two novel liposome production processes, the ultrasound-assisted thin-film hydration and the simil-microfluidic techniques sharing the same size reduction/homogenization preparative step, are presented. The phenomenological aspects involved in vectors constitution through the duty cycle sonication process (bilayer rupture/vesicles formation mechanisms) and through the simil-microfluidic approach (intubated flows interdiffusion mechanisms) are described. Finally, two applications as case histories involving the use of the developed techniques for relevant classes of active molecule delivery are described. In particular, a pharmaceutical application concerns the encapsulation of short-interfering RNA (siRNA) molecule, used for gene therapy, inside cationic nanoliposomes, and a nutraceutical application consists in the production of ferrous sulphate anionic liposomal formulations with improved features compared to those already present on the market.

Keywords: ultrasonic size reduction, simil-microfluidic approach, nanoliposomes delivery systems, personalized carriers, cell-mimetic system, gene therapy, nutraceuticals

1. Introduction

Liposomes are closed vesicular structures, constituted by one or more phospholipid bilayers, which are formed when membrane lipids, such as phosphatidylcholine (PC) and

cholesterol (CHO), are dispersed in an excess of water. Liposomes are efficient delivery systems, which are able to ensure a controlled and targeted release of active molecules due to their high biocompatibility, stability, biodegradability, intrinsic toxicity and immunogenicity [1]. Liposomes are also versatile systems in terms of dimensions and chemical modifications, they can be easily reduced in size and coated with different polymers and their surface can be chemically modified with specific ligands to give active targeting. These characteristics, together with their similarity to biological membranes, make them vectors of great interest when compared with other carriers. In particular, size and size distribution are key parameters determining liposomes performance as delivery systems. Compared with micrometre-sized carriers, produced by traditional microencapsulation techniques, nanoparticles have a larger interfacial surface area and have the potential to improve the solubility, enhance the bioavailability and improve the controlled release of the bioactive principle [2]. In nutraceutical applications, liposomes of nanoscale dimensions can improve taste, flavour, stability, absorption and bioavailability of the bioactive compounds [3–6]. From a pharmaceutical point of view, nanoparticles are preferred for their elongated retention time in the small intestine when compared to the larger structures [7] and are particularly desired due to the enhanced permeability and retention (EPR) effect [8]: liposomes with small dimensions can permeate through membrane fenestrations of diseased blood vessels penetrating into the tumour tissue [9].

Due to their favourable features, liposome-based products to be used in pharmaceutical and nutraceutical field have risen together with the need of large-scale and low-environmental impact techniques capable of producing significant amounts of liposomes in a short time and without the use of drastic conditions. Indeed, according to the Paris Agreement on climate change [10], innovation must go hand in hand with the developing of green products, improving the business processes and scaling up investments through greater energy and material efficiencies [11]. The energy efficiency and emissions reduction in the industrial sectors are the crucial point. All this constitutes the basis of the modern industrial manufacturing and the approach is referred as process intensification PI [12–14].

Nowadays, there are a wide set of possibilities to produce lipid-based drug delivery systems through the use of conventional or more recently discovered techniques [15–17]. The membrane contactor, the supercritical fluid and the microfluidic methods [18–20] are among the most recent.

However, despite the leaps and bounds made with the novel technologies in the last few years, the majority of these methods are characterized by high-energy request, long times of process, the use of toxic solvents together with a low productivity. In particular, the most used techniques, such as the ethanol injection [21] or the thin-film hydration (TFH) method, are bench-scale methods characterized by bulk discontinuous processes. Microfluidics is a relatively new technology used for the production of liposomes on nanometric scale [22]. The latter gives the possibility to produce, in a continuous manner, small unilamellar liposomes (SUVs) with a precise control on liposomes dimensional features by modulating the flows at

micrometric scale; anyway the method is characterized by elevated costs of microfabrication and low-product volumes in output.

To overcome these limitations, in this work, two novel versatile and reliable techniques for nanoliposomes production, based on the use of ultrasound as process intensification tool, have been presented. At first, in order to produce, in a versatile manner, nanometric structures with the desired dimension, an ultrasound-assisted size reduction process was developed and coupled with the conventional thin-film hydration method. Subsequently, due to its reliability and versatility, the ultrasound-assisted process generated was also used for liposomes homogenization operation during vesicles production through a simil-microfluidic approach. In that regard, a semi-continuous apparatus, based on microfluidic principles, was expressly designed and fabricated in order to produce higher volumes of lipid vectors, potentially on production scale, directly of nanometric size, overcoming the limitations of the small output volumes typical of the conventional bench-scale techniques. The phenomenological aspects involved in vectors constitution were investigated and described for both the adopted setup. The two methods were finally adopted for short-interfering RNA (siRNA) and ferrous sulphate encapsulation in ad hoc-formulated nanoliposomes to be used in pharmaceutical and nutraceutical applications, respectively.

2. Novel developed techniques for liposomes production

2.1. Ultrasound-assisted thin-film hydration: layout, principles and phenomenological aspects

A versatile and reliable technique able to produce liposomes of different sizes to be used for disparate applications has been developed by coupling the conventional thin-film hydration method [16], which produces micrometric structures, with an ultrasound-assisted process developed to prepare, in a versatile manner, nanometric structures with the desired dimensions. In particular, the size of liposomes is determined during the production process, decreasing due to the addition of ultrasound energy. The energy is used to break the lipid bilayer into smaller pieces, then these pieces close themselves in spherical structures as phenomenologically detailed in Section 2.1.3.

2.1.1. Layout

Figure 1 shows a schematization of nanoliposomes production process through the ultrasound-assisted TFH technique developed. The setup is composed by four main sections: a feeding section where solutions are stored, an evaporation section, constituted by a rotary evaporator (Heidolph, Laborota 4002 Control), where solvents are removed, a production section composed of a tank where vesicles are formed and then homogenized through the use of an ultrasonic source (VCX 130 PB Ultrasonic Processors of Sonics & Materials Inc., CT, USA; maximum power of 130 W; frequency of 20 kHz), giving nanoliposomes as output product and, finally, a recovery section where vesicles are collected and characterized.

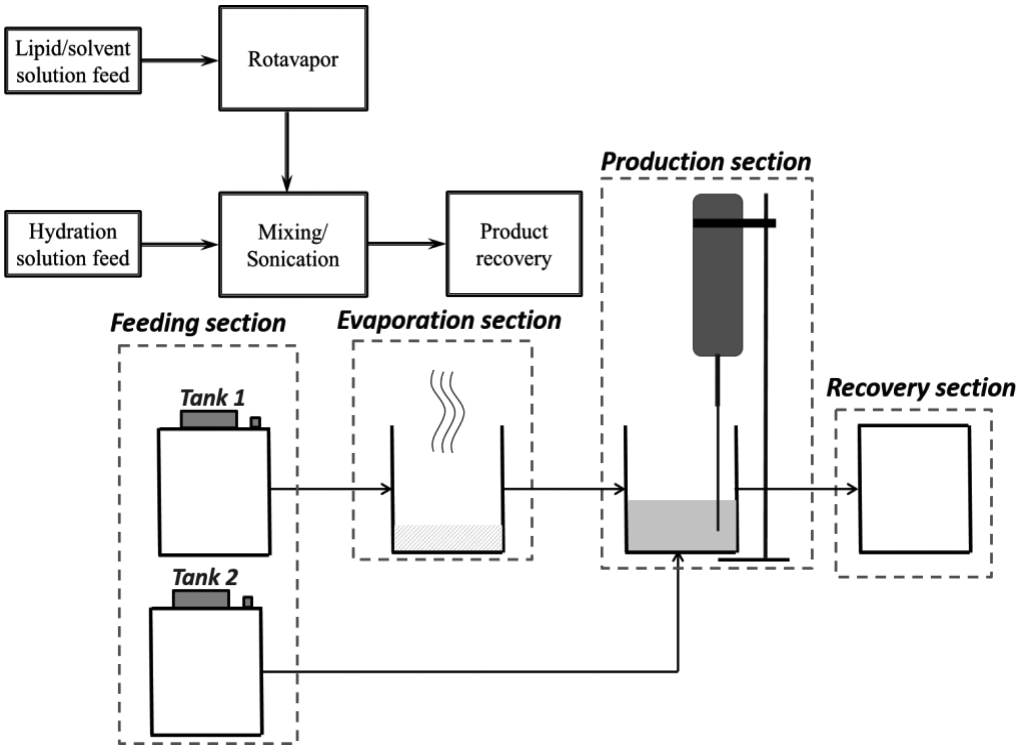

Figure 1. Nanoliposome production through the ultrasound-assisted thin-film hydration method; the main steps are reported: from Tank 1, the lipids/organic solvent solution (eventually containing the hydrophobic molecule to be encapsulated) is introduced in the evaporation section where, by means of a rotary evaporator, solvents are removed leading to the formation of a lipid film. This is then hydrated with a solution (eventually containing the hydrophilic molecule to be encapsulated) stored in Tank 2 of the feeding section. The suspension is homogenized through an ultrasound-assisted process leading to the nanoliposome formation. Finally, the suspension is recovered and characterized.

Briefly, for liposomes production at nanometric scale, at first lipids are dissolved in organic solvents (chloroform/methanol) eventually containing the hydrophobic drug to be encapsulated; after mixing, the solution is vacuum-dried. The dried lipid film, which is generated, is then hydrated at room temperature with water or other hydration solutions eventually containing the hydrophilic drug to be encapsulated and continuously stirred. A suspension containing multilamellar vesicles (MLVs) is produced, maintained at room temperature for several hours and then sonicated by applying a duty cycle purposely developed.

The duty cycle is a discontinuous process by which the liquid sample is sonicated in periodic time intervals followed by switch off in energy supply. It consists of few and short (in the order of seconds) irradiation rounds each followed by few and short pause in order to prevent thermal vesicle disruption, thus obtaining large vesicles (LVs). The sample is stored overnight at 4°C and protected from light in order to stabilize the produced LVs. Subsequently, in order to obtain SUVs, after the stabilization phase, the sample is sonicated again, up to more

http://dx.doi.org/10.5772/intechopen.68157

rounds. The process parameters influencing the sizing process are the ultrasonic amplitude (%), the power (W), the number of sonication cycles, the time of sample exposure to ultrasounds and the volume of the sample treated. As described in detail in Ref. [4] by using a 45% amplitude (percentage of maximum-deliverable power), treating 1-ml volume and by applying the duty cycle, starting from MLVs, after several irradiation rounds, LUVs with 1.416 ± 0.117-μm diameter size are obtained. Subsequently, after more sonication rounds, SUVs with a mean diameter size of 86 ± 33 nm are produced. Finally, after more irradiation rounds, SUVs of 51 ± 28 nm and 49 ± 26 nm are obtained, respectively. In **Figure 2**, produced vesicles from micro- to nanoscale are shown. The duty cycle sonication protocol, coupled with the traditional thin-film hydration method, gives several advantages over conventional liposome-sizing processes as detailed in the next paragraph; first of all, there is the possibility to change liposome dimensions according to the application requirements, avoiding the fixed pore size of the membranes used in the extrusion method.

2.1.2. Principles of the ultrasound process and benefits

Ultrasound is a mechanical vibration phenomenon having a frequency above the range of human hearing (>20 KHz). When ultrasound is adsorbed by a medium, acoustic vibrations increase kinetic energy, producing instantaneous temperature and pressure rise. The explanation of the process can be found in cavitation-wave hypothesis, proposed in 1960. According to this hypothesis, when pressure changes, there is a formation of cavities at liquid–gas interface. The collapse of these cavities generates shock-wave bubbles capable of resonance vibration and producing vigorous eddying or microstreaming. The stresses associated with the propagation of ultrasonic waves may be converted into thermal energy or into chemical energy. Ultrasound-assisted processes can be used for disparate industrial applications, that is, to homogenize, atomize, disperse, deagglomerate and sizing particles, emulsify, disintegrate cells and extracting protein or enzymes from them, to increase reaction speed, to clean and to degas liquids. For example, ultrasonic atomization takes advantage by ultrasound

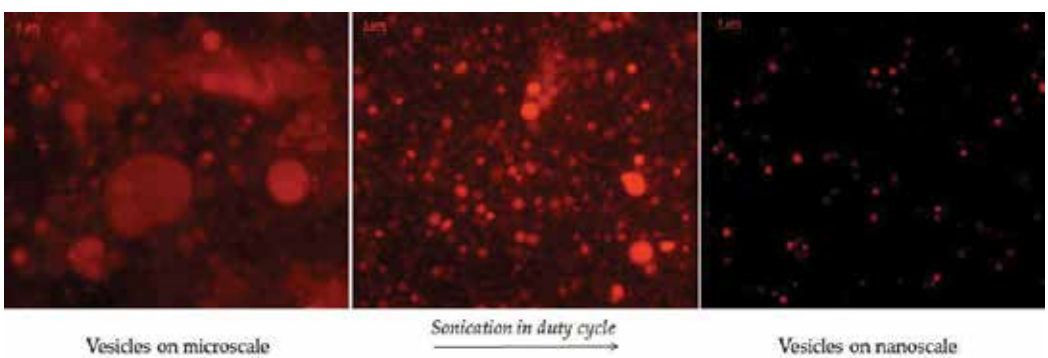

Figure 2. Fluorescence microscopy images of lipid vesicles labelled with Rhodamine B dye (100× objective). Right: Vesicles on microscale not subjected to the size reduction process. Left: Vesicles on nanoscale after sonication in duty cycle.

phenomenon to break up a liquid film into fine droplets. In this case, the phenomenology of the droplets formation process can be explained with cavitation-wave hypothesis or with the capillary-wave hypothesis [23] which analyse the behaviour of a liquid on the solid surface vibrating based on Taylor instability criteria [24]. When the vibration has a frequency of 30 Hz, above a threshold value of amplitude, on the liquid surface capillary waves are formed consisting in crests and troughs. At higher values of amplitude, liquid droplets, separated from the wave crest, are formed [25].

In general, ultrasonication is an easy and scalable process which shows competitive energy costs, applicable in a vast range of fields and for disparate applications. Regarding the particle size reduction, it takes advantage from ultrasound process of the ability to break up lipid structures. In case of nanoliposomes production, the energy is used to break the lipid bilayer into smaller pieces; then these pieces close themselves in spherical structures producing SUVs. In comparison with other sizing techniques, the ultrasonic, which once shows great potential due to reduced time spent and easiness in use, is a simple and efficient method to reduce liposome dimension [26, 27]. Ultrasonic process does not require a number of passages of liposome suspension through a membrane such as extrusion method, and high pressures are not required. Furthermore, the final dimensions of particles are not fixed to the pore size of the membrane, but it is possible to change the vesicle size according to the application requirements. This is possible by controlling the duty cycle, the discontinuous process before described in which the liquid sample is sonicated in periodic time intervals followed by switch off in energy supply. Finally, due to the critical importance to have a sterile environment during loaded SUVs production, another advantage is that sonotrode tip is simpler to clean and sterilize [4].

2.1.3. Phenomenological aspects

As described in Ref. [28], from a thermodynamics point of view, the free energy of the liposome membrane is mainly given by two contributions: the elastic energy due to membrane curvature and the tension energy due to the edge of the layer. Indeed, at the boundary of a bilayer, the polar heads have to be arranged as a semi-circle, in order to connect the two monolayers [29]. The elastic energy has been estimated by Helfrich [30] as proportional to the second power of twice the mean surface curvature, $1/R$ [m^{-1}], and to Gaussian surface curvature, $1/R^2$ [m^{-2}]; through the main elastic moduli, k_c [J] and $\overline{k}_c$ [J], the edge energy are assumed to be proportional to the length of the bilayer edge [30, 31], by the edge tension parameter, γ [J m^{-1}]. On the basis of simple geometrical reasoning [31], a disc initially of radius ρ_D [m], with a surface area $A_D = \pi\rho_D^2$, which is (partially) bended towards forming a sphere (equivalent in area, then with a sphere radius R_S [m] of $R_S = \rho_D/2$), has an edge length equal to $L = (2\pi\rho_D^2)\sqrt{1-(\rho_D^2/(4R^2)}$. Summarizing, for N vesicles with a mean curvature $1/R$, the total free energy could be estimated by Eq. (1) [1]

$$g = N\left(g_{\text{elastic}} + g_{\text{edge}}\right) = N\left\{\left[\frac{1}{2}\left(k_c + \frac{1}{2}\overline{k}_c\right)\frac{4\pi\rho_D^2}{R^2}\right] + \left[\gamma\left(2\pi\rho_D\right)\sqrt{1-\frac{\rho_D^2}{4R^2}}\right]\right\} \quad (1)$$

Therefore, the thermodynamic of the process could be described once the number and the size of the starting discs, N and ρ_D, as well as the curvature of the vesicle, $1/R$, are known;

after the estimation of the material parameters ($2k_c + \overline{k}_c$) and γ. In general, when the energy is supplied to the system, the curvature decreases (the radius of curvature increases), meaning that the spherical vesicles start to open, and the number of liposomes remains constant: for the first second of the process, the supplied energy is used just to increase the free energy of the membrane. During the following 9 s, the radius of curvature remains constant on a very high value because the membrane is flat, the radius of the equivalent disc starts to decrease and the number of structures increases. Both these phenomena are due to the fact that the membrane is being disrupted by the ultrasound energy, thus the total free energy increases, being stored in the structures as edge energy. The magnitude of the phenomena, which happen during this phase, is also dictated by the value of the power parameter $\dot{g}_0$ (the higher the power, the higher the number of discs produced and the smaller their size). During the following 20 s, the relaxation process starts, and the discs bend themselves towards the spherical configuration, since the total free energy in that configuration is lower (the elastic contribution is lower than the edge contribution). During this phase (the bending phase), the radius of curvature decreases (the curvature increases) and the total free energy decreases, no more entities were produced and their size remains constant (N and ρ_D are constants). Subsequently, the cycle starts again. During the first seconds, the discs open (R increases), the entities do not change the number and size (N and ρ_D remain constants) and the total free energy increases. During the remaining of supply-energy phase, the entities were flat discs, and then the energy was used to disrupt them: the curvature does not change, the number of entity increases and their size decreases. The total free energy still increases. Then, the relaxation phase takes place: the discs bend towards sphere, thus the radius of curvature decreases and the total free energy decreases too. The number and the size of entities remain constant.

2.2. Simil-microfluidic method: layout, principles and phenomenological aspects

A simil-microfluidic apparatus was expressly designed and fabricated in order to produce lipid vectors, potentially on production scale, directly on nanometric size, overcoming the limitations of the thin-film hydration technique (and other conventional production methods), which produces small output product volumes in a slow and discontinuous manner. Moreover, the method was developed to avoid the limitations related to the expensive devices needed and microfabrication costs of the microfluidic systems, by transposing their principles to a millimetre scale, drastically reducing the production costs and increasing the yields. With this aim, a new semi-continuous bench-scale apparatus was designed and developed and the ultrasonic energy was used again as an intensification tool for liposome homogenization. The protocol based on the simil-microfluidic approach basically consists in the realization of a contact between two flows, lipids/ethanol and water solutions, inside a millimetric tubular device where interdiffusion phenomena allow the formation of lipid vesicles as detailed in the subsequent paragraphs.

2.2.1. Layout

Figure 3 shows a schematization of the developed simil-microfluidic apparatus. The setup is constituted by five main process sections: a feeding section, a pumping section, a production section, a homogenization section and a recovery section.

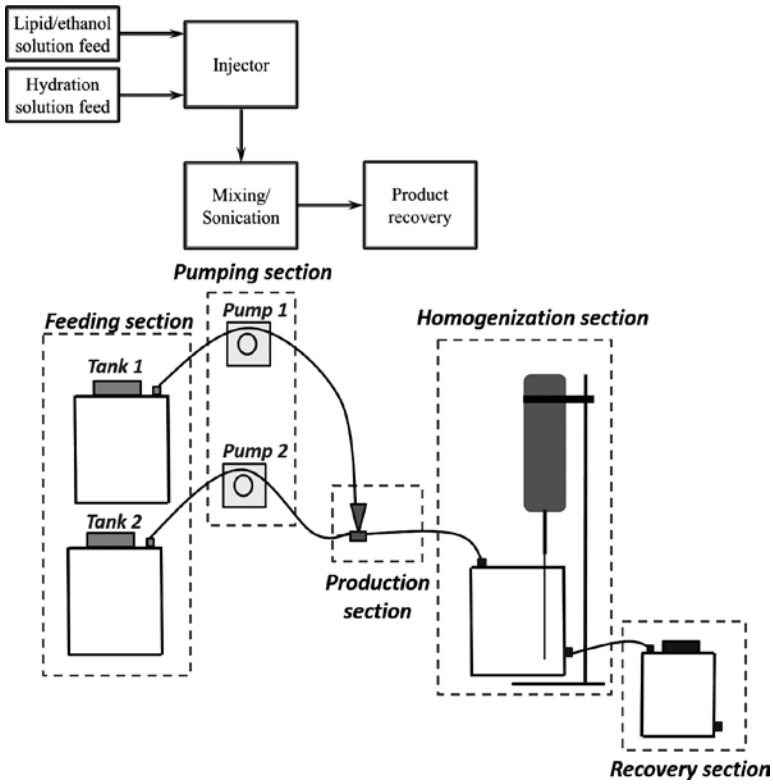

Figure 3. Nanoliposome production through the simil-microfluidic setup. The main sections are reported: feeding, pumping, production, homogenization and recovery. From Tanks [1–2], lipids/ethanol (eventually containing the hydrophobic molecule to be encapsulated) and water (eventually containing the hydrophilic molecule to be encapsulated) solutions are pushed, through peristaltic pumps (Pumps 1–2), to the production section. Here, after the lipid solution injection into the polar phase, nanometric vesicles are formed. The hydroalcoholic solution is then recovered and homogenized through an ultrasound-assisted process. Finally, the suspension is recovered and characterized.

In particular, the feeding section consists in two lines. The first one is made up by a stirred tank filled with lipids/ethanol solution (Tank 1 of **Figure 3**), in which a hydrophobic active molecule to be encapsulated, conveyed in a silicon tube with an internal diameter of about 2 mm, is eventually dissolved. The second line includes a stirred tank filled with the hydration solution (Tank 2 of **Figure 3**), which can be pure water or an aqueous solution, eventually containing the hydrophilic active molecule to be encapsulated, conveyed in a flexible silicone tube with an internal diameter of few millimetres.

The pumping section is composed by two single-head peristaltic pumps (Verderflex OEM mod. Au EZ) indicated as Pumps 1–2 in **Figure 3**.

The lipids/ethanol solution tube ends with several tenths of millimetres internal diameter needle inserted into a silicon tube, an extension of the water tube. This is the production section sketched in **Figure 3**. In this section, an interdiffusion of the two pushed liquids occurs leading to the formation of liposomes on nanometric scale; the suspension is then collected inside a tank and subjected to a homogenization in order to optimize vesicles size distribution. The suspension is finally recovered and characterized.

Briefly, the process starts when lipids/ethanol and water solutions are pushed through peristaltic pumps into the production section, where liposomal vesicles are formed directly on nanometric size (the phenomenology behind vesicles formation through a simil-microfluidic approach will be discussed in the next paragraph). The formed hydroalcoholic solution is recovered and subjected to a homogenization process through the duty cycle sonication protocol, previously described for the ultrasound-assisted thin-film hydration method [28] (Section 2.1.1).

2.2.2. Phenomenological aspects

From a phenomenological point of view, liposome formation is governed by the molecular diffusion between two phases: the organic solvent, in which the lipids are solubilized, and the water; the latter simultaneously diffuses into the organic solvent in order to reduce its concentration below the critical value required for the lipid's solubilization. During the diffusion process, lipid vesicles on nanometric scale start to form through a mechanism called 'self-assembly', according to the theory by Lasic and Papahadjopoulos [32]: lipids dissolved in an organic solvent are in the form of bilayer fragments (phospholipid bilayer fragments, BPFs), the interdiffusion of the water and the organic solvent reduces the solubility of the lipids in the solvent causing thermodynamic instability of BPF edges, inducing the curvature and the closure of bilayer fragments which allow the formation of liposomal vesicles [32]. In the simil-microfluidic setup developed, through the use of constructive expedients (millimetric tubes, peristaltic pumps and injection needle), the reproduction of the laminar flow regime was possible, all the Hagen-Poiseuille assumptions being satisfied, that is, the Reynolds number was found to be less than 2100 for all the volumetric flow rate conditions tested; the piping length in which the two phases interdiffuse was longer than the 'entrance length' required to obtain the parabolic profile [33]. In particular, for a microfluidic system and thus for a laminar flow, liposome formation occurs at the interfaces between the alcoholic and water phases, when they start to interdiffuse in a direction normal to the liquid flow stream. Changes in flow conditions result in size variations of the insertion section of the organic phase reflecting on the vesicles dimensional features. In particular, increasing the volumetric flow rates ratio, the size of the insertion section of the organic phase decreases; this leads to a major dilution of the organic phase limiting the formation of long BPFs, thus inducing the production of liposomal structures of small dimensions. In general, it was shown that the variation in shear forces at the interface of the two fluids has no consequence on liposome structure. In particular, maintaining constant the volumetric flow rates ratio and changing both the buffer and the lipid alcoholic solutions volumetric flow rates, Jahn and collaborators have demonstrated that it is not the magnitude of the shear forces between the parallel-layered stream in having significant impact on liposome's size and size distribution but the stream width (which depends on the volumetric flow rates ratio) [20]. Due to the developed apparatus, the phenomenology connected to the vesicles formation through a microfluidic approach was achieved, exceeding the limit of the bulk methods where a driving force of entropic nature leads to the liposome formation. Local fluctuations of the lipid concentration in a bulk solution make difficult to control the size and the polydispersity of the produced vesicles. On the contrary, the presence of intubated laminar flow with the relative matter diffusive transport allows to minimize the fluctuations of the lipid concentration inside the tubes and to modulate the size and the size distribution of the final vesicles.

2.2.3. Influence of process parameters on liposome dimensional features

When using the simil-microfluidic approach, the lipid concentration and the volumetric flow rate ratio [Vhs/Vls] have a great influence on liposome's size distribution as described in Ref. [34] and also found by Jahn and collaborators for a microfluidic hydrodynamic-focusing platform [35]. In particular, increasing the ratio between the water volumetric flow rate to the lipids-ethanol volumetric flow rate, the PDI value increases as shown in **Figure 4B**. On the contrary, the effect of the ultrasound-assisted process in reducing PDI and thus in ameliorating their size distribution (homogenizing) can be observed (**Figure 4B**).

Another crucial parameter affecting nanoliposome's dimensional features is the lipid concentration. In particular, as visible in **Figure 5A**, increasing lipid concentration, the liposome diameter also increases. This can be explained by the fact that at equal fluid dynamic conditions, a greater number of lipids impact at the same alcohol/water interface area dissolving in the same water volume, thus joining to form larger vesicles. The sample seems to be better homogenized at the higher-tested lipid concentration (**Figure 5B**).

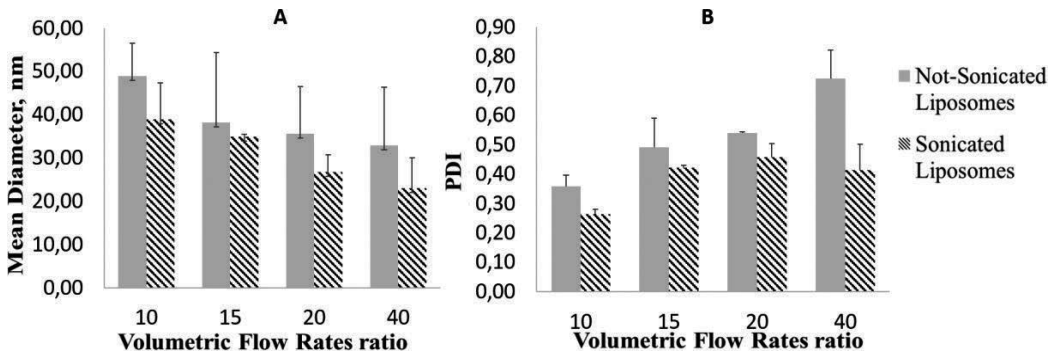

Figure 4. Liposome diameter size (A) and polydispersity index (PDI) (B) before and after sonication treatments at different volumetric flow rates [34].

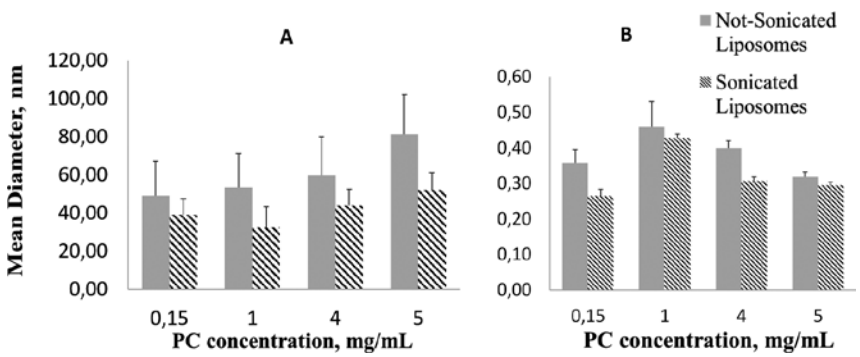

Figure 5. Liposome diameter size (A) and polydispersity index (PDI) (B) before and after sonication treatments at different phosphatidylcholine (PC) concentrations in the hydroalcoholic solution [34].

3. Case histories

3.1. Pharmaceutical application: nanoliposome vectors for siRNAs delivery

The short-interfering RNAs are double-stranded RNA molecules able to target disease components, at genetic level that are considered 'undruggable' with the conventional medicines; thus, their use in the development of innovative gene therapies is growing faster in recent years. Due to their low stability in physiological fluids, low-membrane permeability and their short half-life in the circulatory system, siRNAs are not useable in their naked form and require to be encapsulated in suitable carriers.

As described in Ref. [36], siRNA sequences directed against E2F1 transcription factor (siE2F1-1324) were encapsulated inside positively charged vesicles purposely designed and produced to enhance the interaction with both the negatively charged siRNA, improving its encapsulation efficiency, and the cell-plasmatic membrane, also negatively charged, improving siRNA incorporation in the target cells [37, 38]. It was demonstrated that E2F1 promotes the aggressiveness of human colorectal cancer by activating the ribonucleotide reductase small subunit M2 whose high expression induces cancer and contributes to tumour growth and invasion [39]. Due to the observed correlation, the inhibition of E2F1 expression was studied as a potential way to treat colorectal cancer by encapsulating siE2F1 in cationic nanoliposomes suitably produced by the ultrasound-assisted technique developed. The loaded nanoliposomes were then transfected in human cell lines and in intestinal human biopsy fragments (collected from IBD donors during lower endoscopy performed for colonic cancer screening) to investigate their in vitro and ex vivo silencing activity. In particular, siE2F1 nanoliposomes were transfected in HT29 human colon adenocarcinoma cell line, where conditions are more reproducible, and in cultured human biopsies, in which the cell-cell interactions, thus the human intestinal mucosa cytoarchitecture, are preserved unlike isolated cell cultures.

3.1.1. Materials and methods

Formulation: Nanoliposomes loaded with siRNA sequences for E2F1 expression inhibition were designed and produced by using cholesterol (CAS 57-88-5), L-α-phosphatidylcholine from egg yolk (CAS 8002-43-5) and dioleoyloxy propyl-N,N,N-trimethylammonium propane (DOTAP) (CAS 132172-63-1, >99 % pure), purchased from Sigma-Aldrich (Milan, Italy). In designing the liposome bilayer, the cationic DOTAP phospholipid was chosen to electrostatically interact with the negative siRNA molecules, promoting siRNA encapsulation inside the lipid vesicles, and to interact with the negative cell membrane. The charge ratio between DOTAP and siRNA sequences used was 8.5:1 (±), selected on the basis of previous work [40].

The siRNA sequence direct against E2F1, the siE2F1-1324, was selected [41, 42]. siE2F1-SUV complexes were produced using the thin-film hydration method [16] followed by duty cycle sonication [28]. Briefly, PC, DOTAP and CHOL at 3:0.3:1 (mol:mol) ratio were dissolved in chloroform/methanol at 2:1 (vol/vol). The solvent was removed and the produced lipid film was hydrated with a phosphate buffer solution (PBS; potassium phosphate monobasic of 0.2 M,

sodium hydroxide of 0.2 M, pH 7.4) containing siE2F1-1324 at 8 μM. siRNA-positive and -negative controls (scramble siRNA) were also encapsulated. Finally, the above-described steps were followed also for unloaded liposome production with the only difference in the hydration solution which was pure PBS not containing siRNA sequences. By this way, multilamellar vesicles were achieved, maintained at room temperature for 2 h and then diluted obtaining an siRNA concentration of 4 μM for the loaded samples with a 1:260 (w/w) siRNA/total lipid ratio.

Production: In order to obtain nanoliposomes, samples were subjected to the duty cycle sonication process through the developed ultrasound-based size reduction method and previously described (Section 2.1.1).

Unloaded and siRNA-loaded SUVs were morphologically characterized through an optical microscope, equipped with software to capture the images in the fluorescence field (Axioplan 2- Image Zeiss, Jena, Germany). The size and zeta-potential determinations were performed by using the ZetasizerNano ZS (Malvern, UK) with non-invasive backscatter (NIBS) optics. The resulting particle size distribution was plotted as the number of liposomes versus size. The encapsulation efficiency (E.E.) by spectrophotometric (Lambda 25 UV/VIS Spectrophotometer, $\lambda = 260$ nm for RNA molecules) and electrophoretic assay (run on 1.5% agarose gel) was evaluated. The E.E. was determined as the percentage of siRNA encapsulated into SUVs, calculated subtracting the amount of siRNA present in the supernatant of the centrifuged sample from the total amount of siRNA included in the formulation, to the initial amount of siRNA used.

In order to evaluate siRNA-nanoliposome cytotoxicity and their potential in E2F1 silencing, the complexes were transfected at 200 nM in human colorectal adenocarcinoma cell lines HT29 and in human colon mucosa biopsies, isolated from donors during colonoscopy.

3.1.2. Results and discussion

The production process (formulation and manufacturing) is of crucial importance in preparing siRNA-liposome complexes with the desired shape and size without damaging siRNA's integrity. The shape of liposomes is the main factor affecting carrier's entry in the cellular compartment. Spherical nanoparticle's uptake in mammalian cells was demonstrated to be 3.75–5 times more than rod-shape nanoparticles, indicating that the carrier's curvature can affect the entry in the plasma membrane [43]. In that regard, spherical SUVs were obtained through the ultrasound-assisted method adopted which has been successfully used to produce stable siRNA-SUV complexes on nanometric scale. The achieved siRNA-liposomes, with a mean diameter size of 38 nm (**Table 1**), are useful for the EPR effect, which involves carrier's extravasation through tumour vascular fenestrations of 50–100-nm range size. Another important feature is the surface charge of liposomes. Zeta-potential (ζ) was investigated for both unloaded and SUVs encapsulating siRNA samples; the results are presented in **Table 1**. The positive zeta-potential makes the produced liposomes applicable for the encapsulation of negative siRNA molecules and also promotes the fusion with the negatively charged cell membrane. The ζ-value of the unloaded liposomes (27.90 ± 1.60) appears to be significantly higher than the zeta-potential of the siE2F1-1324-SUV sample (18.02 ± 1.07 mV) suggesting that a strong complexation in addition to the siRNA core encapsulation occurred for the loaded structures.

Properties	siE2F1-1324	Unloaded SUVs
SUVs size [nm] ± SD	38.1 ± 5.6	24.9 ± 5.8
PDI ± SD	0.4 ± 0.02	0.26 ± 0.005
Zeta-potential [mV] ± SD	18.0 ± 1.07	27.9 ± 1.60
Encapsulation efficiency [%]	100	–

Encapsulation efficiency (E.E.) for siRNA-loaded nanoliposomes. Results are expressed as average of three determinations with SD as standard deviation [36].

Table 1. Size, PDI and zeta-potential of unloaded and siE2F1-1324-loaded small unilamellar vesicles (SUVs) produced.

Considering the high degradability of siRNA molecules, thus the difficulty in preserving them during all production steps, one of the main goals was to produce liposomes on nanometric size ensuring the integrity of siRNA's molecular structure at the end of the process as well as preserving their biological activity. siRNA sequences were encapsulated with a 100% E.E. showing the efficacy of both the production technique and the formulation adopted. Moreover, electrophoretic studies have showed the high complex stability, which is a very important parameter to take into account due to the high degradability and toxicity of free siRNA molecules. This result indicates the safety of the developed ultrasound-assisted technique which allows preserving siRNA integrity since no evidence of nucleic acids degradation was visible through the electrophoretic assay.

Regarding the unspecific toxicity of SUVs, results have indicated that siRNA-nanoliposome complexes are far less toxic than Lipofectamine®2000, a commonly used transfection agent which was also investigated in order to have a comparison with the developed liposomal vesicles. siE2F1-SUVs were also able to significantly reduce the vitality of the HT29 colon carcinoma cells, thus proving the effectiveness of the complexes and their ability in siE2F1 delivery, which finally down-regulates cell growth. SUVs were able to enter the cell and release siE2F1 without any toxic effects. Finally, a successful uptake and an E2F1-silencing effect were also observed in cultured human colon mucosa biopsy, achieving an E2F1 protein inhibition till 80.5%, with a patient-dependent response. It can be stated that the size reduction process through sonication in duty cycle is a far less complex and more rapid method for liposome size reduction than the one usually adopted and is able to produce liposomes in the nanometric size range (which can thus take advantage of the EPR effect) with high degree of size homogeneity and 100% encapsulation efficiency, relevant feature that can guarantee a uniform behaviour in terms of delivery properties [36].

3.2. Nutraceutical application: nanoliposome vectors for ferrous sulphate delivery

Anaemia, caused by iron deficiencies, is one of the most widespread nutritional deficiencies, affecting globally two billion people [44]. Despite the success of iron food fortification, particularly in developing countries, the lack of a robust, simple and easy-to-transfer fortification technology has limited this technology [45]. Moreover, the supplementary micronutrient products present on market in the form of tablet or capsules have to be improved in quality and variety in order to increase their availability and access in the commercial

sector [46]. In order to meliorate the supplementary iron products currently on the market, often composed by micrometric particles, sometimes containing the less absorbable ferric form of iron and obtained, in the most of the cases, by using ineffective production processes and drastic conditions, ferrous sulphate nanoliposomes were produced by using the developed simil-microfluidic apparatus.

3.2.1. Materials and methods

Formulation: L-α-phosphatidylcholine from soybean, Type II-S, 14–23% choline basis (CAS n. 8002-43-5), cholesterol (CAS n. 57-88-5), ferrous sulphate heptahydrate (CAS n. 7782-63-0), ascorbic acid (CAS n. 50-81-7) and ethanol of analytical grade (CAS n. 64-17-5) were purchased from Sigma-Aldrich (Milan, Italy) and used for liposome production. Unloaded and ferrous sulphate-loaded nanoliposomes were produced by using the simil-microfluidic bench-scale apparatus developed whose layout and main process steps are described in Section 2.2.1. In particular, a 10:1 (Vhs/Vls) volumetric flow rate ratio and a 5-mg/ml lipid concentration in the final hydroalcoholic solution were used for liposome preparation.

Production: Briefly, a lipid/ethanol solution was obtained by dissolving PC and cholesterol in 10 ml of ethanol. Cholesterol was used at 2.5:1 (mol/mol) PC/CHOL ratio which corresponds to the typical composition of the cell membrane, as suggested by Abbasi and Azari [47] and was added to the formulation in order to stabilize the loaded vesicles. Ferrous sulphate heptahydrate and ascorbic acid were dissolved in 100 ml of deionized water, which was used as hydration solution. Ascorbic acid was added as an anti-oxidant to preserve the ferrous ion against oxidation in a ferrous/ascorbic acid. It has been shown that the co-addition of ascorbic acid and iron in a 2:1 molar ratio (6:1 weight ratio) increases iron absorption from foods twofold to threefold in adults and children [48–50]. In particular, different formulations were produced which differ from each other for the ferrous sulphate/total formulation components (lipids, ascorbic acids and ferrous sulphate) weight ratio (w/w) used. Starting from a 0.06 ferrous sulphate/total components weight ratio, selected from Xia and Xu [51], nanoliposomes were also produced by using a 0.02 ferrous sulphate/total components (w/w) ratio and maintaining all the other chemical and adopted process parameters constant. In order to have a comparison with the ferrous sulphate-loaded particles, unloaded nanoliposomes were produced by adoperating the same formulation and process conditions but using, as hydration solution, pure deionized water without the addition of ascorbic acid and iron.

Unloaded and ferrous sulphate-loaded SUVs were at first characterized in terms of morphology, size and zeta-potential (ZetasizerNano ZS, Malvern, UK). The resulting particle size distribution was plotted as the number of liposomes versus size.

The encapsulation efficiency was determined as the percentage of ferrous sulphate encapsulated in nanoliposomes to the initial amount of ferrous sulphate included in the formulation. Triton X100 at 1% (v/v) was used in order to lyse the nanoliposomes and analyse the encapsulated ferrous sulphate. Iron determination was performed by the 1,10-phenanthroline colorimetric method through UV spectrophotometric assay (Lambda 25 UV/VIS Spectrophotometer, Perkin Elmer, Monza, Italy). A λ = 510 nm, typical of the 1,10-phenanthroline-Fe^{2+} ions complex, was considered.

3.2.2. Results and discussion

The simil-microfluidic bench-scale apparatus developed has allowed to successfully produce iron-loaded nanoliposomes in the desired range size. The method has permitted to produce ferrous sulphate-nanostructured vectors without the use of drastic conditions, such as solvents and/or high pressure, currently used in literature and also at industrial scale for iron particle manufacturing by using discontinuous and laborious processes such as reverse phase evaporation, thin-film hydration and homogenization freeze-thawing production methods [47, 51–53]. A part of the drastic conditions used, limits in the output volumes of final product, usually ranging from 10 to 60 mL with the above-mentioned techniques, represents another crucial problems directly linked with high commercial costs of supplemental products which, for this reason, are not yet widely used as very proper therapies. With the simil-microfluidic setup developed, by using the ultrasound as tool for the process intensification, it was possible to obtain a massive output with the minimum energy, costs and time by operating in a semi-continuous manner. In particular, spherical liposomes were obtained in a nanometric range size as shown in **Table 2**.

Taking into account that the iron solubility is very dependent on the size and the shape of the iron particle complexes, characteristics which are governed by the manufacturing process [45], the simil-microfluidic setup realized was successfully applied for ferrous sulphate nanoliposomes production. In that regard, particles on nanometric scale are required to maintain the transparency of clear beverages during enrichment: carriers have to be small enough so as not to scatter light and be detected by naked eye [54].

The nanoscale plays a crucial role also for other forms of iron supplementation such as oral formulations, the first choice to replace normal iron levels. In this case, the size of nanoparticle systems has a remarkable influence on carrier's uptake after their administration: in many works, it has been proven that nanostructured delivery systems yield an increase in drug uptake, enhancing the intestinal absorption of the active principle [55, 56]. As shown in **Table 2**, vesicles of 48–65-nm diameter range size have been successfully obtained through the developed setup with PDI values of 0.38 ′ 0.01 and 0.63 ′ 0.12, respectively, for the 0.06 and 0.02 (w/w) formulations produced. Due to the presence of polyunsaturated fatty acids (linoleic and oleic acids) composing the phosphatidylcholine, vesicles presented negative zeta-potential values (more negative for the 0.06, w/w formulation due to the presence of large amounts of ascorbic acid which decreases the pH of the sample) and an encapsulation efficiency that increases with

Properties	**0.06 (w/w)**	**0.02 (w/w)**
SUVs size [nm] ± SD	47.80 ± 6.46	65.16 ± 15.48
PDI ± SD	0.38 ± 0.01	0.63 ± 0.12
Zeta-potential [mV] ± SD	−41.05 ± 0.7	−19 ± 0.55
Encapsulation efficiency [%]	22.33 ± 0.58	52.2 ± 1.41

Results are expressed as average of three determinations with SD as standard deviation.

Table 2. Size, PDI, zeta-potential and encapsulation efficiency of loaded small unilamellar vesicles (SUVs) produced, obtained at different weight ratios of ferrous sulphate to the total formulation components.

increasing of the lipid amount with respect to those of iron. In particular, as can be seen in **Table 2**, the encapsulation efficiency increases from about 22 to 52% when the weight ratio between ferrous sulphate and the total lipid decreases from 0.06 to 0.02 (w/w).

4. Conclusions

Based on the use of ultrasound as alternative energy resource, a solid particles size reduction/homogenization process was developed and coupled with the bench-scale conventional thin-film hydration method. The technique was developed in order to produce, in a versatile manner, nanometric structures, with the desired dimension.

Moreover, due to its easiness, reliability, versatility and its great potential in reducing time spent, the ultrasound intensification tool was also used for liposome homogenization operation during vesicles production through the developed simil-microfluidic technique.

The phenomenology involved in liposome formation was described for both the methods; applications regarding the entrapment of active molecules were also described as case histories.

siRNA-nanoliposome complexes (for gene therapy application) were produced for the inhibition of E2F1 protein expression, studied as a potential way to treat colorectal cancer. By the ultrasound-assisted thin-film hydration technique, nanoliposomes with 33–38-nm range size and 100% siRNA encapsulation efficiency were obtained. The produced loaded SUVs demonstrated a very low cytotoxicity in cells when compared with the commercial transfection agent Lipofectamine®2000 and an excellent uptake in the cultured human colon mucosa tissues. A remarkable effect on anti-E2F1 expression after a transfection of siE2F1-1324-SUV sample has been demonstrated also in a dynamic human model such the colon tissue microenvironment.

For nutraceutical application, nanoliposomes loaded with ferrous sulphate with good dimensional features (48–65 nm vesicles) and encapsulation efficiency were successfully produced using the developed simil-microfluidic apparatus, avoiding the use of toxic solvents and drastic conditions.

All the achieved positive results endorse the usefulness of both the formulative and the plant-engineering approaches adopted for nanostructured vectors production to be used in pharmaceutical and nutraceutical applications.

Author details

Sabrina Bochicchio[1,2], Gaetano Lamberti[1] and Anna Angela Barba[2]*

*Address all correspondence to: aabarba@unisa.it

1 Department of Industrial Engineering, University of Salerno, Fisciano, Salerno, Italy

2 Department of Pharmacy, University of Salerno, Fisciano, Salerno, Italy

References

[1] Sawant RR, Torchilin VP. Challenges in development of targeted liposomal therapeutics. The AAPS Journal. 2012;**14**(2):303-15

[2] Singh H. Nanotechnology applications in functional foods; opportunities and challenges. Preventive Nutrition and Food Science. 2016;**21**(1):1

[3] Reza Mozafari M, Johnson C, Hatziantoniou S, Demetzos C. Nanoliposomes and their applications in food nanotechnology. Journal of Liposome Research. 2008;**18**(4):309-27

[4] Bochicchio S, Barba AA, Grassi G, Lamberti G. Vitamin delivery: carriers based on nanoliposomes produced via ultrasonic irradiation. LWT-Food Science and Technology. 2016;**69**:9-16

[5] Srinivas PR, Philbert M, Vu TQ, Huang Q, Kokini JL, Saos E, et al. Nanotechnology research: applications in nutritional sciences. The Journal of Nutrition. 2010;**140**(1):119-24

[6] Putheti S. Application of nanotechnology in food nutraceuticals and Pharmaceuticals. Journal of Science and Technology. 2015;**2**(10):17-23

[7] Huang Q. Nanotechnology in the Food, Beverage and Nutraceutical Industries: Elsevier; 2012, Sawston, Cambrige, UK

[8] Bregoli L, Movia D, Gavigan-Imedio JD, Lysaght J, Reynolds J, Prina-Mello A. Nanomedicine applied to translational oncology: a future perspective on cancer treatment. Nanomedicine: Nanotechnology, Biology and Medicine. 2016;**12**(1):81-103

[9] Kibria G, Hatakeyama H, Sato Y, Harashima H. Anti-tumor effect via passive anti-angiogenesis of PEGylated liposomes encapsulating doxorubicin in drug resistant tumors. International Journal of Pharmaceutics. 2016;**509**(1-2):178-87

[10] Abeysinghe A, Barakat S. The Paris Agreement. Options for an effective compliance and implementation mechanism, 2016, http://pubs.iied.org/pdfs/10166IIED.pdf

[11] Burck J, Bals C, Rossow V. The Climate Change Performance Index: Results 2015: Germanwatch, Berlin; 2014

[12] Dalmoro A, Barba AA, Lamberti G, d'Amore M. Intensifying the microencapsulation process: Ultrasonic atomization as an innovative approach European Journal of Pharmaceutics and Biopharmaceutics. 2012;**80**(3):471-7

[13] Van Gerven T, Stankiewicz A. Structure, energy, synergy, time the fundamentals of process intensification, Industrial & Engineering Chemistry Research; 2009;**48**:2465-74

[14] Charpentier JC. In the frame of globalization and sustainability, process intensification, a path to the future of chemical and process engineering (molecules into money). Chemical Engineering Journal 2007;**134**:84-92

[15] Meure LA, Foster NR, Dehghani F. Conventional and dense gas techniques for the production of liposomes: a review. AAPS Pharmscitech. 2008;**9**(3):798-809

[16] Bangham A, Horne R. Negative staining of phospholipids and their structural modification by surface-active agents as observed in the electron microscope. Journal of Molecular Biology. 1964;**8**(5):660-IN10

[17] Wagner A, Vorauer-Uhl K. Liposome technology for industrial purposes. Journal of Drug Delivery. 2010;**2011**

[18] Jaafar-Maalej, Chiraz, Catherine Charcosset, and Hatem Fessi. A new method for liposome preparation using a membrane contactor. Journal of Liposome Research. 2011;**21**(3):213-20

[19] Sekhon BS. Supercritical fluid technology: an overview of pharmaceutical applications. International Journal of PharmTech Research, 2010;**2**(1):810-26

[20] Jahn A, Vreeland WN, DeVoe DL, Locascio LE, Gaitan M. Microfluidic directed formation of liposomes of controlled size. Langmuir. 2007;**23**(11):6289-93

[21] Pons M, Foradada M, Estelrich J. Liposomes obtained by the ethanol injection method. International Journal of Pharmaceutics. 1993;**95**(1-3):51-6

[22] Yu B, Lee RJ, Lee LJ. Microfluidic methods for production of liposomes. Methods in Enzymology. 2009;**465**:129-41

[23] Avvaru B, Patil MN, Gogate PR, Pandit AB. Ultrasonic atomization: effect of liquid phase properties. Ultrasonics. 2006;**44**(2):146-58

[24] Kull H-J. Theory of the Rayleigh-Taylor instability. Physics Reports. 1991;**206**(5):197-325

[25] Abramov OV. High-intensity Ultrasonics: Theory and Industrial Applications: CRCPress; 1999, Amsterdam, The Netherlands

[26] Huang X, Caddell R, Yu B, Xu S, Theobald B, Lee LJ, et al. Ultrasound-enhanced microfluidic synthesis of liposomes. Anticancer Research. 2010;**30**(2):463-6

[27] Woodbury DJ, Richardson ES, Grigg AW, Welling RD, Knudson BH. Reducing liposome size with ultrasound: bimodal size distributions. Journal of Liposome Research. 2006;**16**(1):57-80

[28] Barba A, Bochicchio S, Lamberti G, Dalmoro A. Ultrasonic energy in liposome production: process modelling and size calculation. Soft Matter. 2014;**10**(15):2574-81

[29] Helfrich W. The size of bilayer vesicles generated by sonication. Physics Letters A. 1974;**50**(2):115-6

[30] Helfrich W. Elastic properties of lipid bilayers: theory and possible experiments. Zeitschrift für Naturforschung Teil C: Biochemie, Biophysik, Biologie, Virologie. 1973;**28**(11):693

[31] Fromherz P. Lipid-vesicle structure: size control by edge-active agents. Chemical Physics Letters. 1983;**94**(3):259-66

[32] Lasic DD, Papahadjopoulos D. Medical Applications of Liposomes: Elsevier; 1998, Amsterdam, The Netherlands

[33] Phenomena T. by RB Bird, WE Stewart, and EN Lightfoot. John Wiley, New York; 1960

[34] Bochicchio S, Dalmoro A, Recupido F, Lamberti G, Barba AA, "Nanoliposomes production by a protocol based on a simil-microfluidic approach", in "Lecture Notes in Bioengineering (LNBE)", Springer Ed.; 2017, Berlin, Germany

[35] Jahn A, Vreeland WN, Gaitan M, Locascio LE. Controlled vesicle self-assembly in microfluidic channels with hydrodynamic focusing. Journal of the American Chemical Society. 2004;**126**(9):2674-5

[36] Bochicchio S, Dapas B, Russo I, Ciacci C, Piazza O, De Smedt S, Pottie E, Barba AA, Grassi G, "In vitro and ex vivo delivery of new designed siRNA-nanoliposomes for E2F1 silencing as a potential therapy for Inflammatory Bowel Diseases-associated colorectal cancer". IJP—International Journal of Pharmaceutics, 2017 in press, doi.org/10.1016/j.ijpharm.2017.02.020

[37] Ibraheem D, Elaissari A, Fessi H. Gene therapy and DNA delivery systems. International Journal of Pharmaceutics. 2014;**459**(1):70-83

[38] Kim H-K, Davaa E, Myung C-S, Park J-S. Enhanced siRNA delivery using cationic liposomes with new polyarginine-conjugated PEG-lipid. International Journal of Pharmaceutics. 2010;**392**(1):141-7

[39] Fang Z, Gong C, Liu H, Zhang X, Mei L, Song M, et al. E2F1 promote the aggressiveness of human colorectal cancer by activating the ribonucleotide reductase small subunit M2. Biochemical and Biophysical Research Communications. 2015;**464**(2):407-15

[40] Bochicchio S, Dalmoro A, Barba A, d'Amore M, Lamberti G. New preparative approaches for micro and nano drug delivery carriers. Current Drug Delivery. 2017;**14**(2):203

[41] Dapas B, Farra R, Grassi M, Giansante C, Fiotti N, Uxa L, et al. Role of E2F1–cyclin E1-cyclin E2 circuit in human coronary smooth muscle cell proliferation and therapeutic potential of its downregulation by siRNAs. Molecular Medicine. 2009;**15**(9-10):297

[42] Poliseno L, Evangelista M, Mercatanti A, Mariani L, Citti L, Rainaldi G. The energy profiling of short interfering RNAs is highly predictive of their activity. Oligonucleotides. 2004;**14**(3):227-32

[43] Chithrani BD, Chan WC. Elucidating the mechanism of cellular uptake and removal of protein-coated gold nanoparticles of different sizes and shapes. Nano Letters. 2007;**7**(6):1542-50

[44] Mellican RI, Li J, Mehansho H, Nielsen SS. The role of iron and the factors affecting off-color development of polyphenols. Journal of Agricultural and Food Chemistry. 2003;**51**(8):2304-16

[45] Mehansho H. Iron fortification technology development: new approaches. The Journal of Nutrition. 2006;**136**(4):1059-63

[46] Mora JO. Iron supplementation: overcoming technical and practical barriers. The Journal of Nutrition. 2002;**132**(4):853S-5S

[47] Abbasi S, Azari S. Efficiency of novel iron microencapsulation techniques: fortification of milk. International Journal of Food Science & Technology. 2011;**46**(9):1927-33

[48] Stekel A, Monckeberg F, Beyda V. Combating iron deficiency in Chile: a case study: International Life Sciences Institute-Nutrition Foundation, 1986, Washington, D.C., USA

[49] Stekel A, Olivares M, Pizarro F, Chadud P, Lopez I, Amar M. Absorption of fortification iron from milk formulas in infants. The American Journal of Clinical Nutrition. 1986;**43**(6):917-22

[50] Lynch SR, Stoltzfus RJ. Iron and ascorbic acid: proposed fortification levels and recommended iron compounds. The Journal of Nutrition. 2003;**133**(9):2978S-84S

[51] Xia S, Xu S. Ferrous sulphate liposomes: preparation, stability and application in fluid milk. Food Research International. 2005;**38**(3):289-96

[52] Kosaraju SL, Tran C, Lawrence A. Liposomal delivery systems for encapsulation of ferrous sulphate: preparation and characterization. Journal of Liposome Research. 2006;**16**(4):347-58

[53] De Paoli T, Hager AA. Liposomes containing bioavailable iron [II] and process for obtaining them. Google Patents; 1996

[54] Danino D, Livney YD, Ramon O, Portnoy I, Cogan U. Beta-casein assemblies for enrichment of food and beverages and methods of preparation thereof. Google Patents; 2014

[55] Desai MP, Labhasetwar V, Amidon GL, Levy RJ. Gastrointestinal uptake of biodegradable microparticles: effect of particle size. Pharmaceutical Research. 1996;**13**(12):1838-45

[56] Hussain N, Jaitley V, Florence AT. Recent advances in the understanding of uptake of microparticulates across the gastrointestinal lymphatics. Advanced Drug Delivery Reviews. 2001;**50**(1):107-42

Chapter 3

Lipobeads

Sergey Kazakov

Additional information is available at the end of the chapter

http://dx.doi.org/10.5772/intechopen.70056

Abstract

A combination of lipid bilayer and cross-linked polymer network is the logical step in development of polymeric and liposomal nanoscopic systems to provide the natural level of functionality. From liposomal systems, lipobeads borrow the well-developed methods for preparation, diversity of lipids to control the properties of a lipid bilayer, biocompatibility of the lipid bilayer, possibility to vary size and morphology (passive targeting), availability of the external surface for attachment of various ligands (active targeting), encapsulation efficiency of both hydrophilic and hydrophobic molecules. Mechanical stability of the lipid bilayer and environmental responsiveness of the whole structure are the properties that hydrogel core brings to the new construct. The reports reviewed in this chapter demonstrate that lipobeads of nanometer and micrometer sizes can be prepared in different media, retain their stimuli responsiveness under physiological conditions, exhibit both reversible and irreversible aggregation, can be loaded with both small and high molecular weight molecules. As a platform for drug delivery systems, lipobeads have already been loaded with chemotherapeutics, malaria vaccine, and dermatological agent providing different controlled release profiles without leakage. Consecutive multistep triggering, new schemes of drug release, combined drug delivery, vesobeads, proteo-lipobeads, enzyme-containing lipobeads, and hemi-lipobeads are the directions for their future development.

Keywords: liposomes, nanogels, supramolecular assembly, lipobeads, preparation, properties, application

1. Introduction: why lipobeads?

In accord with our understanding of complex biological mechanisms prevailing *in situ*, the arrangement of a lipid bilayer/hydrogel assembly—the lipid vesicles filled with polymeric

networks (**Figure 1**) achievable experimentally in laboratory—could be a logical step in the development of polymeric and liposomal-beaded nanoscopic systems.

In the last several decades, different terminology, such as supramolecular biovectors (SMBVs), lipid-coated microgels, lipobeads (LB), gel-filled vesicles, lipogels, gel core liposomes, microgel-in-liposomes, hydrogel-supported lipid bilayer, and nanolipogels particles (nLG), has been utilized to describe these lipid membrane/hydrogel structures. In this chapter, we use the term "lipobeads" for the spherical bipartite structures made of a hydrogel core enclosed within a lipid bilayer.

Actually, the bicompartmental structure of lipobeads mimics natural arrangements of living cells. Just look at the cell envelopes for all three main domains of life (*eubacteria*, *archaea*, and *eukaryotes*). They represent a successive organization of the macromolecular networks (cytoplasm, cell wall, capsule, etc.) and lipid bilayers (cell bilayer membranes and internal membrane system), which Nature uses to provide workability, multifunctionality, and dynamism of living cells of different types.

Evidently, the first synthetic lipid vesicles filled with hydrogel (lipobeads) were reported in 1987, when a successful polymerization within liposomes had been accomplished [1] and microspherules of agarose-gelatin gels filled with gold particles had been mixed with liposomes in the course of their preparation [2]. In 1989, a concept of supramolecular biovectors (SMBVs) was filed as a patent application [3]. The SMBV system was prepared from polysaccharide gel fragments obtained by disruption of a gel of chemically cross-linked maltodextrins and subsequently phospholipidated. In 1994, the SMBVs were reported as new carriers of active substances, such as interleukin-2 (IL-2) [4]. In 1995, lipobeads with Ca-alginate hydrogel core were obtained as a byproduct of a method for the preparation of Ca-alginate hydrogel nanoparticles using the internal compartment of liposomes [5]. In 1996, the spherical hydrogel/lipid bilayer constructs for the first time were named as "lipobeads," and it was shown that a lipid bilayer was formed on the surface of hydrogel polymer beads upon the addition of phospholipids, if their surface had been modified with the covalently attached fatty acids [6]. Lipobeads with an environmentally sensitive hydrogel core prepared by hydration of lipid films with microgel suspension were described as drug delivery systems in 1998 [7]. In the early 2000s, photopolymerization within liposomes was used for preparation of the so-called synthetic polymer complements with imprinted recognition sites [8] and the environmentally responsive nanogels [9]. The latter work contributed toward the characterization of the compatibility of nanogels

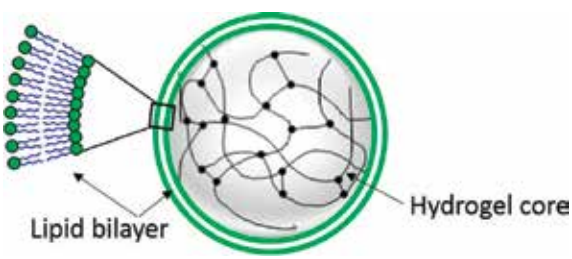

Figure 1. Schematic of a spherical lipid bilayer/hydrogel assembly (lipobead).

and phospholipid bilayer leading to spontaneous phospholipidation of nanogels [10]. Further studies on lipobeads development were devoted either to new methodologies including different compositions of hydrogel core or different agents which could be loaded into the lipobeads.

The chapter has a comprehensive view on (1) synthetic feasibility, functionality and characterization of lipobeads (Sections 2 and 3) and (2) their potential applications as precursors for novel encapsulated and combined drug delivery systems, as microbiochemical reactors, and as an experimental model to study the origin of life (Section 4). It is a useful source of references for the researchers from both academia and industry, who deal with the aforementioned areas of applications. It may be predicted that in the future, the demand in this information will rise dramatically because of a growing interest, especially, in the encapsulated drug delivery systems with tiny bioscopic mechanisms of drug release.

2. Strategies of lipobeads preparation

Two general methods available to date for preparation of artificial bilayer-coated hydrogel particles (lipobeads, giant, or nano) are sketched in **Figure 2**.

The first one (**Figure 2A**) uses the liposomal interior as a chemical reactor for the formation of hydrogel by polymerization [1, 8–22]. In this method, lipid bilayer should be sealed enough to retain the concentration of pregel components and strong enough to withstand the steps preventing polymerization in the surrounding medium.

The second one (**Figure 2B**) is based on the formation of lipid layers around hydrogels after microgel/liposome mixing. In this case, lipid bilayer adsorption on the surface of hydrogel particles prepared separately was promoted via Coulombic attraction between the charged microgels and oppositely charged lipids [7, 23, 24], hydration of lipid films with micro- or nanogel suspension [2, 3], introduction of hydrophobic anchors at the microgel surface around which adsorbing lipids may assemble [6, 25–28], centrifugation of microgels onto a lipid film [29], microfluidic flowing [21], and emulsification [30–32].

In both cases, it is the stability, fluidity, and permeability that are the main properties of a lipid bilayer, which should be governed in the course of lipobeads engineering.

2.1. Effectors of the lipid bilayer fluidity, stability, and permeability

Stability and permeability of a lipid bilayer depend on its fluidity, which can vary with temperature and phospholipid composition. Bilayers undergo a change from liquid to gel (solid) state at the so-called lipid (or order-disorder) phase transition temperature (T_t) characteristic to a phospholipid used (**Figure 3**).

Therein, the shorter the length of hydrocarbon chains, the lower is the T_t, a long hydrocarbon chain at sn-1 position and a short chain at sn-2 position on glycerol exhibit a lower T_t than that of a phospholipid with the opposite arrangement, presence, and position of double bonds in the hydrocarbon chain makes T_t lower than that of the saturated analogue; a bulky

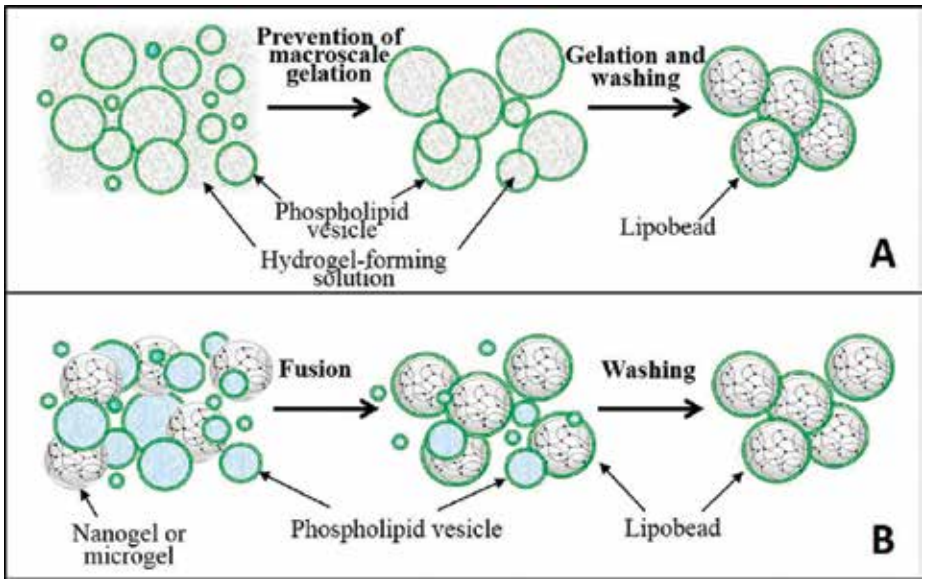

Figure 2. Two methods for lipobeads preparation: (A) formation of hydrogel core by polymerization within vesicle interior and (B) mixing of separately prepared lipid vesicles and hydrogel particles (microgels or nanogels).

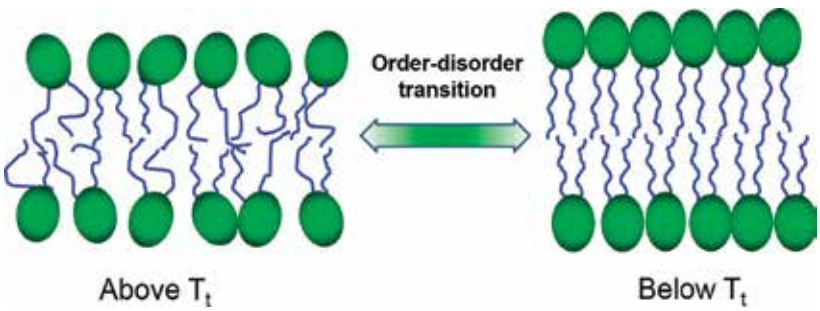

Figure 3. Structure of lipid bilayer below and above the order-disorder transition temperature.

head group confers the lipid a lower T_t than it would be with a smaller head group, the phospholipids with negatively charged head groups favor a lower T_t than that of an uncharged phospholipid. Ionic conditions can modulate this effect, for example, presence of cations in the surrounding water increases T_t.

In the liquid-crystalline "disordered" state, the membrane is fluidic, namely: (i) both alkane chains and head groups of phospholipids are more flexible than in the solid "ordered" state, (ii) the area lipids occupy becomes greater by changing from a 0.48 nm^2/head group to 0.7 nm^2/head group, that is, bilayer expands, (iii) lateral diffusion of phospholipids in the plane of the bilayer and rotation of lipid molecules around C—C bonds accelerate, and (iv) transverse "flip-flop" migration of lipids from one monolayer to the other side of the bilayer becomes more probable.

The factors affecting the lipid phase transition temperature are crucial for lipobeads engineering. Indeed, one can expect the lipid bilayer to be more elastic (favorable for formation of unilamellar membrane) and less sealed (unfavorable for gelation within liposomal interior) above T_t than below T_t. It is known that stability and permeability of naturally occurred membranes can be varied by balancing composition of cholesterol and alcohols. Particularly, cholesterol strongly interacts with phospholipids and inhibits the passive permeability of lipid membrane to water and small electrolytes and nonelectrolytes. The extent of "sealing" directly depends on the amount of cholesterol present, up to moderate levels of cholesterol. However, at very high levels of cholesterol, pure cholesterol phase separates out and leads to an increased leakage through interfacial lipids and unstable aggregates of cholesterol. On the contrary, the insertion of anesthetic molecules, such as alcohols, into the membrane increases the membrane fluidity at a given temperature by depression of the lipid order-disorder transition temperature. Additionally, sphingolipids are commonly believed to protect the cell surface against harmful environmental factors by forming a mechanically stable and chemically resistant outer leaflet of the plasma membrane.

2.2. Polymerization within liposomal nano-/microreactors

In general, preparation of lipobeads using vesicle interior as microreactors includes a number of crucial steps, as shown in **Figure 2A**.

First of all, encapsulation of hydrogel-forming components into liposomes can result from hydration of lipid cast film formed upon solvent evaporation [1, 2, 5, 9, 11, 13, 14, 16, 32], electroformation [12, 22, 33, 34], or rapid phase evaporation [19, 20]. The size of liposomes ensures the final size of lipobeads. Depending on the size, lipobeads can be classified into two groups: nanolipobeads (<1000 nm) and giant lipobeads (>1 μm). Nanolipobeads should be used in realistic drug delivery systems, whereas giant lipogels permit a direct study of structural functionality of the hydrogel/lipid bilayer assemblies, cargo loading, and release mechanisms [12] using optical microscopy.

For 100-nm lipobeads, the liposomal formulations have to be sonicated [1, 9] or extruded through a nanopore filter of a needed pore size [5, 8, 11, 14, 16, 19, 32]. Another approach to control the size of pre-lipobeads is based on hydrodynamic focusing of a stream of the liposome precursor solution by the flow of a hydrogel-forming solution within a microfluidic device [21]. Although the microfluidic-directed approach and electroformation are very elegant methods, they are hardly suitable for a scaled production of lipobeads with regards to pharmaceutical applications.

If the ultimate goal was to engineer the giant lipobeads greater than 1 μm, the gentle hydration of a phospholipid cake [17, 36] or a hybrid agarose/lipid film [unpublished], electroformation [12, 22, 33, 34], emulsification [32], and reverse phase evaporation [1, 13, 30] were used without any agitation of the lipid formulations.

Typical lipid formulations for preparation of lipid vesicles filled with the hydrogel-forming solution are shown in **Table 1**.

Lipid formulation			Method for prelipobead preparation	Size	Ref.
Main phospholipid	T_t	**Other components**			
EPC	−10°C	Cholesterol	Reverse phase evaporation, sonication	~600 nm	[1]
		—	Lipid film hydration, sonication	~150 nm	[9]
		—	Detergent removal or extrusion	~200 nm	[13]
		—	Emulsification	1–40 μm	[32]
		Cholesterol	Reverse phase evaporation	~1–2 μm	[30]
		—	Lipid film hydration, extrusion	~100 nm	[14]
		DOPC/cholesterol		~100 nm	[19]
		NH_2-PEG-DSPE/ cholesterol		~120 nm	[11]
		Cholesterol		0.2–1 μm	[8]
		—		100–200 nm	[37]
DOPC	−22°C	—	Electroformation	10–30 μm	[12]
				0.2–100 μm	[22, 34]
DPPC	42°C	—	Lipid film hydration, extrusion	~800 μm	[5]
		Cholesterol/DCP	Hydrodynamic focusing in microfluidic device	150–300 nm	[21]
SOPC, neutral	6°C	DOTAP, positively charged	Lipid film hydration, extrusion	~350 nm	[16]
Soybean polar lipid extract: PC (45.7%), PE (22.1%), PI (18.4%), PA (6.9%), others (6.9%)	?	–	Lipid film hydration	10–50 μm	[17]
HSPC	52°C	Cholesterol	Lipid film hydration	2–200 μm	[36]

Abbreviations: DCP: dihexadecyl phosphate, DOPC: 1-2 dioleoyl sn-glycero 3-phosphocholine, DOTAP: dioleoyl trimethylammoniumpropane (positively charged), DPPC: 1,2-dipalmotyl-snglycero-3-phosphatidylcholine, DSPE: 1,2-distearoyl-sn-glycero-3-phosphoethanolamine, EPC: Egg chicken L-α-phosphotidylcholine, HSPC: Hydro Soy L-α-phosphotidylcholine, PA: phosphatidic acid, PC: phosphocholine, PE: phosphatidylethanolamine, PEG: polyethylene glycol, PI: phosphatidylinositol, SOPC: 1-stearoyl-*sn*-glycero-3-phosphocholine.

Table 1. Lipid formulations used for preparation of lipobeads by polymerization within lipid vesicles.

Second, when a suspension of vesicles filled with the hydrogel-forming solution is prepared, it is important to prevent cross-linking or polymerization outside those vesicles. This has been done by several methods, such as a 5- to 20-fold dilution [9, 11, 12, 14, 16, 22, 33, 34], gel

filtration [1, 21], centrifugation and dialysis [5, 13, 20, 30], or introduction of polymerization scavengers (e.g., ascorbic acid [19]) into the extravesicular space. In addition, hydrogel-forming solution as well as cross-linker and initiator can be microinjected directly into the internal compartment of a giant unilamellar phospholipid vesicle (GUV) [17].

The third step is gelation of the hydrogel-forming solution entrapped within the closed lipid bilayer. Thermal and ionotropic cross-linking are the examples of physical cross-linking reactions. Some hydrogel cores were made of polysaccharides when temperature changes [2, 5, 32]. Indeed, agarose [5] and κ-carrageenan [32] are the temperature-sensitive polysaccharides which structure in aqueous solutions undergoes a transition from a random-coil conformation to the cross-linked double helixes upon cooling. Agarose is not biodegradable, but its combination with gelatin can bring biodegradability [38]. Gelatin is a thermoresponsive protein, forming a reversible cross-linked network by cooling a water-based solution of the polymer below 35°C. The hydrogel can be liquefied by heating it to physiological temperatures. Interestingly, κ-carrageenan, an anionic polysaccharide carrying one sulfate group, can be cross-linked both thermally (upon cooling) and ionotropically in the presence of divalent or monovalent cations [38]. Similar to alginate, the degradation of carrageenan hydrogels is driven by the exchange of ions with the surrounding fluids. In the course of ionic cross-linking within interior of vesicles, the sections of the polymer backbone carrying the charge bind with ions of opposite charge. For example, when multivalent cations (e.g., Ca^{2+}) were added to a water-based alginate [5] or poly(ethylene dioxythiophene)/poly(styrene sulfonate) [17] solutions, they bound adjacent polymer chains forming ionic interchain bridges that caused a cross-linking. The pH-driven cross-linking inside liposome was carried out by lowering the pH of aqueous solution of poly(acrylic acid) carrying carboxyl groups [20, 30].

The greatest portion of works on gelation within liposomal reactor used photopolymerization to generate a strong covalently cross-linked hydrogel [1, 9, 11, 14, 16, 22, 33, 34, 39]. The monomer and cross-linker depends on the hydrogel core properties required for different applications, as shown in **Table 2**.

Finally, the formulation has to be washed from unreacted chemicals using centrifugation and/or dialysis. In the course of this step, the required medium external to the lipobeads can be introduced. For example, lipobeads could be dispersed in distilled water [13, 30, 36], buffers with pH varied from 7.0 to 7.8 [1, 8, 9, 11, 14, 16, 17, 19–21, 30], or aqueous solutions of sucrose [12, 24, 33, 34]. If necessary, the prepared lipobeads can be dried by gentle evaporation in temperature gradient to be stored at 4°C.

2.3. Hydrogel/liposome mixing

From the general scheme of hydrogel/liposome mixing (**Figure 2B**), one can conclude that hydrogel particles and liposomes should be prepared separately, therein the final size of lipobeads will be defined by the size of hydrogel particles prepared before mixing with liposomes. It has been demonstrated microscopically [40, 41] that hydrophobic modification of the nanogels is not required for spontaneous formation of the bilayer on their surface. Together with the other studies [42], these findings presume that hydrogel/lipid bilayer is an energetically favorable structure.

Monomer.	Cross-linker	Initiator	Prevention of macroscale gelation	Property of hydrogel core	Ref.
PAAm	MBA	ACVA + TEMED	GPC	Not specified	[1]
PSA	BAA	ACVA	GPC	Not specified	[8]
Anchored and nonanchored PNIPA-VI	MBA	DEAP	Dilution 25-fold	Temperature and pH sensitivity	[9]
Anchored PNIPA	TEGDM	DEAP	Dialysis	Temperature sensitivity (probably)	[13]
PNIPA or PAAm	MBA	DEAP	Dilution 20-fold	Temperature sensitive	[14]
PNIPA	MBA	DEAP	Gel filtration	Temperature sensitivity	[21]
dex-HEMA	HEMA	IC2959	Dilution 10-fold	Enzymatically degradable (dextranase)	[16]
PAA	MBA	IC2959	Radical scavenging by AA	pH sensitivity (probably)	[19]
PNIPA	MBA	DEAP	Dilution	Temperature, pH, pI sensitivity	[22, 33, 34]
PLA-PEG-PLA	Diacrylate	IC2959	Dilution 5-fold	Biodegradable	[11]
PAAm	MBA	DEAP	Dilution 20-fold by glucose solution (2.8 M)	Enzymes entrapment, storage, protection, and release	[37]

Abbreviations: ACVA: 4,4′-azobis(4-cyanovaleric acid); BAA: bis-acrylamido acetate; DEAP: 2,2′-diethoxyacetophenone; dex-HEMA: dextran hydroxyethyl methacrylate; GPC: gel permeation chromatography; IC2959: Irgacure 2959; MBA: *N*,*N*-methylenebisacrylamide; PAA: polyacrylic acid; PAAm: polyacrylamide; PEG: polyethylene glycol; PLA: polylactide; PNIPA: poly(*N*-isopropylacrylamide); PSA: sorbitol acrylate; TEMED: *N*,*N*,*N*′,*N*′-tetramethylethylenediamine; TEGDM: tetraethylene glycol dimethacrylate; VI: 1-vinylimidazole.

Table 2. Composition and properties of hydrogel core of lipobeads prepared by polymerization within lipid vesicles.

Lipid formulations used for preparation of lipobeads by hydrogel/liposome mixing are systemized in **Table 3**. Phospholipid with different T_t were employed to prepare conventional liposomes mostly by the lipid film hydration followed by sonication or extrusion in a variety of buffers at pH 7.0–7.6 and deionized water. Nonetheless, the experiments on giant lipobeads show [36, 41] that injection of ethanol solution of phospholipid into hot water is a promising method for preparation of lipidic formulations, which may allow one to exclude the time-consuming steps of lipid film formation and hydration and reduce the time for the scaled fabrication of lipobeads from days to hours.

There are only a few reports (**Table 4**) that deal with nanogels to prepare lipobeads on the nanometer scale: one group employed a high pressure homogenizer to crash bulk polysaccharide hydrogel down to nanosized particles [39, 42], the other group used nanogels extracted from liposomal reactors [9, 10, 26, 27]. In principle, emulsion polymerization

Lipid formulation			Lipid vesicles preparation	Medium (pH)	Ref.
Main phospholipid	**T_t**	**Other components**			
DOPC DOPG	−22°C −18°C	Cholesterol/triolein	w/o emulsion, organic solvent evaporation	5% dextrose HEPES (pH 7.4)	[2]
EPC DPPC	−10°C 42°C	Cholesterol	Injection of ethanol solution of PL in water, homogenization	PBS (pH 7.4)	[3, 4, 40]
EPC	−10°C	–	Lipid film hydration, sonication or extrusion	HEPES (pH 7.4)	[6]
DPPC/DPPG SOPC/DOPG	42°C/41°C 6°C/−18°C	–		Tris (pH 7.0)	[7]
EPC/DMPE	−10°C/50°C	Cholesterol		HEPES (pH 7.0)	[44]
EPC	−10°C	PS/cholesterol		HEN (pH 7.4)	[45]
DMPC/DPPC	24°C/42°C	–		PBS (pH 7.4)	[36]
EPC	−10°C	PS/cholesterol		HEN (pH 8.0)	[46]
PE	63°C	Olein oil/cholesterol		HEPES (pH 7.4)	[47]
SOPC SOPC DOPE	6°C 6°C −16°C	DOPA(−) DOTAP(+) DOTAP(+)		Water	[23]
POPC	−2°C	–		TRIS (pH 7.2)	[28, 48]
DOPC DOPG	−22°C −18°C	DOTAP(+)		HEPES (pH 7.6)	[24]
HSPC	52°C	–	w/o/w microemulsion	Water	[32]
HSPC	52°C	Cholesterol	Injection of ethanol solution of PL in hot water, sonication	Water	[37, 42]

Abbreviations: DMPC: 1,2-dimyristoyl-snglycero-3-phosphatidylcholine, DMPE: 1,2-Dimyristoyl-sn-glycero-3-phosphoethanolamine, DOPA: dioleoyl glycerol phosphate (negatively charged), DOPC: 1-2 dioleoyl *sn*-glycero 3-phosphocholine, DOPE: dioleoyl glycerol phosphoethanolamine (neutral), DOPG: dioleoylphosphatidylglycerol, DOTAP: dioleoyl trimethylammoniumpropane (positively charged), DPPC: 1,2-dipalmotyl-snglycero-3-phosphatidylcholine, EPC: Egg chicken L-α-phosphotidylcholine, HSPC: Hydro Soy L-α-phosphotidylcholine, PE: phosphatidylethanolamine, PL: phospholipid, POPC: 1-Palmitoyl-2-oleoyl-sn-glycero-3-phosphocholine, PS – phosphatidylserine, SOPC: 1-stearoyl-*sn*-glycero-3-phosphocholine.

Table 3. Lipid formulations used for preparation of lipobeads by hydrogel/liposome mixing.

enables preparation of hydrogel particles with a diameter less than 150 nm. However, there is a problem of complete removal of the residual materials. In the absence of an added surfactant, the method is called precipitation polymerization. With the latter two methods, the lipobeads of 1-μm diameter are produced [2, 7, 23, 25, 28, 31]. To prepare giant lipobeads with a diameter up to 100 μm, the inverse suspension polymerization (ISP) method is commonly applied [6, 24, 35, 43–45].

Liposomes can be brought into contact with hydrogel particles by mixing hydrogel particles and liposomes, addition of hydrogel particles into dried lipid film before hydration or

Hydrogel bead composition	Method of bead preparation	Size	Property of hydrogel beads	Ref.
Agarose-gelatin cross-linked by cooling	Emulsification	~1–5 μm	Degradable	[2]
Cross-linked polysaccharide fragments	Extrusion in high-pressure homogenizer	30–60 nm	Temperature, pH, pI: core/bilayer interactions	[39]
Acylated PVA cross-linked by freeze-thaw	ISP	1–100 μm	–	[46]
PMAA-NPMA cross-linked by MBA	ISP	~6 μm	pH sensitivity	[7]
Anchored PDMAA cross-linked by E-BIS	ISP	5–600 μm	– Antibody-antigen interaction [45]	[35, 43–45]
dex-HEMA-MAA (−) or dex-HEMA-DMAEMA (+)	Emulsification	2–5 μm	Degradable	[23]
Acylated PVA cross-linked by freeze-thaw	ISP	~80–100 μm	–	[46]
Anchored PNIPA/P(NIPA-AA) core-shell cross-linked by MBA	Precipitation polymerization	~0.3–2 μm	Temperature, pH sensitivity	[25, 28]
Sodium hyaluronate-PEGDA	Emulsification	1–15 μm	Drying/wetting	[31]
PAAm-allylamine (+) or PAAm-AMPS (−) cross-linked by MBA	ISP	1–100 μm	Electrostatic liposomes/MG interactions	[24]

Abbreviations: AA: ascorbic acid, AMPS: 2-acrylamido-2-methyl-1-propanesulfonic acid, dex-HEMA: dextran hydroxyethyl methacrylate, DMAEMA: dimethylaminoethyl methacrylate, E-BIS: *N*,*N*′-ethylene-bis(acrylamide), ISP: inverse suspension polymerization, MAA: methacrylic acid, MBA: *N*,*N*-methylenebisacrylamide, NPMA: 4-nitrophenyl methacrylate, PAAm: polyacrylamide, PDMAA: polydimethylacrylamide, PEGDA: poly(ethylene glycol) diglycidyl ether, PMAA: polymethacrylic acid, PNIPA – poly(*N*-isopropylacrylamide), PVA: polyvinyl alcohol.

Table 4. Composition and properties of hydrogel particles for lipobeads prepared by hydrogel/liposome mixing.

hydration of the lipid film by aqueous suspension of hydrogel particles. The formation of lipid bilayer around hydrogel particles can be enhanced by shaking, vortexing, pipette agitation, centrifugation, freezing-thawing, heating-cooling, or their combination. The fusion of liposomes will be more advanced at temperatures higher than the T_t of the phospholipid used. Moreover, depending on the electrostatic interaction between bilayer and hydrogel, the liposomes can adsorb on the particles surface, diffuse inside, or/and fuse on the surface with formation of lipobeads [24]. Usually, free liposomes are washed out by centrifugation or removed by ultrafiltration or dialysis. Finally, the lipobeads can be dispersed in a buffer with pH ranged from 7 to 8 or distilled water.

2.4. Modification of hydrogel core and lipid bilayer

To the great extent, the major methods for lipobeads' synthesis (polymerization within liposomal interior and liposome/hydrogel mixing) and further functionalization are analogous to those used for engineering their compartments—conventional nanogels and lipid bilayers.

2.4.1. Hydrogel core

Polymeric nanogels can be synthesized by three straightforward methods: (i) cross-linking polymer chains within already formed nanoparticles using, for example, emulsion polymerization technique [47–49], (ii) polymerization within the liposomal interior followed by the lipid bilayer removal [9], and (iii) photolithographic fabrication of submicrometer hydrogel particles using the PRINT technique [50, 51] or step and flash imprint lithography (S-FIL) [52] as an alternative nanoimprint photolithographic approach.

To engineer the stimuli-responsive nanogels (**Figure 4**), a molecule of interest can be conjugated to the polymer network through a cleavable tether, so that when the tether is cleaved, the drug is allowed to diffuse into the nearby medium. Alternatively, if different molecules are trapped within an environmentally sensitive polymer network with or without environmentally responsive cleavable linkers, the network either changes its volume (swells/shrinks) or degrades when the environmental conditions change, allowing the molecules to be released. For example [53], the doxorubicin-loaded, pH- and redox-sensitive poly(oligo(ethylene glycol) methacrylates-ss-acrylic acid) nanogels exhibited strong internalization by human hepatocellular carcinoma cells (Bel7402) under reduced opsonization and phagocytosis. Herein, the intracellular glutathione (GSH) triggered the release of doxorubicin from the nanogels into cytosol for subsequent entering the nucleus.

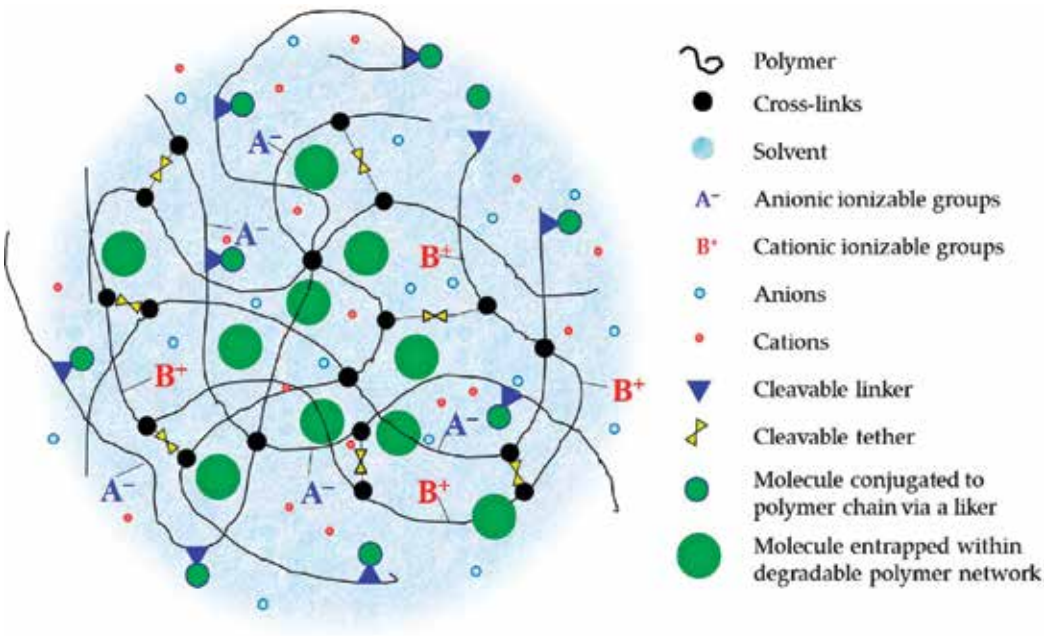

Figure 4. A futuristic view on a stimuli-responsive nanogel with entrapped or/and tethered molecules of interest.

2.4.2. Lipid bilayer

Specific functionality and entrapment of both hydrophilic and hydrophobic molecules into a liposomal interior are the two main objectives of the liposomal system development. Eventually, four types of liposomal systems can be distinguished (**Figure 5**), namely: classical "plain" liposomes, "stealth" liposomes, ligand conjugated liposomes, and stimuli-sensitive liposomes.

The studies on "plain" (traditional) liposomes revealed the difficulty in loading of some types of molecules and leakage of contents from the liposomal interior [54–58]. The further development of the "plain" liposome systems aimed at overcoming these obstacles. In particular, to reduce leakage from liposomes, phospholipids with a higher phase transition temperature [59] were used, and cholesterol [60] and sphingomyelin [61] were incorporated into the lipid bilayer to make it more solid at temperatures of application.

Loading and retention of molecules of interest within liposomes are the molecule dependent processes. For example, weak bases were loaded in response to pH gradients [62–66]. Some molecules, such as doxorubicin, exhibited good retention properties under conditions enhancing their precipitation inside liposomes [67–69], whereas retention of highly hydrophobic molecules, like paclitaxel, was still a challenge [70, 71] until they were converted into the weak bases [72].

Furthermore, the pharmaceutical studies revealed that (i) serum proteins effected on release of drug molecules entrapped into liposomes, (ii) liposomes were cleared very rapidly from

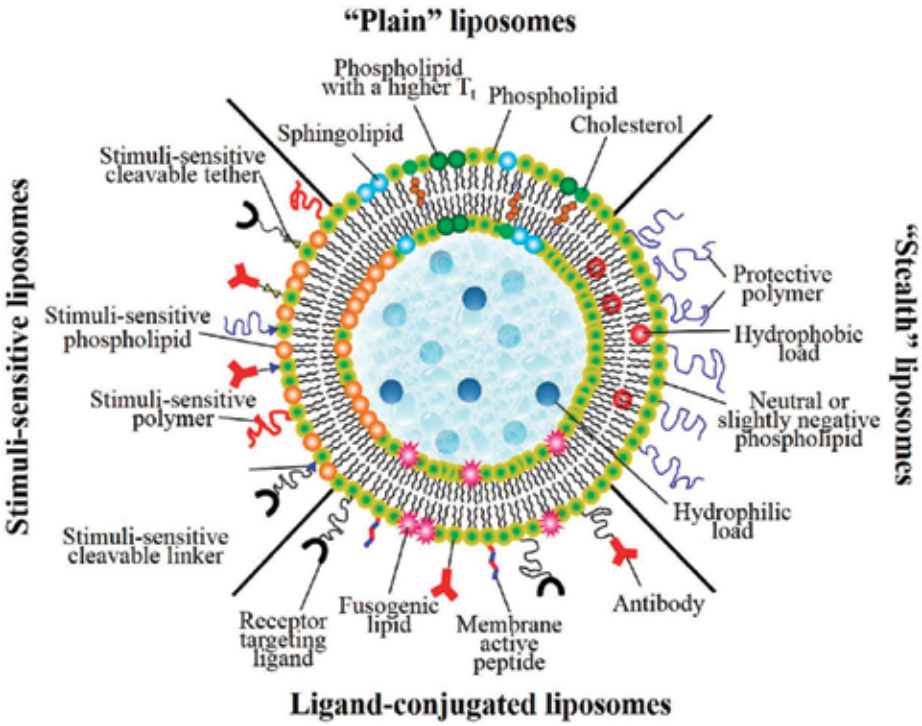

Figure 5. Four evolutionary steps of lipid bilayer modification and functionalization.

circulation by uptake into the cells of the mononuclear phagocyte system (MPS), predominantly in the liver and spleen [73, 74], and (iii) there existed both cellular and intracellular barriers to liposomal delivery [75]. The so-called "stealth" liposomes were developed by stabilizing liposomes with protective polymers (e.g., polyethylene glycol, PEG) [76] in order to increase their circulation time within a biologically active environment, such as blood. In addition, the clearance of liposomes from the body was found [74, 80] to be slower, if they contained neutral or slightly negative phospholipids and their size was around 100 nm. Therefore, the rate of molecules' release should be optimized [77–79].

Ligand-conjugated liposomes were built to target specific cells, intracellular organelles, tumor microenvironment, and/or facilitating receptor-mediated endocytosis (attachment of antibodies, folate, transferrin, tyrosine kinase, vascular endothelial growth factor, introduction of fusogenic lipids, and membrane-active peptides). In particular, three ways to facilitate the intracellular drug delivery include (i) introduction of fusogenic lipids or membrane active peptides into liposomal bilayer enhances fusion or even disruption of cell/organelle membrane and thereby improves cytoplasmic delivery of drug [81–85], (ii) utilization of macrophages for natural endocytosis of drug-loaded liposomes [86], and (iii) receptor-mediated endocytosis of ligand-targeted liposomal drug carriers into the intracellular compartment (see reviews [87–90]).

The release of liposomal contents can be triggered either remotely by heat, radiation, and ultrasound or locally by pH, enzymes, and redox triggers (see review [91] and references therein). For these purposes, the lipid bilayer can be modified with stimuli-sensitive phospholipids, polymers, cleavable tethers, and linkers, as shown in **Figure 5**. Recently, the lipid bilayer consisting of molecules of the temperature-sensitive phospholipid 1-palmitoyl-2-hydroxy-sn-glycero-3-phosphocholine (MSPC) and decorated with gold nanorods was shown to become more permeable for the pain blocking molecules (tetrodotoxin) without a tissue burn when exposed repeatedly to a low intensity near-infrared irradiance [92].

2.5. Encapsulation strategies

2.5.1. Loading during gelation within liposomal interior

Unfortunately, little work has been done so far to test loading capability of lipobeads prepared by polymerization within the lipid vesicles [11, 14, 15, 20, 30]. Typically, a hydrophobic cargo was either incorporated within lipid bilayer at the step of lipid vesicle formation or copolymerized with hydrogel core as an anchor, whereas a hydrophilic cargo was added as a component of the hydrogel-forming solution and incorporated into the intravesicular space before gelation started [9, 11, 13].

The main challenge of the scheme when a load is introduced into the aqueous phase followed by rehydration of a lipid film and further polymerization within a liposomal reactor might be the damage to the loading molecules by toxic ingredients of the hydrogel-forming solution (if any) and/or high temperature and UV radiation initiating polymerization. This approach can be especially problematic for encapsulation of proteins, because of denaturation. Nonetheless, it has been reported that antigen model (BSA) [30] or combination of protein antigen (Pfs25) and oligonucleotide sequence (CpGODN) encapsulated into pH-cross-linked PAA hydrogel core of lipobeads remain intact and active [20]. Moreover, encapsulation efficiencies of lipobeads were shown to be

by 10% higher than those for liposomal carriers. A high encapsulation efficiency of lipobeads has been demonstrated also for hemoglobin [14, 15], which withstands the conditions of free radical polymerization and UV radiation. The other example of successful coencapsulation of hydrophilic proteins (IL-2) and small hydrophobic molecules (TGF-receptor-I inhibitor, SB505124) into the biodegradable hydrogel core of lipobeads has been presented in [11]: encapsulation efficiencies were 80 and 36%, respectively, and UV polymerization did not compromise bioactivity of both immunomodulators. Recently, PAAm lipobeads with a good encapsulation efficiency (37%) of enzymes (bovine Cu, Zn-superoxide dismutase, and bovine milk lactoperoxidase) were synthesized to prove that the UV irradiation used for interior gelation did not cause any reduction in the enzymatic activity of the proteins [37].

2.5.2. Loading of lipobeads prepared by hydrogel/liposome mixing

In the case of lipobeads prepared by hydrogel/liposome mixing, hydrophilic cargos usually are introduced into the interior of hydrogel particles, whereas hydrophobic ones—into the lipid bilayer of liposomes before their mixing. Some molecules can penetrate through the lipid bilayer into the hydrogel core.

Back in 1987, the 200–600-nm agarose-gelatin nanogels were filled with colloidal gold particles prior to mixing with liposomes to form lipobeads [2]. Since colloidal gold particles are very adsorptive for proteins and peptides, their encapsulation into hydrogel core can increase the loading capacity of lipobeads. The cytokine Interleukin-2 (IL-2) plays an important role as an immunostimulator and can be relevant as a treatment by itself for cancer and HIV. However, the difficulties faced today with IL-2 are its toxicity and short half-life. To resolve these problems, this protein was bound to the lipobeads (polysaccharide hydrogel nanoparticles coated with lipid bilayer) [4, 93]. In principle, the lipobeads can be loaded with a number of entities just by their incubation in the corresponding solutions, for example, Ca^{2+} ions and drug mimicking molecules [8], adenosine triphosphate (ATP) [35], and dextran (1.5–3.0 kDa) [44]. Herein, it was found that permeability of the lipid membrane was similar to the free bilayer. To incorporate transmembrane proteins into the peripheral membrane of lipobeads, the hydrogels core particles were mixed and incubated with liposomes containing the proteins of interest within their lipid bilayer [45].

The only chemotherapeutic drug—doxorubicin—was loaded into lipobeads [6, 43]. Encapsulation was performed before lipobeads formation by soaking the dry hydrogel particles in a drug-dissolved solution. The drug diffuses inside in the course of the polymer network swelling and mesh size increase. Further mixing of hydrogel particles with liposomes encapsulates the drug into the lipobeads. As a result, the unbelievably high doxorubicin concentration of ~2 M, which is 10-fold the concentration in liposomes [94], was achieved.

A lecithin-based microemusion method was proposed for fabrication and loading of single-core or multicore lipobeads [31]. The loading efficiency of caffeine into thus prepared sodium hyaluronate lipobeads was obtained to be 30%. A concentration of natural moisturizing factor close to the one present in corneocytes (15%) was encapsulated into the lipobeads, which acquire an enhanced water retention ability similar to corneocytes. This makes them potential for applications in cosmetics and dermatology.

http://dx.doi.org/10.5772/intechopen.70056

Encapsulation of a protein drug into hydrogel particles before lipobeads formation can be performed either by formation of a hydrogel particle in the presence of a protein drug or by incubation of the preformed hydrogel particles in a protein solution. The first approach again could be problematic due to a danger of protein denaturation. The second approach is limited by the size-exclusion effect resulting in a lower loading concentration of proteins. However, encapsulation of proteins into microgels is a promising tool to increase the amount of drug loaded in a prelipobead (loading capacity) by using the "intelligent" properties of polymer networks (swelling/shrinking ability in response to stimuli) [95].

3. Hydrogel core swelling/collapsing and lipobeads properties

The three-dimensional polymer network within a closed lipid bilayer (liposome) can be considered as a gigantic single molecule stabilized by chemical (covalent bonds) or/and physical (ionic bonds, entanglements, crystallites, charge complexes, hydrogen bonding, van der Waals, or hydrophobic interactions) cross-links. The hydrogel core is also an open container with semipermeable boundaries, across which water and solute molecules can move whereas charged (ionizable) groups fixed on the network chains cannot move (**Figure 4**). Herein, the network of cross-linked polymers exhibits both liquid-like and solid-like behavior [96–99]. Therefore, because of its high water content and elastic nature similar to natural tissue, hydrogel core within a liposome is solid enough to support lipid bilayers and liquid enough to keep the membrane intact and functional.

Besides the mechanical stability that hydrogel core provides to the lipid bilayer, the stimuli-sensitivity of the polymer network can be used for managing the environmental responsiveness of lipobeads.

3.1. A variety of possible hydrogel cores

Depending on the composition of a gel/solvent system, the polymer and cross-linking chemistry, nanogels swell or shrink discontinuously or continuously, reversibly or irreversibly in response to many different stimuli (temperature, pH, ion concentration, electric fields, light, reduction/oxidation, enzymatic activity, etc.) [47, 100–105]. In general, various types of hydrogels based upon either natural (e.g., hyaluronic acid, collagen, chondroitin sulfate, alginates, fibrin, and chitosan) and synthetic polymers made of neutral (e.g., 2-hydroxyethyl methacrylate, N-alkylmethacrylamides, N-alkylacylamides, and N,N-dialkylacrylamides), acidic (e.g., acrylic acid, metacrylic acid, and 2-acrylamido-2-methyl propane sulfonic acid), or basic (e.g., N,N-dialkylaminoethyl methacrylate, 1-vinylimidasole, and methacryloyoloxyethyltrialkylammonium bromide) monomers have been prepared, studied, and used in numerous applications (bioseparation, tissue engineering, sensing and molecular recognition, drug and gene delivery, controlled release, artificial muscles, and flow control).

3.1.1. Temperature-sensitive volume change

Typically, the thermoresponsive hydrogels are classified as having either positive or negative volume phase transition with a characteristic temperature (T_V) [106]. Hydrogels exhibiting

positive volume phase transition ("thermophilic" hydrogels) swell upon heating. In contrast, hydrogels exhibiting negative volume-phase transition ("thermophobic" hydrogels) collapse upon heating. The "thermophobic" hydrogels have been studied the most, and a popular example is poly(*N*-isopropylacrylamide) (PNIPA) [107]. In contrast, "thermophilic" behavior in water is not very common for synthetic polymeric materials and likely, because of that, lipobeads with a "thermophilic" hydrogel core have not been attempted yet. Nevertheless, a number of "thermophilic" hydrogels showing a positive thermosensitive volume change have been already fabricated [108–110]. Chitosan cross-linked with glutaraldehyde was found to exhibit the swelling behavior in aqueous media at physiological temperatures and pHs [111]. The graft copolymerization of mixtures of acrylamide (AAm) and acrylonitrile (AN) with *Gum ghatti* (Gg) and cross-linking with MBA resulted in a hydrogel capable of twofold swelling when temperature raised from 30 to 40°C in distilled water [112]. The interpenetrating polymer networks (IPN) composed of poly(acrylic acid) (PAAc) and poly(acrylamide(AAm)-co-butyl methacrylate (BMA), as well as the random poly(AAm-co-AAc-co-BMA) hydrogels cross-linked with MBA also increased their volume (~2.5-fold) within the 30–40°C range in water [113]. Positive thermosensitivity with a twofold swelling ability in the range from 30 to 45°C was reported for a nonionic chemically cross-linked gel made of *N*-acryloylglycinamide as a monomer and MBA as a cross-linker [109]. An abrupt increase in volume to the similar extent within the interval of 30–40°C was observed in the polyzwitterionic hydrogels consisting of N,N′-dimethyl(methacroylethyl)ammonium propanesulfonate or N,N′-dimethyl(acrylamidopropyl) ammonium propanesulfonate cross-linked with EGDM [114]. The gels with positive volume transitions at physiological temperatures, pH and in the presence of salt can be useful in biological or biomedical applications. However, in all abovementioned cases, under physiological pH and salt concentrations, the hydrogels either do not show thermophilic behavior at all or the transition temperature shifted to the nonphysiological values. Nonetheless, recently, hydrogels based on the cross-linked poly(allylurea-co-allylamine) (PAU) copolymers were prepared to unveil a fast and pronounced "thermophilic" increase in volume within the physiological ranges of temperature, pH, and concentration of salt [110].

Thus, first and foremost, a temperature range where the hydrogel shrinks or swells intrinsically depends on the chemical nature of the polymer constituting its network. Herein, the volume changes in a water-swollen hydrogel can be either continuous or discontinuous, as a function of environmental stimuli. If the system remains totally miscible at given thermodynamic conditions, one can expect continuous volume transition. On the contrary, if changes in chemical nature of the polymer network, solvent quality, or environmental stimulus "push" the system into a two-phase (unstable) region of the solubility phase diagram, one can expect that properties of the hydrogel, most notably its volume, change discontinuously. In addition, the studies [115–117] show that increased cross-linking may significantly decrease swelling ability of hydrogel, especially, below T_V, but has a little effect on the value of T_V.

Figure 6 demonstrates that temperature-sensitive shrinking ability of hydrogels depends on their microstructure and method of preparation: the granular hydrogel (A) exhibits a continuous volume decrease with temperature, whereas the denser hydrogels (B and C) exhibit more abrupt changes in volume within the 35–45°C range. Interestingly, the granular structure of the PNIPA hydrogels prepared by thermal polymerization in water (A) can be broken down into separate submicroscopic domains by means of sonication (data not shown). On

http://dx.doi.org/10.5772/intechopen.70056

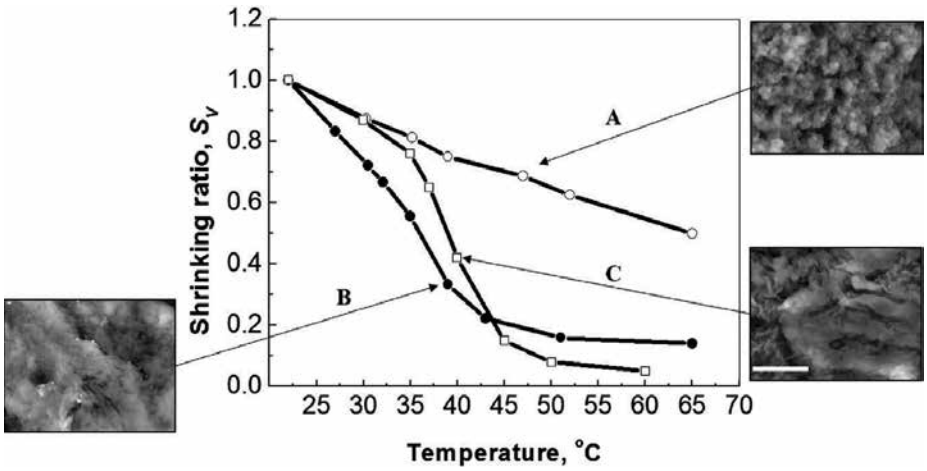

Figure 6. Shrinking abilities S_V and SEM images of the microstructures of PNIPA hydrogels prepared by thermal polymerization in water (A) or DMSO (B), and by UV polymerization in water (C) (scale bar = 5 μm).

the contrary, sonication does not affect the structure of "dense" hydrogels prepared either by thermal polymerization in dimethyl sulfoxide (DMSO) (B) or by photopolymerization in water (C).

It has been shown [118] that incorporation of a small amount of ionizable groups into the nonionic gel network drives the volume phase transition from continuous volume changes toward discontinuous one (**Figure 7**). Moreover, an increase in the portion of sodium acrylate with carboxylic groups on the PNIPA network allowed one to vary the T_V from 34 to 42°C with the increasing extent of swelling ability below the transition temperature.

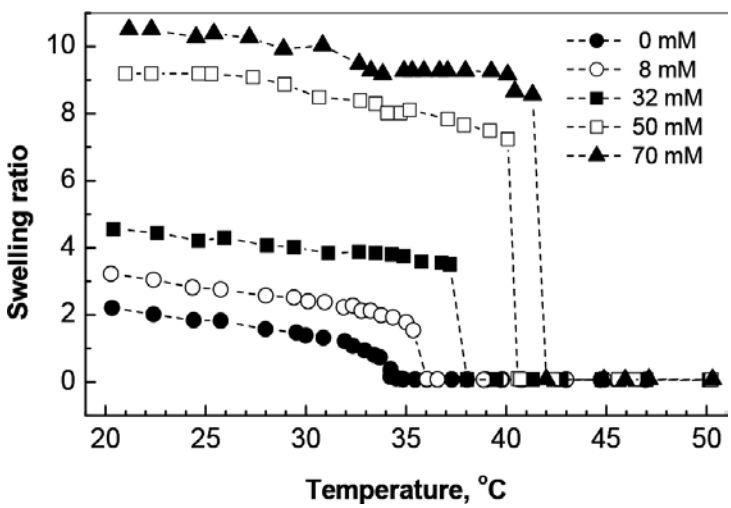

Figure 7. The degree of swelling of the poly(*N*-isopropylacrylamade-co-sodium acrylate) gel in water as a function of temperature. Numbers are the molar fractions of sodium acrylate in the preparations. Data were adopted from [118].

3.1.2. Ionic sensitivity of hydrogels

Figure 7 also suggests that incorporation of charged (anionic, cationic, or both) groups on the polymer network makes the volume transition temperature and degree of swelling dependent on pH and ionic strength. Indeed, the poly(N-isopropylacrylamide-co-methacrylic acid) (PNIPA-MAA) microgel particles [119] at pH 3.4 exhibited a decrease in T_V from 33.5 to 28°C with an increase in MAA content, whereas at pH 7.5, the higher MAA content resulted in the higher T_V. In weakly charged PNIPA hydrogels, addition of ionizable groups on the polymer network pronounced the volume changes when temperature crossed T_V [118, 120, 121]. The experimental studies [122] revealed that distribution of ionic groups in the network affects the temperature of volume change transition.

The type of ionizable groups on the polymer networks makes the maximum swelling ability of a gel strongly dependent on pH. For example, the anioic PNIPA-MAA microgels exhibited the maximum swelling in the range of pHs from 6.5 to 10 [119], whereas for the cationic PNIPA-VI nanogels, the maximum swelling ratio was observed in the range of pHs from 6 to 3.5 [123]. It becomes even more intriguing if the so-called polyampholyte hydrogels are designed [124] by addition of both cationic (VI) and anionic (AA) groups on the network. The polyampholyte gel was in a shrunken state near the isoelectric point (pH ~ pI), and it swelled at both higher and lower pHs. It is interesting that such designed polyampholyte gels can work like biochemomechanical systems in which the enzymatically induced pH changes control the volume of polyampholyte network or, in opposite direction, the pH sensitive volume changes control the activity of enzymes immobilized into the gel [125].

There are experimental evidences [126–130] that different monovalent (Li^+, Na^+, K^+, and Cs^+) and divalent (Ca^{2+}, Mg^{2+}, Sr^{2+}, and Ba^{2+}) ions are able to promote deswelling effects in hydrogels of different chemical nature. Interestingly, at the same molar ratios of divalent to monovalent cations (~1 mM/30 mM), the similar volume changes were observed in biological polyelectrolyte systems during physiological processes like nerve excitation, muscle contraction, and cell locomotion [131–137].

3.1.3. Surfactants as effectors of hydrogel volume change

The extensive theoretical and experimental [138–145] studies have shown that the addition of anionic, cationic, and nonionic surfactants to the solution containing a gel can also influence the T_V and swelling degree of hydrogels depending on their hydrophobicity and charge of the polymer network. In general, addition of anionic or cationic surfactant to the solution of nonionic hydrogel increases T_V as well as the swelling range, whereas the nonionic surfactant does not affect T_V or volume change. The surfactants with ionic head groups when bind to the nonionic polymer networks convert the neutral hydrogels to polyelectrolyte gels and elevate T_V due to introduction of additional osmotic pressure by ionization. The changes in the volume phase transition are also dependent on the length of hydrophobic tail of ionic surfactants and the critical concentration of micelle formation [142]. It was also found [144] that the amount of an ionic surfactant bound onto the swollen network of the nonionic PNIPA hydrogel was much greater than that to the collapsed one. On the contrary, the amount of nonionic

surfactant bound onto the collapsed network of the PNIPA gel was greater than that on the swollen one. Moreover, the changes in T_V with the amount of the anionic surfactants (e.g., sodium dodecyl sulfonate) were more pronounced than for cationic ones (e.g., dodecylamine hydrochloride). Interestingly, the concentration of anionic surfactant (e.g., sodium dodecylbenzene sulfate) bound within the PNIPA hydrogel was found to be higher in the vicinity of the gel surface, whereas a central region of the gel may not contain any bound surfactant molecules [145]. Thus, peripheral layers could be in a more swollen state with a higher T_V in comparison to the central hydrogel core.

3.1.4. Light-sensitive hydrogels

Photosensitive hydrogels with incorporated photosensitive molecules into the gel network have been reported as well. For example, the gels with incorporated leucocyanide and leucohydroxide [146] underwent volume changes upon irradiation and removal of ultraviolet light resulted from ionization reaction and internal osmotic pressure initiated by UV light. Significant volume changes in hydrogels were also induced by visible light [147]. However, the mechanism of volume transition was different—it was due to direct heating of the polymer network by light. Nevertheless, more recent reports [148] showed that a focused laser beam was able to induce reversible shrinking in polymer gels due to radiation forces, rather than local heating, modifying the weak interactions in the gels. Herein, gel shrinkage was observed up to several tens of micrometers away from the irradiation spot. The light-induced contraction was also found in acrylamide gels, which are not temperature sensitive. In hydrogels with temperature-sensitive volume phase transitions, such as PNIPA gel, it was found that the radiation force of the laser beam not only induces the volume phase transition but also lowers the transition temperature T_V by about 10°C at an irradiation power of 1.2 W (λ = 1064 nm).

The fact that the volume change initiated by light is extremely fast seems of great importance for the development of the light-sensitive lipobeads. One could predict that the photosensitive hydrogel cores will also receive an increasing scientific and technological attention due to their capability of serving as the so-called shape-memory polymeric systems [149]. Being exposed to the light with lower wavelengths, the shape-memory materials become deformed and their temporary shape is fixed due to cross-linking. When irradiated with higher wavelengths, they recover their initial shape because of the cross-links cleavage.

3.1.5. Electrical field-induced volume change

Back in the 1950s, it was found that contraction, oscillation, and bending of polyelectrolyte gels can be induced electrically [150–152]. In particular, gels prepared from polymers and copolymers that contain ionizable groups exhibited remarkable contraction when placed between a pair of electrodes connected to a direct current source. Polymer gels containing no ionizable groups showed no volume change under electrical field applied. The extent and rate of volume change of the polyelectrolyte gels were shown to increase with increasing electrical field [153]. An increase in the ionic strength (e.g., an addition of NaCl) also increases the rate of gel shrinkage, whereas an addition of organic solvent (e.g., acetone or

ethanol) decreases both the extent and the rate of shrinking. In different types of hydrogels, an electrically activated volume changes were associated with the induction of the medium pH change by the electric field [154], the electrically initiated volume phase transition [155], and the so-called electrokinetic phenomena—ion transport of counter-ions in the electric field [156].

3.2. Lipobeads by hydrogel/liposome mixing

Success in formation of lipobeads by hydrogel/liposome mixing (see references from **Tables 3** and **4**) is an experimental confirmation of the main property of hydrogel and lipid bilayer—their compatibility. Indeed, the phospholipid bilayer spontaneously self-assembled around a nanogel once extracted from a lipobead (**Figure 8a**) and mixed with liposomes (**Figure 8b**) to form a secondary lipobead (**Figure 8c**) [10].

Moreover, spontaneous formation of the lipid bilayer on the surface of nonanchored microgels was shown microscopically for liposomes made of different phospholipids with or without cholesterol [36, 41]. **Figure 9** represents both laser scanning confocal (**Figure 9A**, **A′**, **A″**) and scanning electron microscopy (**Figure 9B**, **B′**) images evidencing the fusion of liposomes on the hydrogel surface to form a lipid membrane around porous PNIPA-co-FA microgels.

Unilamellarity, continuity, and nonleakiness of the lipid bilayer formed upon microgel/liposome mixing were proven for the micrometer-sized, hydrophobically modified, pNIPAM/p(NIPAM-co-AA) core-shell hydrogel spheres [25, 28]. It was also demonstrated by Dynamic Light Scattering (DLS) and Atomic Force Microscopy (AFM) [40] that hydrophobic modification of the nanogels is not required for spontaneous formation of the bilayer on their surface.

Interesting behavior of the lipobeads was observed when their hydrogel cores change its volume. It was shown (**Figure 10**) that a collapse of the hydrophobically modified PNIPA microgels within the lipid bilayer caused a shape change of the lipobeads from sphere (below T_V) to a small

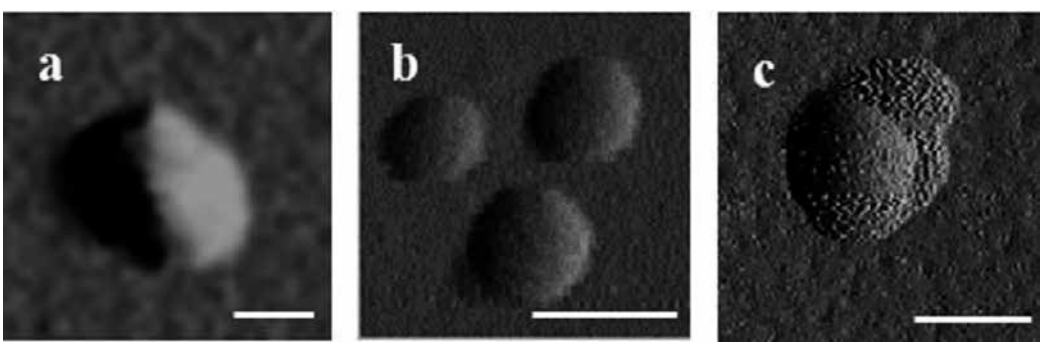

Figure 8. Atomic force microscopy images (amplitude data) of a PNIPA-VI nanogel (a), EPC liposomes (b), and result of their mixture—lipobead flattened on mica surface. Scale bars = 100 nm.

http://dx.doi.org/10.5772/intechopen.70056

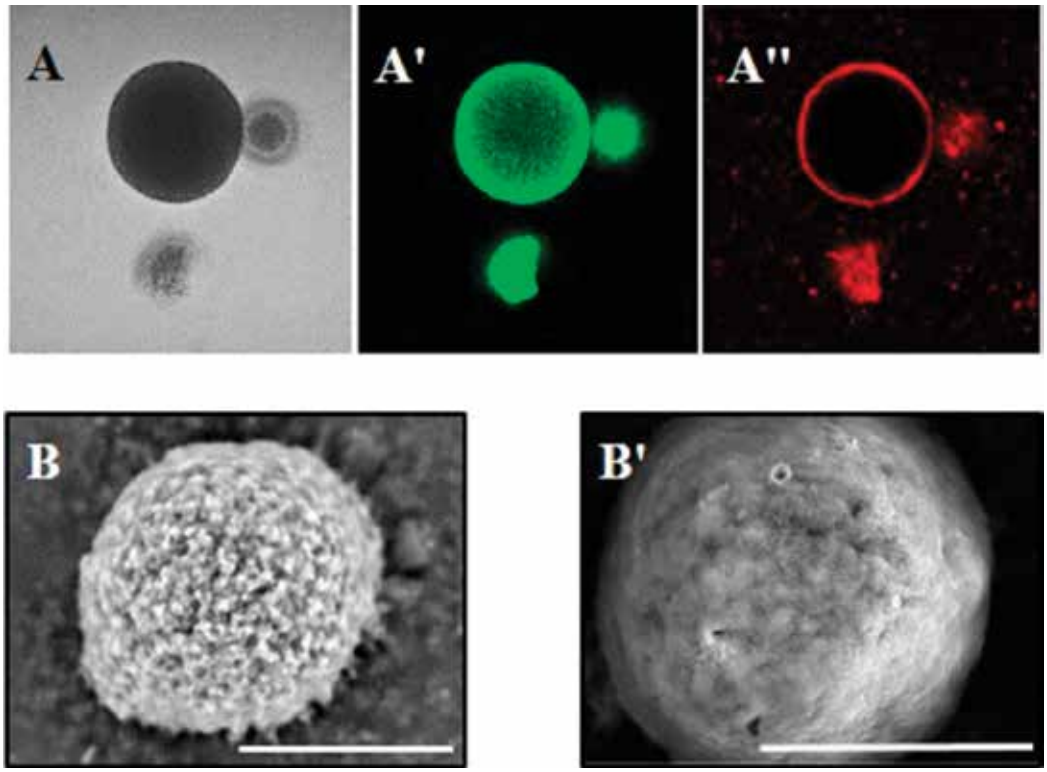

Figure 9. The bright field (A) and confocal laser scanning (A′, A″) microscopy images of PNIPA-co-FA hydrogel microspheres mixed with the liposomes made of HSPC with cholesterol (molar ratio 9:1): Green image (A′) originated from fluorescein-o-acrylate (FA) covalently attached to the PNIPA network within the core. Red image (A″) originated from rhodamine B covalently attached to the heads of PE. Scanning electron micrographs of the PNIPA-co-FA microgel before (B) and after (B′) mixing with liposomes (scale bars = 20 μm).

Figure 10. Fluorescence images of a giant anchored PNIPA lipobead below (left) and above (right) Tv. Red images originated from 0.05 mol% RhodB-PE component within the lipid bilayer. The images were adopted from [25, 28].

central core with high curvature protrusions (above T_V), consisting of the excess lipid bilayer which still adjoin the lipid bilayer remaining bound to the hydrogel via hydrophobic anchors [25, 28]. Importantly, these changes were found to be reversible, and the bilayer remained intact and impermeable.

3.3. Lipobeads by polymerization within liposomal interior

3.3.1. Lipobeads with hydrophobically modified nanogels

As shown by DLS, the size distribution of lipobeads with hydrophobically anchored PNIPA-VI nanogels became bimodal when temperature was raised to 40°C: the position of the first peak corresponded to the initial size of lipobeads at 25°C, while the second peak was assigned to the aggregates of lipobeads. The further cooling back to 25°C restored the original unimodal size distribution of lipobeads, indicating reversibility of anchored lipobeads aggregation. **Figure 11** sketches the behavior of lipobeads resulted from the anchored hydrogel collapsing.

Presumably, the aggregation reduces the hydrophobic/hydrophilic imbalance caused by collapsed nanogels within lipobeads. The reversible dissociation of the lipobead aggregates may evidence that anchored lipobeads do not fuse. The only explanation is that the hydrophobic chains of anchored PNIPA-VI nanogels penetrate into the lipid bilayer and stabilize the liposomal membrane against fusion.

On the contrary to the hydrophobically modified giant lipobeads (**Figure 10**), the anchored PNIPA-VI nanolipobeads did not reveal a size change under temperature or pH variations, as shown by DLS [9]. Probably, on the nanometer scale, a highly curved lipid bilayer is too stiff to follow the collapse of the hydrogel core. This effect remains to be proven.

3.3.2. Lipobeads with nonmodified nanogels

In contrast to the hydrophobically modified lipobeads, the unanchored lipobeads exhibited the unimodal size distribution recorded by DLS at 40°C. The single peak was significantly shifted toward a greater average diameter than that at 25°C. This observation indicated that a more pronounced aggregation occurred in this case. After cooling back to 25°C, the bimodal size distribution of lipobeads was observed. The presence of two peaks indicated that not all aggregates of lipobeads did break up into elementary lipobeads. This pattern of the lipobeads behavior with temperature suggests that the aggregation of lipobeads at elevated temperatures can be irreversible, if lipid bilayers fuse to form a "giant" lipobead containing several nanogels as sketched in **Figure 12**. Herein, the aggregation of unfused lipobeads is reversible (see processes 1 and 2).

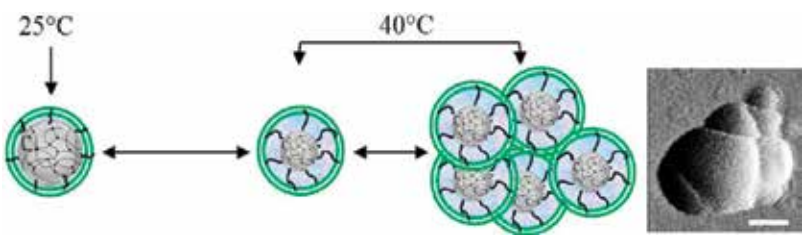

Figure 11. Schematic presentation of the anchored lipobeads and their aggregation in the course of hydrogel core shrinking. AFM image (amplitude data) of an aggregate is shown in the insert. Scale bar = 100 nm. The anchored lipobeads reversibly disaggregate when hydrogel swells back.

http://dx.doi.org/10.5772/intechopen.70056

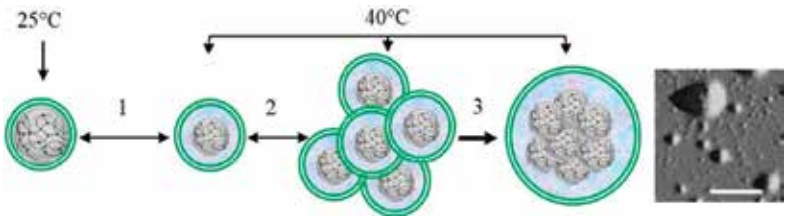

Figure 12. Schematic presentation of the nonanchored PNIPA-VI lipobeads and their aggregation when hydrogel core shrinks. In the course of the liposomal membrane fusion, the collapsed nanogels can aggregate to form a giant lipobead. The processes 1 and 2 are reversible, whereas process 3 is the irreversible one. AFM image (amplitude data) of an aggregate is shown in the insert. Scale bar = 2 μm.

The effect of temperature on shape and size of lipobeads was studied [34] using the giant (not nano-) nonanchored PNIPA lipobeads prepared by polymerization within giant vesicles. As shown microscopically, the giant lipobeads retained their spherical shape when hydrogel core collapsed at high temperature and swelled back after cooling. Their size was found to change reversibly, so that after six cycles of heating/cooling around the volume transition temperature, the lipobeads remained undamaged. The authors postulated that the membrane was coupled to the gel during the volume change, although the study of mechanisms of the gel core/lipid membrane interactions are still in demand.

4. Special applications and new perspectives

4.1. Lipobead-based drug delivery systems

To figure out which properties make lipobeads attractive for the next generation of drug delivery systems, it is worthwhile to consider first their fate in the body once being administered.

4.1.1. From injection to internalization of lipobeads into the cells

Different administration routes including intravenous, intramuscular, pulmonary, and topical could be suitable to deliver drugs by lipobeads. However, the peripheral intravenous injection seems the most reliable and reproducible route for their administration. Once entering the bloodstream after intravenous injection, lipobeads, similar to liposomal or polymeric delivery systems, should withstand a number of environmental (physiological and physicochemical) attacks on the way to targeted organs. The bloodstream is a complex environment of the serum (proteins, electrolytes, etc.) and immune system (macrophages, proteins of complement system, etc.) components, so that interaction of those components with lipobeads could result in either leakage of their content or their removal from the blood circulation as exogenous pathogens. As it was reported for liposomes, the proteins of complement system were able to produce lytic pores and enhance the release of liposomal content [157], whereas blood lipoproteins destabilized liposomes to enhance the leakage of their payload [158]. The opsonins and dysopsonins are another blood proteins, which could be responsible for recognition of

lipobeads and their enhanced uptake by the mononuclear phagocyte system (MPS) cells (neutrophils, monocytes, and macrophages) [159–162].

The effect of physicochemical factors (size, charge, hydrophobicity, surface morphology, and composition) on lipobeads' leakage in and clearance from blood is not known and should be the other target for the future study of lipobeads as a drug delivery system. Nonetheless, even just a few results available on the drug-encapsulated lipobeads (pegylated [11] or not [20]) have already demonstrated their noticeably better stability, biodistribution, nontoxicity, and therapeutic activity than those for liposomes.

Once reaching the heart, the blood with lipobeads is pumped up to organs. Undoubtedly, the mechanical stability of lipobeads in the blood flow will be higher than that of liposomes, since in this construct, a lipid bilayer is supported by hydrogel core and can be strengthened even more by anchoring. The capillaries with a diameter ranging from 2 to 10 μm constitute the first sieving constraint for the lipobead size. The particles of the size between 0.4 and 3 μm would mainly be captured by the liver macrophages. The lipobeads greater than 200 nm [75] would preferentially be filtered by the spleen. The smaller limit comes from the fact that particles less than 40 nm [162] should undergo clearance through metabolism in the liver and excretion through kidneys. Therefore, the diameter of lipobeads is supposed to be in a relatively narrow range from 50 to 180 nm for a longer retention in the bloodstream. Interestingly, it has been proven that formulations of lipobeads were the most reproducible in this range of sizes especially if prepared by polymerization within a liposomal reactor (see **Table 2**).

This range of sizes looks appropriate for lipobeads to exit systemic circulation. To reach interstitial space, lipobeads must cross a thin inner membrane of squamous endothelial cells provided by the capillaries. In normal capillaries, the endothelial cells form uninterrupted linings with typical gaps of 5–10 nm in size. In capillaries associated with pathologies such as tumor and inflammation, the gaps between endothelial cells were reported to vary from 100 to 780 nm for different types of cancer [163]. Due to rapid and imbalanced vessel formation, the tumor neovasculature is chaotic, extremely heterogeneous and "leaky" [164]. The enhanced vascular permeability of the tumor capillaries is the first factor contributing to the phenomenon referred as the enhanced permeation and retention (EPR) effect [165, 166]. The second factor of the EPR effect, an enhanced retention of lipobeads in the interstitial space, can be expected due to a poor lymphatic drainage in the tumor tissue, which results in a slower clearance of drug carriers and their accumulation in the interstitial space [167]. Biodistribution experiments have already performed in mice bearing a distant subcutaneous tumor and in mice with metastatic lung melanoma to show accumulation of drug-loaded lipobeads both in the area surrounding the tumor and within the tumor itself [11]. Therein, the payload is evident in the interstitial spaces between the tumor cells outside the vasculature.

In the interstitial space, lipobeads passively or actively target the cellular surface. Strategies of active cell targeting which has been proposed for liposomal carriers [86–88] could be applicable to lipobeads as well.

The internalization of lipobeads into the cells can proceed via several mechanisms [168, 169] sketched in **Figure 13**. Phagocytosis provides the so-called "cell eating" mechanism by which larger lipobeads can be taken into and degraded within the cells. Using pinocytosis, the cells internalize the fluid surrounding the cell simultaneously with all substances ("cell drinking" mechanism), so that if lipobeads are in the fluid phase area of invagination, they would be taken up to form pinosomes inside. Different endocytic pathways can be distinguished in accord with the specific molecular regulators (not shown in **Figure 13**), such as the clathrin-mediated endocytosis, dynamin-dependent and dynamin-independent mechanisms, as well as receptor-mediated endocytosis. In addition, the mutual fusion of cell membrane and lipid bilayer of lipobeads [170] can occur at the cell surface with internalization of just the drug-loaded nanogels. Understanding the cellular entry of lipobeads, their intracellular trafficking, drug release, and therapeutic action mechanisms are the future topics for studies on lipobeadal drug delivery systems.

4.1.2. New mechanisms of drug release

A drug release profile (the amount of drug released into the bloodstream over time) depends on the properties of the drug itself and drug carrier system. Even a few available examples of drug-encapsulated lipobeads showed that the additional element in their structure, the hydrogel core, significantly prolongs the release time for both high molecular weight (e.g., proteins) and small molecule (e.g., doxorubicin) drugs as compared to conventional liposomes and uncoated hydrogel particles. The characteristic time for release of 50% (D_{50}) of BSA (Mw 66 kDa) from 1-μm lipobeads (~11 days) is 10-fold of that from 1-μm liposomes (~1 day) [20]. For a lighter protein interleukin-2 (IL-2, Mw 17 kDa) [22], D_{50} equals 8, 16, and 52 h for nanogels (Ø150 nm), liposomes (Ø100 nm), and lipobeads (Ø120 nm), respectively, indicating the slower release of the protein drugs from lipobeads. In comparison, the characteristic time (D_{50}) for release of doxorubicin from uncoated microgels (~Ø6 μm) was estimated [6, 43] to be about 1.5 min, whereas the release of doxorubicin from lipobeads was not detected at all within this time scale.

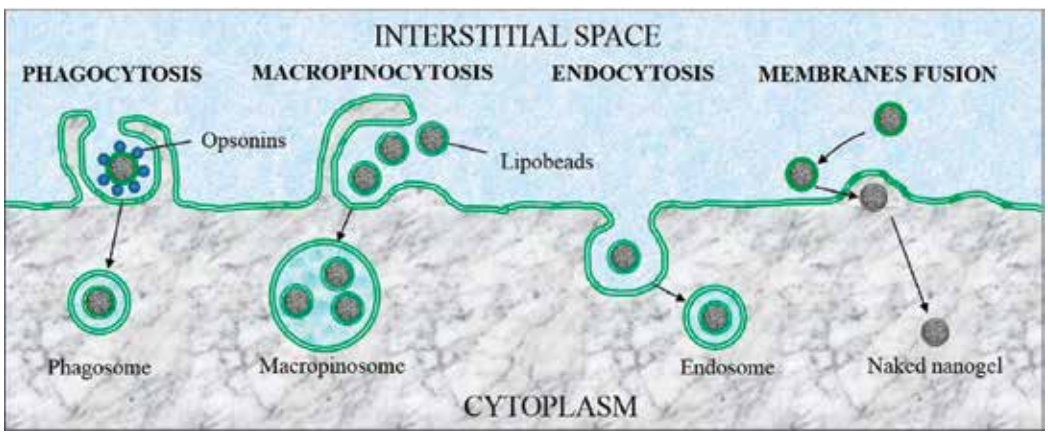

Figure 13. Possible mechanisms of lipobeads' internalization into the cell.

Different applications require different release profiles, and bicompartmental structure of lipobeads brings more options to change the concentration profile of a released drug from a steep rise (burst release) and a cyclic variations (pulsatile release) to a gradual increase up to the value within the therapeutic window is reached (sustained or controlled release). Of particular importance is the capability of lipobeads to provide a better-sustained release, which is the most desirable but more difficult mode to achieve and maintain.

Let us consider the novelty the hydrogel core can bring with regard to drug release mechanisms. Undoubtedly, an advanced property of polymer networks is their responsiveness to environmental stimuli. Depending on possible responses of the hydrogel core (swelling, contraction, and degradation), three mechanisms of drug release from lipobeads could be developed in the future.

In the "sponge-like" mechanism (**Table 5**), hydrogel core initially is in a swollen state. Nevertheless, encapsulated drug molecules release for a prolonged period as compared to conventional liposomes. When the environment changes (temperature, pH, etc.), the polymer network shrinks, so that the hydrogel core, like a squeezed sponge, releases the loaded drug into the space between gel and lipid membrane, and the drug diffuses through the membrane outside the lipobead. This mechanism provides a slow gradual drug release in response to temperature change, for example. The characteristic time of the drug diffusion through the lipid bilayer could be projected to hours.

In the "poration" mechanism, the hydrogel core initially is a shrunken state, and drug molecules are trapped more tightly within the polymer network. Their release can be even more suppressed

Mechanism	Scheme	Characteristic time
"Sponge-like" (diffusion)	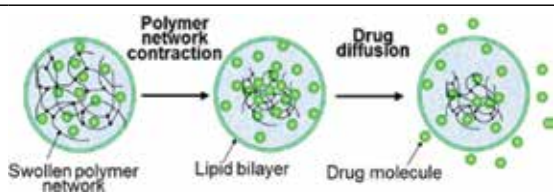	Hours
"Poration"	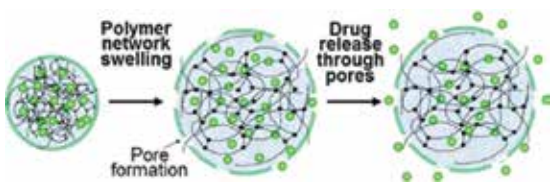	Minutes
"Burst"	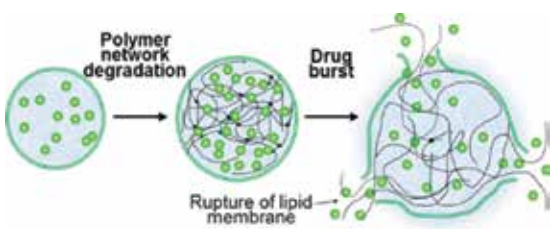	Seconds

Table 5. Mechanisms of drug release from lipobeads with environmentally sensitive or degradable hydrogel core.

in comparison with conventional liposomes. When the environment changes (temperature, pH, etc.), the polymer network swells so much that the volume of hydrogel core becomes greater than the space provided by the closed lipid bilayer. Therefore, a "growing" hydrogel core causes stretching of the lipid bilayer and pore formation ("poration") resulting in the drug release through the pores. This mechanism provides a faster drug release in response to stimuli with the projected characteristic time of minutes.

The "exploding" lipobeads have been discovered [23] as a byproduct of biodegradation of microgels covered with phospholipid membrane. As schematically outlined in **Table 5** (the bottom row), if a polymer network degrades (for example, the interchain cross-links can be cleaved by hydrolysis), the swelling pressure inside increases, because the degradation products are unable to diffuse through the lipid membrane even it stretches. At some point, the internal pressure becomes sufficient to break the membrane. As a result, encapsulated drug falls out of lipobeads with the maximal release rate ("burst" release with the characteristic time of seconds).

4.1.3. Drug combination within lipobeads

In the first example [20], a combination of protein (Pfs25) and oligonucleotide (CpGODN) has been simultaneously encapsulated into lipobeads. The recombinant protein Pfs25 expressed in *Pichia pastoris* is a leading antigen of blocking stage potential and can be used as a vaccine to block malaria transmission by mosquitoes. The antigen Pfs25 has a poor immunogenicity and needs an enhancer of immunological recognition. Unmethylated CpG oligodeoxynucleotide (CpGODN) is a strong stimulator of immune response in mammalian hosts and acts as the adjuvant improving immunogenicity of coadministered protein antigen as well as reducing the amount of protein required. CpGODN stimulates the immune system through a specific receptor TLR9. The immune activity of CpG was monitored by following the levels of nonspecific and specific immunoglobulins, a variety of cytokines, gamma interferon (IFN-γ), and increased lytic activity (see [20] for references). The results of this study were impressive: (i) on the 90th day of storage at 4°C, the detected antigen leakage from lipobeads was significantly lower (5%) than from conventional liposomes (26%), (ii) like the conventional liposomes, no macroscopic sign of adverse reaction (redness, swelling, and formation of granulomas) at the site of intramuscular injection was observed for lipobeads, (iii) lipobead-encapsulated combination of Pfs25 and CpGODN showed the maximal immune response based on serum anti-Pfs25 profile of immunized mice, (iv) significantly higher levels of interferon-γ and interleukin-2 were detected in the spleen if mice immunized with lipobeads carried the drug combination.

In the second scheme [11], hydrophilic protein (IL-2, 17 kDa) and hydrophobic small molecule drug (SB505124, SB, 335 Da) have been coencapsulated into the hydrogel core of 120-nm lipobeads cross-linked by a free radical photopolymerization. The IL-2 belongs to the family of cytokines, soluble proteins that supposedly stimulate natural killer cells (NK) and enhance lytic activity against melanomas and renal cancer. However, efficiency of the IL-2 as an immunotherapeutic agent may be significantly reduced by the ability of tumor cells to secret a number of immunosuppressive factors, such as the transforming growth factor-β (TGF-β) that decreases local immune responses. The SB is a TGF-β antagonist that inhibits TGF-β receptor. The study on coencapsulation into lipobeads and simultaneous sustained

delivery of the aforementioned drugs showed that no toxicity was observed on intravenously administrated mice. Biodistribution analysis of rhodamine-loaded lipobeads in healthy mice indicated that the lipobeads primarily accumulated in lungs, liver, and kidney, the heart and spleen were also reached though. In B16 lung metastatic animals, the highest accumulation of lipobeads and drug was found to occur in the lungs and liver. In comparison to other delivery systems including liposomal, a significantly greater reduction in both tumor growth rate and tumor mass was observed after one-week therapy of the B16/B6 mouse models of metastatic melanoma administered intravenously. It was found that the lipobead-delivered combination immunotherapy stimulated both innate and adaptive immune systems resulting in drastically increased survival.

4.1.4. Combined multifunctional drug containers

As per **Figures 11** and **12**, the nanogel core collapse at elevated temperature causes either reversible or irreversible aggregation of lipobeads depending on whether lipid bilayer fusion occurs or not. Reversible and irreversible aggregation of lipobeads is a key step for designing two types of combined multifunctional containers.

In the system made of anchored lipobeads, the initial formulation may consist of two different drugs entrapped in different lipobeads (**Figure 14**). Under switching condition 1, both drugs can be simultaneously delivered as one aggregate to the targeted organs in the body. At switching condition 2 or 3, either one or the other drug can be released in the desired order.

In the system based on irreversible aggregation of lipobeads (**Figure 15**), several nanogels loaded with different predrug reagents are trapped under the same lipid membrane ("giant lipobeads") to react inside without damaging the surrounding organs and to be delivered to the targeted site in one "giant" container able to release the final product controllably.

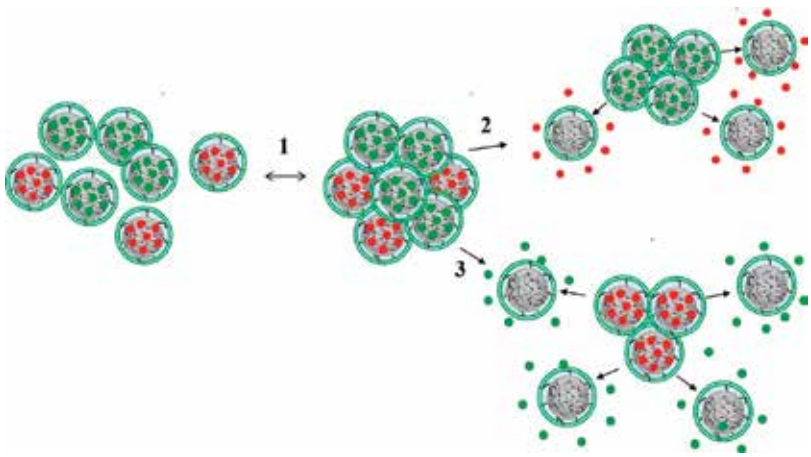

Figure 14. The combined drug delivery system based on reversible aggregation of lipobeads.

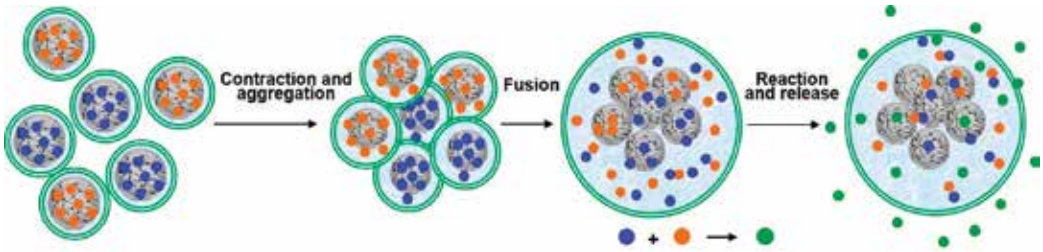

Figure 15. The combined drug delivery system based on irreversible aggregation of lipobeads.

4.1.5. Remarks on lipobead-encapsulated anticancer drugs

Today, cancer is one of the most dangerous illnesses on Earth, because mortality in patients with solid malignant tumors is caused mainly by tumoral metastases, the appearance of new cancerous centers in another organs or different tissues. Administration of anticancer drugs by intravenous route (chemotherapy) is the main treatment aimed at destruction of primary tumor and reduction of the probability of formation of secondary tumors due to metastases. Since single metastatic cells cannot be localized, followed, and monitored so far, a high concentration of an anticancer drug should be systematically distributed throughout the entire human body to increase the probability of the cancer cells' distraction. Being strong poisons and/or cancerogenic themselves, anticancer drugs destroy not only malignant cells but also normal ones giving rise to serious side effects of a chronic and irreversible origin and/or causing the formation of a new malignant tumor even without metastases of the primary one. Moreover, the high concentrations of anticancer drugs can induce a resistance of the malignant cells to these drugs. To reduce the toxicity of the anticancer drugs by controlling their suitable concentrations and reaching the targeted cells without healthy cells being affected, numerous polymeric nanoparticles and liposomal drug delivery systems are under development or undergo clinical trials. However, only two polymer conjugates and six liposome-encapsulated anticancer drugs were approved to market as the most clinically successful liposomal anticancer products so far (for details, see [36] and references therein). Probably, loading drugs into the environmentally responsive hydrogel core covered with the lipid layer is the right way to the chemotherapy with superior tumor response and minimal side effects even at a greater loading concentration.

4.2. Prospective applications and perspectives

4.2.1. Hydrogel/lipid bilayer assembly: Mimicking cell membrane system

Recently developed technologies of using the liposome interior as a microreactor and the concept of lipobeads itself inspire the idea of artificial membrane system with controlled properties. The bottom-up approach to design "liposomes-within-giant vesicle" structures (*vesosomes*) [171, 172] includes a series of structures mimicking cell membrane systems such as shown in **Figure 16** in the order of increase in their complexity: (a) giant vesicles with the size compared to the size of living cells (~5–200 μm), (b) large unilamellar vesicles with the

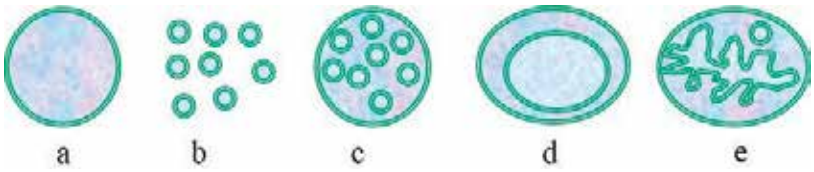

Figure 16. Liposomes-within-giant vesicle structures.

nanometer scale size (<1000 nm), (c) a number of liposomes interior to the single membrane vesicle (cell analogue), (d) a double membrane vesicle with the inner membrane surface lesser than the outer membrane surface (nucleus analogue), and (e) a double membrane vesicle with the inner membrane surface greater than the outer membrane (mitochondrion analogue).

By analogy with vesosomes, it would be intriguing to design the so-called *vesobeads*—hydrogel/membrane structures of different combinations of liposomes, giant vesicles, nanogels, microgels, lipobeads, and giant lipobeads. Some of them shown in **Figure 17** are: (a) giant vesicles with hydrogel core ("giant lipobeads"), (b) hydrogel inside liposomes with the size less than 1 μm, (c) structure that has many lipobeads inside of a giant vesicle, which can also be done by injection. By manipulating the hydrogel, one can cause the lipobeads to aggregate, as shown in structure (d). If the membranes of lipobeads fuse, the structure (e), a number of nanogels inside of a double membrane, can be engineered.

The aforementioned membrane/membrane and hydrogel/membrane structures comprise fusion/fission of LUVs and GUVs and can be served as a model system to study exo- and endocytosis, hydrogel/membrane compatibility, loading ability of the lipid bilayers, polymer networks, and interior of GUVs, and interactions between those assemblages when their surfaces are specifically modified.

Besides all the advantages of conventional lipobeads discussed in this chapter, the multicompartmental structure of vesobeads will provide additional protection against degradation and leakage in bloodstream and greater biocompatibility. Moreover, the structure of a vesobead resembles the structure of a macropinosome (**Figure 13**) and can provide simultaneous internalization of several lipobeads into the cell interior. Indeed, if an external lipid bilayer of vesobead fuses with the cellular plasma membrane, a bunch of loaded lipobeads are injected into cytoplasm.

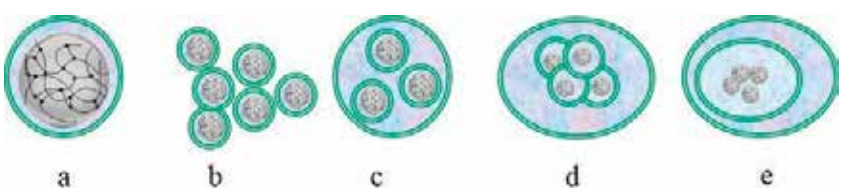

Figure 17. Hydrogel/lipid bilayer assemblies.

4.2.2. Proteo-lipobeads

The next step of lipobead functionalization is incorporation of proteins into their lipid bilayers or/and loading of the hydrogel core with functional proteins. This type of hydrogel/membrane structures has been already named as *proteo-lipobeads*.

4.2.2.1. Proteins within lipid bilayer

The first proteo-lipobeads were prepared when transmembrane receptors were reconstituted into the lipid bilayer of lipobeads [45]. It was found that the receptors retained their native-specific binding. Recently, new proteo-lipobeads with the controlled orientation of the membrane protein and enhanced stability have been developed by modifying agarose beads with linkers, binding membrane proteins to the linkers, and surface coverage with phospholipids [173]. The lipobead incorporated cytochrome c oxidase was shown to be functional in terms of antibody binding and proton transport modulation. The proteo-lipobeads, as alternatives of living cells for monitoring properties of membrane proteins and ion transport through ionic channels and transporters, did exhibit a higher stability, capability of uniform orientation, and functional activity of the membrane proteins in comparison with proteo-liposomes and polymersomes [174]. The further interplay between lipids and the lipobead-encapsulated proteins will allow one to remodel the dynamic cell membrane systems [175] and, despite the increase in complexity of a lipobead structure, will bring about new benefits, such as tiny living cells mimicking mechanisms of drug release regulated by signaling.

If ionic channels (transmembrane proteins) incorporated into the lipid bilayer, it would be necessary to measure ionic transport through the membrane without rupturing the lipid bilayer. For these purposes, one can imagine a hemispherical configuration of the lipobead, which would allow an electrical access to the interior as shown in **Figure 18**. By the way, this device could be used as a biomimetic sensor and a cell analogue, which functional properties could be modeled and studied by changing the inner compartments of the probe.

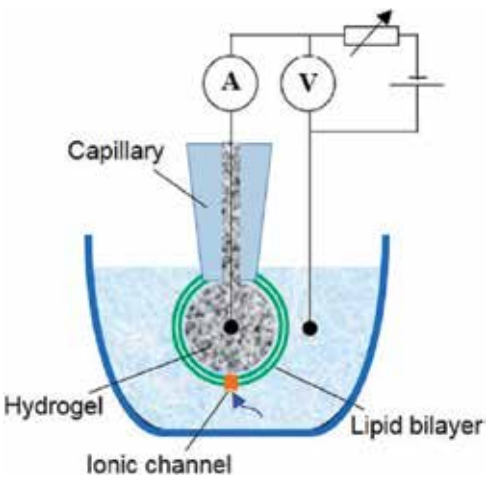

Figure 18. Hemispherical lipobead with electrical access to the interior.

4.2.2.2. Proteins inside hydrogel core

As it was mentioned in Section 2.5.1, so far the only test enzymes were loaded into the lipobeads interior to show retention of their enzymatic activity after release from the hydrogel core [37].

By analogy with the enzyme-containing lipid vesicles (liposomes) [176], one can predict that in turn the near-future development of enzyme-containing lipobeads will follow the same steps and directions, including the studies on (i) methods for adsorption of a variety of enzymes onto the interior or exterior site of the lipid bilayer and for their encapsulation within hydrogel core, (ii) enzyme encapsulation efficiencies, (iii) potential applications, especially, in the biotechnology (e.g., cheese production) and biomedical fields (e.g., enzyme-replacement therapy or for immunoassays). As in the case of liposomes, the enzyme-containing lipobeads could play a twofold role: enzyme carriers and enzymatic nanoreactors. In the first case, the enzyme molecules are expected to be controllably released from the lipobeads at the target site. In the second case, enzymes trapped inside the hydrogel matrix or interspace between the hydrogel core and lipid bilayer catalyze an enzymatic reaction either upon permeation of a substrate across the bilayer or by stimuli-responsive activation of the enzyme molecules.

Obviously, a deeper understanding and modeling of the catalytic activity of the entrapped enzyme molecules will be in demand. In this context, it is worthy to highlight the key property which hydrogel core brings to the enzyme-containing lipobeads: the activity of the enzyme entrapped into the hydrogel can be affected by the 3D-polymeric network density. For example, the studies on activities of enzymes immobilized into the temperature-sensitive hydrogels explicitly indicated that their activity (e.g., urease [177], β-galactosidase [178], α-chymotrypsin [179]) decreased upon PNIPA hydrogel shrinking at elevated temperatures. Since the volume transition in the temperature-sensitive hydrogels is reversible (see Section 3.1.1 for details), the activities of the aforementioned enzymes were restored with temperature decrease beyond the T_V of PNIPA.

There may be another case, when the activity of enzyme immobilized into the hydrogel matrix increases upon a polymer network collapse. In accord with the recently proposed model of electrochemical mechanics of bacterial spores [180], all bacterial spores have a lipobead-like structure consisting of layered protein network (coat), peptidoglycan cross-linked matrix (cortex) enclosed between two lipid membranes, and the spore core containing the genetic information. Some piece of evidence indicates that the co-called cortex lytic enzymes involved into the spore cortex degradation enhance their activity in response to the collapse of the peptidoglycan cortex where these enzymes are located. Note, in this case, the cortex matrix is a substrate for the enzymes, so that its collapse is equivalent to the increase in the substrate concentration, which in turn is responsible for the rate of the degradation reaction.

5. Closing remarks

The concept of lipobeads has been proposed about 30 years ago and the time has come to explore a combination of lipid bilayer and cross-linked polymer network as a logical step of

the development of polymeric and liposomal nanoscopic systems to provide the desired level of functionality, which Nature achieves in living cells. Two general approaches to preparation of lipobeads (polymerization within lipid vesicle interior and mixing of separately prepared lipid vesicles and hydrogel particles) actually are the modified methods for fabrication of liposomes or nanogels. Besides attractive properties from both liposomal and polymeric systems, the mechanical stability of the lipid bilayer and environmental responsiveness of the total structure are the two important properties that hydrogel core brings about to the new construct. Bicompartmental structure of lipobeads predefines their numerous future applications in biotechnology and bioengineering, tissue engineering, sensing and molecular recognition, drug and gene delivery, controlled release, artificial muscles, flow control, and so on.

As a platform for drug delivery systems, lipobeads have already been loaded with chemotherapeutics (doxorubicin, a combination of immunotherapeutic agent and inhibitor of growth factor receptor), malaria vaccine (a combination of stage potential blocker and immunostimulator), and dermatological agent (natural moisturizing factor). In animal experiment, the lipobead-delivered combination chemotherapy demonstrated a drastically increased survival.

Further development of the hydrogel/lipid bilayer assemblies may include vesobeads (e.g., many dispersed lipobeads or their aggregate inside of a giant vesicle, a number of nanogels inside of a double membrane), proteo-lipobeads (lipobeads with functional proteins incorporated into lipid bilayers or/and hydrogel core), enzyme-containing lipobeads (a particular case of proteo-lipobeads with controllable enzymatic activity), and hemi-lipobeads (a cell analogue probe with electrical access to its interior).

This chapter shows that additional technological expenses on production of lipobeads will not be a high cost for the aforementioned advantages of their use in the following Era of the Bioscopic Systems.

Acknowledgements

Financial support for this work was provided by Pace University (Dyson College of Arts and Sciences, Summer Research and Scholarly Research Funds). I would like to thank the entire cohort of my collaborators and all my students participated in this project. I am also grateful to Dr Irina Gazaryan for many comments, which helped clarify my intent.

Author details

Sergey Kazakov

Address all correspondence to: skazakov@pace.edu

Department of Chemistry & Physical Sciences, Pace University, Pleasantville, NY, United States of America

References

[1] Torchilin VP, Klibanov AL, Ivanov NN, Ringsdorf H, Schlarb B. Polymerization of liposome-encapsulated hydrophilic monomers. Makromolekulare Chemie, Rapid Communications. 1987;**8**:457-460

[2] Gao K, Huang L. Solid core liposomes with encapsulated colloidal gold particles. Biochimica et Biophysica Acta (BBA)-Biomembranes. 1987;**897**:377-383

[3] Samain D, Bec J-L, Cohen E, Nguyen F, Peyrot M. Particulate vector useful in particular for the transport of molecules with biological activity and process for its preparation. In: Publication Number WO1989011271; 1989

[4] Castignolles N, Betbeder D, Ioualalen K, Merten O, Leclerc C, Samain D, Perrin P. Stabilization and enhancement of interleukin-2 in vitro bioactivity by new carriers: Supramolecular biovectors. Vaccine. 1994;**12**:1413-1418

[5] Monshpouri M, Rudolph AS. Method of forming hydrogel particles having a controlled size using liposomes. In: US Patent 5464629; 1995

[6] Jin T, Pennefather P, Lee PI. Lipobeads: A hydrogel anchored lipid vesicle system. FEBS Letters. 1996;**397**:70-74

[7] Kiser PF, Wilson G, Needham DA. Synthetic mimic of the secretory granule for drug delivery. Nature. 1998;**394**:459-462

[8] Perrott MG, Barry SE. Liposome-assisted synthesis of polymeric nanoparticles. In: US Patent 6217901; 2001

[9] Kazakov S, Kaholek M, Teraoka I, Levon K. UV-induced gelation on nanometer scale using liposome reactor. Macromolecules. 2002;**35**:1911-1920

[10] Kazakov S, Kaholek M, Kudasheva D, Teraoka I, Cowman KM, Levon K. Poly(N-isopropylacrylamide-co-1-vinylimidazole) hydrogel nanoparticles prepared and hydrophobically modified in liposome reactors: Atomic force microscopy and dynamic light scattering study. Langmuir. 2003;**19**:8086-8093

[11] Park J, Wrzesinski SH, Stern E, et al. Combination delivery of TGF-inhibitor and IL-2 by nanoscale liposomal polymeric gels enhances tumour immunotherapy. Nature Materials. 2012;**11**:895-905

[12] Viallat A, Dalous J, Abkarian M. Giant lipid vesicles filled with a gel: Shape instability induced by osmotic shrinkage. Biophysical Journal. 2004;**86**:2179-2187

[13] Stauch O, Uhlmann T, Frohlich M, et al. Mimicking a cytoskeleton by coupling poly(N-isopropylacrylamide) to the inner leaflet of liposomal membranes: Effects of photopolymerization on vesicle shape and polymer architecture. Biomacromolecules. 2002;**3**:324-332

[14] Patton JN, Palmer AF. Engineering temperature-sensitive hydrogel nanoparticles entrapping hemoglobin as a novel type of oxygen carrier. Biomacromolecules. 2005;**6**:2204-2212

[15] Patton JN, Palmer AF. Photopolymerization of bovine hemoglobin entrapped nanoscale hydrogel particles within liposomal reactors for use as an artificial blood substitute. Biomacromolecules. 2005;**6**:414-424

[16] Van Thienen TG, Lucas B, Flesch FM, Nostrum CF, Demeester J, De Smedt SC. On the synthesis and characterization of biodegradable dextran nanogels with tunable degradation properties. Macromolecules. 2005;**38**:8503-8511

[17] Jesorka A, Markstrom M, Karlsson M, Orwar O. Controlled hydrogel formation in the internal compartment of giant unilamellar vesicles. Journal of Physical Chemistry B. 2005;**109**:14759-14763

[18] Jesorka A, Markstrom M, Orwar O. Controlling the internal structure of giant unilamellar vesicles by means of reversible temperature dependent sol-gel transition of internalized poly(N-isopropyl acrylamide). Langmuir. 2005;**21**:1230-1237

[19] Schillemans JP, Flesch FM, Hannink WE, van Nostrum CF. Synthesis of bilayer-coated nanogels by selective cross-linking of monomers inside liposomes. Macromolecules. 2006;**39**:5885-5890

[20] Tiwari S, Goyal AK, Mishra N, et al. Development and characterization of novel carrier gel core liposomes based transmission blocking malaria vaccine. Journal of Controlled Release. 2009;**140**:157-165

[21] Hong JS, Stavis SM, DePaoli Lacerda SH, Locascio LE, Raghavan SR, Gaitan M. Microfluidic directed self-assembly of liposome-hydrogel hybrid nanoparticles. Langmuir. 2010;**26**: 11581-11588

[22] Pépin-Donat B, Campillo C, Quemeneur F, et al. Lipidic composite vesicles based on poly(NIPAM), chitosan or hyaluronan: Behaviour under stresses. International Journal of Nano Dimension. 2011;**2**:17-23

[23] De Geest BG, Stubbe BG, Jonas AM, Van Thienen T, Hinrichs WLJ, Demeester J, De Smedt SC. Self-exploding lipid-coated microgels. Biomacromolecules. 2006;**7**:373-379

[24] Helwa Y, Dave N, Liu J. Electrostatically directed liposome adsorption, internalization and fusion on hydrogel microparticles. Soft Matter. 2013;**9**:6151-6158

[25] MacKinnon N, Guerin G, Liu B, Gradinaru CC, Rubinstein JL, Macdonald PM. Triggered instability of liposomes bound to hydrophobically modified core-shell PNIPAM hydrogel beads. Langmuir. 2010;**26**:1081-1089

[26] Kazakov S, Kaholek M, Levon K. Lipobeads and their production. In: US Patent 7618565 B2; 2009

[27] Kazakov S, Kaholek M, Levon K. Lipobeads and their production. In: US Patent 7883648 B2; 2011

[28] Saleem Q, Liu B, Gradinaru CC, Macdonald PM. Lipogels: Single-lipid-bilayer-enclosed hydrogel spheres. Biomacromolecules. 2011;**12**:2364-2374

[29] Kiser PF, Wilson G, Needham D. Lipid-coated microgels for the triggered release of doxorubicin. Journal of Controlled Release. 2000;**68**:9-22

[30] Tiwari S, Goyal A, Khatri K, Mishra N, Vyas SP. Gel core liposomes: An advanced carrier for improved vaccine deliver. Journal of Microencapsulation. 2009;**26**:75-82

[31] An E, Jeong CB, Cha C, Kim DH, Lee H, Kong H, Kim J, Kim JW. Fabrication of microgel-in-liposome particles with improved water retention. Langmuir. 2012;**28**:4095-4101

[32] Campbell A, Taylor P, Cayre OJ, Paunov VN. Preparation of aqueous gel beads coated by lipid bilayers. Chemical Communications. 2004;**21**:2378-2379

[33] Campillo CC, Schroder AP, Marques CM, Pépin-Donat B. Composite gel-filled giant vesicles: Membrane homogeneity and mechanical properties. Materials Science and Engineering: C. 2009;**29**:393-397

[34] Faivre M, Campillo C, Viallat A, Pepin-Donat B. Responsive giant vesicles filled with poly(*N*-isopropylacrylamide) sols or gels. Progress in Colloid & Polymer Science. 2006; **133**:41-44

[35] Buck S, Pennefather PS, Xue HY, Grant J, Cheng Y-L, Allen CJ. Engineering lipobeads: Properties of the hydrogel core and the lipid bilayer shell. Biomacromolecules. 2004;**5**: 2230-2237

[36] Kazakov S. Liposome-nanogel structures for future pharmaceutical applications: An updated review. Current Pharmaceutical Design. 2016;**10**:1391-1413

[37] Bobone S, Miele E, Cerroni B, et al. Liposome-templated hydrogel nanoparticles as vehicles for enzyme-based therapies. Langmuir. 2015;**31**:7572-7580

[38] Gasperini L, Mano JF, Reis RL. Natural polymers for the microencapsulation of cells. Journal of the Royal Society Interface. 2014;**11**:20140817

[39] Peyrot M, Sautereau AM, Rabanel JM, Nguyen F, Tocanne JF, Samain D. Supramolecular biovectors (SMBV): A new family of nanoparticulate drug delivery systems. Synthesis and structural characterization. International Journal of Pharmaceutics. 1994;**102**:25-33

[40] Kazakov S, Kaholek M, Levon K. Hydrogel nanoparticles compatible with phospholipid bilayer. Polymer Preprints. 2002;**43**:381-382

[41] Rahni S, Kazakov S. Hydrogel micro−/nanosphere coated by a lipid bilayer: Preparation and microscopic probing. Gels. 2017;**3**:00007

[42] Major M, Prieur E, Tocanne JF, Betbeder D, Sautereau AM. Characterization and phase behavior of phospholipids bilayers adsorbed on spherical polysaccharidic nanoparticles. Biochimica et Biophysica Acta. 1997;**1327**:32-40

[43] Ng CC, Cheng Y-L, Pennefather PS. One-step synthesis of a fluorescent phospholipid-hydrogel conjugate for driving self-assembly of supported lipid membranes. Macromolecules. 2001;**34**:5759-5765

[44] Ng CC, Cheng Y-L, Pennefather PS. Properties of a self-assembled phospholipid membrane supported on lipobeads. Biophysical Journal. 2004;**87**:323-331

[45] Park PS-H, Ng CC, Buck S, Wells JW, Cheng Y-L, Pennefather PS. Characterization of radioligand binding to a transmembrane receptor reconstituted into Lipobeads. FEBS Letters. 2004;**567**:344-348

[46] Umamaheshwari RB, Jain NK. Receptor-mediated targeting of lipobeads bearing acetohydroxamic acid for eradication of *Helicobacter pylori*. Journal of Controlled Release. 2004;**99**:27-40

[47] Shidhaye S, et al. Nanogel engineered polymerics micelles for drug delivery. Current Drug Therapy. 2008;**3**:209-217

[48] JK O, Siegwart DJ, Matyjaszewski K. Synthesis and biodegradation of nanogels as delivery carriers for carbohydrate drugs. Biomacromolecules. 2007;**8**:3326-3331

[49] Shah PP, et al. Skin permeating nanogel for the cutaneous co-delivery of two antiinfmatory drugs. Biomaterials. 2012;**33**:1607-1617

[50] Perry JL, et al. PEGylated PRINT nanoparticles: The impact of PEG density on protein binding, macrophage association, biodistribution, and pharmacokinetics. Nano Letters. 2012;**12**:5304-5310

[51] Perry JL, et al. PRINT: A novel platform toward shape and size specific nanoparticle theranostics. Accounts of Chemical Research. 2011;**44**:990-998

[52] Glangchai LC, Caldorera-Moore M, Shi L, Roy K. Nanoimprint lithography based fabrication of shape-specific, enzymatically-triggered smart nanoparticles. Journal of Controlled Release. 2008;**125**:263-272

[53] Yang H, Wang Q, Chen W, et al. Hydrophilicity/hydrophobicity reversible and redox-sensitive nanogels for anticancer drug delivery. Molecular Pharmaceutics. 2015;**12**: 1636-1647

[54] Gregoriadis G, Ryman BE. Liposomes as carriers of enzymes or drugs: A new approach to the treatment of storage diseases. Biochemical Journal. 1971;**124**:58P

[55] Gregoriadis G. Drug entrapment in liposomes. FEBS Letters. 1973;**36**:292-296

[56] Juliano RL, Stamp D. Pharmacokinetics of liposome-entrapped anti-tumor drugs. Biochemistry & Pharmacology. 1978;**27**:21-27

[57] Mayhew E, Papahadjopoulos D, Rustum YM, Dave C. Use of liposomes for the enhancement of the cytotoxic effects of cytosine arabinoside. Annals of the New York Academy of Sciences. 1978;**308**:371-386

[58] Allen TM, Cleland LG. Serum-induced leakage of liposome contents. Biochimica et Biophysica Acta. 1980;**597**:418-426

[59] Storm G, Roerdink FH, Steerenberg PA, de Jong WH, Crommelin DJ. Influence of lipid composition on the antitumor activity exerted by doxorubicin-containing liposomes in a rat solid tumor model. Cancer Research. 1987;**47**:3366-3372

[60] McIntosh TJ. The effect of cholesterol on the structure of phosphatidylcholine bilayers. Biochimica et Biophysica Acta. 1978;**513**:43-58

[61] Cullis PR, Hope MJ. The bilayer stabilizing role of sphingomyelin in the presence of cholesterol: A 31P NMR study. Biochimica et Biophysica Acta. 1980;**597**:533-542

[62] Mayer LD, Tai LC, Bally MB, et al. Characterization of liposomal systems containing doxorubicin entrapped in response to pH gradients. Biochimica et Biophysica Acta. 1990;**1025**:143-151

[63] Deamer DW, Prince RC, Crofts AR. The response of fluorescent amines to pH gradients across liposome membranes. Biochimica et Biophysica Acta. 1972;**274**:323-335

[64] Mayer LD, Bally MB, Cullis PR. Uptake of adriamycin into large unilamellar vesicles in response to a pH gradient. Biochimica et Biophysica Acta. 1986;**857**:123-126

[65] Madden TD, Harrigan PR, Tai LC, et al. The accumulation of drugs within large unilamellar vesicles exhibiting a proton gradient: A survey. Chemistry and Physics of Lipids. 1990;**53**:37-46

[66] Bolotin EM, Cohen R, Bar LK, Emanuel SN, Lasic DD, Barenholz Y. Ammonium sulphate gradients for efficient and stable remote loading of amphipathic weak bases into liposomes and ligandosomes. Journal of Liposome Research. 1994;**4**:455-479

[67] Drummond DC, Noble CO, Guo Z, Hong K, Park JW, Kirpotin DB. Development of a highly active nanoliposomal irinotecan using a novel intraliposomal stabilization strategy. Cancer Research. 2006;**66**:3271-3277

[68] Maurer N, Wong KF, Hope MJ, Cullis PR. Anomalous solubility behavior of the antibiotic ciprofloxacin encapsulated in liposomes: A 1H-NMR study. Biochimica et Biophysica Acta. 1998;**1374**:9-20

[69] Johnston MJ, Edwards K, Karlsson G, Cullis PR. Influence of drug-to-lipid ratio on drug release properties and liposome integrity in liposomal doxorubicin formulations. Journal of Liposome Research. 2008;**18**:145-157

[70] Bartoli MH, Boitard M, Fessi H, et al. In vitro and in vivo antitumoral activity of free and encapsulated taxol. Journal of Microencapsulation. 1990;**7**:191-197

[71] Cabanes A, Briggs KE, Gokhale PC, Treat JA, Rahman A. Comparative in vivo studies with paclitaxel and liposome-encapsulated paclitaxel. International Journal of Oncology. 1998;**12**:1035-1040

[72] Zhigaltsev IV, Winters G, Srinivasulu M, et al. Development of a weak-base docetaxel derivative that can be loaded into lipid nanoparticles. Journal of Controlled Release. 2010;**144**:332-340

[73] Gregoriadis G, Neerunjun D. Control of the rate of hepatic uptake and catabolism of liposome-entrapped proteins injected into rats. Possible therapeutic applications. European Journal of Biochemistry. 1974;**47**:179-185

[74] Juliano RL, Stamp D. The effect of particle size and charge on the clearance rates of liposomes and liposome encapsulated drugs. Biochemical and Biophysical Research Communications. 1975;**63**:651-658

[75] Mahli S, Dixit K, Sohi H, Shegokar R. Expedition of liposomes to intracellular targets in solid tumors after intravenous administration. Journal of Pharmaceutical Investigation. 2013;**43**:75-87

[76] Gabizon A, Catane R, Uziely B, et al. Prolonged circulation time and enhanced accumulation in malignant exudates of doxorubicin encapsulated in polyethylene glycol coated liposomes. Cancer Research. 1994;**54**:987-992

[77] Laginha KM, Verwoert S, Charrois GJ, Allen TM. Determination of doxorubicin levels in whole tumor and tumor nuclei in murine breast cancer tumors. Clinical Cancer Research. 2005;**11**:6944-6949

[78] Johnston MJ, Semple SC, Klimuk SK, et al. Therapeutically optimized rates of drug release can be achieved by varying the drug-to-lipid ratio in liposomal vincristine formulations. Biochimica et Biophysica Acta. 1758;**2006**:55-64

[79] Charrois GJR, Allen TM. Drug release rate influences the pharmacokinetics, biodistribution, therapeutic activity, and toxicity of pegylated liposomal doxorubicin formulations in murine breast cancer. Biochimica et Biophysica Acta. 1663;**2004**:167-177

[80] Poste G, Bucana C, Raz A, Bugelski P, Kirsh R, Fidler IJ. Analysis of the fate of systemically administered liposomes and implications for their use in drug delivery. Cancer Research. 1982;**42**:1412-1422

[81] Weissmann G, Cohen C, Hoffstein S. Introduction of missing enzymes into the cytoplasm of cultured mammalian cells by means of fusion-prone liposomes. Transactions of the Association of American Physicians. 1976;**89**:171-183

[82] Ozawa M, Asano A. The preparation of cell fusion-inducing proteoliposomes from purified glycoproteins of HVJ (Sendai virus) and chemically defined lipids. Journal of Biological Chemistry. 1981;**256**:5954-5956

[83] Parente RA, Nir S, Szoka FCJ. pH-dependent fusion of phosphatidylcholine small vesicles. Induction by a synthetic amphipathic peptide. Journal of Biological Chemistry. 1988;**263**:4724-4730

[84] Bailey A, Monck MA, Cullis PR. pH-induced destabilization of lipid bilayers by a lipopeptide derived from influenza hemagglutinin. Biochimica et Biophysica Acta. 1997;**1324**:232-244

[85] Torchilin VP, Rammohan R, Weissig V, Levchenko TS. TAT peptide on the surface of liposomes affords their efficient intracellular delivery even at low temperature and in the presence of metabolic inhibitors. Proceedings of the National Academy of Sciences of the United States of America. 2001;**98**:8786-8791

[86] Kelly C, Jefferies C, Cryan SA. Targeted liposomal drug delivery to monocytes and macrophages. Journal of Drug Delivery. 2011;**2011**:727241

[87] Torchilin VP. Recent advances with liposomes as pharmaceutical carriers. Nature Reviews Drug Discovery. 2005;**4**:145-160

[88] Zhao G, Rodriguez BL. Molecular targeting of liposomal nanoparticles to tumor microenvironment. International Journal of Nanomedicine. 2013;**8**:61-71

[89] Allen TM, Cullis PR. Liposomal drug delivery systems: From concept to clinical applications. Advanced Drug Delivery Reviews. 2013;**65**:36-48

[90] Allen TM. Ligand-targeted therapeutics in anticancer therapy. Nature Reviews Cancer. 2002;**2**:750-763

[91] Bibi S, Lattmann E, Mohammed AR, Perrie Y. Trigger release liposome systems: Local and remote controlled delivery? Journal of Microencapsulation. 2012;**29**:262-276

[92] Zhan C, Wang W, Santamaria C, Wang B, Rwei A, Timko BP, Kohane DS. Ultrasensitive phototriggered local anesthesia. Nano Letters. 2017;**17**:660-665

[93] Von Hoegen P. Synthesis biomimetic supra molecular Biovector™ (SMBV™) particles for nasal vaccinedelivery. Advanced Drug Delivery Reviews. 2001;**51**:113-125 and references therein

[94] Lasic DD, Frederic PM, Stuart MCA, Barenholz Y, McCintosh TJ. Gelation of liposome interior. A novel method for drug encapsulation. FEBS Letters. 1992;**312**:255-258

[95] Zhang Y, Zhu E, Wang B, Ding J. A novel microgel and associated post-fabrication encapsulation technique of proteins. Journal of Controlled Release. 2005;**105**:260-268

[96] Harland RS, Prud'homme RK, editors. Polyelectrolyte Gels: Properties, Preparation, and Applications. Washington, DC: American Chemical Society; 1992

[97] Peppas NA. Hydrogels in Medicine and Pharmacy. Boca Raton, FL: CRC Press; 1987

[98] Galaev IY, Mattiasson B. Smart polymers and what they could do in biotechnology and medicine. Trends in Biotechnology. 1999;**17**:335-340

[99] Hennink WE, van Nostrum CF. Novel cross-linking methods to design hydrogels. Advanced Drug Delivery Reviews. 2002;**54**:13-36

[100] Shinoda A et al. Dual cross-linked hydrogel nanoparticles by nanogel bottom-up method for sustained-release delivery. Colloids and Surfaces, B: Biointerfaces. 2012;**99**:18-44

[101] Morimoto N, et al. Hybrid nanogels with physical and chemical cross-linking structures as nanocarriers. Macromolecular Bioscience. 2005;**5**:710-716

[102] Lee ES, et al. A virus-mimetic nanogel vehicle. Angewandte Chemie, International Edition. 2008;**47**:2418-2421

[103] Kopecek J. Polymer chemistry—Swell gells. Nature. 2002;**417**:388-391

[104] Kettel MJ, et al. Aqueous nanogels modified with cyclodextrin. Polymer. 2011;**52**:1917-1924

[105] Shen W, et al. Thermosensitive, biocompatible and antifouling nanogels prepared via aqueous raft dispersion polymerization for targeted drug delivery. Journal of Controlled Release. 2011;**152**:e75-e76

[106] Mah E, Ghosh R. Thermo-responsive hydrogels for stimuli-responsive membranes. Processes. 2013;**1**:238-262

[107] Schild HG. Poly(N-isopropylacrylamide): Experiment, theory and application. Progress in Polymer Science. 1992;**17**:163-249

[108] Yang M, Liu C, Li Z, Gao G, Liu F. Temperature-responsive properties of poly(acrylic acid-co-acrylamide) hydrophobic association hydrogels with high mechanical strength. Macromolecules. 2010;**43**:10645-10651

[109] Liu F, Seuring J, Agarwal S. A non-ionic thermophilic hydrogel with positive thermo-sensitivity in water and electrolyte solution. Macromolecular Chemistry and Physics. 2014;**215**:1466-1472

[110] Shimada N, Kidoaki S, Maruyama A. Smart hydrogels exhibiting UCST-type volume changes under physiologically relevant conditions. RSC Advances. 2014;**4**:52346

[111] Rohindra DR, Nand AV, Khurma JR. Swelling properties of chitosan hydrogels. The South Pacific Journal of Natural and Applied Sciences. 2004;**21**:32-35

[112] Kaith BS, Jindal R, Mittal H. Superabsorbent hydrogels from poly(acrylamide-co-acrylonitrile) grafted *Gum ghatti* with salt, pH and temperature responsive properties. Der Chemica Sinica. 2010;**1**:92-103

[113] Katono H, et al. Thermo-responsive swelling and drug release switching of interpenetrating polymer networks composed of poly (acrylamide-co-butyl methacrylate) and poly (acrylic acid). Journal of Controlled Release. 1991;**16**:215-227

[114] Georgiev GS, Mincheva ZP, Geordieva VT. Temperature-sensitive polyzwitterionic gels. Macromolecular Symposia. 2001;**164**:301-312

[115] Gehrke S. Synthesis, equilibrium swelling, kinetics, permeability and applications of environmentally responsive gels. Advances in Polymer Science. 1993;**110**:81-144

[116] Harsh D, Gehrke SJ. Controlling the swelling characteristics of temperature-sensitive cellulose ether hydrogels. Journal of Controlled Release. 1991;**17**:175-186

[117] McPhee W, Tam KC, Pelton RJ. Poly(N-isopropylacrylamide) latexes prepared with SDS. Journal of Colloid and Interface Science. 1993;**156**:24-30

[118] Hirotsu S, Hirokawa Y, Tanaka T. Volume-phase transition of ionized *N*-isopropyl-acrylamaide. Journal of Chemical Physics. 1987;**87**:1392-1395

[119] Zhou S, Chu B. Synthesis and volume phase transition of poly(methacrylic acid-co-N-isopropylacrylamide) microgel particles in water. Journal of Physical Chemistry. 1998;**102**:1364-1371

[120] Shibayama M, Mizutani S, Nomura S. Thermal properties of copolymer gels containing N-isopropylacrylamide. Macromolecules. 1996;**29**:2019-2024

[121] Hirose T, Amiya T, Hirokawa Y, Tanaka T. Phase transition of submicron gel beads. Macromolecules. 1987;**20**:1342-1344

[122] Kokufuta E, Wang B, Yoshida R, Khokhlov A, Hirata M. Volume phase transition of polyelectrolyte gels with different charge distributions. Macromolecules. 1998;**3**:6878-6884

[123] Kazakov S, Kaholek M, Gazaryan I, Krasnikov B, Miller K, Levon K. Ion concentration of external solution as a characteristic of micro- and nanogel ionic reservoirs. Journal of Physical Chemistry. 2006;**110**:15107-15116

[124] Ogawa Y, Ogawa K, Wang B, Kokufuta EA. Biochemo-mechanical system consisting of polyampholyte gels with coimmobilized glucose oxidase and urease. Langmuir. 2001;**17**: 2670-2674

[125] Eremeev NL, Kukhtin AV, Kazanskaya NF. Enzyme-dependent responses of stimuli-sensitive systems. Bio Systems. 1998;**45**:141-149

[126] Horkay F, Tasaki I, Basser PJ. Effect of monovalent-divalent cation exchange on the swelling of polyacrylate hydrogels in physiological sait solutions. Biomacromolecules. 2001;**2**:195-199

[127] Horkay F, Tasaki I, Basser PJ. Osmotic pressure of polyacrylate hydrogels in physiological salt solutions. Biomacromolecules. 2000;**1**:84-90

[128] Eichenbaum GM, Kiser PF, Shah D, Meuer WP, Needham D, Simon SA. Alkali earth metal binding properties of ionic microgels. Macromolecules. 2000;**33**:4087-4093

[129] Amiya T, Tanaka T. Phase transitions in cross-linked gels of natural polymers. Macromolecules. 1987;**20**:1162-1164

[130] Horkay F, Tasaki I, Basser PJ. Ion-induced volume transition in synthetic and biopolymer gels. Polymer Preprints. 2001;**42**:267-268

[131] Iwasa K, Tasaki I. Mechanical changes in squid giant axons associated with production of action potentials. Biochemical and Biophysical Research Communications. 1980;**95**: 1328-1331

[132] Tasaki I, Iwasa K. Rapid pressure changes and surface displacements in the squid giant axon associated with production of action potentials. Japanese Journal of Physiology. 1982;**32**:69-81

[133] Tasaki I, Nakaye T, Byrne PM. Rapid swelling of neurons during synaptic transmission in the bullfrog sympathetic ganglion. Brain Research. 1982;**331**:363-365

[134] Tasaki I, Byrne PM. Large mechanical changes in the bullfrog olfactory bulb evoked by afferent fiber stimulation. Brain Research. 1988;**475**:173-176

[135] Tasaki I, Byrne PM. Discontinuous volume transitions in ionic gels and their possible involvement in the nerve excitation process. Biopolymers. 1992;**32**:1019-1023

[136] Tasaki I, Byrne PM. Discontinuous volume transitions induced by calcium-sodium ion exchange in anionic gels and their neurobiological implications. Biopolymers. 1994;**34**: 209-215

[137] Tasaki I. Rapid structural changes in nerve fibers and cells associated with their excitation processes. Japanese Journal of Physiology. 1999;**49**:125-138

[138] Kokufuta E, Zhang YQ, Tanaka T, Mamada A. Effects of surfactants on the phase transition of poly(N-isopropylacrylamide) gel. Macromolecules. 1993;**26**:1053-1059

[139] Khokhlov AR, Kramarenko EY, Makhaeva EE, Starodubtsev SG. Collapse of polyelectrolyte networks induced by their interaction with oppositely charged surfactants. Macromolecules. 1992;**25**:4779-4783

[140] Gong JP, Osada Y, Theoretical analysis of the cross-linking effect on the polyelectrolyte-surfactant interaction. Journal of Physical Chemistry. 1995;**99**:10971-10975

[141] Safranj A, Yoshida M, Omichi H, Katakai R. Effect of surfactants on the volume phase transition of cross-linked poly(acryloyl-l-proline alkyl esters). Langmuir. 1994;**10**:2955-2959

[142] Yoshida M, Asano M, Omichi H, Kamimura W, Kumakura M, Katakai R. Dependence of volume phase transition temperature of poly(acryloyl-L-proline methyl ester) gel on hydrophobic tail length of anionic surfactants. Macromolecules. 1997;**30**:2795-2796

[143] Okuzaki H, Osada Y. Effects of hydrophobic interaction on the cooperative binding of a surfactant to a polymer network. Macromolecules. 1994;**27**:502-506

[144] Murase Y, Onda T, Tsujii K, Tanaka T. Discontinuous binding of surfactants to polymer gel resulting from a volume phase transition. Macromolecules. 1999;**32**:8589-8594

[145] Ogawa K, Ogawa Y, Kokufuta E. Effect of charge inhomogeneity of polyelectrolyte gels on their swelling behavior. Colloids and Surfaces. 2002;**209**:267-279

[146] Mamada A, Tanaka T, Kungwatchakun D, Irie M. Photoinduced phase transition of gels. Macromolecules. 1990;**23**:1517-1519

[147] Suzuki A, Tanaka T. Phase transitions in polymer gels induced by visible light. Nature. 1990;**346**:345-347

[148] Juodkazis S, Mukai N, Wakaki R, Yamaguchi A, Matsuo S, Misawa H. Reversible phase transitions in polymer gels induced by radiation forces. Nature. 2000;**408**:178-181

[149] Lendlein A, Jiang H, Junger O, Langer R. Light-induced shape-memory polymers. Nature. 2005;**434**:879-882

[150] Kuhn W, Hargitay B, Katchalsky A, Eisenberg H. Reversible dilation and contraction by changing the state of ionization of high-polymer acid networks. Nature. 1950;**165**:514-516

[151] Steiberg IZ, Oplatka H, Katchalsky A. Mechanochemical engines. Nature. 1966;**210**: 568-571

[152] Sussman MV, Katchalsky A. Mechanochemical turbine: A new power cycle. Science. 1970;**167**:45-47

[153] Osada Y, Hasebe M. Electrically activated mechanochemical devices using polyelectrolyte gels. Chemistry Letters. 1985;**14**:1285-1288

[154] DeRossi DE, Chiarelli P, Buzzigoli G, Domenci C, Lazzeri L. Contractile behaviour of electrically activated mecltanochemical polymer actuators. Transactions—American Society for Artificial Internal Organs. 1986;**32**:157-162

[155] Tanaka T, Nishio I, Sun ST, Nishio SU. Collapse of gels in an electric field. Science. 1982;**218**:467-469

[156] Kishi R, Osada Y. Reversible volume change of microparticles in an electric field. Journal of the Chemical Society, Faraday Transactions 1. 1989;**85**:655-662

[157] Ricklin D, Hajishengallis G, Yang K, et al. Complement: A key system for immune surveillance and homeostasis. Nature Immunology. 2010;**11**:785-797

[158] Allen TM. A study of phospholipid interactions between high density lipoproteins and small unilamellar vesicles. Biochimica et Biophysica Acta. 1981;**640**:385-397

[159] Frank MM. The reticuloendothelial system and bloodstream clearance. Journal of Laboratory and Clinical Medicine. 1993;**122**:487-488

[160] Scherphof GL, Kamps JA. The role of hepatocytes in the clearance of liposomes from the blood circulation. Progress in Lipid Research. 2001;**40**:149-166

[161] Ishida T, Harashima H, Kiwada H. Liposome clearance. Bioscience Reports. 2002;**22**: 197-224

[162] Immordino ML, Dosio F, Cattel L. Stealth liposomes: Review of the basic science, rationale, and clinical applications, existing and potential. International Journal of Nanomedicine. 2006;**1**:297-315

[163] Haley B, Frenkel E. Nanoparticles for drug delivery in cancer treatment. Urologic Oncology. 2008;**26**:57-64

[164] Nagy JA, Chang S-H, Dvorak AM, Dvorak HF. Why are tumour blood vessels abnormal and why is it important to know? British Journal of Cancer. 2009;**100**:865-869

[165] Iwai K, Maeda H, Konno T. Use of oily contrast medium for selective drug targeting to tumor: Enhanced therapeutic effect and X-ray image. Cancer Research. 1984;**44**:2115-2121

[166] Matsumura Y, Maeda H. A new concept for macromolecular therapeutics in cancer chemotherapy: Mechanism of tumoritropic accumulation of proteins and the antitumor agent SMANCS. Cancer Research. 1986;**46**:6387-6392

[167] Noguchi Y, Wu J, Duncun R, et al. Early phase tumor accumulation of macromolecules: A great difference in clearance rate between tumor and normal tissues. Japanese Journal of Cancer Research. 1998;**89**:307-314

[168] Sahay G, Alakhova DY, Kabanov AV. Endocytosis of nanomedicines. Journal of Controlled Release. 2010;**145**:182-195

[169] Iversen TG, Skotland T, Sandvig K. Endocytosis and intracellular transport of nanoparticles: Present knowledge and need for future studies. Nano Today. 2011;**6**:176-185

[170] Düzgüneş N, Faneca H, Pedroso de Lima MC. Methods to monitor liposome fusion, permeability, and interaction with cells. Methods in Molecular Biology. 2010;**606**:209-232

[171] Kisak ET, Coldren B, Evans CA, Boyer C, Zasadzinski JA. The vesosomes—A multicompartment drug delivery vesicle. Current Medicinal Chemistry. 2004;**11**:199-219

[172] Paleos CM, Tsiourvas D, Sideratou Z, Pantos A. Formation of artificial multicompartment vesosome and dendrosome as prospected drug and gene delivery carriers. Journal of Controlled Release. 2013;**170**:141-152

[173] Frank P, Siebenhofer B, Hanzer T, et al. Proteo-lipobeads for the oriented encapsulation of membrane proteins. Soft Matter. 2015;**11**:2906-2908

[174] Geiss AF, Khandelwal R, Baurecht D, Bliem C, Reiner-Rozman C, Boersch M, Ullmann GM, Loew LM, Naumann RLC. pH and potential transients of the bc1 complex coreconstituted in proteo-lipobeads with the reaction center from Rb. Sphaeroides. Journal of Physical Chemistry B. 2017;**121**:43-152

[175] MacMahon HT, Gallop JL. Membrane curvature and mechanisms of dynamic cell membrane remodelling. Nature. 2005;**438**:590-596

[176] Walde P, Ichikawa S. Enzymes inside lipid vesicle: Preparation, reactivity and applications. Biomolecular Engineering. 2001;**18**:143-177

[177] Kukhtina AV, Eremeev NI, Belyaeva EA, Kazanskaya NF. Relationship between state of a termosensitive matrix and the activity of urease immobilized in it. Biokhimiya. 1997;**62**:437-443

[178] Park TG. Stabilization of enzyme immobilized in temperature sensitive hydrogels. Biotechnology Letters. 1993;**15**:57-60

[179] Eremeev NL, Kazanskaya NF. Relationship between the hydration degree of poly-N-isopropylacrylamide gel and activity of immobilized α-chymotrypsin. Russian Chemical Bulletin. 2001;**50**:1891-1895

[180] Kazakov S, Hosein H. Electrochemical mechanics of nanometer-scaled structural layers of bacterial spores. NSTI-Nanotech. 2010;**3**:486-489

Chapter 4

Application of Nuclear Magnetic Resonance Spectroscopy (NMR) to Study the Properties of Liposomes

Anna Timoszyk

Additional information is available at the end of the chapter

http://dx.doi.org/10.5772/intechopen.68522

Abstract

The liposomes are well-known lipid aggregates. The lipid composition and size of the liposomes can be controlled. The method of preparation, lipid composition, temperature, and pH have an influence on the liposome size and bilayer structure. The physicochemical properties of liposomes allow them to various applications. Nuclear magnetic resonance (NMR) is one of the methods used to study liposome properties. The abilities of the method are the high sensitivity and high resolution. Moreover, it provides information about dynamics and structure of molecules. ^{1}H and ^{31}P NMR are most convenient methods to study liposomes, because liposomes are typically formed from phospholipids. Additionally, two-dimensional NMR spectroscopy reveals information about the nature of intermolecular and intramolecular interactions (scalar and dipole-dipole interactions) that makes easier to interpret the structure of molecules. The chapter aims to introduce the NMR phenomenon, interactions between spins in magnetic field, dynamics of molecules and physical parameters of NMR spectra, and the necessary information for analyzing and interpreting high-resolution NMR spectra. It also aims to show how various changes in the bilayer structure or dynamics of lipid molecules are visible in the NMR spectra.

Keywords: liposomes, nuclear magnetic resonance, dynamics, half-width of signal, signal splitting, ^{1}H NMR, ^{31}P NMR, 2D NMR

1. Introduction

Nuclear magnetic resonance (NMR) spectroscopy provides information about the structure and dynamics at the molecular level. The knowledge about the peculiarity of NMR phenomenon and about the physical parameters of NMR spectra would help in analyzing obtained results.

1.1. The magnetic properties and magnetic moment of nuclei

Studies of the atomic structure of discrete spectra have shown that, similar to electrons, nuclei have momentum, which is called nuclear spin. Nuclear spin is directly connected to a given magnetic moment. The values of these magnetic moments can vary. The magnetic moment $\vec{\mu}$ is proportional to momentum $\vec{K}$ (spin) [1]:

$$\vec{\mu} = \gamma \vec{K} \tag{1}$$

where γ is the gyromagnetic ratio, characteristic for a given nucleus (**Table 1**)

1.2. Resonance condition

A given nucleus with its magnetic moment and spin will precess in intense static magnetic field B_0 with frequency ω_0:

$$\omega_0 = 2\pi\nu. \tag{2}$$

The value of the frequency is proportional to γ and to the B_0 field [1]:

$$\omega_0 = \gamma B_0. \tag{3}$$

The frequency of precession in the B_0 field is known as Larmor frequency. In precession, the nuclear dipoles move around a cone in the B_0 field at frequency ω_0. The precessing nuclei transverse magnetic field B_1, which is a linearly oscillating magnetic field along the x-axis, and they then submit to the combined action of both the B_0 and B_1 fields [1]. If B_1 field oscillates at the Larmor frequency, the nuclear magnetic resonance phenomenon will be observed, according to resonance condition as follows:

$$\omega_1 = \omega_0 = \gamma B_0. \tag{4}$$

Nuclei	Nuclear spin	Gyromagnetic ratio [$T^{-1}{\cdot}s^{-1}$]	Resonance frequency in $B_0 = 14.092$ T [MHz]
^{1}H	1/2	2.6752×10^{8}	600
^{13}C	1/2	6.7266×10^{7}	150.9
^{15}N	1/2	-2.7108×10^{7}	60.8
^{17}O	5/2	-3.6267×10^{8}	81.4
^{19}F	1/2	2.5167×10^{8}	564.5
^{25}Mg	5/2	-1.6371×10^{7}	36.7
^{31}P	1/2	1.0829×10^{8}	243.9
^{33}S	3/2	2.0518×10^{7}	46
^{35}Cl	3/2	2.6213×10^{7}	58.8
^{39}K	3/2	1.2482×10^{7}	28

Table 1. The values of nuclear spin ($\vec{K}$), gyromagnetic ratio (γ), and resonance frequency (ω_0) [1, 3].

http://dx.doi.org/10.5772/intechopen.68522

1.3. Nuclear magnetic relaxation

The nuclear magnetic relaxation phenomenon is connected to the interaction between the magnetization vector $\vec{M}$ (equilibrium magnetization) and the B_0 field. The $\vec{M}$ vector is the sum of the magnetic moments of the given nuclei:

$$\vec{M} = \sum_{i=1}^{n} \vec{\mu}_i. \tag{5}$$

The value of magnetization is equal to zero when the nuclei are not in the B_0 field. Then, the $\vec{\mu}$ moments of the nuclei are oriented chaotically in accordance with statistical distribution. In the B_0 field, the $\vec{\mu}$ vectors are ordered, which results in thermodynamic equilibrium. The time in which the equilibrium is set depends on the type of sample and the temperature [2]. In the equilibrium state, more $\vec{\mu}$ moments are oriented parallel to the B_0 field than are antiparallel to it. It is in agreement with the normal Boltzmann equilibrium between the spin states. Thus, the $\vec{M}$ vector is also oriented along the direction of the B_0 field (**Figure 1**).

The $\vec{\mu}$ moments are not coherent in precession; thus, there is no gain in the transverse magnetization $\overrightarrow{M_{xy}}$. When the B_1 field interacts with the precessing spins at the Larmor frequency, the $\overrightarrow{M_{xy}}$ vector gains (**Figure 2**) [2].

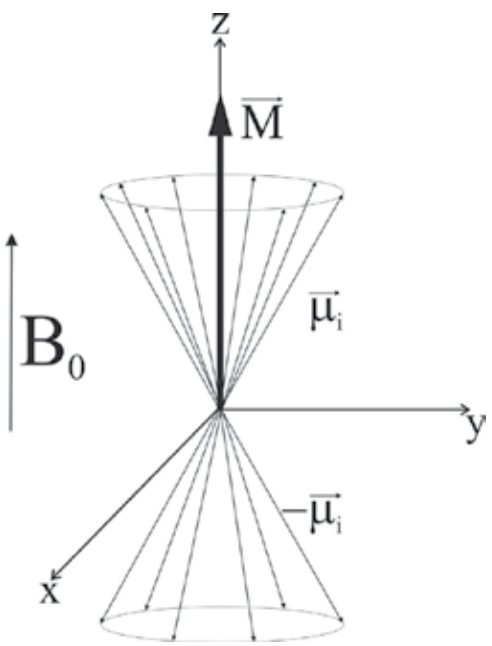

Figure 1. Equilibrium magnetization $\vec{M}$ in B_0 field.

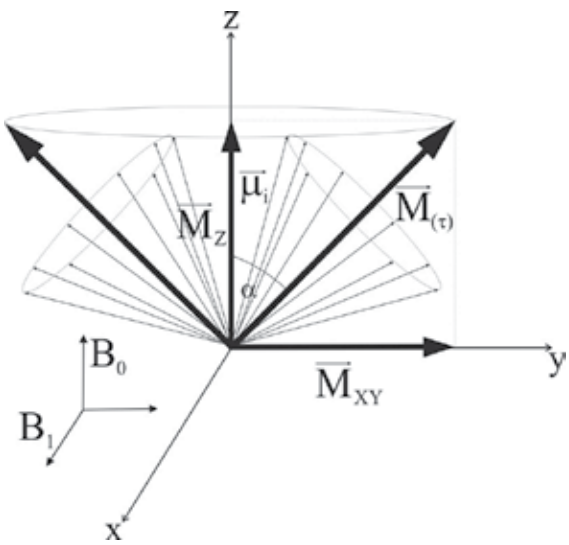

Figure 2. The $\vec{M}$ vector emerged at angle α with respect to the z-axis and the transverse $\vec{M}_{xy}$.

After switching off the B_1 field at time τ, the $\vec{M}$ vector will emerge at angle $\alpha = \gamma B_1 \tau$ with respect to the z-axis. Then, the $\vec{M}$ vector begins to precess around the direction of B_0 field, which is now active [1]. Thus, the transverse $\vec{M}_{xy}$ will lose at time T_2 (transverse relaxation time or spin-spin relaxation time) (**Figure 3**).

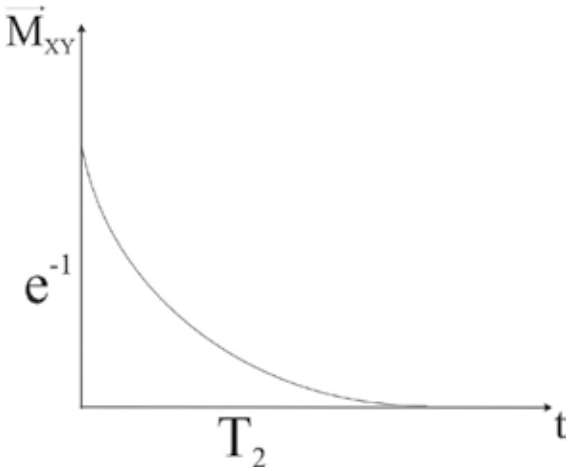

Figure 3. The loss of transverse $\vec{M}_{xy}$ vector at time T_2.

1.3.1. Spin-lattice relaxation process

The orientation of the $\vec{\mu}$ in magnetic field B_0 depends on the value of the interaction energy between $\vec{\mu}$ and B_0 field [3]:

$$E = -\vec{\mu} B_0 = -m\gamma B_0, \tag{6}$$

where m is the magnetic quantum number.

In the equilibrium, the nuclei at every energetic level are in accordance with the normal Boltzmann equilibrium law [3]:

$$\frac{N_1}{N_2} = \exp\frac{\Delta E}{RT} \approx 1 + \frac{\gamma\hbar B_0}{kT_L}, \tag{7}$$

where N_1 is the nucleus population on the energy state, which is less than ΔE energy in comparison to the N_2 population, T_L is the sample temperature, and $\hbar = h/2\pi$ where h is Planck constant.

The B_1 field induces the transition between quantum states, which gives rise to the NMR signal. The equalization of Boltzmann populations (extinction of NMR signal) in the quantum states, known as saturation phenomenon, is accompanied by an increase in the spin temperature T_S. At the same moment, the sample temperature T_L does not change. The condition in which $T_\mathrm{S} > T_\mathrm{L}$means that the equilibrium state has not been archived; however, after switching off the B_1 field, the T_S temperature will equalize with T_L (lattice) temperature. The spin existing in the excited quantum state cannot return to the ground state spontaneously. Thus, forced emission is one way that the spins lose energy [4]. This type of emission is possible only throughout spin-lattice interactions. The transitions between the spin states can be enforced only via the local magnetic field B_loc at the Larmor frequency. Fluctuations of B_loc field are generated by the thermal motion of the atoms and molecules from which a network is formed [1, 2]. Each magnetic moment that participates in random rotational or translational Brownian motion causes a fluctuation of the B_loc field, which causes a Fourier's frequency spectrum for those fields. For the spin ½ nuclei ^{1}H, ^{13}C, and ^{31}P, the dominant mechanism of relaxation is a dipole-dipole interaction, which is a result of the interaction between $\vec{\mu}$ and B_loc that is generated by neighboring magnetic moments. Thus, for the spin ½ nuclei, the dominant mechanism of relaxation is the interaction between the gradient of the electric field generated at the location of the observed nucleus by its electrical surroundings and nuclear electric quadrupole moment [4–6].

The simplest way to describe dipole-dipole interaction is by using the system of two spins. If the spin I $\left(\vec{\mu_I}\right)$ is near the second spin S $\left(\vec{\mu_S}\right)$, then the B_loc field created by the nucleus S at the position of nucleus I is equal to [1–3]

$$B_\mathrm{loc} = \pm\frac{\vec{\mu_S}}{\vec{R_\mathrm{IS}}}\left(3\cos^2\theta - 1\right), \tag{8}$$

where θ is the angle between the B_0 field and the $\vec{R_{IS}}$ vector, and $\vec{R_{IS}}$ vector is the distance between spin I and spin S (**Figure 4**).

If spins S and I are from the same molecule, then the $\vec{R_{IS}}$ is constant, and fluctuations in the B_loc will be associated with random changes in the angle. This mechanism of relaxation is known

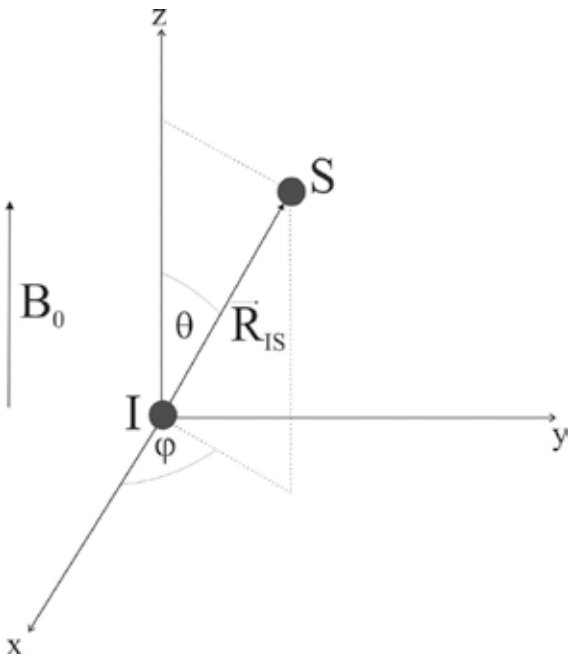

Figure 4. The system of two spins in magnetic field.

as rotational or intermolecular relaxation. If spin I and spin S are not from the same molecule, then the B_{loc} field fluctuations will depend on changes in both angle and the length of the $\vec{R_{IS}}$ [2]. This is called as translational or intramolecular mechanism of relaxation, which primarily relates to a liquid. In fact, in the spin I position, the B_{loc} field is produced by more than one spin S; however, if a system has more than two spins, the calculation of relaxation time rate is limited and the additivity of the effects is assumed. Then, the rate of the spin-lattice relaxation time T_1 can be expressed as the sum of the probabilities of the transitions between spin energy levels [6]:

$$\frac{1}{T_1} = \frac{\sum_{MM'} W_{MM'}(E_M - E_{M'})^2}{\sum_M E_M^2}, \tag{9}$$

where $W_{MM'}$ is the probability of the transition between energy level E_M and level $E_{M'}$.

In the case in which the two protons will be taken into consideration, for example, in an H_2O molecule, then the rate of T_1 can be summarized as follows [2]:

$$\frac{1}{T_1} = 2(W_1 + W_2), \tag{10}$$

where w_1 is the probability of a single spin-flip transition, and w_2 is the probability of a double spin-flip transition.

In a system of *AX* spins, for example, in a CH group, the cross-relaxation effect occurs. In such a case, it is necessary to use the proton-decoupling method to prevent the splitting of signals (multiplets) caused by the spin-spin couplings. Then, the rate of T_1 can be expressed by the formula [2]:

$$\frac{1}{T_1} = W_0 + 2W_1 + W_2, \tag{11}$$

where w_0, w_1, and w_2 represent the probabilities of the two-spin system (**Figure 5**).

After determining the transition probabilities and the perturbation Hamiltonian, it is possible to write the T_1 relaxation time for the homonuclear spins (*II*) and heteronuclear spins (*IS*) as follows [5]:

$$\frac{1}{T_1} = \frac{3}{10}\gamma_I^4\hbar^2 R_{II}^{-6}\left[\frac{\tau_c}{1+\omega_I^2\tau_c^2} + \frac{4\tau_c}{1+4\omega_I^2\tau_c^2}\right] \tag{12}$$

and

$$\frac{1}{T_1} = \frac{1}{10}\gamma_I^2\gamma_S^2\hbar^2 R_{IS}^{-6}\left[\frac{\tau_c}{1+(\omega_S-\omega_I)^2\tau_c^2} + \frac{3\tau_c}{1+\omega_I^2\tau_c^2} + \frac{6\tau_c}{1+(\omega_S+\omega_I)^2\tau_c^2}\right], \tag{13}$$

where τ_c is the correlation time.

The time T_1 is very sensitive to the length of $\vec{R_{IS}}$ between near spins, as directly proportional to its sixth power [7].

The high-temperature approximation is fulfilled, $\omega_0^2\tau_c^2 \ll 1$, for liquids, thus the rate of T_1 is independent of the frequency and Eqs. (12) and (13) are simplified to the following forms [2]:

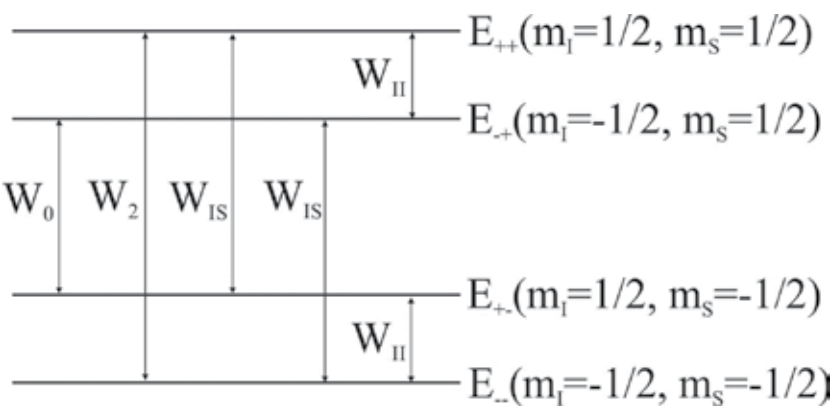

Figure 5. The unlimited transitions in two spin system.

$$\frac{1}{T_1} = \frac{3}{2}\frac{\gamma_I^4 \hbar^2}{\vec{R}_{II}^6}\tau_c \tag{14}$$

and

$$\frac{1}{T_1} = \frac{3}{2}\frac{\gamma_I^2 \gamma_S^2 \hbar^2}{\vec{R}_{II}^6}\tau_c. \tag{15}$$

As a result of the high-temperature approximation, the rate of T_1 increases as the temperature increases.

In general, the total rate of T_1 for protons is the sum of the rates of relaxation times caused by intermolecular and intramolecular factors [2]:

$$\frac{1}{T_1} = \left(\frac{1}{T_1}\right)_{\text{intra}} + \left(\frac{1}{T_1}\right)_{\text{inter}}, \tag{16}$$

where the rate of relaxation time, denoted as intramolecular $(1/T_1)_{\text{intra}}$, fulfills relation (14).

The calculation of the rate of relaxation time caused by the intermolecular factors was presented in reference [8]. The $(1/T_1)_{\text{inter}}$ is directly proportional to the population of spins N_1, and it is inversely proportional to the translational diffusion coefficient D:

$$\left(\frac{1}{T_1}\right)_{\text{inter}} = \frac{17}{30}\frac{\pi\gamma_I^4 \hbar N_1}{aD}, \tag{17}$$

where a is the closest possible distance between two spins belonging to two molecules (a is usually equal to the particle diameter).

Thus, D can be obtained directly while measuring viscosity based on the Stokes-Einstein relationship:

$$D = 6\pi\eta a. \tag{18}$$

The τ_c obtained by measuring the rates of T_1 for each chemical group in the molecule should have the same value when the molecule is subjected to isotropic rotation. In fact, various correlation time values can be observed, and this proves the existence of internal motions in the molecule [4–6].

1.3.2. The Lipari-Szabo model-free approach

In liquids, molecules are subject to rotational motion around the symmetry axis, and individual groups of molecules demonstrate internal movement. A correlation function for this complex motion of the $\vec{R}_{IS}$ vector was derived in reference [9]. The model assumed that the total

rate of the rotational movements is equal to the sum of the rates of the entire molecule (overall rotation—isotropic rotation) and internal rotations:

$$\frac{1}{\tau_i} = \frac{1}{\tau_{i_{\text{all}}}} + \frac{1}{\tau_{i_{\text{inter}}}}, \tag{19}$$

where $\tau_{i_{\text{all}}}$ is the time of isotropic rotation of the entire molecule, and $\tau_{i_{\text{inter}}}$ is the time of the internal isotropic rotation.

According to this model, the rate of T_1 is dependent on the complex motion coefficient C_1[9]:

$$C_1 = \left[1 - \frac{3}{4}\left(\sin^4\beta + \sin^2 2\beta\right)\right], \tag{20}$$

where β is the angle between the axis of rotation and the vector $\vec{R_{IS}}$.

The coefficient C_1 can take any value between 0 and 1 (0> C_1> 1). When $C_1 = 1$, there is no internal movement, when C_1 <1, the vector $\vec{R_{IS}}$ is subject to the movement [9].

1.3.3. Spin-spin relaxation process

The spin-spin relaxation process is associated with losing the phase coherence via the nuclear spin system, which leads to the loss of the $\vec{M_{xy}}$ vector. The effectiveness of the process depends on the rate of the molecular reorientations. In viscous liquids and solids, molecular reorientation is slow, it either takes a few microseconds or it does not occur at all [2]. The strength of magnetic field comes from the $\vec{\mu}$ moments, decreases as the distance between the spins increases. Thus, only the nearest nuclei have a significant contribution to the B_{loc}field. Therefore, from the position of the individual spins, the strength of B_0 field in which they exist differs in the range of B_{loc}, and it may increase by several Gauss. The consequence of this phenomenon is that the resonance frequency of the spins will also be different [1]. Spins can transfer absorbed energy to other spins that are located at a lower state of energy. The rate of T_2 time determines a spin's lifetime at a given energy state. This phenomenon is associated with the broadening of quantum states, which is explained via the Heisenberg uncertainty principle [3]:

$$\Delta\varepsilon t_e \geq \frac{\hbar}{2}. \tag{21}$$

The shorter is the spin's lifetime, the greater the broadening of the quantum states. Therefore, the transverse relaxation time is related to the width of the resonance signal [1, 3]. The dependency of the half-width of the resonance signal $_{1/2}$ and the relaxation time T_2 is

$$\Delta\nu_{\frac{1}{2}} = \frac{1}{2\pi T_2}. \tag{22}$$

The values of the T_2 relaxation times in liquids are similar to the values of the T_1 times and they are relatively long; however, T_2 cannot be greater than T_1[1].

1.4. Spin-spin couplings

The interaction between $\vec{\mu}$ moments, located in the magnetic field B_0, is known as spin-spin coupling J (scalar coupling). Each nucleus interacts with every other nucleus through their valence electrons, and the value of the coupling J depends on the gyromagnetic ratio and the distance between the coupling nuclei (number of bonds). The consequence of the interaction (attraction or repulsion of the moments $\vec{i}$) is the splitting of the quantum states (discrete spectrum). Thus, a given multiplet is found on the spectrum and the distance between the split signals is equal to J. In general, if the proton n is coupled with the other protons, then $(n + 1)$ signals are obtained in the multiplet [1]. Thus, the methyl protons (CH_3) coupled with the two protons of the CH_2 group cause the splitting of the resonance signal on $(2 + 1)$ peaks. In multiplet, the intensity of the signals can differ, and this can be determined using Pascal's triangle. These rules go into effect only if the differences between the chemical shift ranges and the value of spin coupling J are sufficiently large [3].

The spin-spin coupling J of spin Y and spin X can provide a relaxation mechanism for spin Y if spin X undergoes relaxation with time T_1. Spin Y is subjected to a fluctuating field due to the rapid spin X reorientation [1].

1.4.1. Amplifying the signals via polarization transfer

In NMR, the polarization transfer method, or the spin population transfer, is used to amplify the weak resonance signals, for example, in the ^{13}C spectra. The intensity of the signal is directly proportional to the difference between the N_1 and N_2 spin populations at energy levels. The N_1/N_2 ratio fulfils the normal Boltzmann equilibrium between the spin states. The greater the B_0 field, the greater the difference between the spin populations, and this depends on the ratio of the γ of the spins [10]. The nuclei ^{1}H and ^{31}P have large values, hence, the resonance signals are easier to observe than a signal from ^{13}C nuclei. The use of selective pulses of B_1 field might increase signal intensity of the spins in coupled systems. In the case of a system in which a sensitive nuclei A (proton) is coupled with an insensitive nuclei X (^{13}C) in ^{13}C spectra, signals with a coupling value of J(C, H) = 209 Hz (e.g., for $^{13}CHCl_3$) are obtained [10].

Amplifying the parameter signal p may be represented as follows [10]:

$$p = 1 + \frac{\gamma_A}{\gamma_X} \vee p = 1 - \frac{\gamma_A}{\gamma_X}. \tag{23}$$

1.4.2. Nuclear Overhauser effect (NOE)

The nuclear Overhauser effect is a double-coupled nuclei resonance, which results in a change in the signal intensity (typically an increase). Intramolecular and intermolecular factors have an impact on the value of signal amplification [11]. The theoretical maximum value of the signal amplification, in the case of coupling of ^{1}H and ^{13}C nuclei and dipole-dipole relaxation, is 2.989. In fact, the value can change from 1 (which means no gain) to a maximum theoretical value [10]. Because dipole-dipole relaxation is the major relaxation

pathway for protons and the carbons that are directly bonded with protons, the intensity of resonance signals corresponding to them will be more than the intensity from other nuclei. Thus, the spectrum will show signals with various intensities [3]. Therefore, the proton-decoupled resonance technique is used for ^{13}C nuclei. The application of the proton-decoupling method and the NOE effect makes it possible to amplify the signal by up to 200% [10].

The NOE effect can also be observed in the ^{1}H NMR spectroscopy, when two protons, H^{α} and H^{β}, are not directly bonded, but they are sufficiently close to each other. If the signal from H^{α} is gained, then the intensity of the signal corresponding to H^{β} will also increase about 45% [10]. Two mechanisms are responsible for the amplification of the signal, which causes the transfer of polarization:

- dipole-dipole interaction through space and
- chemical exchange (in the two spins system *AX*, the nucleus *A* is polarized and then the polarization is transferred from *A* to *X* with the exchange constant *k*).

1.5. Detection of NMR spectra and NMR spectra parameters

After the discovery of the phenomenon of NMR in solids, it was found that this phenomenon can also be observed by treating the sample with a sequence of short pulses of B_1 field at resonance frequency [12]. After that, the sample can induce alternating voltage with frequency ω_0 in the coil. An increase in the coil-alternating current is observed as a signal of free induction decay (FID).

The pulse duration is given by the following formula [1]:

$$t_i = \frac{\theta}{\gamma B_1}. \tag{24}$$

The selected pulse rotates $\vec{M}$ vector by a given angle θ. The most commonly used pulses are the ones that rotate the $\vec{M}$ vector about 90° ($\pi/2$) or 180° (π) (**Figure 6**). The duration time of the pulses ranges from 1 to 100 μs [3].

The shape of the FID signal is a fading oscillation curve as a function of time. This function is archived in the acquisition time of approximately 1 s. Then, using Fourier transformation, the periodic changes in time are converted to the frequency spectrum. The advantage of using this method is that it enables the fast recording of the spectrum as well as accumulation and averaging, which increases the signal-to-noise ratio [1].

1.5.1. Chemical shift

The chemical shift is the most common parameter analyzed in the ^{1}H NMR spectra. This is due to the fact that the distribution of electrons in the molecule is varied, so the different chemical groups of the same molecule have a different screening constant [1, 3]. Consequently, the same nuclei require a different B_0 field to achieve a resonance condition at a

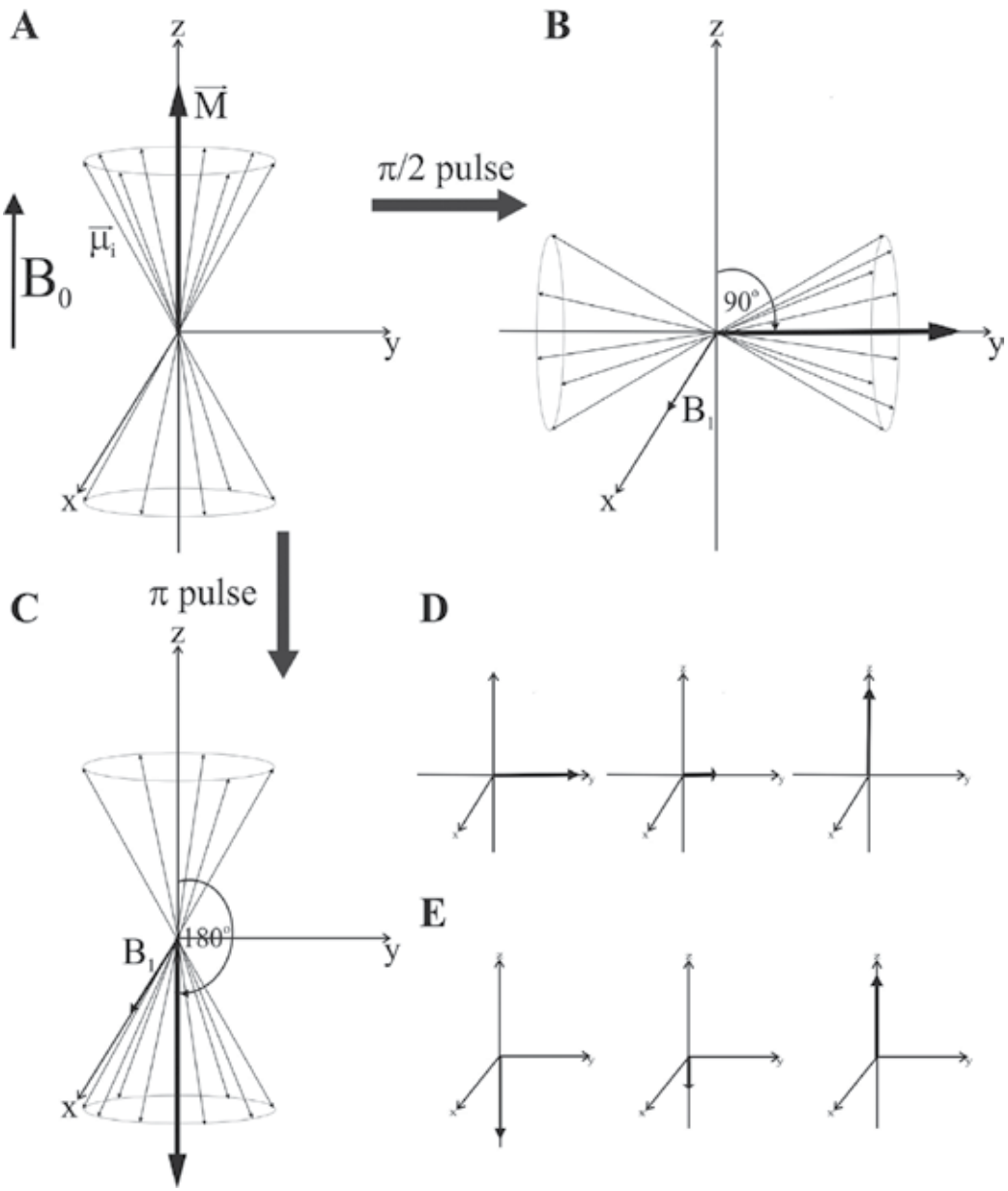

Figure 6. The B_1 field pulses rotate the $\vec{M}$ vector about (B) 90° ($\pi/2$) and (C) 180° (π); (A) the equilibrium state; the evaluation of the $\vec{M}$ vector and return to the equilibrium state in (D) the case (B) and (E) the case (C).

predetermined frequency ω_0.In this situation, the resonance condition must take the following form [1]:

$$B_{\text{ef}}(\text{ofsample}) = B_{\text{st}}(\text{ofstandard}) \tag{25}$$

Thus, the effective field acting on the nucleus must satisfy the following equation [1]:

$$B_{\mathrm{ef}} = B_0(1-\kappa), \tag{26}$$

where κ is the screening constant that is a measure of the density of the electron cloud around the nucleus.

Substituting formula (26) to (25), we get

$$B_0(1-\kappa) = B_{\mathrm{st}}(1-\kappa_{\mathrm{st}}). \tag{27}$$

Assuming, that $(1-\kappa) \approx 0$, because κ is the order of 10^{-6}–10^{-2}, so $\kappa \ll 1$, we then get

$$\frac{B_{\mathrm{st}} - B_0}{B_{\mathrm{st}}} \approx \kappa_{\mathrm{st}} - \kappa = \sigma, \tag{28}$$

where σ is the chemical shift.

However, in the given B_0 field the frequency changes ω_0, and then σ can be presented in the following form [3]:

$$\sigma = \frac{\nu - \nu_{\mathrm{st}}}{\nu_{\mathrm{st}}} \cdot 10^6 \left[\mathrm{ppm}\right]. \tag{29}$$

As the physical parameter used to analyze ^{1}H NMR spectra, σ is defined as the difference between the positions of the sample and standard signals [1]:

$$\sigma = (\nu - \nu_{\mathrm{st}}) \cdot 10^6 \left[\mathrm{ppm}\right]. \tag{30}$$

The measurement range for hydrogen nuclei is about 15 ppm, which is about 3–10% of the spectroscopic range of other magnetic nuclei.

1.5.2. Presence of paramagnetic ions as a factor affecting a value of σ

During the interaction between metals, such as Eu^{3+} or Pr^{3+}, and molecules containing oxygen or nitrogen atoms, metal ions increase their coordination number and form unstable associations [1]. This changes the chemical environment of the protons as well as the dipolar interactions between the unpaired electrons of the metal ions and the protons. This causes a change in the chemical shifts of hydrogen. The value of σ depends on the distance between the proton and the paramagnetic ion, and the value decreases as the distance increases [1].

Paramagnetic ions are used to distinguish the signals assigned to the choline groups of phospholipids. The most frequently used ions are those from the lanthanide group [13]. The concentration of paramagnetic ions added to the external environment of liposomes varies and is unique to each ion. If the concentration is too great, it could broaden all NMR spectra due to the dominant paramagnetic interactions [14].

1.5.3. Intensity of the signal

The intensity of the signals in the ^{1}H NMR spectra is a measure of adsorption, and it is proportional to the number of protons that induced the signal [1]:

$$I = \left(1 + \gamma^2 B_1^2 T_1 T_2\right)^{\frac{1}{2}}. \tag{31}$$

The above formula takes into consideration the relaxation times of different protons in the molecule, and the strength of B_1 field. The physicochemical analysis of the NMR spectrum assumed that the area under the obtained signal is proportional to the number of protons inducing the signals [3]. Therefore, based on the measured area under the signal, the relative number of the protons in the molecule can be determined. Sometimes, the determined relative number of the protons in the molecule is not equal to the number of the protons resulting from the molecular formula. This usually occurs when oxygen, nitrogen, or sulfur are present in a molecular structure; in such a case, the proton may be exchanged for deuterium from the deuterated solvent [3].

1.5.4. Chemical shift anisotropy (CSA)

The ^{31}P lineshape is directly related to the CSA tensor and to the orientation of lipid molecule (relative to the B_0 field) [15]. The value of CSA depends on the phosphate group motion and the temperature. The ^{31}P spectra exhibit a characteristic narrow peak ($\sigma_\perp$—high-field maximum; isotropic part) and a low-field shoulder ($\sigma_\parallel$—anisotropic part). The CSA can be calculated using the fallowing formula [16]:

$$\Delta\sigma = 3\left(\sigma_\parallel + \sigma_\perp\right), \tag{32}$$

where $\sigma_\parallel$ and $\sigma_\perp$ are the values of ^{31}P shielding of the lipid molecules, oriented parallel or perpendicular relative to the magnetic field.

The value of CSA for multilamellar vesicles (MLVs) is about 40–50 ppm, and depends from the size of liposome. For small unilamellar vesicles (SUVs), the CSA value may decrease to 10 ppm [15].

1.6. Two-dimensional (2D) NMR spectra

The two-dimensional NMR experiments are most often used to determine the third and fourth structure of macromolecules.

1.6.1. Two-dimensional correlation spectroscopy (COSY) and total correlation spectroscopy (TOCSY)

The 2D homonuclear (H,H)-COSY experiment showed that the spectra with ^{1}H chemical shifts along the axes were correlated with each other [10, 17]. The pulse sequence of the COSY experiment is shown in **Figure 7A**. In the COSY spectra, the diagonal and cross peaks are visible and they always differ by 90°.

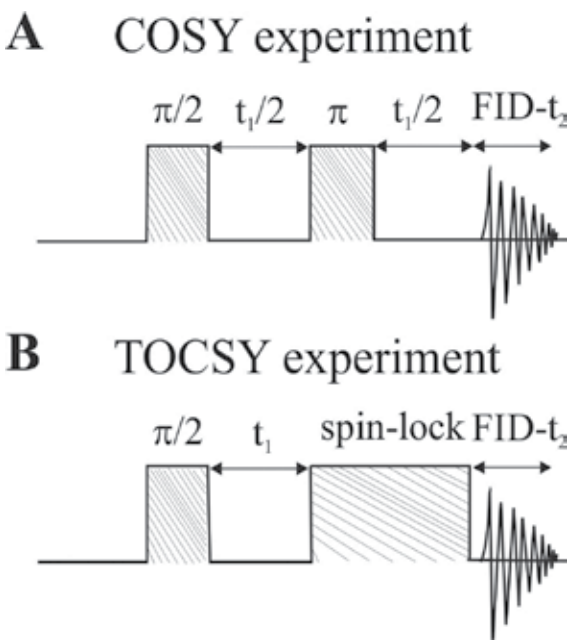

Figure 7. The pulse sequence of (A) the COSY experiment and (B) the TOCSY experiment; t_1 is a time between pulses; t_2 is an acquisition time; π and $\pi/2$ are pulses; spin-lock is a time of the spin states mixing.

When the system of two spins corrects the phase, the absorption signal appears as the cross peak, while the dispersion signal (incorrect phases) appears as the diagonal peak. The cross peaks in the horizontal and vertical directions are the absorption signals with positive and negative amplitudes [10]. When a proton is coupled with more than one proton, the diagonal peak is seen in the corner and it occupies more than one square. This simple rule of spectrum analysis makes the COSY technique an ideal tool for evaluating the ^{1}H spectra. The COSY spectra reveal information about the scalar coupling of protons within a few bonds [10, 17]. One disadvantage of the COSY method is that the cross peaks overlap with the diagonal signal when the chemical shift differences between the coupled nuclei are too small [10]. The 2D homonuclear (H,H)-TOCSY experiment is similar to the COSY experiment, but it exhibits the peaks from all scalar-coupled protons from the spin system [10, 17]. The pulse sequence of the TOCSY experiment is shown in **Figure 7B**. The method used to analyze the TOCSY spectra is similar to the method used to analyze the COSY spectra.

1.6.2. Rotating frame nuclear Overhauser enhancement spectroscopy (ROESY)

The nuclear Overhauser enhancement spectroscopy (NOESY) and ROESY techniques reveal information about the dipole-dipole-coupled protons and the transfer of polarization (the cross-polarization effect) [10, 17]. Usually, the ROESY experiment is used when the studied molecules are large. Then, the dipole-dipole relaxation is less effective because the rotation of the molecule is slow (long τ_c time), which extends the T_1 time [10]. Thus, the ROESY method is more convenient, because it ensures that the NOE effect will be positive [18, 19]. The pulse sequence of the ROESY experiment is shown in **Figure 8**.

Both processes, that is, dipole-dipole interaction through space and cross-polarization, influence the relaxation pathway. The mechanism of magnetization transfer is schematically shown in **Figure 9**.

Dipole-dipole interactions strongly depend on the distance between the coupled protons. Thus, the cross peaks differ in size. The ability to detect the interactions through space and to

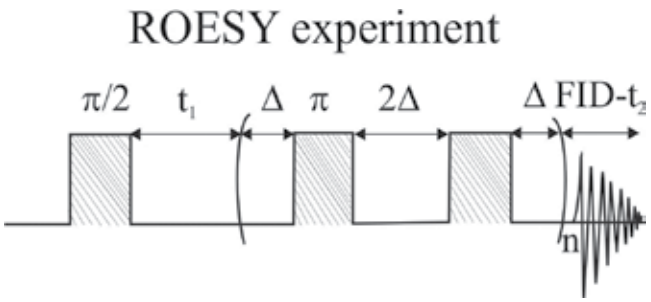

Figure 8. The pulse sequence of the ROESY experiment; t_1 is a time between pulses; t_2 is an acquisition time; π and $\pi/2$ are pulses; Δ is internal fixed time.

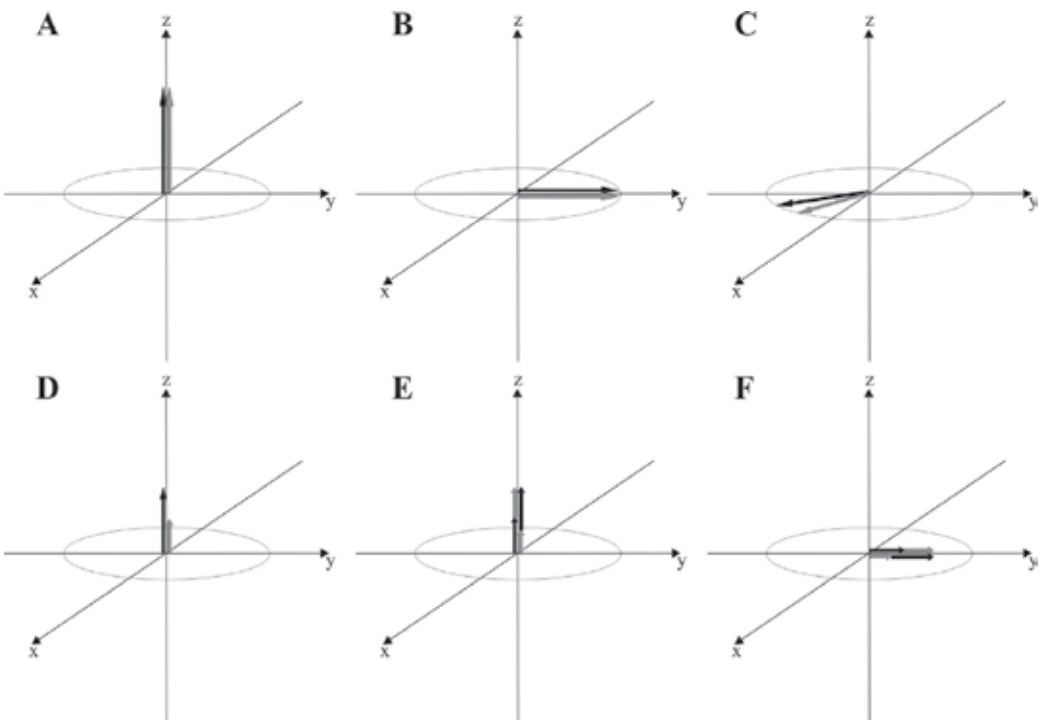

Figure 9. The evaluation of the magnetization vector M_A (black arrow) belonging to A protons and magnetization vector M_X (gray arrow) belonging to X protons. Spins A and X are close enough to interact through space. The diagrams from A to F show evaluation of the M_A and M_X vectors after two gradient pulses ($\pi/2$). The small contreating arrows superposed at the ends of the vectors represent the portion of the magnetization that is transferred from the nuclei of the other sort by cross-polarization during mixing time Δ.

http://dx.doi.org/10.5772/intechopen.68522

obtain general information about the distance between interacting protons provides valuable data about the stereochemistry of a molecule [10].

2. NMR studies of liposomes

The NMR spectra of liposomes differ from typical solution-NMR spectra. It is due to the specificity of lipid aggregates. The size of liposomes, hydration level, and the packing regime of lipid molecules in such structures have an influence on the NMR spectra.

2.1. Analysis of the ^{1}H NMR spectra

MLVs are not suitable for measurements using ^{1}H NMR method due to the large number of lipid bilayers and the large size of the liposomes. In this case, the signals in the ^{1}H NMR spectra are drastically broadened, and it is impossible to analyze any of the physical parameters of the spectrum. Even the signals on the spectrum of SUV/LUV are slightly broadened, and the broadening is not great enough to preclude spectrum analysis. This is due to the fact that liposomes are a kind of lipid aggregate, which distinguishes them from any substance which is soluble in water. From the physical point of view, this kind of sample is neither a homogeneous liquid nor a solid. The diffusion of water molecules and various ions through the lipid bilayer is the basic phenomenon that can be examined by the ^{1}H NMR spectra. The observation of this process is possible, thanks to the use of paramagnetic ions. It changes the chemical environment and the screening constant of each proton from the outer layer, which changes the σ values. Consequently, the choline group signal is split (δ) into two signals and it is assigned to the protons from the outer and inner layers of the liposome (**Figure 10**).

The type and concentration of used lanthanide ions is crucial, for example, if it is too great, the concentration of Eu^{3+} ions may exhibit as broadened ^{1}H spectra or they may even destroy the membrane structure. This effect is associated with the properties of the Eu^{3+} ions, which interact to the same extent with the hydrophilic and hydrophobic part of the liposome membrane. Moreover, the signal corresponded to water is broadened, which means that the Eu^{3+} ions also interact with the water molecules from the hydration shell of the liposome [14]. Thus, Pr^{3+} ions are most often used, which can split the choline signals within a few ppms without the effect of broadening the signals. The preferred concentration of Pr^{3+} ions ranges from 4 to 7 mM [20].

The split signals showed the different intensities. Since the area under a signal is directly proportional to the number of protons that induce the signal, a more intense signal is assigned to the protons from the outer layer and the lower intensity signal is assigned to the protons from the inner layer. This phenomenon is related to the asymmetric distribution of the lipid molecules in each layer. The splitting of the choline group signal creates new possibilities for research. The ratio of the area under the signal corresponds to the outer layer and the area under the signal corresponds to the inner layer (I_o/I_i); this provides information about the size of liposomes (**Figure 11**) [13, 20].

The splitting of the choline signal also offers the possibility to observe the ion transport through the membrane, since every change in the chemical environment of the protons from

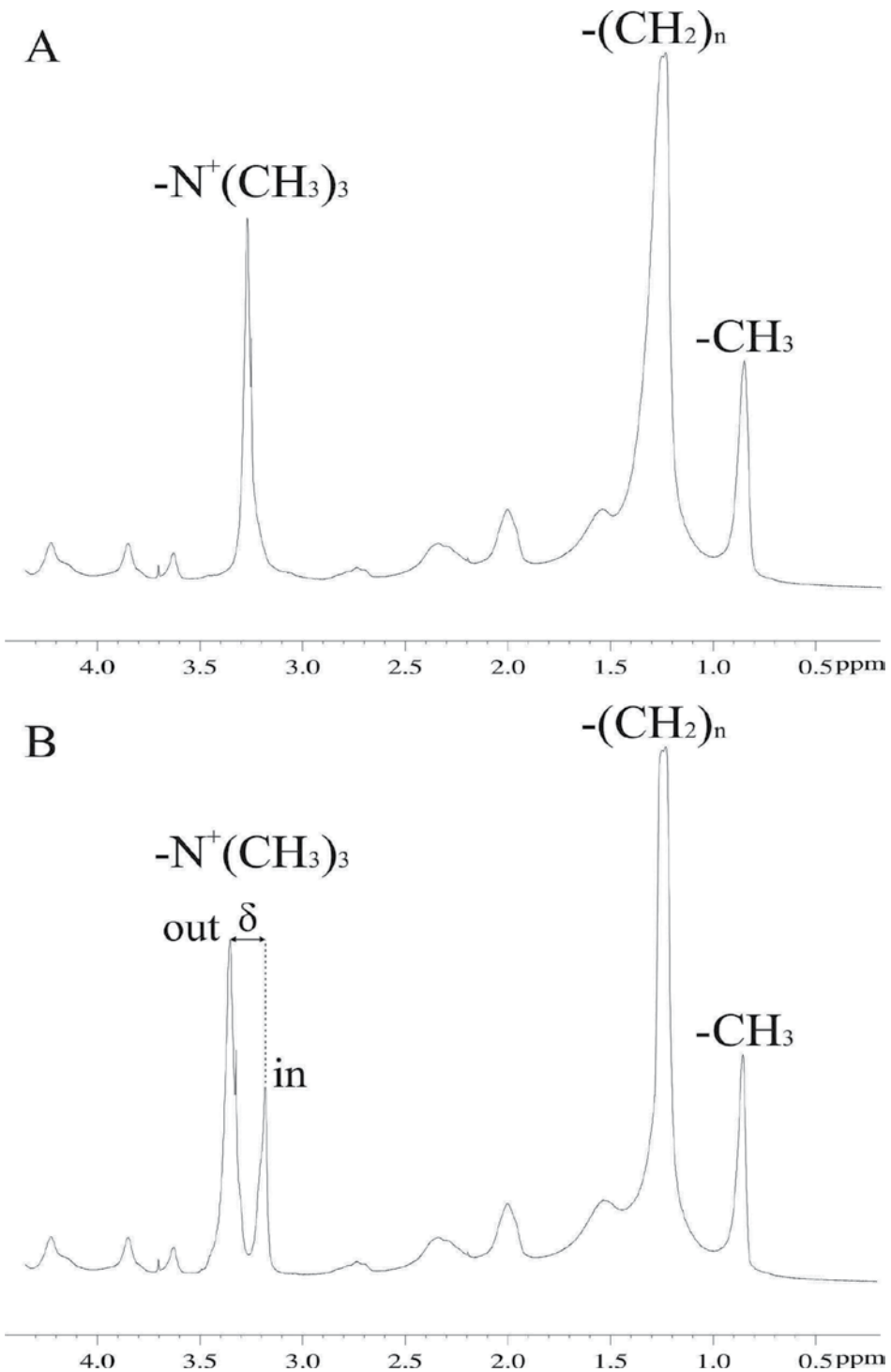

Figure 10. The characteristic ^{1}H spectra of egg-lecithin SUV (A) before and (B) after addition of 5 mM Pr^{3+}ions.

http://dx.doi.org/10.5772/intechopen.68522

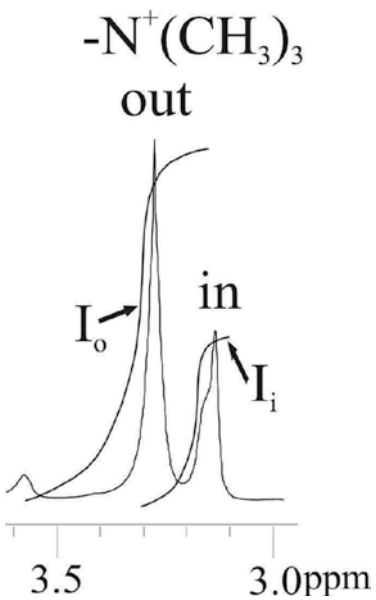

Figure 11. The measure of the area under the signals (integral of the signal) assigned to the protons from the choline groups.

the outer layer and the inner layer will be visible as a change in the σ of the signals. The value of the δ increases as the difference between the chemical environment of the protons from the inner and the outer layer increases [20, 21]. It is very important to maintain a constant temperature and pH for the sample during this kind of experiment because the binding of metal cations is dependent on both of these parameters [22]. The effect is clearly seen in the ^{1}H spectra of PE/PS/PC (phosphatidylethanolamine/phosphatidylserine/phosphatidylcholine) SUV (**Figure 12**).

The splitting of the choline groups is caused by 5 mM of the Pr^{3+} ions. Because the Pr^{3+} is associated only with the outer layer of a liposome, it is easy to observe the changes caused by the diffusion of Ca^{2+}ions in the distance between the splitting signals and the intensity. The value of δ decreased as the concentration of the Ca^{2+} ions increased inside the liposome [21]. The intensity of the signals assigned to the choline groups changed because the fusion process occurred in the SUVs. Ca^{2+} ions are a well-known fusogenic reagent. The fusion process of vesicles caused the increase in their size. Thus, the difference in the intensity of the signals assigned to the choline groups decreased. The fusion process also had an impact on the increase in the concentration of the Ca^{2+} ions in the liposome [21]. In a similar way, it is possible to conduct the experiment with compounds that are adsorbed on the surface of liposomes. Studying the area under each signal may also provide information about the processes that occur in the hydrophilic part of the lipid bilayer.

The half-width of the signal is another parameter that can be analyzed in the ^{1}H NMR spectra (**Figure 13**). The $\Delta\nu_{1/2}$ of the signal is closely related to the dynamics of the chemical groups. The slower the movement, the greater the $\Delta\nu_{1/2}$ of the signal.

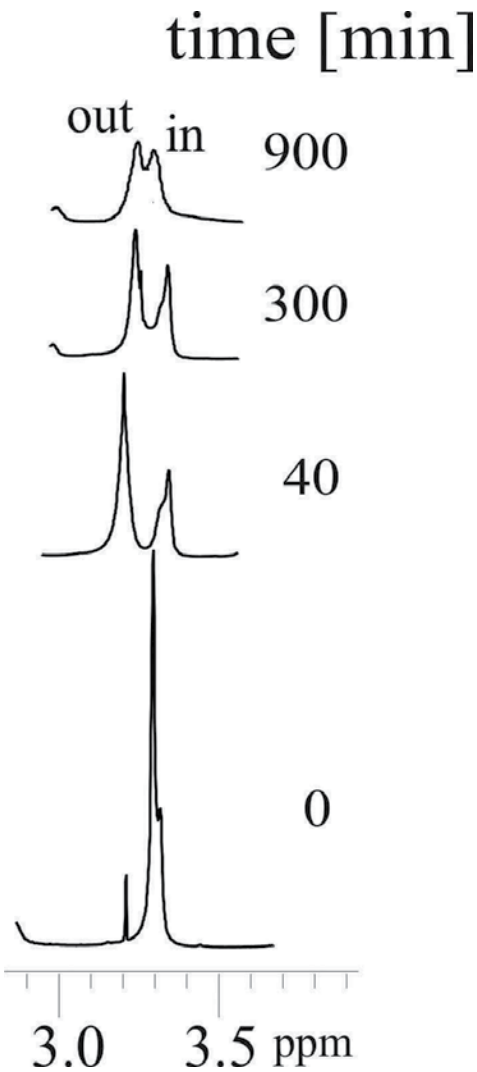

Figure 12. The time-dependent changes of ^{1}H resonance signals assigned to choline groups of PE/PS/PC SUVs after addition of 5.0 mM Pr^{3+} ions in the presence of Ca^{2+}/PS molar ratio of 2.0.

The processes that occur on the surface of the liposomes can cause the choline head to either become rigid or become more fluid, thereby slowing down/speeding up the rotational motion, which results in an increase/decrease in the $\Delta\nu_{1/2}$ of the signal. Additionally, cholesterol, antioxidants, and drugs contained in the liposomal membrane also may increase/decrease the fluidity of the membrane. For instance, the presence of azithromycin molecules increased the fluidity of 1,2-dipalmitoyl-*sn*-glycero-3-phosphocholine (DPPC) liposomes decrease of $\Delta\nu_{1/2}$ below the main phase transition temperature. However, amphotericin B rigidified the hydrophilic part (increase of $\Delta\nu_{1/2}$) of phospholipid bilayer, which increased the fluidity (decrease of $\Delta\nu_{1/2}$) of the hydrophobic core of PC membrane [16]. The opposite effect can be observed in the ^{1}H spectra of PC liposomes in the presence of polysialic acid

http://dx.doi.org/10.5772/intechopen.68522

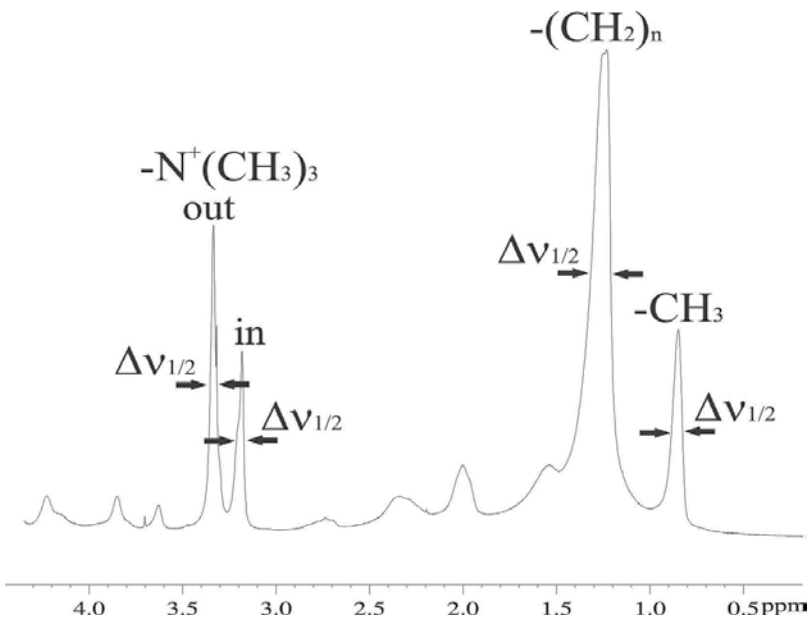

Figure 13. The $\Delta\nu_{1/2}$ of the signals from ^{1}H spectrum of egg-lecithin SUVs.

(**Figure 14**). The interaction of well-hydrated and anionic polysialic acid with the PC headgroups increased the fluidity of the hydrophilic part of the membrane and rigidified the hydrophobic core of the PC bilayer [23, 24].

The effect manifested as a decrease in the $\Delta\nu_{1/2}$ of the signal assigned to the choline groups from the outer layer of the liposome and as an increase in the $\Delta\nu_{1/2}$ of the signal assigned to the choline groups from the inner layer and to the $-(CH_2)_n$ and $-CH_3$ groups from the fatty acid chains. In fact, the observed effect is connected to the restricted motion of lipid molecules in the bilayer structure. The increase of the fluidity of the headgroups is connected to the increase of their rotational motion, their reorientation, and better hydration [17, 24]. The motion of the headgroups is restricted by the hydrophobic interactions, hydrogen bonding, and the intermolecular force between the lipid molecules. Thus, the presence of polysialic acid indicates that the strength of the PO_4^- and $N^+(CH_3)_3$ interactions is weakened. The increase of hydration (unrestricted motion) of headgroups and their reorientation causes the hydrocarbon chains to be more exposed to water molecules. Thus, the membrane polar-apolar interface is more hydrophobic [25].

Studies of liposomes using ^{1}H-NMR can also be conducted with various physical parameters, including temperature. The influence of temperature on the ^{1}H spectra manifests as an increase in the σ values of all the signals (**Figure 15**).

The resonance signals shift toward the direction of the lower magnetic field. This effect is typical for lipid bilayers [26]. The increase in temperature has an impact on the increase in the fluidity of the membrane. It manifests as a decrease of the $\Delta\nu_{1/2}$ of the signals. The ^{1}H NMR temperature-dependent studies may be used to analyze the properties of temperature-sensitive liposomes.

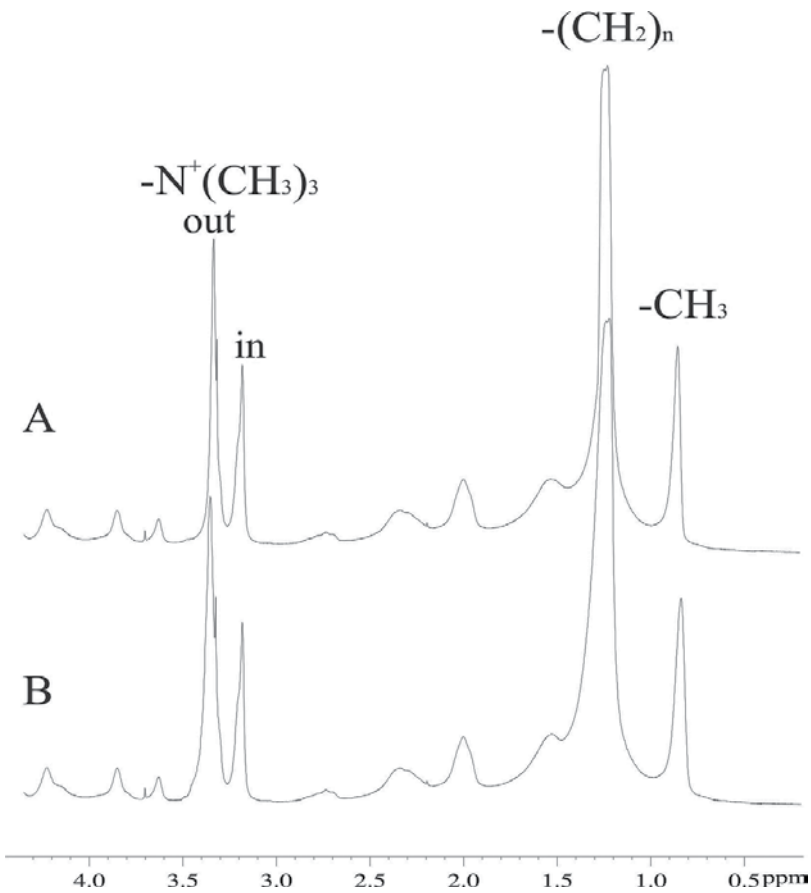

Figure 14. The effect of polysialic acid on changes of the PC SUVs membrane fluidity (the $\Delta\nu_{1/2}$ changes). (A) The ^{1}H NMR spectra of PC SUVs and (B) in the presence of polysialic acid.

The concept of using temperature-sensitive liposomes as drug carriers in local hyperthermia is based on the increase in their therapeutic effect, the ability to reduce drug toxicity for normal cells, and the increase in the permeability of the lipid bilayer at the proper temperature [26, 27]. The release rate of a drug depends on the temperature changes and the serum compounds (lipoproteins); thus, liposomes should be stable in serum and they should release drugs slowly under a proper temperature [28]. The ^{1}H spectra of PC and PC/octadecylamine liposomes (positively charged LUV) showed a narrowing of the resonance signals (decrease in the $\Delta\nu_{1/2}$) assigned to $-N+(CH_3)_3$, $-(CH_2)_n$, and $-CH_3$(**Figure 16**). The largest changes in the $\Delta\nu_{1/2}$ were observed for the signal corresponding to the fatty acid chains, $-(CH_2)_n$groups [26]. The effect was observed in temperatures ranging from 5 to 50°C.

Studies on changes of the splitting and intensity of signals assigned to choline groups revealed that the size of the liposomes increases [26]. In fact, the size of PC liposomes changed from 20–30 nm to 1 μm. Thus, as the temperature increases, the size of the PC liposome also increases. Additionally, when the temperature ranges from 30 to 40°C, the structure of the liposome

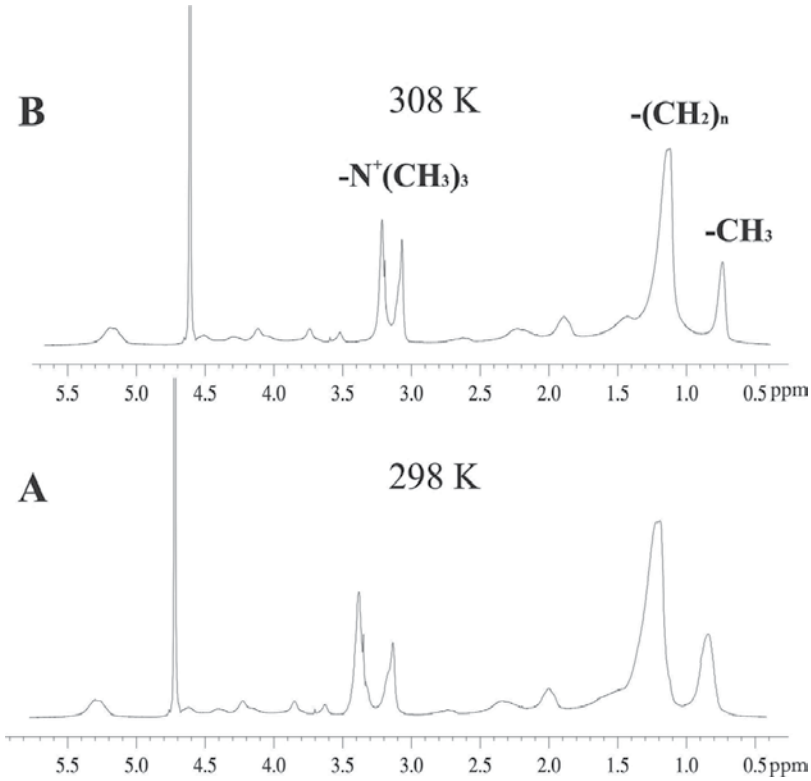

Figure 15. The influence of temperature on the ^{1}H resonance signals shifting. The ^{1}H NMR spectra of PC SUVs at (A) room temperature and (B) 308 K.

membrane is damaged; this makes the PC liposomes completely unstable and useless as thermosensitive drug carriers [26]. Quite the opposite effect was observed in the case of the PC/octadecylamine liposomes. The temperature had a smaller influence on the liposome size changes (from 20 to 60 nm), and the size was changed slowly. The PC/octadecylamine liposomes also seemed to be stable at temperatures ranging from 40 to 50°C [26]. At higher temperatures, the temperature-sensitive liposomes may aggregate or fuse, which makes it possible to transfer the drug to cells by fusion or via an endocytosis process in hyperthermia [26, 29].

2.2. Analysis of the ^{31}P NMR spectra

Liposomes can be composed of one or more kinds of phospholipids. Their molecular structure contains phosphorus atoms, which makes the ^{31}P NMR method extremely useful for studying them. Both MLVs and LUVs/SUVs can be studied using that method. In MLVs, the signal assigned to the phosphate groups is drastically broadened, and its shape is not like the Lorentzian function, unlike the SUVs/LUVs. The ^{31}P NMR spectra are mainly used to study the thermotropic properties of liposomes. The various phases change the structure of membrane, and there are specific transition temperatures for each lipid.

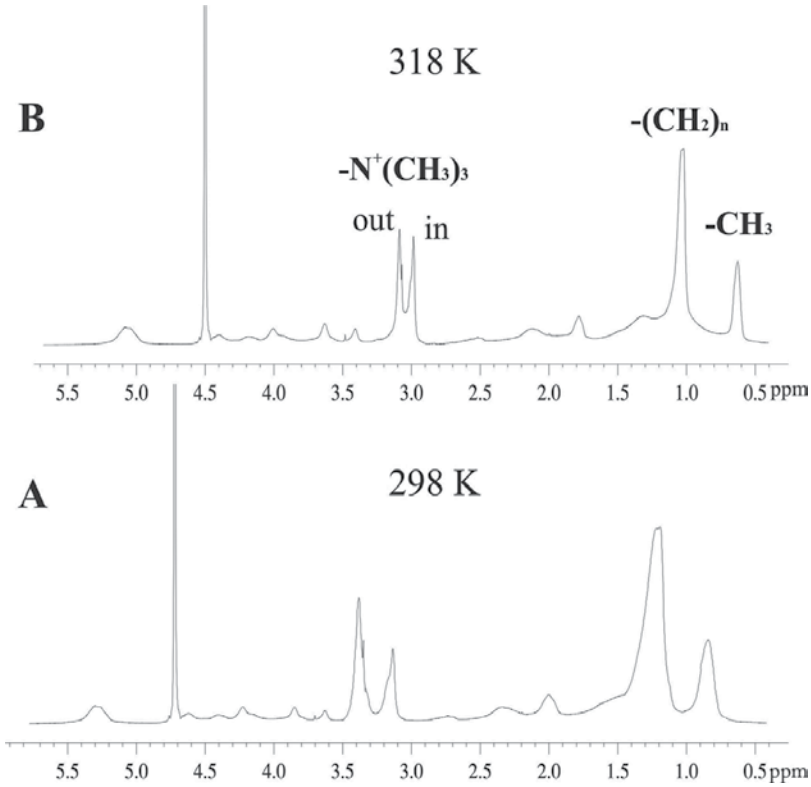

Figure 16. The ^{1}H NMR spectra of PC/octadecylamine liposomes at (A) room temperature and (B) 318 K.

The ^{31}P spectra of PC/Ch MLVs exhibited changes in the lineshape in the temperature range of 10–40°C. The characteristic ^{31}P lineshape of the L_α phase was observed before the phase transition. The monitoring of ^{31}P spectra at short temperature intervals led to observing the intermediate lineshapes between those characteristics for the L_α and H_{II} phases [21]. Substances that are either added to liposome membrane or are found in the liposomal environment can increase/decrease the phase transition temperature. For instance, this can be seen in the effect of the change of phase transition temperature caused by various drugs. The ^{31}P spectra of DPPC MLVs used in various concentrations of Piracetam showed that an additional narrow signal was assigned to the drug [30]. As the concentration of Piracetam increases, the intensity of the signal assigned to that drug also increases. The temperature studies showed that the main phase transition temperature of DPPC MLVs decreased in the presence of Piracetam. The results suggest that hydrophilic Piracetam molecules are associated with the hydrophilic part of the liposome membrane, which increases the fluidity of the membrane. Thus, the temperature of the main phase transition decreases [30].

The ^{31}P NMR method reveals information about the mobility of phosphate groups and about local order. Various substances impact the dynamics of the hydrophilic and hydrophobic part of the lipid bilayer. The number of narrow peaks in the ^{31}P spectra depends on the number of phospholipid types used to form the liposomes [31]. The effect is due to differences in the chemical surroundings of the phosphate groups in each type of phospholipid molecule. In the

^{31}P spectra, the splitting between the signals depends more on the averaged CSA motions than on an isotropic chemical shift [31]. It influences the value of chemical shift, and it may be difficult to assign the signals.

As previously mentioned, the effect of azithromycin on DPPC MLVs [16] was studied. Temperatures ranging between 35 and 45°C did not change the position of the narrow peak and CSA value, but the ^{31}P lineshape in the low-field shoulder was changed, and the presence of azithromycin in the external environment of the liposome decreased the CSA value. In fact, above 40°C, only a narrow peak stays in the spectrum because the CSA value is averaged to zero. The azithromycin caused an increase in the fluidity of the DPPC membrane below the temperature of the main phase transition [16].

When hydrophobic β-carotene is added to a lipid membrane, changes in DPPC membrane fluidity can also be observed. In temperatures above the main phase transition, β-carotene increases the fluidity of the DPPC MLV membrane, and in temperatures below the main phase transition, it decreases the fluidity of that membrane [32].

The opposite effect may be observed for PC MLVs in the presence of polysialic acid (**Figure 17**). In the temperature range of 10–30°C, the ^{31}P spectra show a narrowing of the isotropic part and broadening of the anisotropic part (increase in the CSA value) [23]. The increase of well-hydrated polysialic acid in the membrane increased the fluidity of the headgroups; this resulted in a decrease in the hydrophobic core fluidity.

The ^{31}P NMR spectra also are used to study the fusion process that occurs between liposomes. These types of experiments use fusogenic factors. The ^{31}P NMR is the best method for

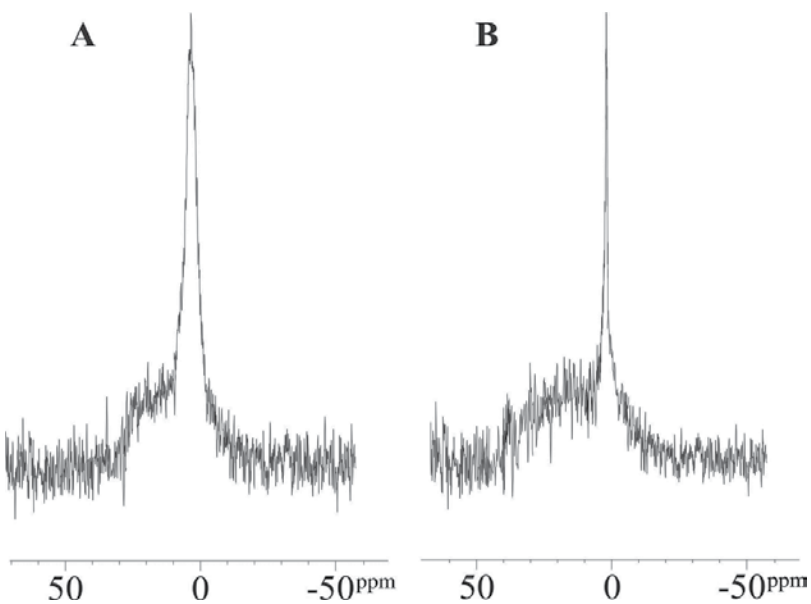

Figure 17. The effect of polysialic acid on ^{31}P NMR spectra of PC MLVs at room temperature. The ^{31}P spectra (A) before and (B) after addition of polysialic acid.

examining the fusion process because it has been proven that the fusion of two vesicles is accompanied by a transient structure, that is, the inverse hexagonal phase [29, 33].

The ^{31}P lineshape of PE/PS/PC MLVs showed changes with an increased molar ratio of Ca^{2+} ions (**Figure 18**). In fact, the Ca^{2+} ions are a well-known fusogenic factor. The characteristic lineshape for the H_{II} phase was obtained when the molar ratio of Ca^{2+}/PS was 2.0 [21]. It means that when the molar ratio of Ca^{2+}/PS is 2.0, the fusion process occurs.

The monitoring of changes in the ^{31}P spectra of PE/PS/PC SUVs after the addition of Ca^{2+} and Pr^{3+} ions showed that the signals were assigned to the choline groups from the inner and outer layers of the membrane. The obtained results revealed the decrease of δ-value and the intensity equalization of the signals corresponded to the choline groups [21]. The Pr^{3+} ions are only associated with the

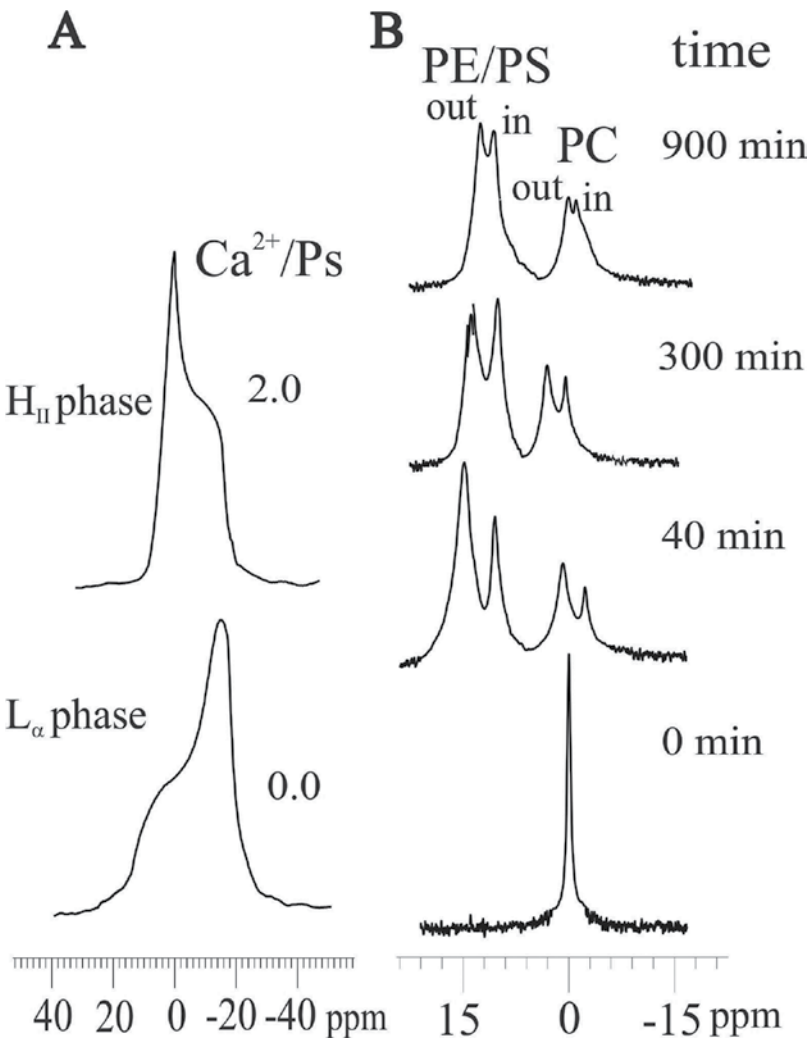

Figure 18. The 31P NMR spectra of PE/PS/PC liposomes; (A) the characteristic ^{31}P lineshape of MLVs in the L_α and H_{II} phase, (B) the time-dependent changes of LUVs after addition of 5.0 mM Pr^{3+} ions in the presence of Ca^{2+}/PS molar ratio of 2.0.

outer layer of a liposome, while the Ca^{2+} ions are not (they can diffuse through the membrane). Thus, the obtained results suggest that during the transient phase (inversed micelle) the fusion process, the lipid molecule transition from the outer to the inner layer and the size of the liposome, increases [21]. These results also confirmed the topological model of the fusion.

2.3. Two-dimensional NMR spectroscopy

2D NMR spectroscopy is the most convenient technique for studying scalar and dipole-dipole couplings. The results obtained using the method are used to study the structure and stereochemistry of molecules [10].

2.3.1. COSY and TOCSY spectra

In the COSY spectra of the PC/octadecylamine SUVs, the signals from the protons coupled within a few of the chemical bonds are visible. The diagonal peaks corresponded to each proton cross-correlated with every other proton from spin system [17, 26]. **Figure 19** depicts the method used to analyze the COSY spectra.

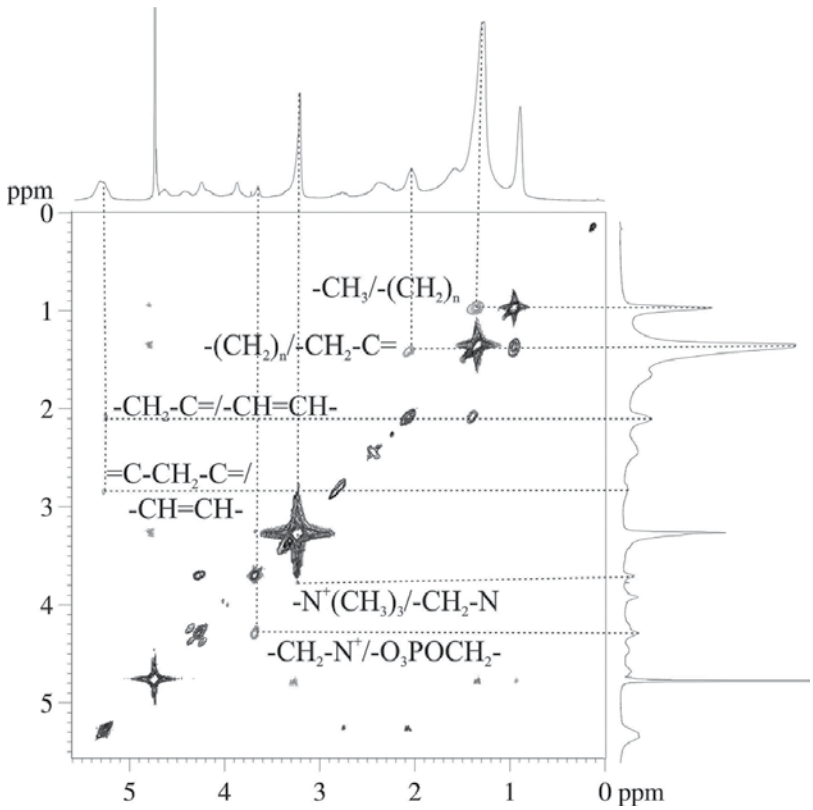

Figure 19. The COSY spectra of PC/octadecylamine SUVs. The cross peaks of scalar-coupled protons from the PC and octadecylamine molecules, and between protons from the PC/octadecylamine and water molecules (unsigned) are depicted in gray.

On comparing the TOCSY and COSY spectra of PC/octadecylamine SUVs, it is possible to determine the differences between them (**Figure 20**). In the TOCSY spectra, all the scalar-coupled protons in the PC molecule can be seen [17]. Both spectra also exhibit the cross peaks between the fatty acid chain groups from the hydrophobic core of the membrane and the water molecules. This is characteristic of well-hydrated membranes in the liquid crystalline phases [17, 26].

2.3.2. ROESY spectra

The ROESY spectra of the PC/octadecylamine SUVs reveal information about the protons coupled through space. Now, the diagonal peaks exhibit dipole-dipole interactions. The observed interactions may occur within one molecule or between neighboring PC molecules. The results also show the interactions between the hydrophilic part (headgroups) and the hydrophobic part (fatty acid chains) of the membrane (**Figure 21**) [17, 26]. The size of the cross-peak is directly proportional to the distance between the coupled protons. This dependency is clearly visible on the ROESY spectra of the PC/octadecylamine liposomes.

The 2D NMR technique is most often used to study the interactions between lipid molecules and substances added to the liposome membrane or to the external environment of liposome. To examine the nature of the interaction (either scalar coupling or through space), COSY/

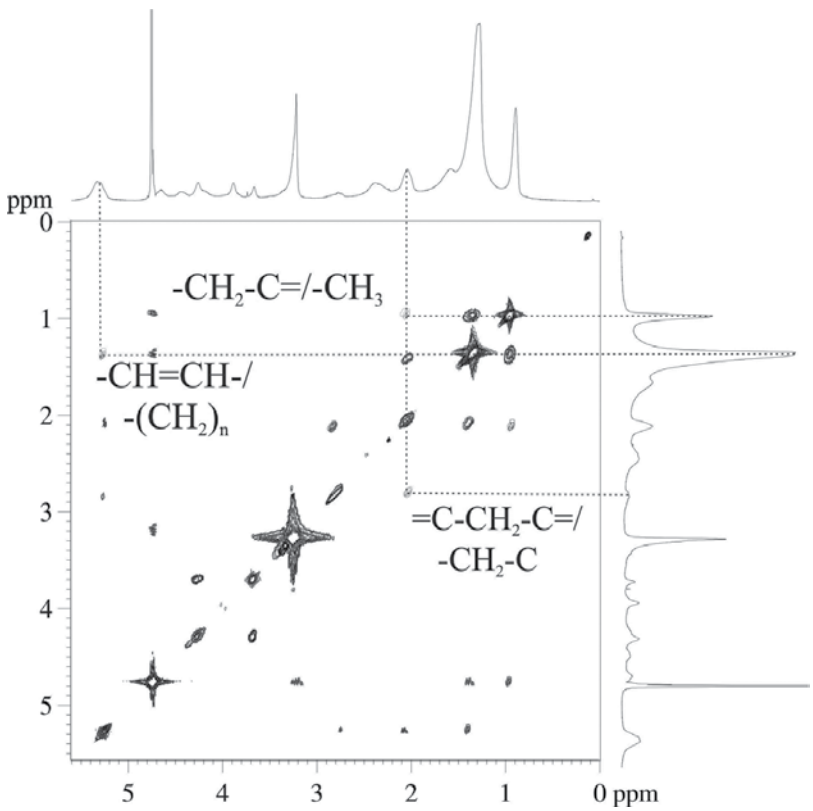

Figure 20. The TOCSY spectra of PC/octadecylamine SUVs. Only new cross peaks are depicted in gray.

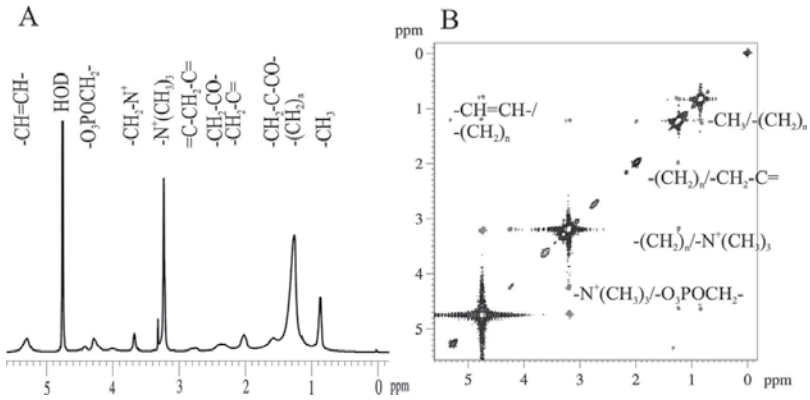

Figure 21. The ROESY spectra of PC/octadecylamine SUVs. (A) The full assigned ^{1}H spectra of the PC/octadecylamine liposomes; (B) The ROESY spectra of the PC/octadecylamine SUVs with assigned dipole-dipole interactions (in gray).

TOCSY or NOESY/ROESY experiments should be used, respectively. An example of this could be the ROESY spectra of PC/octadecylamine SUVs in the presence of sialic acid [17]. When comparing the ROESY spectra of sialic acid and PC/octadecylamine liposomes with PC/octadecylamine SUVs in the presence of sialic acid, it is easy to identify the new cross peaks due to interactions of the protons from the PC/octadecylamine and sialic acid molecules. While the interaction of sialic acid with the PC membrane has a considerable impact on membrane fluidity, the ROESY results only showed one cross peak between sialic acid and the PC molecules [17]. It is interesting to note that the dipole-dipole interaction occurs between the protons from the acyl group of sialic acid and the $(-CH_2)_n$ groups of the PC fatty chains. This result suggests that the other functional groups of sialic acid are well hydrated and, perhaps, the hydrophilic part of the membrane and sialic acid molecule interacts between their hydration shells. The obtained result also explains the strong influence that sialic acid has on decreasing the fluidity of the hydrophobic core of the membrane [17, 26].

Author details

Anna Timoszyk

Address all correspondence to: a.timoszyk@wnb.uz.zgora.pl

Department of Biotechnology, Faculty of Biological Sciences, University of Zielona Góra, Zielona Góra, Poland

References

[1] Hausser KH, Kalbitzer HR. NMR für Mediziner und Biologen. 1st ed. Heidelberg, Germany: Springer-Verlag Berlin Heidelberg; 1989. p. 246

[2] Latanowicz L. Dynamics of proton transfer in solution by NMR relaxation. Berichte der Bunsengeselleschaft für physikalische Chemie. 1987;**91**(3):237-242. DOI: 10.1002/bbpc.19870910314

[3] Lewitt MH. Spin Dynamics: Basics of Nuclear Magnetic Resonance. 2nd ed. New York, NY: Wiley; 2008. p. 740. ISBN 978-0-470-51117-6

[4] Abragam A. The Principles of Nuclear Magnetism. 5th ed. Oxford: Clarendon Press; 1983. p. 618. ISBN 9780198520146

[5] Bloembergen N, Purcell EM, Pound RV. Relaxation effect in molecular magnetic resonance absorption. Physical Review. 1948;**73**(7):679-692. DOI: 10.1103/PhysRev.73.679

[6] Kubo R. Note on stochastic theory of resonance absorption. Journal of Physical Society of Japan. 1954;**9**:935-944. DOI: 10.1143/JPSJ.9.935

[7] Gutowsky HS, Woessner DE. Nuclear magnetic spin-lattice relaxation in liquids. Physical Review. 1956;**104**:843-852. DOI: 10.1103/PhysRev.104.843

[8] Torrey NC. Nuclear spin relaxation by translational diffusion. Physical Review. 1953; **92**(4):962-973. DOI: 10.1103/PhysRev.92.962

[9] Lipari G, Szabo A. Model-free approach to the interpretation of molecular magnetic resonance relaxation in macromolecules.1. Theory and range of validity. Journal of American Chemical Society. 1982;**104**(17):4546-4559. DOI: 10.1021/ja00381a009

[10] Friebolin H. Basic One- and Two-Dimensional NMR Spectroscopy. 5th ed. New York, NY: Wiley; 2010. p. 442. ISBN 978-3-527-32782-9

[11] Overhauser AW. Polarization of nuclei metals. Physical Review. 1953;**92**(2):411-415. DOI: 10.1103/PhysRev.92.411

[12] Hahn EL. Spin echoes. Physical Review. 1950;**80**:580-594. DOI: 10.1103/PhysRev.80.580

[13] Gabrielska J, Gagoś M, Gubernator J, Gruszecki WI. Binding of antibiotic amphotericin B to lipid membranes: A ^{1}H NMR study. FEBS Letters. 2006;**580**:2677-2685. DOI: 10.1016/j.febslet.2006.04.021

[14] Schultze KD, Sprinz H. Electrochemical and NMR spectroscopic investigations of the influence of the probe molecule Eu(fod)$_3$ on permeability of lipid membranes to ions. Biochimica et Biophysica Acta. 2000;**1467**(1):27-38. DOI: 10.1016/S0005-2736(00)00193-0

[15] Leal C, Rögnvaldsson S, Fossheim S, Nilssen EA, Topgaard D. Dynamic and structural aspects of PEGylated liposomes monitored by NMR. Journal of Colloid and Interface Science. 2008;**325**:485-493. DOI: 10.1016/j.jcis.2008.05.051

[16] Fa N, Ronkart S, Schanck A, Deleu M, Gaigneaux A, Goormaghtigh E, Mingeot-Leclercq M-P. Effect of the antibiotic azithromycin on thermotropic behavior of DOPC or DPPC bilayers. Chemistry and Physics of Lipids. 2006;**144**:108-116. DOI:10.1016/j.chemphyslip.2006.08.002

[17] Timoszyk A, Latanowicz L. Interactions of sialic acid with phosphatidylcholine liposomes studied by 2D NMR spectroscopy. Acta Biochimica Polonica. 2013;**60**(4):539-546

[18] Sanders JKM, Hunter BK. Modern NMR Spectroscopy: A Guide for Chemists. 2nd ed. London: Oxford University Press; 1993. p. 328. ISBN 9780198555674

[19] Bax A, Grzesiek S. ROESY. In: Grant DM, Harris RK, editors. Encyclopedia of Nuclear Magnetic Resonance. 1st ed. West Sussex: Wiley; 1996. pp. 4157-4166

[20] Hunt GRA, Tipping LRH. A ^{1}H NMR study of the effects of metal ions, cholesterol and *n*-alkanes on phase transitions in the inner and outer monolayers of phospholipid vesicular membranes. Biochimica et Biophysica Acta. 1978;**507**(2):242-261. DOI: 10.1016/0005-2736(78)90420-0

[21] Osajca A, Timoszyk A. Application of ^{1}H and ^{31}P NMR of topological description of a model of biological membrane fusion. Acta Biochimica Polonica. 2012;**59**(2):219-224

[22] Amari L, Layden B, Rong Q, Geraldes FGC, de Freitas DM. Comparison of fluorescence, ^{31}P and ^{7}Li NMR spectroscopic methods for investigating Li^{+}/Mg^{2+} competition for molecules. Analytical Biochemistry. 1999;**272**:1-7

[23] Timoszyk A, Gdaniec Z, Latanowicz L. The effect of polysialic acid on molecular dynamics of model membranes studied by ^{31}P NMR spectroscopy. Solid State Nuclear Magnetic Resonance. 2004;**25**:142-145. DOI: 10.1016/j.ssnmr.2003.03.023

[24] Timoszyk A, Janas T. Effect of sialic acid polymers on dynamic properties of lecithin liposomes modified with the cationic octadecylamine. Molecular Physics Reports. 2003;**37**:67-70

[25] Walde P, Blöchliger E. Circular dichroic properties of phosphatidylcholine liposomes. Langmuir. 1997;**13**(6):1668-1671. DOI: 10.1021/la9610157

[26] Timoszyk A, Latanowicz L. Physical stability of temperature-sensitive liposomes. In: Bryjak M, Majewska-Nowak K, Kobsch-Korbutowicz M, editors. The impact of membrane technology to human life. 1st ed. Wrocław: Technical University of Wrocław Publishing; 2006. pp. 27-34. ISBN 83-7085-922-4

[27] Gaber MH, Hong K, Huang SK, Papahadjopoulos D. Thermosensitive sterically stabilized liposomes: Formulation and *in vitro* studies on mechanism of doxorubicin release by bovine serum and human plasma. Pharmaceutical Research. 1995;**12**(10):1407-1416. DOI: 10.1023/A:1016206631006

[28] Landon ChD, Park J-Y, Needham D, Dewhirst MW. Nanoscale drug delivery and hyperthermia: The material design and preclinical and clinical testing of low temperature-sensitive liposomes used in combination with mild hyperthermia in treatment of local cancer. Open Nanomedicine Journal. 2013;**3**:38-64. DOI: 10.2174/1875933501103010038

[29] Verkleij AJ, Bombers C, Gerritsen WJ, Leunissen-Bijvelt L, Cullis PR. Fusion of phospholipids vesicles in association with the appearance of lipidic particles as visualized by

freeze fracturing. Biochimica et Biophysica Acta. 1979;**555**:358–361. DOI: 10.1016/0005-2736(79)90175-5

[30] Lindberg G. Resialylation of sialic acid deficit vascular endothelium circulating cells and macromolecules may counteract the development of atherosclerosis: A hypothesis. Atherosclerosis. 2007;**192**(2):243-245. DOI:10.1016/j.atherosclerosis.2007.03.011

[31] Torchilin VP. Recent advances with liposomes as pharmaceutical carriers. Nature Reviews Drug Discovery. 2005;**4**:145-160. DOI: 10.1038/nrd1632

[32] Jeżowska I, Wolak A, Gruszecki WI, Strzałka K. Effect of β-carotene on structural and dynamic properties of model phosphatidylcholine membranes. II. A31P-NMR and 13C-NMR study. Biochimica et Biophysica Acta. 1994;**1194**:143-148. DOI: 10.1016/005-2736(94)90213-5

[33] Siegel DP. Inverted micellar intermediates and the transition between lamellar, cubic, and inverted hexagonal lipid phases. I. Mechanism of L_α H_{II} phase transitions. Biophysical Journal. 1986;**49**(6):1155-1170. DOI: 10.1016/S0006-3495(86)83744-4

Section 2

Liposomes for Drug Delivery

Chapter 5

Liposomes Used as a Vaccine Adjuvant-Delivery System

Ning Wang, Tingni Wu and Ting Wang

Additional information is available at the end of the chapter

http://dx.doi.org/10.5772/intechopen.68521

Abstract

Liposomes, a kind of bilayered vesicles formed by self-assembly of phospholipid molecules in an aqueous medium, are widely used as a vehicle for delivering various therapeutic agents due to their high biocompatibility, diverse and high-loading capacity, and relative ease for preparation and surface decoration to engender multifunctional features. Also, liposomes are a useful carrier for delivering vaccine antigens forming a versatile vaccine adjuvant-delivery system (VADS), which can efficiently fulfill both functions of adjuvancy and delivery when the liposomes are modified with specific functional molecules, such as lipoidal immunopotentiators, antigen-presenting cell (APC) targeting ligands, steric stabilization polymers and charged lipids. In this chapter, liposomes used as a VADS are introduced, including the preparation processes for liposomes, the evaluation methods toward different immunological responses, and also the measures for tracking *in vivo* of the vaccine-carrying liposomes, to provide reader with wide information as a reference related to the liposomal VADS.

Keywords: lipid vesicle, bilayer membrane, vaccine adjuvant-delivery system, vaccination, immune response, mucosal immunity, humoral immunity, cellular immunity, toll-like receptor, pathogen-associated molecular pattern

1. Introduction

Vaccination proves to be the most cost effective and best prophylactic strategy against many types of diseases, such as pathogenic infections, cancerous lesions, and even rheumatoid arthritis [1]. The vaccine concept was first introduced in the late eighteenth century by Edward Jenner, an English physician and scientist who was the pioneer in development of the world's first smallpox vaccine against the fatal virus [1, 2]. All living organisms are continuously exposed to substances including those called pathogens, which may invade, reside in, and eventually damage the organisms as their hosts. Fortunately, the invading pathogens can be prevented by the

organisms in several ways: with physical barriers, for example, or with chemicals that repel or kill invaders; moreover, in vertebrates (the animals with backbones), mammals and, especially, primates (including humans), the pathogens can be further controlled by a more advanced protective system called immune system, which is a complex network of organs containing different types of cells, such as T cells, B cells and antigen-presenting cells (APCs) [including mainly dendritic cells (DCs) and macrophages (MPs)] [2, 3]. Generally, the specific surface structures called antigens (Ags) on the pathogens are first recognized by APCs, which are specialized in uptake and processing the pathogens into fragments to present Ags bound to MHC molecules on APC surface as an epitope, which can interact with and stimulate T cells and B cells into cytotoxic T lymphocytes (CTLs) and plasma cells, respectively [4]. While the plasma cells can secret the Ag-specific antibodies in a substantial amount to neutralize the pathogens into harmless non-infectious organisms, CTLs release the cytotoxins, perforin, granzymes and granulysin, which work together to trigger a series of the caspase cascade and cause apoptosis (programmed cell death) of the pathogen-infected cells, erasing finally the cell-hidden pathogens. This process for pathogen defense will also imprint Ag features in immune system setting up so-called immune memory, which allows the pathogen-experienced survivors to rapidly initiate the immune response toward, and thus erase, the reencountered pathogens bearing the identical Ags [2]. Such ability of immune system obtained after experience to defend pathogens defines the concept of immunity, which underlies the fundamental mechanisms for the Ag-based vaccines to be developed and employed for prophylaxis of various pathogens, including the alien microbes such as viruses, bacteria, fungi, parasites, and even treatment of the neoplasma and cancerous lesions in the body [2].

The conventional vaccines are mainly used for prophylaxis of the infectious diseases and are usually made of live attenuated or inactivated pathogenic organisms, which, after administration, can effectively stimulate the body immune systems to set up robust immunity in recipients against the related microbes [5]. However, the vaccines based on the live attenuated pathogens possess, per se, the potential to cause detrimental infections due to the possible mutation occurrence in the engineered organisms and thus may lead to severe outcomes; while the vaccines made of inactivated microorganisms may stimulate the rather weak and even target-deviated immune response. To enhance the potency of the inactivated microorganism-based vaccines, the products are often added with alum, which were introduced as a vaccine adjuvant in the second decade of last century by Glenny and colleagues [6, 7]. Though alum, together with the undefined complex components, can enhance the efficacy of certain vaccines, it often causes adverse stimulus reactions and even, gives rise to serious side effects. To erase these drawbacks associated with the whole pathogen-based vaccines, researchers have recently developed the subunit vaccines, which contain only the essential antigens with the well-defined components and, thus, are anticipated to be a safe product without the potential risks confronted by the conventional vaccines [8]. Unfortunately, due to lack of other microbial components, which may not only protect the antigens but also be a pathogen-associated molecular pattern (PAMP) for mammalian immune systems, the subunit vaccines are usually unstable and often induce insufficient immune responses against pathogens [9, 10]. To overcome these weaknesses of subunit vaccines, numerous types of nanoparticles with composition mimicking the components of pathogenic organisms have been developed as a vaccine

carrier forming the so-called vaccine adjuvant-delivery systems (VADSs), which can protect antigens from the environmental damage, deliver ingredients to specific lymphocytes, and even enhance, as an adjuvant, the initiation of Ag-specific immune responses [8, 11–14].

Recently, among different types of vaccine carriers, such as emulsions, poly(lactic-co-glycolic acid) (PLGA) particles, silico nanocarriers and virus-like particles (VLPs), liposomes, the vesicles made up of lipid bilayers, were first described by Bangham et al. under an electron microscope in the early 1960s [15], and have ever since attracted much research interests in the development of novel drug delivery system (DDS) or VADS, due to their high biocompatibility, diverse and high loading capacity, and the ease for preparation and surface decoration to engender unique structures bearing the desired functions [16]. In fact, owing to their ability to entrap water- and lipid-soluble molecules in their aqueous and lipid phases, respectively, liposomes have been used since 1970 as a delivery system in therapeutics for a great variety of pharmacologically active agents, including antimicrobial and anticancer therapeutics, vaccines, metal detoxification chemicals, DNA/RNA fragments, enzymes and hormones [17]. As confirmed by researchers, agent delivery with liposomes can circumvent many of the problems associated with direct drug use, for instance, toxicity as a result of indiscriminate drug action, premature drug inactivation or excretion, and inability of drugs to reach the target intracellularly. For medical application, liposomes have proved able to be safely administered by various routes, including the intravenous, intramuscular, subcutaneous, intrathecal, intratracheal, oral, intranasal, and topical (skin and a variety of mucosal tissues) routes, having met with considerable success with several liposome-based products, including several vaccines, already licensed for clinical use in different countries [18].

Particularly, as a vaccine carrier, liposomes have the intrinsic adjuvant properties, which were established as early as 1974 by Gregoriadis and coworkers when strong humoral immune responses to liposome-entrapped diphtheria toxoid were observed after injection into mice, while, unlike other adjuvants, no granulomas at the site of injection were noticed [19–21]. Moreover, there were no hypersensitivity reactions in preimmunized animals when the antigen was entrapped in liposomes and given by intravenous or intra-foot pad injection [20]. In the ensuing years, extensive work in this laboratory and elsewhere has shown that liposomal adjuvanticity applies to a wide variety of bacterial, viral, protozoan, tumor, and other antigens [19, 22]. Now it is generally accepted that liposome can always function the role of adjuvanticity regardless of the type of association of the antigen with liposomes, such as being entrapped within the vesicles, attached onto their surface, and even simply mixed together [23, 24]. To be efficiently recognized and thus taken up by antigen-presenting cells (APCs), liposomes have been explored to be decorated with PAMP molecules and/or the molecules as ligands matching the receptors expressed on the surface of the aimed immunocytes, thus forming a multifunctional targeting VADS [11, 12, 25–27]. To date, various multifunctional liposomes have been developed as a novel VADS targeting APCs to enhance vaccine immunostimulating capacity by utilizing the specific binding affinities between functional molecules on the carrier and special features expressed or engendered by the immune cells. For example, recently, multifunctional liposomes have been successfully constructed being anchored with a toll-like receptor (TLR) ligands, including lipid A for TLR4, CpG-ODN for TLR9, and the synthetic molecules with a distal of mannose group for the C-type receptors on APCs,

such as dendritic cells (DCs), macrophages (MPs), and even been fabricated into microneedles for penetration of skin and mucosa to further enhance delivery efficiency [24]. These kinds of multifunctional liposomes as a VADS proved highly effective in both targeting delivery of vaccine to APCs and enhancing antigen presentation of APCs to T-cells fulfilling a dual function of delivery and adjuvancy for vaccines [11, 24, 25, 27, 28].

2. The components and structure of liposomes used for delivery of vaccines

Common liposomes are the vesicles made up of one or more concentric lipid bilayers alternating with aqueous spaces [17, 21]. The components of liposomes are mainly amphiphilic lipids and include phospholipids such as phosphatidylcholine (PC), phosphatidylserine (PS), phosphatidylglycerol (PG), sphingomyelin (SM), or other lipidic amphiphilies such as polysorbate 80 (SPAN80, nonionic surfactants), often supplemented with cholesterol (CHO) and other charged lipids such as stearylamine (SA), N[1-(2,3-dioleyloxy) propyl]-N,N,N-triethylammonium (DOTMA), 1,2-dioleyloxy-3-(trimethylamonium propane) (DOTAP), and 3 (N,N,-dimethylaminoethane)-carbamyl cholesterol (DMACHO). **Figure 1** shows the molecular structure of some representative lipids.

At ambient temperature, depending on the nature of the lipids, the liposome bilayers may be in a "fluid" or "rigid" state: the fluid state is manifested when liposomes are made with amphiphilic lipids that have a gel-liquid crystalline transition temperature (T_c)— the temperature at which the acyl chains melt—below ambient temperature, whereas the rigid state requires liposomes to be made of amphiphilic lipids with a T_c above ambient temperature [21]. Although liposomes as

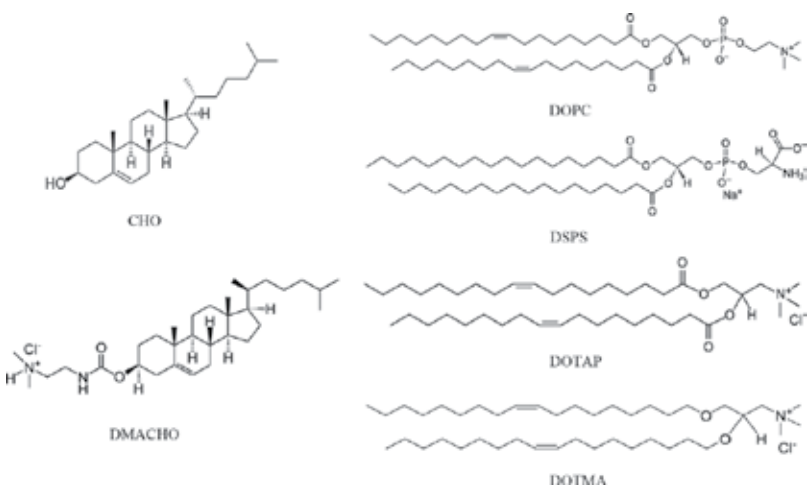

Figure 1. The molecular structure of typical lipids most often used for preparing liposomes. Abbreviations: DOPC, 1,2-dioleoyl-sn-glycero-3-phosphocholine; DSPS, 1,2-distearoyl-sn-glycero-3-phospho-L-serine; DOTAP, 1,2-dioleyloxy-3-(trimethylamonium propane); DOTMA, N[1-(2,3-dioleyloxy) propyl]-N,N,N-triethylammonium; CHO, cholesterol; DMACHO, 3(N,N,-dimethylaminoethane)-carbamyl cholesterol.

an agent carrier bear a common weakness of instability, the pegylation (modification with PEG) to produce a steric stabilization effect, charging with ionic lipids to engender an electrostatic repulsion, and/or lyophilization to form a dry entity renders the liposome-based VADS the stability completely satisfying the shelf-life requirements for a medicinal product [29].

To date, various types of liposomes have been developed for delivery of drugs or vaccines, including unilamellar vesicles, multilamellar vesicles (MLVs), multivesicular liposomes (MVLs) (**Figure 2**) and the liposomes with special structural features, such as cochleates [25, 30], bilosomes [31], niosomes [32], the inorganic nanoparticle-cored liposomes such as phospholipid bilayer-coated aluminum nanoparticles (PLANs) [28], and the interbilayer-crosslinked multilamellar vesicles (ICMVs) [33]. Unilamellar liposomes are a spherical chamber/vesicle, bounded by a single bilayer of an amphiphilic lipid or a mixture of such lipids, containing aqueous solution inside the chamber. Small unilamellar liposomes/vesicles (SUVs) have sizes up to 100 nm; large unilamellar liposomes/vesicles (LUVs) may have sizes more than 100 nm up to few micrometers (μm), and SUVs or LUVs are often used for specific site-targeting delivery of drugs or vaccines. Multilamellar liposomes (MLVs) consist of many Concentric amphiphilic lipid bilayers analogous to onion layers, and MLVs may be of variable sizes up to several micrometers, while multivesicular liposomes (MVLs) are characterized by their unique structure of multiple nonconcentric aqueous chambers surrounded by a network of lipid membranes. Both MLVs and MVLs, with multilayers and multi sub-spherules, respectively, can be employed for sustained delivery of small chemical drugs or other biological agents, e.g. the MVL-based techniques have been developed into a platform of so called DepoFoam for manufacturing the extended-release medicinal products, which may release drugs over a desired period of time from 1 to 30 days [34]. Notably, DepoFoam has already been used in the FDA-approved commercial products, including DepoCyte® (cytarabine liposome injection), DepoDur (morphine

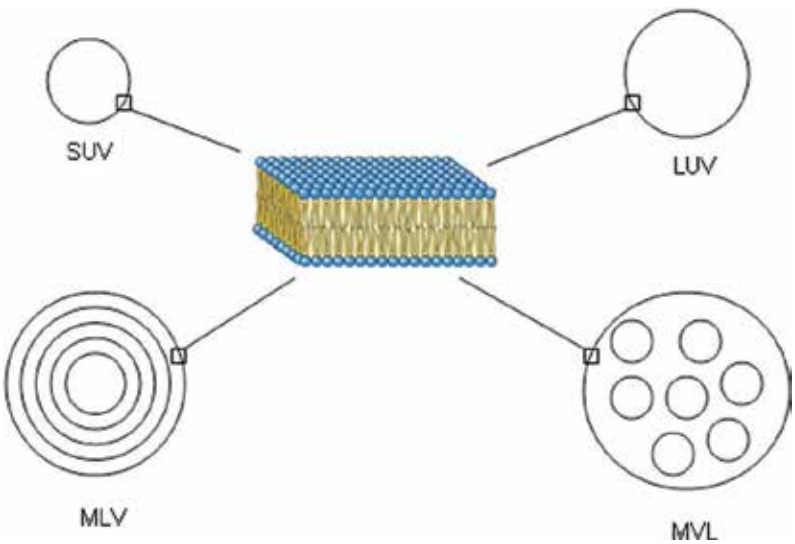

Figure 2. Schematic structure of different types of liposomes. Abbreviations: SUV, small unilamellar vesicles; LUV, large unilamellar vesicles; MLV, multilamellar vesicles; MVL, multivesicular liposomes.

sulfate extended-release liposome injection), and EXPAREL® (bupivacaine liposome injectable suspension) [18].

3. Preparation and characterization of Ag-loaded liposomes

Since first discovery of liposomes, researchers are always trying to set up different ways for preparation of the liposomes that meet the therapeutic demands [35]. Indeed, a variety of methods for production of the drug/vaccine delivery liposomes have been developed and are now so great that no one laboratory has hands-on experience with all of them [21]. Notably, different methods fit different liposomes for entrapping different agents, and, indeed, none of them should be regarded as a versatile procedure that can be employed once and for all to prepare any types of liposomes for entrapping drugs [36]. Moreover, certain agents such as the small compounds that are neutral and nonionizable can hardly be encapsulated in liposomes with a high efficiency by any one of the established processes. Summarily, liposomes used for vaccine delivery can be prepared with high encapsulation efficiency (EE) for Ags by exploiting two strategies: using unique procedures such as emulsification-evaporation or -lyophilization, and constituting special carriers such as charged vesicles. Herein, the method of thin film dispersion-extrusion and the method of emulsification-evaporation or -lyophilization are introduced because they can be safely used to encapsulate Ags without causing chemical/mechanical damage to labile biological agents [11, 36–39].

The method of thin film dispersion-extrusion is regarded as the simplest way to prepare the liposomes with a control size and can be used for entrapping almost all categories of agents if a high EE is not required [15, 36]. This method involves several steps including dissolving lipids organic solvents in a round-bottom flask, removing organic solvent by rotation and evaporation to make a thin lipid film lining the inside walls of flask, rehydration with an aqueous medium of the lipids for dispersion by agitation to engender heterogeneous liposomes, and extrusion several times of the coarse liposomes through a series of polycarbonate membranes with size-defined pores, just obtaining the homogeneous liposomes with a size similar to that of the final membrane pores.

3.1. Materials and equipment used for preparation and characterization of Ag-loaded liposomes

The main materials include sterile ultrapure water, chloroform, phosphate-buffered saline (PBS: 8 g NaCl, 0.2 g KCl, 1.44 g Na_2HPO_4, and 0.24 g KH_2PO_4 in 1000 mL distilled H_2O, pH of 7.4 adjusted with 0.1 M HCl), the PBS sterilized by autoclaving, soy phosphatidylcholine (SPC, molecular weight of 775.04, Avanti Polar Lipids, Inc., Alabaster, Alabama, USA), cholesterol (CHO, molecular weight of 386.65), OVA (ovalbumin) or other Ags, 10 mg/mL of SPC stock solution in chloroform, and 10 mg/mL of CHO stock solution in chloroform, and 2 mg/mL OVA (or other Ags) in PBS containing, or not, 50 mM sucrose, N_2 gas tank, liquid nitrogen, Triton-X100,: Sephadex G-50 (medium) gel (Pharmacia Company), Coomassie Brilliant blue G-250 (Sigma-Aldrich), Bradford reagent: Dissolve 50 mg of Coomassie Brilliant Blue G-250 in 50 mL ethanol, add 100 mL 85% (w/v) phosphoric acid (H_3PO_4). For charged or stealth

liposomes to be used for carrying Ags, 1,2-dioleyloxy-3-(trimethylammonium propane) (DOTAP, a cationic lipid), soy phosphatidylserine (SPS, an anionic lipid), and 1,2-distearoyl-sn-glycero-3-phosphoethanolamine-N-[methoxy(polyethylene glycol)$_{2000}$ (DSPE-PEG$_{2000}$) may be included.

The equipment and apparatus include 50-mL round-bottom flask, vortex mixer, 10-ml LIPEX® Extruders (Transferra Nanosciences Inc., Burnaby, B.C. Canada), membranes with the pore sizes of 400, 200, 100, and 50nm (Avestin, Ottawa, ON, Canada), a rotary evaporator, a probe or water bath sonicator with working frequency of 20 kHz, a vacuum desiccator, and a freeze-dryer, Malvern Zetasizer Nano ZS90 (Malvern instruments Ltd., Malvern, Worcestershire, UK), A FEI Tecnai G2 Spirit—transmission electron microscope (FEI Company, Hillsboro, Oregon, USA) and Vitrobot™ Cryo-TEM sample preparation instrument, a Micro CS150NX Ultracentrifuge (Hitachi, Japan) or other equivalent, 8453 UV-Vis spectrophotometer (Agilent Technologies, Inc., Santa Clara, California, USA) or other equivalent.

3.2. Preparation of Ag-loaded liposomes by thin film dispersion-extrusion method

1. To prepare 2 mL SPC/CHO liposomes (1:1, molar ratio) with lipid concentration of 10 mg/mL, 1330 μL of 10 mg/mL SPC stock solution and 670 μL of 10 mg/mL cholesterol stock solution are mixed in a 50-mL round-bottom flask in a chemical hood, and then organic solvent is removed on a rotary evaporator linked to a recycling water vacuum pump with flask dipped in a water bath at 35–40°C under reduced pressure. (For charged liposomes used for vaccine delivery, the lipid components can be replaced with SPC/CHO/DOTAP (4.5:4.5:1, molar ratio), or SPC/CHO/SPS (4.5:4.5:1, molar ratio); for stealth liposomes, the lipid components may be SPC/CHO/DSPE-PEG$_{2000}$ (9.5:9.5:1, molar ratio), or other combinations depending on the carriers to be used.)
2. The opening of the lipid film-adhering flask is covered with a piece of stretched parafilm to prevent the entry of dusts or contaminants and poke few small holes in the parafilm by a needle, and then the lipid film-adhering flask is put in a vacuum desiccator overnight to remove organic solvent residue.
3. Then 2 mL of PBS containing 2 mg/mL OVA (model Ag) is added to the dry lipid film-containing flask, which is vortexed repeatedly for 10 s on maximum speed until the lipid materials are all suspended in the solution.
4. The sample is sonicated for 5 min at the power of <100 W to disperse all visible precipitates and obtain milky crude liposome sample of mostly MLVs.
5. Repeatedly, the liposome sample is extruded with high pressure N_2 gas to pass through the 400 nm-pore polycarbonate membranes 11 times using the Extruder, which is then re-equipped with polycarbonate membranes of the pore size, in sequence, of 200, 100, and 50 nm, each followed by the due 11-cycle extrusion, and, consequently, resulting in the liposomes with a size of about 420, 220, 120, and 60 nm after each of the 11-cycle extrusion through the corresponding membranes.
6. The liposome preparation is stored in a vial filled with N_2 gas at 4°C in the dark.

3.3. Preparation of Ag-loaded liposomes by emulsification-evaporation/lyophilization method

1. To prepare 2 mL of SPC/CHO liposomes (1:1, molar ratio) with lipid concentration of 10 mg/mL, 1330 μL of 10 mg/mL SPC stock solution and 670 μL of 10 mg/mL cholesterol stock solution are mixed in a 20-mL ample, which contains 4 mL cyclohexane resulting in 6 mL of lipids dissolved in cyclohexane/chloroform (3:1, v/v) to be used as oil phase (O).
2. And 6 mL of O is mixed with 2 mL of 2 mg/mL OVA PBS with (for emulsification-lyophilization method) or without (for emulsification-evaporation method) 50 mM sucrose as water phase (W), and then using an ice/water bath to control the temperature under 30°C, the mixture is emulsified with a sonicator with work frequency of 20 kHz at the power of 50 W to make a W/O type emulsion.
3. By emulsification-evaporation method, the W/O emulsion is evaporated at 35–40°C under a slightly reduced pressure to remove slowly all the organic solvents, and then sample is supplemented with appropriate amount of PBS to obtain finally 2 mL of liposome preparations; otherwise, by emulsification-lyophilization method, the following steps should be completed.
4. The obtained 8 mL of W/O emulsions are mixed with 12 mL of PBS containing 50 mM sucrose and mildly emulsified using homomixer at 5000 rpm for 1 min to form a W1/O/W2 double emulsion, which is quickly subdivided and filled into 5-mL freeze-drying vials with a fill volume of 1 mL per vial.
5. The emulsion-containing vials are immediately put into an ultra-low temperature refrigerator and frozen at −85°C for 4 h, and then transferred into a freeze-dryer and lyophilized with a program as follows: primary drying at −45 and −20°C for 2 h periods, respectively; and secondary drying at 20°C for 4 h.
6. After lyophilization, the vials are immediately filled with nitrogen gas, sealed, and stored at 4°C in the dark.
7. For use, an appropriate amount (0.1–1 mL) of water is added into the dry powder-containing vial, resulting in the Ag-loaded liposomes with lipid concentration of 10–1 mg/mL.

3.4. Characterization of the Ag-loaded liposomes

3.4.1. Test of size and zeta potential

The Ag-loaded liposomes may be characterized in size (mean diameter), zeta potential (ζ), morphology, and structure.

The size (mean diameter) and surface charge (zeta potential, ζ) of the multifunctional liposomes with or without antigen are tested using a Malvern Zetasizer ZS90 (Malvern, Worcestershire, UK) referring to the user manual.

Test of liposome size by DLS (dynamic light scattering) is usually performed using samples with lipid concentration of 1 mg/mL. Thus, 0.2 mL of the prepared liposomes is diluted with 1.8 mL of PBS (with or without sucrose) in a polyacrylate or quartz cuvette and placed in

Zetasizer ZS90, and the particle size is determined by photon correlation spectroscopy (PCS) at 25°C at an angel of 90°, to give the intensity, number or volume mode, which can be used to evaluate the particle size distribution profile which is automatically summarized as parameter of polydispersity index (PDI), while the size is often presented with the average one plus PDI.

For ζ test by electrophoretic light scattering (ELS), 0.7–1 mL of the diluted sample is pipetted into the polyacrylate or quartz cuvette, which is then carefully inserted with the "Dip" cell bearing electrode pair, placed in Zetasizer ZS90 and determined by PCS at 25°C at an angel of 90°.

3.4.2. Cryo-TEM of multifunctional liposomes

The electron microscope is a type of microscope that uses a beam of electrons to create an image of the specimen and has up-to-date the greatest resolving power, allowing it to see nano-sized objects in fine detail [40]. It is large, expensive pieces of equipment, generally standing alone in a small, specially designed room and requiring trained personnel for operation. Recently, the cryo-transmission electron microscopy (cryo-TEM) has gained great development and allows the observation of specimens that have not been stained or fixed in any way, just showing them in their native environment at, notably, even near-atomic resolution [40]. Since early 1990s, the cryo-TEM has been more and more employed by researchers to observe the morphology and structure of the agent-loaded liposomes. Since the liposome surface is always hydrophilic, the hydrophobic carbon grid that used to carry liposomes should be first converted to hydrophilic nature by glow discharge. For cryo-TEM, the sample-holding grid is usually freezed in liquid nitrogen at −196°C for 10 min and transferred to a cryo-holder, which is maintained at ultralow temperature using a liquid nitrogen storage box, and then inserted in the microscope for imaging in the ultralow temperature [39].

The following protocol may apply to observation of the Ag-loaded liposomes by cryo-TEM [39].

1. Using a pipette, 3 μL of the sample is applied to an EM grid that has been converted to hydrophilic nature by glow discharge.
2. After being blotted with filter paper to remove excess sample, the grid is plunged into liquid nitrogen at −196°C for 10 min, and then transferred to a cryo-holder, which can be maintained at ultralow temperature using a liquid nitrogen storage box.
3. Then the cryo-holder is inserted into the EM column that is maintained at liquid nitrogen temperature (77 K), and the liposome sample is imaged at the ultralow temperature.

3.4.3. Determination of EE of the Ag-loaded liposomes

The EE of the Ag-loaded liposomes may be estimated by the following Eq. (1).

$$EE\ (\%) = \frac{\text{Total Ag} - \text{Free Ag}}{\text{Total Ag}} \times 100\% \quad (1)$$

Free Ag may be separated from Ag-associated liposomes by ultracentrifugation and quantitatively determined with the classical Bradford protein assay method [41]. For free Ag separation, the liposome sample is centrifuged at 100,000 × *g* in an ultracentrifuge for 1 h, and then after collection of the free Ag-containing supernatant, the liposomal pellet is suspended with PBS for

washing and centrifuged again. The supernatants are mixed together to adjust protein concentration at a range of 0.1–25 μg/mL, and Ag quantification may be carried out by the following procedure.

1. Five standard solutions (1 mL each) containing 0, 0.1, 0.4, 1.6, 6.4, and 25.6 μg/mL BSA are prepared.
2. And 800 μL of each standard and sample solution (containing for < 25 μg/mL protein) is pipetted into a clean, dry test tube. Protein solutions are normally assayed in duplicate or triplicate.
3. Then 200 μL of Bradford dye reagent concentrate is added to each tube followed by vortex for mixing.
4. The tubes are incubated at room temperature for at least 5 min. Absorbance will increase and changed nonlineally over time, and samples should be incubated at room temperature for not more than 1 h.
5. The standard and sample solutions are transferred into cuvette and measured immediately of the absorbance at 595 nm.
6. The standard curve is obtained and used to quantify free Ags.

3.4.4. Assay of Ag integrity in liposomes using SDS-PAGE

During incorporation in liposomes, the Ag may be damaged due to its possible confrontation of the organic solvents and intense mechanic sonication and therefore should be scrutinized of the integrity. Usually, sodium dodecyl sulfate-polyacrylamide gel electrophoresis (SDS-PAGE) is used to test the integrity of the Ags entrapped in liposomes that are freshly prepared or have been stored in certain conditions for some time for evaluating the stability of the products [42]. The protocol of SDS-PAGE test of the Ags loaded in vaccine carriers has been described in detail in an open access book chapter and is suggested as a reference for investigators [39].

4. *In vitro* and *in vivo* evaluation of the Ag-loaded liposomes

4.1. Materials and equipment used for evaluation of the Ag-loaded liposomes

For assay of the immunity elicited *in vitro* and *in vivo* by vaccination with Ag-loaded liposomes, the following materials should be at hand: HyClone Roswell Park Memorial Institute (RPMI) 1640 medium and fetal calf serum (FCS) by Thermo Fisher Scientific (Waltham, MA, USA), MTT (3-(4,5-dimethylthiazol-2-yl)-2,5-diphenyltetrazolium bromide)) and TMB (3,3,5-tetramethylbenzidine) by Sigma-Aldrich (St. Louis, MO, USA); LysoTracker-red and (4′,6-diamidino-2-phenylindole) DAPI (Thermo Fisher Scientific Inc., Waltham, MA, USA) for label cellular organelles of lysosome and nucleus, respectively; and the biological agents for

assay of immunoglobulins and cytokines, such as IFN-γ and IL-4 assay kits; goat anti-mouse IgG-horse radish peroxidase (HRP), IgG1-HRP, IgG2a-HRP (or IgG2c, if C57BL/6 mice are used) and IgA-HRP with sales package of 200 μg per 0.5 mL, PE-conjugated anti-mouse $CD8^+$ mAb (monoclonal antibody) and FITC-conjugated anti-mouse $CD4^+$ mAb and other fluorescently labeled immunological agents for assay by eBioscience (San Diego, USA), BioLedend (San Diego, USA), or Santa Cruz Biotechnology, Inc. (Dallas, Texas, USA).

For assay of the immunity elicited *in vitro* and *in vivo* by vaccination with Ag-loaded liposomes, the following equipment will be used: a microplate reader (μQuant™, BioTek Instruments, Inc., Vermont, USA), a fluorescent microscope (Olympus IX83, Japan) or other equivalent, a laser scanning confocal microscope (LSCM) (Leica TCS SP5, Wetzlar, Germany) or other equivalent, flow cytometry (BD FACSVerse™, San Jose, CA, USA) or other equivalent, and the flow cytometry data analysis software of FlowJo (Tree Star, Ashland, OR, USA).

4.2. *In vitro* evaluation of vaccine adjuvancy and delivery ability of the Ag-loaded liposomes through cellular experiments

It is believed that after antigen uptake, APCs with normal functions will evolve from immature, antigen-capturing cells to mature, antigen-presenting and T cell-priming cells, and meanwhile able to convert antigens into immunogen epitope and express molecules such as cytokines, chemokines, costimulatory molecules and proteases to initiate an immune response. Thus, the ability of delivery of Ag to APCs is one of the main functions designed to the liposomal carriers and is usually evaluated through assaying enhancement of cellular uptake of the fluorescent agent/Ag-loaded liposomes using mouse bone marrow-derived macrophages (BMMPs) and dendritic cells (BMDCs), both of which are confirmed to be ideal APCs to evaluate vaccine adjuvancy and delivery efficiencies and can be generated from bone marrow precursors as follows [43, 44].

1. The femur bones are first isolated from the euthanized mouse, and then immersed in 75% ethanol for 2 min for disinfection
2. After rinsing thrice with sterile PBS, both ends of femur bones are removed, and bone marrow is flushed out with ice-cold PBS using a hypodermic needle attached to a syringe.
3. The leukocytes obtained are washed thrice with PBS and then transferred into bacteriological petri dishes and cultured in 10 mL of complete RPMI containing 10% heat-inactivated FBS and in the presence of 50 μM 2-mercaptomethanol and 20 ng/mL GM-CSF for 3 days in a cell culture chamber.
4. On days 4 and 6, the culture medium is replaced with the fresh one containing identical ingredients.
5. On day 8, the nonadherent cells in culture medium are used as BMDCs.

Similarly, BMMPs can be obtained using the above protocol with a little modification in Step 4 by replacing GM-CSF with M-CSF, and in Step 5, and, notably, the adherent cells instead of nonadherent cells in culture medium are collected as BMMPs.

The cellular uptake of the fluorescent agent/Ag-loaded liposomes may be assayed by following processes.

1. APCs (BMDCs or BMMPs) are seeded in a 24-well plate with 1 mL of 10^5 cells/well and incubated in a cell culture chamber with 5% CO_2 at 37°C for 24 h.
2. Then each cell well is supplemented with 50 μL of calcein (1 mM)/Ag-loaded liposomes, mixed homogeneously, and incubated continuously in a cell culture chamber at 37°C for various times.
3. After the incubation and removal of the unassociated agents or liposomes through centrifuge at 800 g for 5 min and washing thrice with PBS, the cocultured cells (10^5 cells/mL) are analyzed by flow cytometry for uptake of liposomes with data analysis using FlowJo software; otherwise, a fraction of the cells is imaged using a fluorescent microscope; or to observe the intracellular localization of the agents delivered by liposomes in APCs, the following steps are carried out
4. The cocultured cells are isolated and incubated for 30 min in pre-warmed media (37°C) containing 50 nm LysoTracker-red and DAPI to identify lysosome and nuclei, respectively.
5. After washing thrice, the APCs are observed in a LSCM, and the dissociation of green dots (calcein-liposomes) from red dots, with blue nuclei for cell localization, is considered as the hallmark of lysosome escape by agents delivered by liposomes.

APC activation and maturation induced by the Ag-loaded liposomes can be evaluated by assay of the immunological cytokines and the surface biomarkers secreted or expressed by the APCs in the activated states. The secretion of cytokines, such as tumor necrosis factor (TNF), various interleukins (ILs), IFN-γ and even nitric oxide (NO), is usually enhanced or altered to different degrees by the activated APCs for induction of the subsequent specific immune responses, whereas CD40, CD80, and CD86 are known to be expressed at an enhanced level on the activated APCs and involved in, through binding receptors on T cell surface, providing costimulatory signals necessary for T cell activation and survival, and therefore may be used as markers for evaluating APC activation state. The levels of CDs on surfaces of the activated APCs may be assayed by several steps as follows:

1. The cells seeded in a 24-well plate with 1 mL of 10^6 cells per well are supplemented with 50 μL of soluble Ags (as a control), Ag-loaded liposomes at the dose of 20 μg Ag for up to 30 h for stimulation.
2. After stimulation, the cells are labeled with different color fluorochrome-conjugated Abs against surface biomarkers, such as CD40, CD80, and CD86, at 37°C for 30 min.
3. The cells are quantitatively assayed of the CD levels by flow cytometry.

The levels of cytokines, such as TNF, various ILs and IFN-γ, secreted in culture medium by the activated APCs are first separated in the supernatants by centrifugation and quantified with enzyme-linked immunosorbent assay (ELISA) kits according to product performance

guidance, while the level of secreted NO in cell culture supernatants is usually measured by colorimetric assay with Griess reagents, which react with nitrite forming a colorimetric compound which in turn reflects NO amount in samples [45].

The antigen presentation profile of the liposome-activated APC with MHC-I or -II is usually determined by measuring APC-primed $CD8^+$ and $CD4^+$ T cell proliferation using Ag-specific T cells as the following protocol.

1. To obtain Ag-specific T cells, C57BL/6 mice are immunized subcutaneously in the scruff of the neck with daily dose of 100 μg OVA plus 10 μg Poly (I:C) at injection volume of 100 μL [46], and mice are repeatedly immunized at the same site, at approximately 24-h intervals for 4 consecutive days.
2. Seven days after the first immunization, Ag-specific $CD8^+$ T cells are negatively selected from the spleen of Ag/Poly (I:C)-immunized mice by magnetic bead adsorption using MagniSort® isolation kit.
3. The isolated $CD8^+$ T cells are prelabeled with CFSE (1 μM final concentration for 10^6 cells) at 37°C for 5 min, and then cocultured with the Ag-loaded APCs that are generated by stimulation with free Ag (used as a control) or Ag-loaded liposomes at the ratio of T cell to APC of 10:1, at 37°C for 48 h [47, 48]. To determine MHC II antigen presentation ability of APCs, CD8-depleted splenocytes are prelabeled with CFSE and cocultured with OVA-loaded APCs at the ratio of T cells to APCs at 10:1 at 37°C for 48 h.
4. The proliferation of $CD8^+$ T cells and $CD4^+$ T cells, which, respectively, reflected the MHC I and MHC II antigen presentation by APCs, is determined by measuring the fraction of live cells with decreased CFSE intensity ($CFSE^{low}$ cells) using flow cytometry.

4.3. *In vivo* evaluation of vaccine adjuvancy-delivery ability of the Ag-loaded liposomes through vaccination experiments

4.3.1. Animal vaccination with the Ag-loaded liposomes

The experimental animals, such as mice, rats, rabbits and dogs, can be used as a vaccination model for Ag-loaded liposomes. Though rats, rabbits and dogs can be used for vaccination of Ag-loaded liposomes, mice are a preferred model due to their relatively low price, small body saving liposome samples, and, most importantly, their immune system bearing much-known backgrounds [49]. The vaccination routes are diverse and can be summarized into two ways: injection and noninjection, and the former includes intradermal, intramuscular, intramucosa and intravenous injection, while the later includes intraoral cavity, intravaginal, oral-uptake administration. Notably, intramucosa is a newly developed pathway and has been investigated only for vaccination of the microneedle vaccines, which have also been invented only recently but developed rapidly to show big advantages over the conventional liquid vaccines in the several aspects including the administration convenience, dosage saving, and, especially, efficient delivery of Ags [12–14, 24, 26, 27, 50–52]. The Ag dose given to mice in the formulation of liposomes is often in the range of 0.5–20 μg for injection, but of 5–100 μg for intracavity administration.

4.3.2. Sample collection

Collection of samples, including blood, secreted fluids in reproductive ducts and respiratory tracts, and even contents in digestive lumen and cavities from mice vaccinated with the Ag-loaded liposomes is necessary to obtain the data on a wide range of parameters, such as immunoglobulins, interferons, interleukins and cytokines, to evaluate humoral and cellular immune responses to vaccines. The sample collection from the vaccinated mice is suggested to be carried out 2–4 weeks after vaccination, when the immune responses are thought to be in a prime period. The protocols for collection of various samples, including blood, saliva, pulmonary, respiratory, vaginal and intestinal secretions, are described in detail in an open access book chapter recently published by Springer and suggested here as a reference and guide to performing the corresponding experiments [26].

4.3.3. Isolation of splenocytes from mouse spleen

Proliferation profile of the immunocytes from treated mice reflects the level of the immune responses to a liposomal vaccine and can be sketched using the different types of immunocytes and their fractions in lymphoid tissues, such as spleen, lymph nodes (LNs) and thymus to show the pathways along which the immune responses elicited by a liposomal vaccine have progressed and developed. Therefore, isolation and assay of immune cells from lymphoid tissues are often carried out as one of the fundamental mechanisms underlying the immunological efficacy of certain types of vaccines. Usually, organ, tissue, or cell isolation should be performed with aseptic manipulation in a sterile cabinet or under a sterile condition to avoid contamination for keeping cells alive.

Isolation of mouse splenocytes from spleen is described as follows:

1. The spleen from the abdomen-anatomically opened mouse is isolated using a small pair of hemostatic forceps, and transferred into the cell strainer (200-mesh with pore size of 70 μm) in the Petri dish containing 2 mL sterile PBS.
2. The spleen is ground slightly with the plunger of a 2-mL syringe by grinding circular movements to release the splenocytes into the Petri dish through passing the strainer.
3. Periodically, liquid from outside the strainer is pipetted to wash out the cells from within the strainer. Continuously, the spleen is slightly mashed until all that remains is the white connective tissue of the outer membrane.
4. The splenocyte suspensions are collected, filtered through the strainer twice if necessary, and transferred into a 5-mL tube, and the Petri dish may be washed out with 1-mL PBS twice to maximize the cell recovery.
5. The splenocyte suspensions are centrifuged at 800 × *g* for 5 min at room temperature and discard the supernatant by decant.
6. The splenocyte pellet is fully resuspended in 1-mL red blood cell lysing solution (containing 155-mM NH_4Cl, 12-mM $NaHCO_3$, 0.1-mM EDTA) and left for just 2 min at room temperature to lyse the red cells.

7. The suspensions are diluted immediately with 4 mL PBS, and centrifuged at 800 × *g* for 5 min to discard the supernatant, and the pellet is resuspended in the cells completely in a full volume of PBS and washed twice with PBS following each centrifuge.
8. Finally, the cells are suspended in a proper medium (e.g. RPMI-1640) to a final known volume, and live cells are counted using a hemacytometer under a light microscope after Trypan blue staining.

Mouse lymphoid node immunocytes are isolated using the protocol as follows [28].

1. The anesthetized or euthanized mouse is put on its side to localize the region of the superficial (e.g., inguinal or brachial lymphoid node) to be harvested.
2. After disinfection with chlorhexidine or other disinfectants of the skin region that covers the lymph node, the skin is opened with a tiny incision (about 5 mM) with scissors.
3. The incision is stretched with two forceps to find the lymph node, which may appear grayish or darker than the surrounding fat.
4. The fascia (thin membrane covering the fat and tissue) on top of the lymph node is pinched with one pair of forceps and pulled lightly without breaking the surrounding tissue, then the lymph node is clamped with the second forceps from the underneath and is removed with the first forceps by breaking the fascia.
5. The lymph node is place in a 5- or 10-mL tube containing PBS and should immediately sink to the bottom of the tube, validating that a lymph node but not fat tissue has been extracted.

The obtained lymph nodes can be further subjected to lymphocytes isolation or histological section for immunological assay.

The immune cell proliferation can be tested by MTT (3-(4,5-dimethylthiazol-2-yl)-2,5-diphenyltetrazolium bromide) method.

1. MTT solution is prepared by dissolving 50 mg MTT in 10 PBS followed by filtering through 0.2-μm membranes for sterilization.
2. A cell suspension is adjusted to contain 0.1–1.0 × 10^6 cells/mL in a medium and is seeded with 100 μL of cells per well in a 96-well plate, or with 500 μL of cells per well in a 24-well plate is seeded, with or without the compound to be tested.
3. The seeded cells are cultured for 24–96 h at 37°C and 5% CO_2 in a humidified incubator, and then 10 μL of 5 mg/mL MTT in PBS is added to each well of a 96-well plate, or 50 μL to each well of a 24-well plate.
4. The plate is incubated at 37°C and 5% CO_2 for 3–4 h (resulting in purple precipitates within cells, and the intracellular precipitates can be more precisely visualized under a light microscope).
5. The culture medium is carefully removed using a pipette (after centrifuge at 800 *g* for 5 min for nonadhesive cells), and Dimethyl sulfoxide (DMSO) is added at the amount of

100 μL per well for a 96-well plate, or 500 μL per well for a 24-well plate, which is incubated at room temperature for 2 h in the dark to fully dissolve the intracellular precipitates. (Note: Longer incubations with DMSO in the wells may result in precipitate or turbidity that can increase background. If precipitate is observed, warm the plate at 37°C for 10–20 min and agitate to dissolve the precipitate.)

6. The plate optical absorbance is finally read at a wavelength of 560 nm with a reference wavelength of 650 nm.

4.3.4. Humoral immunity assays

The antigen-specific antibodies, such as IgA, IgG, and IgG2a (or IgG2c in case of samples from C57BL/6 mice), produced in mice vaccinated with Ag-loaded liposomes can be assayed using the method of enzyme-linked immunosorbent assay (ELISA) in a microplate reader (μQuant™, BioTek Instruments, Inc., Vermont, USA) [25, 28]. There are five types of ELISA, including indirect ELISA, direct ELISA, sandwich ELISA, competitive ELISA and ELISPOT, and only a few differences exist amid these ELISA protocols, with the main ELISA principle and lots of procedures being the same. The level of anti-Ag antibody is often determined by the conventional indirect enzyme-linked immunosorbent assay (ELISA) protocol as follows:

1. A 96-well microtiter plate is coated per well with 100 μL of Ag (capture protein) (1 μg/mL) in carbonate buffer (15 mM Na_2CO_3, 35 mM $NaHCO_3$, pH 9.6) and sealed and incubated at 4°C overnight.
2. Each well of the plate is aspirated with pipette to discard the contents and washed three times with 300 μL of PBS containing 0.05% v/v Tween-20 (PBST). After the last wash, the plate is inverted and blotted against clean paper towels to remove any remaining PBST.
3. Each well is blocked by adding 200 μL of PBSTO (PBST containing 1 mg/mL OVA, or protein other than the Ag in liposomes) and then covered and incubated at 37°C for 1 h to prevent the nonspecific binding sites in the coated wells and then blotted on paper towels after discarding of water.
4. Thereafter, 100 μL of samples, which have been collected from mice and diluted appropriately with PBSTO, is added to each well of the plate, sealed, incubated at 37°C for 1 h.
5. After being washed thrice with 200 μL of PBST and blotted on paper towels after last wash, each well is added with 100 μL of the HRP (horseradish peroxidase)-conjugated secondary antibodies that have been diluted with appropriate amount of PBSTO (1:2500) and sealed for incubation at 37°C for 1 h.
6. After being washed with 300 μL of PBST for five times and blotted on paper towels after last wash, each well is supplemented with 100 μL of the freshly prepared TMB (3, 3′, 5, 5′-Tetramethylbenzidine) substrate solution (containing 1 mM TMB, 3 mM H_2O_2 and 0.2 mM Tetrabutylammonium Borohydride (TBABH)) and incubated at room temperature in the dark for 20 min for color development [25, 53].

7. And 20 min later, each well is added with 100 μL of 1 M H_2SO_4 solution to terminate the color development and then immediately determine the optical absorbance at 450 nm, with a reference wavelength at 570 nm, using an automated microplate reader (μQuant™ microplate spectrophotometer, BioTekInstruments, Inc., Winooski, Vermont, USA).

Notably, in above Step 6, TMB substrate solutions should be freshly prepared and used in less than 10 min, because they are chromogenic reagents for peroxidase to develop an intense blue color that can be read directly (at 650 nm), or a deep yellow color (read at 450 nm) after stopping with an acid solution.

And 1 mM TMB substrate solution (containing 1 mM TMB, 3 mM H_2O_2) can be freshly prepared as follows:

1. Preparation of Solution A: Potassium citrate buffer solution (CBS) is prepared by dissolving 2.15 g citric acid in 40 mL H_2O, which is then adjusted of pH 4 with 1 M KOH and diluted with H_2O to 50 mL, and then 50 mL of CBS is then mixed with 15 μL of fresh H_2O_2 (30%), resulting in Solution A.
2. Preparation of Solution B: A total of 10.8 mg TBABH (Tetrabutylammonium Borohydride) is dissolved in 5 mL dimethyl acetylamide (DMA), into which 50.3 mg TMB is then added and dissolved by vertex, resulting in Solution B.
3. Preparation of 1 mM TMB substrate solution: Just before use, 8 mL of Solution A is completely mixed with 200 μL of Solution B, resulting in 8.2 mL 1 mM TMB substrate solution.

4.3.5. In vivo tracking of the Ag-loaded liposomes after vaccination

To track *in vivo* vaccines delivered by liposomes, both *ex-vivo* approaches and *in-vivo* imaging techniques can be used, including *ex-vivo* biodistribution, autoradiography, MRI, optical imaging, PET and single-photon emission computed tomography (SPECT), all of which have their specific advantages and limitations. Consequently, selection of the tracking method should be based on the distinct features of the nanocarriers as well as the specific aims of the experiments [54, 55]. Here, this section introduces a simple fluorescent method that is conveniently applied for tracking vaccine delivery system. For this, the fluorescent agents, such as calcein and sulforhodamine B (SRB), are efficiently entrapped due to their water-soluble properties as a label in the Ag-loaded liposomes, enabling both *ex-vivo* and *in-vivo* imaging approaches to be used for tracking the vaccines.

For *in-vivo* imaging, usually, 0.5, 1, 2, 4, and 8 h after administration of the fluorescent agent/Ag-loaded liposomes via intradermal, intramuscular, intra-mucosal or any other feasible route, mouse is imaged using animal *in vivo* imaging systems; otherwise, mouse is exposed, by anesthetic and anatomic operation, of mucosa, lymph nodes (LNs), or other region wherein vaccines are expected to be delivered by liposomes, to lights with the wavelength matching fluorescent agent entrapped in liposomes for automatic imaging using a camera or a smart phone with lens [24].

For *ex-vivo* imaging and assay, at 0.5, 1, 2, 4, and 8 h after vaccination mice with fluorescent liposomes, the organs, such as spleen, liver, kidney, heart, lung and even brain, and main draining LNs that collect the fluids from the administration site and nearby regions are dissected from the vaccinated mice for further histological section assay. To observe distribution of fluorescent liposomes, the freshly harvested organs and draining LNs should be immediately embedded in the optimum cutting temperature (OCT) compound for cryosection and observation under a fluorescence microscope (IX83, Olympus, Japan). The procedure for cryosectioning is relatively simple and can be performed rather quickly, using the material including necessarily frozen embedding media of OCT, empty slide box, dry ice, cryostat, which is essentially a microtome inside a freezer, disposable blades, specimen mount, slides, and optionally poly-L-Lysine, gelatine, and agarose.

1. The fresh, unfixed tissue sample, up to 2.0 cm in diameter, is frozen in OCT in a suitable tissue mold in liquid nitrogen or at −80°C in an ultralow temperature refrigerator. Certain soft tissues, such as brain, are optimally frozen in M-1 medium at −3°C.
2. The tissue-embedded OCT is fixed and frozen onto the specialized metal grids fitting onto the cryostat.
3. Sections of 5–15 μm thickness are cut in the cryostat at −20°C. If necessary, the temperature of the cutting chamber may be adjusted up or down of ±5°C, depending on the tissue under study. A camel hair brush is useful to help guide the emerging section over the knife blade.
4. Within 1 min of cutting a tissue section, the section is transferred to a room temperature microscope slide by touching the slide to the tissue, avoiding freeze-drying of the tissue. Poly-L-lysine-coated or silanized slides improve the adherence of the section. And to evaluate tissue preservation and orientation, the first slide of each set may be stained with toluidine blue (1–2% w/v in H_2O), hematoxylin, and eosin, or any aqueous stain.
5. The sample-loaded slide is immediately immersed into an appropriate fixative, such as in precooled acetone (−20°C) for 10 min, which is then poured off and allowed to evaporate from the tissue sections for less than 20 min at room temperature, and then rinsed thrice with plentiful PBS.
6. The slide is stained of nucleus with DAPI for immediate observation. Otherwise, the slide may be covered with a layer of OCT to prevent freeze-drying and stored the rest of the sample at −70°C for further assay. For long-term storage, a moistened tissue should be added to the container with the block to prevent desiccation (particularly in a frost-free freezer).

In addition, the draining LN immunocytes that had taken up the liposomes can be sorted out by distinct fluorescent Ab staining using flow cytometry assay as follows.

1. The harvested draining LNs are gently mashed and filtered through a strainer with 70-μm mesh to isolate immune cells.
2. The resulting cells are stained at 4°C for 2 h with different fluorescent dye-conjugated Abs against CD11b, CD11c, F4/80, and CD169.

3. The stained cells are analyzed by flow cytometry to estimate the dLN cells that had engulfed either nanocarriers and their fractions based on fluorescence of liposomes and cells, which can be distinguished according to expressions of $CD11c^{+}F4/80^{-}$ by DCs, $CD11b^{+}F4/80^{-}CD169^{+}$ by subcapsular sinus macrophages (SSMs), $CD11b^{+}F4/80^{+}CD169^{+}$ by medullary sinus macrophages (MSMs), and $CD11b^{+}F4/80^{+}CD169^{-}$ by medullary cord macrophages (MCMs) [24].

4.3.6. In vivo assay of activation of lymphocytes and generation of memory lymphocytes

The immune induction effects by vaccines on lymphocyte activation, memory lymphocyte differentiation, and Ag-specific $CD8^{+}$ T cell production, are also often evaluated by flow cytometry.

1. Three weeks after final immunization with the Ag-loaded liposomes or the control formulations, the treated mice are anesthetized with chloral hydrate and aseptically isolate the splenocytes and LN cells, which, respectively, are seeded in the 24-well plate and cultured at a concentration of 10^6 cells/mL at 37°C in a cell incubator with 5% CO_2.
2. After 24-h incubation, the cells are co-cultured with OVA (10 μg/mL) for further stimulation at a concentration of 10^6 cells/mL at 37°C in a cell incubator with 5% CO_2 [25].
3. After 72-h incubation, the cells are washed (10^5/mL) and stained with fluorescence-labeled anti-mouse Abs (1 μg/mL), including CD4, CD8, CD69, H-$2K^b$-SIINFEKL, CD44 and CD62L for labeling T cells, and CD45R (B220), CD80 and IgD for labeling B cells, at 4°C for 1 h.
4. After washing thrice with PBS, the cells are resuspended in 1 mL PBS and assayed by flow cytometry to measure the percentages of effector memory T cells ($CD44^{high}CD62L^{low}$), central memory T cells ($CD44^{high}CD62L^{high}$), memory B cells ($B220^{+}CD80^{+}IgD^{-}$), and also the Ag-specific $CD8^{+}$ T cells ($CD8^{+}$SIINFEKL-MHC-I^{+}) [56].

Also, the supernatants of the splenocytes culture as well as the sera (1:10 dilution) from treated mice may be subjected to sandwich ELISA assay of the levels of IFN-γ, granuzyme B, IL-4, or other cytokines [25].

4.3.7. Assay of Ag-specific cytotoxicity of CTLs

Production of the Ag-specific cytotoxic T lymphocytes (CTLs) in treated subjects is the required immunity induced by a vaccine to erase the intracellular pathogens and is thus a desired function of a vaccine that has been purposely designed. The *in vivo* Ag-specific cytolysis of induced CTLs in the vaccine-treated mice is regarded as the Ag-specific cytotoxicity of CTLs and is often analyzed using the CFSE-labeled cells bearing the Ag epitopes [57]. Herein, using OVA as the model Ag, the process for assay of the Ag-specific cytotoxicity of CTLs in the vaccinated mice is described as follows [24]:

1. Mice are vaccinated twice with an interval of 3 weeks with the OVA-liposomes by the desired route.

2. The syngeneic splenocytes are isolated from naive mice, washed with PBS, and supplemented with 3% fetal calf serum (FCS) and 5 mM EDTA at 2×10^7 cells/mL in PBS.
3. The splenocytes are equally divided into two populations, which are incubated with CFSE at concentrations of 4 μM ($CFSE^{high}$) and 0.4 μM ($CFSE^{low}$), respectively, for 5 min at room temperature, followed by washing twice with cold PBS.
4. The $CFSE^{high}$ splenocytes are pulsed with 1 μM $OVA_{257–264}$ (SIINFEKL) peptide for 1 h at 37°C in the dark to be target cells identifiable to the OVA-specific CTLs, and then after washing thrice with PBS mixed with $CFSE^{low}$ splenocytes as nontarget cells at equal numbers (2×10^7 total cells).
5. The mixture of the two splenocyte populations is intravenously injected through tail vein into the mice that should have received the second vaccination of OVA-liposomes for 6 days.
6. After 15 h, the draining nodes and spleen from recipient mice are taken to isolate the cells for measuring by flow cytometry the *in vivo* cytolysis effect of CTLs, which is estimated by the loss of the $CFSE^{high}$ antigen-pulsed population relative to the control $CFSE^{low}$ population.

4.3.8. Prophylactic efficacy of the Ag-loaded liposomes tested using pathogen challenge

The prophylactic efficacy of liposomal vaccines can be evaluated using the pathogen challenge experiments using the animals, which should be the hosts that infectious pathogens can lodge at and proliferate in. And the animal models fitting host-pathogen interaction studies are well summarized in a previous paper [58], and the interested readers can refer to the paper for choosing the subjects for carrying out the related research. Notably, the pathogen challenge experiments should be conducted in the laboratory with the necessary biosafety levels (BSLs) that can absolutely guarantee the full protection of the investigators and the complete eradication of the propagation of the pathogens from the laboratory [59]. The requirements of BSLs of the laboratories for carrying out pathogen challenge experiments on various types of pathogens with different infection and lethality abilities are rigorously defined in the guideline book of *Biosafety in Microbiological and Biomedical Laboratories*, which can be freely downloaded from the CDC website and should be at hand for every researcher who conducts related experiments (https://www.cdc.gov/biosafety/publications/bmbl5/bmbl.pdf).

To carry out the pathogen challenge experiments, the model animals with the proper age are vaccinated once or twice at a proper interval by the aimed administration route with the Ag-loaded liposomes at the dose of low, middle and high levels, respectively. And 3 weeks after the (second) vaccination, the animals are challenged with the pathogen in a stock at the challenge dose of 10–50 folds of LD50 (lethal dose 50%) [60]. The animals are weighed once and observed twice daily for certain days to observe the protection efficacy, and the animals may be euthanized before reaching the moribund state due to humane concerns.

5. Conclusions

Liposomes are widely used as a vehicle for delivering various vaccines due to their numerous advantages, including high biocompatibility, diverse and high loading capacity, inherence adjuvanticity, relative ease for preparation and for surface decoration to engender a multifunctional carrier. Particularly, when the liposomes are combined with specific molecules, such as ligands to TLRs, the steric stabilization polymers, and the mannosylated compounds, the carriers are indeed functioning as a stable and effective vaccine adjuvant-delivery system (VADS) to play both the roles of a vaccine adjuvant and a vaccine vehicle. The liposomal VADS can efficiently deliver vaccines to the lymph nodes and even target the APCs to elicit robust humoral as well as cellular immunity against the invading pathogens bearing the surface features matching the loaded antigens, as confirmed by the *in vitro* and *in vivo* experiments, including testing the cellular uptake of liposomes by APCs and the activation of lymphocytes by liposomes, *in vivo* tracking of liposomes, assaying secretion of cytokines and immunoglobulins with liposome stimulation, all of which are described with key steps and key points in this chapter. As researchers are continuously focusing their research interests and efforts on the development of liposomal vaccines, many of the now unknown mechanisms underlying the elicited immunity will eventually be brought to light and may play a crucial role in rational design of the optimal VADSs. Obviously, various types of the liposome-based vaccines may finally be approved by the authorities to enter markets as new products against numerous life-threatening diseases, when many advanced platforms are managed and set up to further explore and constitute the diverse functional liposomes as an effective vaccine adjuvant-delivery system (VADS).

Acknowledgements

The work was supported by the Department of Education of Anhui Province for the University Natural Science Research Project (Grant number KJ2016SD28) and for the Abroad Visiting Scholar Program for the University Key Teachers (Grant number gxfxZD2016045) and also by Hefei University of Technology for the Young Teacher Innovative Project (Grant number JZ2015HGQC0211), and Anhui Natural Science Foundation (Grant number 1708085QH195).

Author details

Ning Wang[1], Tingni Wu[2] and Ting Wang[2]*

*Address all correspondence to: twangcn@hotmail.com

1 School of biological and Medical Engineering, Hefei University of Technology, Hefei, Anhui Province, China

2 School of Pharmacy, Anhui Medical University, Hefei, Anhui Province, China

References

[1] De Gregorio E, Rappuoli R. From empiricism to rational design: A personal perspective of the evolution of vaccine development. Nature Reviews Immunology. 2014;**14**:505-514

[2] Pulendran B, Ahmed R. Immunological mechanisms of vaccination. Nature Immunology. 2011;**12**:509-517

[3] Saalmuller A. New understanding of immunological mechanisms. Veterinary Microbiology. 2006;**117**:32-38

[4] Grimm SK, Ackerman ME. Vaccine design: Emerging concepts and renewed optimism. Current Opinion in Biotechnology. 2013;**24**:1078-1088

[5] Plotkin SA, Plotkin SL. The development of vaccines: How the past led to the future. Nature Reviews Microbiology. 2011;**9**:889-893

[6] Hem SL, HogenEsch H. Relationship between physical and chemical properties of aluminum-containing adjuvants and immunopotentiation. Expert Review of Vaccines. 2007;**6**: 685-698

[7] Glenny A, Pope C, Waddington H, Wallace U. The antigenic value of toxoid precipitated by potassium alum. Journal of Pathology. 1926;**29**:31-40

[8] Moyer TJ, Zmolek AC, Irvine DJ. Beyond antigens and adjuvants: Formulating future vaccines. The Journal of clinical investigation. 2016;**126**:799-808

[9] Sahdev P, Ochyl LJ, Moon JJ. Biomaterials for nanoparticle vaccine delivery systems. Pharmaceutical Research. 2014;**31**:2563-2582

[10] Leroux-Roels G. Unmet needs in modern vaccinology: Adjuvants to improve the immune response. Vaccine. 2010;**28**(Suppl 3):C25-36

[11] Wang N, Wang T, Zhang ML, Chen RN, Niu RW, Deng YH. Mannose derivative and lipid A dually decorated cationic liposomes as an effective cold chain free oral mucosal vaccine adjuvant-delivery system. European Journal of Pharmaceutics and Biopharmaceutics. 2014;**88**:194-206

[12] Wang T, Wang N. Biocompatible matter constructed microneedle arrays as a novel vaccine adjuvant-delivery system for cutaneous and mucosal vaccination. Current Pharmaceutical Design. 2015;**21**:5245-5255

[13] Wang X, Wang N, Li N, Zhen Y, Wang T. Multifunctional particle-constituted microneedle arrays as cutaneous or mucosal vaccine adjuvant-delivery systems. Human Vaccines & Immunotherapeutics. 2016;**12**:2075-2089

[14] Li N, Wang N, Wang X, Zhen Y, Wang T. Microneedle arrays delivery of the conventional vaccines based on nonvirulent viruses. Drug Delivery. 2016;**23**:3234-3247

[15] Bangham AD, Standish MM, Watkins JC. Diffusion of univalent ions across the lamellae of swollen phospholipids. Journal of Molecular Biology. 1965;**13**:238-252

[16] Weissig V. Liposomes came first: The early history of liposomology. Methods in Molecular Biology. 2017;**1522**:1-15

[17] Gregoriadis G. Liposome research in drug delivery: The early days. Journal of Drug Targeting. 2008;**16**:520-524

[18] Allen TM, Cullis PR. Liposomal drug delivery systems: From concept to clinical applications. Advanced Drug Delivery Reviews. 2013;**65**:36-48

[19] Allison AG, Gregoriadis G. Liposomes as immunological adjuvants. Nature. 1974;**252**:252

[20] Gregoriadis G, Allison AC. Entrapment of proteins in liposomes prevents allergic reactions in pre-immunised mice. FEBS Letters. 1974;**45**:71-74

[21] Gregoriadis G, McCormack B, Obrenovic M, Perrie Y, Saffie R. Liposomes as Immunological adjuvants and vaccine carriers. In: O'Hagan DT, editor. Vaccine Adjuvants: Preparation Methods and Research Protocols. New York: Springer; 2000. pp. 137-150

[22] Gregoriadis G, Wills EJ, Swain CP, Tavill AS. Drug-carrier potential of liposomes in cancer chemotherapy. Lancet. 1974;**1**:1313-1316

[23] Perrie Y, Crofts F, Devitt A, Griffiths HR, Kastner E, Nadella V. Designing liposomal adjuvants for the next generation of vaccines. Advanced Drug Delivery Reviews. 2016;**99**: 85-96

[24] Wang N, Zhen Y, Jin Y, Wang X, Li N, Jiang S, Wang T. Combining different types of multifunctional liposomes loaded with ammonium bicarbonate to fabricate microneedle arrays as a vaginal mucosal vaccine adjuvant-dual delivery system (VADDS). Journal of Controlled Release. 2017;**246**:12-29

[25] Wang N, Wang T, Zhang M, Chen R, Deng Y. Using procedure of emulsification-lyophilization to form lipid A-incorporating cochleates as an effective oral mucosal vaccine adjuvant-delivery system (VADS). International Journal of Pharmaceutics. 2014;**468**:39-49

[26] Wang T, Wang N. Preparation of the multifunctional Liposome-Containing microneedle arrays as an oral cavity mucosal vaccine Adjuvant-Delivery system. Methods in Molecular Biology. 2016;**1404**:651-667

[27] Wang T, Zhen YY, Ma XY, Wei BA, Li SQ, Wang NN. Mannosylated and lipid A-incorporating cationic liposomes constituting microneedle arrays as an effective oral mucosal HBV vaccine applicable in the controlled temperature chain. Colloid Surface B. 2015;**126**: 520-530

[28] Wang T, Zhen YY, Ma XY, Wei B, Wang N. Phospholipid Bilayer-Coated aluminum nanoparticles as an effective vaccine Adjuvant-Delivery system. ACS Applied Materials & Interfaces. 2015;**7**:6391-6396

[29] Barenholz Y. Doxil(R)--the first FDA-approved nano-drug: Lessons learned. Journal of Controlled Release. 2012;**160**:117-134

[30] Papahadjopoulos D, Vail WJ, Jacobson K, Poste G. Cochleate lipid cylinders: Formation by fusion of unilamellar lipid vesicles. Biochimica et Biophysica Acta. 1975;**394**:483-491

[31] Senior K. Bilosomes: The answer to oral vaccine delivery? Drug Discovery Today. 2001;**6**: 1031-1032

[32] Moghassemi S, Hadjizadeh A. Nano-niosomes as nanoscale drug delivery systems: An illustrated review. Journal of Controlled Release. 2014;**185**:22-36

[33] Moon JJ, Suh H, Bershteyn A., Stephan MT, Liu H, Huang B, Sohail M, Luo S, Ho Um S, Khant H, Goodwin JT, Ramos J, Chiu W, Irvine DJ. Interbilayer-crosslinked multilamellar vesicles as synthetic vaccines for potent humoral and cellular immune responses. Nature Materials. 2011;**10**:243-251

[34] Ye Q, Asherman J, Stevenson M, Brownson E, Katre NV. DepoFoam technology: A vehicle for controlled delivery of protein and peptide drugs. Journal of Controlled Release. 2000;**64**:155-166

[35] Huang Z, Li X, Zhang T, Song Y, She Z, Li J, Deng Y. Progress involving new techniques for liposome preparation. Asian Journal of Pharmaceutical Sciences. 2014;**9**:176-182

[36] Zhang H. Thin-Film hydration followed by extrusion method for liposome preparation. Methods in Molecular Biology. 2017;**1522**:17-22

[37] Wang T, Wang N, Sun W, Li T. Preparation of submicron liposomes exhibiting efficient entrapment of drugs by freeze-drying water-in-oil emulsions. Chemistry and Physics of Lipids. 2011;**164**:151-157

[38] Wang T, Deng Y, Geng Y, Gao Z, Zou J, Wang Z. Preparation of submicron unilamellar liposomes by freeze-drying double emulsions. Biochimica et Biophysica Acta. 2006;**1758**:222-231

[39] Wang N, Wang T. Preparation of multifunctional liposomes as a stable vaccine Delivery-Adjuvant system by procedure of Emulsification-Lyophilization. Methods in Molecular Biology. 2016;**1404**:635-649

[40] Czarnocki-Cieciura M, Nowotny M. Introduction to high-resolution cryo-electron microscopy. Postepy Biochem. 2016;**62**:383-394

[41] Bradford MM. A rapid and sensitive method for the quantitation of microgram quantities of protein utilizing the principle of protein-dye binding. Analytical Biochemistry. 1976;**72**:248-254

[42] Guo L. Chen J, Qiu Y, Zhang S, Xu B, Gao Y. Enhanced transcutaneous immunization via dissolving microneedle array loaded with liposome encapsulated antigen and adjuvant. International Journal of Pharmaceutics. 2013;**447**:22-30

[43] Lutz MB, Kukutsch N, Ogilvie AL, Rossner S, Koch F, Romani N, Schuler G. An advanced culture method for generating large quantities of highly pure dendritic cells from mouse bone marrow. Journal of Immunological Methods. 1999;**223**:77-92

[44] Zhang X, Goncalves R, Mosser DM. The isolation and characterization of murine macrophages. Current Protocols in Immunology. 2008;**83**:14.1.1-14

[45] Amano F, Noda T. Improved detection of nitric oxide radical (NO.) production in an activated macrophage culture with a radical scavenger, carboxy PTIO and Griess reagent. FEBS Letters. 1995;**368**:425-428

[46] Wick DA, Martin SD, Nelson BH, Webb JR. Profound $CD8^+$ T cell immunity elicited by sequential daily immunization with exogenous antigen plus the TLR3 agonist poly(I:C). Vaccine. 2011;**29**:984-993

[47] Quah BJC, Warren HS, Parish CR. Monitoring lymphocyte proliferation in vitro and in vivo with the intracellular fluorescent dye carboxyfluorescein diacetate succinimidyl ester. Nature Protocols. 2007;**2**:2049-2056

[48] Quah BJ, Parish CR. The use of carboxyfluorescein diacetate succinimidyl ester (CFSE) to monitor lymphocyte proliferation. Journal of Visualized Experiments. 2010;**44**:2259

[49] Wang T, Zhen Y, Ma X, Wei B, Li S, Wang N. Mannosylated and lipid A-incorporating cationic liposomes constituting microneedle arrays as an effective oral mucosal HBV vaccine applicable in the controlled temperature chain. Colloids and Surface B: Biointerfaces. 2015;**126**:520-530

[50] Zhen YY, Wang N, Gao ZB, Ma XY, Wei BA, Deng YH, Wang T. Multifunctional liposomes constituting microneedles induced robust systemic and mucosal immunoresponses against the loaded antigens via oral mucosal vaccination. Vaccine. 2015;**33**:4330-4340

[51] Prausnitz MR, Mikszta JA, Cormier M, Andrianov AK. Microneedle-based vaccines. Current Topics in Microbiology and Immunology. 2009;**333**:369-393

[52] Arya J, Prausnitz MR. Microneedle patches for vaccination in developing countries. Journal of Control Release. 2015;**240**:135-141

[53] Frey A, Meckelein B, Externest D, Schmidt MA. A stable and highly sensitive 3,3′,5,5′-tetramethylbenzidine-based substrate reagent for enzyme-linked immunosorbent assays. Journal of Immunological Methods. 2000;**233**:47-56

[54] Stojanov K, Zuhorn IS, Dierckx RA, de Vries EF. Imaging of cells and nanoparticles: Implications for drug delivery to the brain. Journal of Pharmacy Research. 2012;**29**: 3213-3234

[55] Lee SY, Jeon SI, Jung S, Chung IJ, Ahn CH. Targeted multimodal imaging modalities. Advanced Drug Delivery Reviews. 2014;**76**:60-78

[56] Anderson SM, Tomayko MM, Ahuja A, Haberman AM, Shlomchik MJ. New markers for murine memory B cells that define mutated and unmutated subsets. Journal of Experimental Medicine. 2007;**204**:2103-2114

[57] Clemente T, Dominguez MR, Vieira NJ, Rodrigues MM, Amarante-Mendes GP. In vivo assessment of specific cytotoxic T lymphocyte killing. Methods. 2013;**61**:105-109

[58] Lee A. Animal models for host-pathogen interaction studies. British Medical Bulletin. 1998;**54**:163-173

[59] Burnett LC, Lunn G, Coico R. Biosafety: Guidelines for working with pathogenic and infectious microorganisms. Current Protocols in Microbiology. 2009;**13**:1A.1.1-14

[60] De Vleeschauwer A, Qiu Y, Van Reeth K. Vaccination-challenge studies with a Port Chalmers/73 (H_3N_2)-based swine influenza virus vaccine: Reflections on vaccine strain updates and on the vaccine potency test. Vaccine. 2015;**33**:2360-2366

Chapter 6

Hydrogels and Their Combination with Liposomes, Niosomes, or Transfersomes for Dermal and Transdermal Drug Delivery

Mahmoud Mokhtar Ibrahim, Anroop B. Nair, Bandar E. Aldhubiab and Tamer M. Shehata

Additional information is available at the end of the chapter

http://dx.doi.org/10.5772/intechopen.68158

Abstract

Polymeric networks that retain and absorb substantial amount of water or biological fluids and resemble as a biological tissue are defined as hydrogels. On the other hand, liposomes, transfersomes and niosomes are lipid carriers, which represent one of the major research and development focus areas of the pharmaceutical industry. They have great potential as lipid vehicles that are able to enhance permeation of drugs across the intact skin and can act as local depot for the drug to sustain and control its delivery. Lipid carrier and hydrogel combinations offer transdermal drug delivery of great potential to enhance systemic effects of both hydrophilic and lipophilic drugs. Also, lipid carriers can target drugs to skin appendages and improve transdermal delivery. Lipid carrier proform systems in the form of gelly liquid crystals can also be used transdermally for better drug absorption enhancement. This review highlights the potential of hydrogels and emulgels with or without lipid nanocarriers for dermal and transdermal application.

Keywords: hydrogel, emulgel, liposome, niosome, transfersomes

1. Introduction

Lipid carriers such as liposomes, niosomes, and transferesomes can be brought into gel formulations either in their proforms or in hydrogel vehicles and applied transdermally. They offer the capability of controlling drug release, enhancing drug transdermal absorption and increasing drug bioavailability compared to the plain gels [1]. Pharmaceutical gel preparations such as hydrogels, organogels, and emulgels have been extensively used to deliver both

hydrophilic and lipophilic drugs for dermatological and transdermal use. Gels are cross-linked assembly containing both solid and liquid components within its configuration, which were considered as gelling agents and called gelators [2]. When the gelators are dispersed in appropriate solvent, they were associated together forming network of three-dimensional structure, which immobilize the surrounding aqueous media [2]. These results are followed by a series of the interactions to form the polymeric cross-linked network structures, which retained certain amount of the water [3]. The synthetic or natural gelators have ability to form this series of interactions producing macromolecular chain reaction. It was declared that the hydrophilic groups of the polymers build up gel like structure upon the hydration in the liquid environment. The gelation process stated that the polymer chains connected together to form large branched soluble polymers, which are called 'sol'. Afterward, the aggregation process leads to an increase in the branched polymer length with decreasing of the solubility of the polymers. This macrobranched polymer is called "gel". Then the gelation effect is called 'sol-gel transition' and the gel point is defined as the first point of gel formation [4]. Therefore, it is recognized that the ideal gels were developed following the incorporation of gelator molecules and the proper liquid phase resultant of self aggregation in the environmental medium. Thus, the gels were formed because of physical and chemical interaction between polymers chains. These interactions might form irreversible or reversible links producing permanent or temporary bonds. Hydrogen bonding, van der Waals force, hydrophobic interactions, ð-ð interactions, lamellar microcrystals, glassy nodules or double and triple helices blocks copolymer micelles and ionic associations are the physical interactions included in hydrogel formulations [5].

Hydrogels are polymeric networks, which can absorb and retain substantial amount of water or biological fluids within their porous structure. Several natural and synthetic polymers either solely or cross-linked are used in formulating hydrogels. Crosslinking of polymers provides high physical integrity to the network structure as well as to control the release of drug molecules. Newer ligands and different types of crosslinking allow the development of ideal hydrogel systems with appropriate release characteristics for the successful delivery of drugs, such as nucleic acids, proteins and peptides. The hydrogels have extended their applications in targeted drug delivery and as constituents for preparation of protein or enzyme conjugates. Also, the chemical process may involve a range of interactions such as: formation of covalent bonds always resulting in a strong gel. The three main chemical gelation processes were noticed: (1) condensation, (2) vulcanization, and (3) addition polymerization [5]. These types of bonds have great important roles in the controlling of the physical and chemical characterizations, properties, and structure of the gels. The key for the classification of gels into organogel or hydrogel was based on the type of solvent, polymer used, and polymer chain interactions. If the solvent is organic in nature, then the gel is considered as organogel, else hydrogel [6]. On the other hand, emulgel is a semisolid vehicle that is composed of hydrophilic surfactant (s), oil, water, and gelling agent, "an emulsion transformed to a gel by gelling agent" [7]. Emulgel bases offer the advantage that of being capable of incorporating aqueous and oleaginous ingredients, and their rheological properties can be controlled easily.

The focus of the current chapter in gel drug delivery with or without a carrier system is to increase the range of products, which can effectively deliver the drug with specific release

http://dx.doi.org/10.5772/intechopen.68158

characteristics. The properties of certain gels to undergo sharp volume or sol-gel phase transition in specific environment have provided their importance in drug delivery with new promising applications. Progresses in polymer chemistry and gel technology have extended the prospective of gels in transdermal drug delivery.

2. Hydrogels and lipid carriers for drug delivery

2.1. Hydrogels

Hydrogels offer several favorable characteristics, which are crucial for designing suitable drug delivery systems. Typically, they are polymeric matrices, which are capable of imbibing greater amount of water, due to the good thermodynamic compatability which allow them to swell to a higher extent. These hydrogels emerged as a promising option for drug delivery scientists mainly due to their significant physicochemical and biological properties such as reversible swelling and shrinking, good sorption capacity, mechanical strength, considerable biocompatibility, desired drug release, tissue like physical properties, accommodating wide range of molecules, better compatibility, easy to fabricate, good oxygen permeability, low interfacial tension, nontoxic, etc. In addition, they offer several other characteristics like bioadhesion, mucoadhesion, rapid deformation, ease of surface modification, conforming the shape of surface which they are applied, which make them ideal for drug delivery vehicles for targeted drug delivery [8]. However, the physical properties of hydrogels are usually influenced by the charge of polymer, molecular weight of polymer, density of crosslinking, etc.

The biocompatibility of hydrogels is primarily owing to their higher water content and physicochemical similarity to the native extracellular matrix. They resemble more biological tissues probably due to their high water content, soft consistency and three-dimensional polymeric network. Indeed, the existence of three-dimensional structure of hydrogels could be employed in the design and development of different drug delivery systems. Moreover, the rubbery nature will minimize the mechanical irritation of the polymer to the surrounding body tissues. Further, hydrogels are highly compatible with most of the drugs, proteins and peptides. They can be modified and fabricated into desired formulations of specific size or shape. Thus, hydrogels appeared to be the ideal vehicle for dermal as well as transdermal delivery and different transdermal formulations like matrix patch, reservoir system, gel and carrier system. On the other hand, there are some few limitations, which confine the applications of hydrogels in drug delivery such as relatively low tensile strength, nonuniformity in drug loading of hydrophobic drugs and rapid drug release [9].

2.2. Lipid carriers

Lipid carriers such as liposomes, niosomes, and transfersomes have many applications expanded from conventional drugs to hormones, peptides, immunoglobulin, vaccination, and gene therapy. These drug delivery carriers employ different rate-controlling mechanisms such

as membrane diffusion, diffusion through matrices, osmosis and biodegradation. An explosion in research in drug delivery by nonconventional routes such as transdermal, nasal, ocular, pulmonary, and intraarterial routes has been reported.

2.2.1. Liposomes/niosomes and their pro-forms

Liposomes are the microscopic spherical phospholipids vesicles that form spontaneously when mixed in water under low shear conditions [10]. The phospholipid molecules arranged in layers or sheets and the molecules aligned side by side, in which the hydrophilic heads of phospholipid and their hydrophobic tails down. These phospholipid layers then formed bilayer membranes that encapsulate some of the aqueous vehicles inside a lipid sphere (**Figure 1**).

Liposomes are structurally related to cell membrane "phospholipid bilayer" and have been used in the study of biological membranes instead of using cadaver skin of human [11]. Moreover, liposomes as lipid carriers have been extensively evaluated as delivery vehicles for drugs, genes and/or cosmetics [12]. Liposomes undergo the problem of both chemical and physical instability; hence, the concept of proliposomes was introduced [13]. Proliposomes with least or no water content were prepared in three different forms: dry free-flowing granular product, mixed micellar proliposomes, and liquid crystalline proliposomes for reconstitution immediately at time of use (**Figure 2**). The proliposome liquid crystal type formulae were used successfully for transdermal drug delivery [14].

On the other hand, niosomes are nonionic surfactant vesicles of multilamellar or unilamellar bilayer membrane structures such as liposomes. They can encapsulate both hydrophilic

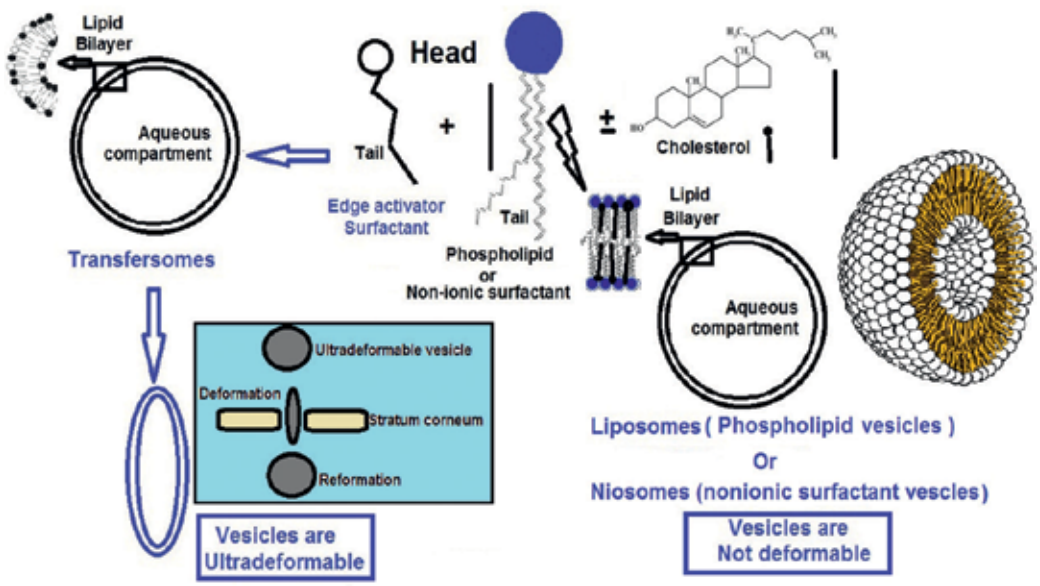

Figure 1. Schematic representation of lipid carriers "liposomes, niosomes, and transfersomes" structure and composition.

http://dx.doi.org/10.5772/intechopen.68158

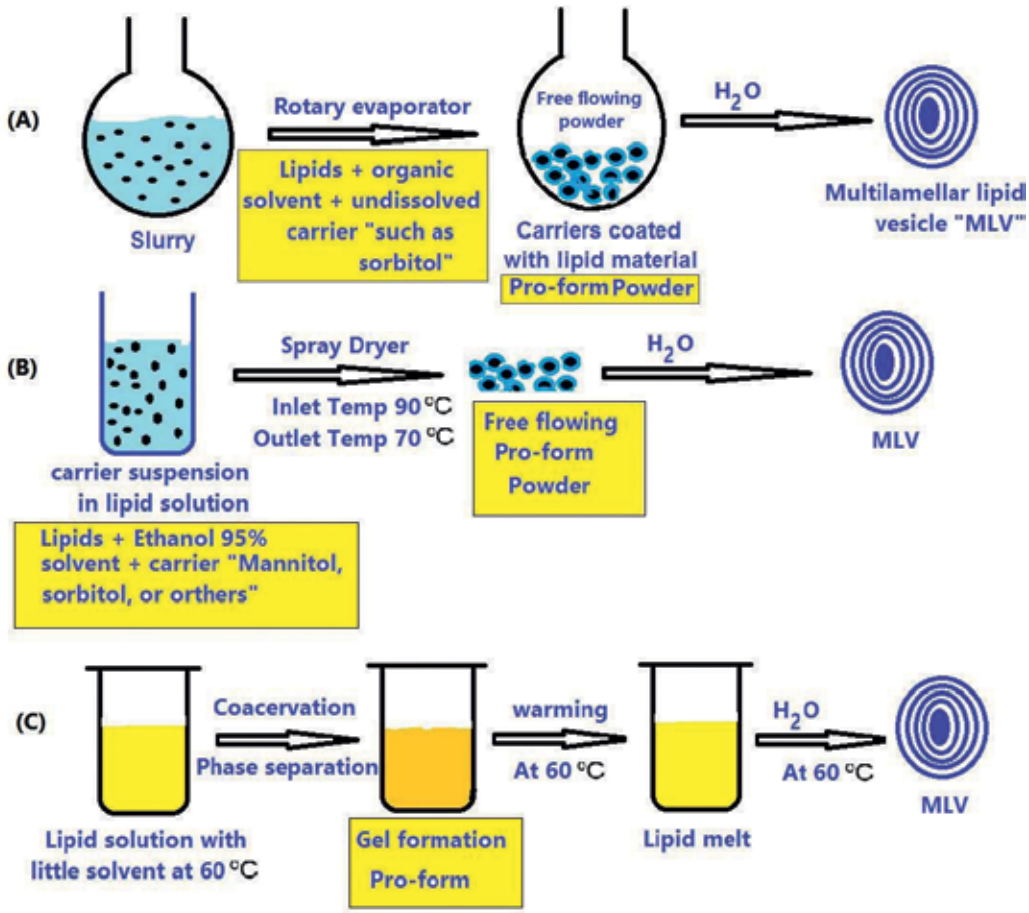

Figure 2. Different procedures of proforms preparation. (A) Slurry method, (B) spray drying method, and (C) coacervation phase separation method.

and hydrophobic molecules in the aqueous compartment and in the bilayer lipid membrane, respectively [15]. These niosomes are chemically stable, and no special conditions are required while preparation or storage, such as nitrogen atmosphere or low temperature. Niosomes are inexpensive alternatives of nonbiological origin to liposomes which are widely studied *in vivo* [16]. Moreover, they are extensively used as lipid carrier similar to liposomes physically, with particular properties, which can be exploited to attain different release characteristics and drug distributions [16]. Preliminary studies indicated that niosomes could prolong the plasma circulation of an entrapped drug and alter its distribution pattern and its metabolic stability [17]. Also, niosomal systems could prolong the contact time of a drug with the applied membranes in case of topical and transdermal applications [18]. Niosomes have many advantages over liposomes such as the lower cost, the greater chemical stability, and the ease of preparation and storage. Theoretically, a niosome formulation requires the presence of a particular class of nonionic amphiphiles dispersed in aqueous vehicle. Cholesterol as well as

fatty alcohols (e.g., myristyl, lauryl, cetyl, steryl, and cetosteryl alcohols) are added in order to prepare vesicles, which are more stable and less leaky [19]. Many investigators had reported a decrease in drug permeability across niosomal membranes as cholesterol concentration increased in the bilayers of niosomal vesicles [20]. In addition, stabilizers to enhance physical stability of niosomal dispersions might be included in formulations of niosomes to inhibit aggregation of vesicles by steric, electrostatic, or repulsive effects. Often a charged surfactant is included in the niosomal bilayers to create electrostatic charges, hence, repulsion between vesicles, thereby increasing their physical stability. The addition of dicetyl phosphate (negatively charging agent) or stearyl amine (positively charging agent) to the bilayers prevents the aggregation of the vesicles [21]. Stability of the niosomal vesicles can also be improved by using a substance (e.g., poly-24-oxyethylene cholesteryl ether (solulan C24)) providing steric barrier on the vesicle surface, which can prevent vesicles aggregation [22].

An increasing number of nonionic surfactants have been found to form niosomes for the encapsulation of hydrophobic and/or hydrophilic solutes [23]. The nonionic surfactants for preparing niosomal vesicles are usually single-alkyl chain surfactant and/or sorbitan esters. There are many examples belonging to different classes of nonionic surfactants that could be used in niosomes production such as crown ethers, glucosyldialkylether, polyglycerol alkylethers, and polyoxyethylene alkyl esters and ethers. These nonionic surfactant vesicles are prepared in the same way like liposomes and under different conditions give rise to either unilamellar type vesicles or multilamellar vesicles according to the method of production [24].

Proliposomes, proniosomes were introduced as free flowing powder and as liquid crystalline preparations for reconstitution just before use [13, 25]. Proniosomes are alternatives to proliposomes and are important from technical view point as they possess greater chemical stability and do not require special preparation or storage conditions as vacuum or nitrogen atmosphere (**Figure 2**).

2.2.2. Transfersomes

Transfersomes "the carrying bodies" are designed lipid vesicles especially for transdermal and/or topical delivery of wide variety of drug molecules. They offer an excellent approach for topical drug application especially the topical immunization. Transfersomes are analogous to liposomes vesicles but contain detergent "the edge activator" in their bilayers composition (**Figure 1**). They are called the ultradeformable carrier systems because they have high capacity of changing their shape via deformation and reformation mechanism, and passing through the natural pores in the stratum corneum (SC) (**Figures 1** and **3**). They can penetrate into the skin deeply and even reach the blood circulation. Transfersomes "the ultradeformable vesicles" containing reasonable amounts of detergent "the edge activator" did not produce lyses of human RBCs. They are very effective in transferring the bioactive drug molecules across the SC. They have the ability to penetrate through small pores "having a diameter of fivefold lower than their own diameter" present in the skin membrane. This indicates that a transfersome vesicle of diameter equaling 500 nm can pass across a membrane pore of 100 nm diameter or more.

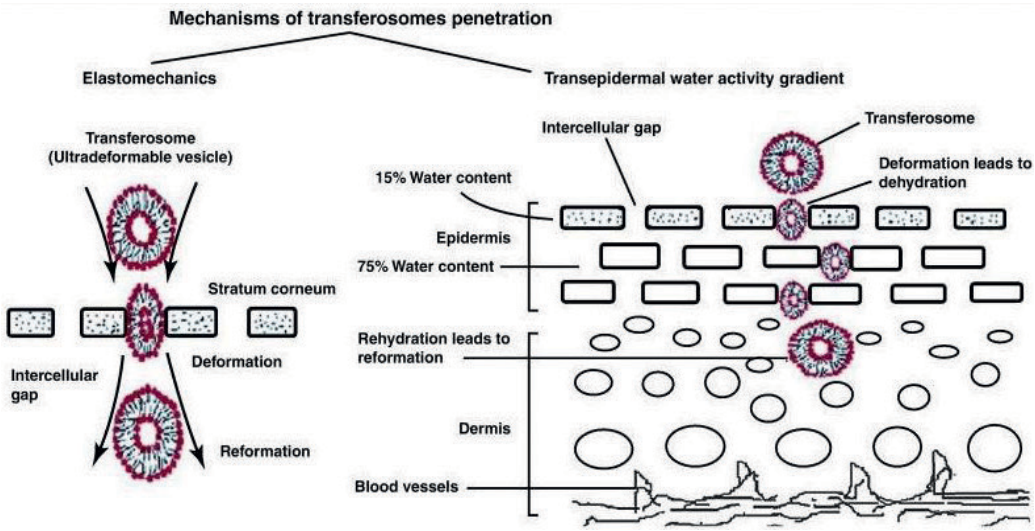

Figure 3. A schematic representation of an ultradeformable, mixed lipid vesicle (transfersome) penetrating a narrow pore. Adapted from Kumar, et al [111].

3. Formulation of gels containing lipid vesicles

For the preparation of gels containing liposomes, transferesomes or niosomes, a portion of the buffer required to form polymer hydrogels will be replaced by concentrated lipid vesicle dispersions loaded with the drug. The gels will be prepared by sprinkling the required amount of gelling agent gradually over the surface of that buffer containing the drug/lipid vesicles and mixed until homogenous gel was obtained [26–27].

3.1. The proposed mechanisms of enhancement of drug permeability using lipid vesicles

Several mechanisms have been proposed in order to explain the enhancement of the drug permeability across the skin membranes using lipid vesicles. El Maghraby et al. had fully described these mechanisms and here we will give short account on it [28].The possible mechanisms for drug and/or vesicular transport through the tough skin layers are shown in **Figure 4**.

1. **Free drug mechanism:** The mechanism concluded that the drug permeates the skin independently after releasing from the vesicles. Thus, the amount of drug that permeated the skin could be due to its own physicochemical properties and not due to the lipid vesicle composition. Many researchers do not support this mechanism as the vast majority recommended the effect of vesicles size and composition on the overall amount of the drug transport [28].
2. **Mechanism of penetration enhancing effects:** It was proven that surface-active agents, which are the backbone of the formulated lipid vesicles, could enhance the transdermal

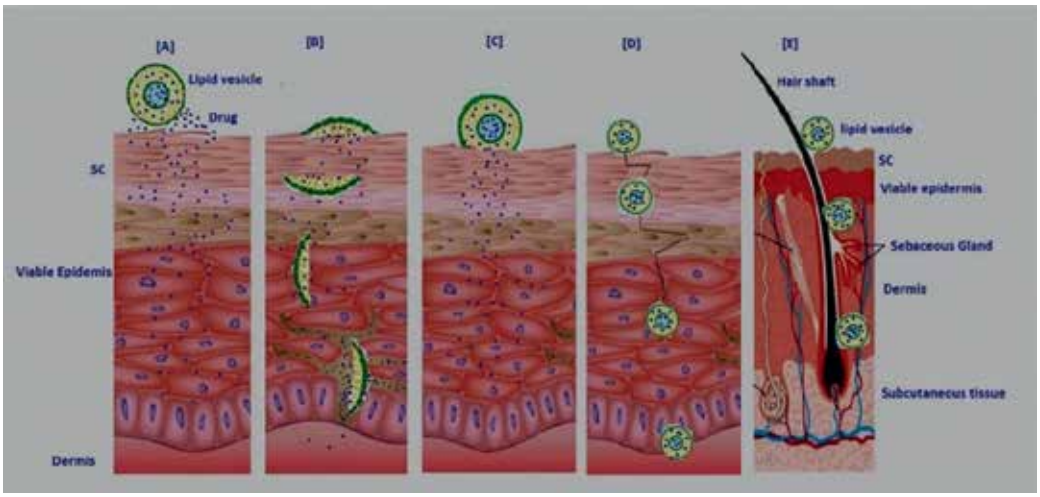

Figure 4. Possible mechanisms of action of liposomes as skin drug delivery systems. (A) It is the free drug mechanism, (B) it is the penetration enhancing process of liposome components, (C) it indicates vesicle adsorption to and/or fusion with the stratum corneum (SC), (D) it illustrates intact vesicle penetration into or into and through the intact skin (not to scale), and (E) Illustrates the penetration of the vesicles through hair follicle. Adapted from El Maghraby et al. [78].

delivery of drugs by lowering the permeability barrier of the skin and interacting with the SC *in vitro* [29]. On the other hand, studies also reported that for the drug molecules to be effectively transported across the SC, they must be entrapped within the lipid vesicles, suggesting that the vesicles are not considered as penetration enhancers, but they act as drug carrier systems [1].

3. **Fusion with the SC and/or vesicle adsorption to cells of SC:** The cells of SC may fuse and mix with lipid vesicles increasing drug partitioning into the skin. Otherwise, the lipid vesicles may adhere to the SC surface via adsorption mechanism and subsequently, drug partition inside the SC cells could happen. Thus, lipid vesicles could fuse with SC where they dissolve and unite with the membrane structure [30].

4. **Intact vesicular penetration mechanism into the skin**: Studies on liposomes based on electron micrography showed intact liposomal vesicles deep in the dermis. In these studies, the authors postulated that liposomal drug carriers could penetrate the epidermis. In addition, it was shown that vesicles can penetrate a ruptured or diseased SC as in case of eczema but cannot transport a skin with psoriasis or hyperkeratosis conditions [31]. On the other hand, Zellmer et al. [32], and Korting et al. [33] indicated that there was no evidence of intact liposomal carrier penetration after skin application of liposomes made from DMPC "1,2-dimyristoyl-sn-glycero-3-phosphocholine" or soy-lecithin.

5. **Mechanism of transfersome transport through the stratum corneum:** Transfersomes are of high surface hydrophilicity which respond to the hydration gradient across dermal tissue. They propel the vesicles through the transcutaneous channels giving transfersome vesicles the chance to act as noninvasive drug carriers. This is due to the fact that transfersome vesicles are of high bilayer membrane flexibility and sufficient skin permeability

where the trans-barrier gradient acts on all skin membrane ingredients simultaneously but not to the same extent. As a result, the membrane changes its local composition under the influence of an anisotropic local (dehydration/hydration) stress, thus acting as a responsible, and smart material. The transfersomal vesicle thus deforms and passes through pores much smaller than the average vesicle diameter spontaneously in a self-regulated manner [34]. Then the hydrostatic pressure difference is responsible for the penetration of intact transfersome vesicles across the SC, i.e., the penetration of ultradeformable vesicles is a result of hydrotaxis and the permeation is governed by principles of elastomechanics [35].

6. **The process of noninvasive transport across the skin consequently involves:**

1. Reversible vesicle mediated opening between epidermal cells and/or lipids "intercellular hydrophilic pathways".
2. Strong response of transfersome vesicles "applied transdermally" to skin hydration gradient which is naturally occurring or an external transdermal electrical gradient.

4. Applications of hydrogels without and with lipid carriers for transdermal delivery of drugs

The different pharmaceutical applications of hydrogels, nanocarriers and their potential combinations are summarized in **Tables 1** and **2**.

4.1. Hydrogels for transdermal delivery of drugs

Application of formulation on skin surface is generally meant for the topical use of dermatological drugs for skin diseases. In this context, hydrogels have been widely studied for topical delivery of drug moieties. Several antifungal and antiinflammatory agents have been successfully formulated into hydrogel products using different polymers [36, 37]. Recently, adhesive hydrogel patches were fabricated, using sodium polyacrylate and carboxymethyl cellulose, for the topical delivery of triclosan in treating acne. *In vitro* permeation studies using hairless mouse skin revealed that a greater amount of drug has been transported into the skin layers [38].

Another application of hydrogel is its usefulness in treating wounds due to burn. The healing rate of these types of wounds is more rapid in a moist environment as compared to the dry technique. Thus, the biocompatible hydrogel polymers are likely to provide moist and healing environment in addition to its potential to protect the wound from bacterial infection. Moreover, these hydrogels could promote fibroblast proliferation and compensate fluid loss from body due to wound exudation. The hydrogels also allow greater entrapment of drug and provide controlled release, which favor rapid healing. Several hydrogel based formulations have demonstrated their potential in healing the skin wounds. Chitosan hydrogels have been widely used in wound healing applications, where they are not only a vehicle but also a medicament [39]. The ideal characteristics such as hemostasis,

Polymer	Type	Drug	Membrane /animal	Formulation type	Inference	References
Agarose	Natural	Alfuzoisn	Sprague-Dawley rats	Hydrogel patch	Prototype transdermal patch prepared with agarose successfully delivered alfuzosin in rats using iontophoresis	[68]
Chitosan	Natural	Berberine	Wistar rat skin	Hydrogel	Increased the permeation and skin deposition in presence of enhancers	[45]
		Liodocaine	Human	Hydrogel	Combination of chitosan membrane and chitosan hydrogel is a good transparent system for controlled drug delivery	[49]
		Diltiazem	Albino rats	Matrix/ membrane	Prolonged steady state drug plasma concentration was observed in membrane permeation controlled system	[46]
		Propranolol	Porcine skin	Hydrogel	Chitosan-laurate and chitosan-myristate hydrogels enhanced the drug diffusion through the skin	[48]
Dextran	Natural	Vitamin E	Rabbit skin	Hydrogel	Enhance the deposition in the skin and increase the stability	[50]
HEC/HPC	Natural	Prochlorperazine	DDY mice	Hydrogel	Pharmacodynamic activity shows the strong inhibitory effects after 4 h of application and extended over a period of time	[52]
Pectin	Natural	Chloroquine	Sprague-Dawley rat	Matrix patch	Plasma concentration of chlorquine by transdermal delivery was comparable to IV infusion	[51]
Poloxamer	Synthetic	Insulin	Sprague-Dawley rats	Hydrogel	Poloxamer hydrogels system could be used for the transdermal iontophoretic delivery of insulin	[119]
		Capsaicin	Wistar rats	Hydrogel	Significant enhancement in capsaicin delivery and greater pharmacodynamic effect by hydrogels compared to cream	[66]

Polymer	Type	Drug	Membrane /animal	Formulation type	Inference	References
Polyvinyl alcohol	Synthetic	Captopril	Wistar rat	Hydrogel	Transdermal delivery of captopril is significantly improved by iontophoresis	[69]
		Testosterone	Sprague-Dawley rats	Hydrogel	Controlled transdermal delivery systems can be developed using polyvinyl alcohol	[57]
Polyacrylamide	Synthetic	Salicylic acid	Hairless pig skin	Hydrogel	The diffusion of salicylic acid from the hydrogel is influenced by the cross-linking density, and applied electric field strength	[70]
pHEMA	Synthetic	Theophylline	Human	Hydrogel disc	Single application of the hydrogel disc provides therapeutically effective concentration of theophylline in 24 h and is maintained for days	[53]
Polyacrylamide, pHEMA, carbopol 934	Synthetic	Peptides	Hairless rat skin	Hydrogel	Permeability coefficient decreases with increase in molecular weight	[71]
PVP, HPC	Synthetic	Nalbuphine	Hairless mice	Hydrogel	Iontophoresis significantly increased the permeation nalbuphine from the formulated hydrogels	[72]
Alginate-Pluronic F127 composite	Semi synthetic	Selegiline	Porcine skin and nude mouse skin	Hydrogel	Linear permeation profile observed suggests the successful transdermal delivery of selegiline	[67]

Abbreviations: HEC, hydroxyethyl cellulose; HPC, hydroxypropyl cellulose; pHEMA, poly(2-hydroxyethyl methacrylate); PVP, poly vinyl pyrrolidone.

Table 1. Particulars of selected transdermal permeation studies carried out using hydrogels.

bacteriostasis, biocompatibility, biodegradability, etc. have made hydrogels an excellent material for wound dressing. Polyvinyl pyrrolidone-based hydrogels were also developed and employed for the successful application of honey in wound treatment, which exhibited greater healing compared with silver sulphadiazine cream [40]. This hydrogel is also utilized in the application of iodine [41]. Hydrogels of alginate, cellulose, and poloxamer were also used in the treatment of wounds [42–44].

The transdermal route is considered a promising path for delivery of molecules into the systemic circulation. This route overcomes major limitations of oral therapy and provides steady state drug delivery. In this context, hydrogels have played an integral role in the progress of

Formulation	Drugs	Model used	Major outcome	References
Chitosan hydrogel	Berberine	*In vitro*	Treatment of Leishmaniasis	[45]
		In vivo		
Chitosan hydrogel	Diltiazem HCl	Diffusion controlled	Systems are capable of achieving the effective plasma concentration for a prolonged period	[46]
		Membrane controlled		
Chitosan hydrogel	Propranolol HCl	*In vitro* permeation	Hydrogels provided more transcutaneous permeation of propranolol hydrochloride than the corresponding solution	[48]
Dextran hydrogels TTS	Vitamin E	*In vitro*	Improved Vitamin E poor stability and increased its topical delivery	[50]
Pectin hydrogel	Chloroquine	*In vivo*	The transdermal management of malaria	[51]
Acrylate hydrogel discs	Theophylline	Clinical study in preterm infants	Therapeutic concentrations of theophylline were achieved and maintained for up to 15 days after repeated application of discs	[53]
Poloxamer hydrogel	Piroxicam	*In vitro*	Various nonionic surfactants improved drug permeation across rat skin	[61]
Liposome suspension	Curcuminoids	*In vitro*	Increased cellular uptake and transdermal delivery of curcuminoids	[76]
			Enhanced and prolonged cytotoxic effects of curcuminoids	
Liposome gel	Triamcinolone acetonide	*In vitro*	Liposomal gel increased the concentration of triamcinolone acetonide five times higher in the epidermis and three times higher in the dermis, than application of the free drug gel	[79]
Liposome suspension and emulsion vehicle	Interferon	*In vivo* antimicrobial activity	Liposomes were better than w/o emulsion for treatment of cutaneous Herpes in guinea pigs	[80]
Liposomes; Cream	Tetracaiene	Clinical study	Liposomal tetracaine-produced anesthesia, which lasted at least 4 h after 1 h application under occlusion	[83]
			The cream formula has no effect	
Liposomal suspension	Miconazole nitrate	*In vitro*	Enhanced skin permeation and retention using liposomes compared to commercial cream	[85]
Liposomes suspension	Carboxyfluorescein	*In vitro*	Selective targeting into pilosebaceous units of hamster ears	[86]
Liposomes in chitosan/gelatin crosslinked with glutaraldehyde hydrogels	Calcein	*In vitro*	Controlled release	[92]

Formulation	Drugs	Model used	Major outcome	References
Liposomes in carbopol hydrogel and hydroxyethyl cellulose gels	Calcein and greseofulvin	*In vitro*	Improved release from carbopol gels compared to hydroxyethyl cellulose gels	[93]
Liposomes in chitosan gel	Carboxyfluorescein	*In vitro*	Delayed release	[94]
Proliposome monophasic system and PEG based ointment	Levonorgestrel	*In vitro* *In vivo*	The higher potential of proliposomal system for efficacious transdermal delivery of hydrophobic drugs compared to PEG ointments	[96]
Proliposomal gel	Exemestane	*In vivo*	Efficient carriers with high potential for the enhanced transdermal delivery	[97]
Niosomes, liposomes, and transferesomes	Tetanus toxoid	*In vivo*	Niosomes and liposomes showed weak immune response transdermally compared to transferesomes in albino rats	[99]
Proniosome gel	Estradiol	*In vitro*	Encapsulation efficiency was 100% High skin permeability	[100]
Niosomes	Lidocaine	*In vitro*	High flux across model lipophilic membrane High flux and shorter lag time across mouse abdominal skin compared with liposomes	[16]
Niosomes in chitosan gel	Methotrexate	Clinical study	Enhanced treatment of psoriasis	[101]
Niosomes in carbopol gel	Celecoxib	*In vitro* *In vivo*	Improved drug localization in deep skin layers and muscles Significant reduction in rat paw edema compared to conventional carbopol gels	[102]
Niosomes and liposomes	Tretinoin	*In vitro* *Ex vivo*	Niosomes give higher cutaneous drug retention than both liposomes and Retin A®commercial formulation	[105]
Proniosome in carbopol, CMC, and HPMC hydrogels	Ketorolac	*In vitro*	Enhanced drug release from niosomes prepared with Span 60 Improved absorption of celecoxib Improved bioavailability	[106]
Niosomes in sodium alginate and CMC hydrogels, emulgels and proniosomes	Ketorolac tromethamine	*In vitro*	Improved skin permeability from niosomal gels and emulgels Delayed drug permeability from proniosomes Enhanced antiinfalmmatory effects using rat paw edema model	[27]

Formulation	Drugs	Model used	Major outcome	References
Transferesomes "Transfersulin"	Insulin	*In vivo*	Only transfersulin produced marked hypoglycaemic effects in mice however, mixed micelles, liposomes, or insulin solution did not produce any hypoglycemic effect after transdermal application	[108]
		Clinical study	Transfersulin could be administered over an area of 40 cm^2 or less to deliver the basal daily supply of insulin to a typical type I diabetes patient	
Transfersomes	Triamcinolone acetonide	*In vivo*	Transfersomes of Triamcinolone-acetonide suppresses arachidonic acid-induced skin edema longer than the marketed products for topical treatment	[113]
Transfersomes	Hydrocortisone	*In vivo*	Therapeutic concentration lowered significantly to 0.1% after topical application to mice	[114]
Transfersomes	Dexamethasone	*In vivo*	Therapeutic concentration lowered to below 0.01% after topical application to mice	[114]
Transfersomes "cationic type"	DNA vaccines	*In vivo*	Induced strong humoral and cellular immune response after topical application to mice	[115]
Tranfersomes in carbopol hydrogel	Sertraline	*In vitro*	Enhanced release and permeability of poor soluble drug	[116]
		In vivo	No skin irritation after topical application to guinea pigs	
			Better antidepressant activity of transferosomal gel compared to the control gel	
Protransfersome gel	Levonorgestrel	*In vitro*	Better entrapment efficiency, better skin permeation and better stability compared to proliposomes	[117]
Proliposomal gel		*In vivo*	Eight-fold increase in peak plasma concentration of levonorgestrel after topical application to female rats	
Protransfersome gel	Cisplatin	*In vitro*	Improved site-specific and localized drug action in the skin	[118]
		In vivo	Protection against cisplatin genotoxicity and cytotoxicity	

Table 2. Pharmaceutical application of hydrogels, nanocarriers and their combinations.

transdermal drug delivery. This versatile hydrogel drug delivery system has been successfully utilized for the delivery of molecules into and through the skin. The use of hydrogels in transdermal delivery is primarily owing to their intrinsic properties such as controlled/sustained drug release for transdermal transport, higher stability, greater percutaneous absorption, desired functionality, and nontoxic nature. Additional advantages such as ease

of application, better skin compliance, skin hydration, improved drug effectiveness, convenience, compliance, safety and ease of fabrication of patch, and greater swelling have made them to triumph over other polymeric materials. Both passive and active delivery approaches have been used for the transdermal delivery of molecules by fabricating patches or gels or carriers using hydrogels (**Table 1**).

Prospective of hydrogels in the transdermal delivery of drug molecules by passive process has been extensively studied in the last few decades. Both natural and synthetic polymers were widely used in developing transdermal delivery system for passive delivery. The potential of chitosan in developing hydrogel-based transdermal drug delivery systems was demonstrated in several investigations. Tsai et al. have successfully delivered berberine through the skin by incorporating in a hydrogel formulation for the treatment of leishmaniasis [45]. This polymer was also utilized in developing hydrogel-based matrix diffusion controlled and membrane permeation controlled transdermal systems of diltiazem. The *in vivo* permeation studies in rat model signified the prospective of this polymer to deliver effective concentration of drug for a prolonged period of time [46]. Several studies were also reported wherein chitosan-based hydrogel transdermal systems have been successfully utilized [47]. Hydrogels of this polymer prepared by physical crosslinking method were utilized for transdermal delivery of propranolol [48]. Multiple functions of chitosan as a rate controlling membrane and as reservoir in the transdermal delivery system were also demonstrated [49].

Cassano et al. have developed dextran hydrogel transdermal system, which deposits greater amount of vitamin E in the skin and enhances the vitamin stability [50]. This transdermal system was prepared by adding the methacrylic groups on dextran and the product (methacrylated dextran) was further copolymerized with aminoethyl methacrylate. This is then esterified with transferulic acid to protect the vitamin E from photodegradation. Pectin, another polysaccharide, was also utilized in developing hydrogel matrix patch for the transdermal delivery of chloroquine [51]. Similarly, hydrogels of cellulose polymers (hydroxyethyl cellulose and hydroxypropyl cellulose) have also demonstrated their prospective in preparing different transdermal delivery systems [52].

Acrylate polymers were also extensively studied for their potential in developing various transdermal systems. A hydrogel disc consisting of 90% w/w poly-2-hydroxyethyl methacrylate, crosslinked with 10% w/w polytetramethylene oxide was used for the transdermal delivery of theophylline in infants (**Figure 5**). The repeated application of discs has delivered therapeutic concentrations of theophylline and maintained for a period of 2 weeks [53]. In another attempt, various poly(hydroxyethyl methacrylate) copolymeric hydrogels were synthesized using 2-hydroxyethyl methacrylate, methacrylic acid and *N*-[3-(dimethylamino)propyl] methacrylamide by redox free radical bulk polymerization technique and assessed for their prospective in transdermal delivery system using salbutamol sulphate [54]. Hydrogel prepared with different latex particles (polyacrylic acid-*co* sodiumacrylate, polyacrylic acid-*co*-2-ethylhexyl acrylate and poly*N*-isopropylacrylamide) within carboxymethyl cellulose matrix displayed thermosresponsive release of caffeine, signifying its potential in developing transdermal delivery systems [55]. There are reports wherein composite membrane of crosslinked poly(2-hydroxyethyl methacrylate) has been developed and successfully employed as rate controlling barrier for membrane transdermal drug delivery systems [56].

Figure 5. Hydrogel disc occluded with a transparent dressing on the abdomen of an infant of 29 weeks gestation. Adapted from Cartwright et al. [54].

Polyvinyl alcohol-based hydrogels were also developed and evaluated for the transdermal delivery of testosterone, both *in vitro* and *in vivo*. It was observed that the prepared hydrogel effectively delivering drug into the systemic circulation indicates the potential of this polymer in developing a transdermal system [57]. pH sensitive hydrogels have also been developed using poly-electrolyte, poly(acrylamide: maleic acid) for the delivery of terbinafine (cationic) wherein drug release was influenced by pH of media [58]. Alternatively, ionic polymers like N vinyl-2-pyrrolidone and methylene succinic acid have been successfully employed in developing the transdermal drug delivery systems [59]. Reports also exist wherein hydrogels are used to fabricate transdermal patch for the delivery of vaccine [60].

Poloxamer is probably one of the most extensively studied polymers in transdermal drug delivery. This polymer has demonstrated its potential as a transdermal vehicle for delivery by passive and active approaches [61, 62]. Several molecules of different categories are successively delivered using this polymer. The ideal concentration for the topical application of this polymer was found to be ~20% [63]. The prospective of this polymer in enhancing the transdermal delivery of molecules, providing controlled zero order release, prolonging therapeutic effect, delivering macromolecules was documented in the literature [64–66]. Composite thermogels of poloxamer were also utilized in transdermal delivery of certain molecules [67–72].

4.2. Liposomes for transdermal delivery of drugs

Liposomes are widely used as carriers due to the small size, both hydrophobic and hydrophilic properties, biodegradability, and high safety [73]. Several studies demonstrated the

great potential of liposomes as lipid vehicles, which are able to enhance drug permeation through the skin and also can act as local depot for the drug to sustain and control its delivery [74, 75].

A recent investigation showed that liposomes were induced to deliver and release very poor water-soluble drugs such as curcuminoids at a controlled rate to targeted cells [76]. Authors have evaluated and proved the contribution of liposomal curcuminoids to the antiproliferation as well as to the apoptosis of breast cancer cell lines. Another investigation done by El Maghraby et al. about the effects of liposomes after topical application indicated that liposomes could exert different functions, which may be local or enhanced systemic absorption [77]. They can improve drug deposition into the skin at the site of action providing local effects and reducing systemic absorption and drug side effects. Moreover, the liposomes as a drug carrier can provide high potential for transdermal delivery and targeted delivery to skin appendages. Liposomes as lipid carriers for triamcinolone acetonide showed increased drug concentration in SC as well as in the dermis by fivefold compared with a standard ointment of the same drug [78]. In one more research by the same authors, the incorporation of these liposomes encapsulating triamcinolone acetonide in a gel dosage form resulted in nonsignificant differences in drug concentrations in SC and dermis when compared with a gel containing liposome components as well as the free drug at the same concentrations [79]. Moreover, the topical delivery of interferon (peptide drug) from liposomes was greater than that from emulsion form (w/o) or aqueous solution when *in vivo* applied to cutaneous herpes simplex virus guinea pig model [80]. Egbaria et al. had employed a tape striping technique on guinea pig skin *in vitro* and liposomes showed increased deposition and accumulation of interferon into SC and deeper stratum [81]. It has been demonstrated that liposomes with lipophilic drugs such as progesterone or hydrocortisone "entrapped in the bilayer structure of the lipid vesicles" permeate the skin like the free drug itself. Conversely, glucose (highly polar molecule) enclosed in the aqueous compartment of liposomal vesicle was found not available for transport across the skin. It was suggested that direct transfer of the drug molecule from liposomal suspension to the skin occurs only when the drug is entrapped within the lipid bilayer [82]. Liposomes can also improve the local anesthetic activity of tetracaine and lidocaine where the cream formula has no effects [83, 84]. Ethanol containing liposomes (Ethosomes) enhanced the intensity and duration of benzocaine local anaesthetic effect [75]. The localizing effects or efficiency of liposomes was dependent on the lipid composition and method of preparation. In addition, the liposomal miconazole nitrate has shown to facilitate the localized drug delivery and improved its availability by a controlled release pattern, which enhanced the treatment of deep fungal infections [85]. In addition to the enhanced localized accumulation effects of liposomes, they can target drugs to skin appendages and improved transdermal delivery of drugs. Lieb et al. showed selective carboxyfluoresce in liposomes targeting into the pilosebaceous follicles of the hamster ears when compared with aqueous or alcoholic solutions containing 10% ethanol or even with 0.05% sodium lauryl sulphate, or propylene glycol donor vehicles [86]. Due to the highest follicular density in hamster skin and hairless mice skin as compared to human skin, a higher drug accumulation was observed in their skin suggesting the drug deposition from liposomes through the

follicular pathway [87]. This is true for hydrophilic drugs encapsulated into liposomes; however, highly lipophilic drugs could target the sebaceous gland and no significant differences in drug accumulation was observed when liposomes were compared with mixed micelles or ethanolic gels [88].

Liposomes as nanocarriers were reported to improve transdermal delivery of drugs. Ganesan et al. observed that after finite dose applications of lipophilic drugs to hairless mouse skin, greater amounts were delivered from liposomal vesicles compared to aqueous vehicles [82]. In addition, vesicles of fluid liposomes produced high percutaneous absorption and tissue distribution rather than skin accumulation [89]. Conversely, there are some reports which generally excluded a liposome transport process across the skin where they attributed their positive influence on increased skin permeability to a localizing effect as the drugs accumulated on skin surface or the upper layers of SC, hence, favoring their diffusion. This was done for lipophilic drugs such as ketoprofen where the drug was first complex with cyclodextrin and then encapsulated into liposomes [90, 91].The major aim of inclusion of liposomes into a hydrogel was to control the release of drugs and to stabilize the liposomal bilayer structure by creating a protective film on surfaces of liposomal vesicles. Ciobanu et al. had formulated chitosan/gelatin hydrogel by double crosslinking with glutaraldehyde and sodium sulphate/sodium tripolyphosphate to be used as matrices for the inclusion of calcein loaded liposomes [92]. Calcein, a model hydrophilic drug in small unilamellar vesicles (SUVs) and multilamellar vesicles (MLVs), was released from polymeric hydrogels for several days to weeks. In another study, liposomes prepared from phosphatidylcholine (PC) or distearoylglycero-PC and cholesterol (DSPC/Chol), and incorporating calcein or greseofulvin were formulated by thin film hydration technique. Calcein and greseofulvin release from liposomal gels using carbopol polymer was faster compared to hydroxyethyl cellulose and mixture gels [93]. Billard et al. prepared an innovative hybrid formulation, which was composed of a water-soluble model molecule "carboxyfluorescein" in liposomal vesicles and dispersed in tridimensional matrix of chitosan hydrogel [94]. Liposome dispersions in chitosan gel in water did not affect the gelation process absolutely. The release of carboxyfluorescein was delayed from the hybrid liposomes in hydrogel systems compared to the hydrogel matrix without lipid vesicles.

Taking into consideration the potential use of proliposomes for transdermal delivery of drugs, topical application of nicotine-loaded proliposomes under occlusive conditions was evident to sustain nicotine delivery across the skin [95]. In addition, Deo et al. had proven that the system proliposomes was superior to PEG-based ointment for the transdermal delivery of levonorgestrel (model hydrophobic drug) [96]. Moreover, proliposomal gels prepared and evaluated for transdermal bioavailability of exemestane (a novel steroidal aromatase inactivator used in the treatment of advanced breast cancer) were compared with control oral suspension of the drug [97]. Proliposomal gels offered high potential and was efficient carriers for the enhanced sustained transdermal delivery of Exemestane. Proliposomal gel showed greater percentage of inhibition of edema when compared to marketed diclofenac gel in the treatment of rheumatoid arthritis. They also exhibited superior stability when compared to traditional liposomes, thereby increasing its potential application in transdermal delivery systems [98].

4.3. Niosomes for transdermal delivery of drugs

One of the most useful advantages of niosomes is that they greatly enhance the uptake of drugs via transdermal route. Transdermal drug delivery using niosomes is widely used in cosmetics. Niosome-entrapped antibiotics were successfully used to treat acne. The penetration of drugs into the skin was greatly enhanced as compared to unentrapped drug. The noninvasive transdermal vaccination via topical application of niosomes is also being researched. Gupta et al. has shown that niosomes of tetanus toxoid (along with liposomes and transfersomes) can be used for transdermal immunization [99]. However, the current results of niosomal topical immunization allow only a weak immune response, and thus more research needs to be done in this field. The encapsulation efficiency of estradiol in proniosomes made from Span 40, Span 60 was 100%, and the permeability of the drug across the nude mouse skin was high as reported by Fang et al. [100]. Lidocaine and lidocaine hydrochloride loaded nonionic surfactant vesicles were formulated using Tween 20 and cholesterol, and tested for their local anesthetic effects [16]. The diffusion experiments indicated high flux of charged lidocaine (lidocaine hydrochloride) through a model lipophilic (Silastic™) membrane and found to be possible only after vesicle formation. In addition, the permeation of the drug from niosomes through mouse abdominal skin showed higher flux and shorter lag times compared with liposome formulations. Methotrexate-loaded niosomal vesicles in chitosan gel were used in the treatment of psoriasis by double blind, placebo controlled study on healthy human volunteers and psoriasis patients [101]. Kaur et al. showed 6.5 times higher drug deposition in deep skin layers and muscles from celecoxib niosomal gels compared with carbopol gel indicating better drug localization with niosomal gel [102]. In the same study, a significant reduction of rat paw edema was resulted after administration of niosomal formulation compared to that of applying conventional gel. Psoriasis area severity index (PASI) was the measure for the severity of the disease. The reduction in PASI scores after 12 weeks of niosomal methotrexate gel topical application was found to be threefold with better clinical efficacy, tolerability and patient compliance. Niosomes were also included in the treatment of vitiligo. Elastic cationic niosomes composed of tween 61/cholesterol/dimethyl dioctadecyl ammonium bromide at 1:1:0.5 molar ratio were effectively used for the dermal delivery of tyrosinase encoding plasmid. Their percutaneous absorption across exercised rat skin showed greater flux compared with the nonelastic niosomes. The application of pMEL34-loaded elastic cationic niosomes in melanoma cell lines gave four times increase in tyrosinase gene expression compared with the free and the plasmid in nonelastic niosomes which lead to efficient topical delivery in vitiligo therapy [103]. Tretinoin (vitamin A metabolite), is topically applied for the treatment of skin diseases such as acne, psoriasis, and photoaging. The drug has high chemical instability and skin irritation, which limited its topical administration [104]. However, the drug transdermal delivery using niosomes and liposomes as vehicle carriers showed more upper cutaneous drug retention than commercial formulation "RetinA®" [105].

Ketorolac proniosomes of Span 60 and Tween 20 and mixed with carbobol, carboxymethyl cellulose (CMC) or hydroxypropylmethyl cellulose (HPMC) hydrogels were evaluated by Alsarra et al. [106]. They found that the drug release was higher from niosomes prepared with Span 60 than from the HPMC gel as control due to the formation of elution channels

and loss of vesicular structure. However, authors did not give any scientific reason for that explanation. Conversely, Mokhtar and Shehata showed the formation of greater vesicles after niosome/hydrogel admixture and explained this by the vesicles crack and reformation during the preparation procedure, which improved ketorolac tromethamine leakage to the outside vehicle (**Figure 6**) [27]. A recent study indicated that no percutaneous permeation

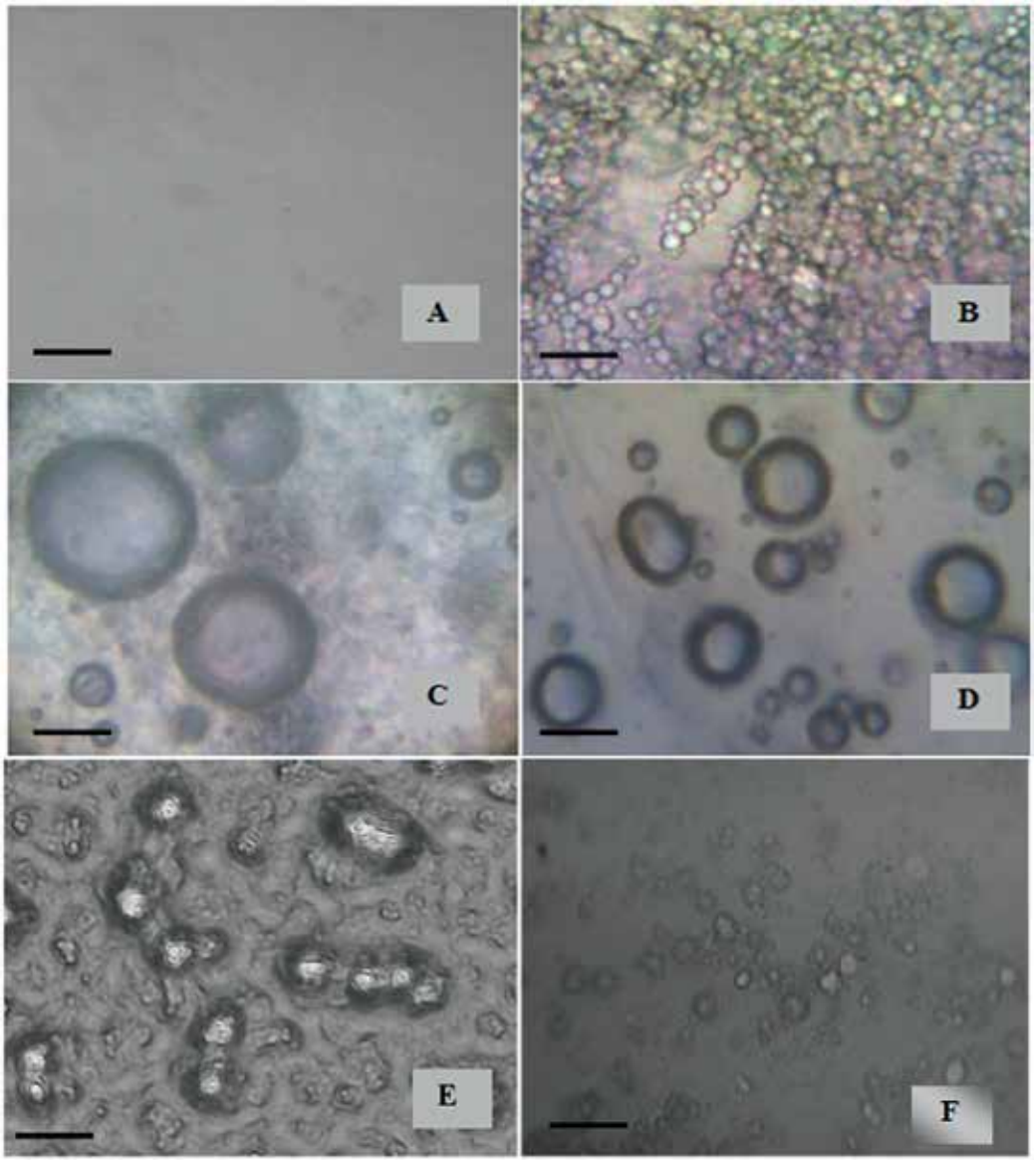

Figure 6. Micrographs (magnification power is 40×) of alginate gel (A), emulgel (B), niosomal gel (C), niosomalemulgel (D), proniosomes (E) and niosomes suspension (F). Adapted from Mokhtar and Shehata, its first publication in J Drug Del Sci Tech. With copywriter permission [27].

was achieved when using submicellar solution of pluronic and sucrose esters containing free Sulfadiazine sodium or when the skin was pretreated with blank niosomes or submicellar solutions of the surfactant free of the drug and only the drug niosomal vesicles can do enhancing the skin permeability [107].

4.4. Transfersomes for transdermal delivery of drugs

The use of transfersomes technology is an innovative approach to increase the transport of substances through the skin. Nonocclusive administration of drug moieties using transfersomes is useful for noninvasive drug delivery of therapeutic proteins transdermally. Transdermal administration of diverse molecules with ultradeformable vesicles also permits targeted skin delivery or preferential delivery into the deep tissue of the dermis under the site of application.

Transferesomes have high suspension-driving pressures, which can eliminate the mismatch effect of carrier and pore size. This can be considered true for the transfersomes with a size not more than threefold the size of transdermal pores. The transcutaneous glands or hair follicles are well known to play a role in the process of molecular diffusion across the skin. However, such channels are too impermeable to large molecule such as insulin transdermally [108]. This could explain why a topically applied insulin in the mixed-lipid micelles or liposomes had nonsignificant antidiabetic effects. Transfersomes have a higher flexibility and stability than liposomes which allows them to penetrate through the human skin. The incorporation of insulin molecules into the vesicle of these lipid particles (transfersulin) results in a considerable insulin transport through the skin into the blood stream in mice and to a lower extent in humans [108]. Moreover, transfersomes can deliver an antigen to the lymphatics from where they can be transferred to lymph nodes. The antigens are then phagocytosed and presented to the T-cells in the lymph nodes. Thus, transfersomes are very important carriers for transdermal delivery of antigens and are under investigation for use in human vaccination development [109–110]. The transdermal enhancement of drug permeability using these ultradeformable vesicles does not depend upon the concentration gradient and mainly work on the principle of hydrotaxis and elastomechanics as reported by Kumar et al. [110].

The transfersomes deform and reform but remain intact during the transportation of the loaded drug to the target tissues under the skin application site. These carriers which are driven by the local water gradient across the skin barrier could be engineered to achieve a localized and high drug concentration at the application sites and deep inside the dermis. This way of drug administration can abolish any local and/or systemic adverse drug effects, and often increase the drug potency. Also, the local clearance through the cutaneous microcirculation is avoided, which permits the drug delivery deep into the muscles or joints. Therefore, transfersomes greatly increase the ratio of drug concentration in the target tissue more than the systemic drug concentration when compared to other formulations "liposomes or niosomes of the drug", which inherently enhances the drug safety profiles. In addition, the transfersomes could be targeted to the macrophages if suitably designed, thus, they have sufficient immune-adjuvant action. After topical application of transfersomes, they showed comparable titer values with their intradermal counterparts; however, they required lesser dosages [109]. Transfersomes encapsulating bacterial gap junction proteins gave rise

to circulatory antibodies against the gap junction proteins when applied topically. It was interesting that the antibodies titer value was found to be greater than that produced after subcutaneous injection of the gap junction proteins [111].

The study done by Kim et al. has vividly shown that the ultradeformable cationic vesicle (cationic transfersomes) formulation has several characteristics of being a good nonviral vector system, for instance, high transfection activity and long retention time [112]. This formulation was prepared using a cationic lipid, 1,2-dioleoyl-3-trimethyl- ammonium propane chloride (DOTAP) and sodium cholate, and it was found to be capable of transfecting several cell lines as well as penetrating the intact skin of mice when transdermally applied. In addition, this formulation is found to be stable and has shown 6 days of gene expression, an essential factor for an efficient gene therapy. Therefore, it is developed further as either invasive or noninvasive gene delivery system.

Topical usage of triamcinolone acetonide with ultradeformable vesicles resulted in reduction of the necessary drug dose to the levels of 0.01 wt% (10-fold lower drug dosage compared to cream or lotion preparations). Epicutaneous drug administration of these highly deformable carriers was also observed to prolong the biological response time markedly and to increase the reproducibility of the biological drug action [113]. In another study done by Cevc and Blume, either hydrocortisone or dexamethasone formulations in a suspension of very deformable vesicles (transfersomes) have significantly lowered the therapeutically relevant concentration range to 0.1 wt% and may be lower than 0.01 wt%, respectively [114]. This is lower than the respective concentrations used in commercial hydrocortisone and dexamethasone products "0.25–2.5 wt% (mainly 1%) and 0.03–0.1 wt%, respectively". The biological response time for the local corticosteroid action was prolonged and the sensitivity of dexamethasone in very deformable vesicles to abrasion was diminished. These findings confirmed the expectation that very deformable carriers offer several advantages for transdermal delivery of corticosteroids into the skin. Cationic transfersomes were formulated and tested for topical immunization using cationic transfersomes based DNA vaccine. They were capable of inducing strong humoral and cellular immune response and offered all the advantages of DNA vaccines, and overcome the disadvantages of classical invasive methods of vaccination [115]. Transfersomal gels prepared by Gupta et al. using Span 80, soya lecithin, and carbopol was found to enhance skin delivery of sertraline (antidepressant drug) due to excellent release and permeation of the drug [116]. They found no skin irritation after transdermal application of the gel formulation containing transfersomes. Since a properly designed ultradeformable vesicles could even claim the transport of drug (of different sizes, even large peptide or DNA) equivalent to the subcutaneous injection and this technology may provide effective tool for noninvasive therapy. The enhanced transdermal delivery of bioactive molecules by transferesomes also opens new challenges for the development of novel therapies.

Protransfersomal gels of levonorgestrel were developed for transdermal contraceptive use [117]. Authors indicated that the protransfersomal gels possessed better stability, better skin permeability, and greater encapsulation efficiency than proliposomal formulation. Recently, protransfersome showed better noninvasive delivery of cisplatin in cutaneous squamous cell carcinoma [118]. They have improved site-specific and localized drug action in the skin; hence, they provide a better option for dealing with serious diseases of skin such as squamous cell carcinoma. In addition, they had high potential as topical drug delivery system with protection against genotoxicity and cytotoxicity of cisplatin.

5. Conclusion

This review article provides valuable information regarding the hydrogels, emulgels and their combination with lipid nanocarriers "liposomes, niosomes and transferesomes" for topical and transdermal drug delivery. It has been shown that all of these systems have great potentials, being able to deliver both lipophilic and/or hydrophilic active ingredient via transdermal route of administration. The inclusion of lipid vesicles into hydrogels could enhance their stability, prolong drug release, enhance transdermal permeability, and increase localization of the drug in the skin. Proforms of the lipid vesicles could also improve site-specific and localized drug action in the skin. In order to optimize these drug delivery vehicles, a greater understanding of polymer and biological interaction mechanisms is required. Hydrogel combinations with lipid nanocarriers could be of great potential for increasing transdermal drug delivery and clinical research in the future.

Declaration of interest

Authors report no conflicts of interest. The authors alone are responsible for the content and writing of this article.

Author details

Mahmoud Mokhtar Ibrahim[1,2]*, Anroop B. Nair[3], Bandar E. Aldhubiab[3] and Tamer M. Shehata[1,3]

*Address all correspondence to: mahmoktar@yahoo.com

1 Department of Pharmaceutics and Industrial Pharmacy, Faculty of Pharmacy, Zagazig University, Zagazig, Egypt

2 Department of Pharmaceutics, Faculty of Pharmacy, Delta University, Egypt

3 Department of Pharmaceutical Sciences, Faculty of Clinical Pharmacy, King Faisal University, Al Hassa, Kingdom of Saudi Arabia

References

[1] Hofland HEJ, Bouwstra JA, Bodde HE, Spies F, Junginger HE. Interaction between liposomes and human stratum corneum *in vitro*: Freeze fracture electron microscopical visualization and small angle X-ray scattering studies. British Journal of Dermatology. 1995;**132**:853-866

[2] Justin-Temu M, Damain F, Kinget R, Van Den Mooter G. Intravaginal gels as drug delivery systems. Journal of Women's Health. 2004;**13**(7):834-844

[3] Calligaris S, Pieve SD, Arrighetti G, Barba L. Effect of the structure of monoglyceride-oil-water gels on aroma partition. Food Research International. 2010;**43**(3):671-677

[4] Rubinstein M, Colby R. Polymer Physics. New York: Oxford University Press; 2003. pp. 1-38

[5] Kim TH, Kim DG, Lee M, Lee TS. Synthesis of reversible fluorescent organogel containing 2-(2′-hydroxyphenyl)benzoxazole: Fluorescence enhancement upon gelation and detecting property for nerve gas simulant. Tetrahedron. 2010;**66**(9):1667-1672

[6] Gronwald O, Snip E, Shinkai S. Gelators for organic liquids based on self-assembly: A new facet of supramolecular and combinatorial chemistry. Current Opinion in Colloid & Interface Science. 2002;**7**(1-2):148-156

[7] Madan M, Bajaj A, Amrutiya N. Formulation and in vitro evaluation of topical emulgel containing combination of a local anaesthetic and an anti-inflammatory drug. Indian Journal of Pharmaceutical Education and Research. 2009;**43**(4):351-359

[8] Peppas NA, Bures P, Leobandung W, Ichikawa H. Hydrogels in pharmaceutical formulations. European Journal of Pharmaceutics and Biopharmaceutics. 2000;**50**(1):27-46

[9] Hoare TR, Kohane DS. Hydrogels in drug delivery: Progress and challenges. Polymer. 2008;**49**(8):1993-2007

[10] Shokri J, AzarmiSh, Fasihi Z, Hallaj-Nezhadi S, Nokhodchi A, Javadzadeh Y. Effects of various penetration enhancers on percutaneous absorption of piroxicam from emulgels. Research of Pharmaceutical Sciences. 2012;**7**(4):225-234

[11] Ostro MJ, Cullis PR. Use of liposomes as injectable drug delivery systems. American Journal of Hospital Pharmacy. 1989;**46**:1576-1587

[12] Macquaire F, Baleux F, Giaccobi E, Huynh-Dinh T, Neumann JM, Sanson A. Peptide secondary structure induced by a micellar phospholipidic interface: Proton NMR conformational study of a lipopeptide. Biochemistry. 1992;**31**:2576-2583

[13] Liu F, Huang, L. Development of non viral vectors for systemic gene delivery. Journal of Controlled Release. 2002;**78**:259-266

[14] Hu C, Rhodes DG. Proniosomes: A novel drug carrier preparation. International Journal of Pharmaceutics. 2000;**206**(1-2):110-122

[15] Shingade GM, AamerQuazi, Sabale PM, Grampurohit ND, Gadhave MV, Jadhav SL, Gaikwad DD. Review on: Recent trends on transdermal drug delivery system. Journal of Drug Delivery and Therapeutics. 2012;**2**(1):66-75

[16] Carafa M, Santucci E, Lucania G. Lidocaine-loaded non-ionic surfactant vesicles: Characterization and in vitro permeation studies. International Journal of Pharmaceutics. 2002; **231**:21-32

[17] Kaur IP, Garg A, Singla AK, Aggarwal D. Vesicular systems in ocular drug delivery: An overview. International Journal of Pharmaceutics. 2004;**269**:1-14

[18] Azmin MN, Florence AT, Handjani-Vila RM, Stuart JF, Vanlerberghe G, Whittaker JS. The effect of non-ionic surfactant vesicle (niosome) entrapment on the absorption and distribution of methotrexate in mice. Journal of Pharmacy and Pharmacology. 1985;**37**(4):237-242

[19] Hofland H, Van der Geest R, Bodde H, Junginger H, Bouwstra J. Estradiol permeation from nonionic surfactant vesicles through human stratum corneum in vitro. Pharmaceutical Research. 1994;**11**:659-664

[20] Devaraj GN, Parakh SR, Devraj R, Apte SS, Rao BR, Rambhau D. Release studies on niosomes containing fatty alcohols as bilayer stabilizers instead of cholesterol. Journal of Colloid and Interface Science. 2002;**251**(2):360-365

[21] Uchegbu IF, Florence AT. Non ionic surfactant, vesicles (niosomes): Physical and pharmaceutical chemistry. Advances in Colloid and Interface Science. 1995;**58**:1-55

[22] Uchegbu IF, Vyas SP. Non-ionic surfactant based vesicles (niosomes) in drug delivery. International Journal of Pharmaceutics. 1998;**172**:33-70

[23] Arunothayanun P, Bernard MS, Craig DQM, Uchegbu IF, Florence AT. The effect of processing variables on the physical characteristics of non-ionic surfactant vesicles (niosomes) formed from a hexadecyldiglycerol ether. International Journal of Pharmaceutics. 2000;**201**:7-14

[24] Yoshioka T, Sternberg B, Florence AT. Preparation and Properties of vesicles (niosomes) of sorbitan monoesters (Span 20, 40, 60 and 80) and sorbitantriester (Span 85). International Journal of Pharmaceutics. 1994;**105**:1-6

[25] Bouwstra JA, Hofland HEJ. Niosomes. In: Kreuter J, editor. Colloidal Drug Delivery Systems. Marcel Dekker Inc.; 1994

[26] Blazek-Welsh AI, Rhodes DG. Maltodextrin-based proniosomes. AAPS Pharmsci. 2001; **3**(1):1-8

[27] Mokhtar M A and Shehata T M. The enhancement of transdermal permeability of water soluble drug by niosome-emulgel combination. Journal of Drug Delivery Science and Technology. 2012;**22**(4):353-359

[28] El Maghraby GM, Barry BW, Williams AC. Liposomes and skin: From drug delivery to model membranes. European Journal of Pharmaceutical Sciences. 2008;**34**:203-222

[29] El Maghraby GM, Williams AC, Barry BW. Skin delivery of oestradiol from deformable and traditional liposomes: Mechanistic studies. Journal of Pharmacy and Pharmacology. 1999;**51**:1123-1134

[30] Honeywell-Nguyen PL, Arenja S, Bouwstra JA. Skin penetration and mechanisms of action in the delivery of the D2-agonist rotigotine from surfactant-based elastic vesicle formulations. Pharmaceutical Research. 2003;**20**(10):1619-1625

[31] Schaller M, Korting HC. Interaction of liposomes with human skin: The role of the stratum corneum. Advanced Drug Delivery Reviews. 1996;**18**:303-309

[32] Korting HC, Zeinicke H, Schafer KM, Falco OB. Liposome encapsulation improves efficacy of betamethasone dipropionate in atopic eczema but not in psoriasis vulgaris. European Journal of Clinical Pharmacology. 1990;**39**:349-351

[33] Zellmer S, Pfeil W, Lasch J. Interaction of phosphatidylcholine liposomes with the human stratum corneum. Biochimica et Biophysica Acta. 1995;**1237**:176-182

[34] Korting HC, Stolz W, Schmid MH, Maierhofer G. Interaction of liposomes with human epidermis reconstructed in vitro. British Journal of Dermatology. 1995;**132**:571-579

[35] Cevc G, Blume G. Lipid vesicles penetrates into intact skin owing to transdermal osmotic gradient and hydration force. Biochimica et Biophysica Acta. 1992;**1104**:226-232

[36] Cevc G. Self-regulating smart carriers for non-invasive and targeted drug delivery. Cellular and Molecular Biology. 2002;**7**(2):224-222

[37] Rodríguez R, Alvarez-Lorenzo C, Concheiro A. Interactions of ibuprofen with cationic polysaccharides in aqueous dispersions and hydrogels. Rheological and diffusional implications. European Journal of Pharmaceutical Sciences. 2003;**20**:429-438

[38] Shishu, Aggarwal N. Preparation of hydrogels of griseofulvin for dermal application. International Journal of Pharmaceutics. 2006;**326**:20-24

[39] Lee TW, Kim JC, Hwang SJ. Hydrogel patches containing triclosan for acne treatment. European Journal of Pharmaceutics and Biopharmaceutics. 2003;**56**:407-412

[40] Wang T, Zhu X, Xue X, Wu D. Hydrogel sheets of chitosan, honey and gelatin as burn wound dressings. Carbohydrate Polymers. 2012;**88**:75-83

[41] Yusof N, Hafiza A, Zohdi RM, Bakar AM. Development of honey hydrogel dressing for enhanced wound healing. Radiation Physics and Chemistry. 2007;**76**:1767-1770

[42] Vogt PM, Reimer K, Hauser J, Rossbach O, Steinau HU, Bosse B, Muller S, Schmidt T, Fleischer W. PVP-iodine in hydrosomes and hydrogel--a novel concept in wound therapy leads to enhanced epithelialization and reduced loss of skin grafts. Burns. 2006;**32**:698-705

[43] Du L, Tong L, Jin Y, Jia J, Liu Y, Su C, Yu S, Li X. A multifunctional in situ-forming hydrogel for wound healing. Wound Repair and Regeneration. 2012;**20**:904-910

[44] Heilmann S, Küchler S, Wischke C, Lendlein A, Stein C, Schäfer-Korting M. A thermosensitive morphine-containing hydrogel for the treatment of large-scale skin wounds. International Journal of Pharmaceutics. 2013;**444**:96-102

[45] Pereira R, Carvalho A, Vaz DC, Gil MH, Mendes A, Bártolo P. Development of novel alginate based hydrogel films for wound healing applications. International Journal of Biological Macromolecules. 2013;**52**:221-230

[46] Tsai CJ, Hsu LR, Fang JY, Lin HH. Chitosan hydrogel as a base for transdermal delivery of berberine and its evaluation in rat skin. Biological and Pharmaceutical Bulletin. 1999;**22**:397-401

[47] Jain SK, Chourasia MK, Sabitha M, Jain R, Jain AK, Ashawat M, Jha AK. Development and characterization of transdermal drug delivery systems for diltiazem hydrochloride. Drug Delivery. 2003;**10**:169-177

[48] Ammar HO, Salama HA, El-Nahhas SA, Elmotasem H. Design and evaluation of chitosan films for transdermal delivery of glimepiride. Current Drug Delivery. 2008;**5**:290-298

[49] Cerchiara T, Luppi B, Bigucci F, Orienti I, Zecchi V. Physically crosslinked chitosan hydrogels as topical vehicles for hydrophilic drugs. Journal of Pharmacy and Pharmacology. 2002;**54**:1453-1459

[50] Thein-Han WW, Stevens WF. Transdermal delivery controlled by a chitosan membrane. Drug Development and Industrial Pharmacy. 2004;**30**:397-404

[51] Cassano R, Trombino S, Muzzalupo R, Tavano L, Picci N. A novel dextran hydrogel linking trans-ferulic acid for the stabilization and transdermal delivery of vitamin E. European Journal of Pharmaceutical Sciences. 2009;**72**:232-238

[52] Musabayane CT, Munjeri O, Matavire TP. Transdermal delivery of chloroquine by amidated pectin hydrogel matrix patch in the rat. Renal Failure. 2003;**25**:525-534

[53] Obata Y, Otake Y, Takayama K. Feasibility of transdermal delivery of prochlorperazine. Biological and Pharmaceutical Bulletin. 2010;**33**:1454-1457

[54] Cartwright RG, Cartlidge PH, Rutter N, Melia CD, Davis SS. Transdermal delivery of theophylline to premature infants using a hydrogel disc system. British Journal of Clinical Pharmacology. 1990;**29**:533-539

[55] Suhag GS, Bhatnagar A, Singh H. Poly(hydroxyethyl methacrylate)-based co-polymeric hydrogels for transdermal delivery of salbutamol sulphate. Journal of Biomaterials Science Polymer Edition. 2008;**19**:1189-1200

[56] Don T, Huang M, Chiu A, Kuo K, Chiu W, Chiu L. Preparation of thermo-responsive acrylic hydrogels useful for the application in transdermal drug delivery systems. Materials Chemistry and Physics. 2008;**107**:266-273

[57] Sun YM, Huang JJ, Lin FC, Lai JY. Composite poly(2-hydroxyethyl methacrylate) membranes as rate-controlling barriers for transdermal applications. Biomaterials. 1997;**18**:527-533

[58] An NM, Kim DD, Shin YH, Lee CH. Development of a novel soft hydrogel for the transdermal delivery of testosterone. Drug Development and Industrial Pharmacy. 2003;**29**:99-105

[59] Sen M, Uzun C, Güven O. Controlled release of terbinafine hydrochloride from pH sensitive poly(acrylamide/maleic acid) hydrogels. International Journal of Pharmaceutics. 2000;**203**:149-157

[60] Ahmad B, Bashir S, Nisar M, Huglin MB. Anionic hydrogels for controlled release of transdermal drug. Journal of Biological Science. 2003;**3**:298-304

[61] Ishii Y, Nakae T, Sakamoto F, Matsuo K, Matsuo K, Quan YS, et al. A transcutaneous vaccination system using a hydrogel patch for viral and bacterial infection. Journal of Controlled Release. 2008;**131**:113-120

[62] Shin SC, Cho CW, Oh IJ. Effects of non ionic surfactants as permeation enhancers towards piroxicam from the poloxamer gel through rat skins. International Journal of Pharmaceutics. 2001;**222**:199-203

[63] Wang YY, Hong CT, Chiu WT, Fang JY. In vitro and in vivo evaluations of topically applied capsaicin and nonivamide from hydrogels. International Journal of Pharmaceutics. 2001;**224**:1-2

[64] Miyazaki S, Tobiyama T, Takada M, Attwood D. Percutaneous absorption of indomethacin from pluronic F-127 gels in rats. Journal of Pharmacy and Pharmacology. 1995;**47**:455-457

[65] Erukova VY, Krylova OO, Antonenko YN, Melik-Nubarov NS. Effect of ethylene oxide and propylene oxide block copolymers on the permeability of bilayer lipid membranes to small solutes including doxorubicin. Biochimica et Biophysica Acta. 2000;**1468**:73-86

[66] Liaw J, Lin Y. Evaluation of poly(ethylene oxide)-poly(propylene oxide)- poly(ethylene oxide) (PEO-PPO-PEO) gels as a release vehicle for percutaneous fentanyl. Journal of Controlled Release. 2000;**68**:273-282

[67] Fang JY, Leu YL, Wang YY, Tsai YH. In vitro topical application and in vivo phramacodynamic evaluation of nonivamide hydrogels using Wistar rat as an animal model. European Journal of Pharmaceutical Sciences. 2002;**15**:417-423

[68] Chen CC, Fang CL, Al-Suwayeh SA, Leu YL, Fang JY. Transdermal delivery of selegiline from alginate-Pluronic composite thermogels. International Journal of Pharmaceutics. 2011;**415**:119-128

[69] Nair AB, Vaka SR, Gupta S, Repka MA, Murthy SN. In vitro and in vivo evaluation of a hydrogel-based prototype transdermal patch system of alfuzosin hydrochloride. Pharmaceutical Development and Technology 2012;**17**:158-163

[70] Wang H, Hou HM. Improvement of transdermal permeation of captopril by iontophoresis. Acta Pharmacologica Sinica. 2000;**21**:591-595

[71] Niamlang S, Sirivat A. Electric field assisted transdermal drug delivery from salicylic acid-loaded polyacrylamide hydrogels. Drug Delivery. 2009;**16**:378-388

[72] Banga AK, Chien YW. Hydrogel-based iontotherapeutic delivery devices for transdermal delivery of peptide/protein drugs. Pharmaceutical Research. 1993;**10**:697-702

[73] Fang JY, Sung KC, Hu OY, Chen HY. Transdermal delivery of nalbuphine and nalbuphine pivalate from hydrogels by passive diffusion and iontophoresis. Arzneimittelforschung. 2001;**51**:408-413

[74] Muthu M S, Singh S. Targeted nanomedicines: Effective treatment and brain disorders. Nanomedicine. 2009;**4**:105-118

[75] Seth A K, Misra A, Umrigar D. Topical liposomal gel of idoxuridine for the treatment of herpes simplex: Pharmaceutical and clinical implications. Pharmaceutical Development and Technology. 2004;**9**:277-289

[76] Mura P, Maestrelli F, Gonzalez-Rodrıguez ML, Michelacci I, Ghelardini C, Rabasco AM. Development, characterization and in vivo evaluation of benzocaine-loaded liposomes. European Journal of Pharmaceutics and Biopharmaceutics. 2007;**67**:86-95

[77] Chang C-C, Yang W-T, Ko S-Y, Hsu Y-C. Liposomal curcuminoids for transdermal delivery: Iontopherisis potential for breast cancer chemotherapeutics. Digest Journal of Nanomaterials and Biostructures. 2012;**7**(1):59-71

[78] El Maghraby GM, Williams AC, Barry BW. Can drug bearing liposomes penetrate intact skin? Journal of Pharmacy and Pharmacology. 2006;**58**:415-429

[79] Mezei M, Gulasekharam V, Liposomes—A selective drug delivery system for topical route of administration. 1. Lotion dosage form. Life Science. 1980;**26**:1473-1477

[80] Mezei M, Gulasekharam V. Liposomes—A selective drug delivery system for topical route of administration: Gel dosage form. Journal of Pharmacy and Pharmacology. 1982;**34**:473-474

[81] Weiner N, Williams N, Birch G, Ramachandran C, Shipman CJR, Flynn G. Topical delivery of liposomally encapsulated interferon evaluated in cutaneous herpes guinea pig model. Antimicrobial Agents and Chemotherapy. 1989;**33**(8):1217-1221

[82] Egbaria K, Ramachandran C, Kittayanond D, Weiner N. Topical delivery of liposomally encapsulated interferon evaluated by in vitro diffusion studies. Antimicrobial Agents and Chemotherapy 1990;**34**(1):107-110

[83] Ganesan MG, Weiner ND, Flynn GL, Ho NFH. Influence of liposomal drug entrapment on percutaneous absorption. International Journal of Pharmaceutics. 1984;**20**:139-154

[84] Gesztes A, Mezei M. Topical anaesthesia of skin by liposome-encapsulated tetracaine. Anesthesia and Analgesia. 1988;**67**:1079-1081

[85] Foldvari M, Gesztes A, Mezei M. Dermal drug delivery by liposome encapsulation: clinical and electron microscopic studies. Journal of Microencapsulation. 1990;**7**(4):479-489

[86] Agarwal R, Katare OP. Preparation and in vitro evaluation of Miconazole nitrate loaded topical liposomes. Journal of Pharmacy Technology. 2002;48-60

[87] Lieb L M, Ramachandran C, Egbaria K, Weiner N. Topical delivery enhancement with multilamellar liposomes into pilosebaceous units. I. In vitro evaluation using fluorescent techniques with hamster ear model. Journal of Investigative Dermatology. 1992;**99**(1):108-113

[88] Du Plessis J, Egbaria K, Ramachandran C, Weiner ND. Topical delivery of liposomally encapsulated gamma-interferon. Antiviral Research. 1992;**18**:259-265

[89] Tschan T, Steffen H, Supersaxo A. Sebaceous-gland deposition of isotretinoin after topical application: An in vitro study using human facial skin. Skin Pharmacology. 1997;**10**:126-134

[90] Fresta M, Puglisi G. Application of liposomes as potential cutaneous drug delivery systems. In vitro and in vivo investigation with radioactivity labelled vesicles. Journal of Drug Targeting. 1996;**4**:95-101

[91] Barry BW. Novel mechanisms and devices to enable successful transdermal drug delivery. European Journal of Pharmaceutical Sciences. 2001;**14**:101-114

[92] Francesca Maestrelli, Maria Luisa Gonz'alez-Rodr'ıguez, Antonio Maria Rabasco, Paola Mura. Effect of preparation technique on the properties of liposomes encapsulating ketoprofen–cyclodextrin complexes aimed for transdermal delivery. International Journal of Pharmaceutics. 2006;**312**:53-60

[93] Ciobanu BC, Cadinoiu AN, Popa M, Desbrières J, Peptu CA. Modulated release from liposomes entrapped in chitosan/gelatin hydrogels. Mater SciEng C Mater BiolAppl. 2014;**43**:383-391

[94] Mourtas S, Fotopoulou S, Duraj S, Sfika V, Tsakiroglou C, Antimisiaris SG. Liposomal drugs dispersed in hydrogels Effect of liposome, drug and gel properties on drug release kinetics. Colloids and Surfaces B: Biointerfaces. 2007;**55**:212-221

[95] Billard A, Pourchet L, Malaise S, Alcouffe P, Montembault A, Ladavière C. Liposome-loaded chitosan physical hydrogel: Toward a promising delayed-release biosystem. Carbohydrate Polymers. 2015;**115**:651-657

[96] Hwang BY, Jung BH, Chung SJ, Lee MH, Shim CK. In vitro skin permeation of nicotine from proliposomes. Journal of Controlled Release. 1997;**49**:177-184

[97] Deo MR, Sant VP, Parekh SR, Khopade AJ, Banakar UV. Proliposome-based transdermal delivery of levonorgestrel. Journal of Biomaterials Applications. 1997;**12**(1):77-88

[98] Jukanti R, Sheela S, Bandari S, Veerareddy PR. Enhanced bioavailability of exemestane via proliposomes based transdermal delivery. Journal of Pharmaceutical Sciences. 2011;**100**(8):3208-3222

[99] Kurakula M, Srinivas C, Kasturi N, Diwan PV. Formulation and evaluation of prednisolone proliposomal gel for effective topical oharmacotherapy. International Journal of Pharmaceutical Science and Drug Research. 2012;**4**(1):35-43

[100] Gupta PN, Mishra V, Rawat A, Dubey P, Mahor S, Jain S, Chatterji DP, Vyas SP. Non-invasive vaccine delivery in transfersomes, niosomes and liposomes: A comparative study. International Journal of Pharmaceutics. 2005;**293**(1-2):73-82

[101] Fang JY, Hong CT, Chiu WT, Wang YY. Effect of liposomes and niosomes on skin permeation of enoxacin. International Journal of Pharmaceutics. 2001;**219**(1-2):61-72

[102] Lakshmi PK, Devi GS, Bhaskaran S, Sacchidanand S. Niosomal methotrexate gel in the treatment of localized psoriasis: Phase I and phase II studies. Indian Journal of Dermatology, Venereology and Leprology. 2007;**73**(3):157

[103] Kaur K, Jain S, Sapra B, Tiwary A K. Niosomal gel for site-specific sustained delivery of anti-arthritic drug: In vitro-in vivo evaluation. Current Drug Delivery. 2007;**4**(4):276-282

[104] Manosroi A, Khanrin P, Lohcharoenkal W, Werner R G, Götz F, Manosroi W, Manosroi J. Transdermal absorption enhancement through rat skin of gallidermin loaded in niosomes. International Journal of Pharmaceutics. 2010;**392**(1):304-310

[105] Ridolfi DM, Marcato PD, Justo GZ, Cordi L, Machado D, Durán N. Chitosan-solid lipid nanoparticles as carriers for topical delivery of Tretinoin. Colloids and Surfaces B: Biointerfaces. 2012;**93**:36-40

[106] Manconi M, Sinico C, Valenti D, Lai F, Fadda AM. Niosomes as carriers for tretinoin: III. A study into the in vitro cutaneous delivery of vesicle-incorporated tretinoin. International Journal of Pharmaceutics. 2006;**311**(1-2):11-19

[107] Alsarra IA, Bosela AA, Ahmed SM, Mahrous GM. Proniosomes as a drug carrier for transdermal delivery of ketorolac. European Journal of Pharmaceutics and Biopharmaceutics. 2005;**59**:485-490

[108] Muzzalupo R, Tavano L, Cassano R, Trombino S, Ferrarelli T, Picci N. A new approach for the evaluation of niosomes as effective transdermal drug delivery systems. European Journal of Pharmaceutics and Biopharmaceutics. 2011;**79**(1):28-35

[109] Cevc G, Gebauer D, Stieber J, Scha¨tzlein A, Blume G. Ultraflexible vesicles, Transfersomes, have an extremely low pore penetration resistance and transport therapeutic amounts of insulin across the intact mammalian skin. Biochimica et Biophysica Acta. 1998;**1368**:201-215

[110] Singh RP, Singh P, Mishra V, Prabakaran D, Vyas SP. Vesicular systems for non-invasive topical immunization: Rationale and prospects. Indian Journal of Pharmacology. 2002;**34**:301-310

[111] Kumar A, Pathak K, Bali V. Ultra-adaptable nanovesicular systems: A carrier for systemic delivery of therapeutic agents. Drug Discovery Today. 2012;**17**(21-22):1233-1241

[112] Paul A, Cevc G, Bachhawat BK. Transdermal immunization with an integral membrane component, gap junction protein, by means of ultra-deformable drug carrier transfersomes. Vaccine. 1998;**16**:188-195

[113] Kim A, Lee EH, Choi S-H, Kim C-K. In vitro and in vivo transfection efficiency of a novel ultra-deformable cationic liposome. Biomaterials. 2004;**25**:305-313

[114] Cevc G, Blume G. Biological activity and characteristics of triamcinolone-acetonide formulated with the self-regulating drug carriers, Transfersomes®. Biochimica et Biophysica Acta. 2003;**1614**:156-164

[115] Cevc G, Blume G. Hydrocortisone and dexamethasone in very deformable drug carriers have increased biological potency, prolonged effect, and reduced therapeutic dosage. Biochimica et Biophysica Acta. 2004;**1663**:61-73

[116] Mahor S, Rawat A, Dubey Praveen K, Gupta Prem N, Khatri K, Goyal Amit K, Vyas SP. Cationic transfersomes based topical genetic vaccine against hepatitis B. International Journal of Pharmaceutics. 2007;**340**:13-19

[117] Jain S, Sapre R, Ashok KT, Narendra KJ. Proultraflexible lipid vesicles for effective transdermal delivery of levonorgestrel: Development, characterization, and performance evaluation. AAPS PharmSciTech. 2005;**6**(3):E513-E522

[118] Gupta V, Agarawal RC, Trivedi P. Reduction in cisplatin genotoxicity (micronucleus formation) in non target cells of mice by protransfersome gel formulation used for management of cutaneous squamous cell carcinoma. Acta Pharmaceutica. 2011;**61**:63-71

[119] Pillai O, Panchagnula R. Transdermal delivery of insulin from poloxamer gel: Ex vivo and in vivo skin permeation studies in rat using iontophoresis and chemical enhancers. Journal of Controlled Release. 2003;**89**(1):127-140

Chapter 7

Thermosensitive Liposomes

Anjan Motamarry, Davud Asemani and
Dieter Haemmerich

Additional information is available at the end of the chapter

http://dx.doi.org/10.5772/intechopen.68159

Abstract

Thermosensitive liposomes (TSLs) are a drug delivery system for targeted delivery that release the encapsulated drug when heated to fever temperatures (~40–42°C). Combined with localized hyperthermia, TSLs allow precise drug delivery to a targeted region. While mostly investigated as cancer therapy, other applications including treatment of local infections and wound healing have been explored. Over the last ~40 years, numerous TSL formulations and payloads have been investigated. As with other nanoparticles, the addition of targeting molecules to TSL has been examined to improve targeted delivery. TSL release kinetics and plasma stability are two important factors that affect efficacy, and new formulations often aim to further improve on these properties. The possibility of encapsulating a magnetic resonance (MR) contrast agent that is released together with the encapsulated drug allows for visualization of drug delivery with MR imaging. Various heating modalities have been examined in combination with TSL. Since the goal is to expose a defined tissue region to uniform temperatures within the range where TSLs release (typically ~40–43°C), the choice of an appropriate heating modality has considerable impact on treatment efficacy. Several ongoing clinical trials with TSL as cancer therapy suggest the potential for clinical impact in the near future.

Keywords: liposomes, thermosensitive liposomes, triggered release, hyperthermia, drug targeting, drug delivery

1. Introduction

Surgical resection, radiation therapy, and chemotherapy are the three primary cancer treatment modalities. While chemotherapy is used in the treatment of almost all cancers, it has challenges and limitations. Most of the chemotherapeutic agents are highly cytotoxic to both cancer and normal tissues. Often chemotherapy is administered systemically, meaning it is

not directed to the cancerous tissues. The drug uptake by normal tissues causes off target effects including severe toxicities to different organs such as heart, liver, or kidneys, immune system, and others. In quite a number of cases, the toxicity profile of the drug limits the maximum tolerated dose (MTD) that can be administered. It is well known that inadequate dose is a primary cause for tumor recurrence and development of drug resistance. Thus, typically the highest possible dose is given to a patient to maximize the amount taken up by the cancerous tissues. All these factors have led to the development of methods to direct the drug to the tumor tissue, including various nanoparticles such as liposomes.

Liposome-encapsulated drug has evolved as a very potent source of directing the drug to the site of tumor. There are several ways by which a drug can be targeted to the tumor using liposomes. Kunjachan et al. review the various methods by which liposomes can be used to target the tumors [1]. Standard chemotherapy involves the administration of free (i.e., unencapsulated) drug (**Figure 1A**). Encapsulating the drug within a liposomal formulation allows prolonged blood circulation with very limited tissue uptake. Liposomes and other nanoparticles are most often based on passive targeting (**Figure 1B**). That is, they rely on the enhanced permeability and retention (EPR) effect resulting from leaky tumor vessels combined with absent lymph drainage in most tumors [2]. As a result, liposomes preferentially accumulate within the tumor over typically 24–48 hours. Tumors can be actively targeted by adding antibodies to the liposome surface, which are specific to either the cancer cells themselves (**Figure 1C**), or specific to the endothelial cells of the tumor vasculature (**Figure 1D**). One limitation of this antibody-based approach is that due to the heterogeneity of tumors, not all tumors or cancer cells have the unique antigen for the targeting antibody to bind. Another targeting method includes the use of an external trigger to release the drug either within the interstitium (i.e., after letting the liposomes accumulate via EPR effect) (**Figure 1E1**) or by releasing the drug within the vasculature of the tumor (**Figure 1E2**). The latter method requires liposomes specifically designed to respond to the specific trigger. Depending on the liposome, various external energy sources or biological signals may trigger drug release; these include heat, light, pH, and ultrasound, among others. In this chapter, we will focus on using heat as trigger, i.e., we will discuss in detail the evolution and current status of thermosensitive (or temperature sensitive) liposomes (TSLs).

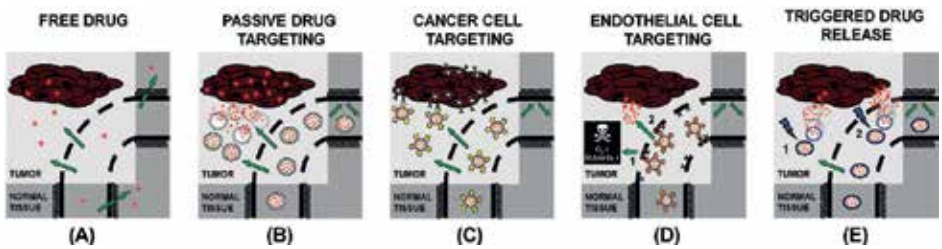

Figure 1. Current drug targeting strategies. (A) Conventional therapy or free drug infusion. (B) Passive targeting by liposomes utilizing EPR effect. (C) Active targeting of liposomes labeled with tumor-specific antibody. (D) Active targeting of liposomes with endothelial cell-specific antibody. (E) Triggered drug release either (1) within the tumor interstitium or (2) intravascular release. TSL fall into this last category reproduced with permission from Ref. [1]. Copyright (2015) American Chemical Society.

http://dx.doi.org/10.5772/intechopen.68159

The strategy is that TSLs are administered systemically, followed by local hyperthermia (>40–42°C). The local hyperthermia triggers drug release within the targeted region, by which the drug becomes bioavailable and can exhibit the intended cytotoxic effect. Thus, the combination of TSL with a localized heating modality allows for localized drug delivery.

Note, however, that TSLs may have additional clinical applications outside cancer therapy, as there are various other clinical indications where it is necessary to deliver a drug targeted to a specific region within the body.

2. Background: evolution of thermosensitive liposomes (TSLs)

Liposomes as carriers of therapeutic drugs have been long investigated as a tool for improving the therapeutic index (i.e., decreasing the toxicity associated with drug delivery, while improving delivery to tumor). In 1995, Doxil [3] became the first nanoliposomal drug to be approved by Food and Drug Administration (FDA). However, with liposomes, a major limitation was directing the liposomes to the tumor. Initial liposomal formulations such as Doxil depend on preferential passive liposome accumulation based on the enhanced permeability of the tumor blood vessels, together with the lack of lymph drainage (EPR effect). However, it takes a considerable time (about 1–2 days) for the liposomal drug to accumulate within tumor. Moreover, the drug accumulated within the tumor is not bioavailable as it is still encapsulated within the liposomes [4]. The result was that Doxil achieved reduced toxicity while efficacy was in general not better than unencapsulated drug.

In 1978, Yatvin et al. [5] suggested for the first time the use of temperature sensitive liposomes (TSLs) (i.e., liposomes that release the encapsulated drug in response to heat) combined with hyperthermia for targeting the drug to tumors or local infections. The basic idea was to administer this liposomal drug systemically, and then expose only the tissue region where drug delivery is intended to hyperthermia. They proposed to use slightly higher temperature (42–44°C) than normal body temperature (37°C) to target drug delivery. This first TSL formulation used the two lipids dipalmitoyl phosphatidylcholine (DPPC) and distearoyl phosphatidylcholine (DSPC) to make liposomes sensitive to heat. DPPC and DSPC have "liquid-crystalline transition temperatures (Tm)" of 41 and 54°C, respectively; here Tm is the temperature at which the lipids undergoe a transformation from a solid gel-like structure (i.e., highly impermeable to hydrophilic substances) to a highly permeable liquid structure. These liposomes are now often termed as traditional thermosensitive liposomes (TTSLs) [6]. The reason that two lipids were used is because TSLs were too leaky when only a single lipid was used. Hence, a combination of DPPC and DSPC (ratio 3:1) was used, and these first TSLs encapsulated the antibiotic neomycin with the aim of treating bacterial infections.

Use of TTSLs for cancer treatment was first tested by Weinstein et al. [7] in 1979 in mice-carrying lung cancer. They showed that there was a fourfold increase in the amount of methotrexate delivered to heated tumors using the initial TTSL composition with slightly varied ratios (DPPC:DSPC = 7:3). A major limitation of this initial formulation was the quick elimination of the liposomes within 1 hour of the infusion.

In the following decades, various modified compositions were proposed based on the original formulation above. The primary goal was to increase the liposome stability and reduce leakage of the contained drug when exposed to serum [8]. This search led to the incorporation of cholesterol to the composition of liposomes [8, 9]. Gaber et al. showed that by using cholesterol, the phase transition can be avoided as the lipids are in liquid-ordered phase [10]. However, the incorporation of cholesterol delayed the complete release of the encapsulated drug doxorubicin to about 30 minutes at 42°C. Also around the same time, strategies were developed for circumventing the reticuloendothelial system and the immune system [11], which was addressed by the incorporation of polyethylene glycol (PEG) in the 1990s. Some studies showed that clearance of TSL was size dependent [12]. Larger liposomes were cleared quickly whereas smaller liposomes took a longer time to be cleared. However, small liposomes are less stable at normal body temperature (37°C). Hence, liposomes in the size range of 50–200 nm were recommended [12]. Around the same time mid-1990s, Kono et al. [13, 14] proposed the incorporation of thermosensitive polymers into liposomes to make them temperature sensitive. TSLs carrying polymers such as poly (N-isopropylacrylamide) were being evaluated [14]. However, a major setback for using these polymers was that they were not biodegradable. The next major breakthrough occurred in 2000 when Needham et al. [15] reported the successful incorporation of lysolipids and PEG into the liposomal lipid composition (DPPC:MPPC:DSPE-PEG2000 in the ratio of 90:10:4). Lysolipids are derivatives of lipid in which acyl derivatives are removed by hydrolysis making them more hydrophilic. The incorporation of lysolipids caused the rapid release of the encapsulated doxorubicin at hyperthermia temperatures (42°C). These have been called as lysolipid temperature-sensitive liposomes (LTSL). LTSL released much more rapidly (seconds) than prior formulations [16]. LTSLs were found to substantially improve delivery efficacy, with 3.5 times enhanced tumor drug delivery compared to TTSL, and ~17 times higher than unencapsulated drug [17]. A formulation similar to the one proposed by Needham is so far the only TSL formulation that made it into human clinical trials. However, the plasma half-life of LTSL is still not ideal with median initial plasma half-life of about 1 hour in humans and 1.5 hours in dogs [18, 19].

In 2004, Lindner et al. proposed a novel formulation based on the new lipid 1.2-dipalmitoyl-sn-glycero-3-phosphoglyceroglycerol ($DPPG_2$) with prolonged plasma half-life and similarly short release rates as LTSL [20, 21]. Initial studies with $DPPG_2$-TSL filled with carboxyfluorescein (CF) demonstrated initial plasma half-life 5 hours in rats [20]. More recent studies with doxorubicin-filled $DPPG_2$-TSL in cats showed plasma half-life of around 1 hour [22], similar to doxorubicin-LTSL.

As naturally occurring lipids were used for making TSL, they are usually considered safe.

2.1. Extravascular release versus intravascular triggered release

Three key requirements must be fulfilled by TSLs to be effective:

- Encapsulation of therapeutically relevant drug payload with minimum leakage.
- Avoidance of mononuclear phagocyte system (MPS) to prolonged circulation.
- Release of the payload (encapsulated drug) at target location (e.g., tumor).

The delivery strategy of initial liposome formulations (nonthermosensitive Stealth liposome, e.g., Doxil) was based on passive accumulation in tumor interstitial space (**Figure 1B**), followed by slow release within the interstitium (extravascular release). Since TSL release is actively triggered, TSL-based delivery may be used based on either of two delivery approaches: extravascular and intravascular triggered release (indicated by (1) and (2) in **Figure 1E**), based on whether release occurs inside the vasculature/blood or in the tumor interstitium. For extravascular triggered release, the targeting is passive and mostly relies on the EPR effect. For intravascular triggered delivery, there is no explicit-targeting mechanism, but rather targeting is based by location where heating is induced.

Since extravascular triggered release requires passive accumulation of TSL in the tumor interstitium before trigger of release, there is a necessary time delay between TSL administration and hyperthermia (typically several hours). This also means that TSLs of adequate plasma stability are required, with a plasma half-life exceeding many hours. Computer models suggest that the optimal release rate for extravascular triggered release is in the order of many minutes to hours [16, 23].

For intravascular triggered release, hyperthermia occurs ideally immediately after, or even during TSL administration [24]. This is because any leakage of drug after delivery is detrimental during intravascular triggered delivery, as it reduces the amount available for release. Thus, plasma stability requirements are less stringent than for extravascular triggered delivery. Release occurs while TSLs transit the heated tumor region; this transit time is in the range of a few seconds for most tumors, and thus ideally TSL should release very rapidly (within seconds).

Both intravascular and extravascular triggered approaches are the subject of ongoing preclinical studies as described in the previous section [25, 26]. It is interesting to note that, while the benefit of faster releasing TSL has been demonstrated in 2000 [17], it was only elucidated recently that intravascular triggered delivery was the dominant delivery mechanism, and responsible for improved delivery with fast-release TSL [16, 27].

Table 1 summarizes the differences between intravascular and extravascular triggered release.

Mathematical models are an effective tool to evaluate different TSL delivery strategies and drug transport kinetics. Such models have several advantages which include: ability to utilize a large body of physiological and physiochemical data, prediction of pharmacokinetics and target tissue dose, and extrapolation of results both across species and routes of administration [28, 29]. The latter point is of relevance since results from experimental animal studies often do not translate into human patients, and models can thus help explain such deviations [30].

Drug delivery system	Tumor targeting	Initiation of heating	Typical TSL leakage rate	Ideal TSL release rate
Extravascular triggered TSL (TSL-e)	Passive (EPR)	Hours after TSL infusion	hours-days	hours
Intravascular triggered TSL (TSL-i)	Active via heat source	During, or immediately after TSL infusion	minutes	seconds

Table 1. Comparison of TSL for intravascular and extravascular triggered release.

In 2012, extravascular and intravascular triggered release approaches were compared using a mathematical model [16]. Specifically, the following drug delivery strategies were compared based on the chemotherapy agent doxorubicin: (1) unencapsulated drug; (2) nonthermosensitive stealth liposomes; (3) intravascular triggered TSL (TSL-i); and (4) extravascular triggered TSL (TSL-e). The models predict that intravascular triggered release results in considerably higher drug uptake by cancer cells (i.e., efficacy) compared to the other delivery modalities (**Figure 2**). During intravascular triggered delivery, new TSLs enter the tumor vasculature and release drug as long as hyperthermia is present. The systemic blood volume thus serves as reservoir of nonbioavailable drug that becomes bioavailable when entering the target tissue region.

2.2. Release kinetics

As described above, the intravascular triggered delivery strategy is most effective when TSLs have very rapid release, within seconds. This is the reason why the later, fast-release formulations that release within seconds greatly improved drug accumulation in tumors compared to early formulations that required many minutes to release (**Figure 3**). Unfortunately, plasma

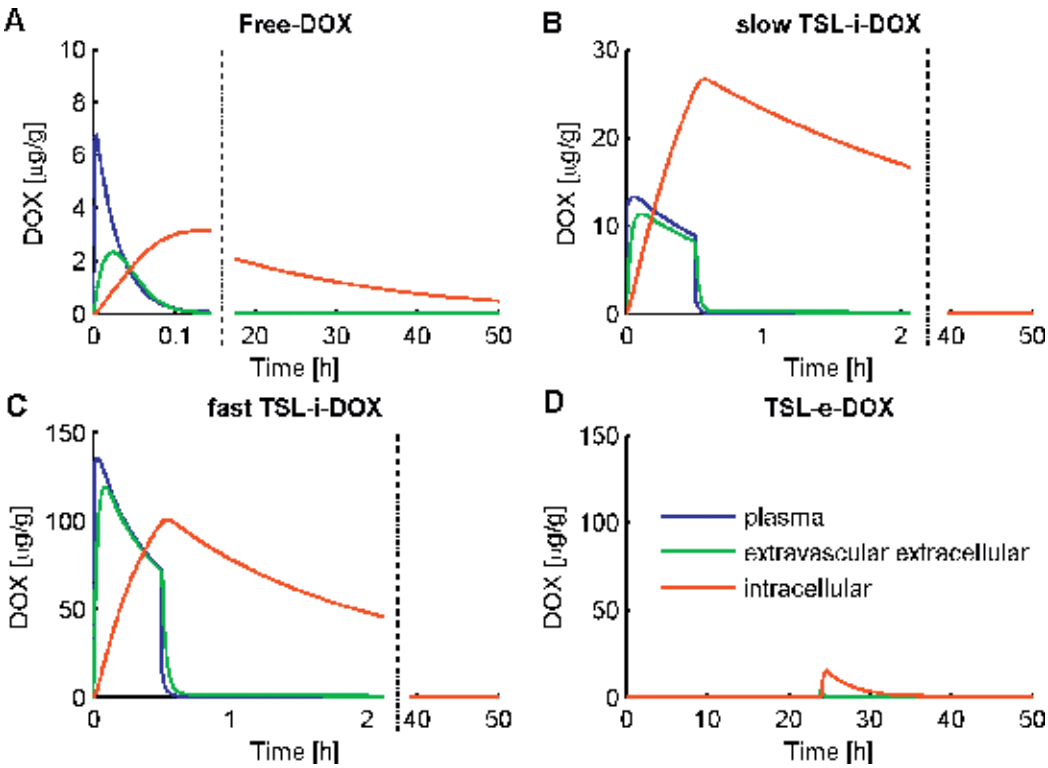

Figure 2. Doxorubicin concentrations (unencapsulated drug) in plasma, extravascular-extracellular space (EES), and inside cells are plotted over time for different delivery systems: (A) free-DOX (unencapsulated drug), (B) slow-release TSL-i-DOX (release rate ~min), (C) fast-release TSL-i-DOX (release rate ~seconds), and (D) TSL-e-DOX [7]. Hyperthermia for 30 minutes was applied immediately for TSL-i, and after 24 hours for TSL-e (to allow for TSL accumulation in EES). Reproduced from Ref. [16].

http://dx.doi.org/10.5772/intechopen.68159

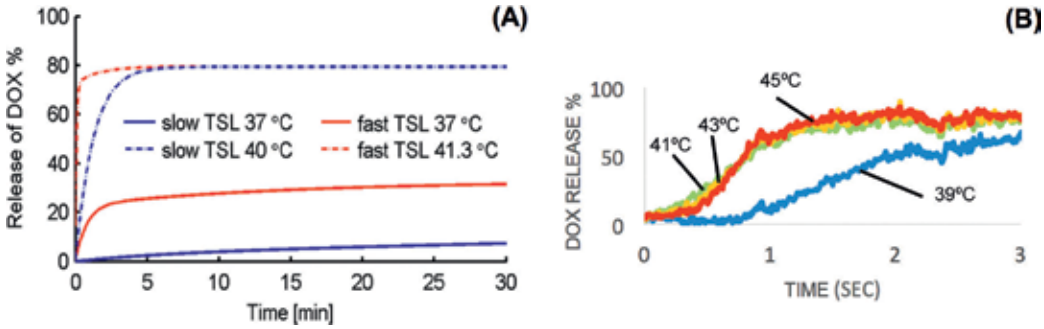

Figure 3. (A) Graph shows release rate during hyperthermia (40–41°C), as TSL stability at body temperature (37°C), comparing a slow-release formulation and a newer fast-release formulation (reproduced from Ref. [16]). (B) Graph shows a release rate within first few seconds between 39 and 45°C of a fast-release formulation in fetal bovine serum (FBS) (unpublished data). TSLs were prepared according to Needham et al. [15] with slight modifications. (DPPC: MSPC: DSPE-PEG2000 85.3:9.7:5), and loaded with Dox using a citrate-based pH gradient.

stability is directly tied to release during hyperthermia, i.e., typically the faster a liposome releases when heated, the more this liposome leaks at body temperature (**Figure 3A**) [26].

2.3. Intravital microscopy

Intravital microscopy is an important technology that enables visualization of drug release and uptake at microscopic scales. This enables better understanding of how the drug is taken up by the tumor once it is released from the TSL. Using fluorescent compounds such as CF or doxorubicin, it is possible to observe the drug in different compartments (e.g., inside vasculature and cells). This imaging methodology requires visual access to tumors, which is typically provided by windows (**Figure 4**).

Figure 4. Window chamber in a mouse. Reproduced with permission from Ref. [32]. Copyright (2013) Nature Publishing.

A detailed procedure of implantation of a window chamber was explained by Ritsma et al. [31]. A small viable piece of tumor (~1–3 mm^3) is transplanted into the fascia of the dorsal skin flap which is placed within a window chamber of the recipient mice [32]. To allow visualization during hyperthermia, the tumor needs to be heated. For this purpose, a special heating coil has been developed that allows the uniform heating of these window chambers carrying tumors. The imaging takes place while animals are under anesthesia, after TSLs have been administered. While tumors are exposed to hyperthermia, tumors are imaged using confocal fluorescence microscopes using appropriate excitation and emission filters depending on fluorescence properties of the molecule. **Figure 5** demonstrates the uptake of doxorubicin released from the TSL within the blood during hyperthermia, and drug uptake by cancer cell nuclei.

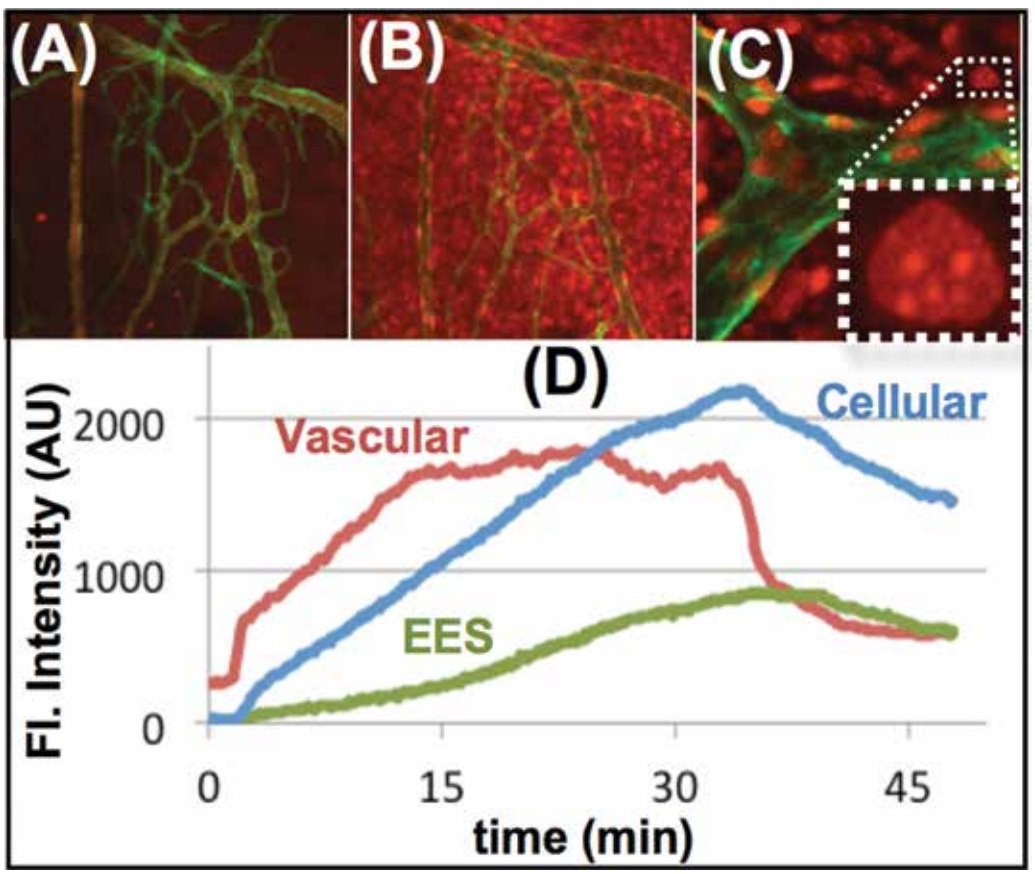

Figure 5. Intravital fluorescence microscopy demonstrates intravascular triggered release. Images show labeled endothelial cells (green) and doxorubicin fluorescence (red). Tissue accumulation and cell uptake are demonstrated during hyperthermia-induced release from TSL (30 minutes, 42°C), (A) after 5 minutes and (B) after 20 minutes (field of view (FOV) 500 × 500 μm). (C) Subcellular doxorubicin localization is observed at higher magnification (inlet). (D) Aggregate fluorescence within vessels, interstitium (EES), and intracellular regions extracted from image data in (A) and (B). These data demonstrate triggered initial intravascular release, followed by tissue uptake within EES and cells. Unpublished data courtesy of Dr. Timo ten Hagen.

2.4. Targeted thermosensitive liposomes

Various targeting moieties such as antibodies are nowadays widely used for targeted delivery of liposomes and other nanoparticles and have also been investigated for TSL. The idea of attaching an antibody to a TSL was reported by Sullivan and Huang [33] as early as 1985. Sullivan and Huang [33] used covalently attached antiH2Kk antibody to a palmitic acid derivative to make heat sensitive immunoliposomes (with DPPC) carrying carboxyfluorescein. They used a similar approach to successfully deliver uridine inhibitors to lymphoma cells *in vitro*. However, *in vivo* evaluation in mice carrying human ovarian cancers did not yield encouraging results. This was attributed to the leakiness of the liposomes, which used egg phosphatidylcholine, egg phosphatidylglycerol, cholesterol, and phosphatidylethanolamine in the ratio 38.1:4:32:1.9 [34].

With the development of newer TSL formulations (e.g., LTSL), there has been an increased interest in conjugating targeting molecules to TSL, particularly to those carrying the chemotherapeutic drug doxorubicin. Antibodies, peptides, and aptamers have been successfully added to TSLs. **Table 2** summarizes the targeting molecules that have been used.

Antibodies targeting common receptors found in cancers such as human epidermal growth factor receptor 2 (HER-2) [35] and epidermal growth factor receptor (EGFR) [36] have been conjugated to LTSL carrying doxorubicin that are being evaluated in animal models. Kullberg et al. [37] showed that adding listeriolysin O along with HER-2 antibody enhanced cytoplasmic delivery of the cargo.

Similarly, Na et al. added elastin-like peptide (ELP), which significantly improved the drug uptake within cells [38].

References	Type	Targeting molecule	Target	Payload encapsulated
[33]	Antibody	Anti H2Kk	H2Kk	Carboxyfluorescein
[35]	Antibody	Anti Her-2	Her-2	Calcein
[36]	Antibody	Anti EGRF	EGFR	Calcein, Dox
[38]	Peptide	Val-Pro-Gly-Val-Gly	Intracelluar delivery	Dox
[39]	Peptide	Cys-Arg-Glu-Lys-Ala	Clotted plasma proteins in tumor vessels	Dox
[40]	Peptide	Arg-Cys-D-Phe-Asp-Gly	tumor and angiogenic endothelial cells	Dox
[41]	Peptide	CCRGDKGPDC	$\alpha v\beta 3$-positive cells	Dox
[42]	Aptamer	AS1411	nucleolin receptors	Contrast agent (Gd-DTPA)
[43]	Peptide cargo		Bone regeneration	107–111 pentapeptide of the parathyroid hormone-related protein

Table 2. Targeted thermosensitive liposomes.

Moreover, peptides that target tumors have also been added to TSLs. Wang et al. added the tumor homing pentapeptide (Cys-Arg-Glu-Lys-Ala) (CREKA) to TSLs and evaluated their efficacy in MCF-7 bearing nude mice [39]. Dicheva et al. [40] added a cyclic pentapeptide to TSL-doxorubicin improving the drug uptake and delivery. Deng et al. [41] improved the anti-tumor efficacy by adding the iRGD peptide.

Most recently, Zhang et al. [42] used an aptamer conjugated TSLs loaded with contrast agent that targeted the nucleoporin receptors. Besides displaying excellent biocompatibility, they showed promise in the early detection of cancers.

In a somewhat different application, Lopez et al. developed a collagen-based scaffold to which TSLs were covalently attached via targeting molecule to slowly release a peptide cargo with proosteogenic effect from the scaffold [43].

3. Payloads

Ever since the initial studies where neomycin was encapsulated in TSL [5], several other drugs and reporter molecules have been encapsulated by various TSL formulations and evaluated. Several combinations have successfully made it to various stages of preclinical and clinical trials. A brief overview of the compounds that have been successfully encapsulated will be reviewed here.

The fluorescent reporter carboxyfluorescein (CF) has been the molecule of choice for studying the release kinetics of TSLs. Starting from the initial studies until today, CF has been used in the study of various TSL combinations. Other fluorescent molecules such as calcein have also been used to study TSL release.

Yatvin et al. encapsulated cisplatin (cis-dichlorodiammineplatinum(II)) in 1981 [44] and evaluated against mice tumor sarcoma. This suggested that a whole array of different compounds could be encapsulated by TSLs. However, until the late 1980s, only water soluble compounds were being encapsulated into TSLs.

Doxorubicin is an amphiphilic compound that was encapsulated into the TSL toward the end of 1980s. Doxorubicin is a highly cytotoxic chemotherapeutic drug belonging to the group of anthracyclines, with several off target effects such as cardiotoxicity and myelosuppression. Tomita et al. encapsulated doxorubicin in DPPC: cholesterol-based TSL to improve stability [45]. Other formulations further attempted to improve TSL stability [10, 46]. Unezaki et al. reported the active loading of doxorubicin against a pH gradient into TSLs [47], which resulted in more than 90% encapsulation efficacy. The TSL composition developed by Needham et al. [15] is the formulation that progressed furthest toward clinical use, with ongoing clinical trials that will be discussed later. One of the significant developments that occurred more recently for TSL-Dox was the incorporation of contrast agents. Several researchers encapsulated doxorubicin along with gadolinium-based contrast agents [48–50]. This provided the ability of monitoring the release of a contrast agent from TSL

and subsequent tissue uptake by magnetic resonance imaging (MRI), indicating the tissue regions where doxorubicin may be delivered to.

Following doxorubicin, several groups encapsulated other drugs belonging to the same family of anthracycline drugs in TSL, including daunorubicin, idarubicin, and epirubicin. The initial studies with daunorubicin in the mid-1990s in mice models of sarcoma were disappointing [51]. However, more recent studies with newer formulations of idarubicin-TSL showed superior survival rate and tumor growth inhibition as compared to free idarubicin [52]. Similar results were demonstrated with epirubicin-TSL in animals [53].

The successful encapsulation of anthracyclines with high efficiency prompted the search for other molecules with high encapsulation efficiency. Liu et al. [54] reported that using metal ions such as Zn or Cu could lead to high efficacy in encapsulation of cisplatin. Moreover, the presence of metal bound liposomes increased the cytotoxicity.

Apart from anthracyclines [65], the drugs bleomycin [55], melphalan [56], placitaxel [57], docetaxel [58], and gemcitabine [59] have been encapsulated into TSL and delivered to tumors, while reducing systemic drug toxicities.

Another fluorescent compound that was successfully encapsulated in TSL is the cancer drug 5-fluorouracil. Sabbagh et al. used a lipid combination containing DPPC, cholesterol, and PEG to encapsulate 5-fluorouracil. They further found that complexing 5-fluorouracil with copper-polyethylenimine improved the stability of the liposomes with a higher encapsulation efficacy [60].

Recently, vinorelbine was encapsulated into a TSL formulation [61]. Vinorelbine is a wide spectrum chemotherapeutic agent used in treatment of breast, lung, and liver cancers. However, free vinorelbine is associated with venous toxicity causing blisters when infused directly into the blood. The authors reported that combining vinorelbine-TSL with hyperthermia resulted in enhanced antitumor activity. In another study, Wang et al. showed that [62] vinorelbine-TSL in combination with radiofrequency ablation (RFA) improved the survival of micecarrying liver tumors.

Another interesting recent application of TSL is the targeted delivery of the antibiotic ciprofloxacin to aid wound healing. Wardlow et al. [63] demonstrated the encapsulation of ciprofloxacin in TSL, and used these for delivery to hyperthermic areas using a rat model. They suggested that this formulation could be used for chronic wound healing. However, work still remains to evaluate these TSLs in an animal model of chronic would healing.

Most recently, it was reported that chemotherapeutic drugs vincristine and doxorubicin were coloaded into TSL in combination. Li et al. showed that multiple drug loading could be achieved to exploit the synergy between drugs [64].

It should be noted that each drug has to be individually tested, i.e., there is no single TSL formulation that would work for all drugs. In addition, the release rate and leakage will vary for different drugs, and it may not always be possible to achieve rapid release within seconds as is ideal for intravascular triggered release. **Table 3** summarizes the drugs that have been encapsulated in a TSL formulation and the liposomal composition.

References	Composition	Ratio	Cargo/payload
[5]	DPPC, DSPC	3:1	Neomycin
[7]	DPPC, DSPC	7:3	Methotrexate
[44]	DPPC, DSPC	7:1	Cisplatin
[45]	DPPC, Cho		Doxorubicin
[10]	DPPC, HSPC, Cho, PEG	100:50:30:6	Doxorubicin
[51]	DSPC:Cho		Daunorubicin
[52]	DPPC:DSPC:DSPE-PEG	6:3.5:0.5	Idarubicin
[53]	DPPC:MSPC:DSPG:DSPE-mPEG2000	82:8:10:4	Epirubicin
[55]	DPPC: DSPC	9:1	Bleomycin
[56]	Phosphatidyl choline, cho		Melphalan
[57]	DPPC:MSPC:DSPE-PEG2000:DSPG	83:3:10:4	Paclitaxel
[58]	DPPC:DSPE:PEG2000:EPC:MSPC: DTX	82:11:4:3:4	Docetaxel
[59]	DPPC:DSPC:$DPPG_2$	50:20:30	Gemcitabine
[60]	DPPC:CHO:DSPE-PEG	90:5:5	5-Fluorouracil
[61]	DPPC:MPPC:DSPE-PEG2000	86:5:4	Vinorelbine
[63]	DPPC:MSPC:DSPE-PEG	85.3:9.7:5.0	Ciprofloxacin
[64]	DPPC: DSPE-PEG2000: MSPC	75:17:8	Doxorubicin & Vincristine
[48]	DPPC:MSPC:DSPE-PEG2000	85.3:9.7:5.0	Doxorubicin & ProHance®

Table 3. Thermosensitive liposomes composition and payloads.

4. Heating modalities

TSLs have been used successfully in combination with various heating modalities in both animal models and in human clinical trials. Some of these heating modalities include devices already in clinical use; others have only been used in animals. Ideally, only the targeted tissue region is exposed to temperatures within the range where TSL release (typically above ~40°C). In addition, higher temperatures (>43–50°C) may result in reduced blood perfusion [66] and should be avoided since without perfusion TSLs are not transported to the target site. Thus, in an ideal case, the targeted tissue region should be exposed to a quite narrow temperature range (~40–43°C). For larger tumors—particularly as can be the case in humans or large animals—achieving this temperature uniformity in large tissue volumes is challenging, and the hyperthermia device becomes an important element affecting TSL-based drug delivery efficacy.

Since deep-seated tumors are typically identified based on medical imaging (e.g., computed tomography (CT), magnetic resonance imaging (MRI), or ultrasound imaging), TSLs may be used for image-guided drug delivery. Here, the intent is to deliver drug to a specific region of the body identified by medical imaging. Since TSLs are administered systemically, image-guided drug delivery is realized by exposing the targeted tissue volume to hyperthermic temperatures by image-guided heating devices. Thus, one important aspect that should guide

the selection of the heating modality is ability to expose only the targeted tumor region to uniformly hyperthermic temperatures.

4.1. Animal hyperthermia systems

4.1.1. Water bath

Water bath as a heat source has been used extensively in preclinical studies, especially involving small animals. Usually the animal is anesthetized, hair removed if necessary and the region surrounding the tumor is immersed in a water bath, which is preheated to the required temperature (usually >40°C). It is essential to make sure that the skin distant from the targeted tumor is not exposed to the heat from the water bath. For example, some researchers used a water bath cover made of material that does not conduct heat, with the other parts of the body covered by a polystyrene cover [50]. Other studies used a plastic syringe to hold the leg of mice in place to expose only the tumor to heated water while protecting the other leg from heat [32]. Ultrasound gel or vaseline has also been applied to protect the tissues surrounding the tumor from heat exposure.

4.1.2. Light sources

Various light sources have been employed to induce hyperthermia, usually for surface heating of subcutaneous tumors. Several groups used a cold lamp, which emits visible light (350–700 nm wavelength) [50, 59]. By adjusting the power of the lamp, a target temperature of ~41–43°C was achieved. White cotton wool was placed around the area surrounding the tumor to avoid heating and drug delivery.

Near infrared (NIR) lasers (~800–1000 nm wavelength) have also been used as a heating sources in nanoparticle-based drug delivery systems, which can penetrate tissue to depths in the range of ~0.5 cm [51, 67, 68]. The diameter of the laser spot can be adjusted by optical lenses to correspond to the targeted area.

4.1.3. Microwave hyperthermia

Microwave devices have a long history for use in hyperthermia studies [69] and have been used in combination with TSLs, for example by the first *in vivo* TSL study by Weinstein et al. in 1979 [7]. They used a system specifically designed to expose subcutaneous rodent tumors to hyperthermia through microwave antennas placed on the skin. Three other studies also used surface microwave applicators: one trial in dogs [19], one in cats [22], and a phase I trial in humans for breast cancer; the latter two used a FDA-approved microwave hyperthermia system [70]. While there are also interstitial microwave antennas for heating deep tissue regions [69], to our knowledge these have not yet been used in combination with TSL.

4.2. Clinically used hyperthermia and thermal ablation devices

4.2.1. Radiofrequency ablation

Thermal tumor ablation is a heat-based cancer therapy, where the cancer is killed by heat alone, by heating above ~50°C. Most widely used is radiofrequency ablation (RFA), where

radiofrequency electric current is applied to tissue via electrode inserted into the tumor under image guidance [71]. The electric current results in localized tissue heating (**Figure 6**). In the clinic, RFA is used guided by medical imaging techniques such as MRI, ultrasound, or CT, and is currently in use for liver, lung, kidney, and other types of cancer.

Since local tumor recurrence often occurs at the margin of the tissue regions killed by heat, TSLs have been combined with RFA to preferentially deliver chemotherapy to these margins that are exposed to sublethal, hyperthermic temperatures (**Figure 7**). This combination is also being examined in clinical trials for treatment of primary liver cancer.

There are other technologies for tumor ablation similar to RFA used clinically, such as microwave ablation and laser. While these could also be combined with TSL, studies on such combinations are not yet available.

4.2.2. High-intensity focused ultrasound (HIFU)

High-intensity focused ultrasound (HIFU) in combination with magnetic resonance imaging (MRgHIFU) is in clinical use for treatment of tumors by heating them to >50°C (i.e., thermal

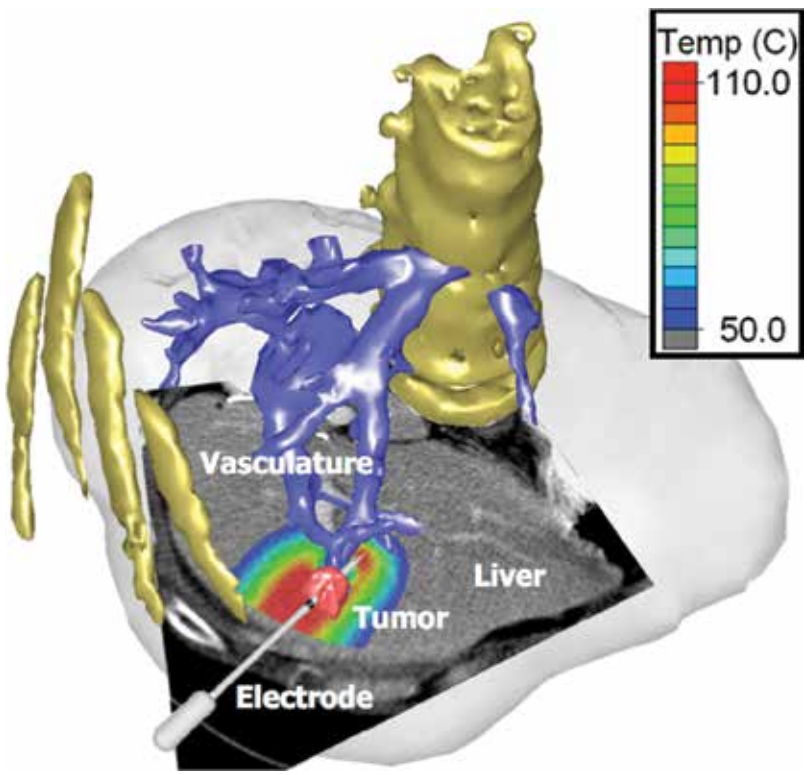

Figure 6. Overview of liver radiofrequency tumor ablation procedure as clinically performed. An RFA electrode is inserted into the tumor under imaging guidance, and the tumor is killed by heat. Tumor recurrences following ablation occur primarily in the margin of the ablation zone, where inadequate temperatures were obtained (<50°C). The combination with TSL delivers drug at high dose to this ablation margin, potentially reducing recurrences. Adapted from Ref. [72].

http://dx.doi.org/10.5772/intechopen.68159

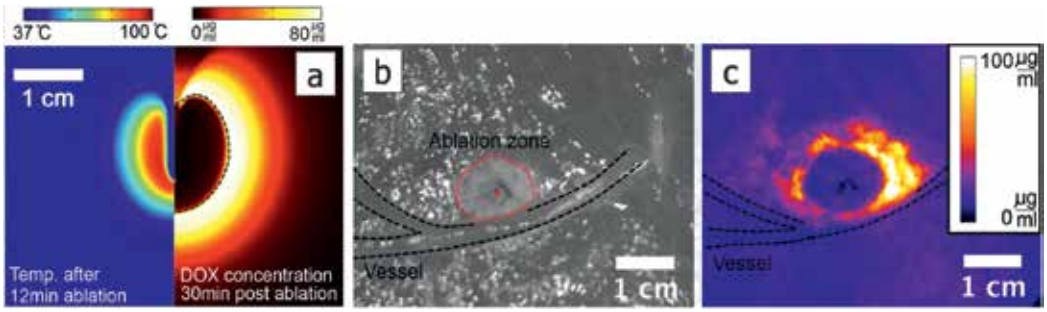

Figure 7. Combination of tumor ablation with TSL. (a) Two-dimensional (2-D) computer simulation of temperature (left), and of drug delivery (right), showing drug uptake in the margin of the ablation zone. Results are based on a prior computer model [73]. (b) Results of a recent porcine animal study (normal liver) demonstrating visible ablation zone, and (c) drug delivery in the margin of the ablation zone visualized by fluorescence imaging (unpublished results), qualitatively similar to computer model prediction in (a).

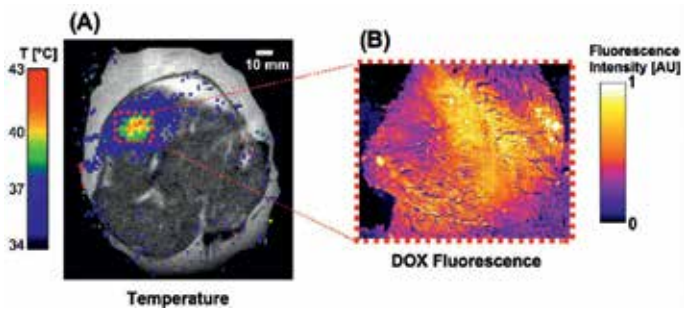

Figure 8. (A) Temperature map during MRgHIFU-hyperthermia measured via MR thermometry, overlaid on preprocedural proton density-weighted image of rabbit thigh muscle. The targeted tissue region is heated to ~40–42°C after administration of TSL-Dox. (B) Doxorubicin distribution visualized via fluorescence microscopy in extracted tissue sample demonstrating localized, image-guided drug delivery. Figure adapted from Ref. [75].

ablation). HIFU employs focusing of ultrasound emitted from external ultrasound transducers into deep tissue regions, resulting in highly localized tissue heating (~mm range diameter of focal spot). The focal spot can be electronically steered, allowing precise spatial targeting with mm accuracy. A technique named magnetic resonance (MR) thermometry allows real-time noninvasive imaging of tissue temperature and is ideally suited to monitor and control HIFU heating (**Figure 8A**) [73]. MRgHIFU thus allows noninvasive targeted heating of deep tissue regions while monitoring and controlling desired temperature, thus being ideally suited for TSL-based drug delivery (**Figure 8B**) [74–76]

5. Clinical trials

TSL formulations have been evaluated in both veterinary trials as well as in human clinical trials as cancer therapy. TSL formulations using doxorubicin have been evaluated in

the veterinary clinic for various cancers. A TSL-doxorubicin formulation (ThermoDox® by Celsion), which is based on the LTSL formulation by Needham et al., has been actively evaluated in the treatment of hepatocellular carcinoma and recurrent breast wall cancers. These clinical trials are briefly discussed below.

5.1. Animal trials

A phase I clinical trial was conducted in companion dogs with solid tumors (carcinomas and sarcomas). Of the 20 dogs that were enrolled in the study, from those that were treated at least twice with TSL-Dox, 12 dogs had stable disease and 6 had partial response. The toxicities observed were manageable [19].

Similarly, TSL-doxorubicin was evaluated in a pilot trial in the veterinary clinic for the treatment of feline soft tissue sarcoma [22]. Eleven cats with advanced sarcoma were divided into three treatment groups with increasing dosage of TSL-doxorubicin. Up to six treatments were delivered every alternate week with a radiofrequency applicator. Two cats in the highest dosage group showed partial response. Dosage was well tolerated in all the cats showing potential for larger studies.

5.2. Human trials

There have been several human clinical trials with TSL-Dox, all with the formulation ThermoDox® (Celsion Corp.), which is based on the LTSL formulation [15].

The furthest progress has been combining TSL with radiofrequency ablation (RFA) in primary liver cancer (i.e., hepatocellular carcinoma). The motivation was delivery of high doses of doxorubicin to the margin of the zone killed by heat, as shown in **Figure 6**. As there was a significant proportion of patients that had local tumor recurrence just outside the ablation zone, there was a strong premise for this approach. Wood et al. [18] reported results at the conclusion of a phase I study involving RFA and TSL-Dox in liver cancer patients. This safety trial showed that TSL-Dox was well tolerated with manageable side effects up to a maximum tolerated dose (MTD) of 50 mg/m^2 (this is in the same range as the MTD for unencapsulated doxorubicin). With the successful completion of this phase I trial, TSL-doxorubicin in combination with RFA was fast tracked to a phase III trial for primary/metastatic liver tumors in the "HEAT trial" (NCT00617981) [77], which unfortunately failed. There have been several possible explanations that have been attributed to this failure, which have been described in detail by Dou et al. [78]. However, a retrospective analysis showed that TSL-Dox in combination with RFA performed better in those patients where the RFA duration was at least 45 minutes [79], which was supported by further animal studies [80]. As a result, a follow-up phase III trial ("OPTIMA trial," NCT0211265) was initiated where required RFA duration was increased, and this trial is ongoing.

Another trial recently initiated in England also focuses on liver cancer (both primary and metastatic cancer) and combines TSL-Dox with HIFU ("TARDOX trial," NCT02181075).

In addition, there have been a few phase I and phase I/II trials where TSL-Dox was combined with microwave hyperthermia for recurrent chest breast wall cancer ("DIGNITY trial,"

NCT00826085). Zagar et al. reported the results of a phase I study using TSL-Dox in recurrent breast wall cancer [70]. Patients who had exhausted all other therapies were enrolled in this trial. Almost 17% of the enrolled patients showed complete remission and another 31% showed partial response. Based on the promising results of these prior phase I/II trials, a follow-up trial has been initiated in Europe ("EURO-DIGNITY," NCT02850419).

Finally, a phase I study has been recently announced in the United States, where TSL-Dox will be combined with MRgHIFU for treating childhood sarcomas (NCT02536183). Thus, at least four different ongoing clinical trials are in various stages of recruiting patients.

1. A phase I study of lyso-thermosensitive liposomal doxorubicin and MR-HIFU for pediatric refractory solid tumors (NCT02536183).
2. Targeted chemotherapy using focused ultrasound for liver tumors (TARDOX) (NCT02181075).
3. Study of ThermoDox with standardized radiofrequency ablation (RFA) for treatment of hepatocellular carcinoma (HCC) (OPTIMA) (NCT0211265).
4. Heat-activated target therapy of local-regional relapse in breast cancer patients (EURO-DIGNITY) (NCT02850419).

6. Conclusion

While TSLs have been first proposed almost 40 years ago, only within the last decade have first results from clinical trials in humans become available. Animal studies have shown that in ideal conditions, up to 20–30 times of bioavailable drug can be delivered to the tumor tissue (measured within a few hours of infusion) as compared to administration of the same dosage of free drug. TSL benefit from reduced off-target toxicity effects, similar to nontemperature sensitive liposomes already in clinical use. The efficacy of TSL depends both on the specific liposomal formulation (e.g., release rate, plasma stability), the encapsulated drug, and on the specific heating modality. Several such heating modalities are clinically available, with MRgHIFU being one of the most attractive methods. HIFU is noninvasive, allows exquisite spatial control of heating with mm accuracy, and combined with MR-thermometry tissue temperature can be monitored and controlled in real time.

Contrary to most other nanoparticle approaches, TSLs can be employed for image-guided drug delivery where the goal is to deliver drug to a region identified by medical imaging. Such an approach may find additional clinical applications apart from cancer. One limitation of many current TSL formulations is the still relatively short plasma half-life (~1 hour), which limits the duration available for delivery, reduces the quantity of encapsulated drug available for release, and also negatively impacts systemic toxicities.

In summary, TSLs represent a highly promising drug delivery approach that has the potential for considerable clinical impact in the near future.

Abbreviations

CF	Carboxyfluorescein
Dox	Doxorubicin
DPPC	Dipalmitoyl phosphatidylcholine
$DPPG_2$	1,2-dipalmitoyl-sn-glycero3-phosphodiglycerol
DSPC	Distearoyl phosphatidylcholine
DSPE-mPEG2000	Distearoyl glycero phosphoethanolamine
DSPE-PEG-2000	1,2-distearoyl-snglycero-3-phosphoethanolamine-N-polyethylene glycol 2000
DSPG	Distearoyl glycero phosphoglycerol
EPR	Enhanced permeability and retention
HIFU	High-intensity focused ultrasound
HSPC	Hydrogenated soy phosphatidylcholine
LTSL	Lysolipid temperature sensitive liposomes
MPPC	Monopalmitoyl phosphatidylcholine
MRgHIFU	Magnetic resonance-guided high-intensity focused ultrasound
MSPC	Myristoyl lyso glycero phosphocholine
MTD	Maximum tolerated dose
PEG	Poly ethylene glycol
RFA	Radiofrequency ablation
TSL	Thermosensitive liposomes
TTSL	Traditional thermosensitive liposomes

Author details

Anjan Motamarry, Davud Asemani and Dieter Haemmerich*

*Address all correspondence to: haemmer@musc.edu

Department of Pediatrics, Medical University of South Carolina, Charleston, SC, USA

References

[1] Kunjachan S, Ehling J, Storm G, Kiessling F, Lammers T. Noninvasive imaging of nanomedicines and nanotheranostics: Principles, progress, and prospects. Chemical Reviews. 2015;**115**:10907-10937. DOI: 10.1021/cr500314d

[2] Maeda H. The enhanced permeability and retention (epr) effect in tumor vasculature: The key role of tumor-selective macromolecular drug targeting. Advances in Enzyme Regulation. 2001;**41**:189-207

[3] Barenholz Y. Doxil(r)—the first fda-approved nano-drug: Lessons learned. Journal of Controlled Release. 2012;**160**:117-134. DOI: 10.1016/j.jconrel.2012.03.020

[4] Park K. Facing the truth about nanotechnology in drug delivery. ACS Nano. 2013;**7**:7442-7447. DOI: 10.1021/nn404501g

[5] Yatvin MB, Weinstein JN, Dennis WH, Blumenthal R. Design of liposomes for enhanced local release of drugs by hyperthermia. Science. 1978;**202**:1290-1293

[6] Ta T, Porter TM. Thermosensitive liposomes for localized delivery and triggered release of chemotherapy. Journal of Controlled Release. 2013;**169**:112-125. DOI: 10.1016/j.jconrel.2013.03.036

[7] Weinstein JN, Magin RL, Yatvin MB, Zaharko DS. Liposomes and local hyperthermia: Selective delivery of methotrexate to heated tumors. Science. 1979;**204**:188-191

[8] Allen TM, Cleland LG. Serum-induced leakage of liposome contents. Biochimica et Biophysica Acta. 1980;**597**:418-426

[9] Lelkes PI, Friedmann P. Stabilization of large multilamellar liposomes by human serum in vitro. Biochimica et Biophysica Acta. 1984;**775**:395-401

[10] Gaber MH, Hong K, Huang SK, Papahadjopoulos D. Thermosensitive sterically stabilized liposomes: Formulation and in vitro studies on mechanism of doxorubicin release by bovine serum and human plasma. Pharmaceutical Research. 1995;**12**:1407-1416

[11] Mumtaz S, Ghosh PC, Bachhawat BK. Design of liposomes for circumventing the reticuloendothelial cells. Glycobiology. 1991;**1**:505-510

[12] Magin RL, Hunter JM, Niesman MR, Bark GA. Effect of vesicle size on the clearance, distribution, and tumor uptake of temperature-sensitive liposomes. Cancer Drug Delivery. 1986;**3**:223-237

[13] Kono K. Thermosensitive polymer-modified liposomes. Advanced Drug Delivery Reviews. 2001;**53**:307-319

[14] Kono K, Zenitani K, Takagishi T. Novel ph-sensitive liposomes: Liposomes bearing a poly(ethylene glycol) derivative with carboxyl groups. Biochimica et Biophysica Acta. 1994;**1193**:1-9

[15] Needham D, Anyarambhatla G, Kong G, Dewhirst MW. A new temperature-sensitive liposome for use with mild hyperthermia: Characterization and testing in a human tumor xenograft model. Cancer Research. 2000;**60**:1197-1201

[16] Gasselhuber A, Dreher MR, Rattay F, Wood BJ, Haemmerich D. Comparison of conventional chemotherapy, stealth liposomes and temperature-sensitive liposomes in a mathematical model. PLoS One. 2012;**7**:e47453. DOI: 10.1371/journal.pone.0047453

[17] Kong G, Anyarambhatla G, Petros WP, Braun RD, Colvin OM, Needham D, Dewhirst MW. Efficacy of liposomes and hyperthermia in a human tumor xenograft model: Importance of triggered drug release. Cancer Research. 2000;**60**:6950-6957

[18] Wood BJ, Poon RT, Locklin JK, Dreher MR, Ng KK, Eugeni M, Seidel G, Dromi S, Neeman Z, Kolf M, Black CD, Prabhakar R, Libutti SK. Phase I study of heat-deployed liposomal doxorubicin during radiofrequency ablation for hepatic malignancies. Journal of Vascular and Interventional Radiology. 2012;**23**:248-255.e7. DOI: 10.1016/j.jvir.2011.10.018

[19] Hauck ML, LaRue SM, Petros WP, Poulson JM, Yu D, Spasojevic I, Pruitt AF, Klein A, Case B, Thrall DE, Needham D, Dewhirst MW. Phase I trial of doxorubicin-containing low temperature sensitive liposomes in spontaneous canine tumors. Clinical Cancer Research. 2006;**12**:4004-4010. DOI: 10.1158/1078-0432.CCR-06-0226

[20] Lindner LH, Eichhorn ME, Eibl H, Teichert N, Schmitt-Sody M, Issels RD, Dellian M. Novel temperature-sensitive liposomes with prolonged circulation time. Clinical Cancer Research. 2004;**10**:2168-2178

[21] Hossann M, Wiggenhorn M, Schwerdt A, Wachholz K, Teichert N, Eibl H, Issels RD, Lindner LH. In vitro stability and content release properties of phosphatidylglyceroglycerol containing thermosensitive liposomes. Biochimica et Biophysica Acta. 2007;**1768**:2491-2499. DOI: 10.1016/j.bbamem.2007.05.021

[22] Zimmermann K, Hossann M, Hirschberger J, Troedson K, Peller M, Schneider M, Bruhschwein A, Meyer-Lindenberg A, Wess G, Wergin M, Dorfelt R, Knosel T, Schwaiger M, Baumgartner C, Brandl J, Schwamberger S, Lindner LH. A pilot trial of doxorubicin containing phosphatidyldiglycerol based thermosensitive liposomes in spontaneous feline soft tissue sarcoma. International Journal of Hyperthermia. 2016;**33**(2):178-190. DOI: 10.1080/02656736.2016.1230233

[23] El-Kareh AW, Secomb TW. A mathematical model for comparison of bolus injection, continuous infusion, and liposomal delivery of doxorubicin to tumor cells. Neoplasia. 2000;**2**:325-338

[24] Chen Q, Tong S, Dewhirst MW, Yuan F. Targeting tumor microvessels using doxorubicin encapsulated in a novel thermosensitive liposome. Molecular Cancer Therapeutics. 2004;**3**:1311-1317

[25] Kneidl B, Peller M, Winter G, Lindner LH, Hossann M. Thermosensitive liposomal drug delivery systems: State of the art review. International Journal of Nanomedicine. 2014;**9**:4387-4398. DOI: 10.2147/IJN.S49297

[26] Lokerse WJ, Kneepkens EC, Ten Hagen TL, Eggermont AM, Grull H, Koning GA. In depth study on thermosensitive liposomes: Optimizing formulations for tumor specific therapy and in vitro to in vivo relations. Biomaterials. 2016;**82**:138-150. DOI: 10.1016/j.biomaterials.2015.12.023

[27] Manzoor AA, Lindner LH, Landon CD, Park JY, Simnick AJ, Dreher MR, Das S, Hanna G, Park W, Chilkoti A, Koning GA, ten Hagen TL, Needham D, Dewhirst MW.

Overcoming limitations in nanoparticle drug delivery: Triggered, intravascular release to improve drug penetration into tumors. Cancer Research. 2012;**72**:5566-5575. DOI: 10.1158/0008-5472.can-12-1683

[28] Gustafson DL, Rastatter JC, Colombo T, long ME. Doxorubicin pharmacokinetics: Macromolecule binding, metabolism, and excretion in the context of a physiologic model. Journal of Pharmaceutical Sciences. 2002;**91**:1488-1501

[29] Yang RS, Andersen ME, Pharmacokinetics, Norwalk: Appleton and Lange; 1994. pp. 49-73

[30] Park K. Lessons learned from thermosensitive liposomes for improved chemotherapy. Journal of Controlled Release. 2014;**174**:219

[31] Ritsma L, Steller EJA, Ellenbroek SIJ, Kranenburg O, Borel Rinkes IHM, van Rheenen J. Surgical implantation of an abdominal imaging window for intravital microscopy. Nature Protocols. 2013;**8**:583-594

[32] Li L, ten Hagen TL, Hossann M, Suss R, van Rhoon GC, Eggermont AM, Haemmerich D, Koning GA. Mild hyperthermia triggered doxorubicin release from optimized stealth thermosensitive liposomes improves intratumoral drug delivery and efficacy. Journal of Controlled Release. 2013;**168**:142-150. DOI: 10.1016/j.jconrel.2013.03.011

[33] Sullivan SM, Huang L. Preparation and characterization of heat-sensitive immunoliposomes. Biochimica et Biophysica Acta. 1985;**812**:116-126

[34] Vingerhoeds MH, Steerenberg PA, Hendriks JJ, Dekker LC, Van Hoesel QG, Crommelin DJ, Storm G. Immunoliposome-mediated targeting of doxorubicin to human ovarian carcinoma in vitro and in vivo. British Journal of Cancer. 1996;**74**:1023-1029

[35] Kullberg M, Mann K, Owens JL. A two-component drug delivery system using her-2-targeting thermosensitive liposomes. Journal of Drug Targeting. 2009;**17**:98-107. DOI: 10.1080/10611860802471562

[36] Haeri A, Zalba S, Ten Hagen TL, Dadashzadeh S, Koning GA. Egfr targeted thermosensitive liposomes: A novel multifunctional platform for simultaneous tumor targeted and stimulus responsive drug delivery. Colloids and Surfaces B Biointerfaces. 2016;**146**:657-669. DOI: 10.1016/j.colsurfb.2016.06.012

[37] Kullberg M, Owens JL, Mann K. Listeriolysin o enhances cytoplasmic delivery by her-2 targeting liposomes. Journal of Drug Targeting. 2010;**18**:313-320. DOI: 10.3109/10611861003663549

[38] Na K, Lee SA, Jung SH, Hyun J, Shin BC. Elastin-like polypeptide modified liposomes for enhancing cellular uptake into tumor cells. Colloids and Surfaces B Biointerfaces. 2012;**91**:130-136. DOI: 10.1016/j.colsurfb.2011.10.051

[39] Wang C, Wang X, Zhong T, Zhao Y, Zhang WQ, Ren W, Huang D, Zhang S, Guo Y, Yao X, Tang YQ, Zhang X, Zhang Q. The antitumor activity of tumor-homing peptide-modified thermosensitive liposomes containing doxorubicin on mcf-7/adr: In vitro and in vivo. International Journal of Nanomedicine. 2015;**10**:2229-2248. DOI: 10.2147/ijn.s79840

[40] Dicheva BM, ten Hagen TL, Seynhaeve AL, Amin M, Eggermont AM, Koning GA. Enhanced specificity and drug delivery in tumors by crgd-anchoring thermosensitive liposomes. Pharmaceutical Research. 2015;**32**:3862-3876. DOI: 10.1007/s11095-015-1746-7

[41] Deng Z, Xiao Y, Pan M, Li F, Duan W, Meng L, Liu X, Yan F, Zheng H. Hyperthermia-triggered drug delivery from irgd-modified temperature-sensitive liposomes enhances the anti-tumor efficacy using high intensity focused ultrasound. Journal of Controlled Release. 2016;**243**:333-341. DOI: 10.1016/j.jconrel.2016.10.030

[42] Zhang K, Liu M, Tong X, Sun N, Zhou L, Cao Y, Wang J, Zhang H, Pei R. Aptamer-modified temperature-sensitive liposomal contrast agent for magnetic resonance imaging. Biomacromolecules. 2015;**16**:2618-2623. DOI: 10.1021/acs.biomac.5b00250

[43] Lopez-Noriega A, Ruiz-Hernandez E, Quinlan E, Storm G, Hennink WE, O'Brien FJ. Thermally triggered release of a pro-osteogenic peptide from a functionalized collagen-based scaffold using thermosensitive liposomes. Journal of Controlled Release. 2014;**187**:158-166. DOI: 10.1016/j.jconrel.2014.05.043

[44] Yatvin MB, Muhlensiepen H, Porschen W, Weinstein JN, Feinendegen LE. Selective delivery of liposome-associated cis-dichlorodiammineplatinum(ii) by heat and its influence on tumor drug uptake and growth. Cancer Research. 1981;**41**:1602-1607

[45] Tomita T, Watanabe M, Takahashi T, Kumai K, Tadakuma T, Yasuda T. Temperature-sensitive release of adriamycin, an amphiphilic antitumor agent, from dipalmitoylphosphatidylcholine-cholesterol liposomes. Biochimica et Biophysica Acta. 1989;**978**:185-190

[46] Merlin JL. Encapsulation of doxorubicin in thermosensitive small unilamellar vesicle liposomes. European Journal of Cancer. 1991;**27**:1026-1030

[47] Unezaki S, Maruyama K, Takahashi N, Koyama M, Yuda T, Suginaka A, Iwatsuru M. Enhanced delivery and antitumor activity of doxorubicin using long-circulating thermosensitive liposomes containing amphipathic polyethylene glycol in combination with local hyperthermia. Pharmaceutical Research. 1994;**11**:1180-1185

[48] Negussie AH, Yarmolenko PS, Partanen A, Ranjan A, Jacobs G, Woods D, Bryant H, Thomasson D, Dewhirst MW, Wood BJ, Dreher MR. Formulation and characterization of magnetic resonance imageable thermally sensitive liposomes for use with magnetic resonance-guided high intensity focused ultrasound. International Journal of Hyperthermia. 2011;**27**:140-155. DOI: 10.3109/02656736.2010.528140

[49] de Smet M, Heijman E, Langereis S, Hijnen NM, Grull H. Magnetic resonance imaging of high intensity focused ultrasound mediated drug delivery from temperature-sensitive liposomes: An in vivo proof-of-concept study. Journal of Controlled Release. 2011;**150**:102-110. DOI: 10.1016/j.jconrel.2010.10.036

[50] Willerding L, Limmer S, Hossann M, Zengerle A, Wachholz K, Ten Hagen TL, Koning GA, Sroka R, Lindner LH, Peller M. Method of hyperthermia and tumor size influence effectiveness of doxorubicin release from thermosensitive liposomes in experimental tumors. Journal of Controlled Release. 2016;**222**:47-55. DOI: 10.1016/j.jconrel.2015.12.004

[51] van Bree C, Krooshoop JJ, Rietbroek RC, Kipp JB, Bakker PJ. Hyperthermia enhances tumor uptake and antitumor efficacy of thermostable liposomal daunorubicin in a rat solid tumor. Cancer Research. 1996;**56**:563-568

[52] Lu T, Lokerse WJ, Seynhaeve AL, Koning GA, ten Hagen TL. Formulation and optimization of idarubicin thermosensitive liposomes provides ultrafast triggered release at mild hyperthermia and improves tumor response. Journal of Controlled Release. 2015;**220**:425-437. DOI: 10.1016/j.jconrel.2015.10.056

[53] Wu Y, Yang Y, Zhang FC, Wu C, Lu WL, Mei XG. Epirubicin-encapsulated long-circulating thermosensitive liposome improves pharmacokinetics and antitumor therapeutic efficacy in animals. Journal of Liposome Research. 2011;**21**:221-228. DOI: 10.3109/08982104.2010.520273

[54] Liu H, Zhang Y, Han Y, Zhao S, Wang L, Zhang Z, Wang J, Cheng J. Characterization and cytotoxicity studies of dppc:M(2+) novel delivery system for cisplatin thermosensitivity liposome with improving loading efficiency. Colloids and Surfaces B Biointerfaces. 2015;**131**:12-20. DOI: 10.1016/j.colsurfb.2015.04.029

[55] Tiwari SB, Udupa VN, Rao S, Devi PU. Thermochemotherapy: Synergism between hyperthermia and liposomal bleomycin in mice bearing melanoma b16f1. Pharmacy and Pharmacology Communications. 2000;**6**:19-23. DOI: 10.1211/146080800128735421

[56] Chelvi TP, Ralhan R. Hyperthermia potentiates antitumor effect of thermosensitive-liposome-encapsulated melphalan and radiation in murine melanoma. Tumour Biology. 1997;**18**:250-260

[57] Wang ZY, Zhang H, Yang Y, Xie XY, Yang YF, Li Z, Li Y, Gong W, Yu FL, Yang Z, Li MY, Mei XG. Preparation, characterization, and efficacy of thermosensitive liposomes containing paclitaxel. Drug Delivery. 2016;**23**:1222-1231. DOI: 10.3109/10717544.2015.1122674

[58] Zhang H, Gong W, Wang ZY, Yuan SJ, Xie XY, Yang YF, Yang Y, Wang SS, Yang DX, Xuan ZX, Mei XG. Preparation, characterization, and pharmacodynamics of thermosensitive liposomes containing docetaxel. Journal of Pharmaceutical Sciences. 2014;**103**:2177-2183. DOI: 10.1002/jps.24019

[59] Limmer S, Hahn J, Schmidt R, Wachholz K, Zengerle A, Lechner K, Eibl H, Issels RD, Hossann M, Lindner LH. Gemcitabine treatment of rat soft tissue sarcoma with phosphatidyldiglycerol-based thermosensitive liposomes. Pharmaceutical Research. 2014;**31**:2276-2286. DOI: 10.1007/s11095-014-1322-6

[60] Al Sabbagh C, Tsapis N, Novell A, Calleja-Gonzalez P, Escoffre JM, Bouakaz A, Chacun H, Denis S, Vergnaud J, Gueutin C, Fattal E. Formulation and pharmacokinetics of thermosensitive stealth(r) liposomes encapsulating 5-fluorouracil. Pharmaceutical Research. 2015;**32**:1585-1603. DOI: 10.1007/s11095-014-1559-0

[61] Zhang H, Wang ZY, Gong W, Li ZP, Mei XG, Lv WL. Development and characteristics of temperature-sensitive liposomes for vinorelbine bitartrate. International Journal of Pharmaceutics. 2011;**414**:56-62. DOI: 10.1016/j.ijpharm.2011.05.013

[62] Wang S, Mei XG, Goldberg SN, Ahmed M, Lee JC, Gong W, Han HB, Yan K, Yang W. Does thermosensitive liposomal vinorelbine improve end-point survival after percutaneous radiofrequency ablation of liver tumors in a mouse model? Radiology. 2016;**279**:762-772. DOI: 10.1148/radiol.2015150787

[63] Wardlow R, Bing C, VanOsdol J, Maples D, Ladouceur-Wodzak M, Harbeson M, Nofiele J, Staruch R, Ramachandran A, Malayer J, Chopra R, Ranjan A. Targeted antibiotic delivery using low temperature-sensitive liposomes and magnetic resonance-guided high-intensity focused ultrasound hyperthermia. International Journal of Hyperthermia. 2016;**32**:254-264. DOI: 10.3109/02656736.2015.1134818

[64] Li M, Li Z, Yang Y, Wang Z, Yang Z, Li B, Xie X, Song J, Zhang H, Li Y, Gao G, Yang J, Mei X, Gong W. Thermo-sensitive liposome co-loaded of vincristine and doxorubicin based on their similar physicochemical properties had synergism on tumor treatment. Pharmaceutical Research. 2016;**33**:1881-1898. DOI: 10.1007/s11095-016-1924-2

[65] AllenTM, Martin FJ. Advantages of liposomal delivery systems for anthracyclines. Seminars in Oncology. 2004;**31**:5-15

[66] Rossmann C, Haemmerich D. Review of temperature dependence of thermal properties, dielectric properties, and perfusion of biological tissues at hyperthermic and ablation temperatures. Critical Reviews in Biomedical Engineering. 2014;**42**:467-492

[67] You J, Shao R, Wei X, Gupta S, Li C. Near-infrared light triggers release of paclitaxel from biodegradable microspheres: Photothermal effect and enhanced antitumor activity. Small. 2010;**6**:1022-1031. DOI: 10.1002/smll.201000028

[68] You J, Zhang P, Hu F, Du Y, Yuan H, Zhu J, Wang Z, Zhou J, Li C. Near-infrared light-sensitive liposomes for the enhanced photothermal tumor treatment by the combination with chemotherapy. Pharmaceutical Research. 2014;**31**:554-565. DOI: 10.1007/s11095-013-1180-7

[69] Ryan TP, Brace CL. Interstitial microwave treatment for cancer: Historical basis and current techniques in antenna design and performance. International Journal of Hyperthermia. 2017;**33**:3-14. DOI: 10.1080/02656736.2016.1214884

[70] Zagar TM, Vujaskovic Z, Formenti S, Rugo H, Muggia F, O'Connor B, Myerson R, Stauffer P, Hsu IC, Diederich C, Straube W, Boss MK, Boico A, Craciunescu O, Maccarini P, Needham D, Borys N, Blackwell KL, Dewhirst MW. Two phase I dose-escalation/pharmacokinetics studies of low temperature liposomal doxorubicin (ltld) and mild local hyperthermia in heavily pretreated patients with local regionally recurrent breast cancer. International Journal of Hyperthermia. 2014;**30**:285-294. DOI: 10.3109/02656736.2014.936049

[71] Rossmann C, Rattay F, Haemmerich D. Platform for patient-specific finite-element modeling and application for radiofrequency ablation. 2012;**1**:0. DOI:10.1615/VisualizImageProcComputatBiomed.2012004898

[72] Gasselhuber A, Dreher MR, Negussie A, Wood BJ, Rattay F, Haemmerich D. Mathematical spatio-temporal model of drug delivery from low temperature sensitive liposomes during radiofrequency tumour ablation. International Journal of Hyperthermia. 2010;**26**:499-513. DOI: 10.3109/02656731003623590

[73] Rieke V, Butts Pauly K. Mr thermometry. Journal of Magnetic Resonance Imaging. 2008; **27**:376-390. DOI: 10.1002/jmri.21265

[74] Gasselhuber A, Dreher MR, Partanen A, Yarmolenko PS, Woods D, Wood BJ, Haemmerich D. Targeted drug delivery by high intensity focused ultrasound mediated hyperthermia combined with temperature-sensitive liposomes: Computational modeling and preliminary in vivo validation. International Journal of Hyperthermia. 2012;**28**:337-348. DOI: 10.3109/02656736.2012.677930

[75] StaruchRM, Hynynen K, Chopra R. Hyperthermia-mediated doxorubicin release from thermosensitive liposomes using mr-hifu: Therapeutic effect in rabbit vx2 tumours. International Journal of Hyperthermia. 2015;**31**:118-133. DOI: 10.3109/02656736.2014.992483

[76] Grull H, Langereis S. Hyperthermia-triggered drug delivery from temperature-sensitive liposomes using mri-guided high intensity focused ultrasound. Journal of Controlled Release. 2012;**161**:317-327. DOI: 10.1016/j.jconrel.2012.04.041

[77] Celsion's phase iii thermodox(r) heat study recommended for continuation by data monitoring committee. 2017. Available from: http://investor.celsion.com/releasedetail.cfm?releaseid=469443 (Accessed: February 2, 2017)

[78] Dou Y, Hynynen K, Allen C. To heat or not to heat: Challenges with clinical translation of thermosensitive liposomes. Journal of Controlled Release. 2017;**249**:63-73. DOI: 10.1016/j.jconrel.2017.01.025

[79] Lencioni R, Tak W.-Y, Chen M. H, Finn R. S, Sherman M, Makris L, O'Neal M, Simonich W, Haemmerich D, Reed R, Borys N, Poon R. T. P, Abou-Alfa G. K: Standardized radiofrequency ablation (srfa) ≥ 45 minutes (m) plus lyso-thermosensitive liposomal doxorubicin (ltld) for solitary hepatocellular carcinoma (hcc) lesions 3-7 cm: A retrospective analysis of phase iii heat study. Journal of Clinical Oncology. 2014; 32:e15143–e15143. DOI:10.1200/jco.2014.32.15_suppl.e15143

[80] Swenson CE, Haemmerich D, Maul DH, Knox B, Ehrhart N, Reed RA. Increased duration of heating boosts local drug deposition during radiofrequency ablation in combination with thermally sensitive liposomes (thermodox) in a porcine model. PLoS One. 2015;**10**:e0139752. DOI: 10.1371/journal.pone.0139752

Chapter 8

Liposomal Drug Delivery to the Central Nervous System

Rita Nieto Montesinos

Additional information is available at the end of the chapter

http://dx.doi.org/10.5772/intechopen.70055

Abstract

Central nervous system diseases represent a huge world of burden of human suffering with negative economic results. Most therapeutic compounds cannot attain the brain because of the blood-brain barrier and its expression of efflux transporters. Among them, the P-glycoprotein plays a significant role leading to failure of various clinical treatments. A non-invasive strategy to circumvent the blood-brain barrier and P-glycoprotein emphasizes on the encapsulation and therefore masking of therapeutic compounds in drug delivery systems. Up to now, liposomes are the most widely studied drug delivery systems due to their biocompatibility, biodegradability, and less toxicity. The incorporation of polyethylene glycol-lipid derivatives within the bilayer of conventional liposomes significantly prolongs liposomal cargo half-life by steric stabilization. Interestingly, an increased brain accumulation of liposomal cargo is achieved by coupling targeting moieties on liposomes surface. These targeting moieties such as peptides or monoclonal antibodies recognize the biochemical transport systems at the blood-brain barrier and mediate the transport of liposomes and their cargo across this barrier. Moreover, stimuli-sensitive liposomes are programmed for cargo release when exposed to a particular microenvironment. Hence, this chapter highlights the potential liposomal applications for delivery of therapeutic compounds as well as diagnostic tools or both, in major central nervous system diseases.

Keywords: central nervous system diseases, blood-brain barrier, P-glycoprotein, liposomes, passive targeting, active targeting, stimuli strategies

1. Introduction

Most neurological disorders compromise the central nervous system (CNS) and its main organ, the brain. These disorders include stroke, brain cancer, Alzheimer's disease, Parkinson's

disease, epilepsy, multiple sclerosis, neuroinfections, and traumatic disorders of the nervous system, among others (http://www.who.int/en/). Because millions of people worldwide are affected by CNS disorders, they constitute 6.3% of the global burden of disease. In other words, CNS diseases are a huge world of burden of human suffering with negative economic results [1]. Most of the therapeutic molecules cannot attain the brain because of the presence of the blood-brain barrier (BBB), which separates the bloodstream from the cerebral parenchyma [2]. This barrier is mainly composed by endothelial cells, which are linked by tight junctions [3]. The BBB also contains a basal membrane, pericytes, and astrocytes [3]. More important is the presence of efflux transporters that perform active back-transport of the therapeutic molecules to the blood lumen. P-glycoprotein (P-gp) is the most important efflux transporter associated to the failure of various therapies to treat CNS diseases [4]. Advances in nanomedicine have created a non-invasive strategy for the management of CNS diseases [5]. This strategy emphasizes on the encapsulation of therapeutic compounds, which are mainly P-gp substrates, in drug delivery systems, also called nanocarriers, such as liposomes, lipid nanocapsules, polymeric nanoparticles, or polymersomes [6–10]. Encapsulation of therapeutic compounds in drug delivery systems improve their solubility and protect them from the biological environment and circumvent the P-gp at the BBB yielding higher concentrations of the therapeutic compounds in the brain parenchyma [5]. Among nanocarriers, liposomes have been the most studied due to their composition, which makes them biocompatible, biodegradable, and less toxic [11]. Liposomes not only hold potential as vehicles for therapeutic compounds (therapeutics) [7] but also for diagnostic tools (diagnostics) [12] directed to the CNS. Interestingly, recent efforts have combined therapeutics and diagnostics in the same unique nanocarrier, thus opening the way to theranostic liposomes, which represent an essential advancement for personalized nanomedicine [13]. To specifically target the therapeutic compound or the diagnostic tool to the pathological site, the CNS, two strategies are usually used [14]: (1) Passive targeting based on the longevity of the pharmaceutical carrier in the blood and its accumulation in pathological sites with compromised vasculature via the enhanced permeability and retention effect and (2) Active targeting based on the attachment of specific ligands to nanocarriers surface to recognize and bind specific biological receptors expressed at the BBB [14]. Later studies propose a new active targeting strategy in which liposomes take advantage of changes in the pathological microenvironment for localized and timely release of their cargo [15]. According to their formulation, stimuli-sensitive liposomes release may obey to internal stimuli such as pH, temperature, redox condition, and enzymatic activity or external stimuli such as magnetic fields, ultrasound, or irradiation [15]. Since innovative strategies are urgently needed to counteract CNS diseases, this manuscript summarizes the most relevant examples of passively and actively targeted liposomes, smaller than 200 nm, for therapeutics, diagnostics, or theranostics of major CNS diseases.

2. The blood-brain barrier

The blood-brain barrier (BBB) is an innate and selective barrier formed by endothelial cells lining ~650 km of microvessels, which constitute by far the largest interface for the blood-brain

exchange (**Figure 1**) [3]. The BBB endothelial cells differ from endothelial cells in the rest of the body by the absence of fenestrations and sparse pinocytic vesicular transport. The BBB endothelial cells display wider tight junctions known as zonulae occludens, and adherens junctions (AJ), which cover the vessels walls as a continuous sheath, leaving no space between cells [16]. Moreover, the BBB is also composed by an extracellular matrix (basal membrane), pericytes, and astrocyte foot processes [2, 4]. Because of this configuration, most molecular traffic takes a transcellular route across the BBB, rather than moving paracellularly as in most endothelia. The presence of specific transport systems on the luminal and abluminal membranes regulates the influx and efflux of various essential endogenous and exogenous substrates [17, 18]. Small gases such as oxygen and carbon dioxide but also small lipophilic agents, such as ethanol, caffeine, nicotine, and drugs like anesthetics and barbiturates, can diffuse freely through the lipid membranes [19]. Small polar molecules, such as glucose, amino acids, organic anions and cations, and nucleosides cross the BBB by carrier-mediated transport. Large solutes, such as proteins and peptides, are transported across the BBB by receptor-mediated or adsorption-mediated endocytic transport [17, 18]. In parallel, it was originally stated that therapeutic compounds transporting across the BBB were dependent on their physicochemical properties such as lipophilicity, molecular weight, and ionic state. However, it is the presence of efflux

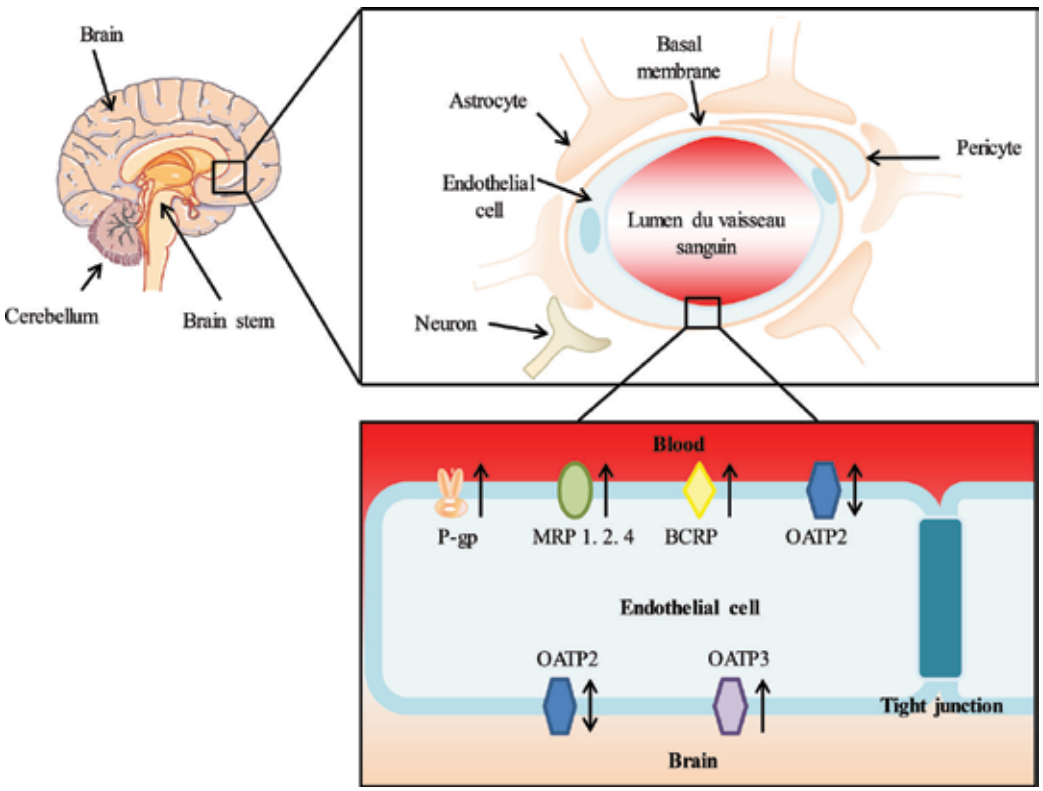

Figure 1. The blood-brain barrier. P-gp = P-glycoprotein, MRP = Multidrug resistance-associated proteins, BCRP = Breast cancer resistance protein, and OATP = Organic anion transporter polypeptide.

transporters at the BBB that limits the brain uptake of a variety of endogenous and exogenous compounds, including relatively lipophilic therapeutic compounds [20]. Most of these efflux transporters belong to the ATP-binding cassette (ABC) transporters super family. ABC transporters are transmembrane proteins that use the energy from the ATP hydrolysis to drive the efflux of their substrates. Based on three critical defining criteria, multi-specificity, location, and energetics; P-glycoprotein is considered to be the most important ABC efflux transporter at the BBB [21].

3. The P-glycoprotein

The expression of P-glycoprotein (P-gp) on endothelial cells at the human BBB was first described in 1989 by Cordon-Cardo et al. and Theibaut et al. [22, 23]. Since then, P-gp has been found at the luminal membrane of the endothelial cells lining the capillaries of the brain [4, 24], in neurons and in astrocytes [25, 26]. The P-gp is also localized at the apical surfaces of the epithelial cells that constitute the ventricular exposed surface of the human choroid plexus [27]. The P-gp was also observed in primary brain tumors [28]. The relevance of the P-gp at the BBB has been properly illustrated in knockout mice lacking the P-gp isoform mdr1a (mdr1a (−/−) mice). The mdr1a (−/−) mice were healthy and fertile and appeared phenotypically normal, but they accumulated much higher levels of P-gp substrates in the brain. A clear example was the increased sensitivity to the centrally neurotoxic pesticide ivermectin [29]. Knockout mice accumulated 100-fold higher concentrations of ivermectin in the brain as compared to wild-type mice; consequently, knockout mice developed a severe neurotoxicity and died [29]. More recently, selamectin, another pesticide also demonstrated to be a P-gp substrate [30]. Meanwhile, pharmacokinetic studies in knockout mice were rapidly extended to therapeutic drugs. Thus, the absence of mdr1a in mice led to highly increased levels of vinblastine, digoxin, and cyclosporin A in the brain [31]. Tissue distribution studies demonstrated that the relative brain penetration of radiolabeled ondansetron and loperamide is increased 4- and almost 14-fold, respectively in mdr1a (−/−) mice. Moreover, a pilot toxicity study showed that the oral administration of loperamide gains potent opiate-like activity in the CNS of mdr1a (−/−) mice. Oral domperidone also showed neuroleptic-like side effects in mdr1a (−/−) mice [31]. Using the same *in vivo* model, it was suggested that antidepressants like levomilnacipran, vilazodone, and escitalopram are P-gp substrates [32], while the modern antiepileptic topiramato is only a weak P-gp substrate [33]. These observations are strongly supported by brain distribution and disease models not only for the above drugs but also for a large list of them [2].

4. Circumventing the BBB

Disruption of the BBB has been observed in various CNS pathologies such as stroke, multiple sclerosis (MS), and amyotrophic lateral sclerosis (ALS) [34]. From these scenarios, it is known that disruption of the BBB leads to increased extravasation of immune cells and

poorly regulated flux of molecules and ions across the BBB with consequent neuroinflammation, neurodegeneration, or infections [35]. Additionally, clinical disruption of the BBB is expensive and requires hospitalization [7]. Therefore, in diseases where the BBB represents an obstacle to attain significant brain concentrations of therapeutic compounds, a less aggressive alternative is by modulating the activity of the P-gp. Nonetheless, we cannot negligate that the P-gp protects the brain from intoxication by endogenous and exogenous harmful lipophilic compounds that otherwise could penetrate the BBB by simple diffusion without any limitation [36]. Therefore, the ideal approach should inhibit the P-gp at the BBB to let the P-gp substrate (therapeutic compound) enter into the brain and then re-induce the P-gp-mediated efflux to hamper the entry of harmful compounds. The development of third-generation P-gp modulators, which transiently and directly inhibit the transport of P-gp substrates, has been a promising approach to modulate the P-gp [37, 38]. Unfortunately, clinical studies suggest high doses of these compounds. These high doses by themselves or in co-administration with P-gp substrates may predict toxic profiles, thus limiting the use of these agents [39]. Several studies have already proposed the use of natural products, the designs of peptidomimetics, and dual activity ligands as a fourth-generation of P-gp modulators [40]. In spite of the countless studies, the effective and safe inhibition of the P-gp at the human BBB is not yet a reality. A non-invasive strategy that takes advantage of the CNS physiology involves nanomedicine [41]. This innovative strategy uses mainly nano-scale drug delivery systems (DDSs) such as liposomes, polymeric nanoparticles, lipid nanocapsules, and polymersomes. Hereafter, DDSs transport small doses of poorly soluble drugs through the body and by-pass the P-gp at the BBB to finally target the brain, thus reducing toxicity in peripheral tissues [5]. A synergistic strategy that had obtained optimistic *in vivo* results tackling the P-gp at the BBB is the concomitant loading of a P-gp substrate and a P-gp inhibitor in the same nanocarrier [42]. Nanomedicine also offers the possibility to transport diagnostic tools as well, thus providing clear benefits to diagnose and treat defiant diseases [43]. Owing to their unique characteristics like biocompatibility, biodegradability, non-inmunogenicity, and less toxicity, liposomes have been the most studied and clinically recognized among nanocarriers [11].

5. Liposomal strategies to target the central nervous system

Nanotechnology is the understanding and control of matters having dimensions roughly within the 1–100 nm range. However, in nanomedicine, particles smaller than 10 nm are quickly cleared by the kidney or through extravasation and particles bigger than 200 nm are efficiently filtered by liver, spleen, and bone marrow, thus a size between 10 and 200 nm would enable liposomes to circulate in the bloodstream [44]. Due to their structure, liposomes have demonstrated their ability as nanocarriers for CNS targeting of hydrophilic or lipophilic cytotoxics, neuroprotectants, antiepyleptics, anti-ischemia, antiretroviral and antifungals drugs among others, and diagnostic agents. Basically, liposomes deliver their cargo across the BBB through passive and active targeting (**Figure 2**). Nonetheless, active targeting goes further, opening a stimuli-responsive strategy.

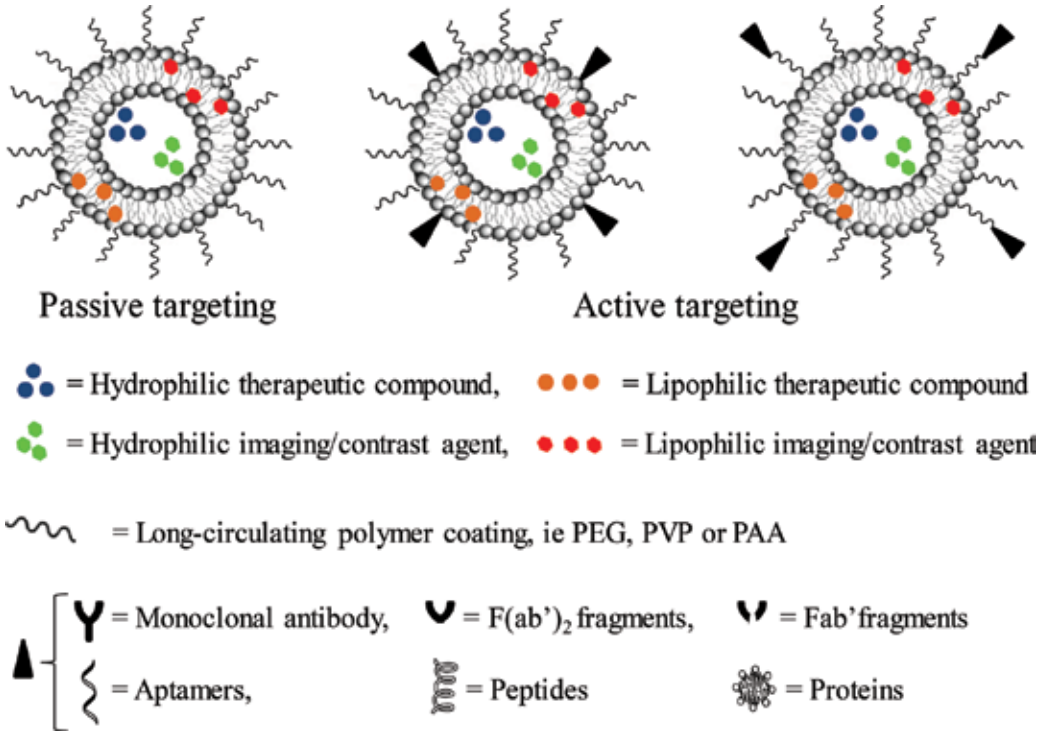

Figure 2. Liposomal strategies for passive and active targeting.

5.1. Passive targeting strategy

Passive targeting is mainly based on the enhanced permeability and retention (EPR) effect. In 1986, Maeda and co-workers named EPR effect to the mechanism in which macromolecules with a high molecular weight, 15000 to 70000 daltons, such as polymers and proteins precipitate and accumulate effectively in tumor tissues [45]. Such high accumulation usually last more than 24 hours [45]. This phenomenon was attributed to the hypervasculature and enhanced vascular permeability in solid tumors, which is due to the overproduction of vascular mediators including bradykinin, nitric oxide (NO), vascular endothelial growth factor (VEGF) and carbon monoxide (CO) [46]. Moreover, solid tumors have defective blood vessels with large gaps, up to 1.0 μm between endothelial cells, whereby macromolecules pass to the tumor [14]. Since solid tumors lack adequate lymphatic drainage, there is therefore a poor circulatory recovery of the extravasated macromolecules, resulting in their accumulation in the tumor microenvironment for long periods [14]. This phenomenon was not observed in healthy blood vessels [45]; hence, it constituted a promising strategy to treat selectively cancer solid tumors using nanocarriers like polymer-coated liposomes [47]. Prolonged blood circulation may allow a longer interaction time between liposomes and the target. The incorporation of soluble, hydrophilic, flexible and biocompatible polymers such as polyethylene glycol (PEG) or its derivatives within the bilayer of conventional liposomes leads to the formation of a protective and hydrophilic layer on their surface. This prevents the recognition

of liposomes by opsonins and reduces their clearance by the reticuloendothelial system (RES) and consequently extends the liposomal half-life [48]. Other prominent synthetic polymers with stealth properties are poly(vinyl pyrrolidone) (PVP) and poly(acryl amide) (PAA) [11]. Liposomes size is another parameter with high impact on the passive targeting through the EPR effect. Long-circulating liposomes also called stealth liposomes should possess a size inferior to 400 nm for effective extravasation [14, 48]. Different studies demonstrated that passive targeting provides promising therapeutic outcomes in diseases where there is a BBB disruption like stroke [49, 50].

5.2. Active targeting strategy

In the last few years, more sophisticated liposomes were designed to actively target the brain. Active targeting lies on the coupling of targeting moieties including small-molecule ligands, peptides, aptamers, monoclonal antibodies (mAbs) or their fragments on the liposomal surface. Then these functionalized liposomes are able to target the brain after recognizing the biochemical transport systems expressed at the brain endothelial cells. Such systems are the adsorptive-mediated endocytosis (AME), the carrier-mediated transport (CMT), and the receptor-mediated endocytosis (RME). Brain targeting through AME is based on the electrostatic interaction between a positively charged moiety and the negatively charged sites on the luminal surface of plasma membrane and brain capillaries. For instance, cationized human serum albumin conjugated to PEGylated liposomes showed a rapidly time-dependent response taken up by cultured porcine brain capillary endothelial cells and by intact brain capillaries [51]. However, *in vivo*, AME also occurs to a large extent in other organs like liver and kidneys, thus decreasing brain specificity [6]. The CMT systems are localized at the brain capillary endothelium and mediate the passage of small molecular weight nutrients across the BBB. The most studied are the transporters for D-glucose (GLUT1), large neutral amino acid (LAT1), small neutral amino acids (EAAT), cationic amino acids (CAT1), monocarboxylic acids (MCT1), and organic cations (OCT) [52]. Although a possible competition with endogenous ligands is predicted, liposomes decorated with LAT1 were able to penetrate the BBB penetration *in vivo* [53]. RME is one of the major mechanisms by which various DDSs can deliver their cargo across the BBB. RME systems require the binding of a ligand to a specific receptor located on the luminal membrane of the BBB [6]. Then, the receptor-ligand binding induces the internalization of receptor-ligand complexes within an endocytic vesicle. From there forward, receptors may mediate different processes including: (1) transcytosis of the ligand from blood to brain, (2) reverse transcytosis from brain to blood, or (3) only endocytosis into the brain capillary endothelium without net transport across the endothelial cell [52]. Specific receptors of the brain capillary endothelium have been identified for low-density lipoproteins (LDL), low-density lipoprotein receptor-related protein 1 (LRP-1), insulin, insulin-like growth factors (IGF-I, IGF-II), interleukin-1 (IL-1), folic acid (FA) and transferrin (Tf) [52]. Hence, attachment of these endogenous ligands to the surface of liposomes has generated promising results [54]. Besides binding endogenous ligands, these receptors also bind mAbs or their fragments (Fab', $F(ab')_2$), which could be grafted on the liposomes surface [6]. The most successful mAb that has been studied and used for brain targeting is OX26 [55, 56], which specifically targets brain capillary endothelial cells, thanks to the high concentration

of the transferrin receptor (TfR) expressed on their luminal side [57]. Thus, OX26 may be able to cross the BBB via the receptor-mediated transcytosis. OX26 does not bind the TfR on the transferrin-binding site but uses another epitope [58]. Given that high doses of insulin are required to target the insulin receptor and that an overdose of insulin could cause hypoglycemia, some studies effectively promote grafting of liposomes with the murine 83–14 mAb to target the BBB via the insulin receptor [59]. The low-density lipoprotein receptor (LDLR) and the LDLR-related protein (LRP) can bind multiple ligands. Among them, the apolipoprotein E grafted to liposomes favored the internalization of the DDS via the LDLR in porcine brain capillary endothelial cells and the rodent cell line RBE4 [60]. Moreover, increased expression of epidermal growth factor receptor (EGFR) [61], vascular endothelial growth factor receptor (VEGFR) [62] and integrins [63] in the brain environment is associated with brain injury or blood-brain barrier (BBB) dysfunction, thus providing more targets in these pathological episodes.

5.3. Stimuli-responsive strategy

Usually the challenge is to formulate liposomes which have the right size and structure to entrap their cargo with high efficiency and in such a way that they do not leak out. On the other hand, it is important to play on the fluidity of the liposomal membrane. A too high liposomal stability is rather disadvantageous than desired. Remaining inside the stable liposomes, the encapsulated compounds are not delivered to the targeted tissue. At that point, it is necessary to find the right balance between stability in the bloodstream and a high delivery of liposomal cargo in the target. In general, the chemical and biophysical properties of lipid molecules primarily dictate the development of tunable (stimuli-sensitive) liposomes [64]. The various types of stimuli that could trigger liposomal cargo release can be classified into internal or intrinsic to the target tissue (changes in pH, temperature, redox condition, or the activity of certain enzymes) and external or artificially applied (magnetic field, ultrasound, and various types of irradiation) [15]. In one example, the lower pH, the higher temperature, and overexpression of several proteolytic enzymes of the tumor microenvironment should trigger the cytotoxic release when liposomes are exposed [14]. More exhaustive literature about stimuli-sensitive liposomes was formerly described [14, 15].

The encapsulation of nanoparticles in liposomes not only adds more stimuli for delivery but also provides more useful properties. For instance, by encapsulating PEG-coated quantum dots (QDs) in the internal aqueous phase of liposomes, a more extensive fluorescent staining is observed in a solid tumor model compared to free PEGylated QDs [65]. Meanwhile, superparamagnetic iron oxide nanoparticles (SPIONs) loaded in liposomes demonstrated to serve as a magnetic resonance imaging *in vivo* tool [66].

6. Liposomes for drug delivery to the central nervous system

More recent and relevant studies applying different liposomal targeting strategies for the treatment of major CNS diseases are summarized herein.

6.1. Stroke

An ischemic stroke occurs because of an obstruction, by a blood clot, within a blood vessel supplying blood to the brain [67]. Ischemic stroke accounts for 87% of all stroke cases. The cerebral ischemic area is composed of the ischemic core, a zone of irreversibly damaged tissue, and the ischemic penumbra, a surrounding zone of less severe and reversible damaged tissue [67]. To date, the only Food and Drug Administration (FDA) approved treatment for ischemic stroke is tissue plasminogen activator (tPA), a proteolytic enzyme. tPA enhances the conversion of plasminogen to plasmin, which subsequently degrades the fibrin matrix in the clot and improves blood flow to the ischemic region [68]. However, its short half-life, 2–6 minutes and therapeutic time window, less than 4.5 hours, elicite its administration in high doses which might lead to significant hemorrhagic complications [69, 70]. Interestingly, hemorrhage was reduced when tPA was loaded in actin-targeted liposomes and intravenously administered by the internal carotid artery in an *in vivo* model bearing clots injected [71]. Other therapeutic approaches have focused on protecting neurons from the main pathogenic mechanisms causing ischemic injury in the penumbra, such as excitotoxicity, oxidative stress, inflammation, or apoptosis [67]. Certainly, loading of these neuroprotective agents in liposomes may return improved results. Various studies emphasized on passive targeting strategies because during stroke the BBB is disrupted. Therefore, the effect of intravenous administration of empty [^{3}H]-labeled PEG-liposomes in a stroke rat model was investigated [50]. One hour after middle cerebral artery occlusion (MCAO), rats received the liposomal formulation and one hour after, reperfusion was started (t-MCAO) [50]. [^{3}H]-labeled PEG-liposomes accumulated in the ischemic brain in a time-dependent manner. Such accumulation at 3 hours post-dosing was significantly higher compared to the one in the non-ischemic side. These results were attributed to the disruption of the BBB and the leakage of liposomes to the brain parenchyma, where they gradually accumulated in the ischemic region via the EPR effect. Usually, once reperfusion is started, secondary cerebral damage known as ischemic/reperfusion (I/R) injury is observed [50]. In the same study, intravenous administration of PEGylated liposomes loaded with tacrolimus, a neuroprotective agent and a P-gp substrate [2] before (I/R) injury significantly suppressed cerebral cell death. While the damage volume for PEG-liposomes encapsulating tacrolimus was about 0.2 cm^3; for free tacrolimus and PBS, it was ~0.3 and ~0.4 cm^3, respectively. This formulation also suppressed superoxidative anions induced-damage in the brain and improved motor function deficits compared to free tacrolimus [50]. Fasudil, a Rho-kinase inhibitor is an approved drug for cerebral vasospasm after subarachnoid hemorrhage but thanks to its neuroprotective properties, it could be a promising candidate for the treatment of ischemic stroke. Phase III clinical trials showed fasudil usefulness and safety [72], however, the clinical trials were finished because of fasudil poor clinical efficacy, short permanence in the bloodstream and difficulty to penetrate the BBB [49]. Hence, it was encapsulated in PEG-liposomes and intravenously administered immediately after reperfusion in t-MCAO rats [49]. Fasudil-loaded PEG-liposomes diffused and accumulated in the I/R region, from an early phase after administration up to 24 hours. Moreover, the aforementioned formulation significantly suppressed the volume of damaged brain tissue, obtaining ~0.2 cm^3, compared to free fasudil, ~0.3 cm^3, and PBS, ~0.4 cm^3. Fasudil-loaded PEGylated liposomes also reduced in a significant manner neutrophil invasion and improved the motor functional

disorder [49]. The success of this study was basically due to PEGylation and liposome size. Using the same stroke *in vivo* model, it was confirmed that~100 nm PEG-liposomes got a high accumulation on the ischemic side, ~200 nm PEG-liposomes showed a lower accumulation and no accumulation was observed for ~800 nm PEG-liposomes [49]. Xenon is a pleiotypic cytoprotective gas, which rapidly diffuses across the BBB. Although xenon has few clinical adverse effects, its administration by inhalation requires intubation and ventilation with a large xenon concentration that reduces the maximum fraction of inspired oxygen [73]. Thus, an ultimate study encapsulated xenon into echogenic liposomes and determined its benefits after systemic administration in t-MCAO rats. Different dosage schemes demonstrated that this formulation effectively reduced ischemic neuronal cell death and improved neurological function. Undoubtely, ultrasound triggered additional liposomal xenon release obtaining still better therapeutic results [73]. Other studies accentuate on the benefits of actively targeted strategies over passively targeted strategies during stroke (**Table 1**). For instance vascular endothelial growth factor (VEGF) was loaded in PEGylated liposomes decorated with transferrin and intravenously administered two days after inducing a t-MCAO model [74]. VEGF confers neuroprotection, promotes neurogenesis and cerebral angiogenesis, and transferrin is an iron-binding glycoprotein with high affinity for the transferrin receptor (TfR) at the BBB [75]. While the damage volume for VEGF-loaded PEGylated liposomes coupled to transferrin was about ~2.5 cm^3, for VEGF-loaded PEGylated liposomes was ~3.0 and for saline ~3.5 cm^3, respectively. VEGF-induced neovascularization in the penumbra zone was significantly higher for the actively targeted formulation (245,873 microvessels per field), than for the passively targeted formulation (139,801.3) and for saline (102,175.5) [74].

6.2. Cancer

Globocan 2012 revealed that the worldwide brain and CNS cancer incidence and mortality in both sexes was 3.4 and 2.5 per 100,000 people, respectively [76]. In parallel, the World Cancer Research Fund International (http://www.wcrf.org) estimated that 256,000 new cases of brain and CNS cancer were diagnosed in 2012. Gliomas are tumors that arise from glial or precursor cells and include astrocytoma, glioblastoma, oligodendroglioma, ependymoma, mixed glioma, malignant glioma, and a few rare histologies. Glioma accounts for 27% of all tumors and 80% of malignant tumors, and among these, glioblastoma is the most common accounting for 46.1% [77]. Unfortunately, the efficacy of conventional chemotherapy is always limited due to the poor specificity in targeting cancer, low circulation time, reduced penetration in the tissue, and most importantly the toxic side effects of anti-cancer drugs [78]. Thus, nanotechnology appeared to help chemotherapy to be reborn and Doxil®, liposomal doxorubicin, received the first approval as a nano-drug in 1995 [79]. Nowadays, several research groups are developing nanocarriers to encapsulate anti-cancer drugs and fight against cancer tumors. Owing to the leaky nature of the tumor-associated blood vessels and lack of adequate lymphatic drainage, nanocarriers may take advantage of the EPR effect to target tumors [14]. However, in the case of brain tumors, nanocarriers must first overcome the BBB, which remains intact at the early stage of the brain tumor development. Only when the tumor grows to a certain volume and angiogenesis begins, the BBB is impaired and the blood-brain tumor barrier (BBTB) then becomes the main obstacle that nanocarriers must

Disease	Year	Size (nm)	Targeting ligand	Drug/diagnose agent	Administration route	Results	Refs.
Stroke	2015	~100	HAIYPRH (T7) peptide	ZL006	Intravenous	Increased liposomal transport across the BBB, reduced infarct volume and improved neurological deficit	[117]
	2013	~160	Anti-NR1-receptor antibody	Superoxide dismutase enzyme	Intracarotid	Reduced infarct volume, inflammatory markers, and improved *in vivo* behavior	[118]
	2010	60–90	*p*-aminophenyl-α-d-mannoside	CDP-Choline	Intravenous	Reduced ischemia-reperfusion in young and aged animals	[119]
	2010	~105	Transferrin	VEGF	Intravenous	Reduced infarct volume and increased neovascularization	[74]
	2003	200–250	Antiactin antibody	tPA	Intravenous	Reduced tPA-induced hemorrhage	[71]
	2013	~100	Anti-HSP72 antibody	Citicoline/gadolinium or rhodamine	Intravenous	Increased liposomal transport across the BBB and reduced infarct volume	[120]

http://dx.doi.org/10.5772/intechopen.70055

Disease	Year	Size (nm)	Targeting ligand	Drug/diagnose agent	Administration route	Results	Refs.
Cancer	2016	~110	PTD peptide	Epirubicine and celecoxib	Intravenous	Increased liposomal transport across the BBB, survival time and anti-vasculogenic mimicry effects	[121]
	2015	100-120	R8-dGR peptide	Paclitaxel	Intravenous	Increased survival time	[122]
	2015	~110	R8-c(RGD)	Paclitaxel	Intravenous	Increased survival time and anti-vasculogenic mimicry and anti-brain cancer stem cells effects	[123]
	2014	~95	Glutathione	Doxorubicin	Intravenous	Increased doxorubicin levels in brain, tumor growth inhibition, and increased survival	[81]
	2014	~100	Glutathione	Doxorubicin	Intravenous	Increased doxorubicin levels in brain	[83]
	2014	105	WGA	Daunorubicin, quinacrine and tamoxifen	Intravenous	Increased liposomal transport across the BBB and survival time	[124]
	2014	~120	RGD and transferrin	Paclitaxel	Intravenous	Increased liposomal transport across the BBB and antiproliferative activity against C6 cells	[125]
	2013	~180	Transferrin and folate	Doxorubicin	Intravenous	Increased tumor growth inhibition, survival time, and apoptotic activity in glioma cells	[54]
	2009	100-110	WGA	Topotecan and tamoxifen	Intravenous	Increased survival time	[86]
	2015	~100	pH-sensitive valve	Gd-DTPA	Intravenous	Improved cargo release in tumor microenvironment	[126]
	2014	~120	Endoglin	Gd	Intravenous	Increased signal emmited by Gd in tumor periphery	[127]
	2016	~180	(RGD-TPGS	Docetaxel/QD	Intravenous	Increased docetaxel levels and QD fluorescence in brain	[128]

Disease	Year	Size (nm)	Targeting ligand	Drug/diagnose agent	Administration route	Results	Refs.
AD	2015	~200	Transferrin	α-Mangostin	Intravenous	Increased α -mangostin levels in brain	[129]
	2015	~110	Glutathione	Amyloid-targeting antibody fragments	Intravenous	Increased amyloid-targeting antibody fragments levels in plasma and brain	[130]
	2013	~180	CPP	Rivastigmine	Intranasal	Increased rivastigmine levels in hippocampus and cortex	[92]
	2012	~150	DSPE-PEG_{3400}-XO4	DSPE-PEG_{3400}-XO4	Intravenous	Liposomal transport across the BBB and binding to Aβ plaques	[131]
PD	2012	~120	OX26	GDNF	Intravenous	A partial rescue of nigra-striatal neurons	[104]
	2011	~110	Chlorotoxin	L-dopa	Intraperitoneal	Increased dopamine levels in substantia nigra and striata and attenuated behavioral disorders	[102]

Abbreviations: CDP-Choline = cytidine 5′ diphosphocholine, VEGF = vascular endothelial growth factor, tPA = tissue plasminogen activator, PTD = glycine-arginine-lysine-lysine-arginine-arginine-glutamine-arginine-arginine-arginine-cysteine-glycine-NH_2 peptide, RGD = arginine-glycine-aspartic acid peptide, WGA = wheat germ agglutinin, Gd-DTPA = gadolinium-diethylendiaminopentaacetic acid, Gd = gadolinium, RGD-TPGS = arginine-glycine-aspartic acid peptide-D-alpha-tocopheryl polyethylene glucol 1000 succinate, QD = quantum dots, CPP = cell penetrating peptide, DSPE-PEG_{3400}-XO4 = 1,2-distearoyl-sn-glycero-3-phosphoethanolamine-N-[methoxy-XO4-(polyethylene glycol-3400)] sodium salt and GDNF = glial-derived neurotrophic factor.

Table 1. Recent studies based in active targeted liposomes for CNS diseases.

http://dx.doi.org/10.5772/intechopen.70055

circumvent. Hence, the presence of receptors on the BBB and BBTB provides a pathway to actively target brain tumors (**Table 1**) [80]. A recent *in vivo* study showed the difference between passive and active brain targeting of doxorubicin, a P-gp substrate [2]. PEGylated liposomal [^{14}C]-labeled doxorubicin similar to Doxil®/Caelyx® was used as the passive targeting formulation, whereas Glutathione PEGylated liposomal [^{14}C]-labeled doxorubicin (2B3-101) was assessed as the active delivery system [81]. Glutathione is an endogenous tripeptide currently used as a drug-targeting ligand because among the nutrient transporters in mammalian species, glutathione transporter has a preferential expression at the BBB [82]. After intravenous administration, both liposomal formulations displayed a similar doxorubicin pharmacokinetic profile and brain exposure during the first 24 hours. However, 4 days post-dosing, the brain doxorubicin concentration as well as its brain-to-plasma ratio was higher for Glutathione PEGylated liposomes. Compared to passive liposomes, active liposomes resulted in a significant inhibition of tumor growth and two animals of this group showed a complete tumor regression. Moreover, the active delivery system exhibited an increase of 16.1% in the median survival compared to the passive delivery system and an increase of 38.5% compared to saline [81]. Later, the same research group, using the sophisticated cerebral open flow microperfusion (cOFM) brain sampling technique, found that Glutathione PEGylated liposomes enhanced doxorubicin concentration in the brain extracellular space ~5-fold relative to PEGylated liposomes [83]. 2B3-101 was recently investigated in a phase I/IIa clinical study in patients with solid tumors, brain metastases, or recurrent malignant glioma (www.clinicaltrials.gov). Another approach emphasized on doxorubicin loaded liposomes dually functionalized with transferrin and folate to actively target an *in vivo* brain C6 glioma-bearing model [54]. While transferrin binds the TfR at the BBB [75], folate or folic acid binds the folate receptor (FR) [84], which is over-expressed in a wide variety of human tumors and whose density increases as the stage of cancer worsens [84]. After four intravenous administrations in 17 days, the mean survival time was 30 days for rats treated with this active targeting formulation, 27 days for doxorubicin-loaded liposomes, 24 days for doxorubicin solution and 20 days for saline. Doxorubicin-loaded liposomes functionalized with transferrin and folate also exhibited the least tumor area and the highest apoptotic activity in the glioma cells among all the treated groups [54] and did not modify liver enzyme levels or heart histology [54]. Due to its active targeting mechanism of receptor-mediated endocitosis and its high affinity for the cerebral capillary endothelium, wheat germ agglutinin (WGA) showed to be a good candidate to target the BBB [85]. Grafted to the surface, WGA favored the transfer of topotecan-tamoxifen-loaded liposomes across the BBB and then targeted brain tumors [86]. Among the four types of topotecan liposomes with or without the P-gp modulator tamoxifen and/or WGA, the one modified with tamoxifen and WGA exhibited the strongest cytotoxic effect against murine glial tumor (C6) cells [86]. Likewise, this formulation achieved the highest inhibitory effect against C6 cells after crossing an *in vitro* BBB (murine brain microvascular endothelial cells/rat astrocytes) model [86]. Moreover, after one week of treatment with the different formulations, the mean survival time of an *in vivo* brain C6 glioma-bearing model was 26 days for topotecan liposomes modified with tamoxifen and WGA, 20 days for topotecan liposomes, 19 days for free topotecan and 15 days for saline. A mean survival time of 31 days was achieved with two weeks of treatment with topotecan liposomes modified with tamoxifen and WGA [86].

6.3. Alzheimer's disease

Alzheimer's disease (AD) is the most common neurodegenerative dementia and contributes to 65% of all cases. AD is substantially increased among people aged 65 years or older, leading to progressive decline in memory, thinking, language, and learning capacity [87]. The pathophysiology of AD is related to the injury and death of neurons caused by the progressive production and accumulation of insoluble proteins aggregates, such as amyloid-β (Aβ) plaques and neurofibrillary tangles of hyperphosphorylated tau [88]. Currently, there is no drug to treat AD; only four FDA-approved compounds are known to relieve AD symptoms. These are donepezil, galantamine, memantine, and rivastigmine [89]. Once donepezil, a weak P-gp substrate [90], was encapsulated in PEGylated liposomes and administered by intranasal route in experimentation animals, it exhibited higher plasma and brain concentrations than free donepezil administered by the same or oral route [91]. In addition, histopathological examination showed that PEGylated liposomal donepezil was safe and non-toxic [91]. Rivastigmine was encapsulated in PEGylated liposomes functionalized with a cell penetrating peptide (CPP), whose proved internalization pathway across the cell membrane is via transduction or endocytosis [92, 93]. This formulation administered by intranasal route demonstrated its capacity to improve rivastigmine distribution and retention in the hippocampus and cortex, which are CNS regions highly affected by AD. This is in comparison with the intravenous administration of rivastigmine solution [92]. The clinical utility of galantamine, which is also a P-gp inhibitor [94], is hampered by its intricate transport across the BBB and its poor retention in the CNS. Hence, galantamine was loaded in PEGylated liposomes functionalized with a synthethic peptide, Lys-Val-Leu-Phe-Leu-Ser [95]. The selected peptide possess a 75% similar sequence to the serpin enzyme complex-receptor (SEC-R), which is expressed on the surface of neural (PC12) cells and may interact with soluble and non-toxic Aβ-peptides [96]. Thus, fluorometry and confocal microscopy confirmed that actively targeted liposomes significantly facilitated a higher uptake and accumulation of galantamine in PC12 neuronal cells related to non-targeted PEGylated liposomes [95]. The utility of neuroprotective agents in AD was also optimized by encapsulating them in actively targeted liposomes (**Table 1**).

6.4. Parkinson's disease

Parkinson's disease (PD) is the second most common progressive neurodegenerative brain disorder of insidious onset. This chronic disease is caused by a selective degeneration of dopaminergic neurons in the substantia nigra pars compacta, which consequently results in a reduction in striatal dopamine levels [97]. PD is generally characterized by primary motor symptoms such resting tremor, bradykinesia, rigidity, and postural instability. Non-motor symptoms experienced by PD patients may include cognitive impairment, mood disorders, and sleep disturbances [98]. Up-to-date, there is no cure for PD, the only available treatment, dopamine, is focused on the signs and symptoms. Since exogenous dopamine cannot cross the BBB, the gold standard therapy for PD is based on the administration of the natural precursor of dopamine, L-dopa, to restore dopaminergic transmission [99]. Because L-dopa is a P-gp substrate [100], it only crosses the BBB to a certain extent and once in the brain, it is

converted to dopamine. However, L-dopa cannot be administered alone because it is catalyzed to dopamine by peripheral dopamine-decarboxylase enzyme and causes peripheral side effects, such as nausea, sleepiness, and dyskinesia [99]. Thus, L-dopa was encapsulated in PEGylated and chlorotoxin-functionalized liposomes and studied in an *in vivo* 1-methyl-4-phenyl-1,2,3,6-tetrahydro pyridine (MPTP)-induced PD model [101]. Chlorotoxin (ClTx) is a 36-amino acid peptide that exhibits high affinity for brain gliomas and other tumors of neuroectodermal origin [102] but it is also able to bind proliferating vascular endothelial cells [103]. After intraperitoneal injection, the aforementioned formulation significantly increased the distribution of dopamine in the substantia nigra and striata and attenuated the behavioral disorders. Besides, it diminished the MPTP-induced loss of tyrosine hydroxylase-positive dopaminergic neurons as compared with L-dopa in PEGylated liposomes and free L-dopa [101]. Glial-derived neurotrophic factor (GDNF), a rescue of nigra-striatal tract agent was encapsulated in PEGylated liposomes functionalized with the mAb OX26 and administered in a 6-hydroxydopamine-induced PD *in vivo* model [104]. Authors explained the partial rescue of the nigra-striatal tract through the two weeks delayed and single liposomal intravenous administration, thus suggesting that future studies should increase and timely synchronize dosing administration with the onset of the disease [104].

6.5. Epilepsy

Epilepsy is a chronic and often progressive brain disorder, characterized by recurrent seizures, which are brief episodes of involuntary movement involving a part or the whole body. These episodes are caused by excessive electrical discharges from cortical neurons, which can cause visual disturbances, loss of control of bowel or bladder function, and consciousness [105]. According to the World Health Organization, epilepsy affects about 50 million people worldwide but only 70% of patients can be successfully treated while about 30% of patients are resistant or refractory to current available antiepileptics [106]. Earlier research has shown that mainly the activity of the P-gp at the BBB is directly related to anticonvulsants resistance [107]. This so-called medically intractable epilepsy is often associated with a poor prognosis, increased morbidity and mortality in patients, and a negative social impact in the life of patients and their family environment [106]. Unfortunately, only few studies have tried to improve the epilepsy therapy by applying nanotechnology. In a pilocarpine-induced seizure *in vivo* model, nimodipine, a neuroprotective agent [108] and a P-gp substrate [109] encapsulated in liposomes prevented epileptic seizures and mortality compared to free nimodipine [110]. In the meantime, curcumin, another neuroprotective agent [111] with ability to inhibit the P-gp [112], encapsulated in liposomes delayed the onset and decreases the duration of epileptic seizures in a pentylenetetrazole-induced seizure *in vivo* model [113]. In the same way, the anticonvulsivant activity of gossypin, a bioflavonoid isolated from *Hibiscus vitifolius* and possible P-gp inhibitor [114], was significantly improved when it was entrapped in liposomes. Liposomal gossypin succeeded in increasing seizures threshold and latency of current electroshock seizures pentylenetetrazole-induced seizure *in vivo* model [115]. Earlier studies demonstrated that liposomal anticonvulsivants as valproic acid and phenytoin exerted more prominent therapeutic efficacy than free drugs [116].

7. Liposomes for diagnostics of central nervous system diseases

Liposomes by themselves do not have any imaging property but various efforts have enabled liposomes to entrap and deliver diagnostic agents in pathological tissues. Most investigations deal with diagnosis of cancer.

7.1. Cancer

By attaching synthetic pH-responsive chemical modulators to an *Escherichia coli* mechanosensitive ion channel of large conductance (MscL), it was properly converted in a pH-sensitive valve able to gate at acidic environments such as solid tumors, sites of inflammation, endosomes, and lysosomes [132]. The sensitivity and pH interval for channel opening were tuned by varying the hydrophobicity and pK_a of the pH modulators. At a pH lower than the pKa of the modulator, the channel acquires a charge in the pore of the channel, which tends to the opening [132]. Later, these pH-sensitive valves were incorporated in PEGylated liposomes loaded with paramagnetic chelate gadolinium-diethylenetriaminepentaacetic acid (Gd-DTPA), which is detectable *in vivo* by magnetic resonance imaging (MRI). The aforementioned formulation, Gd-DTPA-pH-sensitive PEGylated liposomes was compared to Gd-DTPA-pH-insensitive PEGylated liposomes in mice implanted with a C6 glioblastoma tumor which has a pH between 6.6 and 7.0 [126]. While Gd-DTPA-pH-sensitive PEGylated liposomes started to release their cargo ten minutes post-dosing and lasted up to forty minutes, the Gd-DTPA-pH-insensitive PEGylated liposomes showed a slow initial release that only stabilize after ten minutes and was significantly lower than the pH-sensitive formulation. This study demonstrated that only few ion channels per liposome are sufficient to induce the release of content [126]. The strategy used herein is advantageous and highly supported over other pH-sensitive liposomes containing high amounts of negatively charged lipids, polymers, or unsaturated lipids. These materials make liposomes prone to fast bloodstream clearance affecting basically their pharmacokinetic properties and thus those of the encapsulated cargo [126]. Usually, the targeting moiety is conjugated to the liposomal surface and the whole formulation is assessed *in vitro* or *in vivo*. Nonetheless, a two-step active targeting is also possible and it was the case for molecular imaging of delineating tumor margins in a C6 glioma-bearing model [127]. Herein, the biotin-streptavidin ligation technique was used for its reability to attach antibodies on liposomes surface [133]. Gadolinium was used as the imaging agent and endoglin (CD105), a protein involved in angiogenesis, was used as the targeting moiety. Hence, experimentation animals received an intravenous injection of biotin-endoglin and after 24 hours, injection of streptavidin-PEGylated liposomes loaded with gadolinium. In this way, in the tumor periphery, the signal emitted by gadolinium from the two-step targeting was about 59% higher than those obtained for the usual one-step targeted liposomes and non-targeted liposomes [127].

8. Liposomes for theranostics of central nervous system diseases

A major achievement of nanomedicine in the last few years was the development of theranostic delivery systems, which integrate imaging and therapeutic functions in one single but

complex structure, thus providing a powerful approach to improve disease-specific detection, treatment, and follow-up monitoring [134]. The flexible composition of liposomes enables them to be engineered to adsorb, entrap, encapsulate, or conjugate different imaging agents and therapeutic compounds [134].

8.1. Stroke

Citicoline (CDP-Choline), a drug used in the treatment of stroke [135], was loaded in liposomes made of phospholipids containing rhodamine or gadolinium, which enabled the nanocarriers to be traceable by fluorescence or MRI. These liposomes were functionalized with anti-HSP72 antibody, which is able to bind the HSP72 protein. HSP72 protein is a biomarker expressed for up to seven days in the peri-infarct region following cerebral ischemia [120]. This formulation was administered by intravenous route after surgery in an MCA *in vivo* model, where it achieved a damage of 30% volume smaller than the one obtained with free citicoline. This could be attributed to the 80% traceable liposomal localization on the periphery of the ischemic lesion [120].

8.2. Cancer

Liposomes co-encapsulating the cytotoxic and P-gp substrate docetaxel [2] and QDs and actively targeted with arginine-glycine-aspartic acid peptide -*D*-alpha-tocopheryl polyethylene glycol 1000 succinate (RGD – TPGS) were developed and tested *in vivo* for brain targeting [128]. QDs are semiconductor nanocrystals with a photostability up to 100–10000 fold greater than conventional organic dyes. Unluckily, because QDs are heavy metals, they may lead to potential toxicities, but their encapsulation in liposomes may improve their biocompatibility to become a potential tool for diagnostics in *in vitro* and *in vivo* tumor models [136]. TPGS, a derivative of the natural vitamin E (alpha-tocopherol), has shown great potential in overcoming the P-gp via inhibition of its ATPase activity [42]. RGD peptide binds preferentially the $\alpha v\beta 3$ integrin, an adhesion molecule highly expressed on activated endothelial cells, new-born vessels and some tumor cells [137]. In this context, targeting tumor cells or tumor vasculature by RGD-based strategies is a promising approach [138]. Hence, docetaxel-QDs-loaded liposomes functionalized with RGD-TPGS intravenously administered in rats, exhibited a docetaxel brain distribution ~2-fold higher than the value obtained for docetaxel-QDs-loaded liposomes functionalized with TPGS and ~7-fold higher than the value obtained for free docetaxel [128]. These data is in line with the strongest fluorescence of brain sections for docetaxel-QDs-loaded liposomes functionalized with RGD-TPGS, mild fluorescence for docetaxel-QDs-loaded liposomes functionalized with TPGS and no fluorescence for free QDs [128]. Surely TPGS inhibited the P-gp allowing a higher brain distribution of liposomal docetaxel related to free docetaxel [128]. Another study formulated magnetoliposomes co-loaded with doxorubicin and SPIONs and coated with carboxymethyl dextran (CMD), a stealth alternative to PEGylation [139]. Typically, superparamagnetic nanoparticles coated with carboxydextran are used as MRI agents to detect tumors and their microenvironment [140]. Thus, *in vitro*, this formulation demonstrated to be an efficient T_2-weighed contrast agent for MRI but also induced cytotoxicity which could be enhanced by low-frequency

alternating magnetic field [139]. Further *in vivo* data could determine the usefulness of this formulation as a potential carrier for targeting diagnostic and therapy to brain cancer.

8.3. Parkinson's disease

QDs and apomorphine, a rescue medication for Parkinson's disease were encapsulated in PEGylated liposomes [141]. Then, *in vivo* bioimaging analysis determined that the fluorescence emitted from PEGylated liposomal QDs after intravenous administration was higher in the brain than in other organs and it lasted up to 60 minutes. In contrast, the fluorescence derived from free QDs was visualized immediately following the injection, decreased rapidly in the brain but lasted up to 35 minutes in liver [141]. Likewise the brain uptake of liposomal apomorphine at 1 hour post-dosing was 2.4-fold higher than the value obtained for free apomorphine. Cell uptake studies in bEND3 cells suggested that these theranostic liposomes could enter into cells by clathrin-dependent and caveola-mediated endocytosis [141].

9. Future outcomes

Nanomedicine has emerged as the key to open the door of the medicine of tomorrow. Thanks to exponential efforts and improvements, nanomedicine has launched to the clinical field various drug-loaded liposomes for brain targeting (**Table 2**). However, regarding other CNS diseases, nanomedicine has not yet fulfilled its promise. The possible improved brain distribution of various liposomal therapeutic compounds and diagnostic agents remains to be studied. The CNS is so complex that gives us a wide variety of receptors to target. Currently, various targeting moieties such as aptamers, peptides, mAbs, or their fragments have proved their ability to target a specific receptor in the CNS. Thus, future studies should investigate their *in vivo* potential but always paying attention to the grafting itself. Attachment of targeting moieties does not alter the liposomal biodistribution; it only increases the liposomal internalization in targeted cells. Thus, the quantity of targeting

Therapeutic compound	Purpose: to assess	Patients	Phase
Cytarabine (DepoCyte®)	The safety of whole brain radiotherapy	Brain metastases	I
Cytarabine	The effectiveness in co-administration with high doses of methotrexate	SNC metastases	II
Doxorubicin	The effectiveness	Refractory solid brain tumors	I
Vincristine (Marqibo)	The safety, activity, and pharmacokinetics	Refractory solid brain tumors in children and adolescents	I/II
Doxorubicin (2B3-101)	The safety, tolerability, and pharmacokinetics alone or in combination with trastuzumab	Solid tumors and brain metastases or recurrent malignant glioma	I/IIa

Data obtained from www.clinicaltrials.gov

Table 2. Current completed clinical trials based on liposomal formulations for CNS diseases.

ligand should not compromise the liposomal long-circulating properties conferred by PEG or another polymer. The amount of surface PEG-lipid complex necessary for creating stealth liposomes varies between 5 and 10 mol% and the optimal PEG-derivative length should have a molecular weight of 2000 daltons [142]. If a PEG-derivative is used as the spacer to graft the targeting ligand, the amount of PEG molecules to guarantee steric stabilization must not be inferior to 5 mol% [143]. Since steric hindrance of the PEG chains may interfere with the targeting moiety recognition by the targeted tissue, functionalization of liposomes with two PEG chain lengths was proposed. While PEG_{2000} would confer long circulating properties, PEG_{5000} would be used as linker to overexpose the targeting ligand to targeted cells [56]. To ensure sustained cargo release, an alternative to PEGylation, is the integration of pre-encapsulated loaded liposomes within depot polymeric scaffolds. This strategy attempts to provide ingenious solutions to limitations of conventional liposomes such as short plasma half-lives, toxicity, stability, and poor control of cargo release over prolonged periods [144]. The lack of liposomal toxicity information in the pre-clinical stage is another issue that could hamper the success of these DDSs. Liposomal synthesis protocols must ensure the absence of impurities from organic solvents, free surfactants, and heavy metals, which could contribute to bias results. Because, toxic effects could arise from organic solvent residues, latest studies accentuate on liposomes formulations using organic solvents-free methods [145]. Although nanomedicine aims to prolong the half-life of the cargo incorporated in the DDS, some pharmacotherapies would need a chronic administration. In this sense, an exhaustive study of empty liposomes toxicity would help to exploit their best usage in different therapies.

10. Conclusions

Nanomedicine and especially liposomes represent a step forward to deliver diagnostic agents and/or therapeutic compounds in CNS diseases such as stroke, brain cancer, AD, PD, or epilepsy. Therefore, this manuscript outlines the most recent and relevant engineered liposomal strategies to cirvumvent the BBB and its main efflux transporter, the P-gp. Moreover, important aspects to further optimize liposomal strategies are discussed at the end of this chapter.

Author details

Rita Nieto Montesinos

Address all correspondence to: milynm@gmail.com

Laboratorio de Neurociencias, Universidad Catolica de Santa Maria, Arequipa, Peru

References

[1] Organization WH. Neurological Disorders Affect Millions Globally: WHO report. World Health Organization; Switzerland. 2007. http://www.who.int/mental_health/neurology/neurological_disorders_report_web.pdf

[2] Loscher W, Potschka H. Role of drug efflux transporters in the brain for drug disposition and treatment of brain diseases. Progress in Neurobiology. 2005;**76**(1):22-76

[3] McCaffrey G, Davis TP. Physiology and pathophysiology of the blood-brain barrier: P-glycoprotein and occludin trafficking as therapeutic targets to optimize central nervous system drug delivery. Journal of Investigative Medicine. 2012;**60**(8):1131-1140

[4] Schinkel AH. P-Glycoprotein, a gatekeeper in the blood-brain barrier. Advanced Drug Delivery Reviews. 1999;**36**(2-3):179-194

[5] Wong HL, Wu XY, Bendayan R. Nanotechnological advances for the delivery of CNS therapeutics. Advanced Drug Delivery Reviews. 2012;**64**(7):686-700

[6] Beduneau A, Saulnier P, Benoit JP. Active targeting of brain tumors using nanocarriers. Biomaterials. 2007;**28**(33):4947-4967

[7] Vieira DB, Gamarra LF. Getting into the brain: Liposome-based strategies for effective drug delivery across the blood-brain barrier. International Journal of Nanomedicine. 2016;**11**:5381-5414

[8] Tosi G, et al. Potential use of polymeric nanoparticles for drug delivery across the blood-brain barrier. Current Medicinal Chemistry. 2013;**20**(17):2212-2225

[9] Aparicio-Blanco J, Torres-Suarez AI. Glioblastoma multiforme and lipid nanocapsules: A review. Journal of Biomedical Nanotechnology. 2015;**11**(8):1283-1311

[10] Gao HL, et al. Effect of lactoferrin- and transferrin-conjugated polymersomes in brain targeting: *In vitro* and *in vivo* evaluations. Acta Pharmaceutica Sinica. 2010;**31**(2):237-243

[11] Immordino ML, Dosio F, Cattel L. Stealth liposomes: Review of the basic science, rationale, and clinical applications, existing and potential. International Journal of Nanomedicine. 2006;**1**(3):297-315

[12] Fulop A, et al. Molecular imaging of brain localization of liposomes in mice using MALDI mass spectrometry. Scientific Reports. 2016;**6**:33791

[13] Muthu MS, Feng SS. Theranostic liposomes for cancer diagnosis and treatment: Current development and pre-clinical success. Expert Opinion on Drug Delivery. 2013; **10**(2):151-155

[14] Deshpande PP, Biswas S, Torchilin VP. Current trends in the use of liposomes for tumor targeting. Nanomedicine (London). 2013;**8**(9):1509-1528

[15] Torchilin VP. Multifunctional, stimuli-sensitive nanoparticulate systems for drug delivery. Nature Reviews Drug Discovery. 2014;**13**(11):813-827

[16] Luissint AC, et al. Tight junctions at the blood brain barrier: Physiological architecture and disease-associated dysregulation. Fluids Barriers CNS. 2012;**9**(1):23

[17] Wong AD, et al. The blood-brain barrier: An engineering perspective. Frontiers in Neuroengineering. 2013;**6**:7

[18] Abbott NJ, et al. Structure and function of the blood-brain barrier. Neurobiology of Disease. 2010;**37**(1):13-25

[19] Begley DJ, Brightman MW. Structural and functional aspects of the blood-brain barrier. Progress in Drug Research. 2003;**61**:39-78

[20] Golden PL, Pollack GM. Blood-brain barrier efflux transport. Journal of Pharmaceutical Sciences. 2003;**92**(9):1739-1753

[21] Miller DS, Bauer B, Hartz AM. Modulation of P-glycoprotein at the blood-brain barrier: Opportunities to improve central nervous system pharmacotherapy. Pharmacological Reviews. 2008;**60**(2):196-209

[22] Cordon-Cardo C, et al. Multidrug-resistance gene (P-glycoprotein) is expressed by endothelial cells at blood-brain barrier sites. Proceedings of the National Academy of Sciences of the United States of America. 1989;**86**(2):695-698

[23] Thiebaut F, et al. Immunohistochemical localization in normal tissues of different epitopes in the multidrug transport protein P170: Evidence for localization in brain capillaries and crossreactivity of one antibody with a muscle protein. Journal of Histochemistry and Cytochemistry. 1989;**37**(2):159-164

[24] Seetharaman S, et al. Multidrug resistance-related transport proteins in isolated human brain microvessels and in cells cultured from these isolates. Journal of Neurochemistry. 1998;**70**(3):1151-1159

[25] Volk HA, et al. Neuronal expression of the drug efflux transporter P-glycoprotein in the rat hippocampus after limbic seizures. Neuroscience. 2004;**123**(3):751-759

[26] Spiegl-Kreinecker S, et al. Expression and functional activity of the ABC-transporter proteins P-glycoprotein and multidrug-resistance protein 1 in human brain tumor cells and astrocytes. Journal of Neuro-Oncology. 2002;**57**(1):27-36

[27] Rao VV, et al. Choroid plexus epithelial expression of MDR1 P glycoprotein and multidrug resistance-associated protein contribute to the blood-cerebrospinal-fluid drug-permeability barrier. Proceedings of the National Academy of Sciences of the United States of America. 1999;**96**(7):3900-3905

[28] Demeule M, et al. Expression of multidrug-resistance P-glycoprotein (MDR1) in human brain tumors. International Journal of Cancer. 2001;**93**(1):62-66

[29] Schinkel AH, et al. Disruption of the mouse mdr1a P-glycoprotein gene leads to a deficiency in the blood-brain barrier and to increased sensitivity to drugs. Cell. 1994; **77**(4):491-502

[30] Geyer J, Gavrilova O, Petzinger E. Brain penetration of ivermectin and selamectin in mdr1a,b P-glycoprotein- and bcrp- deficient knockout mice. Journal of Veterinary Pharmacology and Therapeutics. 2009;**32**(1):87-96

[31] Schinkel AH, et al. P-glycoprotein in the blood-brain barrier of mice influences the brain penetration and pharmacological activity of many drugs. Journal of Clinical Investigation. 1996;**97**(11):2517-2524

[32] Bundgaard C, Eneberg E, Sanchez C. P-glycoprotein differentially affects escitalopram, levomilnacipran, vilazodone and vortioxetine transport at the mouse blood-brain barrier *in vivo*. Neuropharmacology. 2016;**103**:104-111

[33] Sills GJ, et al. P-glycoprotein-mediated efflux of antiepileptic drugs: Preliminary studies in mdr1a knockout mice. Epilepsy & Behavior. 2002;**3**(5):427-432

[34] Daneman R. The blood-brain barrier in health and disease. Annals of Neurology. 2012;**72**(5):648-672

[35] Obermeier B, Daneman R, Ransohoff RM. Development, maintenance and disruption of the blood-brain barrier. Nature Medicine. 2013;**19**(12):1584-1596

[36] Johnstone RW, Ruefli AA, Smyth MJ. Multiple physiological functions for multidrug transporter P-glycoprotein? Trends in Biochemical Sciences. 2000;**25**(1):1-6

[37] Kuntner C, et al. Dose-response assessment of tariquidar and elacridar and regional quantification of P-glycoprotein inhibition at the rat blood-brain barrier using (R)-[(11) C]verapamil PET. European Journal of Nuclear Medicine and Molecular Imaging. 2010;**37**(5):942-953

[38] Montesinos RN, et al. Coadministration of P-glycoprotein modulators on loperamide pharmacokinetics and brain distribution. Drug Metabolism and Disposition. 2014;**42** (4):700-706

[39] Bauer M, et al. Pharmacokinetics of single ascending doses of the P-glycoprotein inhibitor tariquidar in healthy subjects. Pharmacology. 2013;**91**(1-2):12-19

[40] Palmeira A, et al. Three decades of P-gp inhibitors: Skimming through several generations and scaffolds. Current Medicinal Chemistry. 2012;**19**(13):1946-2025

[41] Krukemeyer MG, Krenn V, Huebner F, Wagner W, Resch R (2015) History and Possible Uses of Nanomedicine Based on Nanoparticles and Nanotechnological Progress. J Nanomed Nanotechnol 6: 336. DOI: 10.4172/2157- 7439.1000336

[42] Nieto Montesinos R, et al. Delivery of P-glycoprotein substrates using chemosensitizers and nanotechnology for selective and efficient therapeutic outcomes. Journal of Controlled Release. 2012;**161**(1):50-61

[43] Boulaiz H, et al. Nanomedicine: Application areas and development prospects. International Journal of Molecular Sciences. 2011;**12**(5):3303-3321

[44] Liu Y, et al. The shape of things to come: Importance of design in nanotechnology for drug delivery. Therapeutic Delivery. 2012;**3**(2):181-194

[45] Matsumura Y, Maeda H. A new concept for macromolecular therapeutics in cancer chemotherapy: Mechanism of tumoritropic accumulation of proteins and the antitumor agent smancs. Cancer Research. 1986;**46**(12 Pt 1):6387-6392

[46] Maeda H, et al. Tumor vascular permeability and the EPR effect in macromolecular therapeutics: A review. Journal of Controlled Release. 2000;**65**(1-2):271-284

[47] Torchilin V. Tumor delivery of macromolecular drugs based on the EPR effect. Advanced Drug Delivery Reviews. 2011;**63**(3):131-135

[48] Huwyler J, Drewe J, Krahenbuhl S. Tumor targeting using liposomal antineoplastic drugs. International Journal of Nanomedicine. 2008;**3**(1):21-29

[49] Fukuta T, et al. Neuroprotection against cerebral ischemia/reperfusion injury by intravenous administration of liposomal fasudil. International Journal of Pharmaceutics. 2016;**506**(1-2):129-137

[50] Fukuta T, et al. Treatment of stroke with liposomal neuroprotective agents under cerebral ischemia conditions. European Journal of Pharmaceutics and Biopharmaceutics. 2015;**97**(Pt A):1-7

[51] Thole M, et al. Uptake of cationzied albumin coupled liposomes by cultured porcine brain microvessel endothelial cells and intact brain capillaries. Journal of Drug Targeting. 2002;**10**(4):337-344

[52] Pardridge WM. Drug transport across the blood-brain barrier. Journal of Cerebral Blood Flow & Metabolism. 2012;**32**(11):1959-1972

[53] Li L, et al. Large amino acid transporter 1 mediated glutamate modified docetaxel-loaded liposomes for glioma targeting. Colloids and Surfaces B: Biointerfaces. 2016;**141**:260-267

[54] Gao JQ, et al. Glioma targeting and blood-brain barrier penetration by dual-targeting doxorubincin liposomes. Biomaterials. 2013;**34**(22):5628-5639

[55] Schnyder A, Huwyler J. Drug transport to brain with targeted liposomes. NeuroRx. 2005;**2**(1):99-107

[56] Nieto Montesinos R, et al. Liposomes coloaded with elacridar and tariquidar to modulate the P-glycoprotein at the blood-brain barrier. Molecular Pharmaceutics. 2015; **12**(11):3829-3838

[57] Jefferies WA, et al. Transferrin receptor on endothelium of brain capillaries. Nature. 1984;**312**(5990):162-163

[58] Jones AR, Shusta EV. Blood-brain barrier transport of therapeutics via receptor-mediation. Pharmaceutical Research. 2007;**24**(9):1759-1771

[59] Zhang Y, Schlachetzki F, Pardridge WM. Global non-viral gene transfer to the primate brain following intravenous administration. Molecular Therapy. 2003;**7**(1):11-18

[60] Hulsermann U, et al. Uptake of apolipoprotein E fragment coupled liposomes by cultured brain microvessel endothelial cells and intact brain capillaries. Journal of Drug Targeting. 2009;**17**(8):610-618

[61] Taylor TE, Furnari FB, Cavenee WK. Targeting EGFR for treatment of glioblastoma: Molecular basis to overcome resistance. Current Cancer Drug Targets. 2012;**12**(3):197-209

[62] Plate KH, et al. Vascular endothelial growth factor and glioma angiogenesis: Coordinate induction of VEGF receptors, distribution of VEGF protein and possible *in vivo* regulatory mechanisms. International Journal of Cancer. 1994;**59**(4):520-529

[63] Tabatabai G, et al. The role of integrins in glioma biology and anti-glioma therapies. Current Pharmaceutical Design. 2011;**17**(23):2402-2410

[64] Mathias Viard AP, Chapter one – stimuli-sensitive liposomes: Lipids as gateways for cargo release. Advances in Planar Lipid Bilayers and Liposomes. 2015;**22**:1-41

[65] Al-Jamal WT, et al. Functionalized-quantum-dot-liposome hybrids as multimodal nanoparticles for cancer. Small. 2008;**4**(9):1406-1415

[66] Martina MS, et al. Generation of superparamagnetic liposomes revealed as highly efficient MRI contrast agents for *in vivo* imaging. Journal of the American Chemical Society. 2005;**127**(30):10676-10685

[67] Anrather J. Iadecola C, Stroke research at a crossroad: Asking the brain for directions. Nature Neuroscience. 2013;**14**(11):1363-1368

[68] Koudelka S, et al. Liposomal nanocarriers for plasminogen activators. Journal of Controlled Release. 2016;**227**:45-57

[69] Davis SM, Donnan GA. 4.5 hours: The new time window for tissue plasminogen activator in stroke. Stroke. 2009;**40**(6):2266-2267

[70] Kim J-Y, Kim J-K, Park J-S, Byun Y, Kim C-K. The use of PEGylated liposomes to prolong circulation lifetimes of tissue plasminogen activator. Biomaterials. 2009;**30**:5751-5756

[71] Asahi M, et al. Antiactin-targeted immunoliposomes ameliorate tissue plasminogen activator-induced hemorrhage after focal embolic stroke. Journal of Cerebral Blood Flow & Metabolism. 2003;**23**(8):895-899

[72] Shibuya M, et al. Effects of fasudil in acute ischemic stroke: Results of a prospective placebo-controlled double-blind trial. Journal of the Neurological Sciences. 2005; **238**(1-2):31-39

[73] Peng T, et al. Therapeutic time window and dose dependence of xenon delivered via echogenic liposomes for neuroprotection in stroke. CNS Neuroscience & Therapeutics. 2013;**19**(10):773-784

[74] Zhao H, et al. Postacute ischemia vascular endothelial growth factor transfer by transferrin-targeted liposomes attenuates ischemic brain injury after experimental stroke in rats. Human Gene Therapy. 2011;**22**(2):207-215

[75] Hatakeyama H, et al. Factors governing the *in vivo* tissue uptake of transferrin-coupled polyethylene glycol liposomes *in vivo*. International Journal of Pharmaceutics. 2004;**281**(1-2):25-33

[76] Ferlay J, et al. Cancer incidence and mortality worldwide: Sources, methods and major patterns in GLOBOCAN 2012. International Journal of Cancer. 2015;**136**(5):E359- E386

[77] Ostrom QT, et al. CBTRUS statistical report: Primary brain and central nervous system tumors diagnosed in the United States in 2008-2012. Journal of Neuro-Oncology. 2015;**17**(Suppl 4):iv1-iv62

[78] Nair BG, et al. Nanotechnology platforms; an innovative approach to brain tumor therapy. Journal of Medicinal Chemistry. 2011;**7**(5):488-503

[79] Chang EH, et al. Nanomedicine: Past, present and future - A global perspective. Biochemical and Biophysical Research Communications. 2015;**468**(3):511-517

[80] Wei X, et al. Brain tumor-targeted drug delivery strategies. Acta Pharmaceutica Sinica B. 2014;**4**(3):193-201

[81] Gaillard PJ, et al. Pharmacokinetics, brain delivery, and efficacy in brain tumor-bearing mice of glutathione pegylated liposomal doxorubicin (2B3-101). PLoS One. 2014;**9**(1):e82331

[82] Kannan R, et al. GSH transport in human cerebrovascular endothelial cells and human astrocytes: Evidence for luminal localization of Na+-dependent GSH transport in HCEC. Brain Research. 2000;**852**(2):374-382

[83] Birngruber T, et al. Enhanced doxorubicin delivery to the brain administered through glutathione PEGylated liposomal doxorubicin (2B3-101) as compared with generic Caelyx,((R))/Doxil((R))—A cerebral open flow microperfusion pilot study. Journal of Pharmaceutical Sciences. 2014;**103**(7):1945-1948

[84] Low PS, Henne WA, Doorneweerd DD. Discovery and development of folic-acid-based receptor targeting for imaging and therapy of cancer and inflammatory diseases. Accounts of Chemical Research. 2008;**41**(1):120-129

[85] Fischer D, Kissel T. Histochemical characterization of primary capillary endothelial cells from porcine brains using monoclonal antibodies and fluorescein isothiocyanate-labelled lectins: Implications for drug delivery. European Journal of Pharmaceutics and Biopharmaceutics. 2001;**52**(1):1-11

[86] Du J, et al. Dual-targeting topotecan liposomes modified with tamoxifen and wheat germ agglutinin significantly improve drug transport across the blood-brain barrier and survival of brain tumor-bearing animals. Molecular Pharmaceutics. 2009;**6**(3):905-917

[87] Alzheimer's A. 2016 Alzheimer's disease facts and figures. Alzheimers & Dementia. 2016;**12**(4):459-509

[88] Bloom GS. Amyloid-beta and tau: The trigger and bullet in Alzheimer disease pathogenesis. JAMA Neurology. 2014;**71**(4):505-508

[89] Tan CC, et al. Efficacy and safety of donepezil, galantamine, rivastigmine, and memantine for the treatment of Alzheimer's disease: A systematic review and meta-analysis. Journal of Alzheimer's Disease. 2014;**41**(2):615-631

[90] McEneny-King A, Edginton AN, Rao PP. Investigating the binding interactions of the anti-Alzheimer's drug donepezil with CYP3A4 and P-glycoprotein. Bioorganic & Medicinal Chemistry Letters. 2015;**25**(2):297-301

[91] Al Asmari AK, et al. Preparation, characterization, and *in vivo* evaluation of intranasally administered liposomal formulation of donepezil. Drug Design, Development and Therapy. 2016;**10**:205-215

[92] Yang ZZ, et al. Enhanced brain distribution and pharmacodynamics of rivastigmine by liposomes following intranasal administration. International Journal of Pharmaceutics. 2013;**452**(1-2):344-354

[93] Trabulo S, et al. Cell-penetrating peptides-mechanisms of cellular uptake and generation of delivery systems. Pharmaceuticals (Basel). 2010;**3**(4):961-993

[94] Namanja HA, et al. Inhibition of human P-glycoprotein transport and substrate binding using a galantamine dimer. Biochemical and Biophysical Research Communications. 2009;**388**(4):672-676

[95] Mufamadi MS, et al. Ligand-functionalized nanoliposomes for targeted delivery of galantamine. International Journal of Pharmaceutics. 2013;**448**(1):267-281

[96] Boland K, Manias K, Perlmutter DH. Specificity in recognition of amyloid-beta peptide by the serpin-enzyme complex receptor in hepatoma cells and neuronal cells. Journal of Biological Chemistry. 1995;**270**(47):28022-28028

[97] Oertel WH, Ellgring H. Parkinson's disease—Medical education and psychosocial aspects. Patient Education and Counseling. 1995;**26**(1-3):71-79

[98] Sprenger F, Poewe W. Management of motor and non-motor symptoms in Parkinson's disease. CNS Drugs. 2013;**27**(4):259-272

[99] Nagatsua T, Sawadab M. L-dopa therapy for Parkinson's disease: Past, present, and future. Parkinsonism & Related Disorders. 2009;**15**(Suppl 1):S3-S8

[100] Vautier S, et al. Interactions between antiparkinsonian drugs and ABCB1/P-glycoprotein at the blood-brain barrier in a rat brain endothelial cell model. Neuroscience Letters. 2008;**442**(1):19-23

[101] Xiang Y, et al. Chlorotoxin-modified stealth liposomes encapsulating levodopa for the targeting delivery against Parkinson's disease in the MPTP-induced mice model. Journal of Drug Targeting. 2012;**20**(1):67-75

[102] Lyons SA, O'Neal J, Sontheimer H. Chlorotoxin, a scorpion-derived peptide, specifically binds to gliomas and tumors of neuroectodermal origin. Glia. 2002;**39**(2):162-173

[103] Kesavan K, et al, Annexin A2 is a molecular target for TM601, a peptide with tumor-targeting and anti-angiogenic effects. Journal of Biological Chemistry. 2010;**285**(7):4366-4374

[104] Xia CF, et al. Intravenous glial-derived neurotrophic factor gene therapy of experimental Parkinson's disease with Trojan horse liposomes and a tyrosine hydroxylase promoter. The Journal of Gene Medicine. 2008;**10**(3):306-315

[105] Browne TR, Holmes GL. Epilepsy. The New England Journal of Medicine. 2001;**344** (15):1145-1151

[106] Ma A, et al. P-glycoprotein alters blood-brain barrier penetration of antiepileptic drugs in rats with medically intractable epilepsy. Drug Design, Development and Therapy. 2013;**7**:1447-1454

[107] Luna-Tortos C, Fedrowitz M, Loscher W. Several major antiepileptic drugs are substrates for human P-glycoprotein. Neuropharmacology. 2008;**55**(8):1364-1375

[108] Nascimento VS, et al. Antioxidant effect of nimodipine in young rats after pilocarpine-induced seizures. Pharmacology Biochemistry and Behavior. 2005;**82**(1):11-16

[109] Zhang L, et al. P-glycoprotein restricted transport of nimodipine across blood-brain barrier. Acta Pharmaceutica Sinica B. 2003;**24**(9):903-906

[110] Moreno LC, et al. Acute toxicity and anticonvulsant activity of liposomes containing nimodipine on pilocarpine-induced seizures in mice. Neurosci Letters. 2015;**585**:38-42

[111] Kiasalari Z, et al. Antiepileptogenic effect of curcumin on kainate-induced model of temporal lobe epilepsy. Journal of Pharmaceutical Biology. 2013;**51**(12):1572-1578

[112] Cheng KK, et al. Highly stabilized curcumin nanoparticles tested in an *in vitro* blood-brain barrier model and in Alzheimer's disease Tg2576 mice. AAPS Journal. 2013;**15**(2):324-336

[113] Agarwal NB, et al. Liposomal formulation of curcumin attenuates seizures in different experimental models of epilepsy in mice. Fundamental & Clinical Pharmacology. 2013;**27**(2):169-172

[114] Rajnarayana K, Venkatesham A, Krishna DR. Influence of some bioflavonoids on the transport of nitrendipine. Drug Metabolism and Drug Interactions. 2008;**23**(3-4):299-310

[115] Nagpal D Agarwal NB, Katare D. Evaluation of liposomal gossypin in animal models of epilepsy. International Journal of Pharmacy and Pharmaceutical Sciences. 2016;**8**(4): 247-251

[116] Oka M, et al. Effect of liposome-entrapped lidocaine on limbic status epilepticus in rats. No To Shinkei. 1991;**43**(8):769-773

[117] Wang Z, et al. Enhanced anti-ischemic stroke of ZL006 by T7-conjugated PEGylated liposomes drug delivery system. Scientific Reports. 2015;**5**:12651

[118] Yun X, et al. Nanoparticles for targeted delivery of antioxidant enzymes to the brain after cerebral ischemia and reperfusion injury. Journal of Cerebral Blood Flow & Metabolism. 2013;**33**(4):583-592

[119] Ghosh S, et al. Mannosylated liposomal cytidine 5′ diphosphocholine prevent age related global moderate cerebral ischemia reperfusion induced mitochondrial cytochrome c release in aged rat brain. Neuroscience. 2010;**171**(4):1287-1299

[120] Agulla J, et al. *In vivo* theranostics at the peri-infarct region in cerebral ischemia. Theranostics. 2013;**4**(1):90-105

[121] Ju RJ, et al. Destruction of vasculogenic mimicry channels by targeting epirubicin plus celecoxib liposomes in treatment of brain glioma. International Journal of Nanomedicine. 2016;**11**:1131-1146

[122] Liu Y, et al. Dual receptor recognizing cell penetrating peptide for selective targeting, efficient intratumoral diffusion and synthesized anti-glioma therapy. Theranostics. 2016;**6**(2):177-191

[123] Liu Y, et al. Multifunctional tandem peptide modified paclitaxel-loaded liposomes for the treatment of vasculogenic mimicry and cancer stem cells in malignant glioma. ACS Applied Materials & Interfaces. 2015;**7**(30):16792-16801

[124] Li XT, et al. Multifunctional targeting daunorubicin plus quinacrine liposomes, modified by wheat germ agglutinin and tamoxifen, for treating brain glioma and glioma stem cells. Oncotarget. 2014;**5**(15):6497-6511

[125] Qin L, et al. A dual-targeting liposome conjugated with transferrin and arginine-glycine-aspartic acid peptide for glioma-targeting therapy. Oncology Letters. 2014;**8**(5): 2000-2006

[126] Pacheco-Torres J, et al. Image guided drug release from pH-sensitive Ion channel-functionalized stealth liposomes into an *in vivo* glioblastoma model. Nanomedicine. 2015;**11**(6):1345-1354

[127] Qiu LH, et al. Molecular imaging of angiogenesis to delineate the tumor margins in glioma rat model with endoglin-targeted paramagnetic liposomes using 3T MRI. Journal of Magnetic Resonance Imaging. 2015;**41**(4):1056-1064

[128] Sonali et al. RGD-TPGS decorated theranostic liposomes for brain targeted delivery. Colloids and Surfaces B: Biointerface. 2016;**147**:129-141

[129] Chen ZL, et al. Transferrin-modified liposome promotes alpha-mangostin to penetrate the blood-brain barrier. Nanomedicine. 2016;**12**(2):421-430

[130] Rotman M, et al. Enhanced glutathione PEGylated liposomal brain delivery of an anti-amyloid single domain antibody fragment in a mouse model for Alzheimer's disease. Journal of Controlled Release. 2015;**203**:40-50

[131] Tanifum EA, et al. Intravenous delivery of targeted liposomes to amyloid-beta pathology in APP/PSEN1 transgenic mice. PLoS One. 2012;**7**(10):e48515

[132] Kocer A, et al. Rationally designed chemical modulators convert a bacterial channel protein into a pH-sensory valve. Angewandte Chemie International Edition England. 2006;**45**(19):3126-3130

[133] Papadia K, Markoutsa E, Antimisiaris SG. A simplified method to attach antibodies on liposomes by biotin-streptavidin affinity for rapid and economical screening of targeted liposomes. Journal of Biomedical Nanotechnology. 2014;**10**(5):871-876

[134] Mura S, Couvreur P. Nanotheranostics for personalized medicine. Advanced Drug Delivery Reviews. 2012;**64**(13):1394-1416

[135] Adibhatla RM. Citicoline in stroke and TBI clinical trials. Nature Reviews Neurology. 2013;**9**(3):173

[136] Yukawa H, Tsukamoto R, Kano A, Okamoto Y, Tokeshi M, et al. (2013) Quantum Dots Conjugated with Transferrin for Brain Tumor Cell Imaging. J Cell Sci Ther 4: 150. DOI: 10.4172/2157-7013.1000150

[137] Liu Z, Wang F, Chen X. Integrin $\alpha v\beta 3$-targeted cancer therapy. Drug Development Research, 2008;**69**(6):329-339

[138] Danhier F, Le Breton A, Preat V. RGD-based strategies to target alpha(v) beta(3) integrin in cancer therapy and diagnosis. Molecular Pharmaceutics. 2012;**9**(11):2961-2973

[139] Guo H, et al. Theranostic magnetoliposomes coated by carboxymethyl dextran with controlled release by low-frequency alternating magnetic field. Carbohydrate Polymers. 2015;**118**:209-217

[140] Mikhaylov G, et al. Ferri-liposomes as an MRI-visible drug-delivery system for targeting tumours and their microenvironment. Nature Nanotechnology. 2011;**6**(9):594-602

[141] Wen CJ, et al. Theranostic liposomes loaded with quantum dots and apomorphine for brain targeting and bioimaging. International Journal of Nanomedicine. 2012;**7**: 1599-1611

[142] Lian T, Ho RJ. Trends and developments in liposome drug delivery systems. Journal of Pharmaceutical Sciences. 2001;**90**(6):667-680

[143] Manjappa AS, et al. Antibody derivatization and conjugation strategies: Application in preparation of stealth immunoliposome to target chemotherapeutics to tumor. Journal of Controlled Release. 2011;**150**(1):2-22

[144] Mufamadi MS, et al. A review on composite liposomal technologies for specialized drug delivery. Journal of Drug Delivery. 2011;**2011**:939851

[145] de Jesus Valle MJ, Sánchez Navarro A. Liposomes prepared in absence of organic solvents: Sonication versus lipid film hydration method. Current Pharmaceutical Analysis. 2015;**11**(2):86-91

Section 3

Liposomes in Therapy

Chapter 9

Liposomal Nanoformulations as Current Tumor-Targeting Approach to Cancer Therapy

Alina Porfire, Marcela Achim, Lucia Tefas and Bianca Sylvester

Additional information is available at the end of the chapter

http://dx.doi.org/10.5772/intechopen.68160

Abstract

The liposomes present great potential for applications in targeted delivery of chemotherapeutics in the treatment of cancer. The use of liposomal drug carriers as vehicles for targeting of chemotherapeutic agents to tumor tissues is based on their advantages over other dosage forms, represented by their low systemic toxicity, their bioavailability, and their possibility to enhance the solubility of different chemotherapeutic agents, due to the ability to encapsulate both hydrophilic and lipophilic drugs. They enhance the therapeutic index of anticancer drugs by increasing the drug concentration in tumor cells through tumor targeting. The available approaches used for tumor targeting using liposomes are passive targeting, active targeting, and triggered drug release. The most advanced targeting strategies proposed for cancer treatment are the development of multifunctional liposomes, having combined targeting mechanism. In this chapter, the tumor-targeting mechanisms are described in detail as well as the possibilities to design the targeted liposomal nanocarrier in order to reach the desired target in the body and minimizing the off-target effects. Moreover, the current status of preclinical and clinical evaluation is highlighted.

Keywords: liposomes, cancer, tumor-targeting, passive targeting, active targeting

1. Introduction

The main characteristic of cancer is the existence of abnormal rapidly proliferating cells. Conventional chemotherapy is based on using chemotherapeutic agents that eliminate these uncontrollably dividing cells [1]. Most currently used anticancer agents are not able to differentiate between cancerous cells and normal ones, resulting in high systemic toxicity and side

effects [2]. Because of the severity of the side effects, often dose reduction or cessation of the treatment is necessary, rendering chemotherapy inefficient [3]. By limiting the administered dose to reduce excessive toxicity, only a small fraction of the drug will reach the target tumor site, whereas the remaining portion of the drug will be distributed to other tissues in the body. This lack of specificity toward cancerous cells translates into an insufficient amount of chemotherapeutic drug reaching the site of action [1]. Liposomal nanosystems can overcome the drawbacks of conventional chemotherapy, by increased drug delivery in the tumor tissue and lower drug concentration in normal tissues. This way, the therapeutic efficiency of chemotherapy is increased, while the toxicity and side effects are reduced [4]. Also, due to their small size, the circulation time of standard chemotherapeutic agents is often short as they are rapidly eliminated from the bloodstream by macrophages, thus reducing the effective drug concentration at the tumor site [3]. Moreover, the majority of current chemotherapeutic agents have poor water solubility and absorption, which result in low bioavailability [2]. The incorporation of the chemotherapeutic drugs in liposomal drug delivery systems offers advantages by protecting the drug from degradation, increasing its circulation time in the bloodstream and overall improving its pharmacokinetic profile [1, 2].

2. Liposomal nanoformulations for tumor targeting

2.1. Liposomes for passive tumor accumulation

Passive targeting consists in the transport of nanocarriers through leaky tumor capillary endothelium into the tumor interstitial space [5]. The underlying mechanism, which makes passive targeting possible, is the enhanced permeability and retention (EPR) effect.

It was observed that certain circumstances, such as inflammation/hypoxia, tumors, or infarcts, can determine an enhanced permeability of the endothelial lining of the blood vessel wall compared with the normal state of the tissue [6]. When reaching a given size, a tumor can no longer rely on the normal vasculature present in its vicinity to provide all the oxygen supply needed for its further proliferation. Therefore, as oxygen-deprived cells start to die, they secrete growth factors that promote the formation of new blood vessels from the surrounding capillaries, process known as angiogenesis [7]. These newly formed irregular blood vessels lack the basal membrane of normal vascular structures, thus presenting a discontinuous epithelium, which allows particles, such as nanocarriers (in the size range of 20–200 nm), to extravasate and accumulate inside the interstitial space [8]. Following permeation into the tumor, the enhanced accumulation of nanocarriers in the tumor microenvironment is favored by the poor lymphatic drainage in the tissue. In tumors, the lymphatic function is defective, resulting in minimal uptake of the interstitial fluid. Therefore, nanocarriers that have reached the perivascular space are not cleared efficiently and accumulate in the tumor interstitium [7]. This spontaneous accumulation or "passive" targeting is currently known as the EPR effect [9]. Utilization of the EPR effect is therefore an effective strategy for targeting nanopreparations, such as liposomes, to the site of a tumor and has been extensively documented using various tumor types and animal models, since its early discovery in 1980s by Matsumura and Maeda [10, 11].

Several factors have been shown to influence and favor the EPR, for example, prolonged systemic circulation that allows longer interaction of liposomes with the target, size of the liposomes, composition, and charge on the surface of liposomes [12]. Longevity in blood is achieved by coating the liposomes with polymers, such as polyethylene glycol (PEG). PEG has been shown to protect liposomes from recognition and rapid removal from the circulation by the mononuclear phagocyte system (MPS), enabling the liposomes to stay in the circulation for a prolonged period of time and allowing them to substantially extravasate and accumulate in tumors, hence giving the liposomes long-circulating properties [13]. PEG prevents opsonization by shielding of the surface charge, enhancing the repulsive interaction between polymer-coated liposomes and blood components, increasing surface hydrophilicity, and forming a polymeric layer over the liposome surface which renders them impermeable to opsonins [14, 15]. Additionally, their accumulation in the tumor is strongly linked on the size of the endothelial gaps in the capillary vasculature, which varies between 200 and 2000 nm, depending on the tumor type, its environment, and its localization [7]. An effective extravasation has been shown to occur for particles averaging from 30 to 100 nm in the case of hyperpermeable tumors such as murine colon adenocarcinoma, whereas for poorly permeable tumors (human pancreatic adenocarcinoma), only particles smaller than 70 nm proved to be effective [16, 17]. Last, the composition and charge on the surface of liposomes have impact on passive targeting. The presence of surface-charged lipids can alter the opsonization profile of the liposomes, their recognition by cells of the MPS, and hence their overall plasma circulation profile [18, 19]. While anionic or neutral liposomes escape from renal clearance, the positive surface charge of cationic liposomes leads to nonspecific interactions with the anionic species in the blood, resulting in rapid clearance from circulation by the reticuloendothelial system (RES), which reduces the EPR effect [11, 12]. Moreover, it has been reported that the aggregation of liposomes occurs with greater amounts of cationic lipids in the liposomal membrane; therefore, an optimization of the composition of the liposomal membrane is crucial for enhancing tumor penetration [20].

Conventional liposome formulation is based on the use of phospholipids and cholesterol, the last playing an essential role in the regulation of liposomal membrane fluidity, affecting vesicles permeability and stability [21]. Unmodified liposomes are rapidly eliminated from the circulation by the macrophages of RES, their main clearance sites being liver and spleen [22]. Grafting of PEG on the surface results in the formation of "stealth" or stabilized liposomes, which have improved *in vivo* stability and increased circulation time, up to 24–48 h (the long-circulating liposomes). PEG performance as stabilizer depends on chain length, optimal surface density, and optimal chain configuration. The percentage of PEGylated phospholipids necessary for stealth behavior is about 5–7% mol. with PEG 2 KDa and 15–25% with smaller PEG 350 Da to 1 kDa. Depending on the PEG density and configuration on the liposome structure, three models are possible: "mushroom" (low-polymer density), "pancake" (high-graft density), or "brush" (ideal model, ensuring efficient coverage of the surface) [11, 23].

It was reported that PEGylated egg phosphatidylcholine-cholesterol liposomes loaded with doxorubicin (DOX), having ~100 nm, passively accumulated in the tumor vessels of a multidrug-resistant breast cancer xenograft model, exhibiting a remarkable antitumor effect, where the free DOX failed to provide any detectable therapeutic effect [24].

Mitoxantrone (MTO), an anthracenedione closely related to anthracyclines, was encapsulated in PEGylated liposomes, and efficacy studies in breast cancer model using liposomal-based MTO chemotherapeutic treatment in comparison with free MTO were realized. MTO encapsulation in liposomes limited the toxicity, which allowed the administration of higher MTO doses in the treatment of breast carcinoma on mice [25].

Recently, scientists reached the conclusion that the EPR effect is much more complex than initially defined, as it encompasses complex biological processes such as angiogenesis, vascular permeability, hemodynamic regulation as well as heterogeneities in tumor genetic profile and in the tumor microenvironment and lymphangiogenesis. As these factors differ from patient to patient and from one tumor type to another, they represent an important source of variability when considering the distribution and accumulation of liposomes in tumors. For these reasons, the sole use of the EPR effect as targeting mechanism may now be considered outdated, leaving the focus on designing actively targeted liposomes and liposomes, which combine the passive tumor accumulation with active targeting and/or stimuli sensitivity [2].

2.2. Actively targeted liposomal systems

The limitations of passive tumor targeting have been addressed by developing another kind of targeted drug delivery named active targeting. Various receptors are known to be involved in the development and progression of cancer, so they can be regarded as potential targets for the development of drug delivery systems. Liposomal drug delivery systems for active targeting are designed to have targeting moieties attached on their surface. The targeting ligands bind to the corresponding receptors or surface molecules which are overexpressed on the surface of the tumor cells or tumor vasculature [2, 26]. As a result, liposomes are internalized in the tumor cells by endocytosis and drug concentration in tumor cells is increased [12]. The targeting moieties can be monoclonal antibodies, fragments of antibodies, peptides, proteins, nucleic acids, carbohydrates, or small molecules [2, 26].

The design of liposomes for active targeting is a complex task in which various factors must be taken into account. For instance, the manufacturing material and the size of the liposomes, the type of ligand, the ligand conjugation method, and the ligand density determine the efficacy of the liposomal system both *in vitro* and *in vivo*. The affinity of a ligand for its target is greatly affected by the density of the ligand on the surface of the liposomes [26]. Generally, an increased ligand density favors the uptake of the delivery system as there is a higher probability of interaction with the target (multivalency) [27]. However, a supplementary increase in ligand density can negatively impact on ligand-substrate interactions due to improper orientation of the ligand, steric hindrance of vicinal molecules, and so on. To bind to its specific substrate, a ligand has to be in the proximity of its target, to be able to recognize and interact with it, so the design of liposomal systems with increased circulation time will favor the interaction [26]. As shown above, modifying the surface of the liposomes with PEG can prolong the blood circulation time by avoiding opsonization, but PEG with long chains can hinder the binding of the ligand to its target and PEGylation can increase the size of the liposomes. Besides PEGylation, the size of the liposomes and the surface and ligand charge have important contributions in the ligand-substrate interactions. The size of the liposomes can influence

cellular uptake and intracellular deposition. The charge of the liposomes and the ligand can determine attractive or repulsive forces, which in turn will affect the degree of conjugation. This problem can be solved by adding a spacer, like PEG. It has been shown that cationic liposomes bind to their targets and are consequently internalized to a greater extent than negatively charged particles [26].

Generally, an active targeting liposomal drug delivery system consists of the following components: (1) the liposomal carrier, (2) a hydrophilic polymer forming a protective layer around the liposome, (3) a ligand specifically targeting a certain substrate, (4) a linker molecule or a functional group that couples the ligand to the liposome, and (5) a drug encapsulated in or bound to the liposomal system. Ligands can be covalently or non-covalently bound to the surface of the liposome. The most extensively used approach is the one based on covalent binding of the ligand to the liposomes, usually done with the aid of a linker through a series of chemical reactions [28].

The ligand can be conjugated to the liposomes' components (e.g., a lipid) either prior to liposome preparation or afterwards. Usually, a pre-liposome preparation conjugation has the advantage of allowing better control of the liposomes' physicochemical properties. On the other hand, the post-liposome assembly strategy is based on coupling the ligand to the already-prepared liposomes, and is applied if the ligand changes the properties of the liposomes' components, the ligand is too large to participate in self-assembly, or has a poor stability in organic solvents [26].

Active targeting can be addressed either to tumor cells or to the tumor endothelium.

2.2.1. Active targeting of tumor cells

In targeting tumor cells, the ligand should have a high affinity for a specific receptor overexpressed by tumor cells in order to bind to the receptor and subsequently be endocytosed into the cells. The receptors most exploited in active targeting include the following discussed below [2].

The folate receptor is overexpressed in various types of cancer such as breast, ovarian, lung, colon, kidney, and brain cancers [29]. It has two isoforms: the alpha isoform, which is overexpressed in most cancers, and the beta isoform, which is expressed on the surface of activated macrophages [2]. Active drug delivery targeting the folate receptor involves conjugating folic acid to the surface of liposomes, usually through a PEG spacer between the lipids and the folate. Several liposomal systems conjugated with folic acid have been developed for the delivery of different anticancer agents, including imatinib [30], docetaxel [31], DOX [32], and daunorubicin [33]:

a. The transferrin receptor (TfR) is a transmembrane glycoprotein involved in cellular iron uptake from transferrin (Tf), a plasma protein, by receptor-mediated endocytosis [34]. The TfR has been explored as a target for cancer treatment due to its accessibility, its pivotal role in cell growth, and proliferation and also its overexpression by various types of malignant cells [35]. Recently, nanoparticulate systems modified with Tf were proposed to deliver the

chemotherapeutic agents across the blood-brain barrier (BBB), for the treatment of brain tumors such as glioma. For instance, Tf was attached to the surface of vincristine and tetrandrine-loaded liposomes [36] and for modifying liposomes loaded with cisplatin [37]. Both liposomal formulations showed a more potent cytotoxic effect on tumor cells than the free drugs and the non-modified liposomal drugs, on C6 glioma cells *in vitro* [36, 37].

b. The epidermal growth factor receptor (EGFR) is a 170-kD glycoprotein which belongs to the ErbB family of tyrosine kinase receptors. The EGFR plays a crucial role in cancer progression and metastasis since it activates signaling pathways responsible for promoting cell proliferation, angiogenesis, and inhibiting apoptosis [38]. Overexpression of EGFR has been observed in various types of cancer, including breast, lung, colon, ovarian, pancreatic, and kidney cancers [2]. EGFR-mediated delivery via liposomes is based on using antibodies or antibody fragments embedded in the lipidic membrane. Several anti-EGFR-liposomal systems have been reported for the delivery of DOX [39, 40]. A work describes the development of a large-scale, Good Manufacturing Practice (GMP) compliant process for manufacturing EGFR-targeted immunoliposomes loaded with DOX, using the already approved Cetuximab (C225) and PEGylated-liposomal DOX (Caelyx®). The liposomal formulation was safe, according to the results of a clinical trial [41]. Cetuximab or Cetuximab fragments (Fab′) were also coupled to oxaliplatin-loaded liposomes for increased selectivity for tumor cells. Both liposomal formulations showed greater cellular uptake than untargeted liposomes in EGFR-positive cell cultures *in vitro*, and *in vivo* experiments on colon cancer-bearing mice indicated improved efficacy over untargeted liposomal oxaliplatin. Liposomes equipped with Fab′ fragments bound to a higher extent to EGFR and had better uptake than liposomes coupled to Cetuximab [42].

c. Glycoproteins expressed on the surface of cancer cells can be bound by lectins which can be used as targeting moieties on liposomes, since the bond between the two is very specific.

A PEGylated-liposomal system functionalized with recombinant human E-selectin for the selective delivery of DOX to tumor cells was designed by attaching E-selectin to the PEG chains of PEG2000-DSPE through a maleimide group. When tested on two circulating malignant cell lines expressing sialylated carbohydrate groups, a significant reduction in cell viability was obtained compared to the control and empty E-selectin-coupled liposomes, which shows that the developed liposomal system could be useful in capturing and eliminating circulating tumor cells under flow conditions [43].

d. CD44 (cluster of differentiation 44) is a transmembrane glycoprotein which contains a specific binding domain for hyaluronic acid. CD44 is involved in a series of biological processes, including proliferation, migration, growth, differentiation, and angiogenesis [44]. Various cancers, such as leukemia, ovarian, colon, gastric, pancreatic, and epithelial cancers, have been documented to overexpress CD44.

Several liposomal systems decorated with hyaluronic acid have been described in literature for the delivery of gemcitabine [45] and DOX [46] to tumor cells. Other reported methods of targeting the CD44 receptor involve using anti-CD44 monoclonal antibodies [44] or RNA aptamers (e.g., Apt1) [47].

2.2.2. Active targeting of the tumor endothelium

This type of nanosystem is capable of binding and destroying tumor vasculature and indirectly limiting the growth of the tumor cells that are supplied with nutrients and oxygen by these blood vessels. Targeting the tumor endothelium is advantageous because the nanosystems do not have to extravasate in order to reach their site of action, and can directly bind to the corresponding receptors which are easily accessible [2]; the risk of developing resistance to chemotherapy is reduced because endothelial cells have less genetic variations than tumor cells, and markers expressed by endothelial cells are not specific for any type of tumor [12]. The main targets of the neovascular endothelial cancer cells are described below:

a. The vascular endothelial growth factor (VEGF) is produced by tumor cells in hypoxic conditions [2]. VEGF and its receptor (VEGFR) play an important role in angiogenesis, inducing the proliferation, migration, and survival of epithelial cells. Also, VEGF increases the permeability of blood vessels [48]. There are two main strategies of targeting VEGF-mediated angiogenesis, namely targeting VEGFR to reduce VEGF binding or targeting VEGF to decrease its binding to VEGFR [2]. A novel PEGylated-liposomal system functionalized with a fully human anti-VEGF 165 monoclonal antibody was proposed for paclitaxel. The PEGylated immunoliposomes showed superior antitumor activity compared to unmodified liposomes and the commercially available paclitaxel (Taxol®) in SGC-7901 human gastric cancer-bearing nude mice [48].

b. The integrins are a family of heterodimeric transmembrane glycoproteins participating in interactions between cells or between cells and extracellular matrix. They are composed of non-covalently bound polypeptide α- and β-subunits [12]. Among these integrins, $\alpha_v\beta_3$-integrin seems to be the most important integrin in angiogenesis. It is an endothelial cell receptor for extracellular matrix proteins, including fibrinogen/fibrin, fibronectin, vitronectin, thrombospondin, and osteopontin. Higher expression of $\alpha_v\beta_3$-integrin has been observed in melanoma, lung, and brain cancers [2, 49]. Research has revealed that the arginine-glycine-aspartic acid (RGD) amino acid sequence is the binding site contained in all ligands bound by $\alpha_v\beta_3$-integrin, and new RGD-containing peptides or derivatives with high affinity and selectivity for $\alpha_v\beta_3$-integrin have recently been proposed. Moreover, the incorporation of cytotoxic drugs in nanosystems decorated with RGD-containing ligands could promote antitumor effect by offering a dual-targeting strategy against tumors [50].

A liposomal system containing DOX was engrafted with three different cyclo-RGD-based peptides: cRGDyC (Arg-Gly-Asp-D-Tyr-Cys), cRGDfK (Arg-Gly-Asp-D-Phe-Lys), and cRGDf[N-Met]K (Arg-Gly-Asp-D-Phe-[N-Methyl]Lys). The latter peptide was synthesized based on Cilengitide, the most selective inhibitor of $\alpha_v\beta_3$-integrin currently evaluated in a phase III clinical trial for glioblastoma therapy. *In vitro* experiments regarding liposome-cell association and cytotoxicity were conducted in human umbilical vein endothelial cells (HUVEC) and emphasized the ability of RGD-targeted liposomes to associate to HUVEC through integrin-mediated endocytosis. The therapeutic efficacy of RGD-targeted liposomes was assessed in C-26 colon carcinoma tumor xenograft model in mice. Among the investigated peptides, RGDf[N-Met]K had the most potent cytotoxic effect and increased the survival of mice [50].

In another study, other three RGD-based peptides were evaluated as potential ligands, coupled to liposomes: a monomeric c(RGDfK) (moRGD), a dimeric c(RGDfK) (diRGD), and a special dimeric c(RGDfK) (P-diRGD) containing a PEG spacer between two cyclic RGD motifs. P-diRGD-modified liposomes exhibited the strongest interaction with and internalization in B16 murine melanoma cells. The targetability of P-diRGD-modified liposomes in B16-bearing mice was approximately 2.4-fold and 2.8-fold more increased than that of moRGD- and diRGD-modified liposomes [49].

2.3. Stimuli-sensitive liposomes

Stimuli-responsive liposomes have been developed with the purpose of overcoming problems associated with conventional and long-circulating liposomes, such as a slow release of the loaded drug or the incapacity to fuse with the endosome after internalization. The concept of increasing drug targeting through triggered release is based on utilizing subtle pathological changes in the tumor microenvironment and has been extensively studied in the past years for improved efficiency of liposomal drug release [12, 51]. The stimuli-sensitive nanocarriers maintain their stealth function throughout circulation, and upon arrival at the specific tumor site, undergo rapid changes, such as aggregation, disruption, and permeability changes, which trigger drug release when exposed to a particular tumor microenvironment [2, 52, 53]. In order to achieve site-specific triggered drug release, several strategies have been investigated, for example, internal stimuli that are characteristic for a tumor microenvironment (low pH, redox potential, high temperature, and enzymes) and external stimuli, such as magnetic fields, ultrasound, or light [54–56]. Both internal and external stimuli-sensitive liposomes will be addressed further, classified according to the mechanism exploited.

2.3.1. Internal stimuli

a. The pH-sensitive triggered release is based on the degradation of the liposomal carriers followed by the release of the entrapped drug in tissues with a low pH, such as tumors, the cell cytoplasm, or the endosome [2, 12]. Although PEGylation increases the longevity of the liposomes in the circulation, in some cases it does not guarantee the escape of liposomes from endosomes, allowing the degradation of their contents prior to achieving their target. With the purpose of overcoming this problem, pH-labile linkers have been introduced between the hydrophilic PEG and the hydrophobic moiety, linkers that are cleaved upon exposure to the relatively low-endosomal pH or the acidotic tumor mass [57].

pH-sensitive dextran liposomes having 3-methylglutarylated residues (MGlu-Dex) were described. Surface modification of phosphatidylcholine liposomes with MGlu-Dex enabled obtaining highly pH-sensitive liposomes that were stable at neutral pH but were strongly destabilized in the weakly acidic pH region (pH ~5.5). *In vivo* data suggested that compared to unmodified liposomes, MGlu-Dex-ovalbumin liposomes efficiently increased the uptake of ovalbumin by dendritic cells and significantly suppressed tumor growth [58].

b. Temperature-triggered drug delivery represents an attractive strategy in cancer therapy, because compared to normal tissues, pathological areas, such as tumors, show a distinctive hyperthermia [2]. Temperature-sensitive liposomes release the encapsulated drugs at the

melting-phase transition temperature (Tm) of the lipid bilayer/the lower critical solution temperature (polymers), temperature at which the membrane changes its permeability, disrupting to release the drug [59]. Temperature-sensitive liposomes have been widely investigated in the last decades and successfully applied in both preclinical and clinical studies in combination with heat-based therapies, such as radiofrequency ablation, ultrasound hyperthermia, and microwave hyperthermia [60]. A temperature-triggered liposomal system, ThermoDox® developed by Celsion Corporation (NJ, USA), has successfully demonstrated its improved efficacy during phase III clinical trials for the treatment of hepatocellular carcinoma and phase II trials for breast cancer and colorectal liver metastases [60].

c. Enzymes, such as matrix metalloproteinases—MMPs (e.g. MMP2), phospholipase A2, alkaline phosphatase, transglutaminase, or phosphatidylinositol-specific phospholipase C, are overexpressed in tumor tissues and have been suggested as potential candidates for enzymatically triggered drug release from liposomes [61]. A hybrid liposome composed of phospholipid (DPPC) and PEGylated block-copolymer (Poloxamer 188) was described for the rapid release of encapsulated DOX in the presence of phospholipase A2 (PLA2). Drug release from liposomes was facilitated by higher PLA2 concentrations and was found to be dependent on the temperature and the presence of calcium ion, partially explaining PLA2-responsive drug release. DOX release from liposomes triggered by PLA2 exhibited enhanced cytotoxic effects on the A549 lung cancer cell line, suggesting that DPPC/P188 liposomes are a promising drug carrier for PLA2-expressing sites such as inflammatory lung cancer [62].

To overcome the fact that conventional liposomes have no mechanism for specifically releasing the encapsulated cargos inside the cancer cells, calcein-loaded liposomes containing a novel destabilization peptide (LMDP) were proposed. This peptide can destabilize liposomal membranes upon cleavage by the intramembranous proteases in cancer cells. *In vitro* tests showed that encapsulated calcein was successfully released in the presence of a membrane fraction containing an LMDP-cleavable protease, proving the responsiveness of the system to the cancer-specific protease [63].

2.3.2. External stimuli

a. The use of activated light, made by the adjustment of parameters such as wavelength, intensity, pulse duration, and cycle, has been recognized as a promising tool for several biomedical applications, including light-triggered drug delivery [12]. Visible light, UV, and near-infrared (NIR) light have been investigated so far as triggers for the drug delivery; however, near-infrared is the most desirable for tumor targeting, since it penetrates deeper into the tissue. Thus, the preparation of porphyrin-phospholipid (PoP)-doped liposomes that are permeabilized by directly near-infrared light was described. Upon systemic administration, laser irradiation-enhanced deposition of actively loaded DOX in mouse xenografts, enabling an effective single-treatment antitumor therapy [64]. Another study reported the incorporation of an unsaturated phospholipid, such as dioleoylphosphatidylcholine (DOPC), in order to accelerate the near-infrared light-triggered DOX release in porphyrin–phospholipid

liposomes. The formulation inhibited human pancreatic xenograft growth in mice following a single intravenous administration of 6 mg kg^{-1} DOX, loaded in liposomes [65].

b. Ultrasound-mediated drug delivery represents an attractive way to achieve noninvasive penetration into deep tissues and produce focused, controlled drug delivery [66]. High-intensity focused ultrasound (HIFU) produces local heating, which can promote phase transition of the lipids, facilitating drug release from liposomes. While HIFU is considered ideal for deeper tumors, low-frequency ultrasound (LFUS) is only appropriate for superficial tumors and has been used to trigger drug release from stealth liposomes without affecting the physicochemical properties of the drug [67]. Moreover, it was demonstrated that tumor vascular endothelium becomes more permeable after ultrasound.

A novel nanocarrier of emulsion liposomes (eLiposomes) composed of a perfluoropentane nanodroplet within the aqueous interior of a DPPC liposome, along with the anticancer drug DOX, was described. *In vitro* studies showed that the liposomes displayed good release of DOX upon the application of low-intensity ultrasound at 20 kHz, 1.0 MHz, and 3.0 MHz. This novel drug delivery system promises to provide enhanced drug delivery of DOX compared to traditional stealth liposomes and has the potential to reduce the side effects of cardiotoxicity caused by DOX [68].

c. Magnetic-triggered drug release has received great attention in the past years, as magnetized liposomes have significant biomedical applications such as magnetic hyperthermia, magnetic transfection, and manipulation of cells and proteins [12]. Liposomes are usually magnetized by the incorporation of Fe_3O_4 or γ-Fe_2O_3, and once exposed to a magnetic field, the chemotherapeutic agent incorporated is completely released. Due to their magnetic properties, nanoscale size (approximately 10 nm), and biocompatible nature, these magnetized liposomes are also referred to as SPIONs [2]. For example, DOX-loaded magnetic liposomes were proposed as strategy for anti-colorectal cancer treatment, using a combination of chemotherapy and thermotherapy. *In vitro* cytotoxicity and hyperthermia studies were evaluated against colorectal cancer (CT-26 cells) with high-frequency magnetic field (HFMF) exposure and was found that the combination between DOX-loaded liposomes and HFMF was more effective than either hyperthermia or chemotherapy treatment individually [69].

2.4. Multifunctional liposomes

The current trend reflected by the scientific publications in the field is to develop liposomal nanoformulations that simultaneously demonstrate more than one useful function, that is, multifunctional liposomes, by combining two (longevity and targetability; targetability and stimuli sensitivity) or even all three functionalities mentioned above (longevity, targetability, and stimuli sensitivity). Thus, an ideal nanoformulation used for tumor-targeting purposes should possess the following properties: long circulation in the body, specificity for the site of the disease, sensitivity to local/external stimuli found in/applied to the tumor tissue, enhanced intracellular delivery of the drug, contrast properties to allow *in vivo* visualization, and others [70].

2.4.1. Liposomes combining in vivo longevity and specific target recognition

This type of liposomal formulations combine the drug delivery advantages of PEGylation, such as longevity in blood and passive tumor accumulation, with tumor cell-specific or tumor endothelium-specific delivery by ligand association at their surface. In spite of the advantages, the specific ligands attached to the surface of liposomes may increase the rate of uptake by the RES, could facilitate the development of unwanted immune response, and their amount must be optimized to ensure successful binding to the target [70].

The majority of research in this field utilizes monoclonal antibodies for the design of PEGylated immunoliposomes. Several PEGylated immunoliposomes designed for specific target of EGFR are described in Section 2.2.1. Others are designed to target the human epidermal growth factor receptor 2 (HER2), a growth hormone receptor overexpressed on the surface of certain types of breast cancer cells. HER2 antibody was used in a recent study as a targeting ligand in PEGylated immunoliposomes loaded with DOX. The formulation was tested for combination therapy in association with liposomal bevacizumab, and animal studies revealed increased accumulation of DOX at the tumor site and a significant delay of tumor growth in the combinational liposomal drug delivery group compared to free DOX, liposomal DOX, immunoliposomal DOX, and liposomal bevacizumab [71].

Several research groups developed long-circulating targeted liposomes as a strategy to transport drugs across the BBB for treating brain glioma. Thus, polyethyleneimine (PEI), a positively charged polymer, and vapreotide (VAP), a synthetic somatostatin analog, were used as targeting molecules for vinorebline and tetrandrine. The multifunctional drug-loaded system demonstrated enhanced antitumor efficacy on glioma-bearing mice, explained by a combination of long circulation time in the blood (PEGylated lipids), enhanced transport of drugs across BBB (absorptive-mediated endocytosis by PEI, blocking the expression of P-gp protein by tetrandrine), and increased intracellular uptake by glioma cells and glioma stem cells (receptor-mediated endocytosis by VAP) [72].

Another group reported the use of stabilized peptide ligands, that is, cA7R (cyclic A7R) and ^{D}A7R, for multifunctional glioma-targeted drug delivery. The mentioned peptides were developed to enhance the proteolytic stability of the linear L-peptide A7R (^{L}A7R), which binds with high affinity and specificity to vascular endothelial growth factor receptor 2 (VEGFR2) and neuropilin-1 (NRP-1), which are overexpressed in glioma. In one study, ^{D}A7R, the retro-inverso derivative of ^{L}A7R, was associated to PEGylated liposomes to achieve multifunctional targeting of DOX to glioma. ^{D}A7R had similar binding affinity to its receptors *in vitro*, but ^{D}A7R-conjugated liposomes were superior to ^{L}A7R-modified liposomes in terms of antitumor efficiency *in vivo*, due to their better serum stability and higher tumor accumulation [73]. The same authors conjugated the cyclic derivative, cA7R, on the surface of DOX-loaded PEGylated liposomes, and the resulted system exhibited excellent antitumor, anti-angiogenesis, and anti-vasculogenic mimicry effects, resulting in improved therapeutic efficacy in U87 xenograft nude mice as compared to other DOX formulations (solution, non-functionalized liposomes, or liposomes functionalized with ^{L}A7R) [74].

2.4.2. Active-targeted, stimuli-sensitive long-circulating liposomes

Many liposomal systems described combine long circulation properties, with active targeting and stimuli-responsive drug release functions. The release of drugs from such carriers is triggered specifically at target sites either by local characteristics specific for the tumor tissue or by the application of stimuli at target tissue from outside of the body [75]. Such multifunctional approach was exploited in EGFR-targeting-thermosensitive liposomes. The liposomes were functionalized with GE11, an EGFR-specific peptide or Cetuximab antibody fragments (Fab') for comparison, and dipalmitoylphosphatidylcholine (DPPC):DSPC:DSPE-PEG:DSPE-PEG-GE11 were used to achieve thermosensitivity. The proposed liposomal formulation released DOX at temperatures above 40°C. Of the two investigated anti-EGFR ligands, Fab' was more potent in terms of cellular uptake. On breast cancer cell lines, targeted liposomes encapsulating DOX proved to be more cytotoxic than the plain liposomal DOX [76]. In another study, multifunctional liposomes with target specificity, temperature-triggered drug release, and near-infrared fluorescence imaging were designed. DOX-loaded stealth liposomes were modified with thermosensitive poly[2-(2-ethoxy)ethoxyethyl vinyl ether] chains, conjugated with the antibody trastuzumab (Herceptin, HER), and furthermore indocyanine green was incorporated for near-infrared fluorescence imaging. The group reported the excellent ability of these liposomes for association and internalization to target cells overexpressing Her-2, when heated at 45°C for 5 min [77].

2.4.3. Multifunctional liposomes for enhanced intracellular delivery

In order to improve the cytotoxicity of the chemotherapeutics loaded in liposomes, the use of cell-penetrating peptides (CPPs), which enhance the transport through the plasma membrane into cells, has been proposed [78]. Among these, the use of transactivator of transcription peptide (TATp) in the design of multifunctional liposomes has been shown to enhance cell uptake and cytotoxicity of the loaded drug, or even to increase the therapeutic efficacy against multidrug-resistant cancer cells [79, 80]. To prevent the proteolytic degradation of TAT, which might alter its targeting properties, it is necessary to shield it, usually through the use of PEG chains.

In a recent study, the advantages of formulating paclitaxel (PTX)-loaded liposomes functionalized with TAT and cleavable PEG via a redox-responsive disulfide linker (PTX-C-TAT-LP) were investigated. At tumor site, in the presence of exogenous reducing agent glutathione (GSH), PEG was detached and TAT was exposed to facilitate cell internalization. Compared to conventional stealth PTX-TAT liposomes, PTX-C-TAT-LP achieved enhanced tumor distribution and demonstrated superior delivery efficiency both *in vitro* and *in vivo* [81]. Another study reports a novel dual-functional liposome system possessing mitochondrial targeting properties and extracellular pH response which has been proved to enhance paclitaxel accumulation into the mitochondria. Peptide *D*[KLAKLAK]2 (KLA) was modified with 2, 3-dimethylmaleic anhydride (DMA) and combined with 1, 2-distearoyl-sn-glycero-3-phosphoethanolamine (DSPE) to yield a DSPE-KLA-DMA (DKD) lipid, which, at tumor extracellular pH (~6.8), reversed the surface charge of liposomes (negative to positive), facilitating

their internalization. *In vitro* studies proved that pH-sensitive-modified liposomes exhibited improved efficacy in treating drug-resistant lung cancer A549/Taxol cells compared to conventional therapy [82].

3. Clinical experience with liposomes for cancer chemotherapy

Research on chemotherapy via liposomal drug delivery has known significant progress in the last decades, evolving from *in vitro* and *in vivo* preclinical studies on animals to numerous clinical trials. There are over 1000 clinical trials containing the terms "liposome" and "cancer," either completed or active, according to The National Institutes of Health's (NIH) web-based database, ClinicalTrials.gov and the EU Clinical Trial Register. There are several ongoing clinical trials investigating the efficiency of liposomal cisplatin, NDDP (cisplatin analog), paclitaxel, mitoxantrone, irinotecan, SN38 (the active metabolite of irinotecan), topotecan, lurtotecan, a camptothecin analog, vinorelbine, annamycin, docetaxel, DOX, and vincristine [83–87]. The association of chemotherapeutic drugs is a frequently used strategy in chemotherapy. In this sense, some clinical trials evaluate the synergistic cytotoxicity of a combination of two agents, such as irinotecan hydrochloride-floxuridine and cytarabine-daunorubicin in liposomal forms [86, 88].

Moreover, liposomes are the first nanoscale systems to be approved in 1995. The first liposomal system approved by the regulatory authorities for the treatment of cancer was liposomal DOX (in 1995), marketed as Doxil® in the USA and Caelyx® in Europe [89, 90]. Other liposomal DOX formulations, such as Myocet® and Lipo-Dox®, have also been introduced into the market [91]. Lipo-Dox®, Doxil®, and Caelyx® are sterically stabilized liposomal DOX formulation having the same clinical indications. In contrast to these products, Myocet® is a non-PEGylated liposome encapsulating DOX, used to treat metastatic breast cancer in association with cyclophosphamide [90].

Other cytotoxic drugs incorporated in approved liposomal products are daunorubicin and vincristine in DaunoXome® and Marqibo®, respectively [91]. DaunoXome® is a conventional liposomal formulation containing daunorubicin as a citrate salt, used in clinical practice in the treatment of Kaposi's sarcoma [91]. Marqibo® is a sphingomyelin and cholesterol-based liposomal formulation of vincristine [90], indicated in acute lymphoblastic leukemia [91].

All aforementioned products are administered intravenously, but other routes of administration are also exploited in liposomal drug delivery. For instance, DepoCyt®, a liposomal system containing cytosine arabinoside (a nucleoside analog of deoxycytidine), is administered spinally/intrathecally in neoplastic meningitis and lymphomatous meningitis [92, 93].

Currently, there are several liposomal systems for active targeting that are being investigated in different stages of clinical trials, but no formulation is commercially available. Most of them refer to liposomal systems modified with a transferrin receptor-targeted ligand.

For instance, MBP-426 is a liposome system conjugated with human transferrin for the delivery of oxaliplatin in patients with advanced or metastatic solid tumors that has completed a phase I clinical trial. It was also investigated in a phase Ib/II clinical trial in combination with leucovorin and 5-fluorouracil in second-line patients with metastatic gastric, gastroesophageal junction, or esophageal adenocarcinoma [94, 95].

Even though liposomes and targeting antibodies are both approved for clinical use, there are few studies on nanosystems which combine these two strategies. For example, anti-EGFR immunoliposomes encapsulating DOX have been shown to target the epidermal growth factor receptor by coupling Fab' fragments of the Cetuximab monoclonal antibody on the surface of the liposomes [96, 97]. MCC-465 is a PEGylated immunoliposome containing DOX, modified with the F(ab')2 fragment of GAH human monoclonal antibody, for the treatment of gastric cancer [97, 98]. The delivery of DOX to the brain via liposomes has been enhanced by conjugation with glutathione. 2B3-101 is a glutathione-PEGylated-liposomal system capable of transporting DOX across the BBB by using the glutathione transporters [97, 99].

4. Conclusions

The liposomes present great potential for applications in targeted delivery of chemotherapeutics in the treatment of cancer. Based on their potential, several formulations are already approved and are clinically used in cancer treatment. However, many more have failed during the preclinical evaluation or early stages of clinical development. Therefore, future development of liposomal-based-targeted chemotherapy should comprise strategies based on deep understanding of the pathophysiological mechanism of the disease, on the preparation process and stability issues, and on the correlation between the physicochemical characteristics of the nanocarrier and its targeting ability.

Acknowledgements

This work was supported by a grant of the Romanian National Authority for Scientific Research and Innovation, CNCS-UEFISCDI, project number PN-II-RU-TE-2014-4-0220.

Author details

Alina Porfire*, Marcela Achim, Lucia Tefas and Bianca Sylvester

*Address all correspondence to: aporfire@umfcluj.ro

University of Medicine and Pharmacy "Iuliu Hatieganu," Cluj Napoca, Romania

References

[1] Estanqueiro M, Amaral MH, Conceição J, Sousa Lobo JM. Nanotechnological carriers for cancer chemotherapy: The state of the art. Colloids Surf B Biointerfaces. 2015;**126**:631-48

[2] Danhier F, Feron O, Préat V. To exploit the tumor microenvironment: Passive and active tumor targeting of nanocarriers for anti-cancer drug delivery. J Control Release. 2010;**148**(2):135-46

[3] Sutradhar KB, Amin L. Nanotechnology in Cancer Drug Delivery and Selective Targeting. ISRN Nanotechnology [Internet]. [cited February 10, 2017]; 2014 [12 p.]. Available from: https://www.hindawi.com/journals/isrn/2014/939378/

[4] Egusquiaguirre SP, Igartua M, Hernández RM, Pedraz JL. Nanoparticle delivery systems for cancer therapy: Advances in clinical and preclinical research. Clin Transl Oncol. 2012;**14**(2):83-93

[5] Haley B, Frenkel E. Nanoparticles for drug delivery in cancer treatment. Urol Oncol. 2008;**26**:57-64

[6] Shaji J, Lal M. Nanocarriers for targeting in inflammation. Asian J Pharm Clin Res. 2013;**6**(3):3-12

[7] Bertrand N, Wu J, Xu X, Kamaly N, Farokhzad OC. Cancer nanotechnology: The impact of passive and active targeting in the era of modern cancer biology. Adv Drug Deliver Rev. 2014;**66**:2-25

[8] Jain RK, Stylianopoulos T. Delivering nanomedicine to solid tumors. Nat Rev Clin Oncol. 2010;**7**(11):653-64

[9] Torchilin VP. Drug targeting. Eur J Pharm Sci. 2000;**11**(2):81-91

[10] Matsumura Y, Maeda H. A new concept for macromolecular therapeutics in cancer chemotherapy: mechanism of tumoritropic accumulation of proteins and the antitumor agent smancs. Cancer Res. 1986;**46**(12):6387-92

[11] Rabanel MJ. Aoun V, Elkin I, Mokhtar M, Hildgen P. Drug-loaded nanocarriers: passive targeting and crossing of biological barriers. Curr Med Chem. 2012;**19**(19):3070-102

[12] Deshpande PP, Biswas S, Torchilin VP. Current trends in the use of liposomes for tumor targeting. Nanomedicine. 2013;**8**(9):1509-28

[13] Gabizon AA. Stealth liposomes and tumor targeting: One step further in the quest for the magic bullet. Clin Cancer Res. 2001;**7**:223-5

[14] Torchilin VP. Targeted pharmaceutical nanocarriers for cancer therapy and imaging. AAPSJ. 2007;**9**(2):128-147

[15] Wang M, Thanou M. Targeting nanoparticles to cancer. Pharmacol Res. 2010;**62**(2):90-9

[16] Sawant RR, Torchilin VP. Challenges in development of targeted liposomal therapeutics. AAPSJ. 2012;**14**(2):303-15

[17] Cabral H, Matsumoto Y, Mizuno K, Chen Q, Murakami M, Kimura M, et al. Accumulation of sub-100 nm polymeric micelles in poorly permeable tumours depends on size. Nat Nanotechnol. 2011;**6**(12):815-23

[18] Immordino ML, Dosio F, Cattel L. Stealth liposomes: Review of the basic science, rationale, and clinical applications, existing and potential. Int J Nanomed. 2006;**1**(3):297-315

[19] He C, Hu Y, Yin L, Tang C, Yin C. Effects of particle size and surface charge on cellular uptake and biodistribution of polymeric nanoparticles. Biomaterials. 2010;**31**(13):3657-66

[20] Xiao K, Li Y, Luo J, Lee JS, Xiao W, Gonik AM et al. The effect of surface charge on in vivo biodistribution of PEG-oligocholic acid based micellar nanoparticles. Biomaterials. 2011;**32**(13):3435-46

[21] Laouini A, Jaafar-Maalej C, Limayem-Blouza I, Sfar S, Charcosset C, Fessi H. Preparation, characterization and applications of liposomes: state of the art. J Colloid Sci Biotechnol. 2012;**1**:147-68

[22] Gabizon AA. Liposome circulation time and tumor targeting: implications for cancer chemotherapy. Adv Drug Delivery Rev. 1995;**16**:285-94

[23] Nogueira E, Gomes AC, Preto A, Cavaco-Paulo A. Design of liposomal formulations for cell targeting. Colloid Surface B. 2015;**136**:514-26

[24] Kibria G, Hatakeyama H, Sato Y, Harashima H. Anti-tumor effect via passive anti-angiogenesis of PEGylated liposomes encapsulating doxorubicin in drug resistant tumors. Int J Pharm. 2016;**509**:178-87

[25] Cordeiro Pedrosa LR, van Tellingen O, Soullié T, Seynhaeve AL, Eggermont AMM, ten Hagen TLM et al. Plasma membrane targeting by short chain sphingolipids inserted in liposomes improves anti-tumor activity of mitoxantrone in an orthotopic breast carcinoma xenograft model. Eur J Pharma Biopharm. 2015;**94**:207-19

[26] Bertrand N, Wu J, Xu X, Kamaly N, Farokhzad OC. Cancer nanotechnology: The impact of passive and active targeting in the era of modern cancer biology. Adv Drug Deliv Rev. 2014;**66**:2-25

[27] Wang M, Thanou M. Targeting nanoparticles to cancer. Pharmacol Res. 2010;**62**(2):90-9

[28] Karra N, Benita S. The ligand nanoparticle conjugation approach for targeted cancer therapy. Curr Drug Metab. 2012;**13**(1):22-41

[29] Zwicke GL, Mansoori GA, Jeffery CJ. Utilizing the folate receptor for active targeting of cancer nanotherapeutics. Nano Rev. 2012;**3**:1-11

[30] Ye P, Zhang W, Yang T, Lu Y, Lu M, Gai Y, et al. Folate receptor-targeted liposomes enhanced the antitumor potency of imatinib through the combination of active targeting and molecular targeting. Int J Nanomedicine. 2014;**9**:2167-78

[31] Li L, An X, Yan X. Folate-polydiacetylene-liposome for tumor targeted drug delivery and fluorescent tracing. Colloids Surf B Biointerfaces. 2015;**134**:235-9

[32] Sriraman SK, Pan J, Sarisozen C, Luther E, Torchilin V. Enhanced cytotoxicity of folic acid-targeted liposomes co-loaded with C6 ceramide and doxorubicin: In vitro evaluation on HeLa, A2780-ADR, and H69-AR cells. Mol Pharm. 2016;**13**(2):428-37

[33] Xiong S, Yu B, Wu J, Li H, Lee RJ. Preparation, therapeutic efficacy and intratumoral localization of targeted daunorubicin liposomes conjugating folate-PEG-CHEMS. Biomed Pharmacother. 2011;**65**(1):2-8

[34] Zhang X, Wu W. Ligand-mediated active targeting for enhanced oral absorption. Drug Discov Today. 2014;**19**(7):898-904

[35] Luria-Pérez R, Helguera G, Rodríguez JA. Antibody-mediated targeting of the transferrin receptor in cancer cells. Bol Med Hosp Infant Mex. 2016;**73**(6):372-9

[36] Song X li, Liu S, Jiang Y, Gu L yan, Xiao Y, Wang X, et al. Targeting vincristine plus tetrandrine liposomes modified with DSPE-PEG2000-transferrin in treatment of brain glioma. Eur J Pharm Sci. 2017;**96**:129-40

[37] Lv Q, Li LM, Han M, Tang XJ, Yao JN, Ying XY, et al. Characteristics of sequential targeting of brain glioma for transferrin-modified cisplatin liposome. Int J Pharm. 2013;**444**(1-2):1-9

[38] Master AM, Sen Gupta A. EGF receptor-targeted nanocarriers for enhanced cancer treatment. Nanomedicine (Lond). 2012;**7**(12):1895-1906

[39] Mamot C, Drummond DC, Greiser U, Hong K, Kirpotin DB, Marks JD, et al. Epidermal growth factor receptor (EGFR)-targeted immunoliposomes mediate specific and efficient drug delivery to EGFR- and EGFRvIII-overexpressing. Cancer Res. 2003;**63**(12):3154-61

[40] Song S, Liu D, Peng J, Sun Y, Li Z, Gu JR, et al. Peptide ligand-mediated liposome distribution and targeting to EGFR expressing tumor in vivo. Int J Pharm. 2008;**363**(1-2):155-61

[41] Wicki A, Ritschard R, Loesch U, Deuster S, Rochlitz C, Mamot C. Large-scale manufacturing of GMP-compliant anti-EGFR targeted nanocarriers: Production of doxorubicin-loaded anti-EGFR-immunoliposomes for a first-in-man clinical trial. Int J Pharm. 2015;**484**(1-2):8-15

[42] Zalba S, Contreras AM, Haeri A, Ten Hagen TLM, Navarro I, Koning G, et al. Cetuximab-oxaliplatin-liposomes for epidermal growth factor receptor targeted chemotherapy of colorectal cancer. J Control Release. 2015;**210**:26-38

[43] Mitchell MJ, Chen CS, Ponmudi V, Hughes AD, King MR. E-selectin liposomal and nanotube-targeted delivery of doxorubicin to circulating tumor cells. J Control Release. 2012;**160**(3):609-17

[44] Arabi L, Badiee A, Mosaffa F, Jaafari MR. Targeting CD44 expressing cancer cells with anti-CD44 monoclonal antibody improves cellular uptake and antitumor efficacy of liposomal doxorubicin. J Control Release. 2015;**220**:275-86

[45] Dalla Pozza E, Lerda C, Costanzo C, Donadelli M, Dando I, Zoratti E, et al. Targeting gemcitabine containing liposomes to CD44 expressing pancreatic adenocarcinoma cells causes an increase in the antitumoral activity. Biochim Biophys Acta Biomembr. 2013;**1828**(5):1396-404

[46] Hayward SL, Wilson CL, Kidambi S. Hyaluronic acid-conjugated liposome nanoparticles for targeted delivery to CD44 overexpressing glioblastoma cells. Oncotarget. 2016;**7**(23):34158-71

[47] Alshaer W, Hillaireau H, Vergnaud J, Ismail S, Fattal E. Functionalizing liposomes with anti-CD44 aptamer for selective targeting of cancer cells. Bioconjug Chem. 2015;**26**(7):1307-13

[48] Shi C, Cao H, He W, Gao F, Liu Y, Yin L. Novel drug delivery liposomes targeted with a fully human anti-VEGF165 monoclonal antibody show superior antitumor efficacy in vivo. Biomed Pharmacother. 2015;**73**:48-57

[49] Guo Z, He B, Jin H, Zhang H, Dai W, Zhang L, et al. Targeting efficiency of RGD-modified nanocarriers with different ligand intervals in response to integrin $\alpha v\beta 3$ clustering. Biomaterials. 2014;**35**(23):6106-17

[50] Amin M, Badiee A, Jaafari MR. Improvement of pharmacokinetic and antitumor activity of PEGylated liposomal doxorubicin by targeting with N-methylated cyclic RGD peptide in mice bearing C-26 colon carcinomas. Int J Pharm. 2013;**458**(2):324-33

[51] Perche F, Torchilin VP. Recent trends in multifunctional liposomal nanocarriers for enhanced tumor targeting. J Drug Deliv [Internet]. 2013;**2013**:705265. Available from: http://www.pubmedcentral.nih.gov/articlerender.fcgi?artid=3606784&tool=pmcentrez&rendertype=abstract

[52] Graham SM, Carlisle R, Choi JJ, Stevenson M, Shah AR, Myers RS, et al. Inertial cavitation to non-invasively trigger and monitor intratumoral release of drug from intravenously delivered liposomes. J Control Release. 2014;**178**(1):101-7

[53] Ta T, Porter TM. Thermosensitive liposomes for localized delivery and triggered release of chemotherapy. J Control Release. 2013;**169**(1-2):112-25

[54] Luo D, Carter KA, Razi A, Geng J, Shao S, Giraldo D, et al. Doxorubicin encapsulated in stealth liposomes conferred with light-triggered drug release. Biomaterials. 2016;**75**:193-202

[55] Agarwal A, MacKey MA, El-Sayed MA, Bellamkonda R V. Remote triggered release of doxorubicin in tumors by synergistic application of thermosensitive liposomes and gold nanorods. ACS Nano. 2011;**5**(6):4919-26

[56] Amstad E, Kohlbrecher J, Müller E, Schweizer T, Textor M, Reimhult E. Triggered release from liposomes through magnetic actuation of iron oxide nanoparticle containing membranes. Nano Lett. 2011;**11**(4):1664-70

[57] Karanth H, Murthy RSR. pH-sensitive liposomes--principle and application in cancer therapy. J Pharm Pharmacol. 2007;**59**(4):469-83

[58] Yuba E, Tajima N, Yoshizaki Y, Harada A, Hayashi H, Kono K. Dextran derivative-based pH-sensitive liposomes for cancer immunotherapy. Biomaterials. 2014;**35**(9):3091-101

[59] Bozzuto G, Molinari A. Liposomes as nanomedical devices. International Journal of Nanomedicine. 2015. p. 975-99

[60] Thanou M, Gedroyc W. MRI-guided focused ultrasound as a new method of drug delivery. J Drug Deliv [Internet]. 2013;**2013**:616197. Available from: https://www.hindawi.com/journals/jdd/2013/616197/

[61] Mura S, Nicolas J, Couvreur P. Stimuli-responsive nanocarriers for drug delivery. Nat Mater. 2013;**12**(11):991-1003

[62] Tagami T, Ando Y, Ozeki T. Fabrication of liposomal doxorubicin exhibiting ultrasensitivity against phospholipase A2 for efficient pulmonary drug delivery to lung cancers. Int J Pharm. DOI: 10.1016/j.ijpharm.2016.11.039

[63] Itakura S, Hama S, Ohgita T, Kogure K. Development of nanoparticles incorporating a novel liposomal membrane destabilization peptide for efficient release of cargos into cancer cells. PLoS One. 2014;**9**(10):e111181

[64] Carter K, Shao S, Hoopes MI, Luo D, Ahsan B, Grigoryants VM, et al. Porphyrin-phospholipid liposomes permeabilized by near-infrared light. Nat Commun. 2014; **5**:3546

[65] Luo D, Li N, Carter KA, Lin C, Geng J, Shao S, et al. Rapid light-triggered drug release in liposomes containing small amounts of unsaturated and porphyrin–phospholipids. Small. 2016;**12**:3039-3047

[66] Schroeder A, Kost J, Barenholz Y. Ultrasound, liposomes, and drug delivery: principles for using ultrasound to control the release of drugs from liposomes. Chem Phys Lipids 2009;**162**(1-2):1-16

[67] Arias JL. Drug targeting strategies in cancer treatment: an overview. Mini-Reviews Med Chem. 2011;**11**:1-17

[68] Lin CY, Javadi M, Belnap DM, Barrow JR, Pitt WG. Ultrasound sensitive eLiposomes containing doxorubicin for drug targeting therapy. Nanomed Nanotechnol Biol Med. 2014;**10**(1):67-76

[69] Hardiansyah A, Huang L-Y, Yang M-C, Liu T-Y, Tsai S-C, Yang C-Y, et al. Magnetic liposomes for colorectal cancer cells therapy by high-frequency magnetic field treatment. Nanoscale Res Lett. 2014;**9**(1):497

[70] Torchilin V. Multifunctional and stimuli-sensitive pharmaceutical nanocarriers. Eur J Pharm Biopharm. 2009;**71**:431-44

[71] Tang Y, Soroush F, Tong Z, Kiani MF, Wang B. Targeted multidrug delivery system to overcome chemoresistance in breast cancer. Int J Nanomedicine. 2017;**12**:671-81

[72] Xue-tao L, Wei T, Ying J, Xiao-min W, Yan-hong W, Lan C, et al. Multifunctional targeting vinorebline plus tetrandrine liposome's for treating brain glioma along with eliminating glioma stem cells. Oncotarget. 2016;**7**(17):24604-22

[73] Ying M, Shen Q, Liu Y, Yan Z, Wei X, Zhan C, et al. Stabilized heptapeptide A7R for enhanced multifunctional liposome-based tumor-targeted drug delivery. ACS Applied Materials and Interfaces. DOI:10.1021/acsami.6b01300

[74] Ying M, Shen Q, Zhan C, Wei X, Gao J, Xie C, et al. A stabilized peptide ligand for multifunctional glioma targeted drug delivery. J Control Release. 2016;**243**:86-98

[75] Ganta S, Devalapally H, Shahiwala A, Amiji M. A review of stimuli-responsive nanocarriers for drug and gene delivery. J Control Release. 2008;**126**:187-204

[76] Haeri A, Zalba S, ten Hagen TLM, Dadashzadeh S, Koning GA. EGFR targeted thermosensitive liposomes: A novel multifunctional platform for simultaneous tumor targeted and stimulus responsive drug delivery. Colloids Surf B Biointerfaces. 2016;**146**:657-69

[77] Kono K, Takashima M, Yuba E, Harada A, Hiramatsu Y, Kitagawa H, et al. Multifunctional liposomes having target specificity, temperature-triggered release, and near-infrared fluorescence imaging for tumor-specific chemotherapy. J Control Release. 2015;**216**:69-77

[78] Koren E, Torchilin VP. Cell-penetrating peptides: breaking through to the other side. Trends Mol Med. 2012;**18**:385-93

[79] Koren E, Apte A, Jani A, Torchilin VP. Multifunctional PEGylated 2C5-immunoliposomes containing pH-sensitive bonds and TAT peptide for enhanced tumor cell internalization and cytotoxicity. J Control Release. 2012;**160**:264-73

[80] Apte A, Koren E, Koshkaryev A, Torchilin VP. Doxorubicin in TAT peptide-modified multifunctional immunoliposomes demonstrates increased activity against both drug-sensitive and drug-resistant ovarian cancer models. Cancer Biol Ther. 2014;**15**(1):69-80

[81] Fu H, Shi K, Hu G, Yang Y, Kuang Q, Lu L, et al. Tumor-targeted paclitaxel delivery and enhanced penetration using TAT-decorated liposomes comprising redox-responsive poly(ethylene glycol). J Pharm Sci. 2015;**104**(3):1160-73

[82] Jiang L, Li L, He X, Yi Q, He B, Cao J, et al. Overcoming drug-resistant lung cancer by paclitaxel loaded dual-functional liposomes with mitochondria targeting and pH-response. Biomaterials. 2015;**52**(1):126-39

[83] Allen TM, Cullis PR. Liposomal drug delivery systems: From concept to clinical applications. Adv Drug Deliv Rev. 2013;**65**:36-48

[84] Chang H-I, Yeh M-K. Clinical development of liposome-based drugs: formulation, characterization, and therapeutic efficacy. Int J Nanomedicine. 2012;**7**:49-60

[85] de Jonge MJA, Slingerland M, Loos WJ, Wiemer EAC, Burger H, Mathijssen RHJ, et al. Early cessation of the clinical development of LiPlaCis, a liposomal cisplatin formulation. Eur J Cancer. 2010;**46**:3016-21

[86] Wicki A, Witzigmann D, Balasubramanian V, Huwyler J. Nanomedicine in cancer therapy: Challenges, opportunities, and clinical applications. J Control Release. 2015;**200**:138-57

[87] A service of the U.S. National Institutes of Health. Accessed 10 Feb 2017. https://clinicaltrials.gov/

[88] Fan Y, Zhang Q. Development of liposomal formulations: From concept to clinical investigations. AJPS. 2013;**8**:81-87

[89] Tejada-Berges T, Granai CO, Gordinier M, Gajewski W. Caelyx/Doxil for the treatment of metastatic ovarian and breast cancer. Expert Rev Anticancer Ther. 2002;**2**(2):143-50

[90] Zylberberg C, Matosevic S. Pharmaceutical liposomal drug delivery: a review of new delivery systems and a look at the regulatory landscape. Drug Deliv. 2016;**23**(9):3319-29

[91] Allen TM, Cullis PR. Liposomal drug delivery systems: From concept to clinical applications. Adv Drug Deliv Rev. 2013;**65**:36-48

[92] Hamada A, KawaguchiT, Nakano M. Clinical pharmacokinetics of cytarabine formulations. Clin Pharmacokinet. 2002;**41**(10):705-18

[93] Riggio C, Pagni E, Raffa V, Cuschieri A. Nano-oncology: clinical application for cancer therapy and future perspectives. J Nanomater [online]. 2011 [cited February 16, 2017];**2011**:164506 [10 p.]. Available from: https://www.hindawi.com/journals/jnm/2011/164506/

[94] Mebiopharm Co., Ltd. Study of MBP-426 in Patients With Second Line Gastric, Gastroesophageal, or Esophageal Adenocarcinoma. Accessed 10 Feb 2017. https://www.clinicaltrials.gov/ct2/show/NCT00964080?term=mbp+426&rank=1

[95] Mebiopharm Co., Ltd. Safety Study of MMBP-426 (Liposomal Oxaliplatin Suspension for Injection) to Treat Advanced or Metastatic Solid Tumors. Accessed 10 Feb 2017. https://www.clinicaltrials.gov/ct2/show/NCT00355888?term=mbp+426&rank=2

[96] Wang X, Lu W. Active targeting liposomes: promising approach for tumor-targeted therapy. J Bioequiv Availab. 2016;**8**(8):13-14

[97] University Hospital, Basel, Switzerland. Anti-EGFR Immunoliposomes in Solid Tumors. Accessed 10 Feb 2017. https://clinicaltrials.gov/ct2/show/NCT01702129

[98] Matsumura Y, Gotoh M, Muro K, Yamada Y, Shirao K, Shimada Y, et al. Phase I and pharmacokinetic study of MCC-465, a doxorubicin (DXR) encapsulated in PEG immunoliposome, in patients with metastatic stomach cancer. Ann Oncol. 2004;**15**(3):517-25

[99] Otilia Dalesio, The Netherlands Cancer Institute. Clinical and Pharmacological Study With 2B3-101 in Patients With Breast Cancer and Leptomeningeal Metastases. Accessed 10 Feb 2017. https://clinicaltrials.gov/ct2/show/NCT01818713?term=2B3-101&rank=1

Chapter 10

Methotrexate Liposomes - A Reliable Therapeutic Option

Anne Marie Ciobanu, Maria Bârcă, Gina Manda,
George Traian Alexandru Burcea Dragomiroiu and
Daniela Luiza Baconi

Additional information is available at the end of the chapter

http://dx.doi.org/10.5772/intechopen.68520

Abstract

Liposomes were proposed as drug vector systems in the treatment of many diseases. The following characteristics recommend the liposomes as attractive candidates for drug transportation: solubilisation, duration of action, targeting potential and internalisation. Methotrexate, a folate antagonist, was originally developed as an antineoplastic agent and subsequently used in inflammatory and/or immunosuppressive diseases. Its side effects have led researchers to direct their efforts to reduce toxicity, while maintaining efficacy of methotrexate. Liposomes with methotrexate as such, as well as its disodium salt, were prepared using two methods. The liposomes were characterized in terms of structure, size, degree of poly-dispersion and encapsulation efficiency. The effect of methotrexate incorporated in liposomes has been investigated *in vitro* on human lymphoblastic cell line K562. Methotrexate incorporated into liposomes moderately reduces the proliferation of K562 cells, but significantly inhibits RNA synthesis. The cellular activation is probably the main target of the drug and not the neoplastic proliferation of cells. The methotrexate liposomes exhibited significant anti-inflammatory activity and showed reduced toxicity. Given that the encapsulating of the drug in vector systems may result in the increasing concentration at the site of action, the methotrexate liposomes represent a targeted therapy with an optimized therapeutic efficacy—risk toxicity ratio.

Keywords: liposomes, methotrexate, rheumatoid arthritis

1. Introduction

Liposomes have been proposed as drug vector systems in the treatment of many diseases. Among the drugs proposed to be encapsulated in liposomes, remarkable are

drugs used in anti-fungal therapy (amphotericin B, nystatin, econazole), in anticancer therapy (doxorubicine, daunorubicin, methotrexate (MTX), cytarabine, vincristine, paclitaxel, mitoxantrone), in the treatment of asthma (albuterol) and in the treatment of some inflammatory diseases (clodronate, methotrexate, lactoferrin), in anti-viral therapy (e.g. for the induction of interferon production), as well as for radio diagnostic purpose (indium-111) [1–9].

The following characteristics recommend the liposomes as attractive candidates for the drug transportation: solubilisation (the liposomes can solubilize lipophilic drugs that would be difficult to administer intravenously), duration of action (the liposomes function as a microreservoir which gradually release the drug into the body), targeting potential (by coupling of some ligands on the liposomes surface, it can direct a drug to a specific target) and internalisation (the liposomes interact with the target cell and may be able to promote intracellular transport of some molecules).

Because they are usually prepared from lipids of natural origin, biodegradable and nontoxic, liposomes are useful as drug vector systems that can reduce systemic toxicity [10]. Side effects associated with anti-tumour drugs administered in conventional dosage forms can be reduced by encapsulating them in liposomes. Therefore, the encapsulation of medicines in liposomes is a tool to increase the therapeutic index by reducing the drug toxicity and targeting the specific cells [11].

Although liposomes were first described by Alec D Bangham in 1965, the first liposomal drug product was approved by the Food and Drug Administration (FDA) in 1995 and contains the anticancer drug doxorubicin (Doxil®, doxorubicin hydrochloride liposome injection) [12]. Currently, several liposome-based drugs containing antifungal drugs (amphotericin B, Ambisome®, Abelcet®, Amphotec®), anticancer drugs (daunorubicine, Daunoxome®; doxorubicine, Doxil®, Lipo-dox®, Myocet®; cytarabine, Depocyt®) and photosensitizer for photodynamic therapy (verteporfin, Visudyne®) are approved for clinical use, mainly for intravenous administration [13].

Methotrexate, a folate antagonist, was originally developed as an antineoplastic agent and subsequently used in inflammatory and/or immunosuppressive diseases [14]. Among the cytotoxic agents, methotrexate has been widely used as an immunosuppressant in autoimmune diseases [15]. In 1951, the proposal for the use of methotrexate in the treatment of rheumatoid arthritis was based on its inhibitory effect on the proliferation of lymphocytes and other cells responsible for inflammation of the joint [16]. However, by 1980 there have not been reported and published any clinical studies regarding the use of methotrexate in rheumatoid arthritis. MTX is currently accepted as the most effective and well-tolerated disease-modifying antirheumatic drug (DMARD) for rheumatoid arthritis [17, 18] with certain effects of slowing the progression of the disease and reducing mortality rate [19]. The broad spectrum of side effects and the relatively high frequency of them have led researchers to direct their efforts to reduce toxicity, while maintaining at the same time the therapeutic efficacy of methotrexate. In this regard, both alternative routes of administration (especially in the treatment of inflammatory

http://dx.doi.org/10.5772/intechopen.68520

diseases) and new pharmaceutical formulations with methotrexate were investigated. It has been suggested that the anticancer drugs formulated in liposomes would be the long-awaited 'magic pill' for cancer therapy, due to their ability to selectively accumulate in tumours; at the same time, toxicological studies indicate that encapsulation in liposomes provides protection against the majority of the adverse effects of chemotherapy drugs. On the other hand, liposomes were shown to give an effective and appropriate delivery of anti-rheumatoid drugs to the synovial fluid [20].

Liposomes with methotrexate as such (further named 'hydrophobic methotrexate' liposomes), as well as its disodium salt (further named 'hydrosoluble methotrexate' liposomes), were prepared using two methods: the lipid film hydration method and reverse-phase evaporation method (REV). The liposomes were characterized in terms of structure, size, and degree of poly-dispersion and encapsulation efficiency. Methotrexate incorporation into liposomes has been achieved by passive loading method which encapsulates the active compound during liposome formation or in a stage of preparation when the liposomal structure is very fluid.

The effect of methotrexate incorporated in liposomes has been investigated *in vitro* on human lymphoblastic cell line K562.

The effects of short-term therapy with methotrexate incorporated into the liposomes have also been demonstrated in an *animal model of rheumatoid arthritis*.

2. Preparation of methotrexate liposomes

Liposomes are phospholipid vesicles made up of one or more concentric phospholipid bilayers alternating with layers of aqueous. Phospholipids are a very attractive transport way of drugs and other molecules not only because they are able to form lamellar phases but also because they are natural components of cell membranes having low allergenic potential; they can be metabolized in a manner similar to the endogenous phospholipid membrane and have the advantage of structural variability which can be used to modify the physical properties of liposomes so as to increase selectivity for target organ.

Liposomal properties depend on both the choice of phospholipids and the addition of sterols, particularly cholesterol, and glycolipids [21].

Over time, the size, number of lamellae and the characteristics of the lipid bilayer were handled depending on the purpose of the liposome. Thus, conventional liposomes, sterically stabilized liposomes ('stealth' liposomes), cationic liposomes or targeted liposomes (by coupling ligands to the surface) have been developed. Sterically stabilized liposomes, undetectable ('stealth'), contain lipid derivatives of a polymer (polyethylene glycol, PEG) inserted into the lipid bilayer, which gives them the advantage of the enhanced circulation times.

Conventional liposomes and sterically stabilized liposomes with the following compositions were prepared:

1. Phosphatidylcholine (PC)
2. Phosphatidylcholine:cholesterol (PC:CH)
3. Phosphatidylcholine:cholesterol:polyethylene glycol-2000-phosphatidylethanolamine (PC:CH:PEG2000-PE).

Liposomes are used to encapsulate both hydrophobic and hydrosoluble drugs within the bilayer and the aqueous core, respectively. Consequently, both methotrexate as such (hydrophobic methotrexate liposomes) and its disodium salt (hydrosoluble methotrexate liposomes) were encapsulates in liposomes. Methotrexate incorporation into liposomes has been achieved by passive loading method which encapsulates the active compound during liposome formation or in a preparation stage when the liposomal structure is very fluid [22].

The following weight ratios between the lipid phase and the active substance methotrexate were used: PC:MTX 10:1; PC:CH:MTX 10:2:1 and PC:CH:MTX 10:1:1 for conventional liposomes and PC:CH:MTX:PEG2000 10:1:1:1 for sterically stabilized liposomes [23].

Also, 'control liposomes' (or empty liposomes, or liposomes unloaded with methotrexate) were prepared using the following compositions: PC or PC:CH (10:1 and 10:2) for conventional liposomes and PC:CH:PEG2000-PE (10:1:1) for sterically stabilized liposomes. In order to track the cellular internalisation, we prepared the 'control liposomes' sterically stabilized with the composition PC:PGPH (polyglycerol 12-hydroxystearic acid ester) (10:1).

Two methods of preparation were used: the lipid film hydration method [24] and reverse-phase evaporation method [25–27].

2.1. Lipid film hydration method

The mechanism of liposome formation by lipid film hydration method, combined with extrusion, consists of the following sequence of steps: initially, thin lipid film is hydrated and lipid layers become fluid, then, hydrated lipid lamellae are detached and self-closed, to form large multilamellar vesicles. In order to reduce the size, extrusion of the liposomes is performed, which determines the conversion of multilamellar liposomes in unilamellar liposomes.

The lipid film hydration method was used for the preparation of liposomes with hydrophobic methotrexate. Soybean lecithin and cholesterol were dissolved in chloroform-methanol (2:1, v/v), then the active substance is added and stirred to mix. The organic solution is then subjected to evaporation under reduced pressure in the rotary evaporator to remove the organic solvent. Thin lipid film displayed on the wall's balloon is hydrated by adding pH 7.4 phosphate buffer. The resulting dispersion is kept at rest for 48 h.

http://dx.doi.org/10.5772/intechopen.68520

2.2. Reverse-phase evaporation method

Reverse-phase evaporation method allows to obtain large unilamellar liposomes (or large unilamellar vesicles, LUV), with a significant aqueous compartment. In this process, phospholipids are dissolved in an organic solvent or in a mixture of organic solvents. Then, the aqueous phase is added to the organic phase. At this stage, phospholipids are placed at the interface between two immiscible phases. A W/O emulsion is formed by ultra-sonication or magnetic stirring. The success of emulsification is a fundamental condition to obtain unilamellar liposomes with high encapsulation capacity. The removal of the solvent by evaporation leads to the closeness of the micelles and, consequently, to the formation of a gel emulsion. During this step, the micelles are forming monolayers surrounding aqueous compartments and aggregate to form a compact gelled network. During the next stage, the pressure is reduced to promote the complete evaporation of the organic solvent, at which the destructuration of the gel occurs and the monolayers are getting closer to form liposomal bilayers. This process can be accelerated by shaking the solution using a vortex.

For the preparation of hydrophobic methotrexate liposomes, soya lecithin and cholesterol or PEG2000-PE were dissolved in chloroform-methanol (2:1, v/v), then the active substance is added and stirred to mix. Equal volumes of the organic solution and phosphate buffer solution pH 6 were mixed under magnetic stirring until a W/O emulsion was obtained. Organic solvents were then evaporated to obtain a gel emulsion. After the destructuring of the gel, pH 6 phosphate buffer was added and stirring was continued until the liposomal dispersion is formed.

For the preparation of hydrosoluble methotrexate liposomes, soya lecithin and cholesterol or PEG2000-PE were dissolved in chloroform-methanol (2:1, v/v), and equal volumes of the organic solution and sodium salt of methotrexate were mixed under magnetic stirring until a W/O emulsion was obtained. Organic solvents were then evaporated to obtain a gel emulsion. After the destructuring of the gel, pH 7.4 phosphate buffer was added and stirring was continued until the liposomal dispersion is formed.

2.3. Reducing the size of liposomes and increasing the uniformity of their size by extrusion

Since the formed liposomes are heterogeneous in size, a uniform dispersion is obtained by extrusion. For particle size reduction, liposome dispersions were passed 10 times through a polycarbonate membrane (Whatman Nucleopore® Tch Track Membrane-E) with a pore diameter of 3 μm and then through a membrane with a pore diameter of 100 nm. The pre-filtration through a filter membrane with larger pores (3 μm) is necessary to prevent clogging of the membrane. In the case of sterically stabilized liposomes, as they have been used in studies *in vivo*, extrusion was carried out through a polycarbonate membrane with a 100-nm pore size.

3. Characterization of methotrexate liposomes

The liposomes were characterized in terms of structure, shape, size and degree of poly-dispersion and methotrexate encapsulation efficiency.

Characterisation of the obtained liposomes was pursued as follows:

- The visualisation and the determination of the type of liposomes using enhanced video microscopy (VEM) and transmission electron microscopy (TEM);
- The determination of the size and size distribution of liposomes by dynamic light-scattering technique (DLS);
- The determination of the encapsulation rate and the determination of the content of active substance in liposomes.

In addition to the general methods for liposomes characterisation, intracellular liposomes transport was studied by fluorescence microscopy, and quantification of cell internalisation of 'control liposomes' was studied by fluorimetric technique.

3.1. The visualisation and the type of liposomes

Microscopy is a method for observing liposomal dispersion and determining the shape and the size of liposomes. The ability of this method to directly visualize colloidal structures in real time allows to observe dynamic changes in the number and size of the vesicles and also offers the possibility of discovering new structures.

Examination by enhanced video microscopy showed in particular the shape, size and state of dispersion, but no information on liposome structure was obtained using this technique.

VEM images of methotrexate hydrophobic liposomes prepared by the two methods, the hydration of the lipid film and reverse-phase evaporation, are shown in **Figures 1** and **2**.

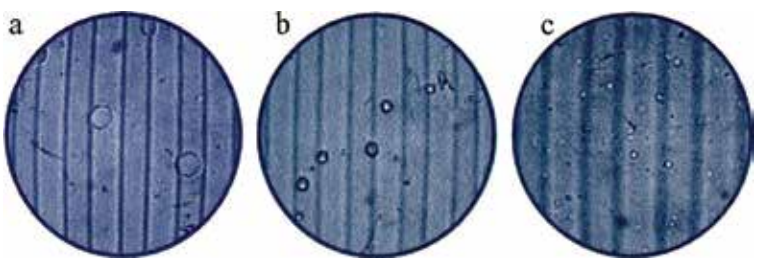

Figure 1. VEM images of hydrophobic MTX liposomes prepared by the method of hydration of the lipid film: PC:MTX = 10:1 (a), PC:CH:MTX = 10:1:1 (b), PC:CH:MTX = 10:2:1 (c).

Hydrophobic methotrexate liposomes prepared by both methods were unilamellar and polydisperse. The presence of cholesterol leads to a decrease of the average diameter of the liposomes. The ratio PC:CH influences the size of liposomes.

Hydrosoluble methotrexate liposomes were prepared only by the reverse-phase evaporation method due to higher encapsulation of methotrexate. In this case, the same change in size of the liposomes in the presence of cholesterol was observed (**Figure 3**).

Variation of liposomes size depending on the lipid layer composition can be explained by the fact that, at the working pH, the phosphatidylcholine polar groups are charged with negative electric charges, which cause electrostatic repulsion between them with the formation of large vesicles; cholesterol, due to its amphiphilic properties, is inserted between phosphatidylcholine molecules shielding the electrostatic repulsion between the polar groups and thereby increase the radius of curvature of the bilayer.

Considering under micron size of the obtained vesicles, transmission electron microscopy was also used. The suspension of liposomes was analysed using the negative staining electron

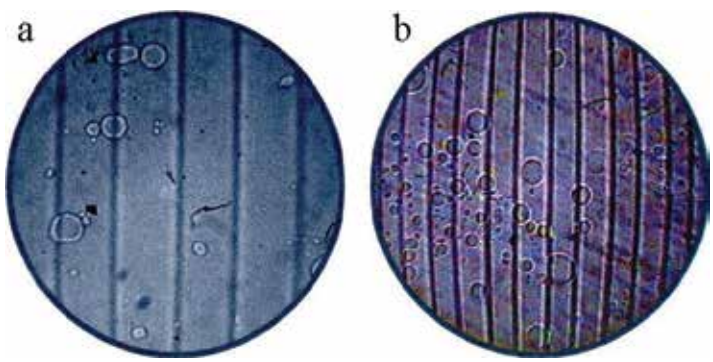

Figure 2. VEM images of hydrophobic MTX liposomes prepared by reverse-phase evaporation method: PC:MTX = 10:1 (a), PC:CH:MTX = 10:1:1 (b).

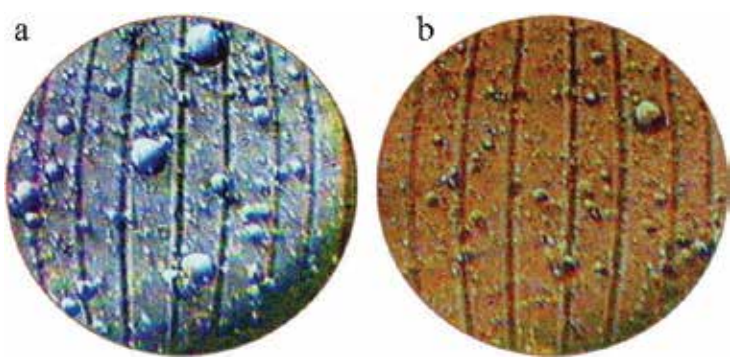

Figure 3. VEM images of hydrosoluble MTX liposomes prepared by reverse-phase evaporation method: PC:MTX = 10:1 (a), PC:CH:MTX = 10:1:1 (b).

microscopy with 1% phosphotungstic acid. Liposomal dispersions with methotrexate (PC:CH:MTX = 10:1:1) were stored at a temperature of 3–5°C and monitored for 3 days (after 48 h, **Figure 4a**, and after 72 h, **Figure 4b**). After 72 h of preparation, TEM images showed a reversible coagulation process, unaccompanied by the membrane destruction. This process is similar to emulsion-clotting process which does not cause the emulsion destruction. The presence of electrical charges on the surface of liposomes explains their electrostatic stabilisation.

The encapsulation of hydrosoluble methotrexate in the internal aqueous liposomal medium results in larger liposomes than those obtained in the absence of MTX (**Figure 5**).

The same effect was observed for liposomes loaded with hydrophobic MTX prepared using pH = 7.4 buffer (**Figure 6**) due to the solubilisation in the aqueous phase of a part of MTX initially encapsulated in liposome membrane. Increasing the size of the liposomes in the presence of methotrexate can be explained also by the osmotic pressure. Due to the hydrophobicity of the lipid bilayer and taking into account that at pH 7.4, both PC and MTX are charged with electrical charges of the same sign, methotrexate diffusion through liposomal membrane is prevented. The pressure difference on both sides of the liposomal membrane occurs due to the difference in the concentration of methotrexate in the inner aqueous phase and in the dispersion medium.

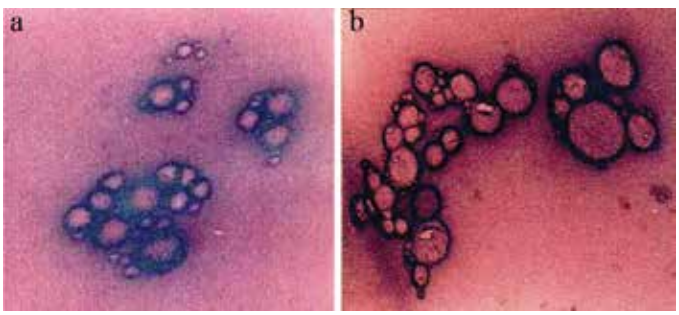

Figure 4. TEM images of the hydrosoluble MTX liposomes, 48 h (a) and 72 h (b) after preparation.

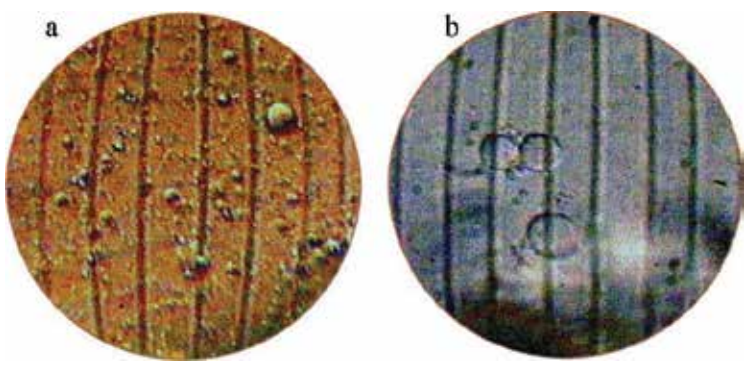

Figure 5. VEM images of 'control liposomes' (PC:CH) (a) and hydrosoluble MTX liposomes (PC:CH:MTX) (b).

In order to reduce the solubilisation of hydrophobic methotrexate in the aqueous medium at pH 7.4, and to increase the efficiency of encapsulation, hydrophobic methotrexate liposomes were prepared by reverse-phase evaporation method, using a pH 6 buffer solution as a dispersion medium. TEM images of the liposomes prepared as such are shown in **Figure 7**.

The results of microscopic examination suggested that the presence of methotrexate in the liposome membrane does not affect the size of the liposomes. It would be expected that the presence of methotrexate in bilayer increases the size of the liposomes. The molecules of organic acids with odd number of carbon atoms are not flat, but have a twisted structure and are not centre-symmetrical, but have a binary axis of symmetry. Carboxyl groups are inclined at an angle of 60° relative to each other and 30° to the plane of zigzag chain of carbon atoms [28]. Given this structure of methotrexate, inserting it between molecules PC would have been expected to result in an increase of lecithin vesicle size.

The methotrexate molecule is not placed between the lecithin molecules due to its pronounced hydrophobic character but it is encapsulated in the hydrophobic region of the bilayer leading

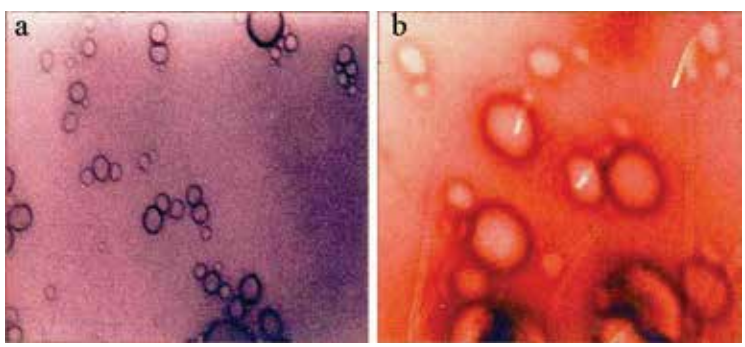

Figure 6. TEM images of 'control liposomes' (PC) (a) and hydrophobic MTX liposomes prepared with pH 7.4 buffer (PC:MTX) (b).

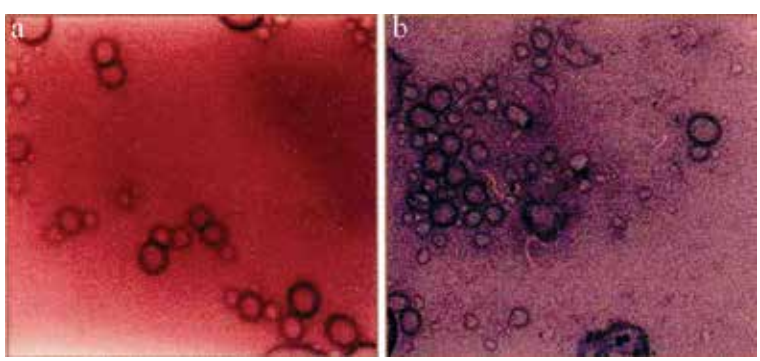

Figure 7. TEM images of 'control liposomes' (PC) (a) and hydrophobic MTX liposomes prepared with pH 6 buffer (PC:MTX) (b).

eventually to an increase in the thickness of the bilayer made, but not in an increase of liposomes size.

In order to reduce the liposomes size and to increase the uniformity of their size, liposomal poly-dispersion was extruded by passing them through polycarbonate membranes with different pore diameters: first membrane with a pore diameter of 3 μm, then a membrane with a pore diameter of 100 nm in the case of sterically stabilized liposomes. Liposomes were extruded to increase their stability and in order to decrease the size under the diameter of capillaries for intravenous administration. Examples of TEM images of the MTX liposomes before and after extrusion are shown in **Figures 8**.

3.2. The determination of the size and size distribution of liposomes

To determine the size and size distribution of the liposomes, dynamic light-scattering technique was used. This technique can be applied to systems in which the average diameter is less than 1 μm. The advantage of the DLS to electron microscopy is that information can be obtained quickly (minutes) and is less expensive. To determine the size distribution of the liposomes by this method, a NICOMP 270 DLS Submicron Particle Sizer (Pacific Scientific® Hiac/Royoco Instruments Division) was used.

The decrease in liposomes diameter when the cholesterol was added in the lipid phase observed by microscopic techniques was confirmed by the results of the DSL determinations. A decrease of approximately 50% in the mean diameter of liposomes was observed for PC:CH formula, from 2502.6 to 1450.2 nm.

The increase of liposomes size after hydrosoluble methotrexate encapsulation observed by VEM and TEM techniques (**Figure 5**) is supported by the DLS results (**Figure 9**). It is noted that the average diameter of the PC:CH:MTX liposomes (4893.2 nm) is superior to that obtained for PC:CH liposomal dispersion (2502.6 nm).

3.3. The determination of the encapsulation rate

Methotrexate liposome encapsulation efficiency was estimated by the determination of loading yield. Load yield is the ratio of the amount of active substance encapsulated in

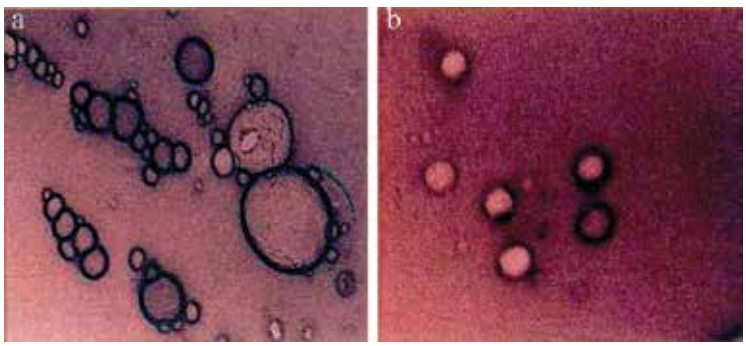

Figure 8. TEM images of PC:CH:MTX liposomes before (a) and after (b) extrusion.

http://dx.doi.org/10.5772/intechopen.68520

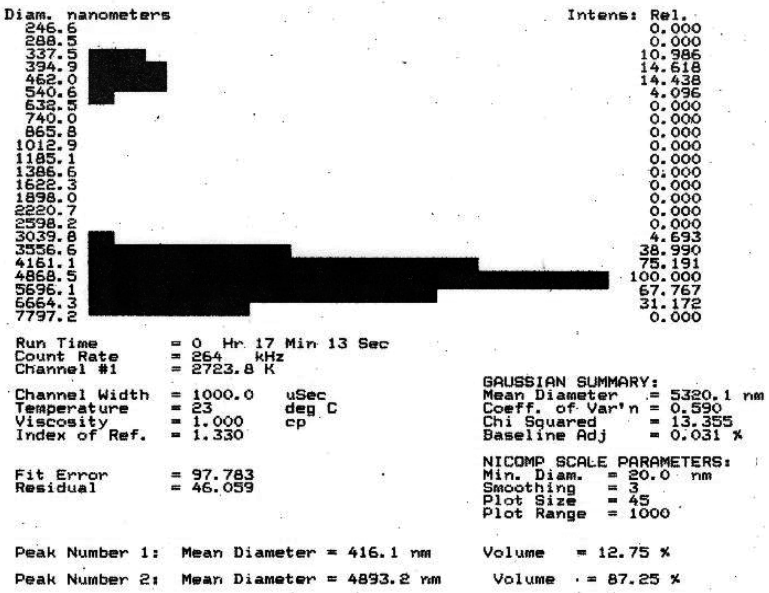

Figure 9. Histogram of PC:CH:hydrosoluble MTX liposomal dispersion.

liposomes and the initial amount of active substance and is calculated using the following formula:

$$R_i = \frac{C_f}{C_0} \times 100 \quad (1)$$

where C_f is the concentration of active substance in the liposome dispersion after the removal of unloaded active substance, and C_0 is the concentration of active substance in the lipid mixture used for liposomes preparation.

In order to determine the concentration of active substance in the liposome dispersion (C_f), the removal of the unloaded active substance was done by dialysis for hydrosoluble methotrexate liposomes and by Sephadex gel filtration for hydrophobic methotrexate liposomes.

The dialysis process was monitored by the UV spectrophotometric determination of the methotrexate in dialysate ('washing water') in order to confirm that all the unloaded methotrexates were removed (**Figure 10**).

After the removal of unloaded active substance, the liposomal dispersion was subjected to lysis with Triton X-100 and methotrexate was quantified by high-performance liquid chromatography (HPLC).

The efficiency of methotrexate encapsulation, measured by loading yield, was similar for hydrosoluble methotrexate liposomes and hydrophobic methotrexate liposomes. However, in the case of hydrophobic methotrexate liposomes slightly higher loading yields were obtained when cholesterol is added in the lipid layer.

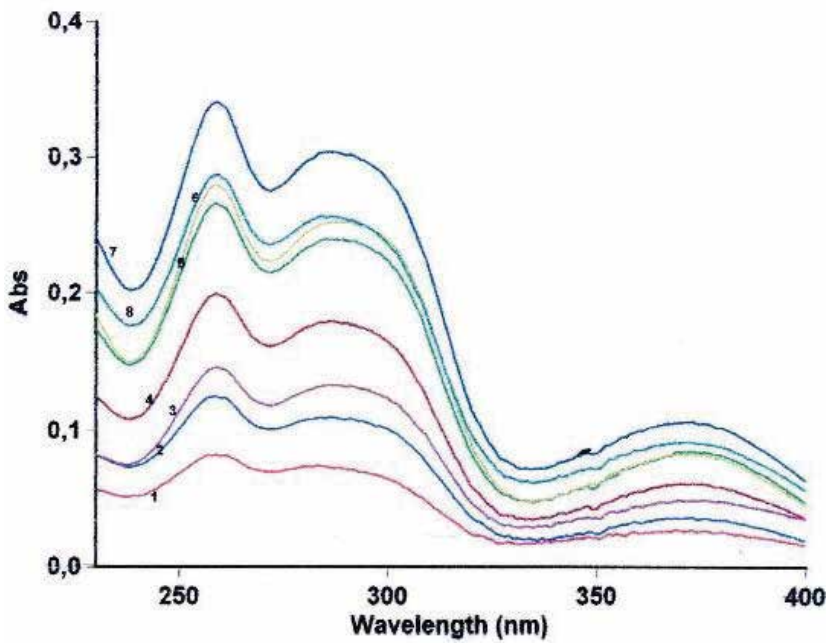

Figure 10. UV-spectrum of methotrexate in dialysate ('washing water').

The electric charge of liposomes is a predictive factor of their lifecycle. Preliminary studies performed on liposomes showed that the presence of lipids with negative electric charge leads to a reduced elimination of the encapsulated substance. The low permeability for hydrosoluble methotrexate of the anionic liposomal membrane explains the high encapsulation efficiency obtained. At the same time, the presence of structures with a large interfacial area per volume unit (cubosomes and hexasomes) in the colloidal dispersions obtained using REV causes a higher encapsulation of hydrophobic substances.

3.4. The determination of content of active substance in liposomes

For the quantitative determination of methotrexate, the liposomal dispersion was subject to ultracentrifugation and the active substance was determined by HPLC after the liposomes lysis with Triton X100. Chromatographic conditions were as follows: HPLC Millenium Waters, Spherisorb 5 ODS 250 × 4.6 mm column, mobile phase 5% tetrahydrofuran in 0.05 M sodium dihydrogen orthophosphate buffer (pH 4.85), flow rate 1.0 mL/min, 20 μL injected volume, UV detection at 313 nm. The concentration of methotrexate in the liposomal dispersion was calculated based on the methotrexate peak area and the obtained calibration curve. The selectivity of the method for the determination of methotrexate in liposomes was demonstrated by analysis of MTX-unloaded liposomes ('control liposomes'). The lipids contained in the liposome membrane do not interfere with methotrexate.

The average methotrexate concentration measured was 196 mg/mL for water-soluble methotrexate liposomes (**Figure 11**) and 200 mg/mL for hydrophobic methotrexate liposomes (**Figure 12**).

3.5. Intracellular transport of liposomes studies

Studies of the interaction between liposomes and cells are of particular importance in order to develop liposomes as vectors with high efficiency for delivering drugs to cells. Therefore, the development of liposomal systems as drug carriers requires detailed understanding of interaction mechanisms between cells and these transporters. Some studies have indicated that the *in vitro* uptake of the liposomes depends on the cell type [29, 30], but the factors that are involved in this uptake are not fully understood. In general, it is believed that the uptake of the liposomes is mediated by nonspecific adsorption to the cell surface [31].

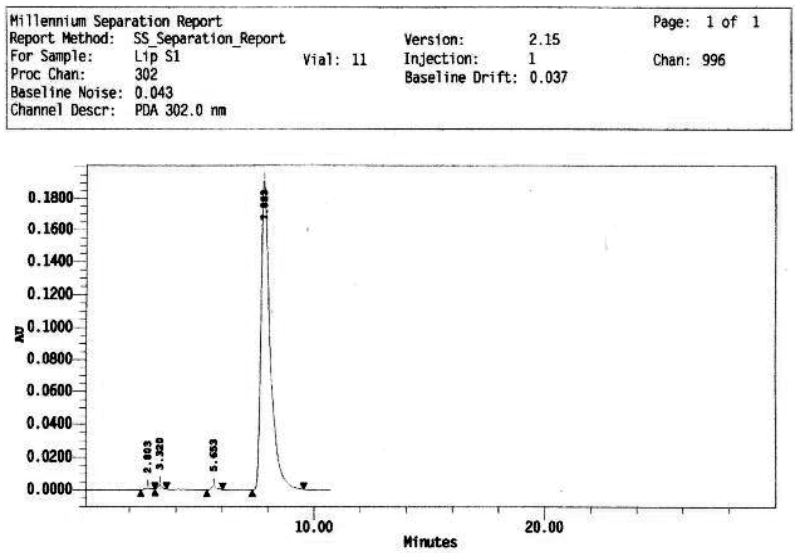

Separation Results

#	Name	Ret Time (min)	Area (uV*sec)	Height (uV)	Amount	Resolution	USP Tangent	Width @ Tang. (min)
1		2.803	18028	900			324	0.623
2		3.320	31347	2683		1.111	1960	0.300
3		5.653	33437	1964		5.891	2498	0.452
4		7.853	5322499	191154		3.739	2221	0.667

Separation Results

#	USP Tailing	K Prime	Selectivity
1		1.80	
2	1.160	2.32	1.29
3	1.235	4.65	2.01
4	1.734	6.85	1.47

Figure 11. Chromatogram of hydrosoluble methotrexate liposomes.

Millennium Separation Report — Page: 1 of 1
Report Method: SS_Separation_Report — Version: 2.15
For Sample: Lip S2 — Vial: 12 — Injection: 1 — Chan: 996
Proc Chan: 302 — Baseline Drift: 0.005
Baseline Noise: 0.016
Channel Descr: PDA 302.0 nm

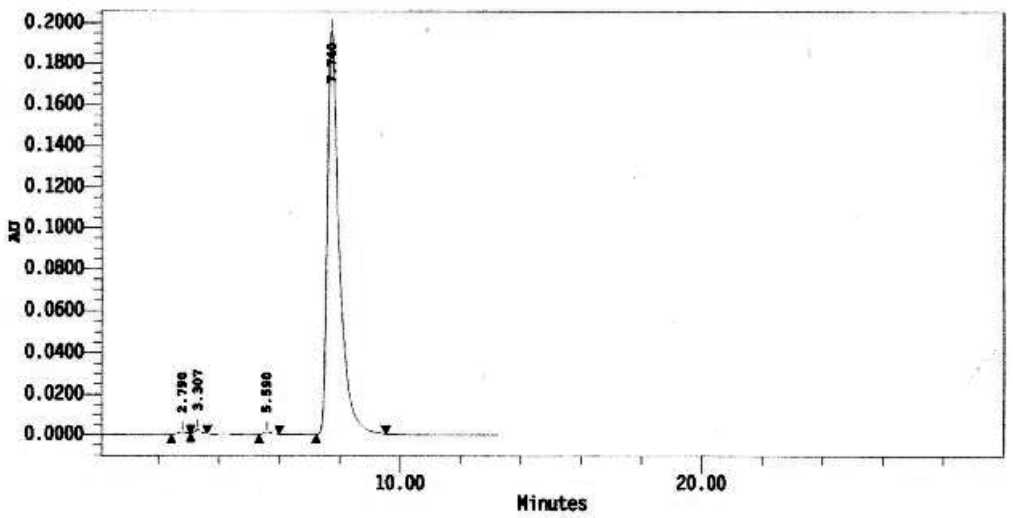

Separation Results

#	Name	Ret Time (min)	Area (uV*sec)	Height (uV)	Amount	Resolution	USP Tangent	Width @ Tang. (min)
1		2.790	25137	1199			199	0.791
2		3.307	29926	2145			1406	0.353
3		5.590	20803	1200		5.258	2452	0.452
4		7.740	5380648	196051		3.694	2227	0.656

Separation Results

#	USP Tailing	K Prime	Selectivity
1		1.79	
2		2.31	1.29
3	1.268	4.59	1.99
4	1.777	6.74	1.47

Figure 12. Chromatogram of hydrophobic methotrexate liposomes.

Given the importance of the liposomes uptaking by macrophages to the elimination from the bloodstream after liposomes intravenous injection, we studied the uptake and the quantification of internalisation of liposomes with different compositions of lipid bilayer by macrophages from tumour line RAW267.4.

The internalisation of the following types of unloaded liposomes was studied: conventional liposomes containing phosphatidylcholine, steric-stabilized liposomes containing phosphatidylcholine, cholesterol, polyethylene glycol 2000 phosphatidylethanolamine

(PC:CH:PEG2000-PE) and PC:PGPH. The cells were incubated for 2 h at 37°C with the Dil-labelled liposomes.

3.5.1. Visualisation of the liposomes internalisation

The internalisation of the methotrexate-unloaded liposomes by macrophages of murine tumour line RAW267.4 was visualized by fluorescence microscopy, using 1,1′-dioctadecyl-3,3,3′,3′-tetramethylindocarbocyanine perchlorate (Dil) as a lipophilic tracer. Images were acquired using a Nikon microscope, in phase contrast or epifluorescence, with a filter that allows 530-nm excitation and observation of emitted fluorescence at 580 nm. Intracellular point-like fluorescence is observed, indicating that the liposomes are internalized (**Figure 13**) [32].

3.5.2. Quantification of liposomes internalisation

Quantitative estimation of the ability of RAW 264.7 tumour macrophages to uptake of various types of liposomes was assessed by fluorimetric measurements. For this purpose, cells were incubated for 2 h at 37°C with methotrexate-unloaded liposomes, labelled with fluorescent Dil tracer (1 μmol liposomes/10^6 cells). After incubation, the liposomes bounded to cell surface were removed by washing with cold PBS buffer.

After washing with trypan blue solution (for complete quenching of extracellular fluorescence), the emitted fluorescence was measured at 580 nm after excitation at 530 nm of samples, using a TECAN spectrofluorimeter. The degree of internalisation of the liposomes (phospholipid nmol/10^6 cells) was calculated using the standard curve obtained from known concentrations of fluorescent liposomes.

The results showed a low uptake of liposomes containing polyethylene glycol-2000-phosphatidylethanolamine (PEG2000-PE) compared to that of conventional liposomes (PC) or PC-PGPH liposomes (**Figure 14**). One possible explanation would be that the presence of PEG2000 on the surface of steric stabilized liposomes hinders their interaction with cells through the barrier formed by hydration of the polymer [32].

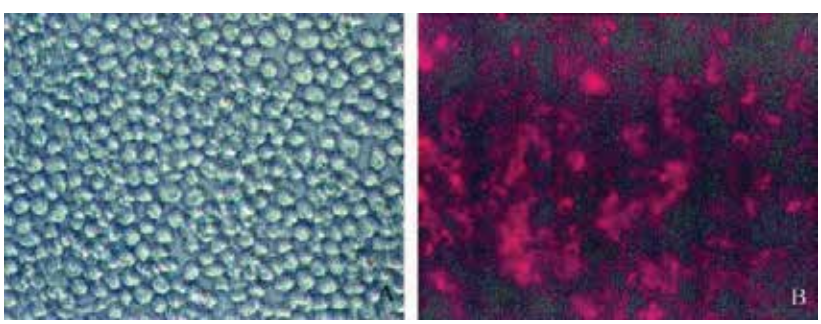

Figure 13. Phase contrast images (A) and fluorescence images (B) obtained in RAW 264.7 macrophages incubated for 2 h at 37°C with PC liposomes, labelled with Dil (20 × objective).

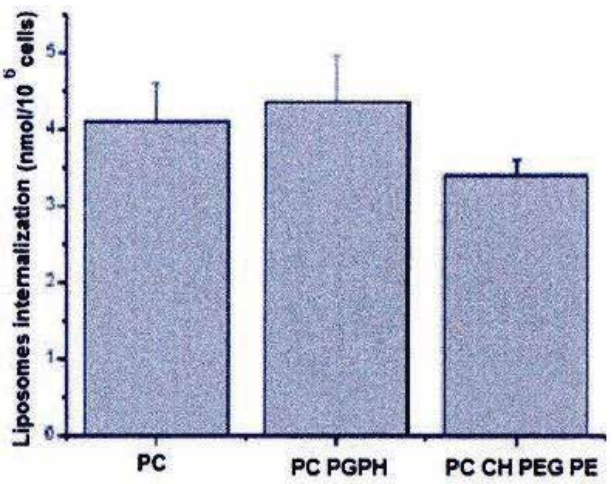

Figure 14. Internalization of PC, PC:PGPH, PC:CH:PEG-PE liposomes by murine macrophages RAW 264.7 after the incubation with 1 μmol liposomes/10^6 cells Phase contrast images (A) and fluorescence images (B) obtained in RAW 264.7 macrophages incubated for 2 h at 37°C with PC liposomes, labelled with DiI (20 × objective).

4. *In vitro* effects of MTX liposomes

The immunosuppressive action exerted *in vitro* by MTX-loaded liposomes was studied.

We compared the effect of hydrosoluble and hydrophobic MTX liposomes (dispersion 200 mg MTX/mL) and MTX solution for injection (concentration 200 mg MTX/mL) on the proliferative capacity of human lymphoblastic cells K562. The preparation and characterisation of MTX-loaded liposomes are presented in Sections 2 and 3.

The human lymphoblastic K562 cell line, purchased from ECACC (the European Collection of Cell Cultures), maintained by *in vitro* cultivation, has been used. Colchicine (standard microtubule disrupter) at a concentration of 10 μM was used as an inhibitor of cell metabolism. Cell proliferation was measured by the MTS reduction test by using CellTiter 96® AQueous Non-Radioactive Cell Proliferation Assay kit (detects the number of viable cells and, consequently, cell multiplication) (Promega Corporation). The cell activation/proliferation was measured by the tritium-labelled uridine (3H-Urd) incorporation test which detects RNA synthesis requiring uridine incorporation via the salvage pathway of nucleotide biosynthesis. The cellular membrane integrity was indirectly evaluated as lactate dehydrogenase (LDH) release, by using Cytotox96® NonRadioactive Cytotoxicity Assay kit (Promega Corporation).

The effect exerted by MTX was calculated as the ratio between the values obtained for MTX and the control value.

Experimental data indicate that MTX solution for injection inhibits neoplastic multiplication (data not shown) and RNA synthesis (**Figure 15**) in lymphoblastic K562 cells, without notably disturbing membrane integrity evaluated as LDH release.

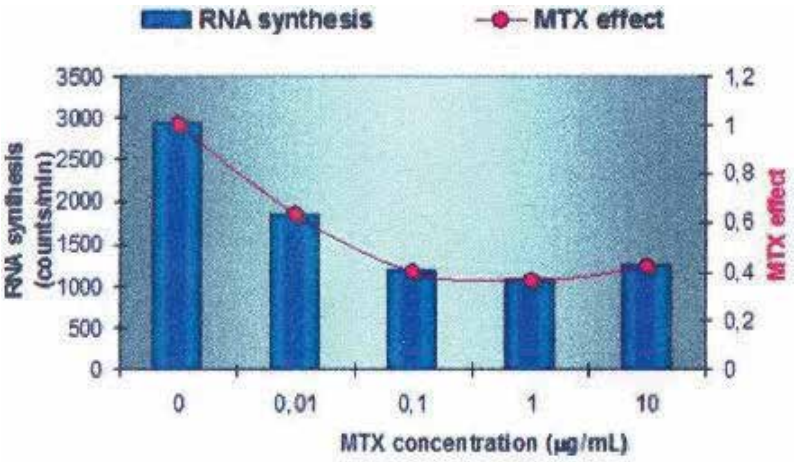

Figure 15. The effect exerted *in vitro* by MTX solution for injection on RNA synthesis by K562 cells.

PC and PC:CH liposomes do not alter significantly the multiplication of K562 cells, but, when loaded with hydrophobic MTX, they tend to hold down the proliferation of tumour cells (**Figure 16**). These results are confirmed by those obtained in the evaluation of RNA synthesis by the tritium-labelled uridine radionuclide technique. Thus, while the unloaded liposomes (PC and PC:CH) tend to stimulate the RNA synthesis, the corresponding MTX-loaded liposomes clearly induce RNA synthesis arrest (**Figure 17**).

The increase of the quantity of liposomal dispersion (treating the cells with a double amount '2×' of liposomal dispersion) does not significantly influence the MTX inhibitory effect. It is worth noticing that hydrosoluble MTX effect (as solution for injection) is also independent on the drug concentration in the range of 0.001–10 μg/mL (data not shown).

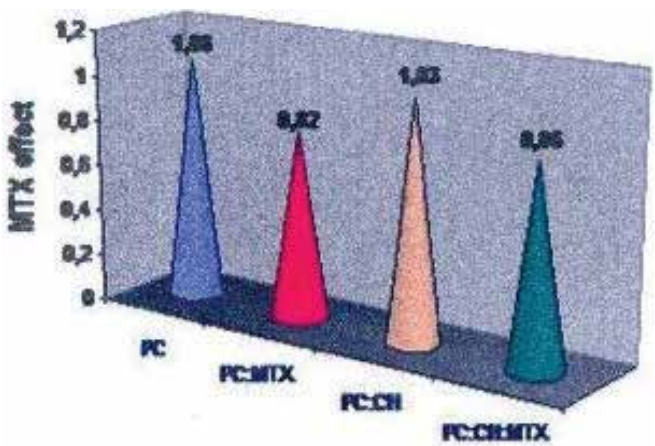

Figure 16. The effect exerted *in vitro* on the multiplication of K562 cells by liposomes loaded with hydrophobic MTX, compared to unloaded liposomes. Cell proliferation has been evaluated by MTS reduction test.

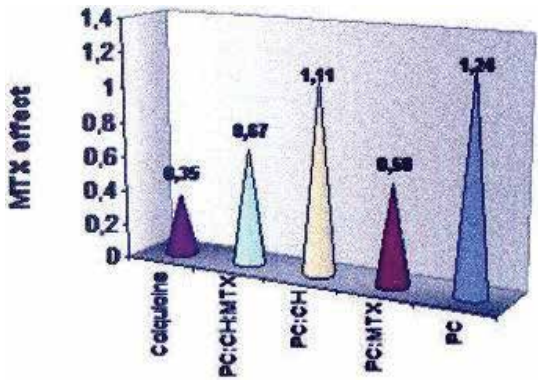

Figure 17. The effect exerted *in vitro* on the multiplication of K562 cells by liposomes loaded with hydrophobic MTX, compared to unloaded liposomes. Cell proliferation has been evaluated by the tritium-labelled uridine incorporation test. The effect has been assessed comparatively to colquicine antimitotic standard.

The inhibitory effect of hydrosoluble or hydrophobic MTX-loaded liposomes on K562 cell multiplication is comparable. However, hydrophobic MTX-loaded liposomes have a little more intense inhibitory effect compared to hydrosoluble MTX-loaded liposomes.

The results indicate that hydrophobic MTX loaded in liposomes tends to restrain the tumoural multiplication of K562 cells and clearly inhibits RNA synthesis, suggesting that activation events are primarily the target of the drug, and not the neoplastic proliferation of lymphoblasts. In addition, the hydrophobic form of MTX loaded in liposomes acts similar to the hydrosoluble one.

5. Investigation of the effects of short-term therapy with methotrexate incorporated into the liposomes in an animal model of rheumatoid arthritis

Rheumatoid arthritis is a chronic, complex, autoimmune disease with plurifactorial etiology. It is characterized by hyperplasia of the synovium of the joint cartilage [33], the infiltration of the synovial cavity with inflammatory cells [33, 34], the presence of autoreactive lymphocytes [35–37] and antibodies with different specifications [38], events that culminates in the gradual erosion of the cartilage/bone and a number of serious extra-articular manifestations [39].

Methotrexate is one of the most widely used disease-modifying anti-rheumatic drugs (DMARDs) in the treatment of rheumatoid arthritis. Although the precise mechanism of action of folate antagonist MTX in the treatment of rheumatoid arthritis is yet unclear [40], the effectiveness of methotrexate is associated with its cytotoxic and anti-inflammatory effects. Clinical and experimental evidence sustain that low-dose MTX has anti-inflammatory effects and a subtle immunomodulatory action [16, 41]. Low dose of methotrexate, orally administrated, weekly, effectively suppresses inflammation in rheumatoid arthritis [42]. However,

systemic toxicity, manifested for instance by stomatitis, nausea, bone marrow depression and liver damage, may limit oral administration of the drug [43].

Methotrexate has also been administered to control intra-articular synovitis in the joints of arthritic patients, but the results have been disappointing due to rapid clearance of the drug from the joint [44].

In order to localize the drug to the site of action and reduce the systemic toxicity, the use of liposomes or polymeric microparticles as carriers for drug delivery systems synovial space was proposed.

Effects of short-term therapy with methotrexate incorporated into the liposomes have also been investigated in an experimental model of arthritis-type inflammation-induced with Freund's adjuvant.

Freund's adjuvant-induced arthritis in the rat is one of the most important experimental models of immune chronic inflammation, with pharmacological relevance in human rheumatoid arthritis. It is most commonly used experimental model for rheumatoid arthritis in screening programmes aimed at finding new-arthritic inflammatory drugs [45].

In a Wistar rat model of arthritis (adjuvant Freund induced), the therapeutic effect and toxicity of MTX as solution for injection or hydrosoluble MTX and hydrophobic MTX-loaded liposomes have been studied [32, 46]. Three different doses of MTX preparations have been administered (i.v.) weekly for 21 days: 0.2. mg/b.w., 0.3 mg/b.w and 0.4 mg/b.w.

The induction of arthritis with Freund's adjuvant and its characterisation was based on the evaluation of the primary oedema due to inflammation (injected paw) and the secondary inflammation (paw contralateral, not injected), using a plethysmometer device (Ugo Basile, Italy) 7 days and 14 days after administration of CFA. The threshold pain response was also assessed after 21 days using an analgesy metre, according to the method of Randall-Selitto [47]. Before the injection of Freund's adjuvant, and 7, 14 and 21 days after induction of arthritis the mobility scale, posture and joint stiffness were evaluated [48]. In addition, the X-ray examination 21 days after administration of CFA has been performed to evaluate the inflammation CFA induced.

The effect of MTX treatment was assessed as threshold of pain sensitivity (Randal-Sellito test) 7, 14 and 21 days of MTX administration, as well as by radiological evaluation 21 days of MTX administration.

The induction of arthritis by Freund adjuvant was confirmed by the statistical results [*t*-Student test and analysis of variance (ANOVA)] of the inflammatory oedema assessment, the clinical assessment and the behaviour of animals (with mobility and posture significantly lower and a marked increase of stiffness), as well as the radiological evaluation of the joints (symmetric arthritogenic disturbances were present after 21 days) [32]. In addition, a marked increase in sensitivity to paw pressure was seen in the affected limb.

A dose-dependent reduction of pain sensitivity in all groups of animals treated with MTX has been shown. In addition, the intensity of the therapeutic effect increased during

treatment (the marked effect has been observed after 21 days of MTX treatment). The effect of MTX treatment has been assessed from the baseline values of the pain sensitivity (determined by Randal-Sellito test) and has been calculated after 7, 14 and 21 days of MTX treatment.

The results of the study indicated that the therapeutic effect of MTX liposomes is superior to that of MTX solution for injection. At the highest dose administered (0.4 mg/kg), the therapeutic effect of hydrosoluble and hydrophobic MTX liposomes is comparable, while at intermediate and low dose, the effect of hydrophobic MTX liposomes is higher than that of the hydrosoluble MTX liposomes. Based on the linear relationships between the MTX effect and log *D* (dose), ED_{50} values have been calculated (**Table 1**). Thus, the lowest efficacious doses of MTX were obtained at all times of the treatment for the MTX-loaded liposomes. The results are in agreement with recent data indicating that MTX encapsulated in liposomes, in contrast to free and generic MTX, proved to have a higher anti-inflammatory and anti-angiogenic efficacy in antigen-induced arthritis model in female C57/Bl6 mice [49].

The immune status of animals was evaluated 7 and 14 days after treatment discontinuation by the following parameters: number of peripheral leucocytes, relative weight of spleen (the ratio spleen weight/body weight), number of splenocytes and the activation potential of splenocytes *in vitro* treated with polyclonal mitogen concanavalin A (ConA) determined by the tritium-labelled uridine incorporation test [50].

Hydrosoluble MTX liposomes particularly tend to enhance the peripheral granulocytes percentage on behalf of the monocyte proportion. Liposome-targeted MTX induces a drop of the monocytes percentage at lower doses than the MTX solution for injection [32]. The mentioned effect ceases 14 days after therapy discontinuation. The effect is less obvious in the case of hydrophobic MTX liposomes. While peripheral monocytes percentage decreases shortly after the withdrawal of the therapy with MTX liposomes, a tendency of up-regulation was noticed 14 days after. Peripheral leukocytes react to lower doses of MTX loaded in liposomes, as compared to MTX solution for injection.

Animals treated with MTX liposomes present lower values of the relative spleen weight. This effect is reversible after 14 days since therapy withdrawal. Similar effects are exerted only by

MTX treatment	**ED_{50} (mg/kg)**		
	7 days of treatment	**14 days of treatment**	**21 days of treatment**
Hydrophobic MTX liposomes	0.338	0.272	0.258
Hydrosoluble MTX liposomes	0.363	0.337	0.285
MTX solution for injection solution	-	0.423	0.387

Table 1. ED_{50} of MTX, determined on the base of pain sensitivity for each group of animal.

http://dx.doi.org/10.5772/intechopen.68520

high doses of MTX solution for injection. The clinical significance of the registered decrease of the relative spleen weight is unclear.

The intermediate doses of MTX-loaded liposomes increase the number of spleen leukocytes, probably on behalf of the peripheral ones.

All MTX formulations induce *in vivo* activation of splenocytes, but only MTX-loaded liposomes restrain the activation potential of splenocytes to exogenous polyclonal mitogens. Seven days after therapy withdrawal, splenocytes are basically activated in the absence of exogenous

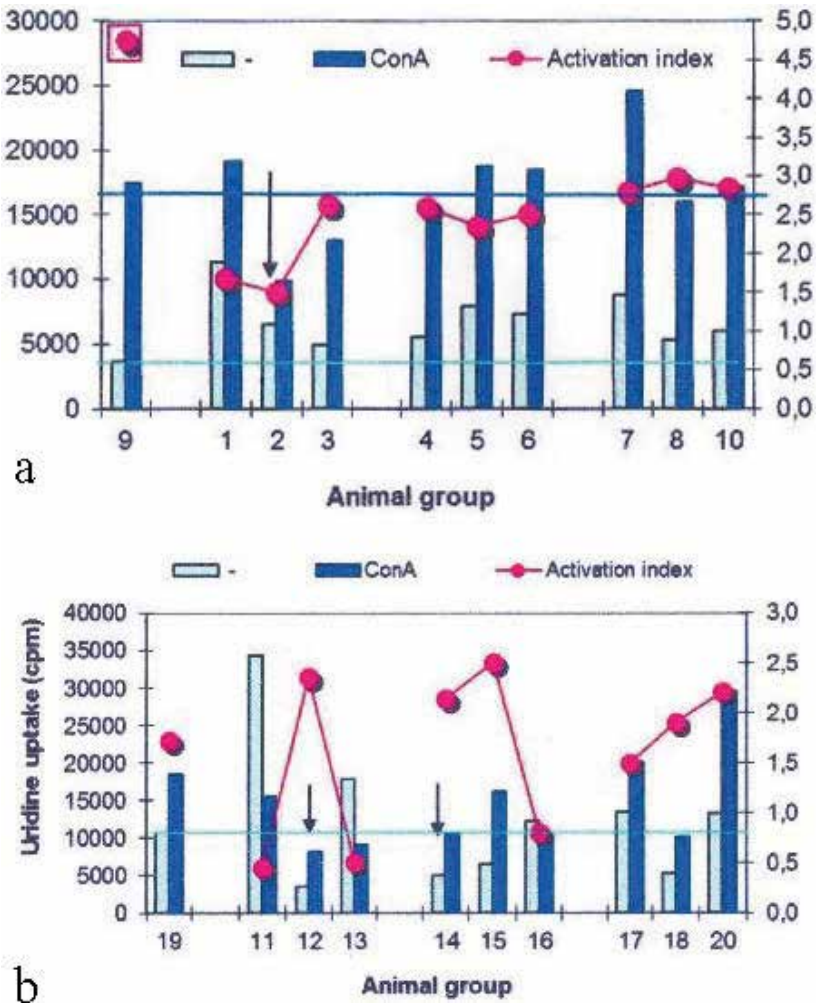

Figure 18. The effect exerted *in vivo* by MTX on the proliferation capacity of the splenic rat lymphocytes (counts per minutes, the tritium-labelled uridine incorporation test); (a) 7 days after therapy withdrawal; (b) 14 days after therapy withdrawal. Legend: The treatment of animal groups: 1;2;3—hydrosoluble MTX-loaded liposomes (0.2;0.3;0.4 mg/kg b.w); 4;5;6—hydrophobic MTX-loaded liposome (0.2;0.3;0.4 mg/kg b.w.); 7;8;10—MTX solution for injection (0.2;0.3;0.4 mg/kg b.w.); 9—control (liposomes, 0.1 mL/100 g/kg b.w.).

stimuli, but the effect is not persistent. Only the MTX-loaded liposomes exert an immunosuppressive action by limiting the *ex vivo* response of splenocytes to ConA. In this case, an anergic state of splenocytes seems to be triggered. Fourteen days after treatment discontinuation, all investigated MTX formulations inhibit splenocytes response to ConA. Accordingly, MTX liposomes exert a lasting antiproliferative action at critical doses. It is worth noticing that low and high doses of hydrosoluble MTX liposomes induce splenocytes anergy, namely activation of resting cells and reduced responses *ex vivo* to Con A. Hydrophobic MTX-loaded liposomes seem to be most efficacious in restraining splenocytes activation.

The results indicate that MTX loaded in liposomes has a more evident impact on the immune status than MTX solution for injection, and hydrophobic MTX incorporated in liposomes seems to be active at the lowest doses (**Figure 18**).

The evaluation of the haematological and biochemical parameters indicates a low toxic effect of MTX in arthritic rats in the applied treatment regimen. Erythrocyte count was not significantly affected and between erythrocyte parameters series good correlation (correlation coefficients of >0.90) was found. Transaminases activities were weak and irregularly affected, registering slight increases (especially AST) at highest MTX doses 7 days after the last administration. The creatinine and urea serum levels were not significantly affected [32].

MTX treatment induced discrete to moderate and reversible histopathological changes in the liver and the kidney. However, a more pronounced impairment in the kidney (glomerular stasis and the increase of the vascular network volume, as a result of circulation disturbances, as well as tubular nephritis and medullary mononuclear cell infiltration), depending on the type of treatment (MTX liposomes or MTX solution for injection) and of the administered dose [46], has been noticed.

6. Conclusion: key results

Several types of poly-disperse liposomal systems containing both hydrosoluble methotrexate and hydrophobic methotrexate were prepared by two methods: lipid film hydration and reverse-phase evaporation. The last one was selected due to the shorter working time and the higher encapsulation efficiency. The liposomal poly-dispersion was extruded to obtain a liposomal monodispersion. MTX liposomes were characterized by VEM, TEM and DLS. The obtained liposomes had the diameters of microns size. The unentrapped drug was removed and the concentration of entrapped MTX was chromatographically determined. The encapsulation efficiency was satisfactory and similar for PC:MTX (10:1) liposomes and for PC:CH:MTX (10:1:1) liposomes. The presence of CH in liposomal membrane increases the rigidity and the hydrophobicity of the membrane. A higher hydrophobic character of liposomal membrane means a larger loading efficiency of hydrophobic MTX.

Hydrophobic MTX loaded in liposomes tends to restrain the tumoural multiplication of K562 cells and clearly inhibits RNA synthesis, suggesting that activation events are primarily the target of the drug, and not the neoplastic proliferation of lymphoblasts.

The methotrexate liposomes exhibited significant anti-inflammatory activity and showed reduced toxicity. Given that the encapsulating of the drug in vector systems may result in the increasing concentration at the site of action, the liposomes with methotrexate represent a targeted therapy with an optimized therapeutic efficacy—risk toxicity ratio.

Acknowledgments

We thank Manuela Florea-Spiroiu, PhD Lecturer, for assistance with liposomes preparation.

Author details

Anne Marie Ciobanu[1], Maria Bârcă[2], Gina Manda[2], George Traian Alexandru Burcea Dragomiroiu[1] and Daniela Luiza Baconi[3]*

*Address all correspondence to: daniela_baconi@yahoo.com

1 Drug Control Department, Faculty of Pharmacy, "Carol Davila" University of Medicine and Pharmacy, Bucharest, Romania

2 Radiobiology Laboratory , "Victor Babes" National Institute of Patholog, Bucharest, Romania

3 Toxicology Department, Faculty of Pharmacy, "Carol Davila" University of Medicine and Pharmacy, Faculty of Pharmacy, Bucharest, Romania

References

[1] Abraham SA, Waterhouse DN, Mayer LD, Cullis PR, Madden TD, Bally MB. The liposomal formulation of doxorubicin. Methods in Enzymology. 2005;**391**:71-97. DOI: 10.1016/S0076-6879(05)91004-5

[2] Pentak D, Kozik V, Bąk A, Dybał P, Sochanik A, Jampilek J. Methotrexate and cytarabine-loaded nanocarriers for multidrug cancer therapy. Spectroscopic Study Molecules. 2016;**21**(12):pii:E1689. DOI: 10.3390/molecules21121689

[3] Popovici A, Antofi N. Lipozomi ca vectori medicamentosi (available in Romanian language). Cluj Napoca: Romsver; 2004

[4] Hong MS, Lim SJ, Oh YK, Kim CK. pH-sensitive, serum-stable and long-circulating liposomes as a new drug delivery system. Journal of Pharmacy and Pharmacology. 2002;**54**(1):51-58

[5] Groll AH, Mickiene D, Piscitelli SC, Walsh TJ. Distribution of lipid formulations of amphotericin B into bone marrow and fat tissue in rabbits. Antimicrobial Agents and Chemotherapy. 2000;**44**(2):408-410

[6] Groll AH, Mickiene D, Werner K, Petraitiene R, Petraitis V, Calendario M, Field-Ridley A, Crisp J, Piscitelli SC, Walsh TJ. Compartmental pharmacokinetics and tissue distribution of multilamellar liposomal nystatin in rabbits. Antimicrobial Agents and Chemotherapy. 2000;**44**(4):950-957

[7] Lim HJ, Masin D, Madden TD, Bally MB. Influence of drug release characteristics on the therapeutic activity of liposomal mitoxantrone. Journal of Pharmacology and Experimental Therapeutics. 1997;**281**(1):566-573

[8] Krishna R, Ghiu G, Mayer LD. Visualization of bioavailable liposomal doxorubicin using a non-perturbing confocal imaging technique. Histology and Histopathology. 2001;**16**(3):693-699

[9] Trif M, Guillen C, Vaughan DM, Telfer JM, Brewer JM, Roseanu A, Brock JB. Liposomes as possible carriers for lactoferrin in the local treatment of inflammatory diseases. Experimental Biology and Medicine. 2001;**226**(6):559-564

[10] Konigsberg PJ, Debrick JE, Pawlowski TJ, Staerz UD. Liposome encapsulated aurothiomalate reduces collagen-induced arthritis in DBA/1J mice. Biochimica et Biophysica Acta. 1999;**1421**:149-162

[11] Akbarzadeh A, Rezaei-Sadabady R, Davaran S, Joo SW, Zarghami N, Hanifehpour Y, Samiei M, Kouhi M, Nejati-Koshki K. Liposome: Classification, preparation, and applications. Nanoscale Research Letters. 2013;**8**:102. DOI: 10.1186/1556-276X-8-102

[12] Bangham AD, Standish MM, Watkins JC. Diffusion of univalent ions across the lamellae of swollen phospholipids. Journal of Molecular Biology. 1965;**13**:238-252

[13] Chang H, Yeh MK. Clinical development of liposome-based drugs: Formulation, characterization, and therapeutic efficacy. International Journal of Nanomedicine. 2012;**7**:49-60

[14] Genestier L, Paillot R, Fournel S, Ferraro C, Miossec P, Revillard JP. Immunosuppressive properties of methotrexate: Apoptosis and clonal deletion of activated peripheral T cells. Journal of Clinical Investigation. 1998;**102**(2):322-328. DOI: 10.1172/JCI2676

[15] Pachner AR, Amemiya K, Delaney E, O'Neill T, Hughes CA, Zhang WF. Interleukin-6 is expressed at high levels in the CNS in Lyme neuroborreliosis. Neurology. 1997; **49**(1):147-152

[16] Cutolo M, Sulli A, Pizzorni C, Seriolo B, Straub RH. Anti-inflammatory mechanisms of methotrexate in rheumatoid arthritis. Annals in Rheumatoid Diseases. 2001;**60**(8):729-735. DOI: 10.1136/ard.60.8.729

[17] Weinblatt ME, Weissman BN, Holdsworth DE, Fraser PA, Maier AL, Falchuk KR, Coblyn JS. Long-term prospective study of methotrexate in the treatment of rheumatoid arthritis: 84-month update. Arthritis & Rheumatology. 1992;**35**(2):129-137

[18] Maetzel A, Bombardier C, Strand V, Tugwell P, Wells G. How Canadian and US rheumatologists treat moderate or aggressive rheumatoid arthritis: A survey. Journal of Rheumatology. 1998;**25**:2331-2338

[19] Krause D, Schleusser B, Herborn G, Rau R. Response to methotrexate treatment is associated with reduced mortality in patients with severe rheumatoid arthritis. Arthritis & Rheumatology. 2000;**43**(1):14-21. DOI: 10.1002/1529-0131(200001)43:1<14::AID-ANR3>3.0.CO;2-7

[20] Kapoor B, Singh SK, Gulati M, Gupta R, Vaidya Y. Application of liposomes in treatment of rheumatoid arthritis: Quo vadis. The Scientific World Journal. 2014;**2014**(ID978351):1-17. DOI: 10.1155/2014/978351

[21] Bader RA. The development of targeted drug delivery systems for rheumatoid arthritis treatment. In: Lemmey AB, editor. Rheumatoid Arthritis – Treatment. InTech; 2012. pp. 111-132. ISBN 978-953-307-850-2 https://www.intechopen.com/books/rheumatoid-arthritis-treatment/the-development-of-targeted-drug-delivery-systems-for-rheumatoid-arthritis-treatment

[22] Cinteză O. Chimia fizică a medicamentului (available in Romanian language). Bucharest: Ars Docenti; 2002

[23] Bârcă M, Bălălău D, Ciobanu AM, Olteanu M, Dudău M, Cinteză O. Preparation and characterization of methotrexate-loaded liposomes. "Ovidius" University Annals of Medical Science – Pharmacy. 2004;**II**(I):137-142

[24] Kono K, Henmi A, Takagishi T. Temperature-controlled interaction of thermosensitive polymer-modified cationic liposomes with negatively charged phospholipid membranes. Biochimica et Biophysica Acta. 1999;**1421**(1):183-197. DOI: 10.1016/S0005-2736(99)00123-6

[25] Szoka F Jr, Papahadjopoulos D. Procedure for preparation of liposomes with large internal aqueous space and high capture by reverse/phase evaporation. Proceedings of the National Academy of Sciences United States of America. 1978;**75**(9):4194-4196

[26] Szoka F Jr, Papahadjopoulos D. Comparative properties and methods of preparation of lipid vesicles (liposomes). Annual Review of Biophysics and Bioengineering. 1980;**9**:467-508. DOI: 10.1146/annurev.bb.09.060180.002343

[27] Paternostre M, Ollivon M, Bolard J. Liposomes: Preparation and Membrane Protein Reconstitution. In: Prasad R, editor. Manual on Membrane Lipids. Springer Lab Manual; 1996. pp. 202-247 ISBN: 978-3-642-48970-9 (Print) 978-3-642-79837-5 (Online)

[28] Nenitescu CD. Chimie organică, vol 1 (available in Romanian language). Bucharest: Editura Pedagogică; 1980

[29] Lee KD, Nir S, Papahadjopoulos D. Quantitative analysis of liposome-cell interactions in vitro: Rate constants of binding and endocytosis with suspension and adherent J774 cells and human monocytes. Biochemistry. 1993;**32**(3):889-899. DOI: 10.1021/bi00054a021

[30] Miller CR, Bondurant B, McLean SD, McGovern KA, O'Brien DF. Liposome-cell interactions in vitro: Effect of liposomes surface charge on the binding and endocytosis of conventional and sterically stabilized liposomes. Biochemistry. 1998;**37**(37):12875-12883. DOI: 10.1021/bi980096y

[31] Pleyer U, Grammer J, Kosmidis P, Ruckert DG. Analysis of interactions between the corneal epithelium and liposomes: Qualitative and quantitative fluorescence studies of a corneal epithelial cell line. Survey of Ophthalmology. 1995;**39**(1):S3-S16

[32] Bârcă M, Baconi DL, Ciobanu AM, Burcea GTA, Bălălău C. Comparative evaluation of methotrexate toxicity as solution for injection and liposomes following a short-term treatment in a murine model of arthritis. Note I. Haematological and biochemical evaluation. Farmacia. 2013;**61**(1):220-228

[33] Firestein GS. Novel therapeutic strategies involving animals, arthritis, and apoptosis. Current Opinion in Rheumatology. 1998;**10**(3):236-241

[34] Youssef PP, Smeets TJ, Bresnihan B, Cunnane G, Fitzgerald O, Breedveld F, Tak PP. Microscopic measurement of cellular infiltration in the rheumatoid arthritis synovial membrane: A comparison of semiquantitative and quantitative analysis. British Journal of Rheumatology. 1998;**37**(9):1003-1007

[35] Goronzy JJ, Weyand CM. T and B cell-dependent pathways in rheumatoid arthritis. Current Opinion in Rheumatology. 1995;**7**(3):214-221

[36] Goronzy JJ, Weyand CM. T cells in rheumatoid arthritis. Paradigms and facts. Rheumatic Disease Clinics of North America. 1995;**21**(3):655-674

[37] Blä S, Engel JM, Buemester GR. The immunologic homunculus in rheumatoid arthritis. Arthritis & Rheumatology. 1999;**42**:2499-2506

[38] Ismail AA, Snowden N. Autoantibodies and specific serum proteins in the diagnosis of rheumatological disorders. Annals in Clinical Biochemistry. 1999;**36**(5):565-578

[39] Bayraktar A, Hudson S, Watson A, Fraser S. Arthritis. Pharmaceutical Journal. 2000; **264**(7078):57-68

[40] Wessels JAM, Huizinga TWJ, Guchelaar H-J. Recent insights in the pharmacological actions of methotrexate in the treatment of rheumatoid arthritis. Rheumatology. 2008;**47**:249-255

[41] Cronstein B. How does methotrexate suppress inflammation? Clinical and Experimental Rheumatology. 2010;**28**(5 Suppl 61):S21-S23

[42] van Ede AE, Laan RF, Blom HJ, De Abreu RA, van de Putte LB. Methotrexate in rheumatoid arthritis: An update with focus on mechanisms involved in toxicity. Seminars in Arthritis Rheumatology. 1998;**27**(5):277-292

[43] O'Dell JR. Methotrexate use in rheumatoid arthritis. Rheumatic Disease Clinics of North America. 1997;**23**(4):779-796

[44] Liang LS, Jackson J, Min W, Risovic V, Wasan KM, Burt HM. Methotrexate loaded poly(L-lactic acid) microspheres for intra-articular delivery of methotrexate to the joint. Journal of Pharmaceutical Science. 2004;**93**(4):943-956

[45] Theisen-Popp P, Muller-Peddinghaus R. Antirheumatic drug profiles evaluated in the adjuvant arthritis of rats by multiparameter analysis. Agents and Actions. 1994;**42**:50-55

[46] Bârcă M, Baconi DL, Ciobanu AM, Militaru M, Burcea GTA, Bălălău C. Comparative evaluation of methotrexate toxicity as solution for injection and liposomes following a short-term treatment in a murine model of arthritis: Note II. Histopathological changes. Farmacia. 2013b;**61**(5):939-947

[47] Randall LO, Selitto JJ. A method for measurement of analgesic activity on inflammed tissue. Archives in International Pharmacodynamics Therapy. 1957;**111**:409-419

[48] Butler SH, Godefroy F, Besson JM, Weil-Fugazza J. A limited arthritic model for chronic pain studies in the rat. Pain. 1992;**48**(1):73-81

[49] Gottschalk O, Metz P, Dao Trong ML, Altenberger S, Jansson V, Mutschler W, Schmitt-Sody M. Therapeutic effect of methotrexate encapsulated in cationic liposomes (EndoMTX) in comparison to free methotrexate in an antigen-induced arthritis study in vivo. Scandinavian Journal of Rheumatology. 2015;**44**(6):456-463

[50] Bârcă M, Ciobanu AM, Bălălău D, Baconi D, Ilie M, Neagu M, Manda G. Short-term treatment with methotrexate-loaded liposomes in a murine model of arthritis. Toxicology Letters. 2005;**158**(Suppl 1):S91-S92

Chapter 11

Liposome-Mediated Immunosuppression Plays an Instrumental Role in the Development of "Humanized Mouse" to Study *Plasmodium falciparum*

Kunjal Agrawal, Vishwa Vyas, Yamnah Hafeji and Rajeev K. Tyagi

Additional information is available at the end of the chapter

http://dx.doi.org/10.5772/intechopen.69390

Abstract

The material world has been getting prone toward infectious diseases, and therefore novel strategies should be devised to treat chronic infectious disorders. The translational biomedical research scientists made early attempts to develop mouse-human chimera (humanized mouse) through the reconstitution of immunodeficient mouse with engraftment of human cells and tissues. Although the humanized mouse proved to be an effective tool in understanding various diseases such as human malaria and hepatitis, however, drug administration, retention capacity of the administered drug, toxicity, and ethical constraints are some of the major issues and need to be objectively addressed. The "humanization" of immunodeficient mouse needs pharmacological immunomodulatory reagents to control the excessively recruited cells of monocyte-macrophage lineage. Therefore, administration of liposome loaded with hydrophobic drug (clodronate) to induce selective apoptosis through "suicidal approach" in myeloid cells plays an instrumental role for controlling residual nonadaptive immune response of the host. Liposomes are spherical and hollow—structures consisting of lipid bilayer—and are used for the delivery of drug and vaccine candidates. The surface-engineered liposomes (ligand anchored) are used for targeted and controlled delivery. Clodronate-loaded liposomes play a pivotal role in developing humanized mouse. This mouse holds relevance to study pathophysiology and immunopathology of human malaria parasite, P. *falciparum*. The liposomal delivery of clodronate administered in immunodeficient mice to modulate their innate immune system is an amenable strategy with the minimal/acceptable range of systemic toxicity.

Keywords: humanized mouse, clodronate, liposomes, interleukin, immunity, innate response

1. Mouse-human chimera(s)

A "humanized mouse" is an immunocompromised mouse carrying identical functions of cell or tissue in origin as seen in humans. The depletion of adaptive immune system allowed sizeable grafting of human cells to understand the biology and pathology of various diseases to developing therapeutic interventions. The nude and severe combined immunodeficiency (SCID) mouse have been used for the humanization, but recently the immunodeficient background of NOG/NSG mouse has shown significant receptivity toward the significant engraftment and repopulation of human cells.

The need of immunodeficient mouse: An immunodeficient mouse is a laboratory mouse from a strain with a genetic mutation that causes a deteriorated or absent thymus, resulting in an inhibited immune system due to a greatly reduced number of T cells. The mouse is invaluable to translational research due to its susceptibility for different types of tissue and tumor grafts with less rejection episodes. These xenografts are commonly used in research to test new methods of imaging, treating tumors as well as understanding infectious diseases. The creation of a reproducible and straightforward animal model is inevitably required as it allows developing in-depth understanding on cellular and molecular mechanisms and pathophysiological manifestation responsible for the cause of systemic inflammatory diseases.

1.1. Human-hepatocyte transplantation

The initial attempt made toward developing a human liver chimeric mouse was the one that would accept human hepatocytes. SCID/bg mouse with the urokinase-type plasminogen activator (uPA) gene linked to an albumin promoter was the first one to be developed. The immunodeficient mice have subacute liver failure and are subjected to transplantation with fresh or cryopreserved human hepatocytes (huHep) via intrasplenic injection. Six to eight weeks after transplantation with human hepatocytes, large islands of human liver tissue are produced within the mouse liver, creating a mouse with a human/mouse chimeric liver [1]. The rate of successful engraftment in terms of huHep repopulation index (RI) is 60–70% as determined by calculating the human serum albumin levels.

The second mouse model that was developed had deficiency in the gene for the tyrosine catabolic enzyme fumarylacetoacetate hydrolase (Fah). These Fah−/− mice could engraft their hepatocytes only in the presence of 2-(2-nitro-4-trifluoromethylbenzoyl)-1,3-cyclohexanedione (NTBC) and lost the engrafted Hepupon drug removal. This gene deficiency was bred into immunodeficient mice to create the FRGN mouse [2]. The mouse also supported the development of *Plasmodium falciparum* sporozoites into exoerythrocytic forms in the liver. Furthermore, when transplanted with human erythrocytes, they proved to be an effective model to study intraerythrocytic stages of *P. falciparum*.

1.2. TK-NOG mice for huHep transplantation

TK-NOG transgenic mouse in which mice express the herpes simplex virus thymidine kinase (HSVtk) transgenic construct containing the mouse albumin enhancer/promoter has drawn

significant attention. HSVtk mRNA is selectively expressed in the liver of NOG mice as a result of which they become prone to severe parenchymal liver damage after ganciclovir treatment

Of late, *reconstitution of TK-NOG mice with human hepatocytes led to orthotopic de novo engraftment and regeneration of huHep islands with controlled immunity and with broad repertoire*. The host is prepared by creating liver stroma with ganciclovir and further reducing their nonadaptive immune responses by clo-lip treatment and deploying immunosuppression strategies through tacrolimus laden polymeric hydrogels, huHep transplantation in TK-NOG mice.

Prkdcscid (protein kinase, DNA-activated, catalytic polypeptide; severe combined immunodeficient mouse *scid*): *Prkdc* plays a crucial role in repairing double-stranded DNA breaks and in recombining the variable (V), diversity (D), and joining (J) segments of immunoglobulin and T-cell receptor genes.

Homozygous mutants do not have mature T and B cells, are not capable to evoke cell-mediated and humoral immune responses, and are supportive to allogeneic and xenogeneic grafts. These models therefore are useful cancer research models. The *SCID* mutation renders NOD mice diabetes-free and thereby makes them useful for adoptive transfer of diabetes through T cell. This mutation in CB17 mice could allow engraftment of human peripheral blood mononuclear cells (PBMC's), fetal hematopoietic tissues, and hematopoietic stem cells (HSCs). The suboptimal engraftment efficiency and their inability to generate a potent and sizeable immune system are some of the striking limitations of this mouse model [3].

The above model proved to be unreliable because of the generation of mouse T and B cells, a phenomenon known as "leakiness," and generation of high levels of host NK cells. Besides, SCID mice resulted in a defective DNA repair system which results in an increased radiosensitivity.

1.3. RAG1 and RAG2 mutation (recombination activating gene 1 and gene 2)

Targeted mutations at gene Rag1 and Rag2 loci prevent mature T-cell and B-cell development in mouse but do not cause leakiness or radiosensitivity. Rag1 is essential for the V(D)J gene rearrangements that generate functional antigen receptors in T and B cells; homozygous $Rag1^{tm1Mom}$ mutants do not mature, functional T and B cells.

NOD-SCID mouse: This model is advantageous over others as it reportedly supported higher levels of engraftment of human PBMCs and showed lower NK-cell activity with additional defects in innate immunity. However, the use of this model has been limited because of the development of thymic lymphomas over the period of time and shorter life span thereby. The residual activity of NK cells and other components of innate immunity are some of the drawbacks of this mouse model

Mutation in (IL-2R) γ-chain: The IL-2Rγ-chain allows signaling through high-affinity receptors such as IL-2, IL-4, IL-7, IL-9, IL-15, and IL-21. The mutation in IL-2Rγ leads to developmental deficiencies in T cell, B cell, and NK cell. Also, this model supports engraftment of human tissues, HSCs and PBMCs. This model supported a remarkable decrease in the inflammation mediators (cytokines/chemokines), which, in turn, helped improve *P. falciparum*

survival. IL-2Rγ mutation on NOD-SCID genetic background conferred an advantage that supported greater and high rising parasitemia which remains stable for weeks with greater reproducibility. Additionally, NSG mice shown lesser effect of aging which was due to the minimalized effect by interposition impact rendered by the IL-2Rγ mutation, along with a small sample size exhibiting marginal benefit of aging in the said mouse strain. The NSG-IV murine model when transplanted with human cells showed a great complementation of IL-2Rγ mutation byclo-lip treatment in controlling inflammation mounted by the cell engraftment which reportedly showed the reduction in the erythrophagocytosis [1, 2, 4–7].

2. Liposomes: versatile carriers

Liposomes are small synthetic vesicles of spherical shape formulated from cholesterol and natural nontoxic phospholipids. The small size and hydrophobic and hydrophilic attributes of liposomes are some of the glaring features in addition to their biocompatibility and sustained release properties [8]. A liposome has an aqueous solution core surrounded by a hydrophobic membrane, in the form of a lipid bilayer, and therefore hydrophilic solutes dissolved in the core cannot readily pass through the bilayer [8].

The nature and attributes of liposomes vary depending upon the method employed for their formulation, lipid composition, and charge present on their surface. Moreover the choice of bilayer components determines the "rigidity" or "fluidity" and the charge of the bilayer [8]. For instance, unsaturated phosphatidylcholine species from natural sources (egg or soybean phosphatidylcholine) renders greater permeability with flexible stable bilayers, whereas the saturated phospholipids with long acyl chains (dipalmitoylphosphatidylcholine) form a rigid rather impermeable bilayer structure [8].

There has been experimental evidence on these phospholipids forming closed structures when mixed rigorously in aqueous phase [8]. These closed structures are hollow and therefore are used to deliver regardless of the nature of selected drug [8].

Hydrophobic chemicals are associated with the bilayer; lipid vesicles may be loaded with hydrophobic and/or hydrophilic molecules. The site-specific and controlled delivery of drugs/candidate vaccines is achieved by the fusion of lipid bilayer with other bilayers such as the cell membrane. However, delivery of entrapped content through liposomal formulations is a complex and non-spontaneous phenomenon [8].

3. Advent of liposomes as delivery vehicle

The origin of liposomal formulation liposomes goes back to the mid-1960s, and when Alec D. Bangham and his coworkers discovered that phospholipids in the presence of suitable solvents form bilayer membranes which beget hollow spheres to form unilamellar or multilamellar vesicles (MLVs) [9]. The background is studied in three phase: "Origin," "Medieval period," and "Modern era."

Origin (1968–1975): The physiochemical characterization of liposomes had been carried out in this period. The approach of thin-film hydration was adopted for the development of multilamellar vesicles (MLVs). The closer resemblance to various biological membranes, liposome, had been a natural choice to study the nature and functions of biological membranes; Bangham had called his lipid structures "multilamellar smectic mesophases" or sometimes "banghasomes" [9]. A more common term liposome was later coined by Weissmann [8].

Medieval period (1975–1985): Liposome's utility was improved following basic research that increased the understanding of their stability and interaction characteristic within the system. There were methodological advancements; so far the formulation of liposomes was concerned further; the in-depth understanding on physiochemical properties of liposomes, their behavior within the body, and their interaction with the cells led scientists to improve upon potential as drug carrier systems.

Modern era (1985 onward): Liposomes have been widely used all across the scientific disciplines including material sciences, mathematics, physics, biophysics, biochemistry, colloid science, and nanobiology for their well-bestowed delivery potential [9]. Ambisome, a parenteral amphotericin-B-based liposomal product, was initially synthesized along with numerous products undergoing clinical trials or licensed for the market [9].

4. Classification of liposomes

The liposome size varies from very small (0.025 μm) to large (2.5 μm) vesicles comprising one or bilayer membranes. The circulation time of liposome is based on the size of the vesicle or in entrapment efficiency. The size and number of bilayers largely affect the amount of drug encapsulated in lipid vesicles, liposomes.

The bilayer behavior and size of liposomes provide an opportunity to categorize them as:

(a) **Multilamellar vesicles** (**MLVs**)

(b) **Unilamellar vesicles**: Unilamellar vesicles can also be classified into two categories: large unilamellar vesicles (LUVs) and [2] small unilamellar vesicles (SUVs). In unilamellar liposomes, the vesicle is surrounded by a single phospholipid bilayer sphere keeping the aqueous solution bound inside it. In multilamellar liposomes, vesicles have a structure similar to that of an onion. The combination of several unilamellar vesicles will give rise to a multilamellar structure of concentric phospholipid separated by water layers [10].

1. **Archeosomes**: Archeosomes are vesicles derived from archaebacteria lipids. These are very different from the eukaryotic and prokaryotic bacteria. They are less sensitive to oxidative stress, high temperature, and alkaline pH [11, 12].
2. **Cochleates**: Cochleates are derived from liposomes, suspended in an aqueous two-phase polymer solution and are subjected to phase separation which allows appropriate partitioning of polar molecule-based structures. When this solution is treated with cations like Ca^{2+} or Zn^{2}, giving rise to cochleate precipitates less than 1 μm in dimension [13].

3. **Dendrosomes**: Dendrosomes are a version of liposomes that along with being nontoxic are biodegradable, self-assembled, hyperbranched, dendritic, spheroidal nanoparticles which are easy to prepare, relatively cheap, and highly stable as well as easy to handle. The dendrosomes have proven for their delivery potential and hold an edge over existing synthetic vehicles for gene delivery. Dried reconstituted vesicles (DRV): This technique allows preparing small, "empty" unilamellar vesicles, containing different lipids or mixtures. Once SUVs are dissolved in solubilized drug, the dehydration is performed. The rehydration then leads to the formation of large quantities of heterogeneous multilamellar vesicles followed by further processing to form liposomal vesicles loaded with drugs [14].
4. **Ethosomes**: The ethosomes (the engineered liposomes) as compared to conventional liposomes have proven efficient so far the delivery attribute is concerned. Also, these carriers have reportedly known to show better entrapment of drug(s) [15]. Ethosomal drug permeation through the skin was demonstrated in diffusion cell experiments. Ethosomal systems were composed of soy phosphatidylcholine, and about 30% of ethanol was shown to contain multilamellar vesicles by electron microscopy.
5. **Immunoliposomes**: Liposomes which are anchored with antibodies, Fabs, or peptide structures can be used in in vitro as well as in vivo applications [16, 17].
6. **Immunosomes**: The glycoprotein molecules attached onto the surface of preformulated liposomes are called "immunosomes." The immunosomes do not vary in their appearances with the prominent presence of spikes evenly distributed on their outer surface [18]. **Immunosomes** have structural and immunogenic characteristics closer to those of purified and inactivated viruses than any other forms of glycoprotein lipid arrangement.
7. **Immune stimulating complex** (**ISCOM**): ISCOMs are made up of saponin mixture Quil A, cholesterol, and phospholipids giving rise to spherical, micellar assemblies of about 40 nm in size. They are constituted of amphiphilic antigens such as membrane proteins. ISCOMs have an inbuilt adjuvant Quillaja saponin, isolated from *Quillaja* [19].
8. **Lipoplexes**: Cationic lipid-DNA complexes, called Lipoplexes, are efficient carriers for cell transfection, but the rendered toxicity limits their applications [20, 21]. These local and systemic toxicities may result from either cationic lipids or nucleic acids.
9. **LUVETs**: Large unilamellar vesicles prepared by extrusion techniques (LUVETs) are chiefly performed with high-pressure systems. These proved to be more stable and did not cause leakage on treatment with detergents [22, 23].
10. **Niosomes**: Niosomes are small unilamellar vesicles made from nonionic surfactants also called novasomes. Their chemical stability is comparable to that of archeosomes [24, 25].
11. **pH-sensitive liposomes**: This class of liposomes is characterized as follows:
    1. This class combines unsaturated phosphatidyl ethanolamine and acidic amphiphiles that render stability at neutral pH [26].
    2. The second class compiles liposomes composed of lipid derivatives which gives increased permeability to encapsulated solutes [26].

3. The third class of pH-sensitive liposomes operates at low pH to destabilize membranes. These are made of pH-sensitive peptides or fusion proteins [26].
4. The fourth class of liposome uses **pH-sensitive liposomes** and has pH-titrable polymers to stabilize membranes which are susceptible to change in shape at low pH [26] (**Figure 1**).

12. **Polymerized liposomes**: Polymerized phosphatidyl choline vesicles (35–140 nm) have been synthesized from lipids bearing one or two methacrylate groups per monomer. These vesicles showed improved stability and controllable time-release properties compared to non-polymeric analogs [27].
13. **Proliposomes**: Proliposomes (PLs) are defined as dry, free-flowing particles that immediately form a liposomal dispersion on contact with water. Proliposomes (PLs) are dry, free-flowing granular products composed of drug(s) and phospholipid(s) which, upon addition

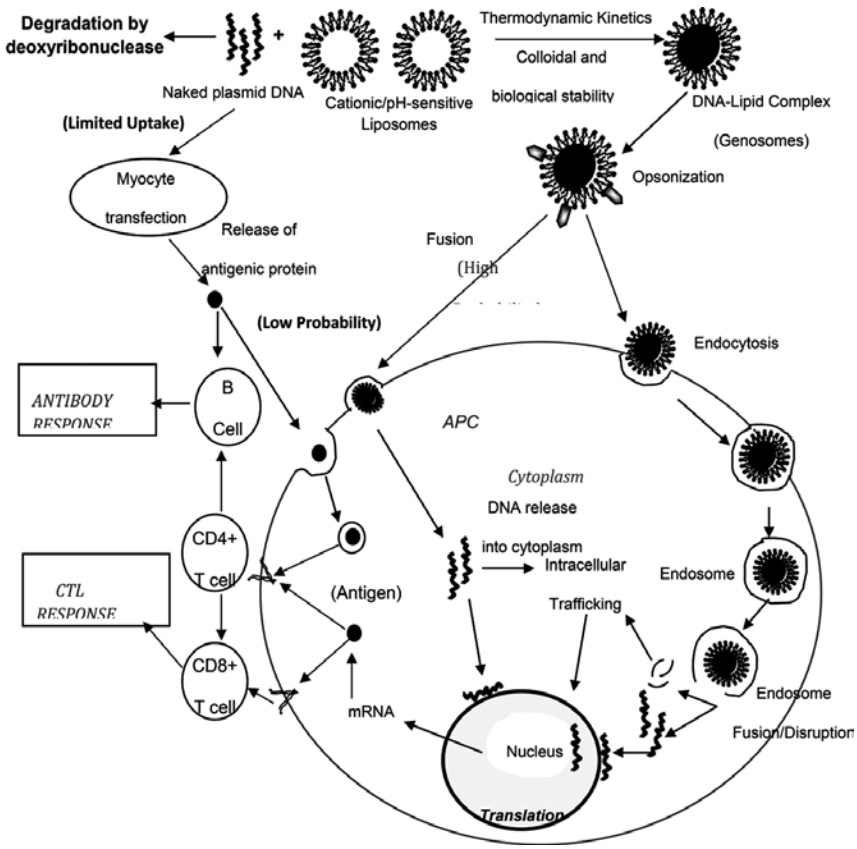

Figure 1. Schematic representation of proposed mechanism of DNA immunization via endocytic pathway. Naked DNA is taken up by a small number of myocytes after i.m. injection, which are then transfected episomally. The produced antigen is released from the cells to interact with APC and thus induce immunity. In contrast, liposomal DNA interacts with APC directly and induces better immune response. It also protects DNA from degradation by deoxyribonuclease attack.

of water, disperse to form a multilamellar liposomal suspension. These are economically feasible to formulate and be used up to a great extent on commercial scale. These hydrated membranes form vesicles upon contact with water. Moreover, the distribution, transfer, and storage become easy due to their availability in lyophilized form [28–30].

14. **Proteasomes**: Vesicles of bacterial origin were solubilized followed by ammonium sulfate precipitation and dialysis against detergent buffer. Proteins and peptides are non-covalently complexed to the membrane making them highly immunogenic [31].

15. **Reverse-phase evaporation vesicles** (**REVs**): Vesicles are formed by evaporation of oil in water emulsions resulting in large unilamellar liposomes. The main problem encountered in the usage of organic solvents is its trace content even after evaporation in the final solution which can be hazardous to human health and also may affect the stability of the vesicles. However, this issue may be addressed by the use of polycarbonate filters which allowed the separation based on their size and entrapment efficiency. Furthermore, as an alternative, diethyl ether can also be used as an organic solvent because of its lesser toxicity [32, 33].

16. **Stealth liposomes**: When liposomes are modified by coating them with polyethylene glycol (PEG), a synthetic hydrophilic polymer can greatly induce stability and their circulation half-life. These advantages have established glycolipids for surface anchoring in order to achieving targeted and sustained delivery. The engineering process of this class of liposome culminated with the observation that coating of liposomes with polyethylene glycol (PEG), a synthetic hydrophilic polymer, would improve their stability and lengthen their half-lives in circulation, rendering the use of glycolipids obsolete [34–38].

    The PEG coating stabilizing effect arises from high concentration of hydrated groups that inhibit both hydrophobic and electrostatic interactions of variety of blood components and thereby limits their recognition by the reticuloendothelial system (RES) [39, 40].

17. **Temperature-sensitive liposomes**: Temperature-sensitive liposomes permit easy gel to liquid crystallization phase transition above the physiological temperatures and are efficient in achieving target-specific drug delivery. This property is achieved by the usage of thermosensitive polymers [41], and therefore, content release, surface properties, and their cell-surface binding may be controlled by the temperature [42].

18. **Transfersomes**: Transfersomes formulated by phosphatidylcholine and cholate are highly deformable making them as preferred choice for transcutaneous delivery of drugs and candidate vaccines. This in contrast to conventional liposomes and niosomes offers needle-free delivery of vaccines and an increased concentration of antibody titer which may suffice the need of systemic and mucosal immunity by provoking humoral and cell-mediated branches of immune system. Moreover, these ultra-deformable carriers can easily overcome the skin barrier and efficiently deliver the antigenic payload [43, 44].

19. **Virosomes**: Virosomes are small unilamellar vesicles containing influenza hemagglutinin, by which they became fusogenic with endocytic membranes. The co-incorporation of other membrane antigens induces enhanced immune responses [10, 45].

5. Engineered version of liposomes

A greater population has relied on the use of antibiotics. However, emergence of resistance against antibiotics has warranted a demand to identify a new class of antibiotics with an efficient mode of delivery.

The scientists engineered an artificial nanoparticles made of lipids, "liposomes," that closely resemble the membrane of host cell which target bacterial toxin [46]. Since bacteria are not targeted directly, the liposomes do not promote the development of bacterial resistance. In clinical medicine, liposomes are used widely as a vehicle to deliver specific medication into the body for achieving extended release [46]. The liposomal formulation, however, act as traps for bacterial toxins, sequesters, and neutralizes them instantly which would be subsequently eliminated by the host's own immune system.

6. Role of clodronate-loaded liposome in global immunosuppression

Clodronate (dichloromethylene bisphosphonate) is a nontoxic drug but impermeable to cell membrane. However, liposomes prepared by using phosphatidylcholine and cholesterol are not toxic and are engulfed by wandering macrophages. The hydrophobic drug clodronate when administered naked will be cleared from the circulation and gets absorbed by the digestive system and may face the leakiness issue. However, when administered through liposomes, it would not easily escape from the cell and is retained [47].

It is evident that clodronate may be delivered into phagocytic cells using liposomes as vehicles, therefore preventing it from being escaped from the cell [47].

The cell enzyme lysosomal phospholipases disrupt the phospholipid layer of liposome and induce release of drug clodronate which gets accumulated sizably within the cell. The free clodronate has an extremely short half-life in the circulation and is cleared from the circulation by the renal system. Therefore, specific entrapment of clo-lip formulation by macrophages induces selective apoptosis of macrophages. Therefore, a technique that involves the macrophage "suicide" approach, using the liposome-mediated intracellular delivery of dichloromethylene bisphosphonate (CI2MBP or clodronate) was deployed. The method is specific with respect to phagocytic cells of the mononuclear phagocyte system (MPS) [47].

7. Autoimmune hemolytic anemia (AIHA) liposome

Autoimmune hemolytic anemia is a disease in which autoantibodies against RBCs lead to their premature destruction. The autoantibodies of the IgG type lead primarily to the uptake and destruction of RBCs by splenic and hepatic macrophages. The current therapies such as corticosteroids and splenectomy are directed at interfering with this process. Clodronate-loaded liposomes (dichloromethylene diphosphonate) selectively deplete macrophages

within 24 h of administration by inducing apoptosis of macrophages. Therefore, liposomal clodronate would be a useful agent for treating sAIHA. This drug formulation was effective within hours by first blocking and then depleting phagocytic macrophages, and its action lasted for 3–4 days in vivo. Thus, in AIHA, liposomal clodronate therapy may act like a temporary, medicinal splenectomy. Therefore, clo-lip treatment may prove useful in situations where rapid response to therapy is critical or other medical therapies are inadequate.

Clodronate-loaded liposomes completely halted the uptake of opsonized RBCs by the spleen in contrast to splenectomy which used corticosteroid treatment. However, this cannot replace the corticosteroid treatment but offers an advantage because the spleen is not removed, and its function is eventually restored by the natural replenishment of macrophages. Clodronate-loaded liposomes undertaken in this treatment are temporary but are spontaneous in treating AIHA as compared to corticosteroids.

8. Immunosuppression by liposome-mediated delivery of specific drugs

Normally, liposomes are now known for immunosuppression. However, liposome loaded with cytostatic drugs for cancer therapeutics is reported to cause more or less immune suppression [48]. These drug-loaded formulations opened new avenues in cancer immunotherapeutics.

The doxorubicin, an anticancer drug, commercially sold as doxil (a liposomal formulation) when administered in vivo, showed macrophage suppression. The immunosuppression was seen from the long-lived persistence of bacteria in the blood stream. We have tried immunomodulatory and pharmacological reagents/chemicals which were used to further suppress the residual innate immune response (**Table 1**) [47–50] of huRBC reconstituted immunodeficient mouse (huRBC-NSG) for the engraftment and survival of *P. falciparum*. Also, immunosuppression of nonadaptive residual immune responses of immunodeficient mouse was contained by clodronate-loaded liposomes in order to achieving significant huRBC grating in immunodeficient animals (NSG) (**Figure 2**).

8.1. Adjuvanticity of liposomes

When bestowed along with clodronate, EDTA, DTPA, or various calcium or metal ion complexes of these chelators have the potential to deplete macrophages in vivo. Liposomal formulations have reportedly enhanced the immune response both at humoral and cell mediated of a vaccine formulation [44, 51]. The adjuvant action of liposomes may be categorized as:

1. The marginal zone antigens of macrophages residing inside the spleen can be targeted through liposomes.
2. The liposomes are used to block or deplete the activity of suppressor alveolar macrophages.

Thus, liposomes offer the advantage of both drug administration and adjuvant [51, 52].

Protocol tested	Dose	No. of mouse	% success (more than 2 days)	Parasitemia length average (days)	Best parasitemia (days)
DMSO	5%	18	88.8	7.18	12
TGFβ	100 ng/day	17	23.5	7.25	8
	1 μg/day	3	66.6	10	13
Splenectomy		5	60	7	10
Cyclophopshamide	75 mg/kg	7	100	7.6	9
	50 mg/kg	12	41.6	6.8	9
Coinfection *P. chabaudi P. falciparum*		7	71.42	11	24
Coinfection *P. yoelii P. falciparum*		52	90.24	11.09	34
NAC	100 mg/kg	25	56	11.07	19
Vitamin E	20 mg/kg	13	77	8.25	34
Trolox	4 mg/kg	5	60	3.85	6
Anti-NK (TMβ-1)	1 mg	15	53.3	4.12	8
Futhan	20 μg/day	4	50	2.75	4
Bleeding		20	35	7.42	14
P. falciparum various amount	0.3%	2	100	2	2
	1%	2	100	4	4
	5%	2	100	5.5	6
	7%	2	100	4	4
	10%	2	100	5.5	6
pABA	400 mg/kg	4	100	4.5	5
Folinic acid	400 mg/kg	4	100	4.5	5

Table 1. Coinfection of *Plasmodium chabaudi* and *Plasmodium yoelii*; NAC and vitamin E seem to have beneficial effect in *P. falciparum* survival; however, results are very heterogenous from one mouse to other and from one experiment to other [5].

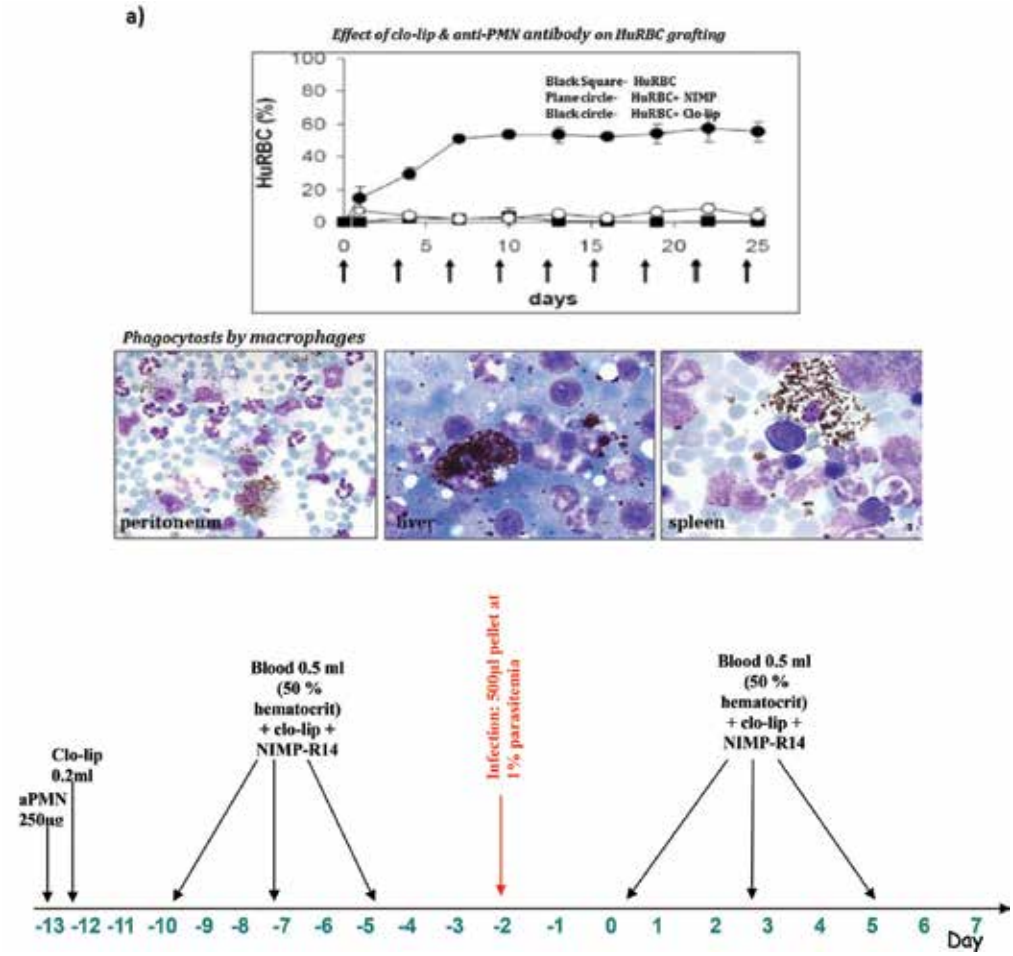

Figure 2. Immunosuppression of nonadaptive residual immune responses of immunodeficient mice by the sustained delivery of (a) clodronate via liposomes and (b) chemical immunomodulation protocol to control residual innate immune responses for robust "humanization".

9. Clodronate-loaded liposomes play a crucial role in host's immunosuppression for sizeable *P. falciparum* grafting in a humanized mouse

To aid in human cell engraftment in recently developed transgenic/immunodeficient strain, TK-NOG [53] mouse is used. Clodronate-loaded liposome will ameliorate the residual nonadaptive immune response by depleting the sizeable number of cells from monocyte-macrophage lineage. The clo-lip (clodronate-loaded liposome) is scavenged by the cells of monocyte-macrophage lineage, triggering their apoptosis and creating stroma for huHep grafting. Recent surge in the usage of humanized mouse models owing to the results from earlier findings [4, 5] in which clodronate-loaded liposome treatment depletes

the macrophage level in an immunodeficient mouse (Pf-NSG-IV) to study of asexual blood stage infection of *P. falciparum* (**Figures 2** and **3**).

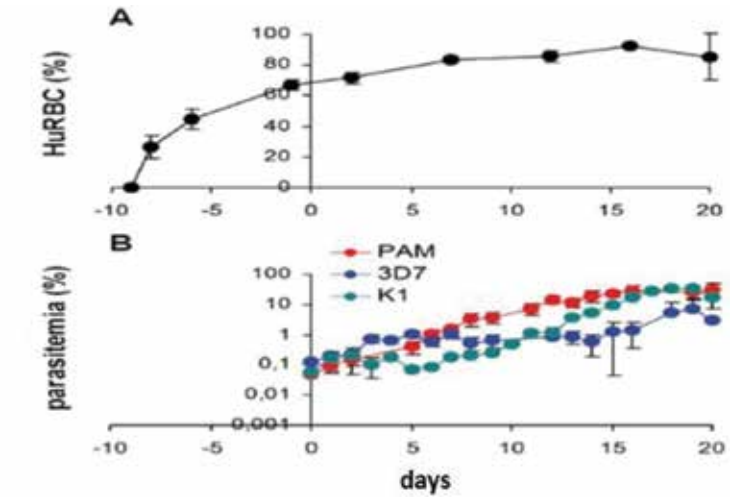

Figure 3. P. *falciparum* engraftment and development in an optimized humanized (PfhuRBC/NSG-IV) mouse [4, 5, 48]. A) Upper panel shows significant human blood chimerism in NSG mice over the period of more than 21 days, and B) lower panel illustrates the sizeable parasitemia using three (PAM, 3D7 and K1) P. falciparum strains in the huRBC reconstituted NSG mice.

10. Human malaria: a systemic inflammatory infectious disease

Malaria is one of the most deadly diseases in terms of mortality and morbidity affecting almost 2 million people worldwide. According to the WHO report, 2015, mortality due to malaria reached 438,000 deaths worldwide, majority of these occurring in African region (90%), followed by the Southeast Asia region (7%) and the Eastern Mediterranean region (2%).

However the malaria incidents dropped drastically by 37% across the globe and by 42% in Africa. Also there was a gradual decrease in the mortality rate by 60% globally and 66% in African region. The life cycle of malaria parasite is shown in **Figure 4**.

P. falciparum has gone to a wider trajectory to develop resistance against all the drugs and more complex patterns of multidrug resistance than anticipated. The suboptimal and uncontrolled use of drugs may lead to severe consequences of drug resistance in the field which could pose threat with unprecedented global health crisis. This scenario gets dangerous in the wake of unavailability of effective vaccines against *P. falciparum*.

10.1. The malaria vaccine development: a challenging task

Malaria is actually caused by the parasite called *Plasmodia* spp. which is highly evolved and a complex organism. The mercurial behavior of parasite because of the secretion of tens of thousands of proteins

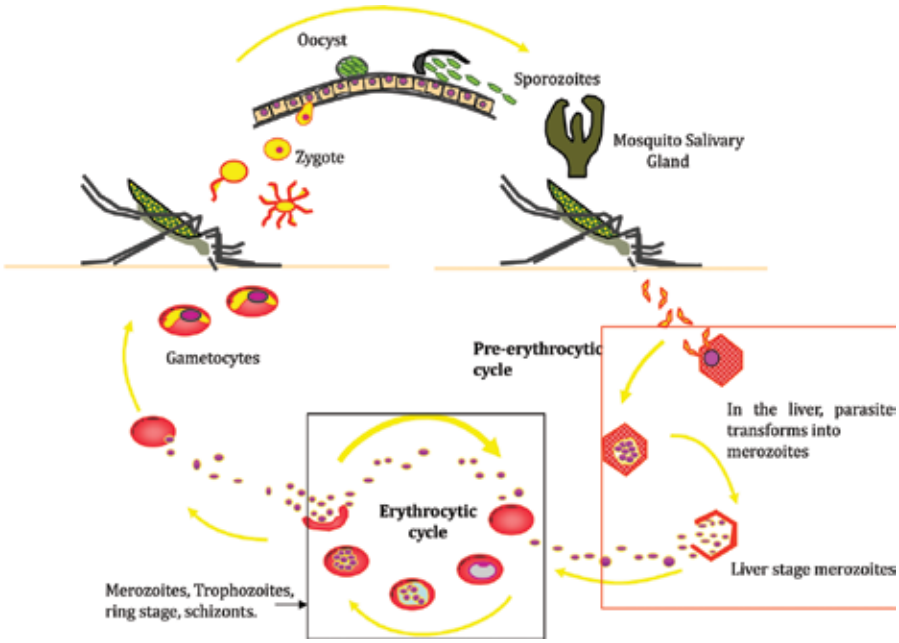

Figure 4. Life cycle of malaria parasite.

at each and every stage establishes it as one of the biggest challenges of humanity. The classical way of making a vaccine is to take the whole organism, the whole bacterium, or the virus and to inactivate it and to inject that as vaccine. That can be done for malaria, but it has been very hard to deploy that into a product—it is actually even harder to cultivate parasite especially liver stage in the lab as the conditions are not commensurate for its replication. The induction of potent and sterile immune responses is very difficult against LS of *P. falciparum*.

Parasite undergoes liver-stage development culminating in the formation and release of tens of thousands of first-generation parasites going undetected as this stage is asymptomatic. The asexual parasite stage can be cultivated in vitro, but the sporogonic stages require a workable humanized mouse model.

The *P. falciparum* consists of about 23 megabase nuclear genomes which has 14 chromosomes and encodes about 5300 genes. For example, two genes mainly Pfmdr1 and Pfmdr2 (*Plasmodium falciparum* multidrug resistance), *Plasmodium falciparum* multidrug resistance-associated protein (Pfmrp), are linked with the amount of drug that accumulates inside the digestive vacuole. Efficacy of drugs is dependent on these transporters as they shuffle them from intravacuolar to extravacuolar and vice versa. This observation suggests the common element of multigenic mechanism associated with mefloquine, halofantrine, and dihydroartemisinin. As the same gene has different effects depending on the type of gene mutation, it becomes difficult to identify any one functional gene emanating resistance. Therefore, vaccine development is a challenging and a herculean task to achieve [54].

11. Liposome as a vaccine candidate

Liposomes are tools that can be used in tumor-targeting, gene-silencing, antisense therapy; immunomodulation; and genetic vaccination [48]. Liposomes (pH-sensitive liposomes) are majorly used for targeted and cytosolic delivery of vaccine candidate for achieving perdurable immune responses as well as delivery of drugs. They can be used as an efficient tool in vaccine development. The mycobacterial lipids when used to formulate liposomes have shown immense potential for mounting upon the sizeable cellular response which are considered as Th1 adjuvant.

The 19 kDa fragment (carboxy-terminal) of merozoite surface protein-1 of *Plasmodium falciparum* (PfMSP-119) is delivered directly into the cytosol with the help of liposomes to enhance immunogenicity. Engineered liposomes are used for sustained release of entrapped content and to increase immunogenicity. The liposomal vesicles have entrapped core of polymer that provides mechanical strength to them.

Gel core liposomes (engineered liposomes) were potentially tested for their utility in intramuscular delivery of transmission blocking antigen Pfs25 (recombinant protein antigen). Further, by using these engineered liposomes, the study evaluated the effect of coadministration of vaccine adjuvants CpG-ODN on the immune system of Pfs25. Liposome formulations of caryostatics, antibiotics, photosensitizers, enzymes, hormones, cytokines, and nucleic acids are being used to achieving some very promising results.

For targeting the DNA vaccine uptake and expression, APC are a preferred alternative to muscle cells. Antigen-coding plasmid DNA when administered via liposomes could bypass the need of muscle involvement and facilitates its uptake by APC, for instance, those infiltrating the site of injection or in the lymphatic, at the same time protecting DNA from nuclease attack [48, 55]. Engineered liposomes show advantage because of their evasion ability to escape the invasive route of administration making it an efficient carrier for the delivery of entrapped contents. Transfection of APC with liposome-entrapped DNA could be rendered by selecting an appropriate vesicle surface charge and lipid composition or by the co-entrapment of other adjuvants together with the plasmid DNA [48, 55–58] (**Figure 5**).

The proposed concepts of antimalarial vaccine based on liposomal construct of various types (cocktail formulation):

a. Recombinant protein-containing liposomes target specific, however, non-pH sensitive to deliver rDNA protein from (CSP 22), SPF 66 form of sporozoites and merozoites, so that proteins are specifically processed through endosomal pathway and presented by APCs through MHC II.

b. The second population of liposomes will contain dendritic cells targeted pH-sensitive liposomes bearing rDNA lipid complexes (target specific and pH sensitive) to deliver them to the cytosol of specific cells, that is, dendritic cells for subsequent expression of liver-stage and erythrocytic stage antigenic cellular expression and MHC I restricted presentation for Th-1 cellular CTL responses.

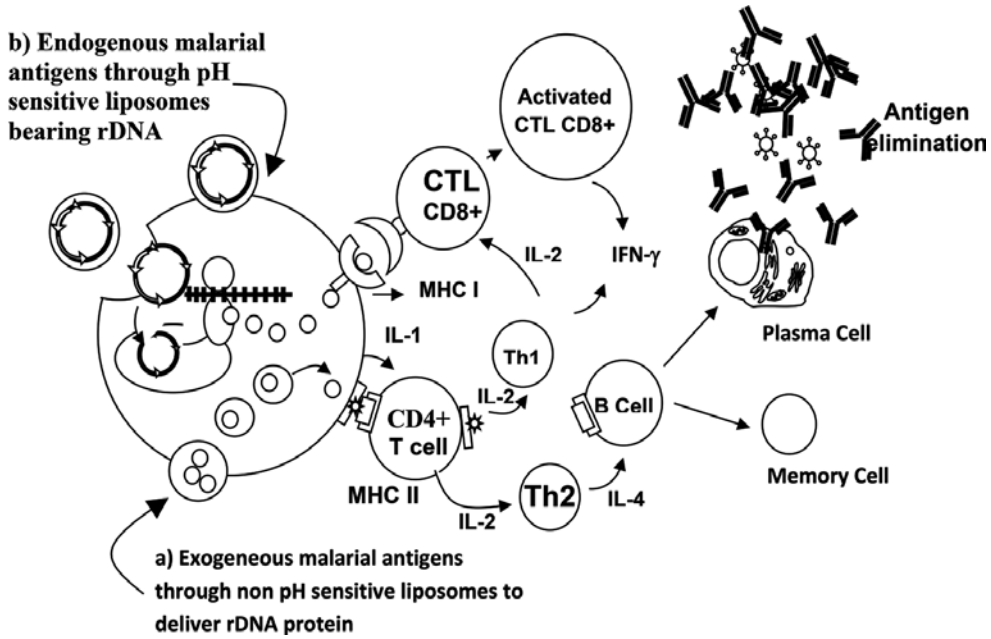

Figure 5. Schematics illustrating the proposed concepts of antimalarial vaccine based on liposomal construct of various types (cocktail formulation).

12. Cytotoxicity rendered by liposomes

1. **Dermal toxicity**: Conventional doxorubicin is used actively in various malignant tumors giving rise to a number of side effects like cardiotoxicity and myelosuppression. A different approach of this chemotherapeutic agent enclosed in PEGylated liposomes, in which liposome encapsulation prevents doxorubicin from penetration to compartments with tight endothelial cells junctions and facilitates its distribution to tissues with abnormal blood vessels [59]. This results in higher drug accumulation within the tumor than normal tissues. Consequently, a decreased incidence of cardiac and hematological toxicity is observed. PEGylated liposomal doxorubicin (PLD) has the ability to deposit itself within the skin and to induce specific mucocutaneous reactions. There are six types of PLD-related dermal disorders, and the most common is palmar-plantar erythrodysesthesia (PPE) [60]. Other less frequent manifestations are intertrigo-like dermatitis, a diffuse follicular rash, a maculopapular rash, melanotic macules, or a recall phenomenon. Dermal toxicity is the most common adverse reaction limiting PLD therapy. Skin lesions usually appear in regions prone to trauma such as the palms and soles. This was reported in a patient suffering from ovarian cancer showing partial response to chemotherapy [61].

2. **PEGylated liposomal doxorubicin (PLD)** was administered in patients. These PEGylated liposomes show a lower rate of cardiotoxicity and myelosuppression but show some obvious adverse effects including palmar-plantar erythrodysesthesia (PPE and some dermal manifestations such as intertrigo-like dermatitis, diffuse follicular rash, melanotic macules,

maculopapular rash [61]. Some studies have advocated that dimethyl sulfoxide or corticosteroids may be beneficial in the treatment of PLD-induced dermal complications as they accelerate skin recovery. The only well-established preventive management includes dose intensity modification or complete chemotherapy discontinuation.

13. Future challenges

For some drugs like DaunoXome, AmBisome, Doxil, Epaxel, etc., liposomes have proved to be a reliable delivery vehicle with some major challenges:

1. **Uptake by reticuloendothelial system**: Liposomes may be formulated as aerosol and as semisolid form such as cream, gel, or dry powder and are administered. They will then be readily taken up by the mononuclear phagocyte system (MPS) such as Kupffer cells of the liver and spleen. This is the natural route for the uptake of liposomes; however, they lack the ability to target site-specific receptors expressed on the surface of diseased cells and hence are inefficient for site-specific delivery. Therefore, liposomes which may evade rapid uptake by MPS need to be developed and further explored. PEG-coated or sterically stabilized liposomes are a few glaring examples.
2. **Large-scale production**: Production of liposomes from small scale (laboratories) to a large scale is a challenging task. The regulatory norms of the use of chloroform and methanol are not recommended more than the permissible limits. Preparation of liposomes also involves various steps like evaporation of solvent system under reduced pressure, preparation of thin lipid film, sonication, etc. These procedural hurdles pose a challenge across the researchers to develop these vehicles on a large scale.
3. **In process stability**: The oxidation and/or hydrolysis of phospholipids used in liposomal preparation does not allow the long-term storage and therefore less shelf-life. The physical and chemical instability of prepared liposomes is something to be explored further. However, fewer formulations are used in a lyophilized form which is to be reconstituted in a suitable buffer before use. Also, liposomes cannot withstand the degradation from proteins and enzymes in an animal model due to electrostatic stabilization.

Author details

Kunjal Agrawal[1,#], Vishwa Vyas[1,#], Yamnah Hafeji[1] and Rajeev K. Tyagi[1,2*]

*Address all correspondence to: rajeev.dbt@gmail.com

1 Institute of Science, Nirma University, Ahmedabad, Gujarat, India

2 Department of Global Health, College of Public Health, University of South Florida, Tampa, FL, USA

# These authors contributed equally to this work.

References

[1] Good MF, Hawkes MT, Yanow SK. Humanized mouse models to study cell-mediated immune responses to liver-stage malaria vaccines. Trends in Parasitology. 2015; **31**(11):583-594

[2] Tyagi RK, Miles B, Parmar R, Garg NK, Dalai SK, Baban B, et al. Human IDO-competent, long-lived immunoregulatory dendritic cells induced by intracellular pathogen, and their fate in humanized mice. Scientific Reports. 2017;**7**:41083

[3] Shultz LD, Brehm MA, Garcia-Martinez JV, Greiner DL. Humanized mice for immune system investigation: Progress, promise and challenges. Nature Reviews Immunology. 2012;**12**(11):786-798

[4] Arnold L, Tyagi RK, Meija P, Swetman C, Gleeson J, Perignon JL, et al. Further improvements of the *P. falciparum* humanized mouse model. PLoS One. 2011;**6**(3):e18045

[5] Arnold L, Tyagi RK, Mejia P, Van Rooijen N, Perignon JL, Druilhe P. Analysis of innate defences against *Plasmodium falciparum* in immunodeficient mice. Malaria Journal. 2010;**9**:197

[6] Hu Z, Van Rooijen N, Yang YG. Macrophages prevent human red blood cell reconstitution in immunodeficient mice. Blood. 2011;**118**(22):5938-5946

[7] Jordan MB, van Rooijen N, Izui S, Kappler J, Marrack P. Liposomal clodronate as a novel agent for treating autoimmune hemolytic anemia in a mouse model. Blood. 2003;**101**(2):594-601

[8] Wagner A, Vorauer-Uhl K. Liposome technology for industrial purposes. Journal of Drug Delivery. 2011;**2011**:591325

[9] Bozzuto G, Molinari A. Liposomes as nanomedical devices. International Journal of Nanomedicine. 2015;**10**:975-999

[10] Akbarzadeh A, Rezaei-Sadabady R, Davaran S, Joo SW, Zarghami N, Hanifehpour Y, et al. Liposome: Classification, preparation, and applications. Nanoscale Research Letters. 2013;**8**(1):102

[11] Conlan JW, Krishnan L, Willick GE, Patel GB, Sprott GD. Immunization of mice with lipopeptide antigens encapsulated in novel liposomes prepared from the polar lipids of various Archaeobacteria elicits rapid and prolonged specific protective immunity against infection with the facultative intracellular pathogen, *Listeria monocytogenes*. Vaccine. 2001;**19**(25-26):3509-3517

[12] Krishnan L, Dicaire CJ, Patel GB, Sprott GD. Archaeosome vaccine adjuvants induce strong humoral, cell-mediated, and memory responses: Comparison to conventional liposomes and alum. Infection and Immunity. 2000;**68**(1):54-63

[13] Gould-Fogerite S, Kheiri MT, Zhang F, Wang Z, Scolpino AJ, Feketeova E, et al. Targeting immune response induction with cochleate and liposome-based vaccines. Advanced Drug Delivery Reviews. 1998;**32**(3):273-287

[14] Gregoriadis G, Davis D, Davies A. Liposomes as immunological adjuvants: Antigen incorporation studies. Vaccine. 1987;**5**(2):145-151

[15] Touitou E, Dayan N, Bergelson L, Godin B, Eliaz M. Ethosomes - novel vesicular carriers for enhanced delivery: Characterization and skin penetration properties. Journal of Controlled Release: Official Journal of the Controlled Release Society. 2000;**65**(3):403-418

[16] Huang A, Kennel SJ, Huang L. Interactions of immunoliposomes with target cells. The Journal of Biological Chemistry. 1983;**258**(22):14034-14040

[17] Sullivan SM, Connor J, Huang L. Immunoliposomes: Preparation, properties, and applications. Medicinal Research Reviews. 1986;**6**(2):171-195

[18] Perrin P, Sureau P, Thibodeau L. Structural and immunogenic characteristics of rabies immunosomes. Developments in Biological Standardization. 1985;**60**:483-491

[19] Kersten GF, Crommelin DJ. Liposomes and ISCOMs. Vaccine. 2003;**21**(9-10):915-920

[20] Audouy S, Hoekstra D. Cationic lipid-mediated transfection in vitro and in vivo (review). Molecular Membrane Biology. 2001;**18**(2):129-143

[21] Khalil IA, Kogure K, Akita H, Harashima H. Uptake pathways and subsequent intracellular trafficking in nonviral gene delivery. Pharmacological Reviews. 2006;**58**(1):32-45

[22] Mayer LD, Hope MJ, Cullis PR. Vesicles of variable sizes produced by a rapid extrusion procedure. Biochimica et Biophysica Acta. 1986;**858**(1):161-168

[23] Tamba Y, Tanaka T, Yahagi T, Yamashita Y, Yamazaki M. Stability of giant unilamellar vesicles and large unilamellar vesicles of liquid-ordered phase membranes in the presence of Triton X-100. Biochimica et Biophysica Acta (BBA): Biomembranes. 2004;**1667**(1):1-6

[24] Vyas SP, Rawat M, Rawat A, Mahor S, Gupta PN. Pegylated protein encapsulated multivesicular liposomes: A novel approach for sustained release of interferon alpha. Drug Development and Industrial Pharmacy. 2006;**32**(6):699-707

[25] Brewer JM, Alexander J. Studies on the adjuvant activity of non-ionic surfactant vesicles: Adjuvant-driven IgG2a production independent of MHC control. Vaccine. 1994;**12**(7):613-619

[26] Drummond DC, Zignani M, Leroux J. Current status of pH-sensitive liposomes in drug delivery. Progress in Lipid Research. 2000;**39**(5):409-460

[27] Regen SL, Singh A, Oehme G, Singh M. Polymerized phosphatidyl choline vesicles. Stabilized and controllable time-release carriers. Biochemical and Biophysical Research Communications. 1981;**101**(1):131-136

[28] Jung BH, Chung BC, Chung SJ, Lee MH, Shim CK. Prolonged delivery of nicotine in rats via nasal administration of proliposomes. Journal of Controlled Release: Official Journal of the Controlled Release Society. 2000;**66**(1):73-79

[29] Payne NI, Timmins P, Ambrose CV, Ward MD, Ridgway F. Proliposomes: A novel solution to an old problem. Journal of Pharmaceutical Sciences. 1986;**75**(4):325-329

[30] Janga KY, Jukanti R, Velpula A, Sunkavalli S, Bandari S, Kandadi P, et al. Bioavailability enhancement of zaleplon via proliposomes: Role of surface charge. European Journal of Pharmaceutics and Biopharmaceutics: Official Journal of Arbeitsgemeinschaft fur Pharmazeutische Verfahrenstechnik eV. 2012;**80**(2):347-357

[31] Lowell GH, Smith LF, Seid RC, Zollinger WD. Peptides bound to proteosomes via hydrophobic feet become highly immunogenic without adjuvants. The Journal of Experimental Medicine. 1988;**167**(2):658-663

[32] Szoka F, Jr., Papahadjopoulos D. Procedure for preparation of liposomes with large internal aqueous space and high capture by reverse-phase evaporation. Proceedings of the National Academy of Sciences of the United States of America. 1978;**75**(9):4194-4198

[33] Cortesi R, Esposito E, Gambarin S, Telloli P, Menegatti E, Nastruzzi C. Preparation of liposomes by reverse-phase evaporation using alternative organic solvents. Journal of Microencapsulationcapsulation. 1999;**16**(2):251-256

[34] Allen TM, Hansen C, Martin F, Redemann C, Yau-Young A. Liposomes containing synthetic lipid derivatives of poly(ethylene glycol) show prolonged circulation half-lives in vivo. Biochimica et Biophysica Acta. 1991;**1066**(1):29-36

[35] Blume G, Cevc G. Liposomes for the sustained drug release in vivo. Biochimica et Biophysica Acta. 1990;**1029**(1):91-97

[36] Klibanov AL, Maruyama K, Torchilin VP, Huang L. Amphipathic polyethyleneglycols effectively prolong the circulation time of liposomes. FEBS Letters. 1990;**268**(1):235-237

[37] Lasic DD, Martin FJ, Gabizon A, Huang SK, Papahadjopoulos D. Sterically stabilized liposomes: A hypothesis on the molecular origin of the extended circulation times. Biochimica et Biophysica Acta. 1991;**1070**(1):187-192

[38] Senior J, Delgado C, Fisher D, Tilcock C, Gregoriadis G. Influence of surface hydrophilicity of liposomes on their interaction with plasma protein and clearance from the circulation: Studies with poly(ethylene glycol)-coated vesicles. Biochimica et Biophysica Acta. 1991;**1062**(1):77-82

[39] Woodle MC, Lasic DD. Sterically stabilized liposomes. Biochimica et Biophysica Acta. 1992;**1113**(2):171-199

[40] Moghimi SM, Szebeni J. Stealth liposomes and long circulating nanoparticles: Critical issues in pharmacokinetics, opsonization and protein-binding properties. Progress in Lipid Research. 2003;**42**(6):463-478

[41] Kono K. Thermosensitive polymer-modified liposomes. Advanced Drug Delivery Reviews. 2001;**53**(3):307-319

[42] Needham D, Dewhirst MW. The development and testing of a new temperature-sensitive drug delivery system for the treatment of solid tumors. Advanced Drug Delivery Reviews. 2001;**53**(3):285-305

[43] Mishra D, Dubey V, Asthana A, Saraf DK, Jain NK. Elastic liposomes mediated transcutaneous immunization against Hepatitis B. Vaccine. 2006;**24**(22):4847-4855

[44] Tyagi RK, Garg NK, Jadon R, Sahu T, Katare OP, Dalai SK, et al. Elastic liposome-mediated transdermal immunization enhanced the immunogenicity of *P. falciparum* surface antigen, MSP-119. Vaccine. 2015;**33**(36):4630-4638

[45] Gluck R. Adjuvant activity of immunopotentiating reconstituted influenza virosomes (IRIVs). Vaccine. 1999;**17**(13-14):1782-1787

[46] Henry BD, Neill DR, Becker KA, Gore S, Bricio-Moreno L, Ziobro R, et al. Engineered liposomes sequester bacterial exotoxins and protect from severe invasive infections in mice. Nature Biotechnology. 2015;**33**(1):81-88

[47] Van Rooijen N, Sanders A. Liposome mediated depletion of macrophages: Mechanism of action, preparation of liposomes and applications. Journal of Immunological Methods. 1994;**174**(1-2):83-93

[48] Tyagi RK, Garg NK, Sahu T. Vaccination strategies against malaria: Novel carrier(s) more than a tour de force. Journal of Controlled Release: Official Journal of the Controlled Release Society. 2012;**162**(1):242-254

[49] van Rooijen N, Sanders A, van den Berg TK. Apoptosis of macrophages induced by liposome-mediated intracellular delivery of clodronate and propamidine. Journal of Immunological Methods. 1996;**193**(1):93-99

[50] Drake RD, Lin WM, King M, Farrar D, Miller DS, Coleman RL. Oral dexamethasone attenuates Doxil-induced palmar-plantar erythrodysesthesias in patients with recurrent gynecologic malignancies. Gynecologic Oncology. 2004;**94**(2):320-324

[51] Allison AG, Gregoriadis G. Liposomes as immunological adjuvants. Nature. 1974;**252** (5480):252

[52] Rosenkrands I, Agger EM, Olsen AW, Korsholm KS, Andersen CS, Jensen KT, et al. Cationic liposomes containing mycobacterial lipids: A new powerful Th1 adjuvant system. Infection and Immunity. 2005;**73**(9):5817-5826

[53] Nishiyama S, Suemizu H, Shibata N, Guengerich FP, Yamazaki H. Simulation of human plasma concentrations of thalidomide and primary 5-hydroxylated metabolites explored with pharmacokinetic data in humanized TK-NOG mice. Chemical Research in Toxicology. 2015;**28**(11):2088-2090

[54] Menard R, Tavares J, Cockburn I, Markus M, Zavala F, Amino R. Looking under the skin: The first steps in malarial infection and immunity. Nature Reviews Microbiology. 2013;**11**(10):701-712

[55] Owais M, Gupta CM. Liposome-mediated cytosolic delivery of macromolecules and its possible use in vaccine development. European Journal of Biochemistry. 2000; **267**(13):3946-3956

[56] Tiwari S, Goyal AK, Khatri K, Mishra N, Vyas SP. Gel core liposomes: An advanced carrier for improved vaccine delivery. Journal of Microencapsulation. 2009;**26**(1):75-82

[57] Tiwari S, Goyal AK, Mishra N, Khatri K, Vaidya B, Mehta A, et al. Development and characterization of novel carrier gel core liposomes based transmission blocking malaria vaccine. Journal of Controlled Release: Official Journal of the Controlled Release Society. 2009;**140**(2):157-165

[58] Tyagi RK, Garg NK, Dalai SK, Awasthi A. Transdermal immunization of *P. falciparum* surface antigen (MSP-119) via elastic liposomes confers robust immunogenicity. Human Vaccines & Immunotherapeutics. 2016;**12**(4):990-992

[59] Mangana J, Zipser MC, Conrad C, Oberholzer PA, Cozzio A, Knuth A, et al. Skin problems associated with pegylated liposomal doxorubicin-more than palmoplantar erythrodysesthesia syndrome. European Journal of Dermatology. 2008;**18**(5):566-570

[60] Green AE, Rose PG. Pegylated liposomal doxorubicin in ovarian cancer. International Journal of Nanomedicine. 2006;**1**(3):229-239

[61] Kubicka-Wolkowska J, Kedzierska M, Lisik-Habib M, Potemski P. Skin toxicity in a patient with ovarian cancer treated with pegylated liposomal doxorubicin: A case report and review of the literature. Oncology Letters. 2016;**12**(6):5332-5334

Edited by Angel Catala

Liposomes have received increased attention in recent years. Nevertheless, liposomes, due to their various forms and applications, require further investigation. These structures can deliver both hydrophilic and hydrophobic drugs. Preparation of liposomes results in different properties for these systems. In addition, there are many factors and difficulties that affect the development of liposome drug delivery structure. The purpose of this book is to concentrate on recent developments on liposomes. The articles collected in this book are contributions by invited researchers with a long-standing experience in different research areas. We hope that the material presented here is understandable to a broad audience, not only scientists but also people with general background in many different biological sciences. This volume offers you up-to-date, expert reviews of the fast-moving field of liposomes.

ISBN 978-953-51-4622-3

Photo by Jezperklauzen / iStock

IntechOpen